Non-Hermitian Quantum Mechanics

NIMROD MOISEYEV

CAMBRIDGE

CAMBRIDGE

www.cambridge.org/9780521889728

NON-HERMITIAN QUANTUM MECHANICS

Non-Hermitian quantum mechanics (NHQM) is an important alternative to the standard (Hermitian) formalism of quantum mechanics, enabling the solution of otherwise difficult problems. The first book to present this theory, it is useful to advanced undergraduate and graduate students and researchers in physics, chemistry and engineering.

NHQM provides powerful numerical and analytical tools for the study of resonance phenomena – perhaps one of the most striking events in nature. It is especially useful for problems whose solutions cause extreme difficulties within the structure of a conventional Hermitian framework. NHQM has applications in a variety of fields, including optics, where the refractive index is complex; quantum field theory, where the parity-time (PT) symmetry properties of the Hamiltonian are investigated; and atomic and molecular physics and electrical engineering, where complex potentials are introduced to simplify numerical calculations.

NIMROD MOISEYEV is Bertha Hartz Axel Professor of Chemistry and Physics and a member of the Minerva Centre for Nonlinear Physics of Complex Systems at the Technion-Israel Institute of Technology. He has won numerous awards for his work, including the Humboldt Prize, the Marie Curie Prize, the Landau Award and the Centre de Mécanique Ondulatoire Appliquée (CMOA) medal for his “major contribution to the development of the non-Hermitian theory of quantum mechanics”.

NON-HERMITIAN QUANTUM MECHANICS

NIMROD MOISEYEV
Technion-Israel Institute of Technology

CAMBRIDGE
UNIVERSITY PRESS

CAMBRIDGE UNIVERSITY PRESS
Cambridge, New York, Melbourne, Madrid, Cape Town, Singapore,
São Paulo, Delhi, Dubai, Tokyo, Mexico City

Cambridge University Press
The Edinburgh Building, Cambridge CB2 8RU, UK

Published in the United States of America by Cambridge University Press, New York

www.cambridge.org
Information on this title: www.cambridge.org/9780521889728

First published 2011

Printed in the United Kingdom at the University Press, Cambridge

A catalogue record for this publication is available from the British Library

Library of Congress Cataloguing in Publication data
Moiseyev, Nimrod, 1947–
Non-Hermitian quantum mechanics / Nimrod Moiseyev.
p. cm.
Includes bibliographical references and index.
ISBN 978-0-521-88972-8 (hardback)
1. Quantum theory – Mathematics. 2. Hermitian structures. 3. Resonance.
4. Hermitian symmetric spaces. I. Title.
QC174.17.M35M65 2011
530.12 – dc22 2010040292

ISBN 978-0-521-88972-8 Hardback

To the memory of my parents Rachel and Itzhak
who taught me to wonder

The Lively Imagination/Zelda

For the lively imagination
Holds a secret key,
Granted to the ignorant and unlettered,
That unlocks the ivory doors of science.
It enters the soaring towers,
Ambles through the equation-teeming dark –
And whistles there in wonder
Like an unruly youth.

Translated from the Hebrew by *Amitai Halevi*

Contents

Preface

This is the first book ever written that presents non-Hermitian quantum mechanics (NHQM) as an alternative to the standard (Hermitian) formalism of quantum mechanics. Previous knowledge of the basic principles of quantum mechanics and its standard formalism is required.

The standard formalism is based on the requirement that all observable properties of a dynamic nature are associated with the real eigenvalues of a special class of operators, called Hermitian operators. All textbooks use Hermitian Hamiltonians in order to ensure conservation of the number of particles. See, for example, the monumental book of Dirac on *The Principles of Quantum Mechanics*.

The motivation for the derivation of the NHQM formalism is twofold.

The first is to be able to address questions that can be answered **only** within this formalism. For example:

- in optics, where complex index of refraction are used;
- in quantum field theory, where the parity–time (PT) symmetry properties of the Hamiltonian are investigated;
- in cases where the language of quantum mechanics is used, even though the problems being addressed are within classical statistical mechanics or diffusion in biological systems;
- in cases where complex potentials are introduced far away from the interaction region of the particles. This approach simplifies the numerical calculations and avoids artificial interference effects caused by reflection of the propagated wave packets from the edge of the grid.

The second is the desire to tackle problems that can, in principle, also be solved within the conventional Hermitian framework, but only with extreme difficulty, whereas the NHQM formalism enables a much simpler and more elegant solution. Moreover it provides the insight that is required in order to predict novel physical phenomena and to design the corresponding experiments. It is most useful in exploration of the **resonance** phenomena, where particles are temporarily trapped by the potential.

In their book on non-relativistic quantum mechanics, Landau and Lifshitz wrote about the need for NHQM:

> Until now we have always considered solutions of the Schrödinger equation with a boundary condition requiring the finiteness of the wavefunction at infinity. Instead of this, we shall look for solutions which represent an outgoing spherical wave at infinity; this corresponds to the particle finally leaving the system when it disintegrates. Since such a boundary condition is complex, we cannot assert that the eigenvalues of the energy must be real. (Section 132 on Resonance at a quasi-discrete level).

The resonance phenomena are some of the most striking phenomena in nature. Resonances are associated with metastable states of a system that has sufficient energy to break up into two or more subsystems. These systems can be nuclei, atoms, molecules, solids, nano-structured materials and condensates. The subsystems may contain elementary particles and/or neutral or negatively/positively charged atomic or molecular ions. The systems whose dynamics is controlled by the resonance phenomena can be as small as protonium (the exotic atom consisting of a proton and an anti-proton) or a helium atom, or as large as a protein.

However, because of the exponential divergence of the asymptotes of the resonance solutions, the derivation of the NHQM formalism became possible **only** after the derivation of the complex scaling transformation by Balslev-Combes and by Barry Simon, with which resonance wavefunctions become square integrable as **bound states** in the standard formalism. The non-Hermitian formalism avoids the need to carry out complicated wave-packet-propagation calculations in order to describe resonance phenomena, and enables the association of a given resonance phenomenon as it appears in an atomic, molecular, nuclear or chemical system with a **single** square-integrable eigenfunction of the complex-scaling Hamiltonian. Therefore, the non-Hermitian formalism, based on this kind of transformation, enables the calculation of cross sections and dynamical properties of systems controlled by their resonance states, by using computational algorithms that were originally developed for bound states in conventional Hermitian quantum mechanics.

Nevertheless, many questions remain unanswered. For example: what is the solution of the time-asymmetric problem in non-Hermitian quantum mechanics? It arises because the time-dependent phase factor, $\exp(-\mathrm{i}Et/\hbar)$, which since $-2\mathrm{Im}(E)$, the decay rate, is necessarily positive, diverges exponentially as $t \to -\infty$. What are the implications and physical manifestations of the incomplete spectrum of a non-Hermitian Hamiltonian that is obtained when two or more eigenstates coalesce to a single self-orthogonal state? What is the physical interpretation of the phase of the complex probability density in non-Hermitian quantum mechanics and how would time-dependent expectations of measurable quantities be calculated?

The answers to these questions that are given in this book are based mainly on my research over the last three decades. It began with my work in Madison, Wisconsin with Phil Certain and Frank Weinhold on the properties of the complex-scaled non-Hermitian Hamiltonian, and then through many years of research with my PhD students and post-doctoral fellows and with my colleagues as well. (I am fortunate to have been surrounded by so many gifted people for such a long period of time.) Thirty years ago, in collaboration with the mathematician Shmuel Friedland, we found that self-orthogonality, the coalescence of two or more eigenstates, is related to the incomplete spectrum of the non-Hermitian complex-scaled Hamiltonian. However, it was not until my most recent series of studies that it was shown to be an observable phenomenon that may have different effects in different fields of physical science.

Aside from presenting the non-Hermitian formalism of quantum mechanics, the purpose of this textbook is to provide many solved problems that will provide a better understanding of the foundations of quantum mechanics, to explain the algorithms for calculating the resonance measurable quantities, and to illustrate the applications of the formalism to physics, chemistry and technology. It should be noted that many of the exercises are not included for honing the skills of the reader, but rather for introducing him/her to additional details of the theory – which can be skipped by readers who may not be interested or conversant with the more technical details.

This textbook is designed for use by graduate and undergraduate students that have already attended a basic course in quantum mechanics. However, for the sake of coherence and in order to make the book more self-contained, the exercises also include problems and solutions for Hermitian cases.

I am grateful to many of my students and colleagues, without whom I would not have been able to do the scientific work that laid the groundwork for this book. Above all, I wish to express my thanks to my student Dr Ido Gilary, who has carefully read the manuscript and checked the solutions given in the book, and whose cogent comments have helped me present the theory more coherently and avoid many pitfalls. Any errors or inaccuracies that remain in the final version are my responsibility alone.

Last but by no means least, I thank my wife Etty, my children Gilead and Hamutal, my daughter and son-in-law Vardit and David, and my grandchildren Noam and Jonathan for their patience, care and love, that gave me the peace of mind needed to do science with joy and fun.

1

Different formulations of quantum mechanics

This book is dedicated to the non-Hermitian formalism of quantum mechanics. In this chapter we wish to give the motivation and the rational for developing a non-Hermitian formalism to quantum mechanics. Therefore this chapter will not explain how non-Hermitian calculations are carried out or in what way the non-Hermitian formalism is analogous to the standard (Hermitian) formalism of quantum mechanics. It is important to emphasize that there is no (known) transformation which enables one to map results which were obtained using one formalism to the other one. Yet, the same physical results should be obtained by studying the same phenomenon using the two formalisms. If this is the case, why should one bother to develop an alternative formalism to the standard Hermitian formalism of quantum mechanics?

There are several reasons for doing this and here we shall focus on five of those reasons.

(1) *There are phenomena which can be explained in a straightforward fashion using the non-Hermitian formalism but are very hard and often impossible to explain within the framework of the standard (Hermitian) formalism of quantum mechanics.*
In particular in Chapter 9 we will describe several physical phenomena which are associated with the self-orthogonality where two or more degenerate resonance states are coalesced.

(2) *There are physical phenomena which one might not immediately associate with quantum behavior where the quantum language can be used to describe the physics.*
The studied problem may be, for example, in systems described in terms of classical statistical mechanics, diffusion in biological systems, or propagation of light in waveguides (WG). In such cases the Hamiltonians are not Hermitian since the system at hand is open to interaction with its environment. For example, when light is propagated in an optical WG within the paraxial approximation the scalar Maxwell equation is like the time-dependent Schrödinger equation with a time-independent Hamiltonian. The square of the index of refraction (with a minus sign) serves as a potential

energy term in quantum mechanics. The propagation axis Z serves as time in quantum mechanics. The imaginary part of the complex index of refraction indicates the amount of absorption loss of the propagated light when it passes through the wave guide. The complex potential renders the Hamiltonian non-Hermitian and therefore such systems can be only studied within the framework of the non-Hermitian formalism discussed here.

(3) *Simplification of numerical propagation of wave packets in time.*
The propagation of matter waves by the Schrödinger equation and the propagation of light in waveguides in the paraxial approximation are associated with two different physical phenomena but they obey the same mathematical equation. The numerical propagation of wave packets is much more simple when taken within the framework of the non-Hermitian formalism of quantum mechanics rather than in the standard (Hermitian) formalism. This is due to the inclusion of a reflection-free complex absorbing potential (RF-CAP) in the Hamiltonian which attains non-zero values only in the non-interacting region in the coordinate space where the physical potentials vanish. This approach enables one to avoid the artificial reflections from the edge of the numerical grid when a finite number of grid points (or a finite number of basis functions) are used to describe a propagated wave-packet. By adding the complex non-Hermitian potential to the Hamiltonian one can carry out numerical calculations using a finite number of grid points or a finite number of basis functions (after all, our computers are finite) and have a numerically exact propagated wave-packet in the region where the RF-CAPs vanish. By numerically exact, we mean that the wave-packet which is obtained by introducing a RF-CAP into the calculations, is exactly as the wave-packet which would be calculated (if it were possible) by computers which are infinite (i.e. infinite capacity, memory and computational power). The derivation of RF-CAPs by carrying out a smooth exterior scaling transformation of the spatial coordinates is presented in Chapter 5.

(4) *Another numerical example for the advantage of the use of the non-Hermitian formalism over the standard one is when the dynamics of a given system can be described by a small number of resonance states.*
Often it is enough to describe the dynamical process and to calculate all possible measurable quantities just from a single resonance state. See, for example, in Chapter 8, the calculations of the high-harmonic-generation (HHG) spectra (i.e. the emitted high frequency radiation) and the calculations of the above-threshold-ionization (ATI) spectra from a single quasi-energy photo-induced resonance state when atoms or molecules interact with strong laser fields.

(5) *Within the framework of the non-Hermitian formalism of quantum mechanics, one can get a better understanding of different methods and theories developed in the standard (Hermitian) formalism of quantum mechanics.*
The first example is the Rayleigh–Schrödinger perturbation theory where the full Hamiltonian is defined as $\hat{H} = \hat{H}_0 + \lambda \hat{V}$, where λ is the perturbation strength parameter. The interesting non-trivial cases occur when $\hat{H}_0$ and $\hat{V}$ do not commute. The radius

of convergence of the perturbation expansion for the eigenvalues and the eigenfunctions is $|\lambda_{\mathrm{bp}}|$, where λ_{bp} is a complex branch point associated with a self-orthogonal state where several (usually only two) eigenfunctions of the full Hamiltonian coalesce. The nature of these branch points and a method to calculate them and thereby to determine the radius of convergence of a perturbational series expansion of the eigenvalues and eigenfunctions is described in Chapter 9. Another example is the calculations of the poles of the scattering matrix for many-body problems. Within the framework of the standard formalism of quantum mechanics it is very difficult, if not impossible (by the available computational facilities), to calculate the poles of the scattering matrix for many-electron atomic or molecular systems. This is particularly true when considering the electronic correlations which are missing in mean field approximations (e.g. Hartree Fock calculations for fermions and Hartree calculations for bosons). In the non-Hermitian formalism the poles of the scattering matrix can be directly obtained by calculating the complex eigenvalues of the non-Hermitian Hamiltonian, as described in Chapters 4 and 5, for time-independent and time-dependent Hamiltonians.

1.1 Hermitian operators: a brief review

A fundamental postulate in standard quantum mechanics is that any measurable dynamical quantity is represented by a Hermitian operator. This postulate results from another postulate in quantum mechanics which states that the quantities we observe are the eigenvalues of operators which represent the measurable quantities. Since measurable quantities such as the momentum of free particles or the energy of stable atoms and molecules are real quantities, the operators which represent them should be Hermitian operators. For example, the x-component of the momentum, $\hat{p}_x$, is represented by $-i\hbar\partial/\partial x$, the Hamiltonian is represented by $\hat{H}$, etc. However, these operators, $\hat{O}$, which represent measurable dynamical quantities, are Hermitian provided that they operate on functions which belong to the Hilbert space $\mathcal{H}$ of square integrable functions such that if f and g are square integrable functions, $f, g \in L_2(\mathbb{R}) = \mathcal{H}$, or have asymptotes which are periodic functions, they satisfy

$$\langle f|\hat{H}|g\rangle = \langle g|\hat{H}|f\rangle^* . \tag{1.1}$$

As a consequence of this postulate there are a series of theorems that serve milestones in the formalism of quantum mechanics. The eigenvalues of Hermitian operators are real and expectation values of any measurable quantity are real. The eigenfunctions of Hermitian operators can serve as a complete set in the series expansion of any wavepacket (including time-dependent wavepackets) that represent the system under study. That is, $|\Psi\rangle = \sum_j c_j|j\rangle$, where $\hat{O}|j\rangle = o_j|j\rangle$. The absolute value of any one of the expansion coefficients, $|c_j|^2$, is the probability of measuring a specific quantity, o_j.

Exercise 1.1

Since the standard formulation of quantum mechanics defines physical operators as Hermitian we have to stress here that **the Hermitian property of an operator is heavily dependent on the basis set which is used to represent a dynamical variable by matrices of infinite order**. It is commonly assumed that these matrices obey the usual laws valid for finite matrices. However, it is obvious that this is not necessarily always true. Show that $\hat{p}_x^3 = (-\mathrm{i}\,\mathrm{d}/\mathrm{d}x)^3 \equiv \mathrm{i}\mathrm{d}_x^3$ is not Hermitian when particle-in-a-box eigenfunctions, $\{\phi_n(x)\}_{n=1,2,\ldots}$, are used as a basis set. Associate it with the fact that $\mathbf{P}\mathbf{P}^2 \neq \mathbf{P}^2\mathbf{P}$, where $\mathbf{P}$ is an infinite order Hermitian matrix that represents the momentum operator for a particle in a box, and its square $\mathbf{P}^2$ is well defined and diagonal.

We should emphasize here that the kind of non-Hermiticity of an operator demonstrated in Ex. 1.1 which is associated with the momentum operator is **not** the type which we commonly discuss in this book. **All the non-Hermitian properties of the Hamiltonian which will be discussed in this book result from the potential energy term in the Hamiltonian**. There are two different types of local potential energy term which render the Hamiltonian of the studied system non-Hermitian. The first type are potentials that in standard (Hermitian) formalism of quantum mechanics support a continuous spectrum. The second type of potentials are complex local potentials.

1.2 Non-Hermitian potentials which support a continuous spectrum

The potentials of open systems describe ionization or dissociation or any other phenomenon where the system under study breaks up into freely moving non-interacting subsystems. When a system is in a metastable state (so called a resonance state) it has enough energy to break up into several subsystems. A given system can arrive at a metastable resonance state in a full collision process where the target and the projectiles form an “activated complex” as they collide, which can be considered as a system that has the energy to break up into subsystems. A more natural way to create a system in a metastable resonance state is in a half collision process. In half collision processes the energy can be pumped into the system by many different ways. For example, by applying a static field, by exposing the system under study to weak or strong lasers, by using accelerators, or by heating. The systems can be, for example: nuclei, atoms, molecules, solids, nano-structured materials, and condensates. The subsystems might contain elementary particles and/or neutral or negative/positive charged atomic or molecular ions. Systems where dynamical behavior is controlled by resonances can be, for example, as small as protonium or helium atoms or as large as proteins.

Different situations where energy is pumped into a system giving it enough energy to break up into subsystems are described in the next chapter. We focus in the next chapter on resonance phenomena which are associated with systems that do not break up immediately into subsystems although they have the energy to do so, but rather remain stable for long periods of time. As time passes the outgoing subsystems reach a detector where the energy and momenta can be measured precisely. Since the momenta are eigenvalues of the momentum operator it seems that the detectors measure the wave-vectors of plane waves, $\{\mathbf{k}_j\}_{j=1,2,\ldots}$, where the measured momentum vector of the j-th particle/subsystem is given by $\hbar\mathbf{k}_j$. Therefore, it is very natural to associate the metastable resonance states of the system with ***stationary*** *solutions of the* ***time-independent*** *Schrödinger equation with* ***outgoing*** *asymptotes rather than with non-stationary wavepacket solutions of the time-dependent Schrödinger equation*. We will show in the following chapters that, even when the system interacts with time periodic electromagnetic fields, resonances can be associated with quasi-stationary solutions.

Exercise 1.2

Often in experiments the detectors measure the momenta of the outgoing particles/subsystems. Because of the uncertainty relation in quantum mechanics we know that it is impossible to measure precisely both the positions and the momenta of the outgoing particles/subsystems. However, it is possible to build detectors (antennas) that measure precisely the momenta of the outgoing particles/subsystems. Is there violation of the uncertainty "principle" since we know precisely the location of the antenna that measures the momenta of the outgoing particles/subsystems?

Here we are coming to a critical point in our discussion of the resonance phenomena. By imposing outgoing boundary conditions on the eigenfunctions of the time-independent Hamiltonian (we will extend this approach also to the time-dependent Hamiltonian in Chapter 4) two kinds of solutions are obtained. The first type of solution is the bound states. The second type of solution is the resonance states which are associated with complex eigenvalues and eigenfunctions which are **not in the Hermitian sector of the domain of the physical Hamiltonian**.

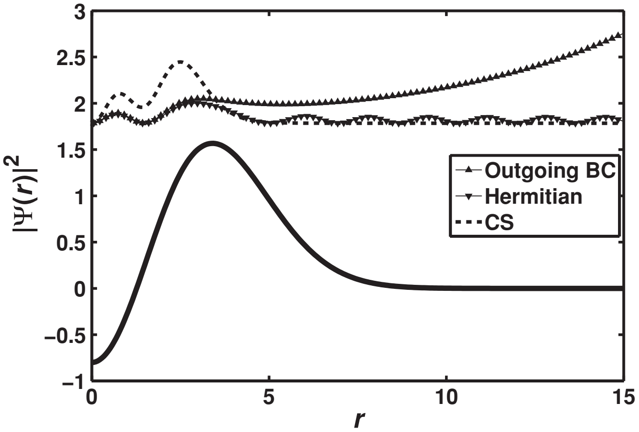

Figure 1.1 The *second* longest living resonance state for a spherical potential, $V(r) = (r^2/2 - 0.8)\exp(-0.1r^2)$, obtained by carrying out three different types of calculation. The model potential is plotted using a full dark line.

These complex resonance eigenvalues are associated with the complex poles of the scattering matrix derived within the framework of the standard (Hermitian) formalism of quantum mechanics. We will explain the properties of the resonance complex eigenvalues and eigenfunctions in detail in Chapters 4–6. As we will show in this book, the use of the resonance states as a basis set in describing full collision and half collision processes has both conceptual and numerical advantages over the standard approach. First, in many cases the dynamical process can be described as a linear combination of a small number of resonance eigenstates (i.e. solutions of the time-independent Schrödinger equation obtained by imposing outgoing boundary conditions). Often only one resonance state dominates the dynamics. In such cases, even without doing any computations one can find out what the potential parameters are which should be varied in order to control the dynamics. The variation of potential parameters can be done by selecting different type of atomic, molecular or mesoscopic systems, or by varying the structure of the system as in the case of quantum dots, quantum wells and waveguides or by varying the laser parameters when photo-induced dynamics is under study. For instance, it is quite difficult and often impossible to explain the results of experiments where the electronic and nuclear coordinates are strongly coupled to one another, such as in the case of scattering of electrons from molecules or in the scattering of anti-protons from atoms. As we will show in Chapters 4–9, within the framework of the non-Hermitian formalism of quantum mechanics we can explain the results of such experiments.

In order to illustrate the advantages in using non-Hermitian quantum mechanics for studying the resonance phenomenon, we show here in Fig. 1.1 the metastable resonance states for a particle in a spherically symmetric potential barrier given by

$$V(r) = (r^2/2 - 0.8)\mathrm{e}^{-0.1r^2} \qquad \{0 \le r \le \infty\}\,. \tag{1.2}$$

Note that the cross section of this potential in any given direction supports two barriers separated by a potential well. The s-waves eigenfunctions which are associated with the resonance phenomenon were calculated numerically by three different approaches: (1) using the Hermitian formalism of quantum mechanics; (2) using the non-Hermitian formalism by imposing outgoing boundary conditions (BC) on the solutions of the time-independent Schrödinger equation; (3) using the complex scaling method (CS) where the Hamiltonian becomes non-Hermitian due to rotation of the coordinate into the complex plane, i.e., $r \to r\exp(+\mathrm{i}\theta)$. In this method we calculate the square-integrable eigenfunctions which decay to zero as $r \to \infty$. These functions are associated with complex eigenvalues which are θ-independent (provided that θ gets to sufficiently large values). In this case the Hamiltonian is non-Hermitian due to the use of the complex scaling technique and not because of the requirement of outgoing boundary conditions.

The non-Hermitian methods for the calculations of resonance energies and wavefunctions will be described briefly in this chapter and in greater detail in Chapters 4–5. The resonance phenomenon in this case is related to the fact that a wavepacket which is initially localized inside the potential well remains localized for quite a long period of time. The different types of physical resonance phenomenon in nature are described in detail in the next chapter since resonances are one of the most interesting phenomena in physical sciences.

We now closely examine the manifestation of the resonance phenomenon in each of the approaches described above.

(1) In the first approach we calculated the s-wave continuum eigenfunctions of the Hamiltonian $\hat{H} = -0.5\partial_r^2 + (r^2/2 - 0.8)\exp(-0.1r^2)$ within the framework of the standard formalism of quantum mechanics. In Figs. 1.1 and 1.2 we show the results obtained by the Hermitian calculations for $E = \mathrm{Re}(E_{\mathrm{res}})$, where E_{res} are complex poles of the scattering matrix. To avoid the relatively complicated calculations of the scattering matrix (we discuss this approach in Chapter 3) we first evaluated the poles of the scattering matrix using the non-Hermitian formalism of quantum mechanics. Knowing the relevant values we proceeded to calculate the relevant continuum functions for two energies. One case is when $E = \mathrm{Re}(E_1^{\mathrm{res}}) = 1.784582\,\mathrm{au}$ and the other case is when $E = \mathrm{Re}(E_2^{\mathrm{res}}) = 2.455696\,\mathrm{au}$. As one can see from the results presented in Fig. 1.1 for the first case, the Hermitian continuum function is localized inside the potential well and has only very weak oscillations outside the potential barrier. However, in the second case, shown in Fig. 1.2, the situation is very different and it is hard to distinguish between the continuum function $\Psi^{QM}_{E=2.455696}(r)$ which is obtained by the

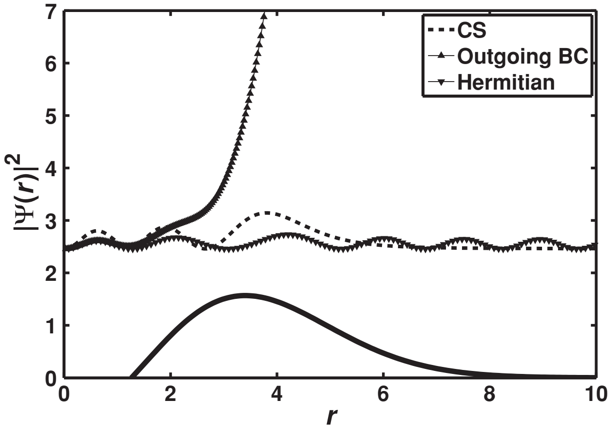

Figure 1.2 The *third* longest living resonance for a spherical potential, $V(r) = (r^2/2 - 0.8)\exp(-0.1r^2)$, obtained by carrying out three different types of calculation. The top of the potential barrier is plotted using a full dark line.

standard (Hermitian) quantum mechanical calculations and any other continuum solution which typically has a larger amplitude in the external region than in the internal region (i.e., inside the potential well). Therefore, within the Hermitian formalism of quantum mechanics the continuum functions associated with energy-eigenvalues which are equal to the real parts of the complex resonance poles are not necessarily localized in the interaction region and are not necessarily very different in their nature from other continuum functions. Note that even for the first case where the Hermitian continuum function is localized inside the potential well there are infinitely many other continuum eigenfunctions that have the same structure. Roughly speaking, any eigenfunction which is associated with an energy-eigenvalue E of the Hermitian Hamiltonian in the range

$$\mathrm{Re}(E_1^{\mathrm{res}}) - \Gamma_1^{\mathrm{res}}/2 < E < \mathrm{Re}(E_1^{\mathrm{res}}) + \Gamma_1^{\mathrm{res}}/2\,, \tag{1.3}$$

where $\Gamma_1^{\mathrm{res}} = 2\mathrm{Im}(E_1^{\mathrm{res}}) = 0.34750\,\mathrm{au}$, looks similar to the Hermitian continuum function shown in Fig. 1.1. This is the reason that within the framework of the standard formalism of quantum mechanics the resonance phenomenon is associated with the dynamical behavior of wavepackets rather than with a single stationary solution of the time-dependent Schrödinger equation.

(2) Now we repeat the calculations while imposing outgoing boundary conditions on the solutions of the time-independent Schrödinger equation. That is, we demand that $\psi(r \to \infty) = C\exp(+ikr)$. As mentioned above and as will be discussed in detail in Chapter 4, in this case the eigenfunctions are not in the Hermitian sector of the domain of the Hamiltonian and E will attain complex discrete values, E_n^{res}, where here, for example, $E_1^{\mathrm{res}} = 1.784582 - 0.173750\mathrm{i}\,\mathrm{au}$ and $E_2^{\mathrm{res}} = 2.455696 - 1.111399\mathrm{i}\,\mathrm{au}$. Note

that the inverse of $\Gamma_n^{\rm res} \equiv -2{\rm Im}(E_n^{\rm res})$ provides the lifetime of the nth resonance state. As $\Gamma_n^{\rm res}$ increases the lifetime of the metastable state is shorter. The calculations are simple and straightforward. Figures 1.1 and 1.2 show the second and third longest living resonance states obtained by the non-Hermitian quantum mechanical calculations. Their asymptotes diverge exponentially and therefore neither of the resonance wavefunctions are embedded in the Hermitian sector of the domain of the Hamiltonian. That is clear in spite of the fact that when outgoing boundary conditions are imposed the resonance states are uniquely defined and can be easily evaluated for one-dimensional, one-particle problems. However, it is hard to develop a coherent quantum mechanical theory using functions which are not bounded and can not be expanded by orthonormal square integrable functions (embedded in the Hilbert space).

(3) The third approach we use here, which will be described in detail in Chapter 5, is in a sense a "trick" to change the asymptotical behavior of the non-Hermitian resonance wavefunctions by rotating the coordinates into the complex plane. For example, the simplest way to perform such a procedure is by taking $r \to r\exp({\rm i}\theta)$. The complex scaled resonance eigenfunction which has been obtained by imposing outgoing boundary conditions on the solutions of the time-independent Schrödinger equation is a square integrable eigenfunction of the complex scaled Hamiltonian. The mathematical justification for the use of this type of non-unitary transformation and its limitations will be discussed in Chapter 5. At this time we wish to point out the motivation for using this approach. The results presented in Figs. 1.1 and 1.2 show that upon complex scaling both of the short-living resonance wavefunctions are square integrable and decay exponentially to zero as $r \to \infty$. Therefore, due to the rotation of the coordinate into the complex plane, both of the resonances are embedded in the generalized Hilbert space and can be expanded by a set of orthonormal square-integrable basis functions. This property enables us to develop a non-Hermitian quantum mechanical theory and computational methods for calculating resonance energies, lifetimes and cross sections. From the results presented in Section 1.1 one might get the (wrong) impression that in the Hermitian and non-Hermitian pictures the resonance wavefunctions look alike. However, they are very different in their nature. The non-Hermitian resonance eigenfunction is associated with a complex eigenvalue whereas the Hermitian solution is associated with a real eigenvalue. The asymptote of the non-Hermitian complex scaled resonance function decays to zero whereas the Hermitian resonance wavefunction oscillates. The results obtained from the Hermitian and the non-Hermitian (complex scaling) calculations for the third longest living metastable (resonance) state in Fig. 1.2 are very different. This resonance has a very short lifetime since $1\,{\rm au} = 2.419 \cdot 10^{-17}\,{\rm s}$ and life-time $= 1/(2 \times 1.111399)$ au in our case. While the Hermitian wavefunction can not be distinguished from any other continuum state, the non-Hermitian resonance function has a sharp and clear nodal structure at the interaction region (inside the potential well), it decays exponentially to zero and therefore it is a square-integrable function which is embedded in the generalized Hilbert space.

We can summarize this by stating that the resonance states are well defined in quantum mechanics within the framework of the non-Hermitian formalism. In non-Hermitian quantum mechanics a resonance is associated with a *single* eigenstate of the Hamiltonian and not with a collection of continuum states (i.e., wavepacket) which is the case in Hermitian quantum mechanics.

1.3 Complex local potentials

In these cases the Hamiltonian is non-Hermitian despite the fact that the eigenfunctions of the time-independent Schrödinger equation are square integrable. The potentials are complex for different reasons. One example is when complex absorbing potentials are introduced in the propagation of waves solving either the Scrödinger equation (or the scalar Maxwell equation in the paraxial approximation) or the vector Maxwell equations. The motivation to introduce complex reflection-free absorbing potentials is to avoid the non-physical interferences which are introduced in conventional calculations by the reflections of the tail of the propagated wave packet from the edge of the grid used in the numerical computations. Physical reasons for introducing complex potentials may arise in optics (due to a complex index of refraction), field theory, and even in cases where the quantum language is used to describe the physics when the studied problems are associated with classical statistical mechanics or with diffusion in biological systems.

As an example of a non-Hermitian Hamiltonian that is not related to the resonance phenomena, let us mention the Hamiltonian that becomes non-Hermitian due to the inclusion of purely imaginary external fields, e.g., $\mathrm{i}gx^3$, where g is a real parameter and the Hamiltonian commutes with the symmetry operator: $x \to -x$ and $\mathrm{i} \to -\mathrm{i}$. This symmetry operator, is known as the $\mathcal{PT}$ symmetry operator, where $\mathcal{P}$ is the parity operator, i.e., $\mathcal{P}x\mathcal{P}^{-1} = -x$ and $\mathcal{T}$ is the time-reversal symmetry operator where $\mathrm{i} \to -\mathrm{i}$, i.e., $\mathcal{T}\mathrm{i}\mathcal{T}^{-1} = -\mathrm{i}$. Note in passing that $\mathcal{T}$ is an anti-linear operator while the Hamiltonian is a linear operator.

Exercise 1.3

Show by using semiclassical arguments that the spectrum of non-Hermitian Hamiltonian $\hat{H} = \hat{p}^2 + \mathrm{i}gx^3$ is real and positive for any value of $g \neq 0$ provided the solution eigenfunctions are defined on the whole real line.

In analogy to quantum-mechanical theory, quantum field theories for such non-Hermitian Hamiltonians possess special properties. The Hamiltonians which commute with the $\mathcal{PT}$ symmetry operator hold additional special properties. For example, although these types of Hamiltonian are non-Hermitian they support a real eigenvalue spectrum provided that the strength parameter of the complex local potential g has values smaller than a critical value. Above the critical value of the complex potential strength parameter the spectrum of the non-Hermitian Hamiltonians which commute with the $\mathcal{PT}$ operator is comprised of real eigenvalues and pairs of complex conjugate energies.

Exercise 1.4

Consider two real operators H_0 and V such that $H_0(x) = H_0(-x)$ and $V(x) = -V(-x)$. The Hamiltonian $H = H_0 + \lambda V$ commutes with the $\mathcal{PT}$ symmetry operator when $\lambda = \mathrm{i}\Gamma$ and Γ gets real values only. That is, $[H(-x, \Gamma)]^* = H(x, \Gamma)$. Prove that the eigenvalues of $H(x, \Gamma)$ are real for $\Gamma < |\lambda_{\mathrm{bp}}|$, where λ_{bp} is a branch point in the complex λ-plane. Note that only inside the circle of $\lambda < |\lambda_{\mathrm{bp}}|$ the eigenvalues are analytical functions and therefore the perturbation series expansion of $E(\lambda)$ converges.

1.4 Physical interpretation of complex expectation values

In non-Hermitian quantum mechanics expectation values of dynamical variables might attain complex values. What is the physical meaning of complex expectation values? Can they provide any measurable quantity? Let us assume that ψ is an eigenfunction of the complex scaled Hamiltonian. As we will explain in Chapter 6, the expectation value of a complex scaled dynamical operator $\hat{O}$ is given by

$$\bar{O} = \frac{\langle \psi^* | \hat{O} | \psi \rangle}{\langle \psi^* | \psi \rangle} \equiv |\bar{O}| \mathrm{e}^{\mathrm{i}\alpha} , \tag{1.4}$$

where here without lost of generality we assume that the eigenfunctions of the unscaled (real) Hamiltonian are real. We postulate here that the absolute value of the complex expectation value of the dynamical operator $\hat{O}$ and its phase α are measurable quantities. For example, in scattering experiments the peaks in the cross sections are obtained when the projectiles have energy which is equal to $|E_{\mathrm{res}}|$ and *not* $\mathrm{Re}(E_{\mathrm{res}}) = E_{\mathrm{r}}$. This feature cannot be explained within the conventional framework of Breit–Wigner theory, and becomes evident once the real part of the energy E_{r} has a sufficiently small value.[1]

Another example for our interpretation of complex expectation values is the complex probability density. The probability density in non-Hermitian quantum

---

[1] Shachar Klaiman, part of a PhD thesis which has been submitted to the senate of the Technion-Israel Institute of Technology.

mechanics is a complex function of the vector positions of the particles, $\rho(\mathbf{r})$. The probability density is given by $|\rho(\mathbf{r})|$. Is there a physical meaning to the phase of $\rho(\mathbf{r}) = |\rho(\mathbf{r})| \exp(\mathrm{i}S(\mathbf{r}))$? Barkay and Moiseyev[2] have shown that the asymptote of the phase of $\sqrt{\rho(\mathbf{r})}$, i.e., $\sqrt{S(\mathbf{r})}$ as $|\mathbf{r}| \to \infty$, provides the phase, $\arg[t(E)]$, of the measurable complex transition probability amplitude in scattering experiments. Specifically, it has been shown that the asymptotes of the eigenfunctions of the non-Hermitian Hamiltonian provide the complex probability amplitudes, $t(E)$, to get specific products in scattering experiments. We postulate that the phase of the complex expectation values of dynamical variables are measurable quantities. In the case that the phase is ± 1 the situation is similar to standard quantum mechanics, i.e., positive and negative momenta are associated with particles which move in opposite directions. However, when within the non-Hermitian formulation the phase is not $n\pi$, where $n = 0, 1, \ldots$; its measurement requires an interference between two waves; for example the experiments of Heiblum and his co-workers which are briefly discussed below.

The phases of the complex probability amplitudes play an important role in the interference between resonance states during scattering experiments. See, for example, the explanation for the sharp structures in cross sections which were measured in electron hydrogen molecule scattering experiments.[3] Another example is the use of non-Hermitian scattering theory for calculating the resonant tunneling probability amplitude in a quantum dot[4] in order to explain the sharp phase change in the transition-probability amplitude of electrons scattered through a quantum dot as measured by Yacoby and Heiblum and co-workers.[5] It is important to mention that the phase of the complex transition probability amplitude is a measurable quantity in electron–quantum dot scattering experiments.[6]

1.5 Concluding remarks

There are different origins for non-Hermitian operators.

(1) One reason is the representation of an operator $\hat{O}$ by square integrable functions $\{\phi_n\}_{n=1,2,\ldots}$ which vanish at the interval endpoints $[-L_1, +L_2]$, such that $\hat{O}\phi_n$ does not vanish at these endpoints. In such a case $\{\phi_n\}_{n=1,2,\ldots}$ does not belong to the domain of $\hat{O}$. This type of non-Hermitian operators are out of the scope and interest of this book.

(2) The second type of non-Hermitian operators are the Hamiltonians of open systems that have a continuous spectrum (they may possess a discrete spectrum as well). In such

---

[2] H. Barkay and N. Moiseyev, *Phys. Rev. A* **64**, 044702 (2001).

[3] E. Narevicius and N. Moiseyev, *Phys. Rev. Lett.* **81**, 2221 (1998); **84**, 1681 (2000); *J. Chem. Phys.* **113**, 6088 (2000).

[4] H. Barkay, E. Narevicius and N. Moiseyev, *Phys. Rev. B* **67**, 045322 (2003).

[5] A. Yacoby, M. Heiblum, D. Mahalu, and H. Shtrikman, *Phys. Rev. Lett.* **74**, 4047 (1995).

[6] R. Schuster, E. Buks, M. Heiblum, D. Mahalu and V. Umansky, *Nature* **385**, 417 (1997).

cases the requirement from the eigenfunctions of the time-independent Schrödinger equation to have asymptotes of outgoing waves (i.e., imposing outgoing boundary conditions on the eigenfunctions) results in complex eigenvalues which are associated with eigenfunctions which are not in the Hermitian sector of the domain of the Hamiltonian. These types of solution are associated with resonance phenomena which are definitely some of the most striking phenomena in physical sciences. This book will focus on the resonance phenomena although our derivations, formulations and concepts hold also for any other case where the system is represented by a finite non-Hermitian matrix.

(3) The third type of non-Hermitian operator we mentioned in this chapter is those which include complex local functions which often serve as potentials which absorb light, or particles. In this chapter we briefly mentioned these types of problem and addressed the readers to references where they can learn more about the physical motivation for constructing these types of non-Hermitian operator. However, as stated above, the derivations, theorems and computational algorithms which are presented in this book are relevant and applicable also for these types of non-Hermitian problem.

1.6 Solutions to the exercises

Answer to Exercise 1.1

The answer to this problem has been given by Alon, Moiseyev and Peres.[7] The matrix elements of **P** and $\mathbf{P}^2$ are Hermitian since it is possible to perform integration by parts, in which the boundary terms vanish. However, for particle-in-a-box functions where

$$\phi_n(x) = \sqrt{\frac{2}{L}} \sin\left(\frac{n\pi x}{L}\right) , \tag{1.5}$$

then

$$\begin{aligned}\int_0^L \phi_m \mathrm{d}_x^3 \phi_n \mathrm{d}x &= -\int_0^L \phi_n \mathrm{d}_x^3 \phi_m \mathrm{d}x - \int_0^L \mathrm{d}_x\phi_m \cdot \mathrm{d}_x^2 \phi_n \mathrm{d}x - \int_0^L \mathrm{d}_x\phi_n \cdot \mathrm{d}_x^2\phi_m \mathrm{d}x \\ &= -\int_0^L \phi_n \mathrm{d}_x^3 \phi_m \mathrm{d}x + [\mathrm{d}_x\phi_m \cdot \mathrm{d}_x\phi_n]_0^L \end{aligned} \tag{1.6}$$

and the last term does not vanish. Therefore,

$$\int_0^L \phi_m \hat{p}_x^3 \phi_n \mathrm{d}x \neq \int_0^\pi \phi_n [\hat{p}_x^3]^* \phi_m \mathrm{d}x \tag{1.7}$$

and $\hat{p}_x^3$ **for a particle-in-a-box function is not Hermitian**. The source of the difficulty is that the domain of P consists of functions on the interval $[0, L]$ which vanish

---

[7] O. E. Alon, N. Moiseyev and A. Peres, Infinite matrices may violate the associative law, *J. Phys. A* **28**, 1765 (1995).

at the interval endpoints. However, $\hat{p}_x\phi_n$ does not vanish at these endpoints, and therefore does not belong to the domain of **P**: the expression $\hat{p}_x(\hat{p}_x\phi_n)$ is not mathematically defined. This does not contradict the fact that $-\mathrm{d}_x^2\phi_n = (n^2\pi^2/L^2)\phi_n$. The point is that when **P** is an infinite order matrix as defined above, the elements of the infinite order matrix $\mathbf{P^2}$ are not the same as $\int_0^\pi \phi_m \hat{p}_x^3\phi_n \mathrm{d}x$. The same difficulty in another form can be written as:

$$\sum_{s=1}^{\infty} \mathbf{P}_{ms}(\mathbf{P}^2)_{sn} \neq \sum_{s=1}^{\infty}(\mathbf{P}^2)_{ms}(\mathbf{P})_{sn}\,. \tag{1.8}$$

It is interesting to see that in this case this difficulty is avoided when, rather than using infinite order matrices, we use finite ones, such that

$$\int_0^L \phi_m \hat{p}_x^3\phi_n \mathrm{d}x = \lim_{N\to\infty} \sum_{r,s}^{N} \mathbf{P}_{mr}\mathbf{P}_{rs}\mathbf{P}_{sn}\,. \tag{1.9}$$

Answer to Exercise 1.2

The answer to this question is that the positions of the detectors/antennas that measure the momenta of the outgoing particles/subsystems do not give us any indication of the positions of the particles/subsystems. The reason is very simple. The positions of the detectors commute with the momenta of the particles/subsystems and there is no violation of the uncertainty “principle” (relation rather than principle). Of course in such cases where the momenta have been measured precisely the uncertainty in the positions of the outgoing particles/susbsystems is infinitely large.

Answer to Exercise 1.3

The eigenvalue problem we wish to solve is

$$\left[-\frac{\mathrm{d}^2}{\mathrm{d}x^2} - \mathrm{i}gx^3\right]\psi(x) = E\psi(x)\,, \tag{1.10}$$

where $\psi(x) \to 0$ as $|x| \to \infty$. The semiclassical solution given below has been borrowed from Bender and Boettcher.[8] The Bohr–Sommerfeld quantization rule implies that

$$\int_{x_-^{\mathrm{ctp}}}^{x_+^{\mathrm{ctp}}} \mathrm{d}x\sqrt{E + \mathrm{i}gx^3} = \pi\left(n + \frac{1}{2}\right)\,, \tag{1.11}$$

where n is the number of bound states associated with classical periodic orbits within the interval of $E \geq E' > 0$. The classical turning points, $x_\pm^{\mathrm{ctp}}$, are calculated

---

[8] C. Bender and S. Boettcher, *Phys. Rev. Lett.* **80**, 5243 (1998).

as usual (under the assumption that indeed the potential supports bound states) from the requirement that

$$E = -\mathrm{i}g\left(x_j^{\mathrm{ctp}}\right)^3 . \tag{1.12}$$

Therefore,

$$x_j^{\mathrm{ctp}} = (E/g)^{1/3}\mathrm{e}^{\mathrm{i}(\pi/2+2\pi j)/3} \tag{1.13}$$

such that $x_-^{\mathrm{ctp}} \equiv x_1^{\mathrm{ctp}}$ and $x_+^{\mathrm{ctp}} \equiv x_0^{\mathrm{ctp}}$. Note that the distance between the two classical turning points has a real value,

$$x_+^{\mathrm{ctp}} - x_-^{\mathrm{ctp}} = 2(E/g)^{1/3}\cos(\pi/6) . \tag{1.14}$$

Since the classical periodic trajectories evolve around the mid-point $x = 0$ the integral given in Eq. (1.11) can be written as

$$\int_{x_-^{\mathrm{ctp}}}^{x_+^{\mathrm{ctp}}} \mathrm{d}x\sqrt{E+\mathrm{i}gx^3} = \int_{x_-^{\mathrm{ctp}}}^{0} \mathrm{d}x\sqrt{E+\mathrm{i}gx^3} + \int_{0}^{x_+^{\mathrm{ctp}}} \mathrm{d}x\sqrt{E+\mathrm{i}gx^3} . \tag{1.15}$$

By substituting in the first integral $x = sx_-^{\mathrm{ctp}}$ and in the second integral $x = sx_+^{\mathrm{ctp}}$ while using the condition of Eq. (1.11) one gets that

$$\int_{x_-^{\mathrm{ctp}}}^{x_+^{\mathrm{ctp}}} \mathrm{d}x\sqrt{E+\mathrm{i}gx^3} = \sqrt{E}(x_+^{\mathrm{ctp}} - x_-^{\mathrm{ctp}})\int_0^1 \mathrm{d}s\sqrt{1-s^3} = \pi\left(n+\frac{1}{2}\right) . \tag{1.16}$$

Consequently, by substituting the result of Eq. (1.14) the energies are given by

$$E_n = \left[\frac{\pi g^{1/3}}{2\gamma\cos(\pi/6)}\right]^{6/5}\left(n+\frac{1}{2}\right)^{\frac{6}{5}} ; \qquad n = 0, 1, 2, \ldots , \tag{1.17}$$

where $\gamma = \int_0^1 \mathrm{d}s\sqrt{1-s^3}$. Since the integrand in γ is positive over all the range of integration, γ is real and positive and therefore so are the energies E_n.

Answer to Exercise 1.4

Since λ_{bp} is a branch point in the complex λ plane of $\hat{H}(\lambda)$ a perturbative expansion of the eigenvalues and eigenfunctions of H in a power series of λ will converge for $|\lambda| < |\lambda_{\mathrm{bp}}|$. We now turn to proving that for $|\lambda| < |\lambda_{\mathrm{bp}}|$ the eigenvalues of $H = H_0 + \lambda V$ are real. That is,

$$(H_0 + \lambda V)\Psi_j = E_j\Psi_j , \tag{1.18}$$

where E_j are real eigenvalues and Ψ_j are square integrable.

It has been proven by Moiseyev and Friedland[9] that when H_0 and V are Hermitian operators/matrices (as in our case) then one can always find at least one complex value of λ for which $H = H_0 + \lambda V$ has a non-diagonalizable spectral representation. For a matrix this implies, e.g., that the number of linearly independent eigenvectors is smaller than the dimension of that matrix (the spectrum becomes incomplete). The spectrum of an operator (matrix) becomes incomplete at a branch point denoted by λ_{bp} where at least two eigenfunctions (eigenvectors) coalesce. Here we restrict ourselves to the class of Hamiltonians for which $\lambda_{\mathrm{bp}} \neq 0$.

The most common situation is that the energy spectrum in the neighborhood of the branch point is associated with the coalescence of two eigenfunctions and the two corresponding eigenvalues. For $\lambda = \mathrm{i}\Gamma$ and $\lambda_{\mathrm{bp}} = \mathrm{i}\Gamma_{\mathrm{bp}}$ we can write in the vicinity of a branch point

$$E(\lambda) = E^{\mathrm{bp}} \pm D\sqrt{(\lambda - \lambda_{\mathrm{bp}})(\lambda - \lambda^*_{\mathrm{bp}})} \tag{1.19}$$

In the case of $|\lambda| > |\lambda_{\mathrm{bp}}|$ this gives a pair of complex conjugate eigenvalues E and E^*, whereas for $|\lambda| < |\lambda_{\mathrm{bp}}|$ the system has two real eigenvalues. These eigenvalues of H are analytical functions of λ and can be described as a power series expansion in λ,

$$E_j(|\lambda| < |\lambda_{\mathrm{bp}}|) = \sum_{n=0}^{\infty} \lambda^n E_j^{(n)}\,, \tag{1.20}$$

where $E_j^{(n)}$; $n = 0, 1, 2, \ldots$ are the *real* energy correction terms to the Rayleigh–Schrödinger perturbation expansion of the eigenvalues of $H = H_0 + \lambda V$. The $(2n+1)$-rule of Wigner states that if the k-th order correction terms $\psi_j^{(k)}$ are known up to the n-th order (i.e., $k = 0, 1, \ldots, n$), then one can calculate the true eigenvalue E_j up to the $(2n + 1)$ correction energy term.[10] The $(2n + 1)$-theorem of Wigner implies that

$$E_j = \langle \chi_j^{(n)} | H_0 + \lambda V | \chi_j^{(n)} \rangle + O(\lambda^{2n+2})\,, \tag{1.21}$$

where

$$\chi_j^{(n)}(x) = \sum_{k=0}^{n} \lambda^k \psi_j^{(k)} \tag{1.22}$$

---

[9] N. Moiseyev and S. Friedland, The association of resonance states with the incomplete spectrum of finite complex-scaled Hamiltonian matrices. *Phys. Rev. A* **22**, 618–623 (1980).

[10] E. P. Wigner, *Hungarian Academy* **53**, 475 (1935). Note that this paper contains Wigner's conclusion and uses it but does not provide the proof. In his letter to Phil R. Certain from the University of Wisconsin at Madison on July 4th, 1972 Wigner wrote "I am afraid that when I wrote this article I was still under the impression that everyone knows everything that can be derived in a few lines, and did not state the theorem explicitly" and added a six-line proof.

and $\langle \chi_j^{(n)} | \chi_j^{(n)} \rangle = 1$. Therefore, following the $(2n+1)$-rule of Wigner,

$$\begin{aligned} E_j^{(2n+1)} &= \langle \psi_j^{(n)} | V | \psi_j^{(n)} \rangle \,, \\ E_j^{(2n)} &= \langle \psi_j^{(n)} | V | \psi_j^{(n-1)} \rangle \end{aligned} \tag{1.23}$$

where the n-th order correction to the exact eigenfunction Ψ_j is the solution of the following equation

$$\psi_j^{(n)}(x) = G_0(E_j^{(0)}) V(x) \psi_j^{(n-1)} - \sum_{k=1}^{n} E_j^{(k)} G_0(E_j^{(0)}) \psi_j^{(n-k)} \tag{1.24}$$

where

$$G_0(E_j^{(0)}) = \sum_{k \neq j} \frac{|\psi_k^{(0)}\rangle\langle\psi_k^{(0)}|}{E_j^{(0)} - E_k^{(0)}} \,. \tag{1.25}$$

The eigenfunctions of the zero-order Hamiltonian,

$$\psi_q^{(0)}(x)\,, \qquad \text{where} \quad q \in \{j, k\}\,, \tag{1.26}$$

are real eigenfunctions which have either *even* or *odd* parity due to the symmetry of $H_0(x) = H_0(-x)$. Consequently, the eigenvalues of the zero-order Hamiltonian and also any n-th order correction energy terms, $\{E_k^{(n)}\}$, are real.

Due to the symmetry properties of $V(x) = -V(-x)$ and of the zero-order eigenfunctions $\psi_k^{(0)}(x) = (-1)^k \psi_k^{(0)}(-x)$, $k = 0, 1, \ldots,$ the n-th order eigenfunction $\psi_j^{(n)}$ is either an *even* or an *odd* parity eigenfunction (i.e., $\psi_j^{(n)}(x) = (-1)^{j+n} \psi_j^{(n)}$) and therefore, following the $(2n+1)$-rule of Wigner,

$$E_j^{(2n+1)} = 0\,. \tag{1.27}$$

This is a crucial point in our proof. Regardless of the odd or even parity properties of $\psi_j^{(n)}$, $[\psi_j^{(n)}]^2$ is an even function and from Eq. (1.23) it is clear that for our class of Hamiltonians $E_j^{(2n+1)} = 0$ and therefore

$$E_j(|\lambda| < |\lambda_{\text{bp}}|) = \sum_{n=0}^{\infty} \lambda^{2n} E_j^{(2n)}\,. \tag{1.28}$$

Consequently, for $\lambda = \mathrm{i}\Gamma$ the series

$$E_j(|\Gamma| < |\Gamma_{\text{bp}}|) = \sum_{n=0}^{\infty} (-1)^n \Gamma^{2n} E_j^{(2n)} \tag{1.29}$$

has real values only. The physical realization of this result can be measured, for example, by considering two coupled two-dimensional waveguides. The propagation of a light beam in a waveguide is obtained by solving the scalar Maxwell equation which is equivalent to the solution of the time-dependent Schrödinger equation where the time t is replaced by Z, the propagation axis of the light in the waveguide. The time-dependent potential in the Schrödinger equation $V(\mathbf{r}, t)$ is replaced by $-(2\pi/\lambda)^2 n^2_{\text{eff}}(X)$, where $n^2_{\text{eff}}(X)$ is the one-dimensional effective index of refraction and λ is the wavelength of the propagated light beam in a vacuum. In our case $-n^2_{\text{eff}}(X)$ consists of two separated equivalent one-dimensional rectangular potential wells. The light irradiated into one waveguide oscillates between the two parallel waveguides with a period which depends on the width and the height of the rectangular potential wells and on the distance between them. The period of oscillation between the two coupled waveguides is inversely proportional to the difference between the almost degenerate propagation constants associated with the eigenvalues of the "Hamiltonian" where the "potential" is linearly proportional to $-n^2_{\text{eff}}(X)$. For more details see the experiment carried out by Vorobeichik and his co-workers which is described in their paper on Electromagnetic realization of orders-of-magnitude tunnelling enhancement in a double well system.[11]

Depending on the material composing the wave guide, the effective index of refraction can be complex where the imaginary part varies with λ. A positive imaginary part of the index of refraction causes absorption loss when the electromagnetic wave propagates through the material. For example, by doping ions of rare earth elements into silica wave guides a trapped optical mode turns into a leaky guiding mode (a so-called resonance state). A negative imaginary part of $n^2_{\text{eff}}(X)$ is obtained when an inverse electronic population occurs and the electrons in the waveguide mostly populate a long-living electronic excited state rather than the ground electronic state. When a laser beam is transferred via this waveguide with a proper wavelength then a stimulated photo-emission occurs due to the electronic relaxation from the long-living excited state into the electronic ground state. In such a case the electric power distribution of the laser is exponentially increased as it propagates through the waveguide.

Now we turn to the realization of the theoretical result above. Let us construct two waveguides as described above from materials with complex index of refraction, *such that in one of them the imaginary part of* $V(x) = -n^2_{\text{eff}}(X)$ *is negative,* $\text{Im}V(x) = -\Gamma$, *while in the second one it is positive and equal to* $+\Gamma$. Following our proof, as Γ is increased the gap between the almost degenerate propagation

---

[11] I. Vorobeichik *et. al.*, *Phys. Rev. Lett.* **90**, 176806 (2003).

constants is reduced and therefore the period of the oscillations of the propagated light beam in between the two waveguides will increase. For proposed experimental setups based on this analysis see Klaiman *et al.*[12]

1.7 Further reading

On the representation of dynamical variables by Hermitian operators and infinite order matrices

P. A. M. Dirac, *The Principles of Quantum Mechanics*, 4th edn., Oxford, Clarendon Press, 1958.

On resonances as the most striking phenomenon is scattering theory

J. R. Taylor, *Scattering Theory*, New York, John Wiley & Sons, Inc., 1972.

On the different types of non-Hermitian operator

E. Balslev and J. M. Combes, Spectral properties of many-body Schroedinger operators with dilatation-analytic interactions, *Comm. Math. Phys.* **22**, 280–294 (1971).

J. Aguilar and J. M. Combes, A class of analytic perturbations for one-body Schrödinger Hamiltonians, *Commun. Math. Phys.* **22**, 269–279 (1971).

B. Simon, Resonances in n-body quantum systems with dilatation analytic potentials and the foundations of time-dependent perturbation theory, *Ann. Math.* **97**, 247–274 (1973).

H. Feshbach, *Theoretical Nuclear Physics*, New York, John Wiley & Sons, Inc., 1992.

H. Feshbach, Unified theory of nuclear reactions, *Ann. Phys.* **5**, 357–390 (1958).

H. Feshbach, Unified theory of nuclear reactions: II, *Ann. Phys.* **19**, 287–313 (1962).

N. Moiseyev, Feshbach resonances: the branching of quantum mechanics into Hermitian and non-Hermitian formalisms, *J. Phys. Chem. A*, **113**, 7660–7666 (2009).

A. Bohm, *Quantum Mechanics: Foundation and Applications*, New York, Springer-Verlag, 3rd edn. 1994.

N. Moiseyev, P. R. Certain and F. Weinhold, Resonance properties of complex-rotated Hamiltonians. *Mol. Phys.* **36**, 1613–1630 (1978).

E. Narevivius and N. Moiseyev, Non-Hermitian quantum mechanics: formalism and applications, *Fundamental World of Quantum Chemistry*, **2**, 1–31 (2003).

E. Narevivius and N. Moiseyev, Non-Hermitian quantum mechanics: theory and experiments not amenable to conventional quantum mechanics, *Prog. Theo. Chem. Phys.* **12**, 311–338 (2003).

H. Barkay and N. Moiseyev, Complex density probability in non-Hermitian quantum mechanics: interpretation and a formula for resonant tunneling probability amplitude, *Phys. Rev. A* **64**, 044702–044705 (2001).

N. Hatano and D. R. Nelson, Localization transitions in non-Hermitian quantum mechanics, *Phys. Rev. Lett.* **77**, 570–573 (1996).

---

[12] S. Klaiman, U. Gunther and N. Moiseyev, Visualization of branch points in PT-symmetric waveguides, *Phys. Rev. Lett.* **101** 080402 (2008).

N. Hatano and D. R. Nelson, Vortex pinnin and non-Hermitian quantum mechanics, *Phys. Rev. B* **56**, 8651–8673 (1997).

D. R. Nelson and N. M. Shnerb, Non-Hermitian localization and population biology, *Phys. Rev. E* **58**, 1383–1403 (1998).

C. M. Bender and S. Boettcher, Real spectra in non-Hermitian Hamiltonians having PT symmetry, *Phys. Rev. Lett.* **80**, 5243–5246 (1998).

C. M. Bender, D. C. Brody and H. F. Jones, Scalar quantum field theory with complex cubic interaction, *Phys. Rev. Lett.* **93**, 251601–251604 (2004).

2

Resonance phenomena in nature

Although the non-Hermitian formalism of quantum mechanics which is developed in this book is not limited to specific examples and is applicable to problems which are not necessarily quantum mechanical (such as problems which require the solution of the Maxwell equation rather than of the Schrödinger equation) we dedicate an entire chapter to resonance phenomena in nature since they are related to a broad range of subjects and fields in physics, chemistry, molecular biology and technology.

In this chapter we will introduce two different types of resonances, so called shape-type and Feshbach-type resonances, as they appear in different fields of science. The resonance phenomenon is associated with metastable states of a system that as time passes breaks into several subsystems. That is, even though the system has sufficient energy to break apart, this does not happen instantly but requires quite a long time with respect to the characteristic time scale of the system.

In Table 2.1 we give several examples of resonance phenomena, where we specify the decaying systems, the resulting subsystems, and classification in terms of shape and Feshbach resonances. (These concepts will be explained more formally later.)

Each of the listed systems has a typical time scale and in some of these cases the lifetime of the system is less than one nano-second while in other cases it takes more than several thousand years for the system to decay. The theory of resonance states (quasi-stationary or metastable states) was first derived by Gamow[1] in 1928 for α decay of heavy nuclei while studying the transition of a particle through a potential barrier.

2.1 Shape-type resonances

Since the transition through a barrier depends on the height and width of the barrier it is clear from simple semiclassical arguments that the life-time of a temporarily

---

[1] G. Gamow, *Zs. f. Phys.* **51**, 204 (1928); *Zs. f. Phys.* **52**, 510 (1928).

Table 2.1 *Examples of resonance phenomena in nature*

phenomenon	system	subsystems	type
radioactive radiation	nuclei	nuclear fragments	shape
Stark effect	atoms/molecules in dc & low frequency ac fields	ions and electrons	shape
photo-ionization	atoms/molecules in high frequency ac fields	ions and electrons	Feshbach
autoionization and Auger	atoms/molecules in excited states	ions and electrons	Feshbach
predissociation	molecules	ions and/or radicals	shape and/or Feshbach
predesorption	atoms/molecules adsorbed on solid surfaces	free atoms/ molecules and solids	Feshbach
High harmonic generation (HHG) and above threshold ionization (ATI)	atoms/molecules in strong laser fields	ions and electrons and high energy photons	Feshbach/shape
Leaking modes in wave guides and optical fibers	light propagated in WG/optical fibers	scattered light and unpopulated WG/optical fibers	Feshbach

trapped particle varies by many order of magnitude as the potential parameters vary from one case to another. The type of resonance which is associated with the shape of the potential the particle has to tunnel through is referred to as a *shape-type resonance* since the shape of the potential heavily affects the rate of decay. A simple example from molecular physics is a potential barrier induced by the rotational motion of a diatomic molecule, AB, about its center of mass. The Hamiltonian within the framework of the Born–Oppenheimer approximation is given by

$$\hat{H}_{\mathrm{AB}}^{(J)} = -\frac{\hbar^2}{2\mu}\frac{\partial^2}{\partial R^2} + V_J^{\mathrm{eff}}(R), \tag{2.1}$$

where

$$V_J^{\mathrm{eff}}(R) = \frac{\hbar^2 J(J+1)}{2\mu R^2} + V(R), \tag{2.2}$$

the rotational quantum number J has values $J = 0, 1, 2, \ldots$, and $\mu = M_{\mathrm{A}}M_{\mathrm{B}}/(M_{\mathrm{A}} + M_{\mathrm{B}})$ is the reduced mass of the diatomic molecule. $V(R)$ is the electronic energy of the diatomic molecule in the ground state as function of the intranuclear distance R. Usually $V(R)$ supports one extremum point where $V(R)$ gets a

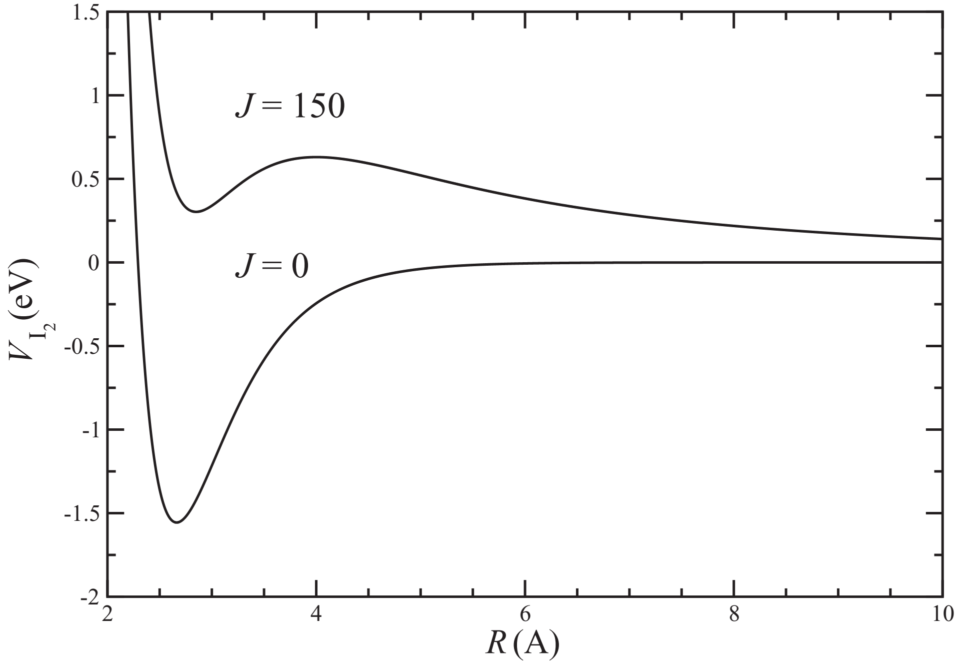

Figure 2.1 The ground state electronic energy of an iodine molecule, I_2, as function of the intranuclear distance R for different values of the rotational quantum number J potential.

minimal value at the equilibrium distance of the non-rotating molecule $R = R_0$. It is convenient to shift the electronic energies by a constant such that the threshold energy is equal to zero, i.e., $\lim_{R\to\infty} V(R) = 0$. In such case the vibrational bound states associated with the rotational quantum number J are the eigenvalues of $\hat{H}_{AB}^{(J)}$ which possess negative values (i.e., below the threshold energy).

As the value of the rotational quantum number J increases a rotational potential barrier emerges: $[\hbar^2 J(J+1)]/[2I(R)]$, where the moment of inertia of the diatomic molecules is $I = \mu R^2$. When this barrier is sufficiently large, two extremum points where $\mathrm{d}V_J^{\mathrm{eff}}(R)/\mathrm{d}R = 0$ are obtained. The first extremum point is a local minimum in the potential energy curve $V_J^{\mathrm{eff}}(R)$, whereas the second extremum point is a local maximum which is associated with the top of the potential barrier. The "classical" dissociation energy is defined as the energy gap between the two extremum points. This is the energy which is required to bring the molecule from the bottom of the potential well to the top of the potential barrier. See, for example, the upper curve in Fig. 2.1 where the ground potential energy curve of I_2 is shown for two different rotational quantum numbers. Due to the rotational excitation the vibrational states which are now located above the threshold energy can tunnel through the potential barrier and dissociate. The fact that the molecule dissociates in energies which are smaller than the "classical" dissociation energy leads to description of this phenomenon as a predissociation.

Let us give a qualitative description of the rotational predissociation phenomenon. The initial state is taken as the ν-th vibrational state of the non-rotating (i.e., $J = 0$) AB molecule, $\Phi_\nu(t = 0)$. The solution of the time-dependent Schrödinger equation for $J > 0$ within the Born–Oppenheimer approximation is given by $\Phi_\nu(t) = \exp(-\mathrm{i}\hat{H}^{(J)}_{\mathrm{AB}} t/\hbar)\Phi_\nu(0)$. Due to the tunneling through the barrier the survival probability which is defined by $|\langle\Phi_\nu(0)|\Phi_\nu(t)\rangle|^2$ decays as $\exp(-\Gamma t/\hbar)$ as $t \to \infty$. The lifetime of the resonance state is defined as

$$\tau = \frac{\hbar}{\Gamma}\,. \tag{2.3}$$

The resonance energy bandwidth $\Delta E = \hbar\Delta\omega$ is defined by using the Fourier transform relation, $\tau\Delta\omega = 1$. Therefore, Γ is the resonance width ΔE.

The resonance tunneling through a potential barrier is also a characteristic mechanism of radioactive decay. However, it should be stressed that shape-type resonances are not necessarily associated with tunneling through potential barriers. Consider a particle moving under the influence of an open rectangular potential well. Slowly moving particles can be temporarily trapped inside the region $-a/2 < x < +a/2$ at quantized energies which are about equal to $-V_0 + (n\pi\hbar/a)^2/(2M) > 0$ where $n = 1, 2, \ldots$ and V_0 is the depth of the rectangular potential well.

The existence of metastable states associated with the shape of the potential of interaction has technological implications. For instance, when a projectile is scattered from a target where the potential of interaction is a potential well embedded between two potential barriers one finds sharp features in the transmission cross section. In fact, when the above mentioned shape-type resonances are narrow (i.e., they live for a long time) one finds that scattering the particle at the resonant energy leads to full transmission through the barrier. This resonance tunneling mechanism is used for constructing diodes and transistors. While the rigorous explanation of this phenomenon is not simple within the standard (Hermitian) formalism of quantum mechanics, as will be shown in Chapter 8 is quite straightforward to explain this phenomenon within the framework of the non-Hermitian formulation of quantum mechanics.

Exercise 2.1

Using semiclassical arguments calculate the lifetime of a molecule which dissociates due to a rotational excitation. Assume that the tunneling is through a parabolic barrier and that the potential well is harmonic.

The problem given in Ex. 2.1 can be associated with a one-dimensional effective potential of a two-dimensional quantum problem where the motion in one dimension varies adiabatically. For example consider a one-dimensional quantum well which is constructed from three different semiconductor layers. The motion of the electron in a direction perpendicular to the layers can be regarded as effectively one dimensional.

2.2 Feshbach-type resonances

This type of resonance can be obtained for many-particle systems (even in a one-dimensional potential) or for a single particle in an n-dimensional potential where $n > 1$. The Feshbach resonance can be described as a bound state embedded in the continuum of an unperturbed Hamiltonian which becomes metastable due to the coupling with the embedding continuum. This state has a finite lifetime and as time passes decays to the reaction products, as described for example in Table 2.1. In this spirit, without loss of generality let us assume that the system under study consists of two subsystems which interact with one another. The Hamiltonian of the full system is described by

$$H(1,2) = h_1(1) + h_2(2) + V(1,2)\,, \tag{2.4}$$

where correspondingly $h_1(1)$ and $h_2(2)$ are the Hamiltonians for the non-interacting subsystems. The interaction potential $V(1,2)$ vanishes when either one of the two particles is removed from the system (for example via ionization or dissociation). For simplicity let's assume that the subsystem that can be removed is subsystem "2". (Another possibility is of one particle in a 2D potential which vanishes as $y \to \infty$ when $a < x < b$ (e.g. see Fig. 2.4).)

The threshold energies are the eigenvalues of the h_2 Hamiltonian,

$$h_2\varphi_n(2) = \epsilon_n^{\text{th}}\varphi_n(2)\,. \tag{2.5}$$

The α-th eigenfunction of the full Hamiltonian given in Eq. (2.4) can be expanded in terms of the eigenfunctions of the h_2 Hamiltonian,

$$\Psi_\alpha(1,2) = \sum_{n=1}^{N} \chi_{n,\alpha}(1)\varphi_n(2)\,, \tag{2.6}$$

where N is the number of the eigenfunctions of h_2 which serve as a basis set and the $\chi_{n,\alpha}(1)$ are the n-th channel functions labelled by the index α.

As usual the exact eigenfunction $\Psi_\alpha(1,2)$ of the full Hamiltonian is obtained when $N \to \infty$ in the variational calculations where a set of coupled secular equations are solved and are represented as an eigenvalue matrix problem,

$$\mathbf{H}\boldsymbol{\chi}_\alpha(1) = E_\alpha \boldsymbol{\chi}_\alpha(1)\,, \tag{2.7}$$

where

$$\boldsymbol{\chi}_\alpha(1) = \begin{pmatrix} \chi_{1,\alpha}(1) \\ \chi_{2,\alpha}(1) \\ \cdot \\ \cdot \\ \chi_{n,\alpha}(1) \\ \cdot \\ \cdot \\ \chi_{N,\alpha}(1) \end{pmatrix} . \tag{2.8}$$

In the basis of the eigenstates of h_2 the operators on the diagonal Hamiltonian matrix **H** are given by

$$H_{n,n} = h_1(1) + \mathcal{V}_n^{\text{eff}}(1)\,, \tag{2.9}$$

where

$$\mathcal{V}_n^{\text{eff}}(1) = h_1(1) + \int \varphi_n(2)^* V(1,2)\varphi_n(2)\mathrm{d}\tau_2 \tag{2.10}$$

Here $\mathrm{d}\tau_2$ represents integration over all space on the coordinates of subsystem “2”. The bound states of the n-th closed channel for decay are associated with the eigenvalues of $H_{n,n}$ which are below the threshold energies ϵ_n^{th}. There are bound states of the n-th channel which are embedded in the continuum of the $H_{n',n'}$ effective Hamiltonian where $n' < n$. The n'-th effective Hamiltonians are defined as the open channels for decay since as the full eigenvalue problem is solved the coupling potential terms between the closed channels and the open channels $H_{n,n'} = \int \varphi_n^*(2)V(1,2)\varphi_{n'}(2)\mathrm{d}\tau_2$ are taken into consideration and therefore the bound states of the $H_{n,n}$ effective Hamiltonians become metastable.

For the sake of clarity let us give two simple examples. The first example is of a helium atom where the two electrons are excited from the ground electronic state to the first doubly excited state. When the electronic repulsion is neglected the ground and the excited energy levels of helium are given by the hydrogen like expression (in au),

$$E_{n,m} = -2\left(\frac{1}{n^2} + \frac{1}{m^2}\right)\,, \tag{2.11}$$

where the first doubly excited electronic state energy is estimated by $E_{2,2} = -1$ whereas the ground state of the ion He$^+$ is given by $E_{\mathrm{He}^+} = E_{1,\infty} = -2$. We will consider the Hamiltonian of the helium atom without the electronic repulsion term as our H_0 Hamiltonian. All the states for which $E_{n>1,m>1} \geq E_{n=k,m=\infty}$ are bound states in the continuum of the H_0 Hamiltonian for the k-th channel.

The exact energy of the first doubly excited state of Helium is obtained by including the electronic repulsion (a positive potential energy) and consequently it is higher than $E_{2,2}$. Therefore $E_{\mathrm{He}}(\text{doubly-excited}) > E_{2,2} > E_{\mathrm{He}^+}$. Here we have shown by exciting helium from its ground electronic state to the first doubly excited electronic state the following autoionization process takes place: He*(doubly-excited) $\to$ He$^+$(1s) $+ e^-$. The metastable state of doubly-excited helium is a Feshbach-type resonance since it can be described as a closed channel (bound state) which becomes metastable due to the interaction with the open channel for ionization (a continuum state).

The second simple example is of a non-rotating HD molecule (i.e. the angular momentum is zero) which is scattered from a flat Pt(111) metallic surface. A possible result of this scattering is an HD molecule that is eventually found far from the solid surface with a rotational quantum number J which can be $J = 0$ but can also get higher values of $J = 1, 2, \ldots$ By repeating the same experiment many times or by scattering simultaneously many HD molecules which do not interact with one another one can measure the different probabilities of rotationally exciting the diatom to a given rotational quantum number as a function of the scattering angle and the translational energy of the incoming molecules. The scattering experiment can be schematically described by

$$\mathrm{HD}\,(J = 0) + \mathrm{Pt}\,(111) \to [\mathrm{HD/Pt}]^{\#} \to \mathrm{HD}\,(J = 0, 1, 2, \ldots) + \mathrm{Pt}\,(111)\,, \tag{2.12}$$

where $[\mathrm{HD/Pt}]^{\#}$ denotes the temporarily trapped HD molecule on the flat Pt surface. In order to simplify the explanation we treat the HD molecule as a rigid rotor assuming that it does not get vibrationaly excited during this experiment. Using Legendre polynomials, $P_J(\cos\theta)$ as a basis set the Hamiltonian of the molecule–surface system is described by

$$\hat{H}_{\mathrm{HD/Pt}} = \sum_{J=0}^{\infty} H_{J',J} |P_{J'}\rangle\langle P_J|\,, \tag{2.13}$$

where

$$H_{J',J} = \left(-\frac{\hbar^2}{2M}\frac{\partial^2}{\partial Z^2} + B_{\mathrm{rot}} J(J+1)\right)\delta_{J',J} + \langle P_{J'}|V_{\mathrm{HD/Pt}}(R,\theta,Z)|P_J\rangle\,. \tag{2.14}$$

Here $B_{\mathrm{rot}} = \hbar^2/[2\mu/R^2]$ is the rotational constant of the HD molecule at the equilibrium intranuclear distance R, and $V_{\mathrm{HD/Pt}}(R, \theta, Z)$ is the interaction potential of the HD molecule with the Pt (111) metallic surface. M and μ are respectively the total mass and the reduced mass of the diatomic molecule HD.

The potentials on the diagonal channels of the Hamiltonian matrix, $H_{J,J}$, are denoted by $V_J(Z) \equiv \langle P_J | V_{\mathrm{HD/Pt}}(R, \theta, Z) | P_J \rangle$ and describe the potential energy of HD molecules as a function of the distance of their center of mass from the flat surface. The index J implies that the molecules rotate freely in the J-th rotational quantum state when they are high above the solid surface where the interaction with the solid surface is negligible.

The eigenvalues of the diagonal channels of the Hamiltonian matrix given in Eq. (2.14),

$$H_{J,J} \equiv \langle P_J | \hat{H}_{\mathrm{HD/Pt}} | P_J \rangle = -\frac{\hbar^2}{2M} \frac{\mathrm{d}^2}{\mathrm{d}Z^2} + V_J(Z) \tag{2.15}$$

are the HD-Pt bound vibrational-translational states. We may consider the discrete eigenvalues of the diagonal Hamiltonian defined in Eq. (2.14) as the vibrational-translational modes of a “diatomic” like complex where one “atom” is the HD molecule whereas the second “atom” is the Pt (111) surface which has an infinitely large mass. The energy gap between two adjacent $V_J(Z)$ and $V_{J-1}(Z)$ potentials is equal to $2JB_{\mathrm{rot}}$ and several or all bound states of the $V_J(Z)$ potential might be embedded in the continuum of the $V_{J'<J}(Z)$ potentials (see Fig. 2.2).

Due to the off-diagonal matrix elements $H_{J',J}$ which couple the bound states of the J-th diagonal Hamiltonian $H_{J,J}$ with the continua of the diagonal Hamiltonians $H_{J',J'}$, where $J' < J$, the bound adsorbed HD/Pt (111) eigenstates of $H_{J,J}$ become resonance states (i.e. metastable states). These metastable states have finite lifetimes on the Pt (111) solid surface. During the time the HD molecules are temporarily trapped on the Pt (111) solid surface they rotate almost freely with the rotational kinetic energy $J(J+1)B_{\mathrm{rot}}$, where the specific value of $J > 0$ depends on the scattering experimental conditions. As the HD molecules get farther apart from the solid surface and their interaction with it vanishes, they attain rotational kinetic energies of $J'(J'+1)B_{\mathrm{rot}}$, where $J' < J$, which would be observed in the lab. The adsorbed HD molecule can be trapped “forever” on the Pt (111) solid surface (neglecting interaction with phonos) in vibrational-translational modes which are associated with the bound states of the $V_0(Z)$ potential (i.e. $J = 0$ and the rotational kinetic energy is equal to zero). However, in scattering experiments the HD-Pt (111) bound states can not be populated. Therefore, there is no way to get adsorbed HD molecules with infinitely long time on the solid surface by carrying out elastic scattering experiments.

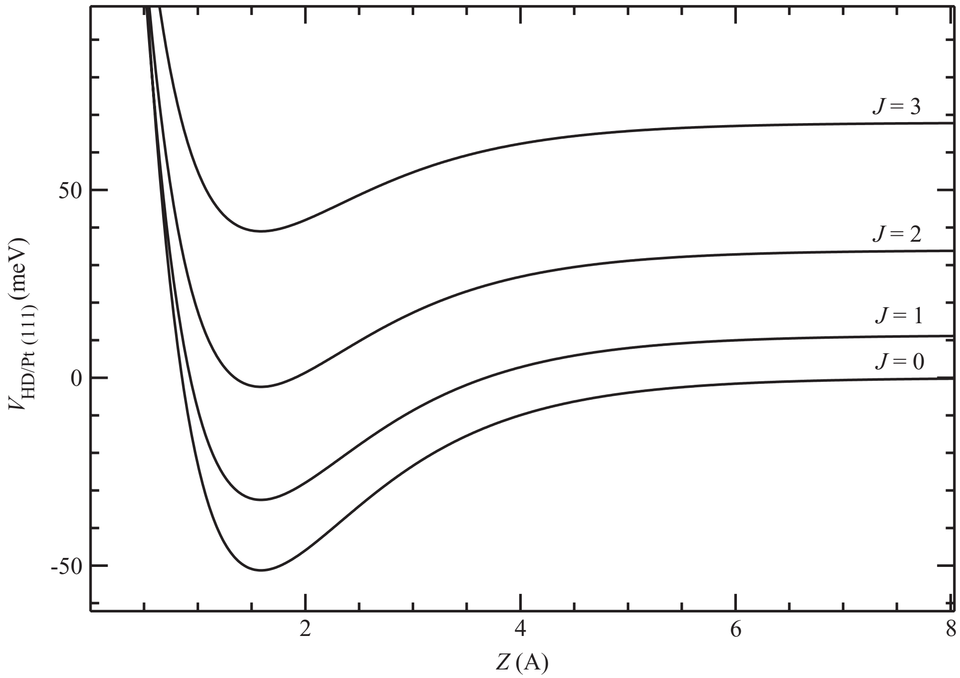

Figure 2.2 The effective potentials of a free-rotating HD molecule as function of the distance of its center of mass from the flat Pt (111) surface $V_J(Z)$. $B_{\mathrm{rot}}J(J+1)$ is the rotational energy of HD molecule at the equilibrium intranuclear distance R. The bound excited states of the $J = 1$ channel are embedded in the continuum of the $J = 0$ channel and the bound states of the $J = 2$ channel are embedded in the continuum of the $J = 1$ and $J = 0$ channels. The bound states embedded in the continuum become resonances as the off-diagonal potential terms $\langle P_{J' \neq J} | V_{\mathrm{HD/Pt}}(R, \theta, Z) | P_J \rangle$, where $V_{\mathrm{HD/Pt}}(R, \theta, Z)$ is the interaction potential of the HD molecule with the Pt (111) metallic surface, are taken into consideration.

The Feshbach predesorption resonances of HD adsorbed on Pt (111) are the bound states of the J-th closed channel for desorption, that become metastable states with finite lifetimes on the solid surface due to couplings of the closed channel J bound states with the continua of the open channels for desorption that are associated with the rotational quantum numbers $J' < J$.

Exercise 2.2

For the 2D potential shown in Fig. 2.4 which describes a 2D slab waveguide (WG) or a 2D quantum dot (QD) the index of refraction of the WG (or the potential energy of the QD) is set to zero for $0 \leq y \leq a(x)$, where $a(x) = [2\cosh^2(x)/(\cosh^2(x) - 2)]^{1/2}/\pi$, and ∞ elsewhere. Calculate the adiabatic potentials assuming that the motion of the light beam in the WG and the motion of the electrons in the QD is much more slowly along the x direction than along the y direction. Estimate the number of Feshbach resonances which have one and two open channels for decay and in the case of electrons in QD estimate the energies of the electrons which “escape” out of the 2D QD into the leads denoted as exit/entrance in Fig. 2.4.

Yet another example of Feshbach resonance is electronic bound states in atoms exposed to intense laser radiation. The bound states of the field-free atom have discrete energy levels, $E_k < 0$, where $k = 1, 2, \ldots$ Let us assume we have a reservoir of an infinitely large number of photons where the energy of a single photon is given by $\hbar\omega_L$. The total energy of the system which consists of an atom and non-interacting photons is the sum of the energies, $\epsilon_{k,n} = E_k + n\hbar\omega_L$, where $n = 1, 2, \ldots, \infty$. Note that under this “zero-order approximation” the atom does not interact with the photons. The threshold energies for ionization are obtained by setting $E_k = 0$ in the expression for $\epsilon_{k,n}$. Therefore the ionization thresholds are $\epsilon_n^{\mathrm{th}} = n\hbar\omega_L$, where $n = N_{\mathrm{ion}}, N_{\mathrm{ion}} + 1, N_{\mathrm{ion}} + 2, \ldots$ and N_{ion} is the minimal number of photons that the atom must absorb for ionization. The bound states associated with the $n \geq N_{\mathrm{ion}}$ channels are embedded in the continuum of the $n < N_{\mathrm{ion}}$ channels. When the interaction between the atom and the laser field is taken into account the bound states which are embedded in the continuum become metastable (Feshbach-type resonances). Using energy conservation arguments the kinetic energy of the ionized electrons which are associated with the k-th electronic state of the field-free atom gets discrete values of $E_{\mathrm{kin}} = \hbar\omega_L n - E_k$, where $n = N_{\mathrm{ion}}, N_{\mathrm{ion}} + 1, \ldots$ In the experiments the peaks in the kinetic energy distribution measurements are at about the same values denoted above and they all have about the same width which is associated with a quantity that is known as the resonance width (which is related to the inverse of the lifetime of the electron in the k-th energy state of the atom interacting with the ac field induced by the laser). The kinetic energy distribution of the photo-ionized electrons is known as the above threshold ionization (ATI) spectrum.

A more rigorous description of the ATI phenomenon which is still quite simple is obtained by using Floquet theory. The Hamiltonian of an atom which interacts with a strong linearly polarized cw laser can be described by

$$\hat{H}(t) = \hat{H}_{\mathrm{FF}} + \epsilon_0 \cos(\omega_L t) \sum_j \mathbf{e}_x^{\mathrm{T}} \cdot \mathbf{r}_j \,, \tag{2.16}$$

where $\hat{H}_{\mathrm{FF}}$ is the Hamiltonian of the field-free atom, and ϵ_0, ω_L and $\mathbf{e}_x$ are respectively the maximum field amplitude, the laser frequency and the polarization direction. The positions of the electrons with respect to the nuclei are denoted by $\mathbf{r}_j$. The quasi-energy solutions (known as Floquet solutions) of the time-dependent

Schrödinger equation are given by

$$\Psi_\alpha(\{\mathbf{r}_j\}, t) = \mathrm{e}^{-\mathrm{i}\mathcal{E}_\alpha t/\hbar}\Phi_\alpha(\{\mathbf{r}_j\}, t)\,,$$

$$\Phi_\alpha(\{\mathbf{r}_j\}, t) = \Phi_\alpha(\{\mathbf{r}_j\}, t + T) = \sum_{n=-\infty}^{+\infty} \varphi_{\alpha,n}(\{\mathbf{r}_j\})\mathrm{e}^{+\mathrm{i}\omega_L nt}\,, \tag{2.17}$$

where $T = 2\pi/\omega_L$ is the time period of the laser-induced oscillating electric field, and $\mathcal{E}_\alpha$ and $\Phi_\alpha(\{\mathbf{r}_j\}, t)$ are respectively the eigenvalues and eigenfunctions of the Floquet operator which is defined by

$$\mathcal{H} = -\mathrm{i}\,\hbar\frac{\partial}{\partial t} + \hat{H}(t)\,. \tag{2.18}$$

Using the functions $\{\exp(+\mathrm{i}\omega_L nt)\}$ as a basis set one gets that the column vectors $\boldsymbol{\varphi}_\alpha(\{\mathbf{r}_j\}) = (\ldots, \varphi_{\alpha,-1}(\{\mathbf{r}_j\}), \varphi_{\alpha,0}(\{\mathbf{r}_j\}), \varphi_{\alpha,+1}(\{\mathbf{r}_j\}), \ldots)$ are the eigenfunctions of the symmetric three-diagonal Floquet matrix where on the diagonal are the shifted field-free atomic Hamiltonian, $\hat{H}_{\mathrm{FF}} + \hbar\omega_L n$, where $n = 0, \pm 1 \pm 2, \ldots$. These diagonal channels are coupled by the components on the two side-bands which are equal to $(\epsilon_0/2)\sum_j \mathbf{e}_x^{\mathrm{T}} \cdot \mathbf{r}_j$. In Fig. 2.3 we show that the diagonal potential terms in the Floquet Hamiltonian which can serve as a field-free effective one-electron, one-dimensional model potentials for a xenon atom are shifted by $n\hbar\omega_L$, where ω_L is the frequency of the cw laser.

2.3 Concluding remarks: on the ambiguity of the definitions of shape- and Feshbach-type resonances

In the previous sections we have shown the differences between shape-type and Feshbach-type resonances, but are these types of resonance uniquely defined? Clearly the resonances associated with a one-dimensional, one-particle system are shape-type resonances regardless of the shape of the potential energy curve and regardless of the question as to whether it supports a potential barrier to tunnel through or not. Shape-type resonances are an exclusively quantum phenomenon. In the semiclassical limit of $\hbar \to 0$ the tunneling shape-type resonances become bound states, that is their lifetime approaches ∞. In such cases the classical particle is trapped forever inside the potential well and does not tunnel through the potential barrier.

On the other hand, it is more difficult to give a unique definition for a Feshbach-type resonance. When an atom is exposed to a time-periodic electric field which is induced by a cw laser, as described above and shown in Fig. 2.3, the bound states of the field-free atom become Feshbach resonances as the field is turned on. This is indeed the situation when the laser frequency ω_L is much larger than the frequency

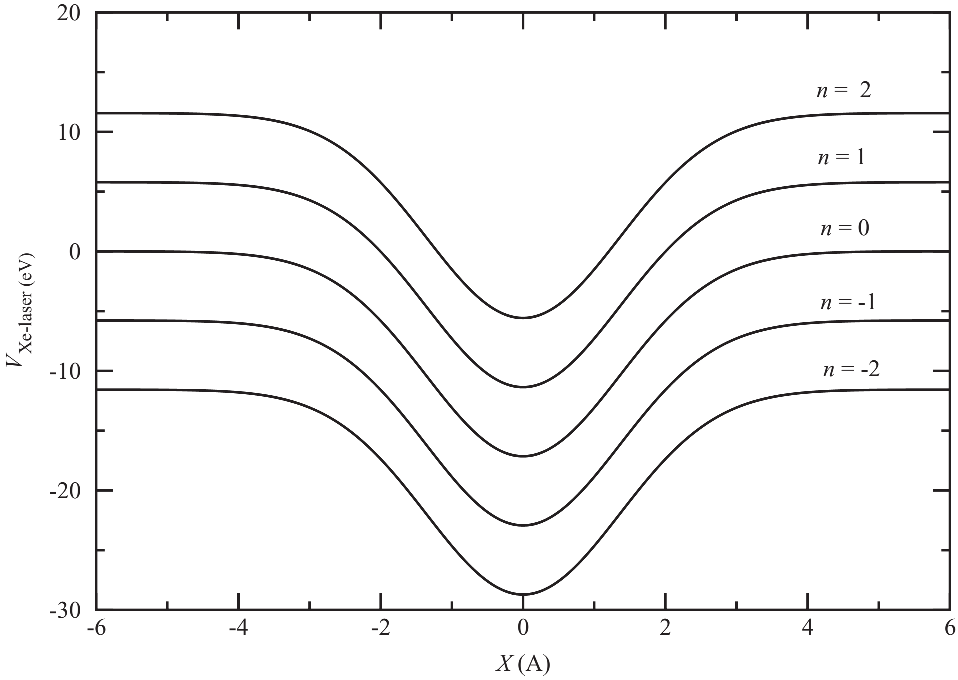

Figure 2.3 The effective potentials for a field-free xenon atom shifted by $\hbar\omega_L n$, where $n = 0, \pm, 1 \pm 2$ and $\omega_L = 0.2$ au. The 1D field-free effective potential is an inverted Gaussian that supports two bound states that mimic the two lowest electronic states of Xe. The bound states of the $n = 2$ channel are embedded in the continuum of the $n \leq -1$ (there are an infinitely large number of open channel for photo-ionization). The bound states embedded in the continuum become resonances as the off-diagonal potential terms in the Floquet Hamiltonian matrix are taken into consideration.

of the electron's motion in the potential of the field-free atom (ω_{atom} can be defined as the electronic excitation energy from the ground state to the first excited state divided by $\hbar$). In the limit of $\omega_L \to \infty$ the resonances return to being the field-free bound states since the electrons oscillate very rapidly due to the driving field with an amplitude given in atomic units by $\alpha_0 = \epsilon_0/\omega_L^2$, where ϵ_0 is the maximum field amplitude. However, in the limit of $\omega_L \to 0$ the ac-field which oscillates as $\cos(\omega_L t)$ behaves much like a static dc-field (substitute $\omega_L \to 0$ in Eq. (2.16)). In such a case the resonances are shape-type resonances due to the tunneling through the quasi-static potential barrier induced by the low frequency laser field. Is there a sharp transition from a shape-type resonance to a Feshbach-type resonance as one varies the laser frequency? The answer is no. Since the Feshbach resonances have a classical analog one can distinguish between Feshbach and shape-type resonances by calculating the lifetime of the particle inside a potential well as function of $\hbar$. If the lifetime adiabatically reduces to zero as $\hbar$ goes to zero then one may define this resonance as a shape-type resonance. However, if the lifetime gets a non-zero value even in the limit of $\hbar \to 0$ it can be considered as a Feshbach-type resonance. This is particularly true when the classical lifetime is very close to the quantum value obtained for $\hbar = 1$ au (i.e., the physical value).

Exercise 2.3

An atom interacts with a cw linearly polarized light that induces an ac field. All the field-free electronic states $|\psi_n^{\mathrm{FF}}\rangle$ become metastable states associated with the photo-ionization decay rate which can be defined as $\Gamma_n^{\mathrm{ac}}(\omega_L) = -\lim_{t\to\infty} \frac{\mathrm{d}}{\mathrm{d}t} \ln(|\langle\psi_n^{\mathrm{FF}}|\Phi_n^{\mathrm{ac}}(t;\omega_L)\rangle|^2)$, where $|\Phi_n^{\mathrm{ac}}(t;\omega_L)\rangle$ is the solution of the time-dependent Schrödinger equation with the time-periodic Hamiltonian that describes the atom which interacts with the ac field as defined in Eq. (2.16). The initial condition is given by $|\Phi_n^{\mathrm{ac}}(t=0;\omega_L)\rangle = |\psi_n^{\mathrm{FF}}\rangle$. Suggest a numerical procedure which "measures" whether the resonances have shape-type character or Feshbach-type character. How does the character of the resonance changes with the laser frequency ω_L?

2.4 Solutions to the exercises

Answer to Exercise 2.1

First we assume that $V(R)$ describes the ground electronic energy of a diatomic molecule as function of the intranuclear distance R. The vibrational and rotational states are obtained by solving the Schrödinger equation within the framework of the Born–Oppenheimer approximation:

$$\left(-\frac{\hbar^2}{2\mu}\frac{\mathrm{d}^2}{\mathrm{d}R^2} + V_{\mathrm{eff}}(R;J)\right)\Psi_{\nu,J}(R) = E_{\nu,J}\Psi_{\nu,J}(R)\,,$$

$$V_{\mathrm{eff}}(R;J) = \frac{\hbar^2 J(J+1)}{2\mu R^2} + V(R)\,. \tag{2.19}$$

The effective potential $V_{\mathrm{eff}}(R;J)$ supports a harmonic-like potential well with the vibrational frequency ω_{well}. This frequency can be approximated by a Taylor series expansion around the position of the minimum of the well, which we will label as R_{min}, where the minimum in the effective potential is $V_{\mathrm{min}} = V_{\mathrm{eff}}(R = R_{\mathrm{min}})$. This means that the lowest energy inside the potential well is about $E_0 = V_{\mathrm{min}} + \hbar\omega_{\mathrm{well}}/2$.

The approximation for the parabolic potential barrier will be derived in a similar manner by expanding $V_{\mathrm{eff}}(R;J)$ around the top of the potential barrier R_{max} where the effective potential is $V_{\mathrm{max}} = V_{\mathrm{eff}}(R = R_{\mathrm{max}})$. Now the dissociation can occur due the tunneling through a potential barrier which is approximated by

$V_{\text{barr}} = V_{\max} - \frac{\mu\omega_{\text{barr}}^2}{2}(R - R_{\max})^2$. In the semiclassical limit the transmission coefficient through a barrier is given by

$$T(E) = \left[1 + \exp\left(+\frac{2}{\hbar}\int_a^b |p|\mathrm{d}x\right)\right]^{-1}$$
$$= \left[1 + \exp\left(+\frac{2}{\hbar}\int_a^b \left|\sqrt{2m(E - V(x))}\right| \mathrm{d}x\right)\right]^{-1}, \tag{2.20}$$

where m is the mass of the tunneling particle and a and b are the classical turning points where $V(x) = E$ and $x = R - R_{\max}$. The dissociation of the diatomic molecule with the reduced mass μ through the parabolic potential barrier can therefore be approximated by[2]

$$T(E) = \left[1 + \exp\left(+\frac{2}{\hbar}\int_{-x_{\text{tp}}}^{+x_{\text{tp}}} \sqrt{2\mu(V_{\max} - \mu\omega_{\text{barr}}^2 x^2/2 - E)}\mathrm{d}x\right)\right]^{-1}, \tag{2.21}$$

where the classical turning points are given by

$$\pm x_{\text{tp}} = \pm\sqrt{\frac{2(V_{\max} - E)}{\mu\omega_{\text{barr}}^2}}. \tag{2.22}$$

The integration results in the following expression for the transmission probability through the barrier:

$$T(E) = \left[1 + \exp\left(\frac{2\pi\Delta}{\hbar\omega_{\text{barr}}}\right)\right]^{-1}, \tag{2.23}$$

where $\Delta = V_{\max} - E$. Now since we assume the molecule is initially situated at the ground state of the well the appropriate energy is $E_0 = V_{\min} + \hbar\omega_{\text{well}}/2$ and thus $\Delta_0 = V_{\max} - V_{\min} - \hbar\omega_{\text{well}}/2$. The probability of passing through the barrier per unit time is given by the frequency of oscillations in the well, $P(t) = \omega_{\text{well}} T(E_0)/(2\pi)$, and therefore the lifetime of the molecule inside the potential well before it dissociates is approximately (assuming that the potential barrier is large enough) given by

$$\tau = \frac{2\pi}{\omega_{\text{well}}} \exp\left(\frac{2\pi\Delta_0}{\hbar\omega_{\text{barr}}}\right). \tag{2.24}$$

As we increase the rotational quantum number J the difference between the bottom of the well ($V_{\min}$) and the top of the barrier ($V_{\max}$) decreases, thus reducing Δ_0 and increasing the probability of the molecule dissociating. Eventually, as the molecule

---

[2] L. D. Landau and E. M. Lifshitz, *Quantum Mechanics*, Pergamon Press Ltd. (1965), Problem 4 in Section 50.

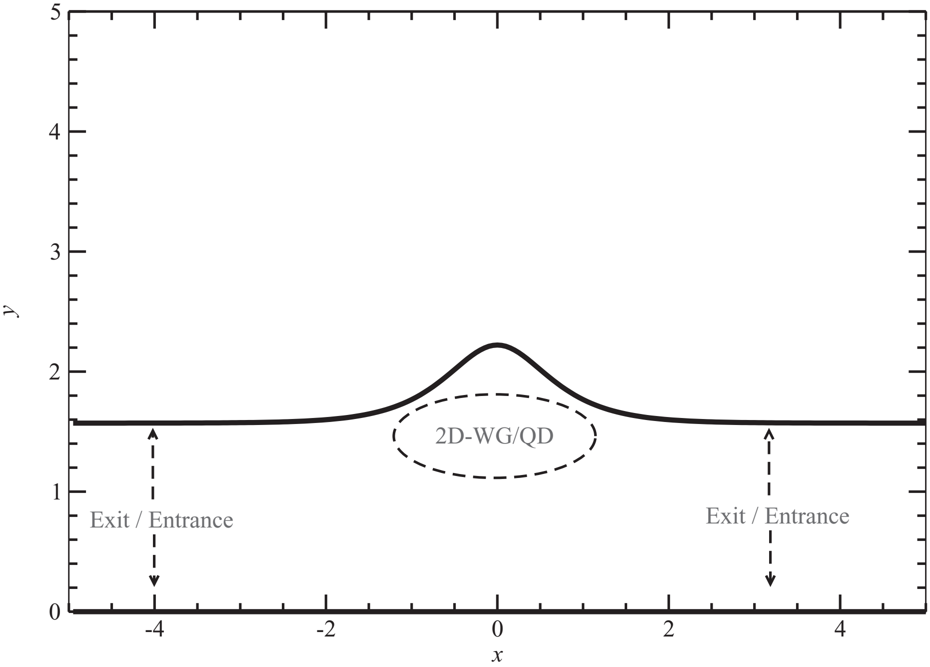

Figure 2.4 A 2D potential which describes a 2D slab waveguide or a 2D quantum dot (refraction index/potential energy is set to zero for $0 \leq y \leq a(x)$, where $a(x) = \pi[\cosh^2(x)/(4\cosh^2(x) - 2)]^{1/2}$ and $\mp\infty$ elsewhere).

goes to higher rotational states, the minimum in $V_{\text{eff}}(R; J)$ will disappear and the molecule will dissociate immediately.

Answer to Exercise 2.2

In Fig. 2.4 a 2D potential is shown which can be used to model either a waveguide (WG) or a quantum dot (QD). Under the adiabatic approximation the light-propagation in the 2D WG or the electrons in the 2D QD move much more slowly along the x-direction than along the y-direction. Two coupled eigenvalue equations are obtained. The first eigenvalue problem is of a particle in a box where the length of the box varies adiabatically with x, which serves here as a parameter.

$$\left(-\frac{1}{2}\frac{\partial^2}{\partial y^2} + V(y;x)\right)\Psi_{n_y}(y;x) = \lambda_{n_y}(x)\Psi_{n_y}(y;x)\,, \tag{2.25}$$

where $V(0 \leq y \leq a(x)) = 0$ and ∞ elsewhere. The eigenvalue equation for the motion in the x-direction is given by

$$\left(-\frac{1}{2}\frac{\partial^2}{\partial x^2} + \lambda_{n_y}(x)\right)\chi_{n_y,n_x}(x) = E_{n_y,n_x}\chi_{n_y,n_x}(x)\,, \tag{2.26}$$

where the adiabatic potential (obtained form the motion in the y-direction) is

$$\lambda_{n_y}(x) = n_y^2 \left(2 - \frac{1}{\cosh^2(x)}\right) . \tag{2.27}$$

Since this potential is, up to a constant, a 1D Rosen–Morse potential, the adiabatic eigenvalues E_{n_y,n_x} have a closed form expression: $E_{n_y,n_x} = 2n_y^2 - \left(\sqrt{1 + 8n_y^2} - 1 - 2n_x\right)^2/8$, where $n_x = 0, 1, 2, \ldots, N_\mathrm{b} - 1$ and the number of the bound states in the Rosen–Morse potential is given by the largest integer N_b satisfying the condition $N_\mathrm{b} \leq \left(\sqrt{1 + 8n_y^2} - 1\right)/2$.[3]

Within the adiabatic approximation the lowest adiabatic channel associated with $n_y = 1$ supports only one bound state (i.e., $N_\mathrm{b} = 1$ and $n_x = 0$) while the first excited adiabatic potential supports two bound states. The adiabatic potentials $\lambda_{n_y}(x)$ and the adiabatic energies E_{n_y,n_x} are shown in Fig. 2.5. As one can see from the results presented in Fig. 2.5, the bound state of $n_y = 1$ is embedded *below* the lowest threshold energy and it can be associated with a true 2D bound state of the system provided that the non-adiabatic couplings can be neglected.

The other bound states, however, are embedded *above* the threshold energies and become Feshbach-type resonances due to the non-adiabatic terms that couple the various adiabatic channels. For example, the energies of the two bound states associated with the $n_y = 2$ adiabatic potential $\lambda_2(x)$ can be taken as estimates for the positions of the Feshbach resonance which have only one open channel to decay. The three bound states associated with the $n_y = 3$ adiabatic potential become Feshbach resonances when the non-adiabatic coupling is taken into account in solving the Schrödinger equation beyond the Born–Oppenheimer approximation. The resonance positions are about equal to $E_{n_y=3,n_x=0,1,2}$ and they have two open channels for decay.

Consider the decay process for an electron which is temporarily trapped in this 2D model potential in a Feshbach resonance associated with some bound adiabatic state. For instance, let it be the state associated with n_y and n_x quantum numbers. As time passes the electron will leak out of the 2D QD and will move outward along the x-direction. In general, we can estimate the exiting electron's velocity through the excess energy it holds above the threshold of the $n_y - k$ potential curve, where $k = 1, \ldots, (n_y - 1)$. This excess energy is converted to kinetic energy as the electron leaks out, which yields an approximated velocity of $v_x \sim \sqrt{2E_{n_x,n_y} - 2(n_y - 1)^2}$. When the electron has several open channels for decay one may detect electrons with different velocities. For example, if one excites an electron to a resonance states with quantum numbers $n_y = 3$ and $n_x = 0$ it can

---

[3] N. Rosen and P. N. Morse, *Phys. Rev.* **42**, 210 (1932). See also L. D. Landan and E. M. Lifshitz, *Quantum Mechanics*, Oxford, Pergamon Press, 1965, Problem 4 in Section 23.

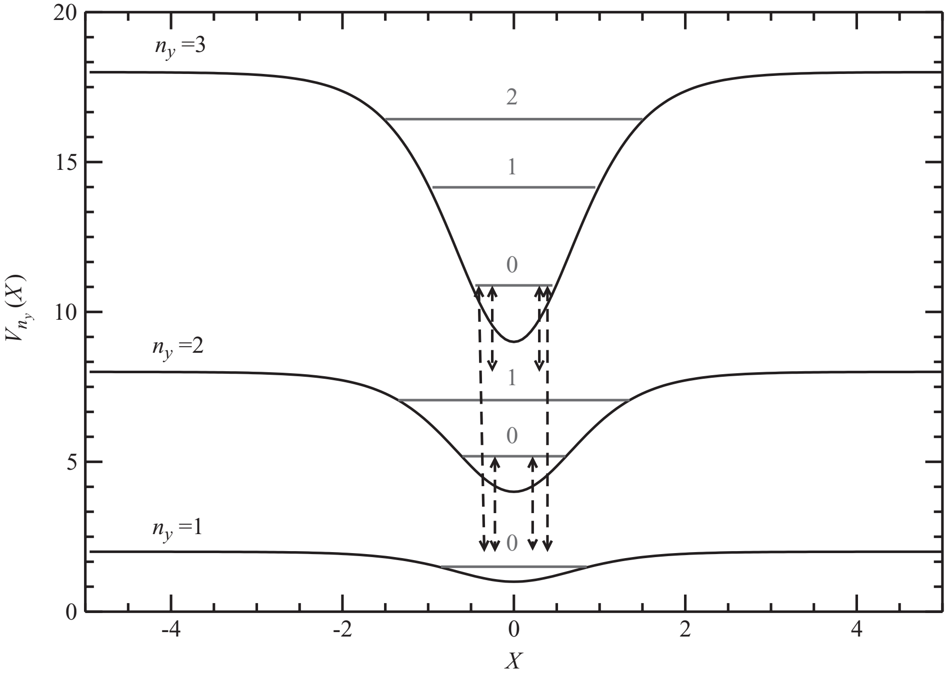

Figure 2.5 The adiabatic potentials $V_{n_y}(X)$ (defined as $\lambda_{n_y}(x)$ in the text) for the 2D waveguide/quantum-dot (WG/QD) which is shown in Fig. 2.4. The length of the arrows indicates the different kinetic energies of the electrons which get out of the 2D WG/QD through the two leads (exits/entrances), due to the decay processes of the populated resonance states, $|n_y = 2, n_x = 0\rangle \rightarrow |n_y = 1, x - \text{threshold}\rangle$ and $|n_y = 3, n_x = 0\rangle \rightarrow |n_y = 2, x - \text{threshold}\rangle$ and to $|n_y = 1, x - \text{threshold}\rangle$. Within the approximation of bound-state embedded in the continuum due to conservation of energy the kinetic energy of the electrons which move freely through the leads in the x-direction are as indicated by the length of the arrows shown in the plot. However, the resonances being metastable states (i.e., states with finite lifetimes) are associate with energies that have widths (that are uniquely defined only within the framework of the non-Hermitian formalism of QM). The variance of the kinetic energies of the electrons that get out of the 2D WG/QD through the leads is linearly proportional to the resonance widths.

decay to the $n_y = 2$ channel producing slow-moving electrons and also to the $n_y = 1$ channel which leads to fast electrons with high kinetic energy. Such decay, however, will not induce current in the lab since the electron in such a QD structure has an equal probability of decaying to both leads, thus one needs to create some asymmetry in the system in order to detect the different decay products.

In a scattering experiment where an electron is transferred via the leads (exits/entrances) through the unoccupied 2D quantum dot resonance state the transmission probability will be almost equal to 100% when the energy of the incoming electron through the lead is equal to the resonance energy which has been roughly estimated as $E_{ny=2,n_x=0}$. In different configurations than the above structure this resonance tunnelling phenomenon can be used for the construction of diodes and transistors.

Answer to Exercise 2.3

It is natural to assume that the field induced resonances are Feshbach-type since they usually result from the coupling of bound states to the continuum via the interaction with the radiation. However, if the frequency of the ac field is very small one may think of it as quasi-static. In such a case the decay will occur due to tunneling through the quasi-static barrier formed and the resonance can be thought of as shape-type.

In order to eliminate the mechanism by which Feshbach-type photo-induced resonances are formed we apply the adiabatic approximation where we treat t (time) in the Hamiltonian defined in Eq. (2.16) as a parameter τ. By doing so we get a time-*independent* Hamiltonian where an atom interacts with a static field of strength $\epsilon_{\rm dc} = \epsilon_0 \cos(\omega_L \tau)$. The solution of the time-dependent Schrödinger equation with the adiabatic time-independent Hamiltonian is defined by $|\Phi_n^{\rm dc}(t; \epsilon_{\rm dc})\rangle$, where $|\Phi_n^{\rm dc}(t = 0; \epsilon_{\rm dc})\rangle = |\psi_n^{\rm FF}\rangle$. The ionization decay rate is obtained by calculating

$$\Gamma_n^{\rm dc}(\epsilon_{\rm dc}) = -\lim_{t\to\infty} \frac{\rm d}{{\rm d}t} \ln(|\langle\psi_n^{\rm FF}|\Phi_n^{\rm dc}(t, \epsilon_{\rm dc})\rangle|^2) \tag{2.28}$$

from $\epsilon_{\rm dc} = 0$ to $\epsilon_{\rm dc} = \epsilon_0$. The rate of ionization results from the tunneling of the electrons through the adiabatic potential barrier created by the static field and therefore can be associated with a shape-type (ST) resonance. We can now average over all the possible field strengths over one cycle of the ac field, $T = \frac{2\pi}{\omega_L}$, to get an effective decay rate which is associated with a shape-type behavior.

$$\Gamma_n^{\rm ST}(\omega_L) = \frac{1}{T} \int_0^T {\rm d}\tau\, \Gamma_n^{\rm dc}(\epsilon_{\rm dc} = \epsilon_0 \cos(\omega_L \tau))\,. \tag{2.29}$$

We can choose the following numerical criterion for the transition from the Feshbach-type to the shape-type resonance phenomenon as we vary ω_L:

$$P(\omega_L) = \left| \frac{\Gamma_n^{\rm ac}(\omega_L) - \Gamma_n^{\rm ST}}{\Gamma_n^{\rm ac}(\omega_L)} \right| , \tag{2.30}$$

which obtains values ranging from 0 to 1 as we increase ω_L. When $P \to 0$ the resonance can be defined as a strictly shape-type resonance since the tunneling rate accounts for the full behavior, whereas when $P \to 1$ it is strictly a Feshbach-type resonance since the tunneling through the quasi-static barrier is negligible.

2.5 Further reading

Shape-type resonances

Alpha decay

R. Neil, Review: Tunnelling phenomena in nuclear physics, *Proceedings of the Second International Conference*, St. Andrews, United Kingdom, Singapore, World Scientific Publishing Co. (2000).

The Stark effect: atoms and molecules in dc fields

S. H. Autler and C. H. Townes, Stark effect in rapidly varying fields, *Phys. Rev.* **100**, 703–722 (1955).

A. D. Buckingham and P. J. Stephens, The Stark effect in molecules with strong nuclear quadrupole coupling, *Mol. Phys.* **7**, 481–191 (1964).

Resonance tunneling in quantum wells and quantum wires

S. Bhattacharyya, S. J. Henley, E. Mendoza, L. Gomez-Rojas, J. Allam and S. R. P. Silva, Resonant tunnelling and fast switching in amorphous-carbon quantum-well structures, *Nature Materials* **5**, 19–22 (2006).

Y. Ji, Y. Chung, D. Sprinzak, M. Heiblum, D. Mahalu and H. Shtrikman, An electronic Mach–Zehnder interferometer, *Nature* **422**, 415 (2003).

A. Yacoby, M. Heiblum, D. Mahalu and H. Shtrikman, Coherence and phase sensitive measurements in a quantum dot. *Phys. Rev. Lett.* **74**, 4047 (1995).

Resonance tunneling: diodes

D. Bohm, *Quantum Theory*, New York, Prentice-Hall, 1951.

K. Ismail, B. S. Meyerson and P. J. Wang, Electron resonant tunneling in Si/SiGe double barrier diodes, *Appl. Phys. Lett.* **59**, 973 (1991).

P. See, D. J. Paul, B. Hollander, S. Mantl, I. V. Zozoulenko and K.-F. Berggren, High performance Si/Si1-xGex resonant tunneling diodes, *IEEE Electron Device Letters* **22**, 182 (2001).

Feshbach-type resonances

Autoionization of atoms and molecules

A. Temkin and Z. J. Horak, Autoionization recent developments and applications. *Astrophys Space Sci.*, **123**, 216 (1986).

G. W. Drake, ed., *Handbook on Atomic, Molecular and Optical Physics*, New York, Springer, 2005.

Predissociation of molecules

H. Lefebvre-Brion and R. W. Field, *The Spectra and Dynamics of Diatomic Molecules*, New York, Academic Press, 2004.

J. Z. H. Zhang, *Theory and Application of Quantum Molecular Dynamics*, Singapore, World Scientific Publishing Co., 1999.

R. Schinke, *Photodissociation Dynamics: Spectroscopy and Fragmentation of Small Polyatomic Molecules*, Cambridge, Cambridge University Press, 1995.

Predesorption of atoms and molecules from solid surfaces

M. J. Cardillo, Helium diffraction as a probe of surface topography, *Faraday Discuss. Chem. Soc.* **80**, 17–27 (1985).

J. Lapujoulade and J. Perreau, The diffraction of molecular hydrogen from copper surfaces, *Phys. Scr.* **T4**, 138–149 (1983).

J. Heidberg, H. Steina, E. Riehla, Z. Szilagyia and H. Weissa, Vibrational predesorption, *Surface Science* **158**, 553–578 (1985).

Atoms and molecules in ac-fields: the above threshold ionization/dissociation and the high order generation phenomena

W. Becker, F. Grasbon, R. Kopold, D. B. Miloševi, G. G. Paulus and H. Walther, Above-threshold ionization: from classical features to quantum effects, *Adv. Atomic Molecular Opt. Phys.* **48**, 35–98 (2002).

T. Brabec and F. Krausz, Intense few-cycle laser fields: frontiers of nonlinear optics, *Rev. Mod. Phys.* **72**, 545 (2000).

Cold atoms in optical and magnetic traps

Ph. Courteille, R. S. Freeland, D. J. Heinzen, F. A. van Abeelen and B. J. Verhaar, Observation of a Feshbach resonance in cold atom scattering, *Phys. Rev. Lett.* **81**, 69–72 (1998).

Modal losses in optical waveguides

A. W. Snyder and J. D. Love, *Optical Waveguide Theory*, London, Chapman and Hall, 1983.

3

Resonances from Hermitian quantum-mechanical calculations

The study of a given system within the scope of Hermitian quantum mechanics conserves the probability of finding a given particle in space. This makes treatment of decaying states with finite lifetime difficult. In this chapter we will show that within the framework of conventional Hermitian quantum mechanics the resonance phenomenon is not a well defined concept. However it is still possible to devise Hermitian quantum mechanical calculations which would reveal the resonant energies and their corresponding lifetimes.

3.1 Resonances as metastable states

In order to illustrate how a decaying state may be obtained in conventional quantum mechanical calculations, we may consider a situation where the Hamiltonian is given by

$$\hat{H} = \hat{H}_0 + \lambda \hat{V} \, . \tag{3.1}$$

Let's assume that we have a special situation where $\hat{H}_0$ supports a true bound state, $|\psi_\mathrm{b}(E_\mathrm{b})\rangle$ that is embedded in the continuum of $\hat{H}_0$. The bound state $|\psi_\mathrm{b}(E_\mathrm{b})\rangle$ is a square integrable function (part of the Hilbert space of our problem) which decays exponentially to zero in the coordinate space. The continuum functions are energy normalized such that $\langle\psi_\mathrm{c}(E')|\psi_\mathrm{c}(E)\rangle = \delta(E - E')$, where $E = 0$ is the threshold energy.

Exercise 3.1

Show that for 1D plane waves $|\psi_\mathrm{c}(E)\rangle = \mathcal{N}\mathrm{e}^{\mathrm{i}px/\hbar}$, where $p = \hbar k$ is the momentum of the free particle and the energy normalization factor is given by $\mathcal{N} = \sqrt{\mu/(2\pi\hbar p)}$.

The perturbation $\hat{V}$ couples the bound state with the continuum. In this special case we get a solution which decays exponentially in time with the decay rate $\Gamma/\hbar$ up to a certain time which is problem dependent. This decay can be exemplified by considering a restricted part of space bounded by a box of size L. As time passes the propagated wavefunction leaks out of the box, which can be taken as large as one wishes. In the limit of $\lambda \to 0$ the decay rate can be obtained from the well known Fermi golden rule,

$$\Gamma \to 2\pi\lambda^2 \rho_c(E_b)|\langle\psi_b(E_b)|\hat{V}|\psi_c(E_b)\rangle|^2 , \tag{3.2}$$

where ρ_c is the density of states in the "white continuum" of the $\hat{H}_0$ Hamiltonian.

Exercise 3.2

Derive the Fermi golden rule from time-dependent perturbation theory.

This result shows that, unlike the situation in non-Hermitian quantum mechanics, in conventional quantum mechanics the resonance phenomenon is not associated with an isolated uniquely defined eigenfunction of the full Hamiltonian $\hat{H}$. Instead it is represented by a *wavepacket* of continuum states. Moreover, this wavepacket may exhibit a non-exponential decay in time. The rate of decay is defined by the Fermi golden rule only for small values of λ and within a certain time period which is problem dependent. As one reduces λ this period of time increases. This point is briefly reviewed below.

As discussed in the previous chapter, the fact that in the above example the spectrum of the zero-order Hamiltonian consists of a bound state embedded in the continuum implies that the resonance, which is born as the coupling potential term, $\hat{V}$, is turned on and a wavepacket is created, is a Feshbach-type resonance. However, shape-type resonances are also associated in conventional Hermitian quantum mechanics with wavepackets and are not uniquely defined, in particular when the resonance decay rate is not sufficiently small. As a matter of fact, in conventional quantum mechanics a clear direct indication of the resonance phenomenon is usually possible only when the resonances are isolated and narrow. Let us briefly explain what we mean by narrow and isolated resonances. Γ can be considered as the energy uncertainty of the resonance state which is termed the *resonance width*. This statement is based on the uncertainty relationship

$$\Delta\omega\Delta t = 1 \tag{3.3}$$

which is based on the Fourier transformation of a signal from the time domain to the frequency/energy domain. Δt is the duration of the signal and $\Delta\omega = \Delta E/\hbar$ is

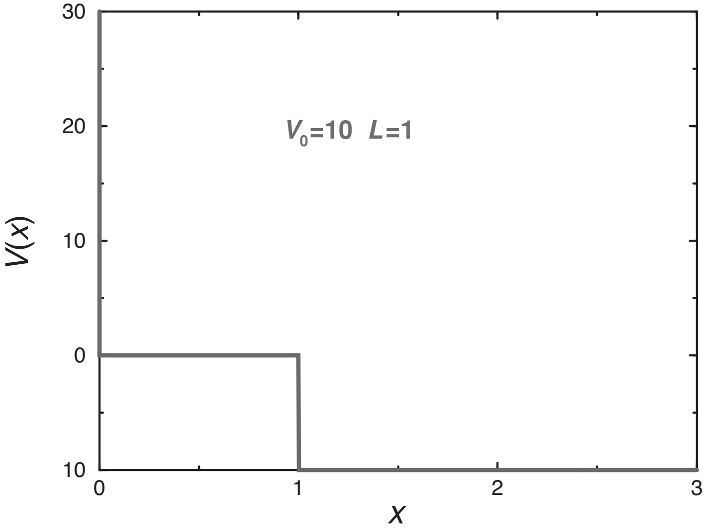

Figure 3.1 The potential barrier given in Eq. (3.5).

the band width of the signal. The lifetime of the resonance state can be taken as Δt where the energy "uncertainty" is defined as the resonance width Γ. Therefore, from Eq. (3.3) one gets that the resonance lifetime, τ, can be defined as the inverse of Γ. That is,

$$\tau = \frac{\hbar}{\Gamma} \, . \tag{3.4}$$

A narrow resonance is one with a small width, i.e. a long lifetime. Isolated resonances are those for which the difference in the energy to adjacent resonances is much smaller than the corresponding resonance widths.

As an illustrative example for the calculations of resonance properties within the framework of conventional Hermitian quantum mechanics, we choose a simple analytically solvable one-dimensional repulsive potential which is shown in Fig. 3.1 and given by:

$$V(x) = \begin{cases} 0 \, , & 0 \le x \le L \, , \\ -V_0 \, , & x > L \, . \end{cases} \tag{3.5}$$

We chose this potential as a case study in order to emphasize the fact that bound states and resonances are not necessarily associated with potential wells. In this model the interaction region can be defined in the interval where $x \le L$. Note that this problem is the same as a spherically symmetric potential with zero angular momentum (i.e. the eigenfunctions for the 1D Hamiltonian that we chose to study are the s-waves in a 3D Hamiltonian with a radial potential).

As will be shown below, the resonances are metastable states of a quantum particle which is temporarily trapped at the step $0 < x \leq L$ at energies $E > 0$. Up to an energy dependent normalization constant the solution to the time-independent Schrödinger equation for $E > 0$ is given by

$$\Psi_E(x) = \begin{cases} \psi_{\text{in}}(x) = \sin(kx)\,, & 0 \leq x \leq L\,, \\ \psi_{\text{out}}(x) = A(k)\mathrm{e}^{-\mathrm{i}q(x-L)} + B(k)\mathrm{e}^{+\mathrm{i}q(x-L)}\,, & x \geq L \end{cases} \tag{3.6}$$

where

$$k = \sqrt{2ME}/\hbar\,, \qquad q = \sqrt{2M(E+V_0)}/\hbar\,. \tag{3.7}$$

From the the continuity of the wavefunction and its derivative at $x = L$,

$$\begin{aligned} \psi_{\text{in}}(x=L) &= \psi_{\text{out}}(x=L)\,, \\ \left.\frac{\partial \psi_{\text{in}}(x)}{\partial x}\right|_{x=L} &= \left.\frac{\partial \psi_{\text{out}}(x)}{\partial x}\right|_{x=L}\,, \end{aligned} \tag{3.8}$$

one gets that

$$A(k) = \frac{1}{2}\left(\sin(kL) + \frac{\mathrm{i}k}{q}\cos(kL)\right) = |A|\mathrm{e}^{-\mathrm{i}\delta(k)} \tag{3.9}$$

and

$$B(k) = \frac{1}{2}\left(\sin(kL) - \frac{\mathrm{i}k}{q}\cos(kL)\right) = |A|\mathrm{e}^{+\mathrm{i}\delta(k)}\,, \tag{3.10}$$

where

$$\delta(k) = \arctan\left(\frac{-k}{q}\cot(kL)\right)\,. \tag{3.11}$$

The ratio between the amplitudes of the outgoing and the incoming waves in this case is the so-called scattering matrix (S-matrix). In our 1D studied case there is only one S-matrix element, $S(k) = B(k)/A(k)$. Substituting $A(k)$ from Eq. (3.9) and $B(k)$ from Eq. (3.10) we get that

$$S(k) = \mathrm{e}^{\mathrm{i}2\delta(k)}\,, \tag{3.12}$$

which is a general property of the S-matrix.

Exercise 3.3

A stationary state of a particle moving in one dimension behaves in the asymptote (i.e. far from the potential of interaction) as a free particle $\psi = [A(k)\mathrm{e}^{-\mathrm{i}kx} + B(k)\mathrm{e}^{+\mathrm{i}kx}]\mathrm{e}^{-\mathrm{i}Et/\hbar}$. Show that when the wavefunction is invariant under time reversal the particle flux (number of particles per unit time that pass through a unit area perpendicular to the direction of motion) is zero and therefore $|S(k)| = |B(k)/A(k)| = 1$ (i.e. the S-matrix is unitary).

$\delta(k)$ is termed the *phase shift* of the *unitary* S-matrix. It is clear that the phase shift is defined up to addition of an arbitrary integer multiple of π. By substituting Eqs. (3.9) and (3.10) into Eq. (3.6) one gets that the asymptotic form of the continuum wavefunction in our model problem is given by

$$\psi_{\text{out}}(x) = A_{\text{out}} \sin\left(qx + \delta(k) - \frac{1}{2}\pi - qL\right) , \tag{3.13}$$

where

$$A_{\text{out}} = 2|A(k)| \tag{3.14}$$

and $A(k)$ is given by Eq. (3.9). The phase shift associated with the wavefunction in the non-interacting region is defined according to Eq. (3.13) by

$$\delta_{\text{out}}(k) = \delta(k) - \frac{1}{2}\pi - qL\,. \tag{3.15}$$

Note that in our studied case $\delta(k) \to \pi/2$ as $q \to 0$ and therefore $\delta_{\text{out}}(k) \to 0$. This fact will be used later when we discuss resonance to bound state transitions in slow particle scattering experiments.

How will the resonance phenomenon be reflected in conventional Hermitian quantum mechanics calculations? Below we present various approaches for extracting the resonance positions/energies and widths, i.e. inverse lifetimes (applied to our model problem) from conventional quantum mechanical calculations where the Hamiltonian is Hermitian.

3.2 The poles of the S-matrix

The fingerprints of resonance states in the cross sections measured in scattering experiments are reflected in the structure of the energy profile of the cross sections. Narrow resonances are manifested by sharp features associated with the complex poles of the scattering matrix.

The poles in the S-matrix are obtained in two cases:

1. When the amplitude of the outgoing waves, $B(k)$, has poles. These are "false" poles which are not associated with the resonance phenomena. "False" poles are independent of the potential strength parameter, $V = \lambda v(\vec{r})$, and exist even when λ approaches zero.[1]
2. When the amplitude of the incoming waves, $A(k)$, vanishes. When these poles are concentrated on the positive imaginary axis of k they are associated with bound states. As will be shown later, the poles which are embedded in the fourth quadrant of the *complex* k-plane (i.e., $\mathrm{Re}(k) > 0$, $\mathrm{Im}(k) < 0$) are associated with the resonance phenomenon. Near the n-th simple isolated pole $S(k)$ can be written as[2]

   $$S(k) \propto \frac{k - k_n^*}{k - k_n} . \tag{3.16}$$

   In order to eliminate the proportionality factor dependence we take the derivative,

   $$\frac{\mathrm{d}lnS(k)}{\mathrm{d}k} = \frac{1}{k - k_n^*} - \frac{1}{k - k_n} , \tag{3.17}$$

   where k_n is a complex pole with $\mathrm{Re}(k_n) > 0$, $\mathrm{Im}(k_n) < 0$.

In the following paragraphs we will show that these poles are associated with the peaks in the density of states in the continuum. In non-Hermitian quantum mechanics these poles emerge as complex eigenvalues of the Hamiltonian. In this chapter, however, we discuss the resonance phenomenon using Hermitian quantum mechanics formalism.

3.3 Resonances from the spectra of density of states

The resonances are associated with the peaks in the density states spectra, $\rho(E)$. We will show here that, under the assumption that the poles are isolated and close to the real axis, the Lorentzian peaks in the plot of the density of continuum states vs. the energy of the decaying particle are a fingerprint of the complex pole in the scattering matrix.

Considering a closed contour of integration, $\mathcal{C}$, in the lower half complex k-plane, then following the residue theorem,

$$N = \frac{1}{2\pi \mathrm{i}} \oint_{\mathcal{C}} \frac{\partial lnS(k)}{\partial k} \mathrm{d}k , \tag{3.18}$$

where N is the number of poles in the lower half of the complex k-plane. From Eq. (3.17) one gets that the integrand is a purely imaginary function of k on the real

---

[1] H. J. Korsch, R. Möhlenkamp and H. D. Mayer, *J. Phys. B* **17**, 2955 (1984) and references therein.

[2] See, for example, A. I. Baz', Ya. B. Zel'dovich and A. M. Perelomov, *Scattering, Reactions and Decay in Nonrelativisitic Quantum Mechanics* and V. I. Kukulin, V. M. Krasnopol'sky and J. Horáček, *Theory of Resonances: Prinicples and Applications*.

axis. When all the poles of $S(k)$ are embedded in a *bounded* region in the lower half complex k-plane (i.e., all of them are at a finite "distance" from the real k-axis) the closed contour of integration $\mathcal{C}$ can be replaced by a contour along the real k-axis (k varies from $-\infty$ to ∞) and, consequently, the integrand divided by the $1/(2\pi \mathrm{i})$ factor is a continuous real function of k which is defined as

$$\frac{\partial N}{\partial k} = (2\pi \mathrm{i})^{-1} \frac{\partial ln S(k)}{\partial k} . \tag{3.19}$$

Let us study the variation of $\partial N/\partial k$ as a function of real k assuming that there is a single isolated pole very close to the real axis. The derivative of N with respect to the energy E is interpreted as the density of states ρ close to the isolated narrow pole (a support for this definition is the Fermi golden rule where the decay rate is proportional to the density of states),

$$\rho \equiv \frac{\mathrm{d}N}{\mathrm{d}E} = \left[\frac{\partial \mathcal{N}}{\partial k}\right]\left[\frac{\partial k}{\partial E}\right] . \tag{3.20}$$

Since in one-dimensional problems $E = (\hbar k)^2/(2M)$,

$$\rho = \left[\frac{M}{2\pi \mathrm{i}\hbar^2 k}\right] \frac{\partial ln S(k)}{\partial k} = \frac{1}{2\pi \mathrm{i}} \frac{\partial ln S(E)}{\partial E} . \tag{3.21}$$

Near an isolated resonance we can express the scattering matrix in a similar manner to Eq. (3.16) as

$$S(E) \propto \frac{E - E_n^*}{E - E_n} , \tag{3.22}$$

and by substituting this expression into Eq. (3.21) we get that the density of states has a Lorentzian shape:

$$\rho(E) = \frac{1}{2\pi \mathrm{i}}\left[\frac{1}{E - E_n^*} - \frac{1}{E - E_n}\right] = \frac{1}{2\pi} \frac{-2\mathrm{Im}(E_n)}{(E - \mathrm{Re}(E_n))^2 + (\mathrm{Im}(E_n))^2} . \tag{3.23}$$

By substituting Eq. (3.17) into Eq. (3.21), one can see that when $k = \mathrm{Re}(k_n)$, the local maxima of the density of states is obtained for the value of $\rho = \rho_{\max}$, where

$$\rho_{\max}(k = \mathrm{Re}(k_n)) = \frac{M}{\pi\hbar^2}\left[-\frac{1}{\mathrm{Re}(k_n)\mathrm{Im}(k_n)}\right] = -\frac{1}{\pi \mathrm{Im}(E_n)} . \tag{3.24}$$

The complex n-th pole of the S-matrix in the complex energy plane is given by

$$E_n = E_{\mathrm{t}} + \frac{(\hbar k_n)^2}{2M} \tag{3.25}$$

with E_t being the threshold energy. Since the peak in the density of states is Lorentzian due to Eq. (3.23), its width is related to the complex part of the pole by

$$\Gamma_n \equiv -2\mathrm{Im}(E_n)\,. \tag{3.26}$$

$\Gamma_n = 2/(\pi\rho_\mathrm{max})$ is the full-width at half maximum of the n-th Lorenzian peak in $\rho(E)$ centered around $E = \mathrm{Re}(E_n)$. Only in the non-Hermitian formalism of quantum mechanics the information regarding Γ_n can be extracted from the energy of the resonance manifested by the pole in the scattering matrix.

We should stress again that the peaks in the plot of the density of states are fingerprints of the resonance phenomenon and for a "white continuum", as in the case of a constant potential, there is no structure in the plot of $\rho(E)$ vs. the energy.

Exercise 3.4

Derive the expressions for the density of states of 1D, 2D and 3D particle-in-a-box problems.

Exercise 3.5

Using the variational method calculate the density of states for our model Hamiltonian for $V_0 = 10$ and $V_0 = 100$ within the framework of the finite box quantization condition.

In Fig. 3.2 we show the density of states for our model Hamiltonian with $L = 1$ au and $V_0 = 10$ au. For the sake of simplicity we will work with energy $\tilde{E}$ in scaled units of

$$\tilde{E} = \frac{2ML^2}{\hbar^2\pi^2}E\,. \tag{3.27}$$

For these potential parameters the non-monotonic behavior of $\rho(E)$ "pops out" only when we calculate the third-order derivative of $\rho(\tilde{E})$. This non-monotonic behavior of $\rho(\tilde{E})$ at $\tilde{E} \sim 1$ is an indication to the resonance phenomenon. As we will show later in this chapter, the resonance phenomenon is reflected in the continuum at energies $\tilde{E} \sim 1$ by states which are localized in the interaction region (i.e., the step in our model potential). When a wavepacket is prepared at that energy (when the standard deviation of the energy of the wavepacket (WP) is smaller than Γ) its decay rate is $\Gamma/\hbar$. In other words, the survival probability of the WP is approximately given by $|\langle\Psi_\mathrm{WP}(t = 0)|\Psi_\mathrm{WP}(t)\rangle|^2 \sim \mathrm{e}^{-\Gamma t/\hbar}$). The difficulty of observing the resonance phenomenon for the chosen potential parameters is due to the large width (i.e., short lifetime) of the WP initially prepared in the interaction region.

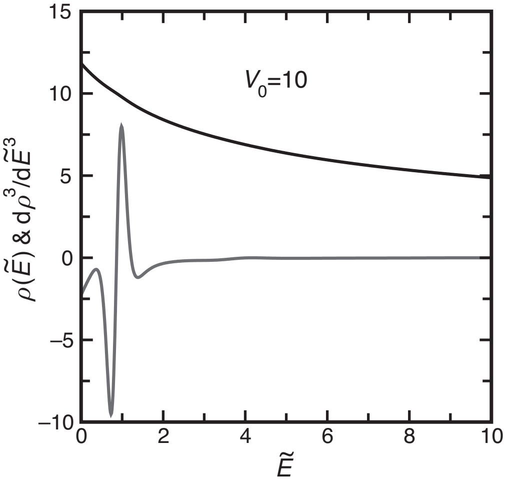

Figure 3.2 Density of states, $\rho(\tilde{E})$, as function of $\tilde{E}$ (given in scaled units defined in Eq. (3.27)) for the model potential in Fig. 3.1 with the potential parameters $L = 1$, $V_0 = 10$. The structure in $\rho(\tilde{E})$ is explored by calculating the high order energy derivatives of $\rho(\tilde{E})$.

One might expect that the resonance phenomenon will become more pronounced in the plot of $\rho(E)$ as the value of V_0 is increased. The idea is simple. The reflection of the quantum particle from the edge of the step in the potential given in Fig. 3.1 increases with V_0. This is due to the fact that in one-dimensional problems the density of states in the continuum is proportional to the inverse of the square root of the kinetic energy of the particle. As V_0 gets larger, the density of states at a fixed energy above the step reduces. Therefore, from the Fermi golden rule formula (Eq. (3.2)) the resonance width will decrease as well since $\Gamma \propto \rho(E)$.

The bound-continuum transition matrix element in Eq. (3.2) also reduces as V_0 is increased due to the fact that the relevant continuum function (that has the same energy as the bound state) oscillates more rapidly. Therefore, as V_0 is increased the resonance width decreases and, as we will show in the next section, *in the limit of $V_0 \to \infty$ a bound state spectrum of a particle in a box is obtained*. About the application of the Fermi golden rule to our model Hamiltonian (i.e., where only shape-type resonances are supported) see Section 3.7.

In Fig. 3.3 we plot the density of states for the case where $V_0 = 100$. Indeed, now the resonance phenomenon is easily observed. Peaks in the density of states $\rho(\tilde{E})$ are obtained at the scaled energies, $\tilde{E} \sim 1, 4, 9$ with widths corresponding to the lifetime of the resonances.

Here we have shown that the resonance phenomenon is associated with high density of states in the continuum of scattering states. It is now important to show

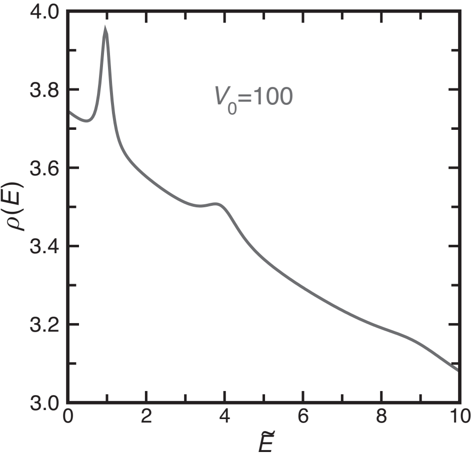

Figure 3.3 Density of states, $\rho(\tilde{E})$, as function of $\tilde{E}$ (given in scaled units defined in Eq. (3.27)) for the model potential given in Fig. 3.1 with the potential parameters $L = 1$, $V_0 = 100$.

that the continuum states which are associated with the resonance phenomenon are localized in the coordinate space within the interaction region (i.e., $x < L$ in our case).

3.4 Resonances from the asymptotes of continuum eigenfunctions

As argued in the previous section, the structure of the scattering continuum states changes in the vicinity of a resonant energy. Around such an energy these states become localized in the relevant region of interaction. For example, in our model case it will be the potential step in the region $0 < x < L$. In this section we wish to show that one can extract the information regarding the position of the resonant energies as well as their corresponding widths from the behavior of the scattering states.

First we normalize the solutions of the time-independent Schrödinger equation by dividing $\psi_E(x)$ as defined in Eq. (3.6) by a factor $\mathcal{N}$ which establishes the degree of localization of the continuum state in the interaction region. This factor is given by

$$\mathcal{N}^2 \equiv \int_0^L |\psi_E(x)|^2 \mathrm{d}x \, . \tag{3.28}$$

By doing this we keep the contribution of the particle in the interaction region constant and we can study the changes in the amplitude of the scattered part. Therefore,

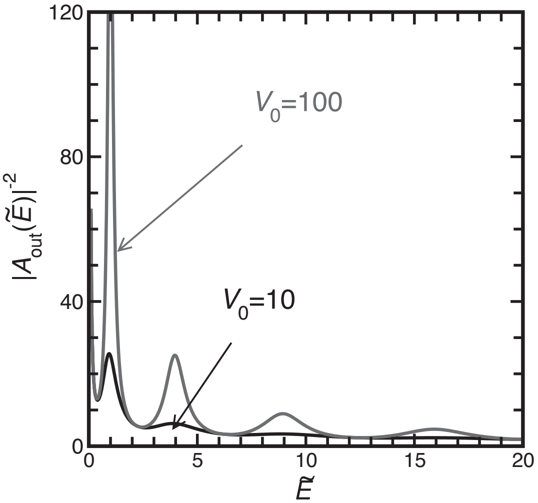

Figure 3.4 The inverse of the "probability" of finding a particle in the "external region" (i.e., out of the interaction region associated with $x < L$), $|A_{\rm out}(\tilde{E})|^2$, as function of the scaled energy $\tilde{E}$, when initially (when the interaction potential is an infinite square potential well) the probability of having the particle in the interaction region (i.e. $0 < x \leq L$ in Fig. 3.1) is unity.

the normalized value of $|A_{\rm out}(E)|^2 = |A(k_E)|^2/\mathcal{N}^2$ provides the maximal probability for a particle which was initially in the interaction region to escape. In Fig. 3.4 we plot the inverse of the re-normalized amplitude outside the interaction region $|\bar{A}_{\rm out}(\tilde{E})|^2$.

As one can see from the results presented in Fig. 3.4, when the scattering amplitude is small there are continuum functions that are localized in the interaction region. The peaks in the spectra are obtained for the scaled energies at $\tilde{E} \sim n^2$, where $n = 1, 2, 3, 4, \ldots$, which are associated with the resonances. In our studied model Hamiltonian the resonances energies are very close to the bound states of a particle-in-a-box problem where the box size is $L = 1$.

Exercise 3.6

Prove that in the limit of $V_0 \to \infty$ the repulsive potential shown in Fig. 3.1 supports a bound state spectrum which is exactly that of a particle in a box of size $L = 1$.

The threshold energy is defined in our case as $E_{\rm th} = -V_0$. In Ex. 3.6 we proved that as $V_0 \to \infty$ the resonances become bound states. That is, the rate of the resonance decay reduces to zero as $V_0 \to \infty$. However, we wish to stress that the effect of the variation of the threshold energy on the resonance rate of decay is problem dependent.

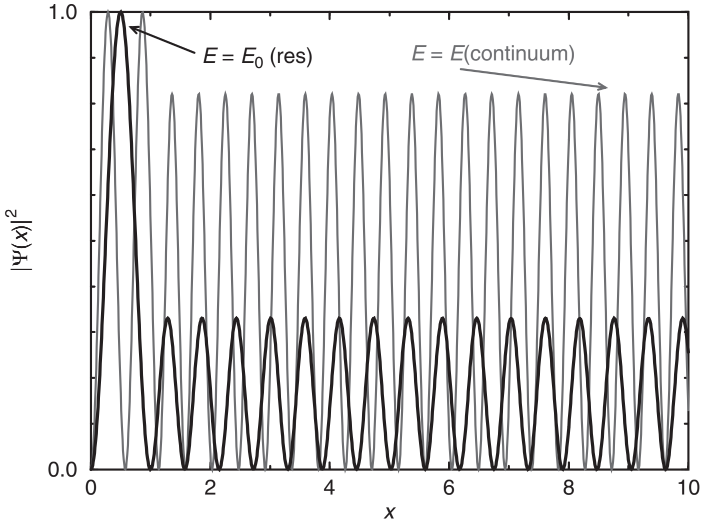

Figure 3.5 $|\Psi_E(x)|^2$ as given in Eq. (3.6) for two different energies: $\tilde{E} = 1$ which is associated with a resonance state and $\tilde{E} = (1 + 2^2)/2$ which is embedded in between two adjacent resonances (see Fig. 3.4). The potential parameters are $L = 1$, $V_0 = 10$, $M = 1$.

Exercise 3.7

Using semiclassical arguments show that the transition through a smooth potential barrier, $V(x)$, which is a slowly varying function of x is not effected by the position of the threshold energy (even when $V(x)$ is described as juxtaposition of rectangular potential barriers). How is this result associated with Gamow's formula for the decay rate through a potential barrier?

In Fig. 3.4 we clearly see that as V_0 is increased the peaks in the spectra become higher and narrower, which implies that the resonances are more localized in the interaction region. This conclusion is supported by the results presented in Fig. 3.5 and Fig. 3.6 where we present the shape of the continuum functions at the scaled energy $\tilde{E} = 1$ (associated with the resonance phenomenon) and at the energy $\tilde{E} = (1^2 + 2^2)/2 = 2.5$ (which is right between two resonant energies) for two different values of V_0. The localization of the continuum states which are associated with the resonance phenomenon can be obtained for any stationary solutions with energy inside the width of the resonance, i.e. any energy in the range $E_{\text{res}} - \Gamma/2 < E < E_{\text{res}} + \Gamma/2$. Therefore, *the resonance phenomenon is associated with a collection of continuum states (i.e., wavepacket) and not with a single stationary solution of the Schrödinger equation.*

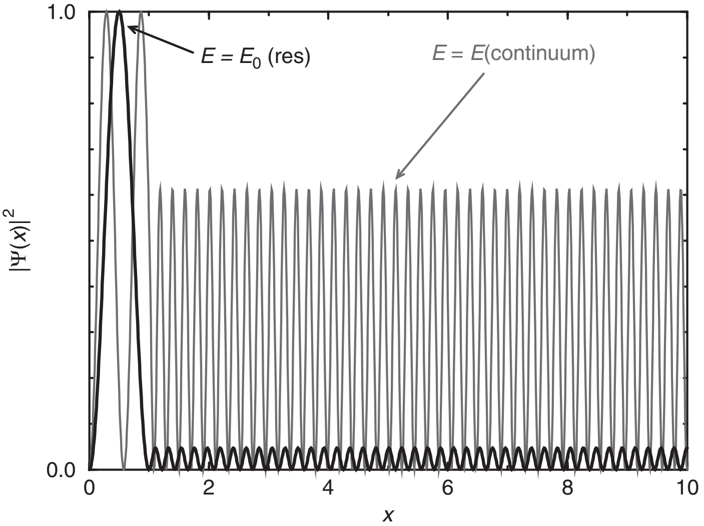

Figure 3.6 $|\Psi_E(x)|^2$ as given in Eq. (3.6) for two different energies: $\tilde{E} = 1$ which is associated with a resonance state and $\tilde{E} = (1 + 2^2)/2$ which is embedded in between two adjacent resonances (see Fig. 3.4). The potential parameters are $L = 1$, $V_0 = 100$, $M = 1$.

The heights of the peaks of $|\Psi(\tilde{E} = 1)|^2$ outside the interaction region (i.e., $x > L$) which are shown in Figs. 3.5 and 3.6 are related to the resonance widths. How can we get the resonance widths from the values of $|A_{\text{out}}(\tilde{E})|^2$? As we will show in Chapter 8, the rate of decay is associated with the energy normalized outgoing waves. Therefore, in the asymptote the outgoing wave defined in Eq. (3.13) should be energy normalized to provide the probability amplitude of the particle to escape,

$$A_{\text{out}}(E) = \gamma(E)\sqrt{\frac{M}{2\pi\hbar^2 q}}\,, \tag{3.29}$$

where q is the wave number of the particle outside the interaction region, as defined in Eq. (3.7).

Exercise 3.8

Derive the flux normalization constant given in Eq. (3.29).

Therefore, the rate of decay from the interaction region is given by

$$\Gamma(E) = |\gamma(E)|^2 = \frac{2\pi\hbar^2 q}{M}|A_{\text{out}}(E)|^2\,. \tag{3.30}$$

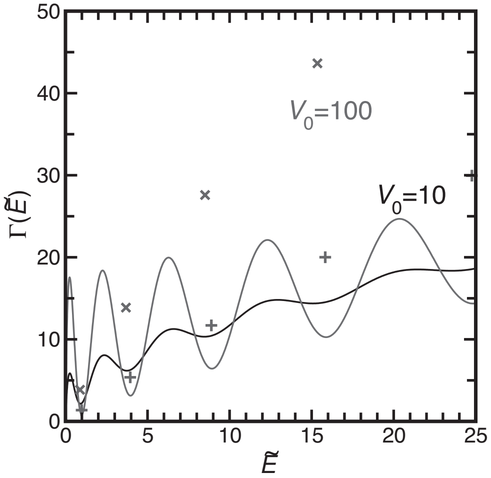

Figure 3.7 The resonance widths associated with the local minima of $\Gamma(\tilde{E}) \equiv |\gamma(\tilde{E})|^2$ as function of the scaled energy $\tilde{E}$ (see Eq. (3.30)). The × and + symbols stand for the resonance energies and widths that were obtained by calculating the poles of the scattering matrix for the two potential parameters $V_0 = 10$, $V_0 = 100$ respectively and are given as reference values.

Only at the energies for which the corresponding continuum states are localized in the interaction region (i.e., $\tilde{E} \equiv E_{\text{res}} \sim n^2$ where $n = 1, 2, \dots$) the resonance width can be defined as

$$\Gamma(E_{\text{res}}) = |\gamma(E = E_{\text{res}})|^2 . \tag{3.31}$$

The reason for this identity is based on a proof which will be given in Chapter 5 where we will discuss the properties of the resonance wavefunctions. See the results presented in Fig. 3.7 where we plotted $\Gamma(E)$ as defined in Eq. (3.30). Let us compare the estimates of the resonance positions (i.e., energies) and widths obtained by the conventional quantum mechanical calculations (presented in Fig. 3.7 and Fig. 3.8) with the resonance energies and widths that are obtained by non-Hermitian quantum mechanical calculation (presented in the next chapter). Such a comparison shows that the correspondence between the Hermitian and the non-Hermitian results for the resonance positions and widths is obtained when V_0 reaches a sufficiently large value and the resonance width is sufficiently narrow.

3.5 Resonances from the phase shifts

In Eq. (3.12) we show the relationship between the phase shift and the scattering matrix elements. The scattering matrix as mentioned above provides the ratio between the incoming and outgoing waves. The S-matrix is a unitary matrix,

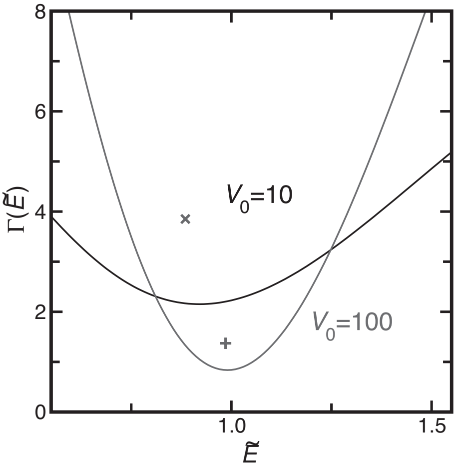

Figure 3.8 A zoom in on the first resonance in Fig. 3.7.

$S(E) = \mathrm{e}^{\mathrm{i}\delta(E)}$, and can be written as

$$S(E) = \frac{E - E_c^*}{E - E_c} = \mathrm{e}^{2\mathrm{i}\delta}\,, \tag{3.32}$$

where

$$E_c = E_r - \frac{\mathrm{i}}{2}\Gamma \tag{3.33}$$

is a complex pole of the S-matrix. Here we assume that the poles are isolated. As we will see later, this approximation holds only when the poles are embedded in the complex "energy" plane sufficiently close to the real axis. These poles are associated in time-independent scattering theory with the resonance positions and widths, as will be discussed later. *In non-Hermitian quantum mechanics the properties of the complex poles can be analyzed and studied as the complex eigenvalues of the Hamiltonian*. From a comparison between Eqs. (3.32)–(3.33) and Eq. (3.12) one gets that

$$\tan 2\delta(E) = \frac{-(E - E_r)\Gamma}{(E - E_r)^2 - \frac{\Gamma^2}{4}}\,. \tag{3.34}$$

As one can see from Eq. (3.34), $\delta(E)$ changes by π as E crosses the value of E_r. The analytical form of the phase shift for our studied case is given in Eq. (3.11). Indeed, the plot of the phase shift as function of E presented in Fig. 3.9 clearly shows a change of the phase shift by π as E passes through the resonant energies $\tilde{E} \sim n^2$; $n = 1, 2, \ldots$ Here the change is rather slow due to the broadness of the resonances; however, when the resonances are narrow this changes is abrupt. The

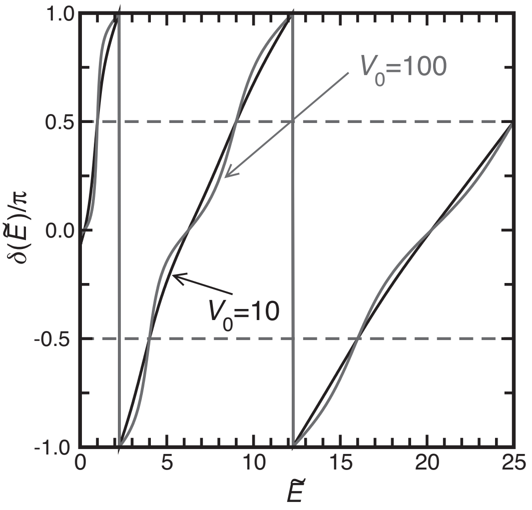

Figure 3.9 The phase shift, $\delta(\tilde{E})$, for the model potential presented in Fig. 3.1 for $V_0 = 10$ and $V_0 = 100$. The resonance positions/energies are obtained when the phase shift changes by π (denoted by crossings with the dashed lines in the plot).

sudden change of the phase shift by π seems to be a sensitive computational procedure for calculating the resonance positions.

The resonance widths can also be evaluated from the energy-dependent phase shift. Using Eq. (3.34) we readily get that

$$\frac{\mathrm{d}E}{\mathrm{d}\delta} = \frac{4(E - E_\mathrm{r})^2 + \Gamma^2}{2\Gamma} . \tag{3.35}$$

Therefore, the resonance width is given by

$$\Gamma = 2\frac{\mathrm{d}E}{\mathrm{d}\delta}|_{E=E_\mathrm{r}} , \tag{3.36}$$

which occurs at the local minima of $\mathrm{d}E/\mathrm{d}\delta$. Since in our case we derived an analytical expression for the phase shift which is given in Eq. (3.11) it is straightforward to derive the analytical expression for the derivative of the phase shift with respect to the energy for our studied model Hamiltonian and get that

$$\frac{\mathrm{d}E}{\mathrm{d}\delta} = \frac{\hbar^4 kq}{M}\left[\frac{q^2\sin^2(kL) + k^2\cos^2(kL)}{\hbar^2 kq^2 L - MV_0\sin(2kL)}\right] , \tag{3.37}$$

where k and q are defined in Eq. (3.6). The local minima in the plot of $2\mathrm{d}E/\mathrm{d}\delta$ as a function of $\tilde{E}$ presented in Fig. 3.10 provide quite accurate values for the resonance positions and widths for our studied case *only* when the resonances are sufficiently narrow (i.e., a small value of Γ). Note also that these results are quite similar to

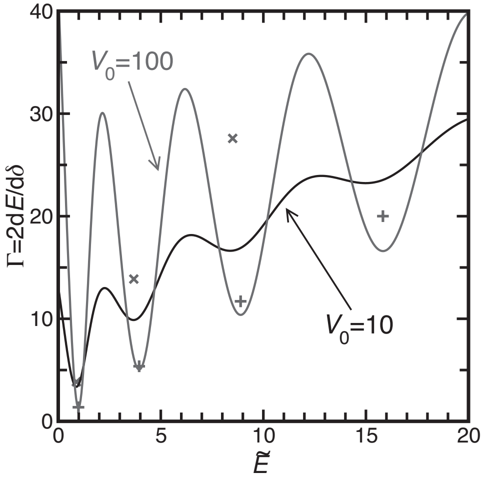

Figure 3.10 The resonance widths for the model potential presented in Fig. 3.1 when $M = 1$, $L = 1$ and $V_0 = 100$ as obtained from the calculations of the energy derivative of the phase shift. The × and + symbols stand for the values obtained from non-Hermitian quantum mechanical calculations for the complex poles of the scattering matrix, $S(E)$, for the two potential parameters $V_0 = 10$ and $V_0 = 100$ respectively.

those presented in Fig. 3.7 due to the behavior of the denominator in Eq. (3.37). In Hermitian quantum-mechanical calculations the resonance is not uniquely defined as in non-Hermitian quantum mechanics and this is the source of the deviation between the Hermitian and non-Hermitian results. Thus such a calculation will provide meaningful values only for isolated narrow resonances.

3.6 The scattering length

When a three-dimensional Hamiltonian has a spherical symmetry the problem can be reduced to the solution of the radial Schrödinger equation for every angular momentum quantum number, l.

$$\left[-\frac{\hbar^2}{2M}\frac{1}{r^2}\frac{\partial}{\partial r}\left(r^2\frac{\partial}{\partial r}\right)+V(r)+\frac{\hbar^2 l(l+1)}{2Mr^2}\right]\Psi(r)=E\Psi(r)\,. \tag{3.38}$$

By substituting $\Psi(r) = \chi(r)/r$ into Eq. (3.38) one gets an equation with a kinetic operator in the form of a one-dimensional Schrödinger equation such that

$$\left[-\frac{\hbar^2}{2M}\frac{\partial^2}{\partial r^2}+V(r)+\frac{\hbar^2 l(l+1)}{2Mr^2}\right]\chi(r)=E\chi(r)\,. \tag{3.39}$$

Let us consider incoming particles along the x-axis with momentum $\hbar k$ which are scattered from a target with a radial interaction potential. The wavefunction for large values of r can be written as

$$\Psi = \mathrm{e}^{-\mathrm{i}kx} + f_k(\theta)\frac{\mathrm{e}^{+\mathrm{i}kr}}{r}\,, \tag{3.40}$$

where $f_k(\theta)$ is the scattering amplitude. Since we considered here a spherically symmetric potential, the amplitude $f_k(\theta)$ depends on the direction only through the scattering angle θ, which is the angle between the directions of the incoming and the outgoing beams of particles. Since the amplitudes of the outgoing and incoming waves are the same, the only effect of the scattering potential is to shift the phase of the outgoing asymptotic wave by an amount we denote by δ_l where each term is the partial wave (the $l = 0$ wave is termed an s-waves, $l = 1$ a p-wave, etc.). In our case study problem the angular momentum is zero and only the s-wave scattering is considered. This assumption holds also in more general cases at very low energies. In the limit of $k \to 0$ the scattering amplitude approaches a constant a_0 and Eq. (3.40) becomes

$$\Psi(k \to 0) = 1 + \frac{a_0}{r}\,. \tag{3.41}$$

From Eq. (3.41) one gets that the probability of observing the scattered particles at the target in a slow particle scattering experiment is given by $4\pi a_0^2$ (in order to calculate the probability we multiply $\lim_{k\to 0}|f_k(\theta)|^2$ by $4\pi r^2$). Therefore a_0 can be interpenetrated as the effective impact parameter or the effective range of interaction. Indeed, by applying the method of partial waves the total cross section (i.e. the total number of particles scattered per second) is given by

$$\sigma = 4\pi a_0^2\,. \tag{3.42}$$

From this it is clear why the effective range of interaction a_0 is termed the *scattering length*. This concept is commonly applied to different types of scattering experiment. For example, it plays a key role in the study of Bose–Einstein condensates (BEC) and in the derivation of the mean field theory for BEC (known as the Gross–Pitaevskii non-linear Schrödinger equation).

From Eq. (3.42) one gets that for s-waves experiments ($l = 0$)

$$a_0 = -\lim_{k\to 0}\frac{\tan\delta_0(k)}{k}\,. \tag{3.43}$$

In our illustrative model Hamiltonian we considered only the s-waves and therefore the phase shift δ_0 is defined by δ_{out} (see Eq. (3.15) and Eq. (3.11)) and k in Eq. (3.43) should be replaced by q, where q and k are as defined in Eq. (3.7). Since $\tan\delta_{\mathrm{out}} \to 0$ as $q \to 0$, we get from Eq. (3.43) that the scattering length is associated with the energy derivative of the phase shift,

$$a_0 = -\lim_{E\to 0} \frac{\hbar^2 k}{M\cos^2\delta_0}\frac{\mathrm{d}\delta_0}{\mathrm{d}E}\,, \tag{3.44}$$

where $2\mathrm{d}\delta/\mathrm{d}E$ at $E = E_\mathrm{r}$ is the resonance width Γ. See, for example, in Eq. (3.37) the analytical expression, $2\mathrm{d}\delta/\mathrm{d}E$, for our model problem. In the off-resonance condition where the phase shift tends to zero or an integer multiple of π, the scattering length attains a constant finite value. However, when the resonance position is at the threshold energy $E = 0$ the phase shift is equal to an odd multiple of $\pi/2$ and then $\tan(\delta_\mathrm{out})$ is infinite and so is the value of the scattering length. In our model problem there are no transitions from bound to resonance states as V_0 is varied. Thus, we modify our model Hamiltonian from a square barrier potential to an open square well potential. The potential is then equal to $-V_0$ when $0 < x \leq L$ and equal to 0 when $x > L$. In this case, as will be discussed in the next chapter, the number of bound states depends on the depth of the potential well, V_0, and by reducing the value of V_0 bound to resonance transitions occur. These transitions are reflected in calculations of the scattering length as a function of V_0.

Exercise 3.9

Derive the scattering length of particles scattered from attractive/repulsive potential well/barrier of depth/height V_0 and range L, representing the force between the projectile and the target.

The dependence of the scattering length on the depth of the well for a open square well potential ($L = 1$) is presented in Fig. 3.11. From Fig. 3.11 one can see that the scattering length exhibits a transition from $+\infty$ to $-\infty$ as a bound state turns into a resonance upon changing the potential parameter V_0. The number of bound states in the potential well increases as the scattering length changes in sign from $+\infty$ to $-\infty$. $a_0 = +\infty$ implies that the effective impact parameter is ∞ and the scattering length is repulsive. *At this specific value of V_0 where the scattering force is $+\infty$ the resonance position is at $E = 0$.* The value of $a_0 = -\infty$ implies that the particle is trapped by the short range potential. *At the value of V_0 where the scattering length is $-\infty$ a new bound state with energy $E = 0$ is born.* In between these two values of V_0 one can observe a transition from a resonance to a bound state. *As will be shown in the next chapter, this transition can be quite complicated and can be analyzed only within the framework of non-Hermitian quantum mechanics.*

This phenomenon of transition from a resonance state to a bound state occurs also when the resonances are Feshbach-type. Let us consider a situation where a bound state of a singlet electronic potential curve ${}^1V(R)$ (where R represents the

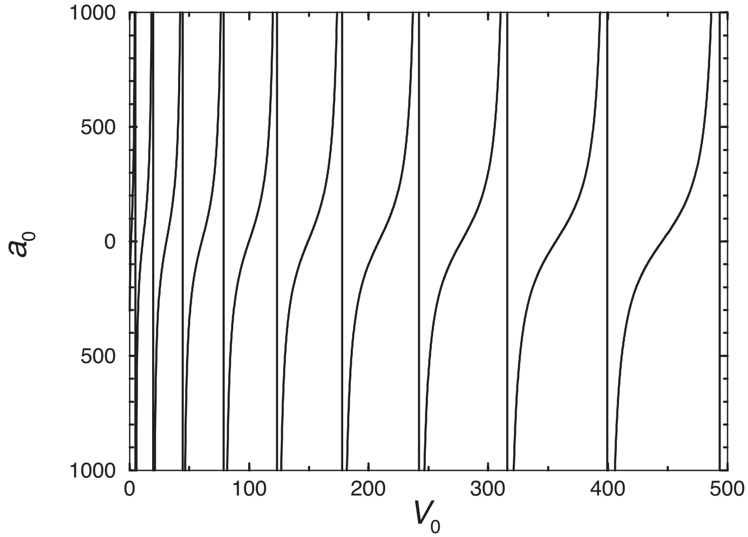

Figure 3.11 The scattering length for particles scattered from an attractive square-well potential. The depth of the potential well is V_0 and the range is $L = 1$.

nuclear coordinates, for instance the intranuclear distance in a diatomic molecule) is embedded in the continuum of the triplet electronic potential curve ${}^3V(R)$. By introducing a magnetic field the coupling between the singlet bound state and the triplet continuum states is turned on and the bound state becomes a resonance state. The resonance position and widths depend on the strength of the magnetic field. For a particular magnetic field $B = B_0$ the resonance position will be at the threshold energy $E = 0$. Therefore, by varying the strength of the magnetic field to cross this resonance/bound state transition the scattering length can be changed from being repulsive to an attractive one.

3.7 Resonances from stabilization calculations

One convenient method to reveal the energies of the resonant states in Hermitian computations is to perform a stabilization calculation. This method relies on the high density of states in the continuum around the resonance energy. The procedure is rather simple; the variational energy levels of a given Hamiltonian are calculated depending on given parameter λ in the basis set. When this parameter is varied continuously the energy levels will change but will be stable around the resonance energies. In terms of the variational energies, $E_j(\lambda)$, obtained as a function of the parameter λ, this phenomenon is manifested by avoided crossings between adjacent variational solutions $E_j(\lambda)$ and $E_{j+1}(\lambda)$.

The continuum spectrum can be discretized by using a box quantization condition for calculating the energy spectra. This is achieved by confining the problem inside a box of length L_{box} and requiring that the solutions of the time-independent Schrödinger equation vanish at the edges such that $\psi_E(x = L_{\text{box}}) = 0$. The variation of L_{box} will affect the discrete quasi-continuum energy spectra of our studied Hamiltonian by lowering the discrete energies as L_{box} is increased.

As discussed above and shown in Figs. 3.5 and 3.6, the stationary continuum solutions of the time-independent Schrödinger equation which are associated with the resonance phenomenon are localized in the interaction region. The interaction region is determined by the shape of the potential. It is expected that as the continuum functions are more localized in the coordinate space then they will be less affected by the variation of L_{box} and thus the resonance state will be narrower (i.e., smaller values of Γ). On the other hand, the delocalized non-resonant continuum functions (see Figs. 3.5 and 3.6) should be strongly affected by the change in L_{box} due to the large amplitude oscillatory behavior. Consequently, we expect to observe energy level crossings in the quasi-continuum as we plot the energies as function of L_{box}. However, since it is unlikely that levels with the same symmetry will cross, avoided crossings rather than crossings are obtained. These avoided crossings in the so-called stabilization plots are associated with the resonance phenomenon. The energies at which the avoided crossings occur provide the approximate values for the resonance position in the continuum. See, for example, the stabilization plot for our studied case presented in Fig. 3.12.

Exercise 3.10

Calculate the stabilization plot for our model potential for different values of the potential parameters V_0 and L and for different values of the mass M by using the variational principle with $\sqrt{2/L_{\text{box}}}\sin(n\pi x/L_{\text{box}})$, $n = 1, 2, \ldots, N$ as a basis set. The Hamiltonian matrix elements were derived in Ex. 3.4.

The results presented in Fig. 3.12 clearly show many avoided crossings at $\tilde{E} \approx 1$, which is the position/energy of the narrowest (i.e., longest lived) resonance state for this problem. For a sufficiently large basis set (assuming the basis set is close to completeness for any selected value of L_{box}) the deviation in the energy values at which these avoided crossings occur is an indication of the lifetime of the associated resonance state. As the lifetime is longer (Γ is smaller) the deviation in the energy positions of the avoided crossings is smaller. As a matter of fact, for sufficiently long lived resonances the resonance position is accurately obtained from the stable plateau energy curves which appear in between two adjacent avoided crossings. In our studied case the resonances are quite broad (i.e., Γ has large values in

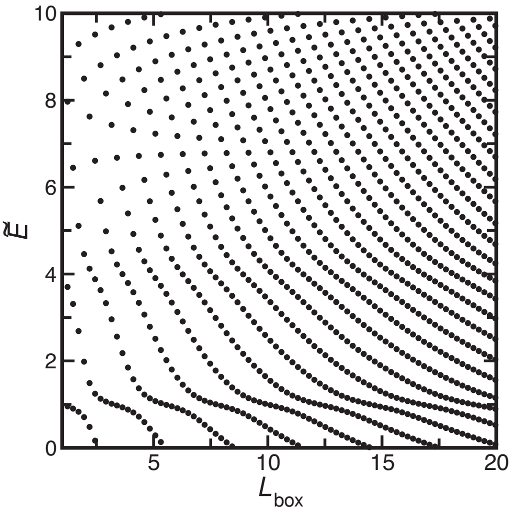

Figure 3.12 Stabilization plot for the model potential presented in Fig. 3.1 when $M = 1$, $L = 1$ and $V_0 = 100$. The energy spectrum is discrete due to the use of the box-quantization condition where $\psi_E(x = L_{\text{box}}) = 0$.

comparison to the difference in the positions of two adjacent resonances) and therefore one can only see in the results presented in Fig. 3.12 the fingerprints of the resonance state at $\tilde{E} \approx 4$. It is quite impossible to observe by this method the presence of resonances for the case where $V_0 = 10$.

We will now show that from a stabilization plot one can get a good estimate for the width of relatively narrow resonances such as the low-lying resonance ($\tilde{E} \approx 1$) in Fig. 3.12. As described above, the avoided crossings are associated with the interaction of a bound state which is embedded in the continuum (and almost unaffected by the variation of the box size) with a continuum state with the same energy (which is very strongly affected by the value of the box size). From this it is quite clear how to identify the "quasi-bound" and the "quasi-continuum" states before or after the avoided crossing region. The "quasi-bound state" energy is hardly affected by the variation of L_{box} whereas the the energy of the "quasi-continuum state" is strongly affected. How can they be defined in the avoided crossing region? In the case of Feshbach resonances it is easy to define the H_0 Hamiltonian of the bound state which is embedded in the continuum. In the case of shape-type resonances there is not a simple way to define H_0. However, since the stabilization plots obtained for Hamiltonians that support Feshbach resonances are very similar in their nature to the stabilization plots for Hamiltonians which support shape-type resonances, we assume here that by taking the linear combinations of the two stationary solutions, $\Psi_{E_1}(x)$, $\Psi_{E_2}(x)$, which converge to the avoided crossing we can select a proper relative phase to yield an approximate bound state $\psi_{\mathrm{b}}(E_{\mathrm{r}})$,

$$\psi_{\mathrm{b}}(E_{\mathrm{r}}) = [\Psi_{E_1}(x) + \mathrm{e}^{\mathrm{i}\alpha}\Psi_{E_2}(x)]/\sqrt{2}\,. \tag{3.45}$$

This state is embedded in the continuum and interacts with a state in a continuum:

$$\psi_{\mathrm{c}}(E_{\mathrm{r}}) = [\Psi_{E_1}(x) - \mathrm{e}^{\mathrm{i}\alpha}\Psi_{E_2}(x)]/\sqrt{2}\,, \tag{3.46}$$

where

$$E_{\mathrm{r}} = (E_1 + E_2)/2 \tag{3.47}$$

is the estimate of the resonance position which is taken as E_{b} in Eq. (3.2). Let us assume that ψ_{b} and ψ_{c} are two degenerate eigenstates of $\hat{H}_0 = E_{\mathrm{b}}|\psi_{\mathrm{b}}\rangle\langle\psi_{\mathrm{b}}| + E_{\mathrm{b}}|\psi_{\mathrm{c}}\rangle\langle\psi_{\mathrm{c}}|$, and thus are orthognal, i.e. $\langle\psi_{\mathrm{b}}|\psi_{\mathrm{c}}\rangle = 0$. (In the case where the Hamiltonian supports only shape-type resonances H_0 is somewhat abstract.) Therefore, the potential that couples the bound state with the continuum is $\hat{V} = \hat{H} - \hat{H}_0$. By substituting Eqs. (3.45) and (3.46) in Eq. (3.2) one gets

$$|\langle\psi_{\mathrm{b}}(E_{\mathrm{b}})|\hat{V}|\psi_{\mathrm{c}}(E_{\mathrm{b}})\rangle|^2 = |\langle\psi_{\mathrm{b}}(E_{\mathrm{b}})|\hat{H}|\psi_{\mathrm{c}}(E_{\mathrm{b}})\rangle|^2|E_1 - E_2|^2/4 \equiv (\Delta E)^2/4\,. \tag{3.48}$$

As shown in Ex. 3.2, in the Fermi golden rule expression the continuum is a "white continuum" that does not contain any information regarding the resonances. Therefore, we associated the "white continuum" with the quasi-continuum energy levels, $E = [\hbar^2\pi^2/(2ML_{\mathrm{box}})^2)]n^2$. Therefore, the density of states in this "white continuum" is given by

$$\rho_{\mathrm{c}}(E) = \frac{\mathrm{d}n}{\mathrm{d}E} = \frac{\sqrt{M}}{\sqrt{2}\pi\hbar}\frac{L_{\mathrm{box}}}{\sqrt{E}}\,. \tag{3.49}$$

Using the Fermi golden rule we get that the estimate for the resonance width from stabilization plots for our model problem can be taken as

$$\Gamma = 2\pi\rho_{\mathrm{c}}(E_{\mathrm{b}})|\langle\psi_{\mathrm{b}}(E_{\mathrm{b}})|\hat{V}|\psi_{\mathrm{c}}(E_{\mathrm{b}})\rangle|^2 = L_{\mathrm{box}}\frac{(\Delta E)^2}{2\hbar}\sqrt{\frac{M}{2(E_{\mathrm{r}} + V_0)}}\,, \tag{3.50}$$

where $E_{\mathrm{r}} + V_0$ is the energy of the "white continuum" state, $\psi_{\mathrm{c}}(E_{\mathrm{b}})$ which interacts with the bound state, $\psi_{\mathrm{b}}(E_{\mathrm{b}})$. For $V_0 = 100$ we get (see Fig. 3.12) that at $L_{\mathrm{box}} = 7$ the energy splitting is given by $\Delta E \approx 0.5\pi^2/2$ and $E_{\mathrm{r}} \approx \pi^2/2$. Using Eq. (3.50) one gets that the estimate for the resonance width for this state is $\Gamma \approx 1.47$. This result is in remarkable agreement with the values of $\Gamma = 1.37$ obtained from non-Hermitian quantum mechanical calculations and also agrees with the result obtained in Fig. 3.8.

3.8 Decay of resonance states

The different approaches applied in the previous sections show that for our model problem the resonance positions are approximately at $\tilde{E}_n \approx n^2$ where $n = 1, 2, 3 \ldots$. The stationary continuum solutions at these energies are localized in the interaction region of the potential. The resonance widths can be estimated from the stationary solutions of the time-dependent Schrödinger equation. However, for stationary solutions we cannot demonstrate the nature of the exponential decay of the resonance state. The resonance phenomenon should be associated in Hermitian quantum mechanics with a wavepacket which evolves in time rather than a stationary state which only changes its phase. A simple way to create a wavepacket which is centered at E_n is by integrating over the continuum functions in an energy range around the resonant energy:

$$\Psi_{E_n}^{\mathrm{WP}}(x, t) = \frac{1}{2\Delta E} \int_{E_n - \Delta E}^{E_n + \Delta E} \mathrm{d}E \, \Psi_E(x) \mathrm{e}^{-\mathrm{i}Et/\hbar} \, , \tag{3.51}$$

where $\Psi_E(x)$ is an eigenfunction of the time-independent Schrödinger equation (Eq. (3.6) for our studied case). Let ΔE be so small that the energy dependence of the amplitudes of the incoming and the outgoing waves associated with $\Psi_E(x)$ (for the model problem this applies to the coefficients $A(E)$ and $B(E)$ defined in Eqs. (3.9) and (3.10)) can be ignored and the wave vector $k = \sqrt{2ME}/\hbar$ (see Eq. (3.7)) can be approximated by the following expression:

$$k = k_n + (E - E_n) \frac{\mathrm{d}k}{\mathrm{d}E}|_{E_n} + \cdots \simeq k_n + \frac{E - E_n}{\hbar v_n} \, , \tag{3.52}$$

where $\hbar k_n$ is associated with the momentum of the quantum particle.

Exercise 3.11

Show that within the approximation given in Eq. (3.52) the WP portrayed in Eq. (3.51) moving in a constant potential travels at a velocity $v_n = \hbar k_n / M$, i.e. the maximum of $|\Psi_{E_n}^{\mathrm{WP}}(x, t)|^2$ moves as $x_{\max} = v_n t$.

For the model problem the velocity of the quantum particle in the interaction region is given by

$$v_n = \frac{\hbar k_n}{M} \, , \tag{3.53}$$

whereas the velocity in the "external region" (i.e., $x > L$) is

$$v_n^{\mathrm{out}} = \frac{\hbar q_n}{M} \tag{3.54}$$

and the corresponding wave vectors are given by $k_n = \sqrt{2ME_n}/\hbar$, $q_n = \sqrt{2M(E_n + V_0)}/\hbar$.

By using this expansion and by substituting Eqs. (3.6)–(3.13) into Eq. (3.51) one gets the time dependence of the wavepacket,

$$\Psi_{\mathrm{WP}}(x,t) = \Psi_{\mathrm{in}}^{\mathrm{WP}}(x,t) + \Psi_{\mathrm{out}}^{\mathrm{WP}}(x,t)\,, \tag{3.55}$$

where

$$\begin{aligned}\Psi_{\mathrm{in}}^{\mathrm{WP}}(x \le L, t) = {} & \frac{\mathrm{i}}{2}\frac{\sin[(x + v_n t)\Delta_{\mathrm{in}}]}{(x + v_n t)\Delta_{\mathrm{in}}}\mathrm{e}^{-\mathrm{i}k_n x - \mathrm{i}E_n t/\hbar} \\ & - \frac{\mathrm{i}}{2}\frac{\sin[(x - v_n t)\Delta_{\mathrm{in}}]}{(x - v_n t)\Delta_{\mathrm{in}}}\mathrm{e}^{+\mathrm{i}k_n x - \mathrm{i}E_n t/\hbar}\,,\end{aligned} \tag{3.56}$$

where $\Delta_{\mathrm{in}} = \Delta E/(\hbar v_n)$ and similarly,

$$\begin{aligned}\Psi_{\mathrm{out}}^{\mathrm{WP}}(x > L, t) = {} & B(E_n)\frac{\sin[(x - L - v_n^{out} t)\Delta_{\mathrm{out}}]}{(x - L - v_n^{\mathrm{out}} t)\Delta_{\mathrm{out}}}\mathrm{e}^{+\mathrm{i}q_n(x-L) - \mathrm{i}E_n t/\hbar} \\ & + A(E_n)\frac{\sin[(x - L + v_n^{\mathrm{out}} t)\Delta_{\mathrm{out}}]}{(x - L + v_n^{\mathrm{out}} t)\Delta_{\mathrm{out}}}\mathrm{e}^{-\mathrm{i}q_n(x-L) - \mathrm{i}E_n t/\hbar)}\,,\end{aligned} \tag{3.57}$$

where $\Delta_{\mathrm{out}} = \Delta E/(\hbar v_n^{\mathrm{out}})$. Note that the wavepacket is square integrable due to its $\mathrm{sinc}(\alpha x)$ profile.

When E_n is a resonant energy the wavepacket $\Psi_{E_n}^{\mathrm{WP}}(x,t)$ defined in Eq. (3.51) is initially localized inside the interaction region. In order to show this we can examine what happens when we construct wavepackets according to Eq. (3.51) around any given energy in the continuum and not only for those around $E = E_n$ which are associated with the resonance phenomenon. In other words we can study a generalized form of Eq. (3.51),

$$\Psi_E^{\mathrm{WP}}(x,t) = \frac{1}{2\Delta E}\int_{E-\Delta E}^{E+\Delta E} \mathrm{d}E'\,\Psi_{E'}(x)\mathrm{e}^{-\mathrm{i}E't/\hbar}\,. \tag{3.58}$$

In order to determine which WP is a resonance state we define a localization parameter, $LP(t,E)$, by the ratio between the part of the wavepacket localized inside the interaction region and the total probability.

$$LP(t,E) = \frac{\rho_{\mathrm{in}}(t,E)}{\rho_{\mathrm{in}}(t,E) + \rho_{\mathrm{out}}(t,E)}\,, \tag{3.59}$$

where the interaction region is bounded by in the region $|x| < L$ such that

$$\rho_{\mathrm{in}}(t,E) = \int_0^L |\Psi_E^{\mathrm{WP}}(x,t)|^2 \mathrm{d}x \tag{3.60}$$

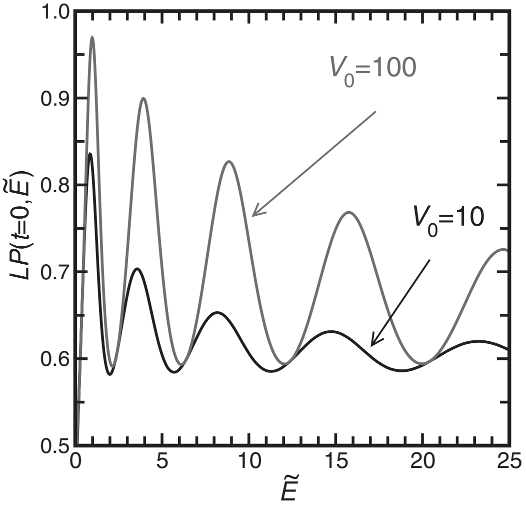

Figure 3.13 The localization parameter in Eq. (3.59) at $t = 0$ as a function of the energy in the continuum constructed according to Eqs. (3.58)–(3.61).

and

$$\rho_{\text{out}}(t, E) = \int_L^\infty |\Psi_E^{\text{WP}}(x, t)|^2 \text{d}x \, . \tag{3.61}$$

For our model problem the localization parameter LP attains local maximal values at the resonance energies, $\tilde{E} \approx n^2$. The energy dependence of the localization parameter at $t = 0$, $LP(t = 0, E)$, presented in Fig. 3.13, clearly provides the resonance positions. This plot, however, does not yield new information since we have already demonstrated that the continuum solutions at the resonance energies are localized at the interaction region.

The evolution of the wavepacket $\Psi_{E_n}^{\text{WP}}$ in time is portrayed in Fig. 3.14 where the initial wavepacket and its evolution at $t = 5/v$ are shown. Here $v = \hbar\sqrt{2M(E + V_0)}/M$ is the velocity of the particle outside the interaction region. It is evident that the wavepacket which was initially localized in the interaction region gradually leaks out, leaving behind a small fraction in the interaction region which diminishes as time passes.

The exponential decay of the wavepacket $\Psi_E^{\text{WP}}(x, t)$ at the interaction region can be observed only after sufficiently long time of propagation. This decay is manifested in the decay of the localization parameter $LP(E_n, t)$ in time. In Fig. 3.14 we can see the evolution of $LP(\tilde{E}_1, t)$ for two different values of the potential parameter V_0.

This is the new information we get from Hermitian quantum mechanics calculations. See the results presented in Fig. 3.15, where the time dependence of

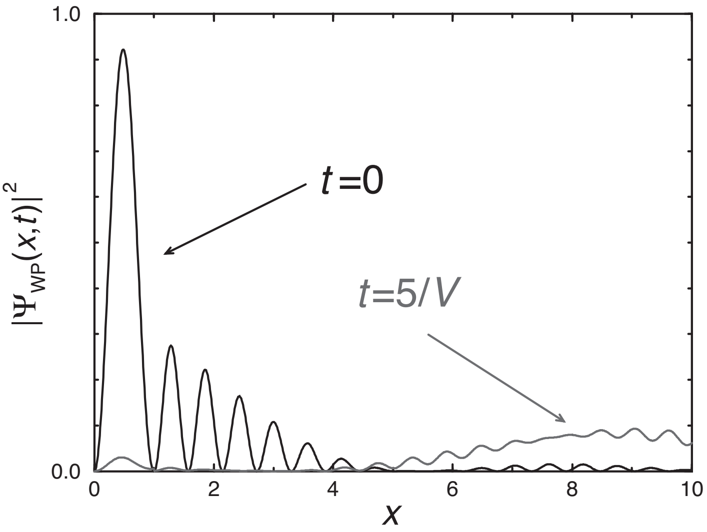

Figure 3.14 $|\Psi_E(x)|^2$ for the intial ($t = 0$) and the propagated wavepacket at $t = 5/v$, where $v = \hbar k/M$. This wavepacket was constructed from the stationary continuum states around $\tilde{E} \approx 1$ for the studied model Hamiltonian with $V_0 = 10$.

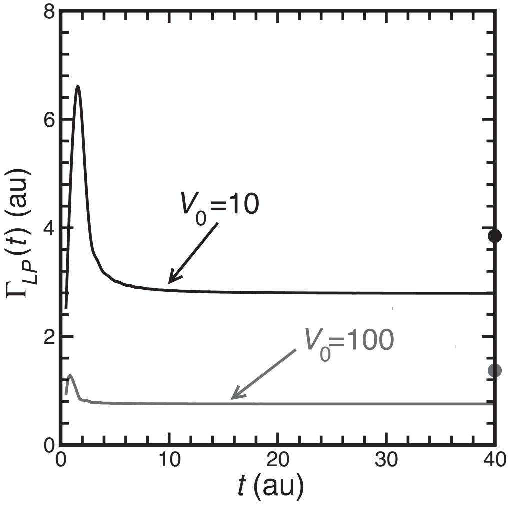

Figure 3.15 The decay rate of the wavepacket constructed from continuum states around $\tilde{E} \approx 1$. The results are shown after smoothing the oscillations induced by the approximations used in the evaluation of the analytical expression for the time-dependent wavepacket. The results are given for two potential parameters, $V_0 = 10$ and $V_0 = 100$, $\Gamma_{LP}(t, \tilde{E} = 1)$. After a sufficiently long period of time the exponential decay of $\Gamma(t)$ is exposed and is found to be in a qualitative agreement with the exact values of the resonance widths obtained from the non-Hermitian quantum mechanical calculations (marked by circles).

the localization parameter associated with a continuum function which is initially localized in the interaction energy is plotted. As time passes the exponential nature of the decay is exposed. Assuming ρ_{in} for a resonance decays exponentially we get that also the localization parameter decays exponentially, and thus

$$\ln[LP(t)] = \ln[LP(0)] - \frac{\Gamma_{LP}(t)}{\hbar}t\,. \tag{3.62}$$

Consequently, at long times where LP is linear on a logarithmic scale the decay is exponential. The decay rates for $V_0 = 10$ and $V_0 = 100$ presented in Fig. 3.15 at $t =$ "∞" where Γ_{LP} is constant are in a qualitative agreement with the accurate resonance widths obtained from non-Hermitian quantum mechanical calculations. As shown in Ex. 3.6, as $V_0 \to \infty$ the resonance widths for the step-like potential vanish. Therefore, the difference between the estimated value of the resonance width obtained within the standard (Hermitian) formalism of quantum mechanics and the exact value obtained by using the non-Hermitian formalism becomes smaller as V_0 is increased. The results presented in Fig. 3.15 support this claim.

We shall now follow the derivation of the exponential decay of a resonance state given in some text books on scattering theory (*Scattering Theory* by J. R. Taylor for example). Near an isolated resonance the energy-normalized stationary continuum wavefunctions are given by

$$\begin{aligned}\psi_{\text{c}}(x,t) &= (\mathrm{e}^{-\mathrm{i}kx} + S\mathrm{e}^{+\mathrm{i}kx})\mathrm{e}^{-\mathrm{i}Et/\hbar} \\ &= 2\cos(kx)\mathrm{e}^{-\mathrm{i}Et/\hbar} + \mathrm{i}\frac{\Gamma}{E - E_{\text{r}} + \frac{\mathrm{i}}{2}\Gamma}\mathrm{e}^{+\mathrm{i}kx-\mathrm{i}Et/\hbar}\,.\end{aligned} \tag{3.63}$$

Here, E_{r} and Γ are the resonance position and width of the complex "energy" associated with the complex pole of the S-matrix, as discussed above. Note that although we associate the resonance phenomenon with the complex poles we are still within the framework of conventional Hermitian quantum mechanics.

In Eq. (3.63) two terms appear. The first one describes a standing wave and the second describes an outgoing wave associated with a simple single pole of the S-matrix. Let us assume that the initial wavepacket, $\Phi(E)$, is initially prepared such that it peaks at the resonance energy, $E = E_{\text{r}}$, associated with the wave vector, $k = k_{\text{r}} \equiv \sqrt{2ME_{\text{r}}}/\hbar$. Hence, the scattering wavepacket which is associated with the second term in Eq. (3.63) is given by

$$\Psi_{\text{sc}}(x,t) = \mathrm{i}\Gamma\int_0^\infty \mathrm{d}E\frac{\Phi(E)}{E - E_{\text{r}} + \frac{\mathrm{i}}{2}\Gamma}\mathrm{e}^{+\mathrm{i}kx-\mathrm{i}Et/\hbar}\,. \tag{3.64}$$

Using the expansion for the wave vector given in Eq. (3.52) (while replacing E_n, k_n and v_n in that equation by E_r, k_r and $v_\mathrm{r} = \hbar k_\mathrm{r}/M$ correspondingly) one gets,

$$\Psi_\mathrm{sc}(x,t) \approx \mathrm{i}\mathrm{e}^{+\mathrm{i}k_\mathrm{r}x - \mathrm{i}E_\mathrm{r}t/\hbar}\Gamma\Phi(E_\mathrm{r})\int_0^\infty \mathrm{d}E\,\frac{\mathrm{e}^{-\mathrm{i}(E-E_\mathrm{r})(t-\frac{x}{v_\mathrm{r}})/\hbar}}{E - E_\mathrm{r} + \frac{\mathrm{i}}{2}\Gamma}\,. \tag{3.65}$$

Here we assumed that

$$|E - E_\mathrm{r}| \gg \Gamma \tag{3.66}$$

and

$$[t - x/v_n] \tag{3.67}$$

is large at any given time t. In performing the integral in Eq. (3.65) we make two approximations. First, we assume that $\Phi(E)$ is well peaked around E_r and thus since the spread of the wavepacket extends much beyond the width of the resonance it can be taken out of the integral and replaced by $\Phi(E_\mathrm{r})$. The second approximation is that the integral in Eq. (3.65) can be extended from $\int_0^\infty$ to $\int_{-\infty}^\infty$ without significantly affecting its values. This is, however, a very delicate point, as we will discuss below. For $t > x/v_\mathrm{r}$ the integration of Eq. (3.65) gives the following expression:

$$|\Psi_\mathrm{sc}(x,t)|^2 = \frac{2\pi M\Gamma^2}{\hbar^2 k_\mathrm{r}}|\Phi(k_\mathrm{r})|^2\mathrm{e}^{-\Gamma t/\hbar}\mathrm{e}^{+\frac{\Gamma x}{\hbar v_\mathrm{r}}}\,. \tag{3.68}$$

Exercise 3.12

Using contour integration derive Eq. (3.68) by showing that

$$\int_{-\infty}^{+\infty} \mathrm{d}x\,\frac{\mathrm{e}^{-\mathrm{i}x\tau}}{x + \mathrm{i}\Gamma/2} \tag{3.69}$$

vanishes when $\tau \leq 0$ and equals $-2\pi\mathrm{i}\mathrm{e}^{-\Gamma\tau/2}$ for $\tau > 0$.

The scattered wavepacket in Eq. (3.68) has two features: (1) an exponential decay in time of a wavepacket that populates a metastable state at energy E_r with a mean lifetime $\hbar/\Gamma$; (2) spatial exponential divergence of the wavefront of the scattered wavepacket as $\mathrm{e}^{+\Gamma x/(\hbar v_\mathrm{r})}$. As time passes the probability density, $|\Psi_\mathrm{sc}(x,t)|^2$, decays to zero at *any* given point in the coordinate space. Therefore, in order to conserve the number of particles the probability density has to diverge exponentially as $x \to \infty$ such that the integral of $|\Psi_\mathrm{sc}(x,t)|^2$ over time *and* coordinate space will be preserved. The divergent behavior of $|\Psi_\mathrm{sc}(x,t)|^2$ implies that particles that leaked out from the interaction region an infinitely long time ago are accumulated at $x = \infty$.

How is it possible that from a conventional quantum-mechanical analysis a non-square integrable function which does not belong to the Hilbert space is obtained? The answer is that in our derivation we get into the non-Hermitian domain of the Hamiltonian when we assume that we can take an initially prepared wavepacket $\Phi(E)$ out of the integration while we change the lower limit of the integral over E in Eq. (3.65) from $E = 0$ to $E = -\infty$. If, for example, one describes $\Phi(E)$ as a Gaussian $(2\alpha/\pi)^{1/4}\mathrm{e}^{-\alpha E^2}$ and does *not* take it out of the integral as we did before, then a wavepacket which is embedded inside the Hilbert space will be obtained.

By replacing the contour of integration to be from $E = -\infty$ to $E = +\infty$ while keeping $\Phi(E_\mathrm{r})$ out of the integration we avoid the interference of the resonance complex pole with other states in the continuum and associate the wavepacket with a single isolated complex energy pole of the S-matrix. This is how we get a solution in the non-Hermitian domain of the operator. The fact that the wavepacket $|\Psi_{\mathrm{sc}}(x, t)|^2$ decays exponentially with the rate of $\Gamma/\hbar$ indicates the physical nature of the complex poles of the S matrix, where Γ is associated with the imaginary part of the complex poles. This type of analysis which associates the complex poles of the S-matrix with the resonance phenomenon may explain the motivation to derive a non-Hermitian quantum-mechanical formalism.

3.9 Real and complex poles of the scattering matrix from wavepacket propagation calculations

For the sake of simplicity and without loss of generality let us first discuss the propagation of a initial one-dimensional wavepacket for a time-independent *Hermitian* Hamiltonian given by

$$\phi(x, t) = \mathrm{e}^{-\mathrm{i}\hat{H}t/\hbar}\phi(x, 0) \tag{3.70}$$

where the time-independent potential $V(x)$ and the initial wavepacket vanish when $|x| \geq L$. For any time $t, \phi(x, t)$ is a square integrable function. However, the wavepacket expands in time and therefore its asymptote, in the non-interacting region $|x| \geq L$, consists of *outgoing plane waves only* such that

$$\begin{aligned}\phi(x \geq L, t) &= \int_{k=0}^{\infty} \mathrm{d}k C_+(k)\mathrm{e}^{+\mathrm{i}kx}\,,\\ \phi(x \leq -L, t) &= \int_{k=0}^{\infty} \mathrm{d}k C_-(k)\mathrm{e}^{-\mathrm{i}kx}\,.\end{aligned} \tag{3.71}$$

The conclusion is clear.

After a sufficiently long time propagation (yet not too long) the time-propagated wavepacket (WP) in the interaction region $-L \leq x \leq L$ where $V(x) \neq 0$ can be described quite accurately as[3]

$$\phi(x,t) = \sum_n D_n(x) e^{-iE_n t/\hbar} \psi_n(x)\,, \tag{3.72}$$

where E_n and $\psi_n(x)$ are respectively the eigenvalues and eigenfunctions of the time-independent Hamiltonian $\hat{H}$ when we impose outgoing boundary conditions on the solutions of the time-independent Schrödinger equation (TISE). This is a remarkable fact since the only solutions of the TISE with *zero amplitude incoming waves* are the poles of the scattering matrix. As we will show in the next chapter, the poles of the scattering matrix are discrete and have either real values $\mathrm{Im}(E_n) = 0$ (associated with square integrable bound states), or complex eigenvalues $\mathrm{Im}(E_n) < 0$ which are associated with eigenfunctions $\psi_n(x)$ which are not in the Hilbert space and have exponentially diverging asymptotes. These solutions which are embedded in the non-Hermitian sector of the domain of the physical Hamiltonian $\hat{H}$ are the resonance states which are associated with the finite lifetime metastable states that will be described in Chapters 4–6.

3.10 Concluding remarks

(1) Resonances are associated with metastable states of a system which has sufficient energy to break into two or more subsystems. The subsystems can be neutral or ionic atoms and/or molecules, electrons, photons or other types of particle.

(2) The fingerprints of the resonances in spectroscopic and scattering experiments depend not only on the studied system but also on the chosen measurement. It is possible that for one kind of experiment the resonances are more pronounced (for example by sharp Lorenzian peaks in cross section measurements) than in another type of experiment.

(3) The resonances are not well defined in Hermitian quantum mechanics and are associated with wavepackets. Each such wavepacket is localized in the interaction region and can be constructed from a collection of continuum eigenstates of the time-independent Hamiltonian.

(4) The scattering matrix calculated *within the framework of Hermitian quantum mechanics* has real and complex poles. The poles embedded in the fourth quadrant of the complex energy plane are associated with the decay resonance phenomenon. We stress the fact that the poles can be calculated from the S-matrix and therefore in principle their calculations do not require the derivation of a non-Hermitian quantum-mechanical formalism.

---

[3] R. Santra, J. M. Shainline and C. H. Greene, Siegert pseudostates: completeness and time evolution, *Phys. Rev. A* **71**, 032703–12 (2005).

(5) For a specific choice of the initial WP, the solution of the *time-dependent* Schrödinger equation within the framework of the Hermitian formation of quantum mechanics is equal to the longest living resonance wavefunction, which is an eigenfunction of the non-Hermitian Hamiltonian (a non-Hermitian operator due to the requirement of outgoing boundary conditions).

(6) Only the bound state poles (i.e. those associated with square integrable eigenfunctions) can be obtained by Hermitian (conventional) quantum-mechanical calculations (solving the time-independent Schrödinger equation). All the other poles (either real or complex eigenvalues of the time-independent Hamiltonian) are associated with exponentially divergent solutions and therefore cannot be calculated by the conventional (Hermitian) quantum-mechanics formalism, but their calculations require the derivation of a non-Hermitian quantum-mechanical formalism.

3.11 Solutions to the exercises

Answer to Exercise 3.1

The free particle wavefunction,

$$\Psi_E(x) = \mathcal{N} \exp(\mathrm{i}kx) \tag{3.73}$$

is energy normalized when

$$\langle \Psi_{E'} | \Psi_E \rangle = \delta(E' - E) \tag{3.74}$$

and therefore

$$\int_{-\infty}^{+\infty} \mathrm{d}E' \langle \Psi_{E'} | \Psi_E \rangle = 1\,. \tag{3.75}$$

Since $E' = (\hbar k')^2/(2M)$ we can substitute in the above equation $\mathrm{d}E' = \hbar^2 k' \mathrm{d}k'/M$. Using the definition of a delta function,

$$\int_{-\infty}^{+\infty} \mathrm{d}x \mathrm{e}^{\mathrm{i}(k-k')x} = 2\pi\delta(k - k')\,, \tag{3.76}$$

we get that

$$\mathcal{N}^2 \int_{-\infty}^{+\infty} \mathrm{d}k' \frac{\hbar^2 k'}{M} 2\pi\delta(k - k') = 1 \tag{3.77}$$

and therefore the energy normalization factor is given by

$$\mathcal{N} = \sqrt{\frac{M}{2\pi\hbar^2 k}}\,. \tag{3.78}$$

Answer to Exercise 3.2

The Fermi golden rule for the state-to-state transition probability is derived from the first-order time-dependent perturbation theory. Consider the following Hamiltonian,

$$\hat{H}(t) = \hat{H}_0 + \hat{V}(t)\,, \tag{3.79}$$

where the unperturbed (zero-order) Hamiltonian is given by

$$\hat{H}_0 = \sum_n E_n^{(0)} |n\rangle\langle n|\,. \tag{3.80}$$

Here we use a box quantization condition and therefore the continuum states are described as discrete quasi-continuum states. By increasing the size of the box the energy gap between adjacent continuum energy levels can be as small as one wishes. Therefore, the quasi-continuum states are normalized as bound states. In the limit of an infinitely large box the spectrum of $\hat{H}_0$ will have a discrete part and a continuous part and then one needs to consider the density of states in a given energy in the continuum.

In order to describe a decaying state we assume we start initially at some discrete bound eigenstate $|\Psi(t=0)\rangle = |m\rangle$ of $\hat{H}_0$ which is embedded in the continuous part of the spectrum. Within first-order time-dependent perturbation theory the solution of the time-dependent Schrödinger equation is given by

$$|\Psi(t)\rangle = |m\rangle \mathrm{e}^{-\mathrm{i}E_m^{(0)}t} + \sum_n C_n(t)\mathrm{e}^{-\mathrm{i}E_n^{(0)}t}\,, \tag{3.81}$$

where

$$C_n(t) = \frac{1}{\mathrm{i}\hbar}\int_0^t \mathrm{d}\tau\, \langle n|\hat{V}(\tau)|m\rangle \mathrm{e}^{\mathrm{i}\omega_{nm}\tau} \tag{3.82}$$

and $\omega_{nm} = (E_m^{(0)} - E_n^{(0)})/\hbar$. The probability to be in a state $|n\rangle$ due to the transition from $|m\rangle \to |n\rangle$ is thus given by

$$P_{m\to n}(t) = |C_n(t)|^2\,. \tag{3.83}$$

We now assume that the perturbation $\hat{V}$ is turned on at $t = 0$ and remains constant in time up to some time $t = T$ and since

$$\int_0^T \mathrm{e}^{\mathrm{i}\omega_{nm}\tau}\mathrm{d}\tau = \frac{\mathrm{e}^{\mathrm{i}\omega_{nm}T} - 1}{\mathrm{i}\omega_{nm}} = \frac{\mathrm{e}^{\mathrm{i}\omega_{nm}T/2}}{\omega_{nm}/2}\left[\frac{\mathrm{e}^{+\mathrm{i}\omega_{nm}T/2} - \mathrm{e}^{-\mathrm{i}\omega_{nm}T/2}}{2\mathrm{i}}\right] \tag{3.84}$$

we get that after the perturbation is turned off the probability to be in a state $m \neq n$ for $t > T$ is

$$P_{m\to n}(t \geq T) = \frac{|\langle n|\hat{V}|m\rangle|^2}{\hbar^2(\omega_{nm}/2)^2}\sin^2\left(\frac{\omega_{nm}T}{2}\right). \tag{3.85}$$

We now wish to see what happens if the perturbation is kept on. This means that $T \to \infty$ and since

$$\lim_{T\to\infty}\frac{\sin^2(\alpha T)}{T\alpha^2} = \pi\delta(\alpha), \tag{3.86}$$

for sufficiently large T,

$$P_{m\to n}(T \to \infty) = T\frac{\pi|\langle n|\hat{V}|m\rangle|^2\delta(\omega_{nm}/2)}{\hbar^2}. \tag{3.87}$$

From the $\delta(\omega_{nm}/2)$ term in this expression we can infer that the bound state $|m\rangle$ can only couple to continuum states at the same energy. Note that in the limit of infinitely large box one has to consider the density of states $\rho(E)$ in the continuum around the final energy $E_n^{(0)}$. Now we consider the probability, δP_{mn}, of the transition from the $|m\rangle$ bound state to a small energy interval in the continuum from $E_n^{(0)}$ to $E_n^{(0)} + \mathrm{d}E_n^{(0)}$. If the density of states and $\langle n|\hat{V}|m\rangle$ vary slowly over this range then the probability is given by

$$\begin{aligned}\delta P_{mn} &\equiv \int_{E_n^{(0)}}^{E_n^{(0)}+\mathrm{d}E_n^{(0)}} P_{m\to n}(T \to \infty)\rho(E)\mathrm{d}E \\ &= \frac{2\pi}{\hbar}T|\langle n|\hat{V}|m\rangle|^2\rho(E_n^{(0)} = E_m^{(0)}).\end{aligned} \tag{3.88}$$

For long enough times the transition probability increases linearly with the time the perturbation is turned on and therefore we can define the probability *per unit time* (i.e. the rate of transition) by

$$\frac{\mathrm{d}(\delta P_{mn})}{\mathrm{d}T} = \frac{2\pi}{\hbar}|\langle n|\hat{V}|m\rangle|^2\rho(E_n^{(0)}). \tag{3.89}$$

The transition from a bound state to a scattering state in the continuum is simply a decay process induced by the perturbation $\hat{V}$. Thus the rate of decay of the m-th bound state $\Gamma_m/\hbar$ due to the coupling with the continuum in the same energy is

$$\frac{\Gamma_m}{\hbar} = \frac{2\pi}{\hbar}\rho(E_n^{(0)})|\langle n|\hat{V}|m\rangle|^2. \tag{3.90}$$

This expression gives the resonance width Γ according to the Fermi golden rule. Note that the density of states is of the zero-order Hamiltonian where we describe a bound state embedded in the continuum. Therefore, $\rho(E)$ is the density of states of the "white continuum" of the $\hat{H}_0$ Hamiltonian and does not contain any information on the decay process which is taken into consideration only when the perturbation potential term $\hat{V}$ is included in the Hamiltonian. Another point which should be emphasized is that the bound state $|m\rangle$ and the continuum function $|n\rangle$ are *two degenerate states of the zero order Hamiltonian* with the energy $E_m^{(0)}$.

Answer to Exercise 3.3

First we briefly derive the flux operator for a one-dimensional real Hermitian Hamiltonian. Multiplying the time-dependent Schrödinger equation from the left by $\psi^*(x,t)$ and its complex conjugate by $\psi(x,t)$ we get the following two equations:

$$\begin{aligned}\psi^*\hat{H}\psi &= \mathrm{i}\hbar\psi^*\frac{\partial}{\partial t}\psi\,,\\ \psi\hat{H}\psi^* &= -\mathrm{i}\hbar\psi\frac{\partial}{\partial t}\psi^*\,.\end{aligned} \tag{3.91}$$

Subtracting the two equations we get the local change in probability density $\rho(x,t) = |\psi(x,t)|^2$, which is given by

$$\frac{\partial}{\partial t}\rho(x,t) = \frac{\hbar}{2M\mathrm{i}}\left(\psi^*\frac{\partial^2}{\partial x^2}\psi - \psi\frac{\partial^2}{\partial x^2}\psi^*\right)\,. \tag{3.92}$$

Since

$$\psi^*\frac{\partial^2}{\partial x^2}\psi - \psi\frac{\partial^2}{\partial x^2}\psi^* = \frac{\partial}{\partial x}W[\psi,\psi^*]\,, \tag{3.93}$$

where $W[\psi,\psi^*]$ stands for the Wronskian of the two functions,

$$W[\psi,\psi^*] = \psi^*\frac{\partial}{\partial x}\psi - \psi\frac{\partial}{\partial x}\psi^*\,, \tag{3.94}$$

this gives a continuity equation which relates the local change in density to the current of probability at that point:

$$\frac{\partial}{\partial t}\rho(x,t) = -\frac{\partial}{\partial x}J(x,t)\,, \tag{3.95}$$

where the *current density* at a given point x is defined as

$$J(x,t) = \frac{\hbar}{2M\mathrm{i}}W[\psi,\psi^*]\,. \tag{3.96}$$

The integral $\int|\psi(t)|^2\mathrm{d}x$ taken over some finite interval (volume in a three-dimensional problem) $x_0 - \Delta_x/2 \le x \le x_0 + \Delta_x/2$ is the probability of finding the particle in this volume. Therefore, in our case $J(x_0,t)$ is the number of particles which pass through an interval $x_0 - \Delta_x/2 \le x \le x_0 + \Delta_x/2$ per unit time. $J(x_0,t)$

is defined as the particle flux (in 3D the flux through a surface bounding the volume is related to the change in the density in that volume through the divergence theorem).

$$\frac{\mathrm{d}}{\mathrm{d}t}\int_{x_0-\Delta_x/2}^{x_0+\Delta_x/2} \mathrm{d}x|\psi(x,t)|^2 = J(x_0-\Delta_x/2,t) - J(x_0+\Delta_x/2,t)\,. \quad (3.97)$$

The flux operator is defined such that $J(x_0,t) = \langle\psi|\hat{F}_{x_0}|\psi\rangle$. Therefore,

$$\hat{F}_{x_0} = \frac{\hat{p}_x\delta(x-x_0) + \delta(x-x_0)\hat{p}_x}{2M}\,, \quad (3.98)$$

where $\hat{p}_x$ is the momentum in the x-direction.

Far enough from the interaction region any stationary scattering state behaves as a free particle $\psi = [A(k)\mathrm{e}^{-\mathrm{i}kx} + B(k)\mathrm{e}^{+\mathrm{i}kx}]\mathrm{e}^{-\mathrm{i}Et/\hbar}$. The Wronskian in this region is equal to

$$W[\psi,\psi^*] = 2(|A(k)|^2 - |B(k)|^2)\,. \quad (3.99)$$

However, for a stationary solution $\rho(x,t) \equiv |\psi(x,t)|^2$ is a time-independent function and therefore the flux $J(x_0,t)$ is constant. Therefore,

$$|A(k)|^2 - |B(k)|^2 = \text{const}\,. \quad (3.100)$$

If the solution is also invariant under the reversal of time it means that the motion is symmetrical when both time and the momentum of the particle are reversed. In terms of the wavefunction it amounts to demanding that $\psi(x,t) = \psi^*(x,-t)$. In other words, in the asymptote we get that $A(k) = B^*(k)$ and thus $|A(k)|^2 - |B(k)|^2 = 0$ and there is no flux. This proves that for stationary solutions the S-matrix, $S^\dagger S = I$. This proof can be readily extended to three dimensions by evaluating the flux through a surface bounding the volume containing the interaction region. This flux can be related to change in the density using a similar continuity equation which can be derived from the Schrödinger equation using the divergence theorem.

Answer to Exercise 3.4

The kinetic energy of a free particle is $E = (\hbar k)^2/(2M)$ and therefore the wave vector is given by $k = \sqrt{2ME}/\hbar$. Therefore, $\mathrm{d}k = \sqrt{M/(2\hbar^2 E)}\mathrm{d}E$. When the particle is confined to a box of length L_{box} its energy levels also become quantized such that

$$E_n = \frac{\hbar^2}{2M}\left(\frac{\pi n}{L_{\text{box}}}\right)^2\,. \quad (3.101)$$

Thus, the momentum is also quantized with values $k = -n\pi/L_{\text{box}}, \ldots, n\pi/L_{\text{box}}$. The volume in k-space depends on the dimensionality. In an n-dimensional problem ($n = 1,2,3$) $V(nD) = [2\pi/L_{\text{box}}]^n$. In a 1D problem (which is equivalent to the s-waves of a 3D spherically symmetric problem) the states associated with energy which is less than or equal to E are on a line from $-k$ to $+k$ and therefore $N = 2k/V(1D) = kL_{\text{box}}/\pi$. The density of states $\rho = \mathrm{d}N/\mathrm{d}E = \mathrm{d}N/\mathrm{d}k \cdot \mathrm{d}k/\mathrm{d}E$ is given by

$$\rho_{1\mathrm{D}}(E) = \frac{L_{\text{box}}}{\hbar\pi}\sqrt{\frac{M}{2E}}\,. \tag{3.102}$$

The density of states in the 1D problem is infinitely large at the threshold energy $E = 0$. As E increases, $\rho_{1\mathrm{D}}(E)$ decreases. Therefore it is expected that when a bound state in one potential energy surface is embedded in the continuum of another potential surface and becomes a resonance due to a coupling potential term, the resonance width (inverse lifetime) will be *larger* as the bound state is embedded closer to the threshold energy of the second potential energy surface. This situation is relevant to the discussion regarding Feshbach-type resonances only and will be discussed in Chapter 4. For shape-type resonances this is not the case and the width of the resonances which are embedded closer to the threshold energy is the smallest.

In two dimensions the number of states with energy less than E is given similarly by $N = \pi k^2/V(2D)$. Therefore

$$\rho_{2\mathrm{D}}(E) = \frac{L_{\text{box}}^2 M}{2\pi\hbar^2}\,. \tag{3.103}$$

Thus in two dimensions the density of states is energy independent.

Along the same line of thought, in 3D the number of states associated with energy less than E is $N = 4\pi k^3/(3V(3D)$, and therefore

$$\rho_{3\mathrm{D}}(E) = \frac{L_{\text{box}}^3}{2\pi^2\hbar^3}\sqrt{2M^3E}\,. \tag{3.104}$$

In 3D the density of states increases as the energy increases.

Answer to Exercise 3.5

Confining the problem to a finite box, we use the eigenstates of the box as a basis set $\sqrt{2/L_{\text{box}}}\sin(n\pi x/L_{\text{box}})$, $n = 1, 2, \ldots, N$. The degree of quantization of space is set by the size of the box, L_{box}. Since our model potential is non-zero only for

$L \le x \le \infty$ the potential matrix elements are given by

$$\begin{aligned} V(n', n) &= -\frac{2V_0}{L_{\text{box}}} \int_L^{L_{\text{box}}} \mathrm{d}x \sin\left(\frac{n'\pi x}{L_{\text{box}}}\right) \sin\left(\frac{n\pi x}{L_{\text{box}}}\right) \\ &= -V_0 \left[\frac{\sin[(n'+n)\pi L/L_{\text{box}}]}{\pi(n'+n)} + \delta_{n',n}\frac{L_{\text{box}} - L}{L_{\text{box}}}\right] \\ &\quad + V_0[1-\delta_{n',n}]\left[\frac{\sin[(n'-n)\pi L/L_{\text{box}}]}{\pi(n'-n)}\right]. \end{aligned} \tag{3.105}$$

Here V_0 is the height of the potential barrier. The Hamiltonian is now represented by an $N \times N$ matrix $[H(n', n) = \delta_{n',n}(n\pi\hbar/L_{\text{box}})^2/(2M) + V(n', n)]$. The variational solutions of the Schrödinger equation are the eigenvalues of the Hamiltonian matrix. The number of the basis functions, N, must be taken large enough to get converged results to the desired accuracy for a given box size. The plot of the eigenvalues as function of L_{box} provides the stabilization plot presented in Fig. 3.12.

Answer to Exercise 3.6

The continuum wavefunction outside the interacting region of the potential in Fig. 3.1 is given by Eq. (3.6). We impose on the continuum solutions outgoing wave boundary conditions, i.e., $A(k) = 0$, where $A(k)$ is defined in Eq. (3.9). Bound states are associated with a positive imaginary wave vector $k_{\text{b}} = \mathrm{i}|k_{\text{b}}|$ (in such cases the asymptote decays exponentially and the eigenfunction is a square integrable function) and therefore the energies of the bound states are given by $E_{\text{b}} = -(\hbar|k_{\text{b}}|)^2/(2M)$. Resonances (as will be discussed in the following chapter) are the solutions of the equation $A(k) = 0$ where k has complex values. What are the conditions under which one gets bound states for our model potential? From Eq. (3.9) one gets that $A(k) = 0$ with k purely an imaginary number implies that

$$\sin(k_{\text{b}}L) + \frac{\mathrm{i}k_{\text{b}}}{q_{\text{b}}}\cos(k_{\text{b}}L) = 0\,. \tag{3.106}$$

As $V_0 \to \infty$ also $q = \sqrt{2M(E+V_0)}/\hbar \to \infty$ and therefore bound states are obtained when

$$\sin(k_{\text{b}}L) = 0\,. \tag{3.107}$$

Equation (3.107) is satisfied when $k_{\text{b}} = n\pi/L$, where $n = 1, 2, \ldots$ *Here we prove that, the repulsive potential presented in Fig. 3.1 where* $V_0 = \infty$ *supports bound states of a particle-in-a box problem.* That is, $E_{\text{b}} = [\hbar^2/(2M)](n\pi/L)^2$ where $n = 1, 2, \ldots$ These states are located, however, in the “un-physical” region of infinitely large kinetic energies above the threshold. In the “real world” these bound states are actually very long living (narrow) resonances. It might happen that their lifetime is so large that it will be hard to measure and in most types of experiment they will behave like true bound states.

Answer to Exercise 3.7

The height of the potential barrier is V_0 and its width is given by $2L$ (i.e., $-L \leq x \leq +L$). The transition probability for a free particle with the energy $E = (\hbar k)^2/(2M) < V_0$ to cross the potential barrier is equal to

$$|T(E)|^2 = \left[1 + \left(\frac{k^2+\alpha^2}{2k\alpha}\right)^2 \sinh^2(2\alpha L)\right]^{-1}, \tag{3.108}$$

where

$$k = \sqrt{2ME}/\hbar \quad \text{and} \quad \alpha = \sqrt{2M(V_0 - E)}/\hbar\,. \tag{3.109}$$

Let us assume that $\alpha L \gg 1$. In such a case the semiclassical approaches are applicable. The transmission probability given above is reduced to

$$|T(E)|^2 \sim \left(\frac{4k\alpha}{k^2+\alpha^2}\right)^2 \exp(-4\alpha L)\,. \tag{3.110}$$

In the spirit of the derivation given in Ex. 3.6 it is indeed expected that $|T(E)|^2$ vanishes as $V_0 \to \infty$ even when E is larger than V_0. However, in many cases where the pre-exponential factor is almost V_0-independent the well-known quasi-classical expression for the transmission probability through a potential barrier is obtained (see, for example, Section 50 in Landau and Lifshitz' text book on *Quantum Mechanics*). When $\alpha \sim (\sqrt{5}-2)k$ the pre-exponential factor is close to unity and then

$$|T(E)|^2 \sim \exp(-4\alpha L) \tag{3.111}$$

is V_0-independent.

Therefore, if $T^2 = \exp(-4\alpha L) = \exp(-2\alpha \int_{-L}^{+L} \mathrm{d}x)$ is the transmission probability of a particle to get through a potential barrier when the barrier's width is L, then the transmission probability to get through a potential barrier when the barrier's width is ηL is given by $T^{2\eta} = \exp(-2\alpha \int_{-L\eta}^{+L\eta} \mathrm{d}x)$. When the potential barrier is a smooth function of x, $V(x)$, then when $V(x)$ is varied sufficiently slowly with x one can approximately describe $V(x)$ by a juxtaposition of rectangular potential barriers. That is, $V(x) = \sum_j V_j(x)$, where $V_j(x) = V(x_j)$ when $x_{j-1} \leq x < x_j$ and V_j vanishes elsewhere. Therefore, due to the scaling law of T^2 mentioned above, $|T|^2 = \exp(-2\sum_j k(x_j)(x_j - x_{j-1})$, where $k(x_j) = \sqrt{2M(V(x_{j-1}) - E)}/\hbar$. Here

$k(x_j)$ replaces α in the transmission through a single rectangular potential barrier. The slowly varying condition is important in order to satisfy the semiclassical (quasi-classical) condition that $k(x_j)(x_j - x_{j-1}) \gg 1$ while at the same time replacing the summation over j by an integral to yield

$$|T(E)|^2 \sim \exp\left(-2\int_{\text{barrier}} k(x)\mathrm{d}x\right), \tag{3.112}$$

where $k(x) = \sqrt{2M(V(x) - E)}/\hbar$.

Gamow's expression for the resonance decay rate for a particle in a potential well supported by a potential barrier (as, for example, $V(x) = -V_0$ for $x \le x_0$ and $V(x) = a/x$ for $x > x_0$ (see Problem 2 in Section 50 in Landau and Lifshitz, *Quantum Mechanics*) is given by $\Gamma = \hbar\omega \exp(-2\int_{\text{barrier}} k(x)\mathrm{d}x)$, where ω is the frequency of the classical periodic motion in the well (i.e., the number of particles colliding in unit time with the left wall of the barrier). For the example mentioned above, $\omega = x_0/v$, where $v = \sqrt{2(E + V_0)/m}$.

Answer to Exercise 3.8

For a free particle $\psi = \mathcal{N}\exp(\mathrm{i}kx - \mathrm{i}Et/\hbar)$, flux normalization implies that we normalize the current of particles such that $J(x,t) = \frac{\hbar}{2M\mathrm{i}} W[\psi, \psi^*] = 1$. Therefore the flux normalization factor $\mathcal{N}$ is given by

$$\mathcal{N} = \sqrt{\frac{M}{\hbar k}}\,. \tag{3.113}$$

Answer to Exercise 3.9

The scattering length is associated with the phase shift. The phase shift for a radial square-barrier potential was derived in Eq. (3.11). For a radial square-well potential the depth of the potential well is $-V_0$ and the threshold energy is taken as $E = 0$. For $E > 0$ the solution in the interaction region ($0 \le x < L$) is given by $\psi_{\text{in}} = \sin(kx)$, where $k = \sqrt{2M(E + V_0)}/\hbar$ and outside the interaction region $\psi_{\text{out}} = A\sin(qx + \delta)$, where $q = \sqrt{2ME}/\hbar$ and δ is the phase shift. From the conditions that $\psi_{\text{in}}(x = L) = \psi_{\text{out}}(x = L)$ and $\mathrm{d}\psi_{\text{in}}/\mathrm{d}x|_{x=L} = \mathrm{d}\psi_{\text{out}}/\mathrm{d}x|_{x=L}$ one gets $k\tan(qL + \delta) = q\tan(kL)$. Consequently (using the identity $\tan(x + a) = (\tan(x) + \tan(a))/(1 - \tan(x)\tan(a))$),

$$\tan\delta = \frac{q\tan(kL) - k\tan(qL)}{k + q\tan(qL)\tan(kL)}\,. \tag{3.114}$$

Since $k \to k_0 = \sqrt{2MV_0}/\hbar$ as $q \to 0$ and $\tan(qL) \to qL$ we can substitute into Eq. (3.43) and get that

$$a_0 = -\lim_{q\to 0} \frac{\tan\delta}{q} = L - \frac{\tan(k_0 L)}{k_0} . \tag{3.115}$$

The $\tan(k_0 L)$ term is responsible for the changes in a_0 from $-\infty$ to $+\infty$ when V_0 or L is varied.

Answer to Exercise 3.10

Taking the free particle solutions of the form $\mathrm{e}^{\mathrm{i}kx}$ and using the expansion in Eq. (3.52) one gets

$$\begin{aligned} &\frac{1}{2\Delta E}\int_{E_n-\Delta E}^{E_n+\Delta E} \mathrm{d}E\,\mathrm{e}^{\mathrm{i}(\pm kx - Et/\hbar)} \\ &\quad\approx \mathrm{e}^{\mathrm{i}(\pm k_n x - E_n t/\hbar)} \frac{1}{2\Delta E}\int_{-\Delta E}^{+\Delta E} \mathrm{d}\tilde{E}\,\mathrm{e}^{\mathrm{i}(\pm x - v_n t)\tilde{E}/(\hbar v_n)} , \end{aligned} \tag{3.116}$$

where $\tilde{E} = E - E_n$. By carrying out the integration the desired result is obtained,

$$\begin{aligned} \frac{1}{2\Delta E}\int_{E_n-\Delta E}^{E_n+\Delta E} \mathrm{d}E\,\mathrm{e}^{\mathrm{i}(\pm kx - Et/\hbar)} &\approx \mathrm{e}^{\mathrm{i}(\pm k_n x - E_n t/\hbar)} \operatorname{sinc}[(\pm x - v_n t)\Delta] \\ &= \mathrm{e}^{\mathrm{i}(\pm k_n x - E_n t/\hbar)} \operatorname{sinc}[(x \mp v_n t)\Delta] , \end{aligned} \tag{3.117}$$

where

$$\Delta = \frac{\Delta E}{\hbar v_n} . \tag{3.118}$$

Answer to Exercise 3.11

By assuming that the integral in Eq. (3.65) can be extended to $-\infty$ without significantly changing its value, it takes the following form:

$$\Psi_{\mathrm{sc}}(x,t) \approx \mathrm{i}\mathrm{e}^{+\mathrm{i}k_r x - \mathrm{i}E_r t/\hbar}\,\Gamma\Phi(E_{\mathrm{r}}) \int_{-\infty}^{\infty} \mathrm{d}E' \frac{\mathrm{e}^{-\mathrm{i}E'(t-\frac{x}{v_{\mathrm{r}}})/\hbar}}{E' + \frac{\mathrm{i}}{2}\Gamma} , \tag{3.119}$$

where $E' = E - E_{\mathrm{r}}$. The integral we wish to solve has the form

$$I = \int_{-\infty}^{+\infty} \frac{\mathrm{e}^{-\mathrm{i}x\tau}}{x + \mathrm{i}a}\mathrm{d}x . \tag{3.120}$$

where $a = \Gamma/2 > 0$. By defining a new variable $z = x\tau$ this integral transforms to

$$I = \pm e^{-a\tau} \int_{-\infty}^{+\infty} F(z)dz\,, \tag{3.121}$$

where

$$F(z) = \frac{e^{-i(z+z_0)}}{z + z_0} \tag{3.122}$$

and $z_0 = ia\tau$. The "+" sign applies to $\tau > 0$ and the "−" sign to $\tau > 0$. In the complex plane the function $F(z)$ has a pole at $z = -z_0$ which is along the imaginary axis, Im(z). For $\tau < 0$ the pole is embedded on the positive side of the imaginary part of z (i.e. $\mathrm{Im}(-z_0 = a|\tau|) > 0$), whereas for $\tau > 0$ the pole is on the negative part of the imaginary axis of z, $\mathrm{Im}(-z_0) < 0$. This is a crucial point in our proof since $F(z)$ vanishes as $\mathrm{Im}(z) \to -\infty$ and diverges exponentially as $\mathrm{Im}(z) \to +\infty$. Therefore, the contour of integration has to be in the lower half of the complex z-plane. This reflects the asymmetry in time with respect to $t = 0$, where for a resonant state the probability decreases when going forward in time and increases when going backward in time. This property, which is inherent in non-Hermitian quantum mechanics, will be discussed extensively in the following chapters.

Let us choose a closed contour, $\mathcal{C}$, which consists of the real z axis from $-R \leq z \leq +R$ and a half a circle $z = R\exp(-i\alpha)$, where $0 < \alpha < \pi$. By taking R to ∞ all the points on the semi circle have $F = 0$ and thus the value of the integral over the closed contour is the desired result of the integration on the real axis. There are now two possibilities.

(I) $\tau < 0$ and the pole is embedded outside the closed contour, $\mathcal{C}$. In such a case $I = 0$.

(II) $\tau > 0$ and the pole is embedded "inside" the closed contour, $\mathcal{C}$. In such a case, due to the residue theorem,

$$\oint_{\mathcal{C}} F(z)dz = 2\pi i \tag{3.123}$$

and therefore $I = -2\pi i e^{-a\tau}$. Applying this result to Eq. (3.119) and taking an energy normalization condition one immediately obtains the results of Eq. (3.68),

$$|\Psi_{sc}(x,t)|^2 = \frac{2\pi M\Gamma^2}{\hbar^2 k_r}|\Phi(k_r)|^2 e^{-\Gamma t/\hbar} e^{+\frac{\Gamma x}{\hbar v_r}}\,. \tag{3.124}$$

3.12 Further reading

A. I. Baz', Ya. B. Zel'dovich and A. M. Perelomov, *Scattering, Reactions and Decay in Nonrelativisitic Quantum Mechanics*, Jerusalem, Israel Program for Scientific Translation, 1969.

A. M. Perelomov and Ya. B. Zel'dovich, *Quantum Mechanics*, Singapore, World Scientific Publishing Co., 1998.

V. I. Kukulin, V. M. Krasnopol'sky and J. Horáček, *Theory of Resonances: Principles and Applications*, Prague, Kluwer Academic Publishers, 1989.

J. R. Taylor, *Scattering Theory: the Quantum Theory on Nonrelativistic Collisions*, New York, John Wiley & Sons, Inc. 1972.

L. D. Landau and E. M. Lifshitz, *Quantum Mechanics*, New York, Pergamon, 1965.

4

Resonances from non-Hermitian quantum mechanical calculations

The Hermitian properties of the Hamiltonian are related not only to the operator itself but also to the functions on which it acts. Hermitian Hamiltonians operate on functions in the L^2 Hilbert space which correspond to boundary conditions which vanish at infinity. In this chapter, in order to move into the non-Hermitian domain, we will impose on the solutions to the time-independent Schrödinger equation (TISE) different boundary conditions which lead to solutions which can be associated with different types of the complex poles of the scattering matrix. These solutions will contain information which was not available within the scope of functions in L^2.

By imposing *outgoing* boundary conditions on the eigenfunctions of the time-independent Hamiltonian complex eigenvalues, $E_{\rm res} = \varepsilon - ({\rm i}/2)\Gamma$, are obtained. These complex energies are associated with decaying resonance states which were discussed in the previous two chapters. The bound states (if they exist) appear as real eigenvalues since they result from exactly such outgoing boundary conditions which appear under the threshold energy. When *incoming* boundary conditions are imposed two kind of solution are obtained. One type of solution is the complex conjugates of the decay resonance solutions mentioned above. In scattering theory text books (see Taylor[1] for example) the physical resonance solutions are associated with the poles of the scattering matrix which are embedded in the lower half of the complex energy plane. However, in nuclear physics the *complex* poles embedded in the upper half of the complex energy plane, so-called *virtual states*, are denoted as *capture resonances*. The other type of solution obtained by imposing incoming boundary conditions on the TISE is the *anti-bound states* which are often denoted as *virtual states*. The anti-bound states are associated, similarly to bound states, with real eigenvalues of the Hamiltonian.

---

[1] J. R. Taylor, *Scattering Theory: the Quantum Theory on Nonrelativistic Collisions*, New York, John Wiley & Sons, Inc., 1972.

Resonances are obtained by imposing outgoing boundary conditions on the solutions of the TISE for 1D, 2D and 3D problems, for one-body or for many-body problems, for short and for long range potentials. The resonances can be shape-type resonances or Feshbach-type and often it is hard to distinguish between the two. However, there are no general analytical solutions of the TISE for all possible problems and therefore for the sake of simplicity and coherence of our representation we will discuss the situation in specific problems. In order to emphasize the fact that resonances appear in almost any studied problem (of course not always but it is hard to avoid them) we have chosen to open our discussions with a simple 1D case where the potential does not support wells and the shape-type resonances are formed due to the presence of potential barriers. The bound states are square integrable states which belong to the L^2 Hilbert space. All the other poles are associated with wavefunctions that diverge exponentially and are not part of the Hilbert space. Under variation of the given potential parameters the bound, anti-bound as well as the decay and capture resonances move in the complex energy plane. In the potential barrier problem we studied in the previous chapter there are no bound/anti-bound states and only decay and capture resonances appear. However, for a rectangular potential-well problem the situation is richer. As one reduces the depth of the potential well the bound states inside the well move up in energy and eventually become anti-bound states. As the depth of the potential is further reduced, these poles transform into decay and capture resonances. These resonances are born in this problem at energies *below* the threshold energy. These phenomena will be discussed in this chapter.

As stated above, the resonances are associated with *complex* eigenvalues of the Hamiltonian. In conventional quantum mechanics the Hamiltonian is Hermitian and therefore the eigenvalues must be real. How can the same Hamiltonian used in conventional (i.e., Hermitian) quantum mechanics lead to complex energies? The explanation is simple. The non-Hermitian properties of an operator depend not only on the operator itself but also on the properties of the wavefunctions. For the sake of clarity let us remind the reader (without loss of generality) that, for example, in the one-dimensional case an operator $\hat{H} = \hat{p}^2/(2M) + V(x)$ is Hermitian provided that

$$\hat{H}^\dagger = \hat{H}\,, \tag{4.1}$$

where $\hat{H}^\dagger$ is an operator which satisfies the following equation:

$$\int_{-\infty}^{+\infty} f(x)\hat{H}^\dagger g(x)\mathrm{d}x = \int_{-\infty}^{+\infty} g(x)\hat{H}^* f(x)\mathrm{d}x\,. \tag{4.2}$$

By carrying out the integration by parts one gets that when $V(x)$ is real this equation is satisfied when

$$\left[g(x)\frac{\mathrm{d}f(x)}{\mathrm{d}x} - f(x)\frac{\mathrm{d}g(x)}{\mathrm{d}x}\right]_{-\infty}^{+\infty} = 0\,. \tag{4.3}$$

Consequently, the Hermitian property of $\hat{H}$ depends also on the boundary conditions of $f(x)$ and $g(x)$. When, for example, $f(x)$ and $g(x)$ are in the L^2 Hilbert space, then $f(x = \pm\infty) = 0$ and $g(x = \pm\infty) = 0$. In such a case Eq. (4.3) is satisfied and $\hat{H}$ is an Hermitian operator. Equation (4.3) is also satisfied for periodic functions where $f(x) = f(x + L)$ and $g(x) = g(x + L)$ and therefore we replace the integration limits from $\pm\infty$ to $\pm NL$ where N is an integer. It is clear that when $f(x)$ and $g(x)$ diverge exponentially the Hamiltonian is non-Hermitian, which gives rise to complex eigenvalues. Thus, a new quantum mechanical formalism should be developed.

4.1 Resonances for a time-independent Hamiltonian

The Hermitian quantum mechanical calculations presented in Chapter 3 explored the association of the resonance energies and decay rates with the real and imaginary parts of the complex poles of the scattering matrix. The poles of the S-matrix are associated with eigenfunctions with zero incoming amplitudes. Therefore, unlike the situation in Hermitian quantum mechanics, in the non-Hermitian formalism these poles can be associated with discrete complex eigenvalues of the Hamiltonian. These solutions can be obtained by solving the TISE with outgoing boundary conditions. The solutions of any differential equation are subject to the constraints of boundary conditions. For the TISE, imposing outgoing boundary conditions means that, while the discrete bound state spectrum is obtained for real eigenvalues lying below the threshold, energy resonances are obtained for complex eigenvalues with real parts embedded in the continuum. The asymptotic form of the general solution in the continuum for a one-dimensional problem is given by

$$\Psi_E(x \to \infty) = A_+(E)\mathrm{e}^{-\mathrm{i}k^+x} + B_+(E)\mathrm{e}^{+\mathrm{i}k^+x}\,, \tag{4.4}$$

$$\Psi_E(x \to -\infty) = A_-(E)\mathrm{e}^{+\mathrm{i}k^-x} + B_+(E)\mathrm{e}^{-\mathrm{i}k^-x}\,, \tag{4.5}$$

where $k^{\pm}$ is the momentum of the free particle at $\pm\infty$ respectively. Requiring outgoing waves only means that at the resonance energies,

$$A_{\pm}(E = E_n) = 0\,, \tag{4.6}$$

where n is an index counting the discrete states in the continuum. If the threshold energy as $x \to \infty$ approaches a constant value E_+^{th} then the eigenvalues of the

Hamiltonian under this restriction attain discrete values, $E_n = (\hbar k_n^+)^2/(2M) + E_+^{\mathrm{th}}$. As will be shown shortly, the index n counts the number of nodes in the interaction region of the real part of the eigenfunction which is associated with the eigenvalue E_n.

There are two ways by which Eq. (4.6) can be satisfied for $\mathrm{Re}(k^+) > 0$.

(1) $k_n^+ = \mathrm{i}|k_n^+|$ and therefore $E_n = E_+^{\mathrm{th}} - |\hbar k_n^+|^2/(2M)$. These solutions are bound states. (Here if we set the threshold energy to 0 these eigenvalues will be negative.)

(2) $k_n^+ = |k_n^+|\mathrm{e}^{-\mathrm{i}\alpha_n}$. These values which correspond to the resonance solutions are complex and are given by

$$E_n = \varepsilon_n - \mathrm{i}/2\Gamma_n = E_+^{\mathrm{th}} + |\hbar k_n^+|^2 \mathrm{e}^{-2\mathrm{i}\alpha_n}/(2M)\,, \tag{4.7}$$

where

$$\alpha = \frac{1}{2}\arctan\frac{\Gamma_n/2}{\varepsilon_n - E_+^{\mathrm{th}}}\,. \tag{4.8}$$

Note that when the threshold energy is 0 (the first threshold can always be shifted to $E = 0$) then these decaying states lie in the fourth quadrant of the complex energy plane where $\alpha \in [0, \pi/4]$.

When Eq. (4.6) is satisfied the 1D resonance wavefunction (also known as a Siegert or Gamow state) has an outgoing asymptote which is given by

$$\lim_{x\to\infty}\Psi_{\mathrm{res}}(x) = B_+(E_n)\mathrm{e}^{\mathrm{i}k_n^+ x}\,, \tag{4.9}$$

where the resonance complex eigenvalue E_n is defined in Eq. (4.7). In 1D problems where the potential $V(x)$ has different asymptotes at ±∞ the threshold energy at $x \to -\infty$ will be labeled by E_-^{th}. The asymptotic behavior at $-\infty$ in such a case is

$$\lim_{x\to-\infty}\Psi_{\mathrm{res}}(x) = B_-(E_n)\mathrm{e}^{\mathrm{i}k_n^- x}\,, \tag{4.10}$$

where

$$k_n^- = \sqrt{2M(E_n - E_-^{\mathrm{th}})}/\hbar\,. \tag{4.11}$$

Exercise 4.1

Following the definition of the complex energy E_n given in Eq. (4.7), show that when the threshold energies at ±∞ are equal to zero then the decay rate of the resonance can be expressed as

$$\Gamma_n = -\frac{2\hbar^2}{M}\mathrm{Re}(k_n)\mathrm{Im}(k_n) \tag{4.12}$$

and the coefficient $B(k_n)$ of the outgoing wave is given by

$$B(k_n) = \gamma_n \sqrt{\frac{M}{\hbar k_n}}\,, \tag{4.13}$$

where γ_n is a complex constant associated with the n-th resonance eigenfunction.

Prove also that as $\Gamma_n \to 0$ then

$$\hbar|\gamma_n|^2 \to \Gamma_n\,. \tag{4.14}$$

Solve this problem for a spherically symmetric potential where $0 \le x \le \infty$ and the resonance eigenfunctions vanish at $x = 0$.

As we have shown in Ex. 3.6 for the model Hamiltonian studied in Chapter 3, by imposing outgoing boundary conditions on the eigenfunctions of the time-independent Hamiltonian, bound states are obtained when the height of the potential barrier, V_0, is taken to be infinitely large. For any finite value of V_0, which can be as large as one wishes, we get narrow resonances which are “almost” bound states in the continuum. It is possible to get bound states in the continuum in higher dimensional problems due to special symmetry properties. It is clear, however, that any infinitesimally weak perturbation which breaks the symmetry of the Hamiltonian will couple between such bound states and the continuum in which they reside and thus a resonance with finite lifetime will be created (see the discussion on the Fermi golden rule given in Ex. 3.2 and the derivation of a lower bound for the number of bound states in the continuum in 2D waveguides and quantum dots[2]).

When we impose outgoing boundary condition on the solutions of our studied model Hamiltonian with a potential barrier complex eigenvalues are obtained. The height of the potential barrier is V_0 and its width is labelled by L. From the analytical solutions presented in Eqs. (3.4)–(3.8) one gets that the requirement of zero amplitude for the incoming waves (i.e., $B(k) = 0$ in Eq. (3.8)) leads to the condition

$$\tan(kL) = \mathrm{i}\frac{k}{q}\,. \tag{4.15}$$

The solutions of Eq. (4.15) are discrete and can be labelled by an index n counting the number of nodes in the interaction region.

Tables 4.1 and 4.2 list the first ten resonance positions and widths for potential parameter $V_0 = 10$ and $V_0 = 100$ respectively. The quantum number n stands for the number of nodes in the resonance wavefunction. Here the resonance positions

---

[2] N. Moiseyev, *Phys. Rev. Lett*, **102**, 167404 (2009).

Table 4.1 *The complex energies of the first ten resonant states of the model potential barrier given in Chapter 3 with potential parameter* $V_0 = 10$ *and* $L = 1$.

n	0	1	2	3	4	5	6	7	8	9
$\tilde{\varepsilon}_n$	0.89	3.68	8.50	15.35	24.22	35.11	48.01	62.92	79.84	98.76
$\tilde{\Gamma}_n$	1.23	4.41	8.78	13.89	19.54	25.60	32.00	38.70	45.65	52.83

Table 4.2 *The complex energies of the first ten resonant states of the model potential barrier given in Chapter 3 with potential parameter* $V_0 = 100$ *and* $L = 1$.

n	0	1	2	3	4	5	6	7	8	9
$\tilde{\varepsilon}_n$	0.99	3.95	8.89	15.83	24.76	35.70	48.64	63.58	80.53	99.48
$\tilde{\Gamma}_n$	0.44	1.71	3.72	6.37	9.53	13.13	17.10	21.38	25.93	30.72

are scaled by, $\tilde{\varepsilon} = \varepsilon/\alpha$ and the resonance width is defined as $\tilde{\Gamma}_n = [-2\mathrm{Im}(E_n)]/\alpha$, where $\alpha = [(\hbar\pi/L)^2]/[2M]$. As $V_0 \to \infty$ the resonance positions converge to $\tilde{\varepsilon}_n = (n+1)^2$, where $n = 0, 1, 2, \ldots,$ while the resonance widths converge to $\tilde{\Gamma}_n = 0$ (see Ex. 3.6). Note that in this simple example $\tilde{\Gamma}_n$ grows when we move to higher energies. However, $\tilde{\Gamma}$ does not always increase monotonically with the resonance position ε and this behavior depends very much on the studied problem at hand.

What happens to the resonances when the height of the potential barrier is reduced and where are they accumulated in the limit of $V_0 \to 0$ when the potential is constant throughout? Figure 4.1 shows V_0-trajectory calculations which demonstrate the motion of the decay resonances (poles of the S-matrix) in the complex energy plane as V_0 is varied. As one goes to lower values of V_0 the resonance goes down as well while the resonance width, Γ, increases.

For each resonance there is a critical value of V_0 where it crosses the threshold energy $E = 0$ and eventually they move below the second threshold energy, $E = -V_0$ (shown in Fig. 3.1). When V_0 is small there are an infinite number of decay resonances with energy positions above the potential barrier ($E = 0$) while a finite number of resonances are embedded below at $E < 0$. Presumably as $V_0 \to \infty$ the resonances below the threshold energy accumulate at $E = -\infty$ with infinitely large widths. This phenomenon is hard to demonstrate for numerical reasons but it is illustrated in Fig. 4.1 where we obtained converged results for $V_0 \geq 10^{-12}$. All poles in Fig. 4.1, including those located below $E_{\mathrm{th}} = -V_0$, are obtained for outgoing boundary conditions (i.e. solutions of Eq. (4.15)). Are all of these poles

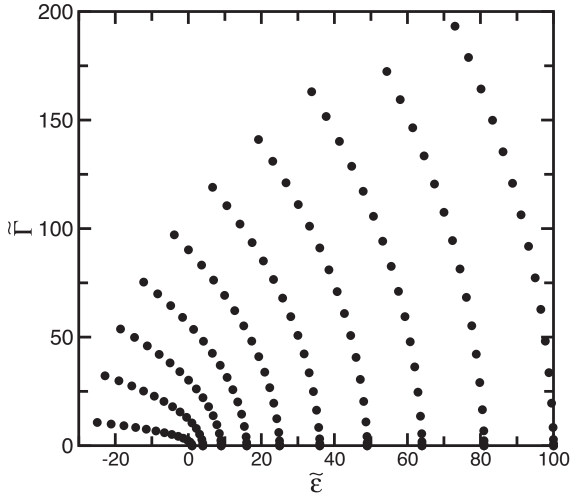

Figure 4.1 The dependence of the first ten resonance positions and widths on the height of the potential barrier described in Eq. (3.5). The width of the potential barrier is $L = 1$ au and the mass of the particle is $M = 1$ au. The results presented here are for the height of the potential barrier $V_0 = 10^{15-j}$ where $j = 0, 1, \ldots, 27$. Note that for $V_0 \to \infty$ the resonances become bound states of a particle-in-a-box problem. As we decrease V_0 the decay resonance states move below the top of the potential barrier ($E = 0$) and eventually move below the threshold energy $E = -V_0$. Presumably as $V_0 \to \infty$ they will accumulate at $E = -\infty$ with infinitely large width.

observable? There is no simple answer to this question. It depends heavily on the experimental setup. For example, consider the situation where we initially inject particles into the system at large V_0 and then by adiabatically decreasing the value of V_0 we may populate a resonance state which eventually will lie below $E_{\text{th}} = -V_0$. If we measure the number of the free particles detected far from the interaction region it will be smaller than the number of particles initially injected into the system due to the populated resonance state. This point will be discussed in the next chapter more elaborately.

Decay resonances which are positioned inside a potential barrier are sometimes referred to as barrier resonances. For example, for an Eckart potential barrier, $V(x) = V_0/\cosh^2(\alpha x)$, this type of resonance has been analytically calculated.[3] Often one might consider these resonances as non-observable poles of the S-matrix and thus not physically interesting. However, it was shown that they can also be used to describe the trapping of a light particle in between two heavy atoms such as in the case of ArHCl[4] (see later Ex. 4.6).

---

[3] V. Ryaboy and N. Moiseyev, *J. Chem. Phys.* **98**, 9618 (1993).

[4] E. Narevichius and N. Moiseyev, *Mol. Phys.* **94**, 897 (1998); *Chem. Phys. Lett.* **287**, 250 (1998).

4.2 Transitions of bound states to anti-bound and resonance states

We start this discussion by describing a "trick" we employed in calculating the decay resonances for the Eckart potential barrier mentioned above. The same method we have used there can be applied to *any* potential, $\hat{V}$, whose inverse, $-\hat{V}$, provides a potential well which supports bound states that can be calculated analytically.

Let us assume that for a given system an analytical expression for the bound state discrete spectrum, $E(n, \lambda)$, is known, where λ is some potential parameter. The bound state spectrum is derived by solving the time-independent Schrödinger equation while imposing outgoing boundary conditions on the solutions under the threshold energy. This implies that the momentum is purely imaginary. Although the distinction between the boundary conditions as outgoing or incoming depends on the sign of the real part of the wave vector, we use it here also for complex values of the momentum. Bound states are associated here with outgoing boundary conditions with $k = \mathrm{i}|k|$ rather than incoming waves with $k = -\mathrm{i}|k|$ in accordance with the accepted terminology in time-independent scattering theory.

We claim that for potentials which support a finite number of bound states, $n = 0, 1, 2, \ldots, N$, and for which the energies have an analytical formula, by increasing the value of n, $n = N + 1, N + 2, \ldots,$ an additional infinite number of discrete states are obtained. These states can be associated either with anti-bound (virtual) states (i.e., the asymptotes of the solutions are incoming waves with positive purely imaginary momentum) *or* with decay resonance states.

The transition from bound to resonance states can be observed by varying the potential parameter λ continuously. However, for the type of potential where the energy is known analytically, by making the transformation

$$\lambda \to -\lambda \tag{4.16}$$

one turns the potential upside down such that $\hat{V} \to -\hat{V}$, and if $\hat{V}$ had the shape of a well it is now a potential barrier. In such a case, by analytical continuation of the energy $E(n, \lambda) \to E(n, -\lambda)$ one gets discrete *complex* eigenvalues which are associated with the decay and capture resonances. In principle also anti-bound states can be obtained for specific values of the potential parameters.

The main conclusion from this analysis is that for a given model Hamiltonian there is a *single* expression for the discrete energy spectrum associated with the poles of the S-matrix. By varying either the quantum number n or one of the *real* potential parameters (λ in our above discussion) the nature of the poles can be changed.

In order to demonstrate the above arguments consider the Hamiltonian of the well-known Morse potential

$$V(x) = V_0(1 - \mathrm{e}^{-bx})^2 - V_0 \,, \tag{4.17}$$

where $E = 0$ is the threshold energy. The solutions with outgoing boundary conditions are discrete and can be found by solving the following differential equation:

$$\frac{\partial^2 \psi(x)}{\partial x^2} + \frac{2MV_0}{\hbar^2}\left(\mathrm{e}^{-2bx} - 2\mathrm{e}^{-bx} + \frac{E}{V_0}\right)\psi(x) = 0 \,. \tag{4.18}$$

By carrying out the transformations $z = 2\kappa \exp(-bx)$ and $\phi(z) = \sqrt{z}\psi(z)$, where

$$\kappa = \frac{\sqrt{2MV_0}}{b\hbar} > 0 \,, \tag{4.19}$$

one gets Whittaker's equation:

$$\frac{\partial^2 \phi(z)}{\partial z^2} + \left(-\frac{1}{4} + \frac{\kappa}{z} + \frac{1/4 - \lambda^2}{z^2}\right)\phi(z) = 0 \,, \tag{4.20}$$

where

$$\lambda = \mathrm{i}\frac{\sqrt{2ME}}{\hbar b} \,. \tag{4.21}$$

The quantization is obtained for outgoing waves when $1/2 + \lambda - \kappa = -n$, where $n = 0, 1, 2, \ldots$, which leads to the following eigenvalues:

$$E_n = -V_0\left(1 - \frac{n + 1/2}{\kappa}\right)^2 \,. \tag{4.22}$$

Consequently, the eigenfunctions of the Morse potential are given by

$$\psi_n(z) = N_n \mathrm{e}^{-z/2} z^{\kappa - n - 1/2} L_n^{(2\kappa - 2n - 1)}(z) \,, \tag{4.23}$$

where $L_n^{(2\kappa-2n-1)}(z)$ are generalized Laguerre polynomials and N_n is a normalization factor. Since $z = 2\kappa \exp(-bx)$, when $x \to \infty$, $z \to 0$. Therefore, the asymptotic behavior of ψ_n is dominated by the $z^{\kappa-n-1/2} = z^{\lambda}$ term which means that

$$\lim_{x\to\infty} \psi_n(x) \propto \mathrm{e}^{-\lambda bx} = \mathrm{e}^{\mathrm{i}kx} \,, \tag{4.24}$$

where $k = \sqrt{2ME}/\hbar$ is the momentum attributed to the wavefunction. The bound states are associated with square integrable functions (i.e., the wave vector is equal to $k = +\mathrm{i}|k|$). This condition puts a limit on the number of the bound states located inside the Morse potential well. The $N + 1$ bound states are labelled by the number of the nodes, $n = 0, 1, 2, \ldots, N$, where N is the largest integer smaller than $\kappa - 1/2$.

The ground state, $|n = 0\rangle$, is situated below the threshold energy slightly above the bottom of the Morse potential well. The energy increases with the quantum number n up to E_N, which is the highest excited bound state which is embedded just below the threshold energy $E = 0$.

What happens if we keep increasing the quantum number n? The energies of solutions obtained for $n = N + 1, N + 2, \ldots$ in Eq. (4.22) decrease and eventually attain values below the minimum of the potential well (up to $E = -\infty$). These states are associated with incoming asymptotes where $k = -\mathrm{i}|k|$. Therefore, these solutions diverge exponentially and are considered as *anti-bound* states which are also known as *virtual* states. Often these solutions are denoted as the non-physical poles of the S-matrix. Here we showed that the Morse potential does not support decay and capture resonances (no states with outgoing boundary conditions with $E > 0$). Note that in a very similar way it is possible to prove that the symmetric Rozen–Morse potential $V = -V_0 \cosh^2(ax)$ supports only bound and anti-bound states. In the absence of decay resonances there is no sharp structure (e.g., peaks) in the density of states or in the cross section. However, it does not imply that these potentials are always reflection-less potentials.

Now, when we vary the potential strength parameter V_0 by carrying out the transformation $V_0 \to -V_0$ we get from Eq. (4.22) an infinite number of discrete complex eigenvalues

$$E_n = V_0 \left[1 - (\frac{n + 1/2}{\kappa})^2 \right] \pm 2\mathrm{i} V_0 \frac{n + 1/2}{\kappa} \,. \tag{4.25}$$

The different sign of the imaginary part of the complex energy corresponds to the two different types of boundary conditions. The positive imaginary part corresponds to incoming waves solutions associated with capture-resonances, whereas the negative imaginary part corresponds to decay resonance solutions with outgoing boundary conditions.

Exercise 4.2

Calculate the poles of a parabolic potential barrier (the inverse of the harmonic oscillator potential, $V = kx^2/2$ where the potential strength parameter is $k = M\omega^2$). Explain why these poles can't be considered as barrier resonances.

Other examples for analytical expressions for barrier resonances can be derived for the potentials in the following exercises.

Exercise 4.3

Find the energies of the barrier resonances for the inverted symmetric Rosen–Morse potential given by $V = V_0/\cosh^2(ax)$. This potential is also known as the Eckart potential barrier in chemical reactions.

Exercise 4.4

Find the energies of the barrier resonances for an inverted non-symmetric Rosen–Morse potential $V = -V_0 \cosh^2 b[\tanh(ax - b) + \tanh(b)]^2 + V_0 \exp(-2b)$.

Exercise 4.5

Find the energies of the barrier resonances for the following spherically symmetric potential: $V = V_0(-\gamma/r^2 + 1/r)$. The solution for the bound states of such a potential were introduced for the inverted potential by Landau and Lifshitz in their quantum mechanics textbook.[5] Such a potential provides a model Hamiltonian of an electron scattering from negative ions).

Barrier resonances are quite often very broad ones (in particular for "Gaussian" like potentials) and are regarded as non-physical solutions. However, as mentioned above, this is not necessarily the situation and these resonances might be related to observable phenomena. To further illustrate this point consider the following exercise.

Exercise 4.6

Let A be a light particle with the mass M = 2000 au (approximately that of an hydrogen atom), which moves freely in a plane excluding two disk areas (i.e., $V = \infty$, when $x^2 + (z \pm R/2)^2 \leq r^2$, where x, z denote the coordinates of A in the plane). The two disks each have a radius r with their centers separated by a distance R. The two disks describe two heavy atoms B and C.

Evaluate the 1D effective model Hamiltonian $H(x, z)$ by treating the x coordinate as a slowly varying parameter. Take $R = 8$ au to be the distance between the centers of mass of the two heavy atoms and their radius to be equal to $r = 2.5$ au. Under what conditions is the adiabatic approximation valid in such case? Calculate the adiabatic

---

[5] L. D. Landau and E. M. Lifshitz, *Quantum Mechanics*, New York, Pergamon, 1965.

potentials, $E_{n_z}(x); n_z = 1, 2, \dots, 5$. What are the resonance positions and widths when the dynamical potential barriers, E_{n_z}, are approximately described by Eckart potential barriers, $V_0/\cosh^2(\alpha x)$? Note that by fitting E_{n_z} to an analytical smooth function, such as the Eckart potential, we remove from the problem the artificial discontinuity of E_{n_z} which results from the description of the two atoms as two hard disks (or spheres in 3D calculations).

4.3 Bound, virtual and resonance states for a 1D potential

To illustrate the behavior of the different poles of the scattering matrix we will now discuss the transitions between bound and resonance states in a one-dimensional symmetric rectangular well. We will show that as a one-dimensional symmetric rectangular well becomes shallower, the bound states move up to the threshold and eventually disappear, but not without leaving a trace. Shortly after a bound state ceases to exist, a new resonance state appears above the well. In the interim a virtual state (anti-bound state) is formed at the threshold energy which then coalesces on its way down (along the energy axis) with another virtual state that is moving up towards it. This coalescence gives rise to a pair of complex energy states inside the well which eventually become a resonance above the well and its conjugate virtual state. All this is readily deduced from the work of H. M. Nussenzveig,[6] which may be rightfully considered a quite exhaustive though rather intricate treatment of the problem. In contrast to it the analysis we present here,[7] which is mainly a quasi-analytical study, is distinguished by its extraordinary simplicity which offers an excellent visualization and a thorough grasp of the subject.

A one-dimensional symmetric rectangular potential-well is defined by

$$V(x) = \begin{cases} 0 & (x < 0 \text{ or } x > L), \\ -V_0 & (0 < x < L), \end{cases}$$

where V_0, the depth of the well, is a positive number. The corresponding time-independent Schrödinger equation is

$$\begin{cases} \Psi'' + k_0^2 \Psi = 0, \quad k_0 = \sqrt{2ME}/\hbar & (x < 0 \text{ or } x > L), \\ \Psi'' + k^2 \Psi = 0, \quad k = \sqrt{2M(E + V_0)}/\hbar & (0 < x < L), \end{cases}$$

---

[6] H. M. Nussenzveig, *Nucl. Phys.* **11**, 499 (1959).

[7] Based on R. Zavin and N. Moiseyev, *J. Phys. A* **37**, 4619 (2004).

and its general solution is given by

$$\begin{cases} \Psi = C\mathrm{e}^{\mathrm{i}k_0x} + C'\mathrm{e}^{-\mathrm{i}k_0x} & (x < 0)\,, \\ \Psi = A\mathrm{e}^{\mathrm{i}kx} + B\mathrm{e}^{-\mathrm{i}kx} & (0 < x < L)\,, \\ \Psi = D\mathrm{e}^{\mathrm{i}k_0x} + D'\mathrm{e}^{-\mathrm{i}k_0x} & (L < x)\,, \end{cases}$$

where A, B, C, C', D and D' are some constants which are subject to boundary conditions and the functions $\mathrm{e}^{\mathrm{i}k_0x}$ and $\mathrm{e}^{-\mathrm{i}k_0x}$ represent waves moving to $+\infty$ and $-\infty$ respectively. By requiring $C = D' = 0$ (or, alternatively, $C' = D = 0$) together with the continuity of Ψ and Ψ' a transcendental equation for the outgoing (incoming) waves is obtained.

As previously discussed, outgoing waves are represented by $\mathrm{e}^{\mathrm{i}k_0x}$ when $x \to +\infty$ and by $\mathrm{e}^{-\mathrm{i}k_0x}$ when $x \to -\infty$. However, real solutions of the transcendental equation are possible only for $E < 0$, when k_0 is pure imaginary ($k_0 = \mathrm{i}|k_0|$), in which case the outgoing waves become decaying exponents pertaining to the bound states. That is, $\Psi \to \mathrm{e}^{-|k_0|x}$ as $x \to \infty$.

Incoming boundary conditions stand for an inward flow and therefore are represented by $\mathrm{e}^{-\mathrm{i}k_0x}$ when $x \to +\infty$ and by $\mathrm{e}^{+\mathrm{i}k_0x}$ when $x \to -\infty$.

In general, the transcendental equation for the outgoing waves (associated with the "+" sign) and for the incoming waves (associated with the "−" sign) is

$$2\cot kL = \frac{\pm\mathrm{i}(k^2 + k_0^2)}{kk_0}\,. \tag{4.26}$$

The complex equation (4.26) can only be solved numerically. One way to do so is by substituting k_0 and k in Eq. (4.26) when one gets that the solution is obtained for

$$\Delta(E) = \Delta(E) = \tan(\sqrt{2M(E+V_0)}L) \pm 2\mathrm{i}\frac{\sqrt{E(E+V_0)}}{2E+V_0} = 0\,. \tag{4.27}$$

For bound and anti-bound states $\mathrm{Im}(E) = 0$ while for decay resonance states $\mathrm{Im}(E) < 0$ and for the conjugate virtual states (so-called capture resonances) $\mathrm{Im}(E) > 0$. The "+" sign in Eq. (4.27) stands for the bound and decay resonance states and the "−" sign is for the virtual states (including the anti-bound states and the so-called capture resonances). For example, the bound and resonance states in the interval of $E_0 < \mathrm{Re}(E) < E_\mathrm{f}$ and $\Gamma_\mathrm{f} < -2\mathrm{Im}(E) \leq 0$ can be obtained by dividing the given complex E-plane into a finite number of grid points. For each of the grid points the phase of $\Delta(E)$ is calculated. The results are divided into four different groups according to the four possible quarters in the complex E-plane. When different colors are associated with different quarters in the complex plane a four color map is obtained. *The desired solutions are the points where all four colors intersect*. See, for example, the results presented in Fig. 4.2.

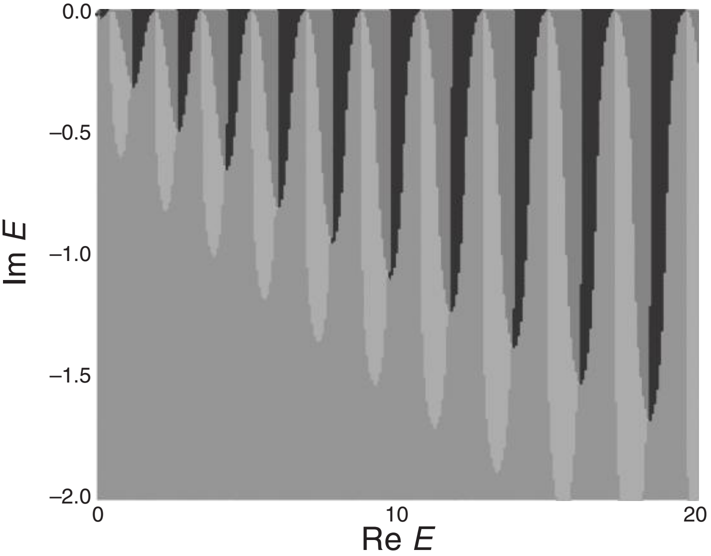

Figure 4.2 The error in the calculations of decay resonances, see Eq. (4.27), for a symmetric rectangular potential well with the depth $V_0 = 10$ and width $L = 10$ ($\hbar = 1$, $M = 1$). The decay resonances are obtained at the intersection points of the four shades. Each shade is associated with the phase of the errors. All errors which are embedded within the same quarter in the complex E-plane are assigned the same shade.

Refined calculations and plots provide the resonance positions and widths within a desired accuracy. Such a procedure, however, does not provide us with the mechanism for the transitions from bound to resonance state as the potential parameter V_0 is varied. A careful variation of V_0 shows that the ground bound state never disappears, the first excited bound state disappears at a critical value of V_0 but never returns as a decay resonance state, whereas all other excited bound states disappear at critical values of V_0 but reappear as resonances at smaller critical values of V_0.

4.4 The mechanism of transition from a bound state to a resonance state

The mechanism of transition from a bound state to a resonance becomes evident when introducing two new variables in the solution of Eq. (4.26):

$$\alpha = \sqrt{1 + \frac{E}{V_0}} \quad \text{and} \quad \gamma = \sqrt{\frac{2MV_0L^2}{\hbar^2}}\,, \tag{4.28}$$

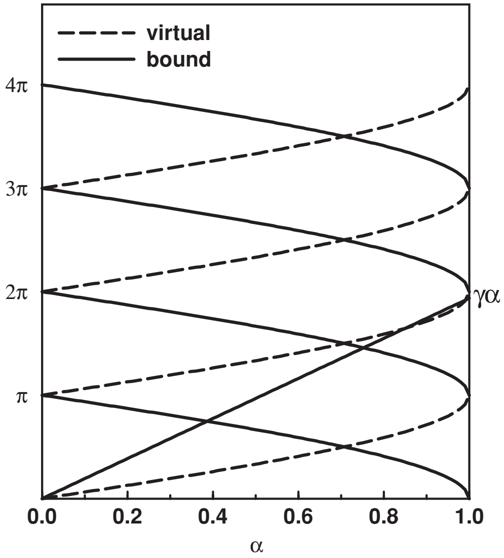

Figure 4.3 The virtual, anti-bound and bound states obtained by varying the depth of the rectangular potential well. α is defined in Eq. (4.28).

in terms of which Eq. (4.26) for the bound states is expressed as

$$\gamma\alpha = (n-1)\pi + 2\cos^{-1}\alpha\,, \quad (n = 1, 2, \ldots)\,. \tag{4.29}$$

Exercise 4.7

Show that in the variables defined in Eq. (4.28) the bound states solutions of Eq. (4.26) are given by Eq. (4.29).

Since the right hand side of Eq. (4.29) is independent of γ, varying the depth of the well leaves it unaltered while the slope of the straight line on the left changes. In Fig. 4.3 the graphical solution (solid lines) is plotted for three different γs. Values of α at the points of intersection of the straight line with the branches of $2\cos^{-1}\alpha$ give the energies of the corresponding bound states according to the formula

$$E = -V_0(1-\alpha^2)\,. \tag{4.30}$$

It is immediately evident from the graph that as the well becomes shallower, the bound states move towards the threshold where they eventually disappear, with the exclusion of the first bound state which always remains inside the well. The number of the bound states for a given well depth is clearly the greatest integer contained in the quantity $(\gamma/\pi + 1)$.

A graphical solution for real virtual states described by Eq. (4.26) can be done in an analogous manner to that of the bound states. Using the same definition for α and γ, the transcendental equation for virtual states transforms to

$$\gamma\alpha = (n-1)\pi + 2\cos^{-1}\sqrt{1-\alpha^2}\,, \quad (n = 1, 2, \ldots) \tag{4.31}$$

Exercise 4.8

Show that in the variables defined in Eq. (4.28) the virtual states solutions of Eq. (4.26) are given by Eq. (4.31).

The graphical solution of this equation is portrayed in Fig. 4.3 by dashed lines. It should be noted that the parity of the real virtual states corresponding to consecutive branches of the right hand side of Eq. (4.31) is in reversed order to that of the bound states. Namely, for bound states *odd* numbers of nodes are associated with *even* quantum number n, whereas for anti-bound states even numbers of nodes are obtained for odd values of n. The real part of the energy of complex virtual state is, of course, identical to the real part of the corresponding conjugate resonance state and the imaginary part has a phase equal to π relative to the resonance.

To get an insight into what happens as the depth of the well is varied, the graphical solutions for the bound and for the real virtual states are combined on one diagram (see Fig. 4.3). By inspecting the diagram it can be readily concluded that every time that an nth bound state with $n \geq 3$ reaches the threshold as a result of diminishing the depth of the well, a new $(n-1)$th virtual state is formed there in addition to an already existing $(n-1)$th virtual state. As the depth of the well is further decreased these two virtual states move toward each other, coalesce and then disappear. Solving simultaneously the complex transcendental equation for the incoming waves, we find that right after the two real solutions merge into one, subsequent decrease of the depth of the well makes this solution complex. At first the new complex virtual state sits inside the well, but as the bottom of the well is continuously pushed up, it eventually crosses the threshold. Of course, in the moment when a new complex incoming wave state is formed its complex conjugate appears as a new solution for the outgoing wave transcendental equation. Thus a disappearing bound state turns into a resonance via a virtual state collision. This is true for any $n \geq 3$. Figure 4.4 shows these transitions for the $n = 3$ bound state. The $n = 2$ bound state never becomes a resonance, consistently with the fact that the $n = 1$ real virtual state is essentially different from those above it, as is apparent from the graphical solution.

The values of the potential depths at which branch points, the points of coalescence of two virtual states, occur can be determined by demanding the two sides

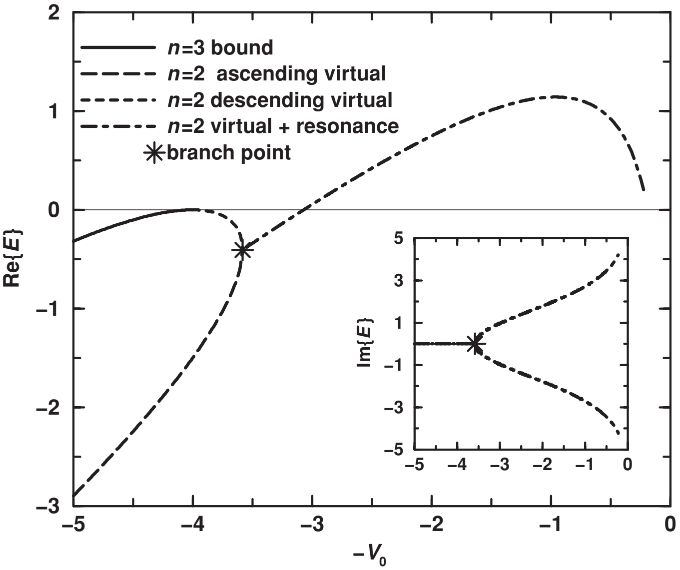

Figure 4.4 Disappearance of the $n = 3$ bound state and the formation of a new decay (shape-type) resonance as a result of diminishing the depth of the rectangular potential well. The parameters are given by $M = 0.5$, $L = \pi, \hbar = 1$.

of Eq. (4.31) to be tangent to each other at the point of their intersection. The tangency requirement alone yields that the energy of the branch point's virtual state is independent of n and is given by

$$E_{\text{bp}} = -\frac{2\hbar^2}{ML^2}\,. \tag{4.32}$$

As discussed above, the branch points (bifurcation points) where the resonances are "born" are at real energies embedded below the threshold energy of the rectangular potential well. The transcendental equation obtained when the intersection is also taken into account is

$$\sqrt{\gamma^2 - 4} = (n-1)\pi + 2\cos^{-1}\frac{2}{\gamma}\,. \tag{4.33}$$

For $n = 1$ this equation is very easy to solve ($\gamma = 2$) and it corresponds to $-V_0 = E_{\text{bp}}$, which means that after the $n = 2$ bound state turns into the $n = 1$ virtual state it moves down towards the bottom of the well until it collides with it and disappears.

It also maybe interesting to note from Fig. 4.3 that for certain well depths some n-th bound state will have the same energy as the n-th virtual state. The relation that must hold between V_0 and n for this to happen is

$$V_0 = \frac{\hbar^2\pi^2(n-\frac{1}{2})^2}{ML^2}\,, \tag{4.34}$$

and the energy of the n-th bound and virtual states will then be

$$E = -\frac{1}{2}V_0\,. \tag{4.35}$$

The bound to resonance state transformation is quite vivid and rich. In the next section we emphasize the fact that there is no way to understand or explain this physically observable phenomenon without the use of the so-called non-physical virtual states.

4.5 Concluding remarks on the physical and non-physical poles of the S-matrix

(1) The so-called physical poles of the S-matrix are the eigenvalues of the time-independent Schrödinger equation which are obtained by imposing outgoing boundary conditions on the corresponding eigenfunctions. These solutions are embedded in the fourth quadrant of the complex energy plane. The real eigenvalues are the bound states and the complex ones are the decay resonance states. In principle the bound states are associated with real eigenvalues embedded below the threshold energy of the system (i.e., the energy where the potential vanishes). However, it might happen due to very specific symmetry properties of the studied Hamiltonian that the bound states are embedded in the continuum. Of course, any infinitesimal small perturbation which does not commute with this special symmetry operator will transform the bound states in the continuum into decay resonance states.

(2) The so-called non-physical (virtual) poles are also obtained by imposing incoming boundary conditions on the solutions of the time-independent Schrödinger equation. These eigenvalues can be either real or complex. The real non-physical eigenvalues are the anti-bound states. The non-physical complex eigenvalues are embedded in the first quadrant of the complex energy plane and are the complex conjugates of the eigenvalues of the decay resonance eigenvalues. These non-physical complex eigenvalues are associated with exponential divergent asymptotes and are referred to as "capture resonance states".

(3) The transition between bound and decay resonance solutions can be a complicated phenomenon. For a square rectangular potential well it is shown that these transitions happen via the transformation of bound states into anti-bound states. The decay and capture resonances are created in this case upon coalescence of two anti-bound states. It is a point of interest that the resonances are "born" while the resonance positions (i.e., the real part of the complex eigenvalues) are below the threshold energy and therefore the new born resonances are not embedded in the continuous part of the spectrum.

4.6 Resonances for a time-dependent Hamiltonian

The above introductory considerations have been focused on the resonance states associated with the solutions of the time-independent Schrödinger equation. We should emphasize here, however, that there is no need to limit ourselves to time-independent Hamiltonians. The case of generally time-dependent Hamiltonians can be treated in an entirely analogous fashion to the time-independent case using the so-called (t, t') formalism. A detailed self-contained discussion of the (t, t') method is beyond the scope of the present work. For more information, the reader is referred to the fundamental work on this subject.[8] Here we provide only a very brief sketch of the underlying theory.

The solution of the time-dependent Schrödinger equation (using atomic units where $\hbar = 1$, $e = 1$ and $m_\mathrm{e} = 1$)

$$\hat{H}(\mathbf{r}, t)\psi(\mathbf{r}, t) = \mathrm{i}\partial_t \psi(\mathbf{r}, t) \tag{4.36}$$

can be expressed as a special case of a more general solution

$$\psi(\mathbf{r}, t) = \left[\Psi(\mathbf{r}, t', t)\right]_{t'=t} , \tag{4.37}$$

where $\Psi(\mathbf{r}, t', t)$ is the solution of the time-dependent Schrödinger equation for the time (t) independent Hamiltonian $\mathcal{H}(\mathbf{r}, t')$,

$$\Psi(\mathbf{r}, t', t) = \mathrm{e}^{-\mathrm{i}\mathcal{H}(\mathbf{r},t')t}\,\Psi(\mathbf{r}, t', t = 0) \,. \tag{4.38}$$

Here the physical time-dependent Hamiltonian $\hat{H}(t)$ is replaced by the generalized Floquet-type time-independent Hamiltonian operator where t has been replaced by t':

$$\mathcal{H}(\mathbf{r}, t') = -\mathrm{i}\partial_{t'} + \hat{H}(\mathbf{r}, t') \,. \tag{4.39}$$

The incorporation of the additional coordinate t' enables us to obtain an analytical expression for the time evolution operator of a time-dependent Hamiltonian. The "trick" we are using here is based on the fact that in the time-dependent Schrödinger equation, the energy operator $\mathrm{i}\partial_t$ is a first order derivative operator (unlike the kinetic energy operator which is a second order derivative operator $-\nabla^2_{x,y,z}$). This fact enables us to use the so-called chain rule for derivatives (for the sake of clarity we replace ∂_t by $\mathrm{d}/\mathrm{d}t$ in the Schrödinger equation, keeping in mind that there are spatial variables which are held fixed):

$$\frac{\mathrm{d}F(t)}{\mathrm{d}t} = \left[\frac{\partial G(t, t')}{\partial t} + \frac{\partial G(t, t')}{\partial t'}\right]_{t'=t} , \tag{4.40}$$

---

[8] U. Peskin and N. Moiseyev, *J. Chem. Phys.*, **99**, 4590–4596 (1993).

where

$$\left[G(t,t')\right]_{t'=t} = F(t)\,. \tag{4.41}$$

It is possible to add additional auxiliary coordinates provided we require that

$$\left[G(t,t',t'',\ldots)\right]_{t'=t''=\cdots=t} = F(t)\,. \tag{4.42}$$

The above generalized Hamiltonian $\mathcal{H}$ depends not only on the position and momentum operators of different spatial degrees of freedom of the studied system, but also on an additional coordinate t' and on its "canonical conjugate momentum", $-\mathrm{i}(\partial/\partial t')$. Each particular solution of the time-dependent Schrödinger equation,

$$\mathrm{i}\,\frac{\partial}{\partial t}\,|\Psi(t)\rangle = \hat{H}(t)\,|\Psi(t)\rangle\,, \tag{4.43}$$

can be then expressed in an equivalent form,

$$|\Psi(t)\rangle = |\Phi(t'=t,t)\rangle\,; \tag{4.44}$$

where

$$|\Phi(t',t)\rangle = \mathrm{e}^{-\mathrm{i}\mathcal{H}(t-t_0)}\,|\Psi(t_0)\rangle\;\delta(t'-t_0)\,. \tag{4.45}$$

Reflections in the spatial space are due to the fact that outgoing plane waves, $\mathrm{e}^{+\mathrm{i}kx}$, and incoming waves, $\mathrm{e}^{-\mathrm{i}kx}$, are degenerate states of the kinetic energy operator. Due to the potential energy operator an eigenstate of the Hamiltonian is a linear combination of the outgoing and incoming states. For example, in 1D problems where a particle with the momentum $\hbar k > 0$ is scattered from a static potential barrier centered at $x = 0$ the eigenfucntion in the asymptotic region (i.e., eigenfunction of the kinetic energy operator) are given by $\Psi_k(x<0) = \mathrm{e}^{\mathrm{i}kx} - R(k)\mathrm{e}^{-\mathrm{i}kx}$, where $|R(k)|^2$ is the reflection factor. Can we have reflections along the new additional coordinate t' when the potential is time dependent? The answer is no. Unlike the situation in the spatial domain, $-\mathrm{i}\frac{\partial}{\partial t'}$ is a first order differential operator, and therefore $\mathrm{e}^{+\mathrm{i}\omega t'}$ and $\mathrm{e}^{-\mathrm{i}\omega t'}$ are *not* two degenerate states and cannot be mixed by the presence of a potential barrier which will appear at later times. Hence, there are no interferences between the forward and backward time-propagated state vectors even when the physical Hamiltonian is time dependent. This is the reason why there are no reflections at the present time from future events. Due to the absence of reflections along the t' coordinate, we can impose periodic boundary conditions on the eigenstates of $\mathcal{H}$, without distorting the given physical problem, even when the physical Hamiltonian $\hat{H}(t')$ is not time periodic (e.g., when the atomic or the molecular systems are exposed to pulsed laser fields). That is,

$$\mathcal{H}\,|\Phi_\alpha(t')\rangle = \mathcal{E}_\alpha\,|\Phi_\alpha(t')\rangle\,; \tag{4.46}$$

with

$$0 \leq t' \leq T_{\mathrm{p}}\,, \quad |\Phi_\alpha(t')\rangle = |\Phi_\alpha(t' + T_{\mathrm{p}})\rangle\,; \tag{4.47}$$

where the period T_{p} is much larger than the duration of the laser pulse. The above eigenvalues $\mathcal{E}_\alpha$ of $\mathcal{H}$ are termed the quasi-energies of the studied problem and are defined modulo $(2\pi/T_{\mathrm{p}})$.

In the case of time-periodic Hamiltonians, $\hat{H}(t) = \hat{H}(t + T)$, the eigenstates of $\mathcal{H}$ are known as the Floquet quasi-energy states. Therefore one can chose $T_{\mathrm{p}} = NT$, where $N \geq 1$.

When outgoing boundary conditions are imposed on the spatial dependence of the eigenfunctions of $\mathcal{H}$, the complex Floquet quasi-energy eigenvalues are obtained in a similar manner to that described above for time-independent Hamiltonians. The $(t,\, t')$ procedure enables us to apply formalisms and methods which were developed for time-independent problems to time-dependent problems in a quite straightforward manner.

One common application of such time-dependent formalism is the study of matter–radiation interaction. For instance, in systems of atoms or molecules interacting with intense laser fields the complex Floquet quasi-energy eigenvalues are associated with the photo-induced resonance phenomenon. That is,

$$\mathcal{E}_\alpha = E_\alpha - \mathrm{i}/2\Gamma_\alpha\,, \tag{4.48}$$

where Γ_α provides the rate of the photo-induced decay of the particles (e.g. electrons) at the energy E_α.

4.7 Conservation of number of particles

In their book on quantum mechanics Landau and Lifshitz[9] wrote “At large distances the wavefunction of the quasi-stationary state (the outgoing wave) contains the factor

$$\mathrm{e}^{\mathrm{i}r\sqrt{2m(E_0 - \frac{1}{2}\Gamma)}/\hbar} \tag{4.49}$$

which increases exponentially as $r \to \infty$. The imaginary part of the root $\mathrm{Im}\sqrt{2m(E_0 - \frac{1}{2}\Gamma)} < 0$. Hence the normalization integral $\int |\psi|^2 \mathrm{d}V$ for these functions diverges. It may be noted, incidentally, that this resolves the apparent contradiction between the decrease with time of $|\psi|^2$ and the fact that the normalization integral can be shown from the wave equation to be a constant”.

---

[9] L. D. Landau and E. M. Lifshitz, *Quantum Mechanics*, Section 132, Oxford, Pergamon Press, 1965.

Let us explain this point in greater detail. The physical interpretation of the divergence property of the resonance wavefunction

$$\phi_{\text{res}}(x) \to e^{+ik_{\text{res}}x} \to \infty \tag{4.50}$$

as $x \to +\infty$ and where

$$E_{\text{res}} \equiv \epsilon - \frac{i}{2}\Gamma = \frac{(\hbar k_{\text{res}})^2}{2M} \tag{4.51}$$

was that at $x = \infty$ one observes "particles" which formed a long time ago.

However, this exponential divergence property of the resonance asymptote at $x \to \infty$ is balanced by the exponential decay of the resonance at long times $t \to \infty$. This fact made me write without giving a detailed explanation that "due to the exponential divergence of ϕ_{res} the number of particles is conserved *only* when *both* the reaction coordinate, r, and the time, t, approach the limit of infinity".

Here we wish to elaborate the discussion on the conservation of number of particles in the extended coordinate–time space. Up to some normalization factor, the asymptote of the solution of the time-dependent Schrödinger equation which is associated with the resonance phenomenon is given by

$$\Psi_{\text{res}}(x > 0, t) = e^{-iE_{\text{res}}t/\hbar} e^{+ik_{\text{res}}x} \tag{4.52}$$

and similarly the resonance asymptote at $x \to -\infty$ is given by

$$\Psi_{\text{res}}(x < 0, t) = e^{-iE_{\text{res}}t/\hbar} e^{-ik_{\text{res}}x} . \tag{4.53}$$

If we think of the resonance phenomenon in terms of a wavepacket evolving in conventional quantum mechanics, then it is initially localized in the interaction region. Eventually this wavepacket escapes the interaction region and becomes a free wave in the asymptotes. Thus the resonance state is confined in a region

$$-\frac{L(t=0)}{2} \le x \le +\frac{L(t=0)}{2} . \tag{4.54}$$

As the wavepacket evolves in time the confinement region expands and $L(t) \to \infty$ as $t \to \infty$.

If we think of the resonance in terms of a discrete eigenvalue with complex energy which is confined in a relevant area bounded by $L(t)$, then in order to conserve the momentum of the free particle in the extended coordinate–time space we should take the limit of $L(t) \to \infty$ and $t \to \infty$ such that

$$\frac{L(t)}{t} = \frac{\hbar k_{\text{res}}}{M} . \tag{4.55}$$

This means that the boundary $L(t)$ is moving with velocity corresponding to the momentum of the resonance state, i.e. $L(t) = [\hbar k_{\text{res}}/M]t$. Therefore, the resonance wavefunction at the edge of the box, $x = L(t)/2$, at time t is given by

$$\Psi_{\text{res}}(x = L(t)/2, t) = \mathrm{e}^{-\frac{\mathrm{i}t}{\hbar}E_{\text{res}}}\mathrm{e}^{+\frac{\mathrm{i}t}{\hbar}\frac{(\hbar k_{\text{res}})^2}{2M}} = 1\,. \tag{4.56}$$

This shows that the spatial divergence of the resonance wavefunction is compensated by its temporal decay, thus making its use to describe physical phenomena possible.

This result is identical to the result which is obtained for a free particle when the standard formalism of quantum mechanics is used. However, within the standard formalism of quantum mechanics this result is obtained without the need to treat time as an additional coordinate which is coupled to the spatial coordinates. In the standard quantum mechanical formalism time serves as a parameter rather than as an additional coordinate. However, this is not a severe problem, and by using the (t, t') method which has been presented in the previous section of this chapter, the extension of the definition of space to include also the t' coordinate can be carried out in the standard quantum mechanics formalism as in the non-Hermitian formalism of quantum mechanics. What is unique in the non-Hermitian formalism of quantum mechanics is that the spatial and the t' coordinates are coupled to one another even when the Hamiltonian is time independent. As has been shown here this coupling is introduced in non-Hermitian quantum mechanics when t'(time) $\to \infty$ and when the spatial coordinate $x \to \infty$, in order to conserve the number of particles in the coordinate–time extended space.

4.8 Solutions to the exercises

Answer to Exercise 4.1

When the asymptotes at both thresholds are $E^{\text{th}}_{\pm} = 0$, then

$$\frac{(\hbar k_n)^2}{2M} = \varepsilon_n - \frac{\mathrm{i}}{2}\Gamma_n \tag{4.57}$$

and therefore since $k_n = \mathrm{Re}(k_n) + \mathrm{i}\mathrm{Im}(k_n)$ we get that

$$\frac{\hbar^2}{2M}\left([\mathrm{Re}(k_n)]^2 - [\mathrm{Im}(k_n)]^2 + 2\mathrm{i}\mathrm{Re}(k_n)\mathrm{Im}(k_n)\right) = \varepsilon_n - \frac{\mathrm{i}}{2}\Gamma_n\,. \tag{4.58}$$

By comparing the imaginary part of the two sides of Eq. (4.58) we obtain that

$$\Gamma_n = -\frac{2\hbar^2}{M}\mathrm{Re}(k_n)\mathrm{Im}(k_n)\,. \tag{4.59}$$

We shall now prove that the coefficient $B(k)$ of the outgoing wave of the resonance is associated with the flux normalization constant as appearing in the standard formalism of quantum mechanics, although here k attains a complex value.

We start by multiplying the TISE for the resonant state by $\Psi_n^*(x)$ from the left,

$$\Psi_n^*(x)\hat{H}\Psi_n(x) = \left(\varepsilon_n - \frac{\mathrm{i}}{2}\Gamma_n\right)|\Psi_n(x)|^2 \, . \tag{4.60}$$

and similarly we multiply for the TISE for the complex conjugate state, $\Psi_n^*(x)$, by $\Psi_n(x)$,

$$\Psi_n(x)\hat{H}\Psi_n^*(x) = \left(\varepsilon_n + \frac{\mathrm{i}}{2}\Gamma_n\right)|\Psi_n(x)|^2 \, . \tag{4.61}$$

Subtracting the two equations results in

$$\begin{aligned}
\frac{\hbar^2}{2M}\left(\Psi_n^*(x)\frac{\mathrm{d}^2}{\mathrm{d}x^2}\Psi_n(x) - \Psi_n(x)\frac{\mathrm{d}^2}{\mathrm{d}x^2}\Psi_n^*(x)\right) &= \mathrm{i}\Gamma_n|\Psi_n(x)|^2 \, , \\
\frac{\hbar^2}{2M}\frac{\mathrm{d}}{\mathrm{d}x}\left(\Psi_n^*(x)\frac{\mathrm{d}}{\mathrm{d}x}\Psi_n(x) - \Psi_n(x)\frac{\mathrm{d}}{\mathrm{d}x}\Psi_n^*(x)\right) &= \mathrm{i}\Gamma_n|\Psi_n(x)|^2 \, , \\
\frac{\hbar^2}{2M}\left[\Psi_n^*(x)\frac{\mathrm{d}}{\mathrm{d}x}\Psi_n(x) - \Psi_n(x)\frac{\mathrm{d}}{\mathrm{d}x}\Psi_n^*(x)\right]_0^{x_0} &= \mathrm{i}\Gamma_n\int_0^{x_0}|\Psi_n(x)|^2\mathrm{d}x \, .
\end{aligned} \tag{4.62}$$

In the asymptote $\Psi_n(x)$ has the form

$$\Psi_n(x \geq x_0) = \gamma_n\sqrt{\frac{M}{\hbar k_n}}\mathrm{e}^{+\mathrm{i}k_n x} \tag{4.63}$$

and its value at the origin $\Psi_n(x = 0) = 0$. By substituting into Eq. (4.62) one gets that

$$\Gamma_n = \hbar|\gamma_n|^2\frac{\mathrm{Re}(k_n)}{|k_n|}\frac{\mathrm{e}^{-2(\mathrm{Im}(k_n))x_0}}{\int_0^{x_0}\mathrm{d}x|\Psi_n(x)|^2} \, . \tag{4.64}$$

In the derivation of Eq. (4.64) we assume that γ is a constant. In order to justify this conjecture we will prove now that

$$\Gamma_n[\text{Eq. (4.64)}] = \Gamma_n[\text{Eq. (4.59)}] \, . \tag{4.65}$$

Since $\mathrm{Im}(k_n) < 0$ the asymptote of the resonance wavefunction exponentially diverges and therefore, as $x_0 \to \infty$,

$$\begin{aligned}\int_0^{x_0} \mathrm{d}x |\Psi_n(x)|^2 &= \int_0^{x'} \mathrm{d}x |\Psi_n(x)|^2 + \int_{x'}^{x_0} \mathrm{d}x |\gamma_n \sqrt{\frac{M}{\hbar k_n}} \mathrm{e}^{\mathrm{i}k_n x}|^2 \\ &= \int_0^{x'} \mathrm{d}x |\Psi(x)|^2 + |\gamma_n|^2 \frac{M}{2\hbar |k_n| \mathrm{Im}(k_n)} \left(\mathrm{e}^{-2(\mathrm{Im}(k_n))x_0} - \mathrm{e}^{-2(\mathrm{Im}(k_n))x'}\right) \\ &\simeq |\gamma_n|^2 \frac{M}{2\hbar |k_n| \mathrm{Im}(k_n)} \mathrm{e}^{-2(\mathrm{Im}(k_n))x_0}\,, \end{aligned} \tag{4.66}$$

where x' in Eq. (4.66) divides the spatial region into two: the interaction region where the resonance wavefunction is localized and the external region where the resonance wavefunction reaches its asymptotic form. Since the asymptote of the resonance wavefunction exponentially diverges when $x_0 \gg x'$, the following approximation holds:

$$\begin{aligned}|\gamma_n|^2 \frac{M}{2\hbar |k_n| \mathrm{Im}(k_n)} \mathrm{e}^{-2(\mathrm{Im}(k_n))x_0} \\ \gg \int_0^{x'} \mathrm{d}x |\Psi_n(x)|^2 - |\gamma_n|^2 \frac{M}{2\hbar |k_n| \mathrm{Im}(k_n)} \mathrm{e}^{-2(\mathrm{Im}(k_n))x'}\,. \end{aligned} \tag{4.67}$$

By substituting Eq. (4.66) into Eq. (4.64) one gets the equality we have proved above and given in Eq. (4.59). QED.

The last proof of this exercise is: $\hbar|\gamma_n|^2 \to \Gamma_n$ *as* $\Gamma_n \to 0$.

When $\Gamma_n \to 0$ then

$$\frac{\mathrm{Re}(k_n)}{|k_n|} \to 1 \tag{4.68}$$

and

$$\mathrm{Im}(k_n) \to 0\,. \tag{4.69}$$

Under these conditions, for a sufficiently large value of x_0,

$$\int_0^{x_0} |\Psi(x)_n|^2 \mathrm{d}x \to 1 \tag{4.70}$$

and Eq. (4.64) is reduced to $\Gamma = \hbar|\gamma|^2$.

Answer to Exercise 4.2

In terms of the variable $z = (M\omega/\hbar)x$ the eigenfunctions of the harmonic oscillator are a product of an exponentially decaying function, $\exp(-z^2)$ (for positive values of k the frequency ω gets real values) and Hermite polynomials $H_n(z)$. Solutions with outgoing boundary conditions are obtained at energies:

$$E_n = \hbar\omega(n + 1/2); \qquad n = 0, 1, 2\ldots \tag{4.71}$$

The inverted potential implies that $k \to -k$ and therefore $\omega \to \pm \mathrm{i}\omega$ and the exponential factor in the eigenfunctions changes to $\exp(\pm\mathrm{i}(M|\omega|/\hbar)x^2)$, where the corresponding eigenvalues are given by

$$E_n = -\mathrm{i}\hbar\omega(n + 1/2)\,. \tag{4.72}$$

The positions of these poles (i.e., $\mathrm{Re}(E_n)$) are all equal to zero (note that the top of the potential barrier is located at $V = 0$) whereas the $-2\mathrm{Im}(E_n)$ are given by

$$\Gamma_n = \hbar\omega(2n + 1)\,. \tag{4.73}$$

One may think that the $n = 0$ pole can be associated with an activated complex in a chemical reaction which is localized at a saddle point in the potential energy surface and is in a transition state with the lifetime $\tau = \hbar/\Gamma_0$. However, this is a pathological case since as $x \to \infty$, $V(x) \to -\infty$ and therefore these poles can't be considered as resonances. Compare these poles with the shape-type potential-barrier resonances obtained for the Eckart potential barrier in Ex. 4.3.

Answer to Exercise 4.3

The barrier resonances for the symmetrical Eckart potential barrier

The Eckart potential is one of the most commonly used models for the description of a chemical potential barrier. Following the strategy to obtain analytical expressions for the resonance position and widths described in the text we use here the expression for the bound-state spectra of the Rosen–Morse Hamiltonian.[10]

The Rosen–Morse potential is symmetric, $V(x) = -V_0/\cosh^2(ax)$. By making the transformation $V_0 \to -V_0$ we get an inverted Rosen–Morse potential which is the symmetric Eckart potential barrier. The solutions of the time-independent Schrödinger equation for the Rosen–Morse potential well for which the asymptotes are outgoing waves associated with an *infinite* number of discrete real eigenvalues are

$$E_n = -\frac{\hbar^2 a^2}{8M}\left[-(1 + 2n) + \sqrt{1 + \frac{8MV_0}{a^2\hbar^2}}\right]^2, \tag{4.74}$$

where $n = 0, 1, 2, \ldots$ The bound states (i.e., square integrable functions) are associated with a *finite* number of levels, determined by the condition $n < N$,

---

[10] N. Rosen and P. N. Morse, *Phys. Rev.* **42**, 210 (1932).

where the maximal number of bound states N is determined by the condition $N(N+1) = 2MV_0/(a\hbar)^2$. Note that $E_0 < E_1 < \cdots < E_N$, where E_0 is the ground bound state and E_N is the highest excited bound state. However, the real negative eigenvalues obtained for $n > N$ are ordered differently. Such that $E_{N+1} > E_{N+2} > \cdots > E_{N+m} > \cdots$ these eigenvalues are associated with anti-bound states and the corresponding eigenfunctions have an exponentially divergent asymptote, $\exp(+\mathrm{i}kx)$, where $k = -\mathrm{i}\sqrt{-2ME_{n>N}}$.

In order to invert this potential and create a barrier, let us carry out the transformation $V_0 \to -V_0$ in Eq. (4.74). We obtain an infinite number of resonances which can be assigned good quantum numbers $n = 0, 1, \ldots$ These are barrier resonances and are often considered as non-physical broad resonances, although as shown in Ex. 3.6 they might be observed in experiments. When substituting V_0 by $-V_0$ in Eq. (4.74), provided that $8MV_0 > \hbar^2 a^2$, the energy positions are given by

$$\mathrm{Re}(E_n) = V_0 - \frac{\hbar^2 a^2}{4M}(2n^2 + 2n + 1) \tag{4.75}$$

and the resonance widths are given by

$$\Gamma_n = -2\mathrm{Im}(E_n) = \frac{\hbar^2 a^2}{2M}\left[(2n+1)\sqrt{\frac{8MV_0}{\hbar^2 a^2} - 1}\right]. \tag{4.76}$$

Note again that the decay resonances of the symmetrical Eckart potential barrier are obtained from the expressions derived for the bound and anti-bound states of the Rosen–Morse potential well.

Answer to Exercise 4.4

The barrier resonances for the non-symmetrical Eckart potential barrier

The energies of the bound states of a non-symmetrical Rosen–Morse potential are given by[11]

$$E_n = -\frac{\hbar^2 a^2}{2M}\left[\alpha - (n + 1/2) - \frac{\beta/2}{\alpha - (n+1/2)}\right]^2, \tag{4.77}$$

where

$$\alpha = \sqrt{\frac{2MV_0\cosh^2(b)}{a^2\hbar^2} + \frac{1}{4}}; \qquad \beta = \frac{2MV_0\sinh(2b)}{a^2\hbar^2}. \tag{4.78}$$

By carrying out the transformation $V_0 \to -V_0$ we get a non-symmetric Eckart potential barrier with a height which equals $V_0\exp(-2b)$. When $b = 0$ the symmetrical potential barrier which has been discussed in Ex. 4.4 is obtained. Using

---

[11] P. M. Morse and H. Feshbach, *Methods of Theoretical Physics*, New York, McGraw-Hill, 1953.

the expression in Eq. (4.77) derived for bound states we see that when inverting the potential $\beta \to -\beta$ and when $8MV_0\cosh^2(b) > a^2\hbar^2$ then $\alpha \to \pm i\tilde{\alpha}$, where $\tilde{\alpha}$ is given by

$$\tilde{\alpha} = \sqrt{\frac{2MV_0\cosh^2(b)}{a^2\hbar^2} - \frac{1}{4}}\,. \tag{4.79}$$

Consequently the complex energies for the corresponding barrier resonances are

$$E_n = -\frac{\hbar^2 a^2}{2M}\left[i\tilde{\alpha} - (n+1/2) + \frac{\beta/2}{i\tilde{\alpha} - (n+1/2)}\right]^2, \tag{4.80}$$

which gives a corresponding width of

$$\Gamma_n = \frac{2\hbar^2 a^2}{M}\frac{\tilde{\alpha}(n+1/2)\left([(n+1/2)^2+\tilde{\alpha}^2]^2 - \beta^2/4\right)}{[(n+1/2)^2+\tilde{\alpha}^2]^2}\,. \tag{4.81}$$

Answer to Exercise 4.5

The barrier resonances for a model Hamiltonian of an electron scattering from a negative ion

One of the examples which were given by Landau and Lifshitz for analytically soluble problems is that of a particle moving in a centrally symmetric field with potential energy $V(r) = V_0[\gamma/r^2 - 1/r]$. The bound state energy levels for $V_0 > 0$ are given by

$$E_{n,l} = -\frac{2V_0^2 M/\hbar^2}{[2n+1+\sqrt{(2l+1)^2 + 8MV_0\gamma/\hbar^2}]^2}\,, \tag{4.82}$$

where $l = 0, 1, 2, \ldots$ and $n = 0, 1, 2, \ldots$ are two good quantum numbers. By making the transformation of $V_0 \to -V_0$ one gets the barrier resonances provided that V_0 gets sufficiently large values such that

$$\Delta \equiv 8MV_0\gamma/\hbar^2 - (2l+1)^2 \geq 0\,. \tag{4.83}$$

When V_0 has small values and $\Delta < 0$ we get the anti-bound states (real energies but exponentially divergent corresponded eigenfunctions). The complex eigenvalues obtained when $\Delta > 0$ are given by

$$E_{n,l} = -\frac{2MV_0^2}{\hbar^2}\frac{(2n+1)^2 - \Delta + 2i(2n+1)\sqrt{\Delta}}{[(2n+1)^2+\Delta]^2}\,. \tag{4.84}$$

The real part of $E_{n,l}$ is associated with the resonance position and is decreasing with the quantum number n up to $-\infty$. The imaginary part of the complex energy which is associated with the resonance width increases with the quantum number

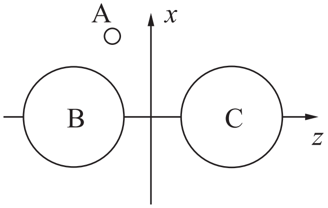

Figure 4.5 Scattering of a light atom from two heavy atoms which are depicted by two discs.

n and thus the resonances at lower energies have decreasing lifetimes. Note that in this special case the resonance states can decay to $r \to \infty$ and to $r \to 0$ due to the nature of the potential at $r \to 0$ which approaches ∞ as $1/r^2$.[12]

Answer to Exercise 4.6

When a light atom is temporarily trapped in between two heavy atoms it implies that it moves much faster along its "molecular" B–C axis (which is labelled here as the z-axis) in comparison to its motion along the perpendicular axis denoted here as the x-axis (see the schematic picture given in Fig. 4.5). Thus by treating the x coordinate as an adiabatic parameter we reduce the problem from a two-dimensional problem to an effective one-dimensional particle-in-a-box problem. The length of the box along the z-coordinate depends on x according to $L(x) = R - 2(r^2 - x^2)^{1/2}$, when $-r \le x \le +r$ and $L = A_{\text{box}}$ elsewhere. A_{box} can be large as one wishes (it stands for the size of the box used in the numerical calculations). The adiabatic potentials are accordingly given by

$$E_{n_z}(x) = \frac{\hbar^2 \pi^2}{2ML(x)^2} n_z^2 ; \qquad n_z = 1, 2, \ldots \tag{4.85}$$

The adiabatic potentials, $E_{n_z}(x)$, describe the situation where the light atom is repelled from both heavy atoms but can be trapped between the two prior to dissociation. As an example of a real physical problem see the calculations of ArHCl resonance.[13] These adiabatic potentials are similar in their shape to Eckart potential barriers. Therefore let us approximate $L(x)$ by

$$L_{\text{eff}}(x) = (R - 2r)\cosh(\alpha x) . \tag{4.86}$$

Since $\mathrm{d}L^2/\mathrm{d}x^2|_{x=0} = 2/r$ and correspondingly $\mathrm{d}L^2_{\text{eff}}/\mathrm{d}x^2|_{x=0} = \alpha^2(R - 2r)$ we define $\alpha = \sqrt{2/[r(R - 2r)]}$. The Eckart potential barrier (inverse of the

---

[12] Read more about this "black hole" phenomenon in S. Klaiman, I. Gilary and N. Moiseyev, *Phys. Rev. A* **70**, 012709 (2004).

[13] E. Narevichius and N. Moiseyev, *Mol. Phys.* **94**, 897 (1998); *Chem. Phys. Lett.* **287**, 250 (1998).

Rosen–Morse potential) is given by $V(x) = V_0 \cosh^2(\alpha x)$, where $V_0 = [\hbar \pi n_z/(R-2r)]^2/[2M]$. From Ex. 4.4 one gets the resonance positions and widths as function of the quantum numbers n_z and n_x,

$$\varepsilon_{n_x,n_z} = \frac{\hbar^2\pi^2}{2M(R-2r)^2} n_z^2 - \frac{\hbar^2}{2Mr(R-2r)}(2n_x^2 + 2n_x + 1)\,,$$

$$\Gamma_{n_x,n_z} = \frac{\hbar^2(2n_x+1)}{2Mr(R-2r)}\sqrt{\frac{2\pi^2 r}{R-2r} n_z^2 - 1}\,. \tag{4.87}$$

In this case barrier resonances will exist when $2\pi^2 r n_z^2 > R - 2r$.

Answer to Exercise 4.7

Graphical solution for the bound states of a symmetric rectangular well

When $E < 0$ then $k_0 = \mathrm{i}\kappa$, where $\kappa = \sqrt{-2ME}/\hbar$. Using the trigonometric identity

$$\cot 2\alpha = \frac{1}{2}\left(\cot\alpha - \frac{1}{\cot\alpha}\right)\,,$$

Eq. (4.26) transforms to

$$\cot(ka/2) - \frac{1}{\cot(ka/2)} = \frac{k}{\kappa} - \frac{\kappa}{k}\,,$$

which can be split in two,

$$\cot\frac{ka}{2} = \frac{k}{\kappa} \quad \text{or} \quad \cot\frac{ka}{2} = -\frac{\kappa}{k}\,.$$

The first of the two equations corresponds to the even states (cosines inside the well) and the other one corresponds to the odd states (sines inside the well). These equations are further transformed into

$$\cos\frac{ka}{2} = \pm\sqrt{\frac{k^2}{\kappa^2+k^2}} \quad \text{or} \quad \sin\frac{ka}{2} = \pm\sqrt{\frac{k^2}{\kappa^2+k^2}}\,,$$

each of which contains two spurious solutions, one for + and one for −, to be excluded so that $\cot(ka/2)$ will have positive values in the first equation and negative values in the second one.

From the definition of k and κ it can be readily seen that

$$\frac{k^2}{\kappa^2+k^2} = \frac{E+V_0}{V_0} = 1 + \frac{E}{V_0}\,.$$

Therefore, by defining two new variables

$$\alpha = \sqrt{1 + \frac{E}{V_0}} \quad \text{and} \quad \gamma = \sqrt{\frac{2mV_0a^2}{\hbar^2}}\,,$$

the above two equations can be written as

$$\cos\frac{\gamma\alpha}{2} = \pm\alpha \quad \text{or} \quad \sin\frac{\gamma\alpha}{2} = \pm\alpha\,,$$

and after excluding the spurious solutions

$$\frac{\gamma\alpha}{2} = \cos^{-1}\alpha + n\pi \quad \text{or} \quad \frac{\gamma\alpha}{2} = \cos^{-1}\alpha + n\pi + \frac{\pi}{2}\,,$$

where $n = 0, 1, 2, \ldots$

Finally, the two equations can be combined into one:

$$\gamma\alpha = (n-1)\pi + 2\cos^{-1}\alpha\,, \quad (n = 1, 2, \ldots)\,.$$

The bound state poles are the intersection points of the curve $(n-1)\pi + 2\cos^{-1}\alpha$, $(n = 1, 2, \ldots)$ and the straight line $\gamma\alpha$ which are plotted as functions of α.

Answer to Exercise 4.8

Graphical solution for the real virtual states (so-called anti-bound states)

To obtain the solutions for the real virtual states from the bound states equations the transformation $\kappa \to -\kappa$ should be performed, so that the even and odd states equations become

$$\cot\frac{ka}{2} = -\frac{k}{\kappa} \quad \text{or} \quad \cot\frac{ka}{2} = \frac{\kappa}{k}\,.$$

Similarly to the bound states, these can be written as

$$\sin\frac{ka}{2} = \pm\sqrt{\frac{\kappa^2}{\kappa^2 + k^2}} \quad \text{or} \quad \cos\frac{ka}{2} = \pm\sqrt{\frac{\kappa^2}{\kappa^2 + k^2}}\,,$$

and since

$$\frac{\kappa^2}{\kappa^2 + k^2} = -\frac{E}{V_0} = 1 - \alpha^2$$

these equations can be rewritten as

$$\sin\frac{\gamma\alpha}{2} = \pm\sqrt{1-\alpha^2} \quad \text{or} \quad \cos\frac{\gamma\alpha}{2} = \pm\sqrt{1-\alpha^2}\,,$$

and then combined into one,

$$\gamma\alpha = (n-1)\pi + 2\cos^{-1}\sqrt{1-\alpha^2}\,, \quad (n = 1, 2, \ldots)\,.$$

The anti-bound state poles are the intersection points of the curve $(n-1)\pi + 2\cos^{-1}\sqrt{1-\alpha^2}$, $\quad (n = 1, 2, \ldots)$ and the straight line $\gamma\alpha$ which are plotted as functions of α.

4.9 Further reading

A. I. Baz', Ya. B. Zel'dovich and A. M. Perelomov, *Scattering, Reactions and Decay in Nonrelativisitic Quantum Mechanics*, Jerusalem, Israel Program for Scientific Translation, 1969.

A. M. Perelomov and Ya. B. Zel'dovich, *Quantum Mechanics*, Singapore World Scientific Publishing Co., 1998.

N. Moiseyev, Quantum theory of resonances: calculating energies, widths and cross-sections by complex scaling, *Physics Reports*, **302**, Issue 5–6, 211–293 (1998).

5

Square integrable resonance wavefunctions

As discussed in the previous chapter, the poles of the S-matrix are identified with discrete eigenvalues of the time-independent Schrödinger equation, where the asymptotes of the corresponding eigenfunctions are either purely outgoing waves or purely incoming waves. More specifically, the bound and decay resonance poles are obtained by imposing the outgoing boundary conditions on the solutions of the time-independent Schrödinger equation, while the anti-bound and virtual states (sometimes referred to as capture resonances) are associated with the solutions obtained under the requirement of the incoming boundary conditions. Except for the bound states, all other poles of the S-matrix are associated with exponentially divergent wavefunctions which by definition do not belong to the Hilbert space of conventional Hermitian quantum mechanics.

This fact represents a major difficulty for the development of a non-Hermitian quantum mechanical formalism. Consequently, one may wonder, for example, how to properly define an inner product in non-Hermitian quantum mechanics (NHQM) if the wavefunctions diverge asymptotically. We recall in this context that the concept of an inner product constitutes a fundamental building block of standard (Hermitian) quantum mechanics (QM), by means of which one defines the quantum mechanical expectation values of physically observable quantities over the quantum states under consideration. An inner product for NHQM is necessary in order to accommodate the tools of conventional QM. Furthermore, one might anticipate that an appropriate NHQM inner product would also facilitate practical numerical calculation of the S-matrix poles for those cases where the eigenvalues of the Hamiltonian do not possess an analytical closed form expression (unlike the cases studied in the previous chapter). An inspiration for this comes, of course, from well-established methods in Hermitian QM such as variational and perturbational basis set expansion methods. Various related questions arise immediately. Are different poles of the S-matrix orthogonal to each other? Is the spectrum of the Hamiltonian in NHQM complete? Are the expectation values of the physical quantities within the NHQM formalism real or complex? And if they are complex, what is the physical meaning of the real and imaginary parts? More specifically, we can ask what is the physical interpretation of the complex density probability? All these important questions are addressed in the current and following chapters.

The first step towards an appropriate reconciliation of the above-mentioned problems is to force the NHQM wavefunctions (i.e. the eigenfunctions associated with the S-matrix poles) to be square integrable by carrying out a suitable mathematical transformation. As shown below, there are various different (although in fact mutually equivalent) ways in which such a transformation can be introduced. Each transformation of this kind converts the original exponentially divergent NHQM wavefunction into a bounded normalizable function which can be considered as a part of a "generalized" Hilbert space. On the other hand, it turns out that applying this transformation to the continuum scattering states (which are not associated with the poles of the S-matrix) leads to additional difficulties which must be overcome by an adequate redefinition of the continuum states themselves.

It is hard to separate the discussion on these transformations of the divergent resonance eigenfunctions from the discussion on the definition of the inner product in NHQM. Let us first describe the source of the problem in NHQM which lies in the exponentially divergent asymptotes of the eigenfunctions of the Hamiltonian associated with the poles of the S-matrix. For the sake of simplicity we define the resonance eigenfunction of a 3D spherically symmetric *real* Hamiltonian $\hat{H}$ as $\Psi_{\text{res}}(r) \to A\mathrm{e}^{(\mathrm{i}kr}/r$ when $r \to \infty$, where $k = |k|\mathrm{e}^{-\mathrm{i}\alpha}$. It is clear that $\Psi_{\text{res}}(r) \to +\infty$ as $r \to \infty$ since $\mathrm{Im}(k) < 0$. For the bound states of $\hat{H}$ the norm of $\Psi_{\text{bound}}(r)$ is defined as an integral over the entire space of $|\Psi_{\text{bound}}|^2$, where $\Psi^*_{\text{bound}}(r)$ and $\Psi_{\text{bound}}(r)$ are two states which are associated with the *same* real eigenvalue E_{bound}. The "bra" and "ket" states which are used for the calculations of expectations values of any given operator should be associated with the same eigenvalue. This is an essential requirement from the calculations of a norm. As we will discuss later, in linear algebra the norm is obtained by calculating the scalar product between the left and right eigenvectors of a given matrix, where the corresponding eigenvalues are equal.

Can we define the norm of the resonance eigenfunctions in a similar way (i.e. $\langle\Psi_{\text{res}}|\Psi_{\text{res}}\rangle$)? The answer to that question is *no* since $\Psi^*_{\text{res}}(r)$ and $\Psi_{\text{res}}(r)$ are *not* two eigenstates of the Hamiltonian which are associated with the same complex eigenvalue. Indeed, both $\Psi^*_{\text{res}}(r)$ and $\Psi_{\text{res}}(r)$ are eigenfunctions of $\hat{H}$. However, if $E_{\text{res}} = E - \mathrm{i}/2\Gamma$ is the corresponding complex eigenvalue of $\Psi_{\text{res}}(r)$, then the complex eigenvalue which is associated with $\Psi^*_{\text{res}}(r)$ is E^*_{res}. Therefore it seems that for the functions associated with the poles of the S-matrix which are not bound states, the norm should be taken as the integral over the entire space of $\Psi^2_{\text{res}}(r)$ and not of $\Psi^*_{\text{res}}(r)\Psi_{\text{res}}(r)$. However, the integral $\langle\Psi^*_{\text{res}}|\Psi_{\text{res}}\rangle = 4\pi\int_0^\infty r^2\Psi^2_{\text{res}}(r)\mathrm{d}r$ is also meaningless due to the divergence of the integrand. Only after applying one of the transformations which will be described below will the functions associated with the divergent states become square integrable, and in this sense they become part of the generalized Hilbert space where the definition of the norm has been modified. Note, however, that bound states can always be described by real functions and therefore the same definition of the norm can be applied to the calculation of the norm of bound states as for the other poles (after applying the suitable transformation).

Exercise 5.1

Prove that for a real and Hermitian Hamiltonian $\hat{H}$ all the eigenfunctions (including the excited states) can be taken as real functions.

In the following sections we will discuss different similarity transformations, $\hat{S}$, which render the resonance wavefunctions and other exponentially divergent solutions square integrable. That is, we look at the solutions of the following eigenvalue equation:

$$\hat{H}_S\Psi_S = E\Psi_S\,, \tag{5.1}$$

where

$$\hat{H}_S = \hat{S}\hat{H}\hat{S}^{-1} \tag{5.2}$$

and

$$\Psi_S = \hat{S}\Psi \tag{5.3}$$

such that the asymptote of Ψ_S at $r \to \infty$ decays to zero,

$$\Psi_S \to 0\,, \tag{5.4}$$

while the asymptote of Ψ at $r \to \infty$ diverges exponentially,

$$\Psi \to \infty\,. \tag{5.5}$$

5.1 The Zel'dovich transformation

As explained above, the norm of a resonance state can not be defined simply as $\langle\Psi^*_{\text{res}}|\Psi_{\text{res}}\rangle = 4\pi\int_0^\infty r^2\Psi^2_{\text{res}}(r)\mathrm{d}r$ since the integrand diverges exponentially as $r \to \infty$. However, a general definition of an inner product can be of the form

$\langle \Psi^*_{\text{res}}|F|\Psi_{\text{res}}\rangle$, where $F(r)$ is a positive definite function (a matrix in linear algebra). Since the resonance asymptotes oscillate and diverge, $F(r)$ can be defined such that the oscillations are suppressed and $r^2F(r)\Psi^2_{\text{res}}(r)$ decays exponentially to zero, thus becoming an integrable function. Accordingly, a Gaussian function, $e^{-\epsilon r^2}$, is a good candidate for $F(r)$ since the divergence is exponential. The problem with such a choice for $F(r)$ is that it reduces and even washes out physical information which is embedded at large distances of r. To avoid this problem Zel'dovich proposed to take the limit of the integral when $\epsilon \to 0$.[1] This approach is analogous to that taken in time-independent scattering theory when multiplying the stationary solutions of the Scrödinger equation by $e^{-i\epsilon t}$ in order to suppress the e^{-iEt} oscillations.

Is it possible to associate the Zel'dovich inner product with a similarity transformation of the type mentioned above? The answer to this question is positive and can be achieved by defining the operator $\hat{S}$ as a multiplication by a Gaussian, $e^{-\epsilon r^2}$. Therefore, for sufficiently small value of ϵ,

$$\hat{H}_S = \hat{S}\hat{H}\hat{S}^{-1} = e^{-\epsilon r^2}\hat{H}e^{+\epsilon r^2} = \hat{H} + \hat{V}_{\text{zel}} ,$$

where the absorbing potential (AP) corresponding to the Zel'dovich inner product as a result of the transformation of the kinetic energy operator is given by

$$\hat{V}_{\text{zel}} = -\frac{\hbar^2\epsilon}{M}\left[\sum_{j=1}^{3}\left(\zeta_j\frac{\partial}{\partial\zeta_j} + \frac{\partial}{\partial\zeta_j}\zeta_j\right)\right] , \tag{5.6}$$

where $\zeta_1 = x$, $\zeta_2 = y$ and $\zeta_3 = z$. Note that this additional potential term is non-Hermitian. The eigenfunctions of $\hat{H}_S$ are given by $\Psi_S = e^{-\epsilon r^2}\Psi$. When Ψ is associated with a sufficiently narrow resonance then Ψ_S decays to zero as $r \to \infty$.

Exercise 5.2

Derive the absorbing potential $\hat{V}_{\text{zel}}$ given in Eq. (5.6) for a general one-dimensional problem and show that it is a non-Hermitian operator.

In the calculations of any quantity using such an inner product the limit of $\epsilon \to 0$ should be taken only after the integral $\int_0^\infty r^2\Psi^2_S(r)\mathrm{d}r$ has been computed. Note that $\hat{V}_{\text{zel}}$ given in Eq. (5.6) holds for any 3D problem and not necessarily for spherically symmetric potentials.

---

[1] I. Baz', Ya. B. Zel'dovich and A. M. Perelomov, *Scattering, Reactions and Decay in Nonrelativistic Quantum Mechanics*, Moskva, Fiziko-Matematicheskoi Literatury, 1966 and translation from Russian by the Israel Program for Scientific Translations, Jerusalem 1969.

Exercise 5.3

For a potential with a 3D spherical symmetry the asymptote of a resonance wavefunction, $\Psi_{\mathrm{res}}(r) \to \mathrm{e}^{+\mathrm{i}kr}/r$ diverges exponentially since $k = |k|\mathrm{e}^{-\mathrm{i}\alpha}$, where $E_{\mathrm{res}} = (\hbar k)^2/(2M)$ and $\alpha > 0$. Prove that by using the Zel'dovich inner product the asymptote of $\Psi_{\mathrm{res}}(r)$, i.e., $\mathrm{e}^{+\mathrm{i}kr}/r$, is a normalizable function provided that the resonance width is not too large. In other words the resonances should be embedded sufficiently close to the real energy axis.

An interesting numerical result of Ex. 5.3 is that the norm of a sufficiently narrow resonance state which is calculated by the Zel'dovich inner product approach is obtained by calculating the indefinite integral $\mathcal{N}^2 \int \mathrm{e}^{+2\mathrm{i}kr}\mathrm{d}r$ and substituting only the lower limit of $r = 0$. As we will see later, this result is very typical of all the approaches which enable us to calculate the norms of the exponentially diverged wavefunctions which are associated with the resonance, virtual and anti-bound poles of the scattering matrix.

5.2 The complex scaling transformation

A convenient and efficient method to divert the divergent resonance wavefunctions into the physical domain of square integrable wavefunctions is to rotate the coordinate along which the divergence occurs into the complex plane. By appropriate rotation the divergence at the asymptotes can be negated and thus evaluation of observables can be achieved through the resonance wavefunction.

This approach is also known as complex scaling or the complex coordinate method. The transformations which correspond to this method scale the coordinate x by a complex phase, $x \to \mathrm{e}^{\mathrm{i}\theta}x$. Similarly, the y and z coordinates are scaled by the same complex factor such that as a whole the complex scaling transformation amounts to

$$\mathbf{r} \to \mathbf{r}\mathrm{e}^{\mathrm{i}\theta} \,. \tag{5.7}$$

In a more general manner one can choose where in space the scaling will begin according to physical or numerical considerations. This can be done by using a shifted complex scaling transformation where

$$\mathbf{r} \to (\mathbf{r} - \mathbf{r_0})\mathrm{e}^{\mathrm{i}\theta} + \mathbf{r}_0 \,. \tag{5.8}$$

The parameter θ does not have to be a real number. This point becomes relevant when the resonances are computed by carrying out complex variational calculations based on a non-Hermitian variational principle which will be described in Chapter 6.

For the evaluation of the exact complex scaled resonance solutions θ can be taken as a real parameter since the imaginary part of θ implies that $\mathrm{e}^{-\mathrm{Im}(\theta)}$ stretches the coordinates (this is in fact equivalent to changing the length units). When θ attains real values it can be defined as the rotational angle of the coordinates in the complex plane. The motivation for applying the complex scaling transformation is obvious. Under this transformation the resonance wavefunctions become square integrable provided that the scaling parameter θ satisfies the condition

$$\theta \geq \phi_{\mathrm{res}} \,, \tag{5.9}$$

where ϕ_{res} is associated with the phase of the complex resonance wavevector k_{res} defined as

$$k_{\mathrm{res}} = |k_{\mathrm{res}}|\mathrm{e}^{-\mathrm{i}\phi_{\mathrm{res}}} = \frac{\sqrt{2m(E_{\mathrm{res}} - E_{\mathrm{t}})}}{\hbar} \,, \tag{5.10}$$

where

$$E_{\mathrm{res}} = \varepsilon - \mathrm{i}/2\Gamma \tag{5.11}$$

and E_{t} is the threshold energy where the potential interaction vanishes and the particle becomes embedded in the continuous part of the energy spectrum of the unscaled Hamiltonian. Following these definitions one gets that

$$\phi_{\mathrm{res}} = \arctan\left(\frac{\Gamma}{2(\varepsilon - E_{\mathrm{t}})}\right) . \tag{5.12}$$

By substituting Eq. (5.12) into Eq. (5.10) a critical value of the scaling parameter (i.e., rotational angle), θ_{c}, is obtained. For $\theta > \theta_{\mathrm{c}}$ the complex scaled resonance wavefunction becomes square integrable where the critical value θ_{c} is given by

$$\theta_{\mathrm{c}} = \arctan\left(\frac{\Gamma}{2(E - E_{\mathrm{t}})}\right) . \tag{5.13}$$

Exercise 5.4

The asymptote of a one-dimensional resonance wavefunction has the form $\Psi_{\mathrm{res}}(x \to \infty) = \gamma \mathrm{e}^{+\mathrm{i}k_{\mathrm{res}}x}$. Prove that upon complex scaling this function becomes square integrable when the rotational angle θ has a sufficiently large value defined in Eq. (5.13).

It is now imperative to associate the complex scaling transformation with the family of similarity transformations discussed in Eqs. (5.1)–(5.3). For this task we need to define an operator which will scale any function of the coordinate by a complex factor. A general operator scaling a coordinate x by η is given by

$$\hat{S} = \mathrm{e}^{\frac{1}{2}\ln\eta(x\frac{\partial}{\partial x}+\frac{\partial}{\partial x}x)} = \sqrt{\eta}\,\mathrm{e}^{\ln\eta(x\frac{\partial}{\partial x})} . \tag{5.14}$$

Upon operating with the scaling operator defined in Eq. (5.14) on an analytic function a scaled function is obtained,

$$\hat{S}\Psi(x) = \sqrt{\eta}\,\Psi(\eta x) , \tag{5.15}$$

where η can be a real, imaginary or complex factor.

Exercise 5.5

Prove that applying the scaling operator in Eq. (5.14) to an analytic function (which can be expanded in a Taylor series), one gets the the function in the scaled coordinate as depicted in Eq. (5.15).

When we rotate the coordinate into the complex plane we are scaling it by a complex phase and thus $\eta = \mathrm{e}^{\mathrm{i}\theta}$ and the scaling operator in Eq. (5.14) takes the following form

$$\hat{S} = \mathrm{e}^{\mathrm{i}\frac{\theta}{2}}\mathrm{e}^{\mathrm{i}\theta x\frac{\partial}{\partial x}} . \tag{5.16}$$

For a many-particle three-dimensional (3D) system the scaling operator is defined by the scaling of all the different spatial coordinates of all the particles:

$$\hat{S} = \Pi_j \mathrm{e}^{\mathrm{i}\frac{\theta}{2}}\mathrm{e}^{\mathrm{i}\theta\,\mathbf{r}_j\cdot\nabla_j} . \tag{5.17}$$

The fact that the complex scaling operator can be applied only to analytical functions restricts the evaluation of resonances by the complex scaling method as described above to analytical potentials. It implies that the complex scaled Hamiltonian given in Eq. (5.2) is a well-defined operator if, and only if, *the potential* $\hat{V}$ *is an analytic function* for which all the high-order derivatives are well defined. For this reason one may wonder whether atomic auto-ionization resonances can be computed by this method since the Columbic potential $1/r$ is singular at $r = 0$. This, however, is not a serious problem since the amplitude of atomic eigenfunctions vanishes at the nucleus and also when the intra-electronic distance is small.[2]

---

[2] For a rigorous mathematical study of the application of the complex coordinate method to atoms see the fundamental works of E. Balslev and J. M. Combes, *Commun. Math. Phys.* **22**, 280 (1971) and B. Simon, *Commun. Math. Phys.* **27**, 1 (1972); *Ann. Math.* **97**, 247 (1973).

When applying the complex scaling method to atoms, due to the nature of the Coulombic interactions the Hamiltonian takes the following form:

$$\hat{H}_{\text{atom}} = \mathrm{e}^{-2\mathrm{i}\theta}\hat{T}_{\mathrm{e}} + \mathrm{e}^{-\mathrm{i}\theta}(\hat{V}_{\mathrm{eN}} + \hat{V}_{\mathrm{ee}}), \tag{5.18}$$

where $\hat{T}_{\mathrm{e}}$ is the kinetic energy operator which is scaled by $\mathrm{e}^{-2\mathrm{i}\theta}$ whereas $\hat{V}_{\mathrm{eN}}$, $\hat{V}_{\mathrm{ee}}$ are respectively the electron–nucleus and electron–electron potential energy operators which are both scaled by $\mathrm{e}^{-\mathrm{i}\theta}$. In a similar fashion, when applying the complex scaling method to molecules we carry out the following transformations:

$$\begin{aligned} \mathbf{r}_j &\to \mathrm{e}^{\mathrm{i}\theta}\mathbf{r}_j\,, \\ \mathbf{R}_\alpha &\to \mathrm{e}^{\mathrm{i}\theta}\mathbf{R}_\alpha\,, \end{aligned} \tag{5.19}$$

where $\{\mathbf{r}_j\}$ and $\{\mathbf{R}_\alpha\}$ are respectively the electronic and the nuclear coordinates, and consequently the complex scaled molecular Hamiltonian is given by

$$\hat{H}_{\text{mol}} = \mathrm{e}^{-2\mathrm{i}\theta}(\hat{T}_{\mathrm{e}} + \hat{T}_{\mathrm{N}}) + \mathrm{e}^{-\mathrm{i}\theta}(\hat{V}_{\mathrm{eN}} + \hat{V}_{\mathrm{ee}} + \hat{V}_{\mathrm{NN}}), \tag{5.20}$$

where $\hat{T}_{\mathrm{N}}$, $\hat{V}_{\mathrm{NN}}$ are respectively the nuclear kinetic energy and the nuclear–nuclear potential energy operators.

The fact that the complex scaling transformation requires the potential to be an analytic function within the spatial region where the resonance wavefunctions are localized raises the following question: is it possible to evaluate molecular resonances by the complex coordinate method within the framework of the commonly used Born–Oppenheimer approximation? The problem lies in the coupling between electronic and nuclear coordinates through the electron–nuclei potential energy terms which are non-analytical operators. Therefore it is *not* possible to obtain complex potential energy surfaces by applying the transformation $\mathbf{r}_j \to \mathrm{e}^{\mathrm{i}\theta}\mathbf{r}_j$ while keeping the nuclei positions $\{\mathbf{R}_\alpha\}$ fixed and unscaled.

Exercise 5.6

Explain why within the framework of the Born–Oppenheimer approximation the electron–nuclei potential energy terms are not analytical operators.

Exercise 5.7

The association of the non-analytical properties of a function with its singularity can be illustrated by the following example.

The Taylor series expansion of a given function F(x) around $x = 0$ is equal to $1 + x + x^2 + x^3 + x^4 + \cdots$. However, the value of $F(x)$ at $x = 2$ is equal to $F(2) = -1$. Explain this result. How is it possible that the infinite sum of positive numbers provides a negative number?

Nevertheless, it was shown by Moiseyev and Corcoran in 1979[3] that molecular autoionization resonances can be calculated within the framework of the Born–Oppenheimer approximation by carrying out analytical continuation of the Hamiltonian matrix elements rather than by scaling the Hamiltonian by $\eta = \mathrm{e}^{i\theta}$. The representation of the complex scaled Hamiltonian by a matrix is based on the complex variational principle, which will be described in Chapter 7 where the properties of the complex scaled Hamiltonians are discussed.

There is, however, another straightforward procedure by which complex molecular potential energy surfaces can be calculated by applying the complex scaling transformation within the framework of the Born–Oppenheimer approximation. The motivation is to have electronic resonance complex energies which are functions of the molecular geometry but are θ-independent. These complex θ-independent energies must be equal to the eigenvalues of the unscaled Born–Oppenheimer electronic Hamiltonian, provided that the outgoing boundary conditions are imposed on the corresponding electronic wavefunctions. The mentioned θ-independent complex electronic energies would then serve as complex potential surfaces when either the time-independent or time-dependent nuclear Schrödinger equation is solved.

Let us sketch the mathematical formulation underlying the approach just discussed. As the first step we re-write Eq. (5.20) into

$$\hat{H}_{mol} = e^{-2i\theta}\hat{T}_N + \hat{H}^{BO}_{mol}(\{\mathbf{r}_j e^{i\theta}\}, \{\mathbf{R}_\alpha e^{i\theta}\}) \,. \tag{5.21}$$

Note that we scale here both the electronic and nuclear coordinates, since then all the potential energy terms are homogenous functions of the scaling parameter. As the second step, the complex scaled electronic molecular Hamiltonian is diagonalized while holding the nuclear geometry fixed. That is,

$$\left[\hat{H}^{BO}_{mol}(\{\mathbf{r}_j e^{i\theta}\}, \{\mathbf{R}_\alpha e^{i\theta}\}) - E^{BO}_{mol}(\{\mathbf{R}_\alpha\})\right] \Psi^{BO}_{mol}(\{\mathbf{r}_j e^{i\theta}\}, \{\mathbf{R}_\alpha e^{i\theta}\}) = 0 \,. \tag{5.22}$$

Importantly, the electronic energies $E^{BO}_{mol}(\{\mathbf{R}_\alpha\})$ come out complex for two reasons: *(i)* because of the analytical continuation of the electronic coordinates which is carried out in order to suppress an exponential divergence of the electronic resonance eigenfunctions; *(ii)* owing to the fact that the nuclei are shifted from the physical real domain into the complex domain.

Now we are coming to the third step of our procedure, aimed at eliminating the effect of *(ii)* and thereby restoring the complex resonance energies as they would emerge in an unscaled calculation, based upon imposing the outgoing boundary conditions on the electrons. We shall accomplish the task just mentioned by shifting

---

[3] N. Moiseyev and C. T. Corcoran, Autoionizing states of H_2 and H_2^- using the complex scaling method. *Phys. Rev. A* **20**, 814–817 (1979).

the nuclei from the complex domain back to the real domain. This back-rotational transformation

$$\mathbf{R}_\alpha \to \mathbf{R}_\alpha\, e^{-i\theta} \tag{5.23}$$

can be carried out assuming that $E^{BO}_{mol}(\{\mathbf{R}_\alpha\})$ is an analytical function of the nuclear coordinates. Since even the broad molecular electronic resonances become square integrable for rotational angles $\theta \ll 1$ rad, a Taylor series expansion of the complex electronic eigenvalues $E^{BO}_{mol}(\{\mathbf{R}_\alpha\})$ in the parameter $x \equiv e^{-i\theta} - 1$ is expected to converge. Written explicitly, our Taylor series prescription for the back-rotation transformation reads as

$$\begin{aligned} E^{BO}_{mol}(\{\mathbf{R}_\alpha e^{-i\theta}\}) &= E^{BO}_{mol}(\{\mathbf{R}_\alpha\}_{\alpha=1,2,\dots}) + (e^{-i\theta} - 1)\sum_\beta \mathbf{R}_\beta \frac{\partial E^{BO}_{mol}(\{\mathbf{R}_\alpha\}_{\alpha=1,2,\dots})}{\partial \mathbf{R}_\beta} \\ &\quad + \frac{(e^{-i\theta} - 1)^2}{2} \sum_{\beta\gamma} \mathbf{R}_\beta \mathbf{R}_\gamma \frac{\partial^2 E^{BO}_{mol}(\{\mathbf{R}_\alpha\}_{\alpha=1,2,\dots})}{\partial \mathbf{R}_\beta \mathbf{R}_\gamma} + \cdots\,. \end{aligned} \tag{5.24}$$

Note that for narrow electronic resonances $x \simeq -i\theta$ and it might be enough to include only the first two leading Taylor expansion terms. On the other hand, we note in passing that it is not necessary to rely on convergence of the Taylor series expansion. One may use instead other numerical techniques of analytical continuation. In any case, one always needs to ensure that all the complex scaling angles θ for which the electronic structure calculation is made are large enough as to make the corresponding electronic resonance wavefunctions square integrable. If this condition is not fulfilled, the back rotation would inevitably lead to a wrong outcome.

We can summarize our considerations by saying that the complex scaled back-rotation approach outlined above enables one to calculate the molecular electronic resonances (pertaining e.g., to autoionization, Auger or inter-Coulombic-Decay [ICD] processes) in a conceptually clean way without using complex absorbing potentials which numerically can never be reflection-free even if they are introduced far from the molecular region.

Since the scaling of the coordinate is essentially a technical procedure, there are limitations on the calculations of resonances for analytical potentials by the complex scaling method. These limitations restrict the maximal value of the rotational angle (scaling factor) θ. The scaling factor $\mathrm{e}^{\mathrm{i}\theta}$ is limited to values of $\theta < \pi/2$, since the kinetic operator is scaled by $\eta = \mathrm{e}^{-2\mathrm{i}\theta}$ and we want to keep it as a positive definite operator. However, the maximal value of θ is often much smaller than $\pi/2$. The maximal value of θ (and therefore the broadest resonances that can be calculated by the complex scaling method as presented in this section) depends on the mathematical properties of the potential at hand. For example, the potential $V(x) = (x^2/2 + 0.8)\mathrm{e}^{-0.1x^2}$ possesses resonances which are localized in a parabolic-like potential well, x^2, and in order to keep the $(\mathrm{Re}[x\mathrm{e}^{\mathrm{i}\theta}])^2$ positive as in the case of $\theta = 0$, one should limit the calculations to the values of the rotational angle for which $\cos(2\theta) > 0$ while $\theta < \pi/2$. Therefore, the resonances of this potential that can be evaluated using the complex scaling technique are those which become square integrable for $\theta < \pi/4$. This 1D model potential served as a test case for the study of new methods for calculating resonances. See, for example, several publications.[4]

Exercise 5.8

Show that when scaling the coordinates by $r \to r\exp(\mathrm{i}\theta)$ for a bound potential behaving as $V(r) = r^n$ the bound states remain square integrable and remain on the real energy axis only when $\theta < \pi/(n + 2)$).

The complex scaled Hamiltonian has a discrete eigenvalue spectrum that consists of two classes of solutions. The first class contains the real spectrum comprised of the bound state point spectrum identical to that of the unscaled Hamiltonian. This spectrum is obtained provided that the scaling angle, θ, is not too large, as discussed above. The second class of solutions contains discrete complex eigenvalue spectra which are associated with resonances.

The complex scaling transformation will expose those resonances for which the rotation of the coordinate will compensate for the asymptotic exponential divergence due to the complex momentum discussed in Chapter 4, that is, the condition to observe a certain resonance is:

$$\tan\theta > \frac{\Gamma}{2\varepsilon}\,. \tag{5.25}$$

When θ is large enough to expose all the decay resonance poles, the continuum becomes a "white" continuum without structure and is rotated into the complex energy plane by an angle 2θ. By white continuum we mean that the behavior is similar to that of a free particle.

The reason for this is that in a "white" continuum the eigenfunctions, $\Psi_\mathrm{c}(x)$, consist of linear combinations of incoming and outgoing waves,

$$\Psi_\mathrm{c}(x) = A(k)\mathrm{e}^{-\mathrm{i}kx} + B(k)\mathrm{e}^{\mathrm{i}kx}\,, \tag{5.26}$$

---

[4] N. Moiseyev, P. R. Certain and F. Weinhold, *Mol. Phys.* **36**, 1613 (1978); N. Lipkin, N. Moiseyev and E. Brändas, *Phys. Rev. A* **40**, 549 (1989); N. Moiseyev, *Mol. Phys.* **47**, 585 (1982); H. J. Korsch, H. Laurent and R. Möhlenkamp, *Mol. Phys.* **43**, 1441 (1981); M. Rittby, N. Elander and E. Brändas, *Phys. Rev. A* **24**, 1636 (1981); I. Gilary, A. Fleischer and N. Moiseyev, *Phys. Rev. A* 72, 012117 (2005).

where the energy in the continuum, E_c, is related to the momentum, k, of the particle through $E_c = E_{th} + (\hbar k)^2/(2M)$ when E_{th} is the threshold energy. When we scale the "white" continuum functions by $e^{i\theta}$ they will be given by

$$\Psi_c(xe^{i\theta}) = A(k)e^{-ikxe^{i\theta}} + B(k)e^{ikxe^{i\theta}}. \tag{5.27}$$

The only solutions which do not diverge exponentially are those solutions for which the corresponding wave vectors attain the values of $k = |k|e^{-i\theta}$. For any other value of k one of the two terms in Eq. (5.27) will diverge. Consequently, the energy of the continuum is given by $|E_c - E_{th}|e^{-2i\theta}$ and is thus rotated into the lower half of the complex energy plane by an angle 2θ.

In the following sections we will show how to evaluate the resonances for non-analytic potentials.

5.3 The exterior scaling transformation

The application of the complex scaling technique encounters serious numerical difficulty in the study of problems where the potential is not dilation analytic. One such example is the calculations of the resonances as functions of the nuclear coordinates which are associated with the molecular auto-ionization phenomenon. Simpler examples are the rectangular potential well and the one-dimensional step potential which was presented in Chapter 3 and used throughout the previous chapters as a model problem. In an attempt to avoid the need to scale the entire potential it was proposed to keep the coordinates unscaled in the region where the potential is not dilation analytic (i.e., can not be expanded in the Taylor series expansion) and rotate the coordinates into the complex plane in the external region/s where the potential is dilation analytic.[5]

Such a procedure is often referred to as exterior complex scaling. The exterior scaling method is based on the fact that the role of the similarity transformation operator $\hat{S}$ is to correct the asymptote of the resonance wavefunctions (see Eqs. (5.1)–(5.4)), and therefore it is possible to define the exterior-scaled (ES) operator $\hat{S}$ as a piecewise operator

$$\hat{S}_{ES}(r_j < r_0) = 1\,, \tag{5.28}$$

whereas

$$\hat{S}_{ES}(r_j \geq r_0) = e^{i\theta(r_j - r_0)\frac{\partial}{\partial r_j}}\,, \tag{5.29}$$

---

[5] B. Simon, *Phys. Lett. A* **71**, 211 (1979); C. A. Nicolaides and D. R. Beck, *Phys. Lett. A* **65**, 11 (1978); B. Gyarmati and R. T. Vertse, *Nucl. Phys. A* **160**, 523 (1971).

where r_j stands for the radial coordinate of the j-th particle in a many-body problem.

Exercise 5.9

The potential energy for a given one-particle problem is $V(x, y, z)$, where x and y are dissociative coordinates. The asymptotic behavior of the potential at hand is given by $\lim_{x\to\infty} V(x, y, z) = 0$, $\lim_{x\to-\infty} V(x, y, z) = \infty$, $\lim_{y\to\pm\infty} V(x, y, z) = 0$ and $\lim_{z\to\pm\infty} V(x, y, z) = \infty$. It is also known that the potential is continuous but its first derivative is not well defined at $x = x_0$, $y = \pm y_0$ and $z = \pm z_0$. What similarity transformation operator $\hat{S}$ should be used in order to correct the asymptotic behavior of the resonance wavefunction in order to obtain a square integrable function with outgoing boundary conditions?

For cases such as the model problem presented in Chapter 3, the resonance solutions can be obtained in an analytical form. If we apply the exterior complex scaling transformation to these problems the same complex energies are obtained. One may wonder why should we apply the complex scaling or the exterior scaling methods for such problems.

It might be assumed that the only advantage of solving the complex scaled Schrödinger equation is that the complex scaled resonance wavefunctions can be expanded in square integrable functions of the coordinate provided that the scaling angle is large enough. However, as we will show in the following chapters, the application of the exterior scaling transformation is important for fundamental reasons. It enables us to show that all poles of the scattering matrix which are associated with the solution of the time-independent Schrödinger equation with either incoming or outgoing boundary conditions (i.e., bound, antibound, resonance and virtual states) form an ortho-normal set.

Exercise 5.10

Show that for a rectangular potential well the transcendental equations which yield the resonance complex eigenvalues are invariant under the exterior scaling transformation.

Let us apply the exterior complex scaling transformation to a single-particle one-dimensional problem (note that it is straightforward to extend this to higher dimensional many-body problems) where the potential $V(x)$ is a continuous piece wise potential and its first-order derivatives are not well defined at N points, $x = x_j\,;\, j = 1, 2, \dots, N$. The exterior complex scaling transformation (ES) implies that $x \to x$ if $x < x_0$ and $x \to (x - x_0)e^{i\theta} + x_0$ if $x \geq x_0$, where $x_0 \geq x_N$. Therefore, we can define a complex path in the complex coordinate plane, $z = F_{\mathrm{ES}}(x)$, such that

$$z = F_{\mathrm{ES}}(x) = \begin{cases} x & \text{if } x < x_0\,, \\ (x - x_0)\mathrm{e}^{\mathrm{i}\theta} + x_0 & \text{if } x \geq x_0\,. \end{cases} \tag{5.30}$$

The transformed Hamiltonian is given by

$$\hat{H}_\theta = -\frac{\hbar^2}{2M}\frac{\mathrm{d}^2}{\mathrm{d}z^2} + V(z)\,. \tag{5.31}$$

By substituting $z = F_{\mathrm{ES}}(x)$ into Eq. (5.31) one gets that

$$\hat{H}_\theta = -\frac{\hbar^2}{2M}\left[f_{\mathrm{ES}}^2(x)\frac{\mathrm{d}^2}{\mathrm{d}x^2} + (\mathrm{e}^{-\mathrm{i}\theta} - 1)\delta(x - x_0)\frac{\mathrm{d}}{\mathrm{d}x}\right] + V(F_{\mathrm{ES}}(x))\,. \tag{5.32}$$

In the case where $V(x \geq x_0) = 0$ the potential $V(F_{\mathrm{ES}}(x))$ in Eq. (5.32) is equal to the unscaled potential $V(x)$. The function $f_{\mathrm{ES}}(x)$ is given by

$$f_{\mathrm{ES}}(x) \equiv \frac{\mathrm{d}x}{\mathrm{d}z} = \begin{cases} 1 & \text{if } x < x_0\,, \\ \mathrm{e}^{-\mathrm{i}\theta} & \text{if } x \geq x_0\,. \end{cases}$$

Note that for the price of using the exterior scaling transformation which is very simple to apply to short range potentials for which $V(F_{\mathrm{ES}}(x)) \cong V(x)$ the kinetic energy operator is much more complicated than before and requires the inclusion of another term which conserves the flux at the point x_0 where the complex scaling is introduced.

Exercise 5.11

Show how the Hamiltonian presented in Eq. (5.32) is derived from Eq. (5.31) by using the contour $z = F_{\mathrm{ES}}(x)$ given in Eq. (5.30).

5.4 The smooth exterior scaling transformation

It is at times complicated to carry out the numerical calculations of resonances by the exterior scaling method. This is especially true in three-dimensional many-body problems. These numerical difficulties arise from the presence of a delta function potential term in the scaled Hamiltonian (see Eq. (5.32)). An alternative approach is to smooth out the transition from a non-scaled region to the scaled region of the coordinate space. Applying such a smooth exterior scaling transformation is in turn equivalent to adding a complex absorbing potential to the the Hamiltonian which is free of any reflections.[6] The main advantage of applying such a transformation is that under specific conditions discussed below one avoids the need to scale the potential and thus it means that the reflection-free absorbing potential (RF-CAP) we are adding to the Hamiltonian is universal and is problem-independent and energy-independent.

Let us first consider a one-particle three-dimensional Hamiltonian with spherical symmetry. When the total angular momentum is equal to zero this problem reduces to a 1D problem and r can be replaced by x in all equations for the RF-CAP. We begin with the Hamiltonian in the complex variable ρ:

$$\hat{H}(\rho) = -\frac{\hbar^2}{2M}\frac{\partial^2}{\partial \rho^2} + V(\rho)\,. \tag{5.33}$$

Now we define the smooth exterior scaling transformation by choosing a smooth path, $F(r)$, in the complex ρ plane that is as close as possible to the real axis r in the region where the interaction potential $V(r) \neq 0$, i.e., $\rho \cong r$. However,

$$\rho = F(r) \to r\mathrm{e}^{\mathrm{i}\theta} \quad \text{as} \quad r \to \infty\,. \tag{5.34}$$

Next, in order to simplify the expression for the volume element such that it will be equal to $\mathrm{d}\rho = \mathrm{d}r$ rather than $\mathrm{d}\rho = f(r)\mathrm{d}r$ we carry out the transformation

$$\hat{H}_f = f^{+1/2}(r)\hat{H}(\rho)f^{-1/2}(r)\,, \tag{5.35}$$

where

$$f(r) = \frac{\partial}{\partial r}F(r)\,. \tag{5.36}$$

This leads to the following transformed Hamiltonian:

$$\hat{H}_f = \hat{H}(r) + \hat{V}_{\text{RF-CAP}}(r)\,, \tag{5.37}$$

where the reflection-free absorbing potential, $\hat{V}_{\text{RF-CAP}}(r)$ contains two contributions,

$$\hat{V}_{\text{RF-CAP}} = \Delta V_f(r) + \hat{V}^{(f)}_{\text{CAP}}\,. \tag{5.38}$$

The first contribution $\Delta V_f(r)$ comes from the difference in the potential $V(\rho)$ along $F(r)$ and along the real axis,

$$\Delta V_f(r) = V(F(r)) - V(r)\,. \tag{5.39}$$

This term vanishes when we are dealing with a short-range potential and the scaling is carried far enough from the relevant region of interaction of the potential. The second contribution to $\hat{V}^{(f)}_{\text{CAP}}$ comes from the scaling of the kinetic energy operator

---

[6] N. Moiseyev, *J. Phys. B* **31**, 1431 (1998).

and is independent of the analyzed potential, thus producing an effective absorbing potential given by

$$\hat{V}^{(f)}_{\mathrm{CAP}} = V_0(r) + V_1(r)\frac{\partial}{\partial r} + V_2(r)\frac{\partial^2}{\partial r^2}\,, \tag{5.40}$$

where

$$V_0(r) = \frac{\hbar^2}{4M} f^{-3}(r)\frac{\partial^2 f}{\partial r^2} - \frac{5\hbar^2}{8M} f^{-4}(r)\left(\frac{\partial^2 f}{\partial r^2}\right)^2\,, \tag{5.41}$$

$$V_1(r) = \frac{\hbar^2}{M} f^{-3}(r)\frac{\partial f}{\partial r}\,, \tag{5.42}$$

$$V_2(r) = \frac{\hbar^2}{2M}(1 - f^{-2}(r))\,. \tag{5.43}$$

Now we can introduce the smooth-exterior-scaling (SES) Hamiltonian as

$$\hat{H}_{\mathrm{SES}} \equiv \hat{H}_f = \hat{T}_r + \hat{V}^{(f)}_{\mathrm{CAP}}\,, \tag{5.44}$$

where $\hat{T}_r$ is the unscaled kinetic energy operator as defined in the standard (Hermitian) formalism of quantum mechanics.

Any contour $F(r)$ for which $F(r) \to r\mathrm{e}^{\mathrm{i}\theta}$ as $r \to \infty$ can be used to calculate the resonances, each contour leading to an absorbing potential which is in principal free of reflections. For example, the RF-CAP can be constructed with the following contour (see Fig. 5.1),

$$F(r) = r + (\mathrm{e}^{\mathrm{i}\theta} - 1)\left[r + \frac{1}{2\lambda}\ln\left(\frac{\cosh[\lambda(r - r_0)]}{\cosh[\lambda(r + r_0)]}\right)\right]\,. \tag{5.45}$$

So far we refer to θ as a real parameter. However, in variational calculations which will be described in the next chapter one may define θ as a complex parameter where the variation of $\mathrm{Im}(\theta)$ when a finite number of basis functions are used is equivalent to the variation of the box-size in the box-quantization calculations.

A simple variation of this contour provides a shifted RF-CAP (SRF-CAP) which will later be shown to be preferable for numerical evaluation of resonances. The SRF-CAP is defined by using

$$F(r) = r + (\mathrm{e}^{\mathrm{i}\theta} - 1)\left[r - r' + \frac{1}{2\lambda}\ln\left(\frac{\cosh[\lambda(r - r' - r_0)]}{\cosh[\lambda(r - r' + r_0)]}\right)\right]\,. \tag{5.46}$$

Exercise 5.12

Show how the Hamiltonian given in Eq. (5.44) is derived from Eq. (5.33) by using a contour $\rho = F(r)$ in Eq. (5.45).

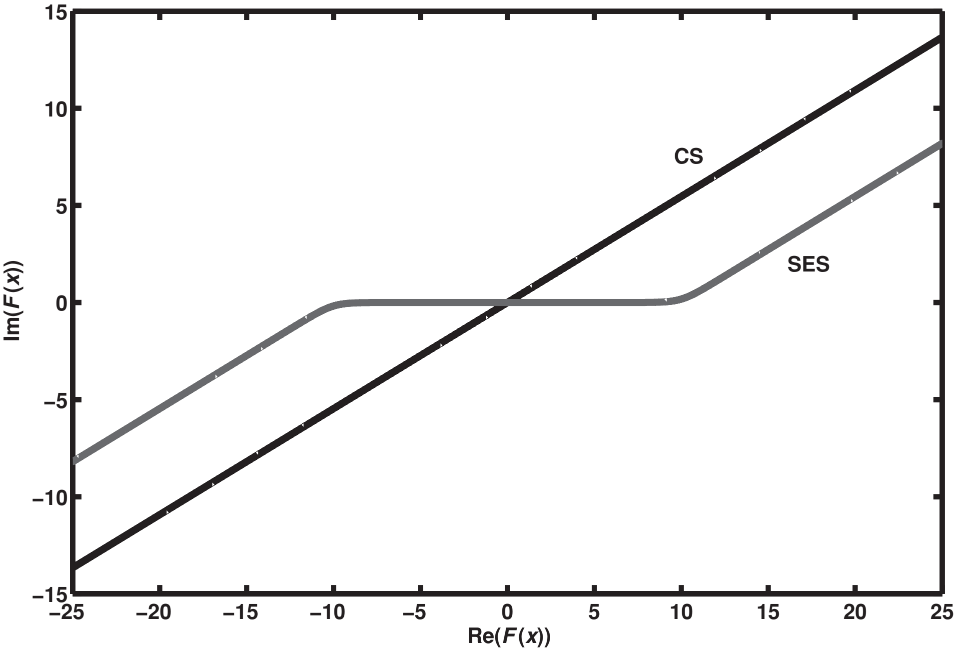

Figure 5.1 The complex scaling (CS) and the smooth-exterior-scaling (SES) transformations which correspondingly are defined by $F(x) = x\mathrm{e}^{\mathrm{i}\theta}$ and by Eq. (5.45) for spherically symmetric potentials. Note that for general 3D problems different types of SES transformation can be used for the different cartesian coordinates.

It is evident that the shifted RF-CAP (SRF-CAP) reduces to the RF-CAP when $r' = 0$.

As discussed above, when ΔV_{f} vanishes it is possible to ignore the scaling of the potential $\hat{V}_{\text{RF-CAP}} = \hat{V}^{(f)}_{\text{CAP}}$. This condition usually holds when short range potentials (SRP) are considered. For piecewise potentials this condition will always hold when $|r| > r_0$ for given values of r_0 and therefore $\Delta V_f = 0$. For a general SRP, ΔV is not strictly equal to zero in the neighborhood of $r = r_0$ and therefore the use of the problem-independent and energy-independent CAP, denoted above as $\hat{V}^{(f)}_{\text{CAP}}$, is an approximation to the RF-CAP. However, when dealing with long-range potentials the situation isn't so simple and we must consider the case where $\Delta V_f = \epsilon$, where ϵ can not be taken as small as one wishes. It should be stressed here that, when solving a many-body problem, it is hard to take into consideration the electronic repulsion in $\Delta V_f(r)$ (i.e. $|f(\mathbf{r}_i) - f(\mathbf{r}_j)|^{-1} - |\mathbf{r}_i - \mathbf{r}_j|^{-1}$) unless one assumes that the electronic repulsion vanishes when the molecule is ionized.

RF-CAP is useful not only for calculating resonances but also in avoiding the artificial reflections in the propagation of wavepackets. Such reflections result from the use of a finite number of basis functions or a finite number of grid points in the numerical time-evolution calculations. For an absorbing potential to be free of reflection it must have little or no effect on the part of the wavepacket propagating in the relevant region of space that is of interest to us. This can be explained as follows. Let us denote the exact propagated wavefunction by

$$\Psi_{\text{exact}}(r,t) = \mathrm{e}^{-\mathrm{i}Ht/\hbar}\Psi(r,0)\,. \tag{5.47}$$

Now we assume that the propagation is limited to the time $t \le T$ where $\Psi_{\text{exact}}(r > L < r_0, t \le T) = 0$, above which numerical errors start to accumulate due to distortion resulting from the parts of the wavepacket which reach $r > L$. The addition of an RF-CAP where $\hat{V}_{\text{RF-CAP}} = 0$ for $r \le L < r_0$ enables us to calculate $\Psi_{\text{exact}}(r \le L, t)$ for times which exceed the limit of $t = T$. This is achieved by suppressing the parts of the wavepacket which pass $r = L$ and thus preventing interference with the wavepacket at $r \le L$.

Exercise 5.13

Consider a wavepacket $\Psi_{\text{exact}}(r,t)$ initially localized in a region bounded by L such that $\Psi_{\text{exact}}(r > L, 0) = 0$. Show that by using the RF-CAP defined above the evolution of the wavepacket far after the RF-CAP will behave as $\Psi_{\text{RF-CAP}}(r \gg L, t) \cong 0$, while in the interaction region where $r < L$ it will behave as $\Psi_{\text{RF-CAP}}(r \le L, t) = \Psi_{\text{exact}}(r \le L, t)$ for *any* given time t.

5.5 Dilation of the Hamiltonian matrix elements into the complex plane

In many practical applications, one needs to represent the Hamiltonian by some matrix either in a basis set or on a grid. The transformation of the coordinate into the complex plane will manifest itself in the matrix elements. Without loss of generality let us assume that the non-Hermitian operator we are dealing with is a single-particle one-dimensional operator,

$$\hat{H}_\theta = -\frac{\hbar^2}{2M}\frac{\mathrm{d}^2}{\mathrm{d}z^2} + V(z)\,, \tag{5.48}$$

where z is a path in the complex coordinate plane, $z = F(x)$. The simplest complex scaling transformation is rotation by θ, $F(x) = x\mathrm{e}^{\mathrm{i}\theta}$. The smooth exterior scaling requires that $F(x) \sim x$ in the interaction region where the potential is varied and $F(x) \to x\mathrm{e}^{\mathrm{i}\theta}$ as $x \to \pm\infty$ in the non-interaction region. Since due to the transformation $x \to z$ the bound and resonance states are associated with exponentially decaying wavefunctions, we can describe them as linear combinations of some complete set of basis functions in the Hilbert space. We now expand the bound and resonance states of the non-Hermitian Hamiltonian, denoted by $\Psi_j(F(x))$, by real orthonormal basis functions, $\{\phi_n(x)\}$, such that

$$\Psi_j(F(x)) = \sum_{n=1}^{\infty} C_{n,j}\phi_n(x)\,, \tag{5.49}$$

where $C_{n,j} = \langle\phi_n|\Psi_j\rangle$. Since $\hat{H}_\theta\Psi_j = E_j\Psi_j$ (where E may attain complex values) by substituting the series expansion of Ψ_j and by multiplying the left-hand side of the time-independent Schrödinger equation by $\langle\phi_n|$ one gets the following matrix eigenvalue equation:

$$\mathbf{H}\mathbf{C}_j = E_j\mathbf{C}_j\,, \tag{5.50}$$

where the matrix elements of the Hamiltonian, $\mathbf{H}$, are given by

$$\begin{aligned}\mathbf{H}_{n',n} &= \langle\phi_{n'}|\hat{H}|\phi_n\rangle \qquad\qquad (5.51)\\ &= \int_{-\infty}^{+\infty} \mathrm{d}x\phi^*_{n'}(x)\left[-\frac{\hbar^2}{2M}\frac{\mathrm{d}^2}{\mathrm{d}(F(x))^2} + V(F(x))\right]\phi_n(x)\,.\end{aligned}$$

When the complex scaling transformation is used where $z = F(x) = x\mathrm{e}^{\mathrm{i}\theta}$, and the potential is an analytical function of x, then the Hamiltonian matrix can be presented by

$$\mathbf{H}_{n',n} = \mathrm{e}^{-\mathrm{i}\theta}\int_F \mathrm{d}z[\phi_{n'}(z^*\mathrm{e}^{+\mathrm{i}\theta})]^*\left[-\frac{\hbar^2}{2M}\frac{\mathrm{d}^2}{\mathrm{d}z^2} + V(z)\right]\phi_n(z\mathrm{e}^{-\mathrm{i}\theta})\,. \tag{5.52}$$

Since the potential is an analytical function of z we can replace the complex integration contour from $F = x\mathrm{e}^{\mathrm{i}\theta}$ by integrating over the real z line: $-\infty \le z \le +\infty$. In this case complex scaling implies that we perform an analytical continuation of the Hamiltonian matrix elements to the complex plane by substituting $\eta = \mathrm{e}^{\mathrm{i}\theta}$ in the expression we obtained for $\mathbf{H}_{n',n}(\eta)$,

$$\mathbf{H}_{n',n}(\eta) = \left\langle[\phi_{n'}(x/\eta^*)]^*\left|-\frac{\hbar^2}{2M}\frac{\mathrm{d}^2}{\mathrm{d}x^2} + V(x)\right|\phi_n(x/\eta)\right\rangle\,. \tag{5.53}$$

Sometimes for numerical reasons we will enable θ to be complex, or alternatively we define the scaling parameter as $\eta = \alpha\mathrm{e}^{\mathrm{i}\theta}$. The use of this option will be demonstrated below in Ex. 5.15 for the application of the complex scaling method to the study of molecular resonances within the framework of the Born–Oppenheimer approximation. Under this approximation the nuclear–electron attraction integral can be written as

$$\mathbf{V}_{\text{nuc-elec}}(n,n') = -\int \frac{\phi_n^*(\mathbf{r})\phi_{n'}(\mathbf{r})}{\sqrt{(\eta x - X)^2 + (\eta y - Y)^2 + (\eta z - Z)^2}} \mathrm{d}\mathbf{r}$$
$$\equiv -\eta^{-1} \int \frac{\phi_n^*(\mathbf{r})\phi_{n'}(\mathbf{r})}{\sqrt{(x - X/\eta)^2 + (y - Y/\eta)^2 + (z - Z/\eta)^2}} \mathrm{d}\mathbf{r}\,, \tag{5.54}$$

where $\mathbf{r} = (x, y, z)$ stands for the electronic coordinates and $\mathbf{R} = (X, Y, Z)$ for the nuclear coordinates. One may raise the question whether the nuclear–electron attraction integral given above is well defined for $\eta = e^{i\theta}$, since the integrand has a square-root branch point when the position of an electron coincides with the position of the nucleus. Therefore the analytical continuation of η is limited to a sphere whose radius is the distance between the electron's position and the position of the nucleus. To avoid this problem we carry out the analytical continuation of the scaling parameter after taking into consideration the volume element.

Actually there are two questions we need to answer. The first one is how to uniquely define the complex-valued integrand. Clearly, one needs to choose the correct sign of the square root such that one obtains the standard Hermitian formula when $\theta = 0$. The second question concerns the singularity of the integrand at the branch point. In fact, this singularity becomes extinguished by the spatial volume element (as long as we are in 3D space). Thus, in summary, the formula (5.54) is always finite and well defined. Using this approach molecular autoionization resonances were first calculated by the analytical continuation of Hamiltonian matrix elements.[7]

Exercise 5.14

Show that numerical difficulties can arise in the calculations of the nuclear attraction integral given in Eq. (5.54) for s-type Gaussians.

The difficulty in applying the complex scaling method to non-analytic potentials can be overcome (with some limitations) by carrying out the dilation of the Hamiltonian matrix elements instead of the kinetic and potential energy operators. In the following exercise we provide an illustrative example showing that this approach holds only for the calculations of sufficiently narrow resonances.

In the following exercise we show that one can never get the exact values of the resonance positions and widths by this method when the potential is a piecewise potential and therefore it is preferable to calculate the resonances for non-dilation analytic potentials by the exterior complex scaling or the smooth exterior

---

[7] N. Moiseyev and C. T. Corcoran, *Phys. Rev. A* **20**, 814 (1979).

scaling methods. The only motivation of using this approach for estimating the resonances for non-dilation analytic potentials is to reduce the computational effort by using a small number of grid points or basis functions and limiting the numerical calculations to the interaction region of the potential under study.

Exercise 5.15

(a) Calculate the resonances for our "toy" problem (presented in Fig. 3.1) where the potential is given by $V(x=0)=\infty$, $V(x \leq L)=0$ and $V(x>L)=-V_0$ (for the values of $L=1$ and $V_0=100$), by carrying out an analytical continuation of the Hamiltonian matrix elements into the complex plane. Use the particle-in-a-box as a basis set to construct the Hamiltonian matrix elements and carry out the analytical continuation by replacing the size of the box A_{box} as it appears in the Hamiltonian matrix elements by $A_{\mathrm{box}}\mathrm{e}^{\mathrm{i}\theta}$.

(b) Consider the solution of the same problem on equally spaced grid points $\{x_i\}_{i=1,\ldots,N}$. Under what conditions can the resonances obtained by carrying out analytical continuation of the Hamiltonian matrix be taken as adequate estimates for the exact values obtained by imposing outgoing boundary conditions on the original problem? To answer this question one should realize that the calculations of resonances by the analytical continuation of the Hamiltonian matrix elements is based on the assumption that we can replace the discontinuous potential by some smooth potential that attains approximately the same values as the original potential at the grid points $\{x_i\}_{i=1,\ldots,N}$. Consider, for example, a smooth potential which is given by $V(x)=-V_0/(\mathrm{e}^{\alpha(L-x)}+1)$.

5.6 Square integrability of field induced resonances

Within the framework of the dipole approximation the Hamiltonian for an atom in cw linearly polarized radiation can be given in four different representations: the length gauge (LG), the velocity gauge (VG), the reduced velocity gauge (RVG) and the acceleration representation(ACC) which is known also as the Kramers–Henneberger representation. These four different representations describe the *same* physical phenomenon where the electrons of a given system interact with the external ac field which is induced by the laser. Indeed, one can move from one representation of the system–laser Hamiltonian to another by carrying out a unitary transformation. We do not present these transformations here but they can be easily derived using the proof that the complex scaled field-induced resonance wavefunctions are square integrable, which is given below. Each one of the gauge representations of the system–laser Hamiltonian has its own advantages and disadvantages. The LG describes the system–laser interaction as a dipole which oscillates in time and for sufficiently small laser frequencies can be regarded as a static dc field that is varied adiabatically. The disadvantage of the LG representation is that the ionized electrons are not moving freely in space as long as the laser is on. Moreover the effective system–laser interaction parameter is increased as the electrons get farther from the nuclei of the molecular system. The RVG has the advantage that the effective system–laser interaction parameter does not increase as the electrons get farther from the nuclei of the molecular system. In the ACC representation the system–laser interaction is described as oscillating electrons which move in the field-free potential. This approach is very useful when the laser frequency is much larger than the frequency of the oscillations of the electrons in the time-averaged ACC potential. However, it is much less efficient in the calculations of the photo-induced dynamics when the laser frequency is lower than the frequency of the oscillations of the electrons in the time-averaged potential or lower than the frequency of electronic oscillations in the field-free potential.

In the LG representation the time-dependent Hamiltonian is given by

$$\hat{H}_{\mathrm{LG}}(t) = \hat{H}_0 + e\epsilon_0 f(t)\cos(\omega t)\mathbf{r}\cdot\mathbf{e}_z\,, \tag{5.55}$$

where $\hat{H}_0$ is the field-free time-independent atomic, molecular or mesoscopic Hamiltonian, ϵ_0 is the maximum field amplitude, e is the electron charge and $\mathbf{r}$ stands for the electronic atomic or molecular coordinates. The fundamental laser frequency is ω, $\mathbf{e}_z$ is the polarization direction of the propagating laser field and $f(t)$ is the laser envelope. When the duration of the laser envelope supports more than ten optical cycles (an optical cycle is defined as $T = 2\pi/\omega$) we can assume that the system interacts with a continuous-wave (cw) laser where $f(t) = 1$.

In the velocity gauge representation the time-dependent Hamiltonian is given by

$$\hat{H}_{\mathrm{VG}}(t) = \hat{H}_0 + \frac{(\hat{\mathbf{p}} - e\epsilon_0\int_0^t \mathrm{d}t' f(t')\cos(\omega t')\mathbf{e}_z)^2}{2M} - \frac{\hat{\mathbf{p}}^2}{2M}\,, \tag{5.56}$$

where the electronic momentum operator has been replaced by the vector potential operator.

In the reduced velocity gauge representation Eq. (5.56) is simplified to

$$\hat{H}_{\mathrm{RVG}}(t) = \hat{H}_0 - \frac{e\epsilon_0\int_0^t \mathrm{d}t' f(t')\cos(\omega t')\mathbf{e}_z\hat{\mathbf{p}}}{M} - \frac{\hat{\mathbf{p}}^2}{2M}\,, \tag{5.57}$$

whereas in the acceleration representation the time-dependent Hamiltonian is given by

$$\hat{H}_{\mathrm{ACC}}(t) = \hat{H}_0 + V_0(\mathbf{r} + (e\epsilon_0/M)\mathbf{e}_z\int_0^t \mathrm{d}t''\int_0^{t''}\mathrm{d}t' f(t')\cos(\omega t')) - V_0(\mathbf{r})\,, \tag{5.58}$$

where the atomic, molecular or mesoscopic field-free potential $V_0(\mathbf{r})$ has been replaced by a time-dependent potential where the electrons are driven by the laser field (time periodic ac field when a cw laser is applied and $f(t) = 1$).

As we will show below, in the LG the photo-induced resonance wavefunctions (for any one of the complex scaling transformations presented in this chapter) are square-integrable only for sufficiently narrow resonances or for very broad resonances for which the resonance lifetime $\hbar/\Gamma$ is much smaller than one optical cycle, $T = 2\pi/\omega$, where ω is the cw laser frequency (i.e., $\Gamma \gg \hbar\omega$). However, using the other types of representation the photo-induced resonance wavefunctions are square integrable regardless of the magnitudes of the resonance widths. Photo-induced resonances can be associated with the eigenfunctions of the complex scaled Floquet operator,

$$\hat{H}_{\mathrm{F}}^{\theta}(t) = \hat{S}_\theta \hat{H}_{\mathrm{F}}(t)\hat{S}_\theta^{-1}\,, \tag{5.59}$$

where $\hat{S}_\theta$ is one of the complex scaling transformations described above. The photo-induced decay rate $\{\Gamma\}$ is associated with $\{-2E_{\mathrm{res}}\}$, where $\{E_{\mathrm{res}}\}$ is a θ-independent complex eigenvalue of $\hat{H}_{\mathrm{F}}^{\theta}(t)$ (assuming that θ gets a sufficiently large value, as described above). The Floquet operator is defined by

$$\hat{H}_{\mathrm{F}}(t) = -\mathrm{i}\hbar\partial_t + \hat{H}_0 + \hat{V}(t)\,, \tag{5.60}$$

where $\hat{H}_0$ is the field-free Hamiltonian. The definition of the time-dependent interaction term $\hat{V}(t) = \hat{V}(t+T)$ varies from one representation of the Floquet operator to another. In the ACC representation it is equal to

$$\hat{V}_{\mathrm{ACC}}^{\theta}(t) = V_0(\mathbf{r}_\theta - \alpha_0\mathbf{e}_z\cos(\omega t)) - V_0(\mathbf{r}_\theta)\,, \tag{5.61}$$

where $V_0(\mathbf{r}_\theta)$ is the complex scaled field-free potential energy term in the Hamiltonian (in atoms it is the electron–nucleus attractive potential term), and $\alpha_0 = e\epsilon_0/(M\omega^2)$, where ϵ_0 is the maximum field amplitude. Here $\mathbf{r}_\theta = \hat{S}_\theta\mathbf{r}\hat{S}_\theta^{-1}$ stands for the complex scaled coordinate. In the RVG the interaction with the field is given by

$$\hat{V}_{\mathrm{RVG}}^{\theta}(t) = \frac{e\epsilon_0}{M\omega}\sin(\omega t)\mathrm{i}\partial_{z_\theta}\,. \tag{5.62}$$

In the VG representation the time-dependent potential is given by

$$V_{\mathrm{VG}}^{\theta}(t) = V_{\mathrm{RVG}}^{\theta}(t) + \frac{e^2\epsilon_0^2}{2M\omega^2}\sin^2(\omega t)\,. \tag{5.63}$$

and in the LG it is

$$V_{\mathrm{LG}}^{\theta}(t) = e\epsilon_0\mathbf{r}_\theta\cdot\mathbf{e}_z\cos(\omega t)\,. \tag{5.64}$$

The resonance Floquet solutions have the following form:

$$|\Psi_\theta(t)\rangle = \mathrm{e}^{-\mathrm{i}E_{\mathrm{res}}t/\hbar}|\Phi_\theta(t)\rangle\,, \tag{5.65}$$

where respectively $\{E_{\mathrm{res}}\}$ and $\{|\Phi_\theta(t)\rangle\}$ are the complex eigenvalues and eigenfunctions of $\hat{H}_{\mathrm{F}}^{\theta}(t)$. The resonance Floquet solutions are gauge variant. However, one can transform the solution obtained in one representation to another in the following way:[8]

$$\begin{aligned}
|\Psi_\theta^{\mathrm{RVG}}(t)\rangle &= \exp\left(-\frac{e\epsilon_0}{M\omega^2}\cos(\omega t)\partial_{z_\theta}\right)|\Psi_\theta^{\mathrm{ACC}}(t)\rangle\,, \\
|\Psi_\theta^{\mathrm{VG}}(t)\rangle &= \exp\left(-\mathrm{i}\frac{e\epsilon_0}{2M\omega^2}\int_0^t \mathrm{d}t'\,\sin^2(\omega t')\right)|\Psi_\theta^{\mathrm{RVG}}(t)\rangle\,, \\
|\Psi_\theta^{\mathrm{LG}}(t)\rangle &= \exp(-\mathrm{i}e\epsilon_0 z_\theta \sin\omega t/\omega)|\Psi_\theta^{\mathrm{VG}}(t)\rangle\,.
\end{aligned} \tag{5.66}$$

Since $\hat{V}_{\mathrm{ACC}}(t) = (V_0(\mathbf{r}_\theta + \alpha_0\mathbf{e}_z\cos(\omega t)) - V_0(\mathbf{r}_\theta) \to 0$ as $|z_\theta| \to \infty$ the asymptotes of the resonance quasi-energy solutions obtained for the complex scaled Floquet operator in acceleration representation are the complex scaled out going square-integrable waves:

$$\langle \mathbf{r}_\theta, t|\Psi_\theta^{\mathrm{ACC}}(t)\rangle \to \mathrm{e}^{-\mathrm{i}E_{\mathrm{res}}t/\hbar}\sum_n \gamma_n \mathrm{e}^{\mathrm{i}\omega n t}\sqrt{\frac{M}{\hbar^2 k_n^{\mathrm{res}}\mathrm{e}^{\mathrm{i}\theta}}}\,\mathrm{e}^{+\mathrm{i}k_n^{\mathrm{res}}z_\theta} \to 0 \tag{5.67}$$

as $|\mathbf{r}_\theta| \to \infty$, where

$$\frac{(\hbar k_n^{\mathrm{res}})^2}{2M} = E_{\mathrm{res}} + \hbar\omega n = E_{\mathrm{r}} + \hbar\omega n - \mathrm{i}\frac{\Gamma}{2} \tag{5.68}$$

and $E_{\mathrm{r}} + \hbar\omega n > 0$. Note that

$$k_n^{\mathrm{res}} = |k_n^{\mathrm{res}}|\mathrm{e}^{-\mathrm{i}\varphi_n^{\mathrm{res}}}\,, \tag{5.69}$$

where $\varphi_n^{\mathrm{res}} > 0$. In Eq. (5.67) we assume that the electrons are ionized along the direction where the laser induced linearly polarized electric field oscillates. The resonances are square integrable when

$$\theta > \frac{1}{2}\arctan\frac{\Gamma/2}{\hbar\omega n + E_{\mathrm{r}}}\,. \tag{5.70}$$

---

[8] U. Peskin, O. E. Alon and N. Moiseyev, The solution of the time-dependent Schrödinger equation by the (t, t') method: multiphoton ionization/dissociation probabilities in different gauges of the electromagnetic potentials, *J. Chem. Phys.* **100**, 7310 (1994).

Using Eqs. (5.66) one gets that the photo-induced resonance states in the RVG are square integrable functions as well,

$$\langle \mathbf{r}_\theta, t|\Psi_\theta^{\mathrm{RVG}}(t)\rangle \to$$

$$\mathrm{e}^{-\mathrm{i}E_{\mathrm{res}}t/\hbar}\sum_n \gamma_n \mathrm{e}^{\mathrm{i}\omega nt}\mathrm{e}^{-i\frac{e\epsilon_0}{M\omega^2}\cos(\omega t)k_n^{\mathrm{res}}}\sqrt{\frac{M}{\hbar^2 k_n^{\mathrm{res}}\mathrm{e}^{\mathrm{i}\theta}}}\mathrm{e}^{+\mathrm{i}k_n^{\mathrm{res}}z_\theta} \to 0\,. \tag{5.71}$$

Since the transformation from the RVG to the VG resonance wavefunctions is a multiplication of the square-integrable RVG resonance wavefunctions by a time-dependent oscillating function, it is obvious that the complex scaled photo-induced resonances in the VG are square-integrable functions as well. From Eq. (5.66) one gets that the asymptote of the photo-induced resonance function in the LG is given by

$$\langle \mathbf{r}_\theta, t|\Psi_\theta^{\mathrm{LG}}(t)\rangle \to \mathrm{e}^{-\mathrm{i}E_{\mathrm{res}}t/\hbar}\sum_n \gamma_n \mathrm{e}^{\mathrm{i}\omega nt}\mathrm{e}^{-\mathrm{i}\frac{e\epsilon_0}{M\omega^2}\cos(\omega t)k_n^{\mathrm{res}}}$$

$$\cdot\sqrt{\frac{M}{\hbar^2 k_n^{\mathrm{res}}\mathrm{e}^{\mathrm{i}\theta}}}\mathrm{e}^{+\mathrm{i}(k_n^{\mathrm{res}}-e\epsilon_0\sin\omega t/\omega)z_\theta} \to 0\,. \tag{5.72}$$

When examining the asymptotic behavior of the resonance Floquet states in the length gauge the situation appears to be different. When $t = T/2$ the asymptote of the resonance wavefunction in the LG representation is proportional to a product of decay terms $\mathrm{e}^{-|k_n^{\mathrm{res}}|\sin(\theta-\varphi_n^{\mathrm{res}})z}$ (note that $\theta - \varphi_n^{\mathrm{res}} > 0$) and when $\sin\omega t = 1$ an exponentially divergent term $\mathrm{e}^{+e\epsilon_0\sin\theta z/\omega}$. Therefore, the photo-induced resonance wavefunction in the LG representation is a square-integrable function if:

(1) the resonance lifetime $\hbar/\Gamma$ is much smaller than a half optical cycle $T/2$ and therefore

$$\Gamma \gg \frac{\hbar\omega}{\pi}\,; \tag{5.73}$$

(2) the resonance lifetime is small enough to ensure that $\exp(-|k_n^{\mathrm{res}}|\sin(\theta - \varphi_n^{\mathrm{res}})z)\exp(+e\epsilon_0\sin\theta z/\omega) \to 0$ as $z \to \infty$ and therefore the localization condition (i.e., the resonance wavefunction is square integrable) when

$$\frac{|k_n^{\mathrm{res}}|\sin(\theta-\varphi_n^{\mathrm{res}})}{\sin\theta} \geq \max\left[-\frac{e\epsilon_0\sin(\omega t)}{\omega}\right] = \frac{e\epsilon_0}{\omega}\,. \tag{5.74}$$

For sufficiently large rotational angle θ for which $\theta \gg \varphi_n^{\mathrm{res}}$ then $|k_n^{\mathrm{res}}|$ should be larger than $e\epsilon_0/\omega$. The conclusion is clear: photo-induced resonances should be calculated within the framework of the RVG (or VG and AC) where they are square-integrable functions regardless of the resonance lifetimes. *The analysis given here is applicable not necessarily only to atoms in AC (alternating current) external field* *but for all other cases where the potential is time periodic*. For example, when light propagates in waveguides where the index of refraction varies periodically along the light propagation axis, within the framework of the paraxial approximation the scalar Maxwell equation reduces to an equation which is equivalent to the time-dependent Schrödinger equation with time-periodic Hamiltonian. The resonances in this case correspond to leaking modes of the light in the waveguide. It is important to mention that in the analysis given above we discuss only the conditions for which the asymptotes of the resonance functions are square integrable and therefore our proof holds for any one of the complex scaling transformations presented above.

From AC to DC field

In an ac field, within the LG representation the interaction of an atom/molecule system with continuous wave laser is described by $e\epsilon_0 z\cos(\omega t)$. When the field varies sufficiently slowly in time the trapped particles in the atomic/molecular potential well tunnel through a quasi-static potential barrier induced by the field. The height of this barrier decreases as the field intensity is increased. In the limit of $\omega \to 0$ a transition form an AC-field to a DC-field occurs and $\hat{H}_{\mathrm{LG}} \to \hat{H}_0 + e\epsilon_0 z$. We have shown that the resonance wave function induced by a AC-field is a square-integrable function provided that the resonance lifetime $\tau\hbar/\omega < T/2$, where $T = 2\pi/\omega$. Since in the limit of DC-field $T \to \infty$ following condition (1) given above, all types of resonance (narrow, broad or overlapping) are associated with square-integrable complex scaled wavefunctions and therefore

$$\lim_{|z|\to\infty}\lim_{\omega\to 0}\Psi^{\theta}_{\mathrm{LG}}(z_\theta, t) = 0\,. \tag{5.75}$$

We proved here that in the adiabatic limit the AC resonance solution obtained in the length gauge representation of the Hamitonians decays to zero. Our proof[9] is in agreement with the proof of Herbst and Simon when the system is exposed to a dc field.[10] From condition (2) in Eq. (5.74) one gets that in the limit where

$$\lim_{\omega\to 0^+}\frac{\sin(\omega t)}{\omega} = t\,, \tag{5.76}$$

the asymptote of the Stark resonances (dc field induced resonances) decays to zero as long as

$$\frac{|k_n^{\mathrm{res}}|\sin(\theta - \varphi_n^{\mathrm{res}})}{\sin\theta} \geq -e\epsilon_0 t\,. \tag{5.77}$$

---

[9] N. Moiseyev, *Int. J. Quantum Chem.* **63**, 279–285 (1997).

[10] I. W. Herbst and B. Simon, *Phys. Rev. Lett.* **41**, 67 (1978); *Commun. Math. Phys.* **80**, 181 (1981); I. W. Herbst, *Commun. Math. Phys.* **64**, 279 (1979).

Since $t \geq 0$ the resonance obtained by applying the exterior scaling transformation is square integrable when $\theta \geq \varphi_n^{\text{res}}$.

5.7 Partial widths from the tails of the wavefunctions

When a resonance state decays it may generate various products, that is there are different channels to which it can decay. Each one of the open channels defines a product of the decay process. The products in one open channel can be very different from the products in other open channels. They can be different atoms, molecules, radicals or the same atomic or molecular species but in different electronic and/or vibrational and rotational quantum states.

By analyzing the asymptotic behavior in each of the decay channels we can deduce which of the channels is preferable. The tendency to decay to a certain channel is portrayed in its partial width, i.e. the part of the resonance width belonging to that specific channel. The partial width which is associated with a given open channel provides the decay rate of the system which is in a metastable resonance state into the specific products which are defined by the given open channel.

The complex scaling transformation renders the resonance wavefunction square integrable and thus enables us to extract from the asymptotic behavior of each channel its corresponding partial width. For example, consider a particle with mass M which moves in a 3D potential $V_{3\text{D}}(x, y, z)$. The resonance states are the solution of the 3D potential problem with outgoing boundary conditions. Let us discuss the evaluation of the partial widths of a resonance state, $\Psi_j^{\text{res}}(x, y, z)$ which is associated with the complex eigenvalue $E_j^{\text{res}} = \epsilon_j - i/2\Gamma_j$, that has only m open channels to decay. Namely, if $V_{2\text{D}}^{\pm}(y, z) = \lim_{x\to\pm\infty} V_{3\text{D}}(x, y, z)$ and the lowest m-th bound state eigenfunctions of the 2D potential are given by $\{\phi_n(y, z)^{\pm}\}_{n=1,2,\ldots,m}$ and are associated with the real eigenvalues $\{E_{\pm,n}^{\text{th}}\}_{n=1,2,\ldots,m}$ then the asymptote of the j-th resonance eigenfunction is given by

$$\lim_{x\to\pm\infty} \Psi_j^{\text{res}}(x, y, z) = \sum_{n=1}^{m} a_{n,j}^{\pm} \phi_{n_j}^{\pm}(y, z) \mathrm{e}^{\pm \mathrm{i} k_{n,j}^{\pm} x}\,, \tag{5.78}$$

where

$$k_{n,j}^{\pm} = \frac{1}{\hbar}\sqrt{2M\left(\epsilon_j - \frac{\mathrm{i}}{2}\Gamma_j - E_{\pm,n}^{\text{th}}\right)} \tag{5.79}$$

complex values and therefore the asymptote of the resonance wavefunction diverges exponentially. We can normalize the resonance wavefunctions by using one of the complex scaling transformations presented in this chapter. For example, we can scale only the dissociative x-coordinate where the particles are bounded in the other directions, i.e., $x \to F_\theta(x)$ where $\lim_{x\to\pm\infty} F_\theta(x) = x\mathrm{e}^{\mathrm{i}\theta}$. The resonance functions can be expanded in a basis which consists of the eigenfunctions of the Hermitian 2D Hamiltonian,

$$\Psi_j^{\mathrm{res}}(F_\theta(x), y, z) = \sum_{n=1}^{\infty} \phi_n^{\pm}(y, z)\chi^{\theta}_{\pm,n,j}(x)\,, \tag{5.80}$$

where we assign the labels ($\pm$, $n \leq m$) to the open channels for which

$$\lim_{x\to\pm\infty} \chi^{\theta}_{\pm,n,j}(x) = a^{\pm}_{n,j}\mathrm{e}^{\pm \mathrm{i}k^{\pm}_{n,j}x\exp(\mathrm{i}\theta)}\,. \tag{5.81}$$

The probability of having a particle in the open channel $n, \pm$ is given by

$$P_{\pm,n,j} = \frac{|a^{\pm}_{n,j}|^2}{\sum_{n=1}^{m}|a^{+}_{n,j}|^2 + \sum_{n=1}^{m}|a^{-}_{n,j}|^2}\,. \tag{5.82}$$

The coefficients $|a^{\pm}_{n,j}|^2$ are obtained by plotting

$$G^{\theta}_{\pm,n,j}(x) = |\chi^{\theta}_{\pm,n,j}(x)\mathrm{e}^{\mp\mathrm{i}k^{\pm}_{n,j}x\exp(\mathrm{i}\theta)}|^2 \tag{5.83}$$

as function of x, where

$$\chi^{\theta}_{\pm,n,j}(x) = \langle\phi_n^{\pm}(y, z)|\Psi_j^{\mathrm{res}}(F_\theta(x), y, z)\rangle_{y,z} \tag{5.84}$$

and

$$a^{\pm}_{n,j} = \lim_{x\to\infty} G^{\theta}_{\pm,n,j}(x)$$

Therefore, one may define the partial width as

$$\Gamma^{\pm}_{n,j} = P_{\pm,n,j}\Gamma_j\,, \tag{5.85}$$

Following this definition, the sum of the partial widths is equal to the total width. However, this definition for the partial widths does not necessarily associate $\Gamma_{\pm,n,j}$ with the corresponding rates of decay to each of the open channels.

Another approach is to associate the partial widths with rates of decay to the open channels. Under this assumption the partial width is the number of particles passing through a unit surface area in the $(y - z)$ plane per time unit which is associated with the n-th open channel to decay. This number is equal to $N^{\pm}_{n,j} = |a^{\pm}_{n,j}|^2 v^{\pm}_{n,j}$, where $v^{\pm}_{n,j}$ are respectively the velocities of the free particles which "escape" to $+\infty$ (while they are moving from left to right) and the free particles which "escape" to $-\infty$ (while they are moving from right to left). The velocity of a beam of free particles in one dimension is given by the ratio $F/\rho(x)$, where $F(x) = \hbar/(2M\mathrm{i})(\psi^*\partial_x\psi - \psi\partial_x\psi^*)$ is the particle flux which measures the number of the particles per unit time through a unit area perpendicular to the direction of motion x, and $\rho(x) = |\psi(x)|^2$ is the probability density of the particles. In the case where the free particles are associated with the $(\pm, n)$ open channel of the j-th resonance state, $\psi(x) = \mathrm{e}^{\pm \mathrm{i} k^{\pm}_{n,j} x}$ and therefore $v^{\pm}_{n,j} = \frac{F(x)}{\rho(x)}$ is given by

$$\begin{aligned} v^{\pm}_{n,j} &\equiv \frac{\hbar \mathrm{Re}(k^{\pm}_{n,j})}{M} \\ &= \sqrt{\frac{2}{M}} \left[(\epsilon_j - E^{\mathrm{th}}_{\pm,n})^2 + (\Gamma_j/2)^2 \right]^{1/2} \cos\left(\frac{1}{2} \arctan\left(\frac{\Gamma_j}{2(\epsilon_j - E^{\mathrm{th}}_{\pm,n})} \right) \right) . \end{aligned} \tag{5.86}$$

In order to avoid the dependence of the number of particles which are detected per time unit on the velocity of the particles we should normalized the asymptotes of $\chi^{\theta}_{\pm,n,j}(x)$ such that $a^{\pm}_{n,j}$ in Eq. (5.78) are defined by

$$a^{\pm}_{n,j} = \frac{\gamma^{\pm}_{n,j}}{v^{\pm}_{n,j}} . \tag{5.87}$$

Consequently, one might expect that the partial widths should be defined as

$$\Gamma^{\pm}_{n,j}/\hbar = \left| \gamma^{\pm}_{n,j} \right|^2 = v^{\pm}_{n,j} \lim_{x \to \pm\infty} \mathrm{e}^{\mp \mathrm{i} k^{\pm}_{n,j} \mathrm{e}^{\mathrm{i}\theta} x} \chi^{\theta}_{\pm,n,j}(x) , \tag{5.88}$$

where the resonance wavefunction is c-normalized. However, there is no guarantee that the sum of the partial widths as defined in Eq. (5.88) is equal to the total width.

Note that for sufficiently narrow resonances the velocity which appears in Eq. (5.88) can be calculated by $v^{\pm}_{n,j} = (\hbar k^{\pm}_{n,j})/M$ (here the velocity gets a complex value with a very small imaginary part). This result is obtained in Chapter 8 using the complex non-Hermitian scattering theory when the energies of the incoming particles are taken as the resonance complex eigenvalues $\epsilon_j - \frac{\mathrm{i}}{2}\Gamma_j$ (an approximation which is justified only for narrow resonances which are embedded close to the real energy axis).

We now describe another possibility for calculating partial widths, $\Gamma^{\pm}_{n,j}$, associated with the j-th resonance state from the exponentially divergent wavefunction of the unscaled resonance state.[11] It is sufficient to calculate the unscaled resonance eigenfunction in a finite volume in space which includes part of the exponentially diverging asymptotic region. This can be achieved, for example, by carrying out a back rotation transformation $\mathbf{r} \to \mathbf{r} \exp(-\mathrm{i}\theta)$ of the complex scaled square integrable resonance function. The continuity equation in standard quantum mechanics is given by

$$\frac{\partial}{\partial t} |\Phi(\mathbf{r}, t)|^2 + \nabla \cdot \mathbf{J}(\mathbf{r}, t) = 0 , \tag{5.89}$$

---

[11] T. Goldzak, I. Gilary, N. Moiseyev, *Phys. Rev. A* (in press).

where

$$\mathbf{J}(\mathbf{r}, t) = \frac{\hbar}{m}\mathrm{Im}\big[\Phi^*(\mathbf{r}, t)\nabla\Phi(\mathbf{r}, t)\big] \,. \tag{5.90}$$

Integrating Eq. (5.89) over a finite volume Ω in space which is bounded by a surface $\mathcal{S}$ we get, using the divergence theorem, that

$$\frac{\partial}{\partial t}\mathcal{N}_\Omega(t) = -\oint_{\mathcal{S}} \mathbf{J}(\mathbf{r}, t)\cdot\hat{\mathbf{n}}\,\mathrm{d}s \,. \tag{5.91}$$

Here $\hat{\mathbf{n}}$ is a unit vector normal to the surface $\mathcal{S}$ and $\mathcal{N}_\Omega(t)$ is the total probability density inside the volume Ω, given by

$$\mathcal{N}_\Omega(t) = \int_\Omega |\Phi(\mathbf{r}, t)|^2\mathrm{d}V \,. \tag{5.92}$$

Now we reach the point where we introduce the difference between the standard (Hermitian) formalism of quantum mechanics and the non-Hermitian formalism. Within the framework of the Hermitian formalism of quantum mechanics $\mathbf{J}(\mathbf{r}, t) = 0$ when $\Phi(\mathbf{r}, t)$ is the stationary solution of the time-dependent Schrödinger equation. However,within the non-Hermitian formalism of quantum mechanics $\mathbf{J}(\mathbf{r}, t) \neq 0$ when $\Phi(\mathbf{r}, t)$ is the resonance stationary solution of the time-dependent Schrödinger equation which is obtained by imposing outgoing boundary conditions on the solution. This is due to the exponential divergence of the asymptote of the resonance wavefunction which must allow outgoing flux for the resonance to decay. The resonance stationary solution of the (unscaled) time-dependent Schrödinger equation for a one-particle system is given by

$$\Phi_j^{\mathrm{res}}(x, y, z, t) = \mathrm{e}^{-\mathrm{i}(\epsilon_j - i\Gamma_j/2)t/\hbar}\Psi_j^{\mathrm{res}}(x, y, z) \,. \tag{5.93}$$

If, for the sake of simplicity of the discussion, we assume that the decay is in the x coordinate and the resonance has the asymptotic form of Eq. (5.78) we can consider Ω to be a box with length $L = L_+ + L_-$ along the x coordinate. Here $L_\pm$ indicates the edges of the box in the two asymptotes along the x coordinates. Since there is no flux in y and z we can integrate over these coordinates and Eq. (5.91) reduces to

$$\Gamma_j = \sum_n \left(\Gamma_{n,j}^+ + \Gamma_{n,j}^-\right) \,, \tag{5.94}$$

where

$$\Gamma^{\pm}_{n,j} = \hbar|\gamma^{\pm}_{n,j}|^2 \frac{\mathrm{e}^{+2\mathrm{Im}(k^{\pm}_{n,j})L_{\pm}} N^{\pm}_n}{\rho(-L_-, +L_+)}\,,$$

$$\rho(-L_-, +L_+) = \int_{-L_-}^{+L_+} \mathrm{d}x \int_{-\infty}^{+\infty}\int_{-\infty}^{+\infty} \mathrm{d}y\mathrm{d}z|\Psi^{\mathrm{res}}_j(x, y, z)|^2\,,$$

$$N^{\pm}_n = \int_{-\infty}^{+\infty}\int_{-\infty}^{+\infty} \mathrm{d}y\mathrm{d}z|\phi_{n_j}(y, z)|^2\,. \tag{5.95}$$

Although $\Gamma^{\pm}_{n,j}$ depends on the values of $L_{\pm}$, the sum of them is equal to the total resonance width which is $L_{\pm}$-independent. Since the branching ratios

$$\mathcal{R} = \frac{\Gamma^{\pm}_{n',j}}{\Gamma^{\pm}_{n,j}} \tag{5.96}$$

are measurable quantities which should be $L_{\pm}$-independent, we must ensure that

$$\mathrm{Im}(k^{\pm}_{n',j})L_{\pm} - \mathrm{Im}(k^{\pm}_{n,j})L_{\pm} = 0\,; \tag{5.97}$$

and similarly the branching ratios

$$\mathcal{R} = \frac{\Gamma^{\pm}_{n',j}}{\Gamma^{\mp}_{n,j}} \tag{5.98}$$

are $L_{\pm}$-independent if

$$\mathrm{Im}(k^{\pm}_{n',j})L_{\pm} - \mathrm{Im}(k^{\mp}_{n,j})L_{\mp} = 0\,. \tag{5.99}$$

Every one of these conditions can be satisfied separately when we assume that the surface $\mathcal{S}$ which bounds the volume Ω expands in time according to the velocities $v^{\pm}_{n,j}$ in each of the channels,

$$L_{\pm} = v^{\pm}_{n,j}\tau = \frac{\hbar\mathrm{Re}(k^{\pm}_{n,j})}{M}\tau\,. \tag{5.100}$$

For a sufficiently large value of a τ (to ensure that $L_{\pm}$ are in the asymptotic region of the resonance wavefunction) the branching ratios are constants, since for any open channel

$$\mathrm{Im}(k^{\pm}_{n,j})L_{\pm} = \frac{\hbar t}{M}\,\mathrm{Re}(k^{\pm}_{n,j})\,\mathrm{Im}(k^{\pm}_{n,j}) = \frac{\hbar\tau}{2M}\Gamma_j\,, \tag{5.101}$$

which does not depend on the channel but only on the total width of the resonance. Here we have shown that the sum of the partial widths is equal to the total width which associated with the imaginary part of the complex resonance eigenvalue.

Exercise 5.16

Photo-induced resonances are associated with the couplings of bound states in the $n = 0$ Brillouin zone (defined as the $n = 0$ Fourier transform of the atom/laser interaction potential $V_{\mathrm{ACC}}^{\theta=0}(t)$) with the continuum of the dressed potentials in the n-th Brillouin zones (defined as the $n > 0$ Fourier components of $V_{\mathrm{ACC}}^{\theta=0}(t)$, i.e., $\mathcal{V}_n(\mathbf{r}) = T^{-1}\int_0^T \mathrm{d}t\mathrm{e}^{-\mathrm{i}\omega n t} V_{\mathrm{ACC}}^{\theta=0}(\mathbf{r}, t)$. Within the Fermi golden rule approximation the values of the partial widths, Γ_n, are linearly proportional to the values of these coupling matrix elements when the energy of the continuum states is equal to the energy of the bound states. That is, if the energy of a bound state of $\mathcal{V}_0$ is $E_0^{\mathrm{bound}} < 0$ then the energy of the continuum state of $\mathcal{V}_{n>0}$ that is most strongly coupled to the bound state is $E_n^{\mathrm{cont}} = \hbar\omega n + E_0^{\mathrm{bound}}$.

1. Show that under the Fermi golden rule approximation *the partial widths oscillate as* $\alpha_0 = e\epsilon_0/(M\omega^2)$ *is varied.*
2. Explain why *there is a structure in the kinetic energy distribution of the fragmented particles (electrons in the photo-ionization process and atoms or molecular radicals in the case of photo-dissociation process)* and explain the expected effect of the variation of the laser parameters (frequency and intensity) on this structure.

This oscillatory behavior of the partial widths and of the kinetic energy distribution of the fragmented particles in the photo-induced process results from the oscillations of the electron induced by the external ac field. The phase modulation of the oscillating electron in the bound state of the $n = 0$ Floquet channel (so-called Brillouin zone) is different from the laser-induced modulation of the electron in the continuum states in the $n \neq 0$ open Floquet channels for decay.

5.8 Concluding remarks

Except for the bound states, all other poles of the S-matrix are associated with exponentially divergent wavefunctions which by definition do not belong to the Hilbert space of the conventional Hermitian quantum mechanics. In this chapter we presented several similarity transformations which convert the original exponentially divergent resonance wavefunctions into a bound-like functions which can be considered as part of the "generalized" Hilbert space. In the next chapter we will discuss different aspects of this issue in some more details. The Zel'dovich and complex scaling transformations are applicable to the resonance poles only. However, in the next chapter, where we discuss the inner product in

NHQM, we will show how the use of the exterior scaling enables the study of the orthogonality properties of all poles of the S-matrix (i.e., in addition to the resonance poles, also the anti-bound poles and poles which are associated with virtual states).

In this chapter we have shown that the complex scaling technique can be applied also to many electron problems, as for example to atoms, for the calculations of autoionization resonances. We show here that the molecular autoionization resonances can be calculated within the framework of the Born–Oppenheimer approximation by dilation of the Hamiltonian matrix elements, instead of dilation of the kinetic and the molecular potential operators, or alternatively by using the smooth-exterior-scaling transformation. The smooth-exterior-scaling transformation is equivalent (under some conditions) to the inclusion of reflection-free one-electron energy-independent and problem-independent complex absorbing potentials (so-called RF-CAPs). It is a point of interest that, by introducing the RF-CAPs into the Hamiltonian, one can propagate wavepackets for long periods of time since the artificial reflections of the waves from the edge of the grid are suppressed. In this context (see also Ex. 5.17 below) we would like to stress again the fact that the complex scaled outgoing wave components of a propagated wavepacket, $\Phi_{\mathrm{WP}}(x, t) \rightarrow \int_0^\infty \mathrm{d}k \phi(k, t) \exp(+\mathrm{i}k e^{\mathrm{i}\theta} x)$ as $t \rightarrow \infty$, are suppressed more rapidly at a given value of x as the quantum particles move faster (i.e., k gets larger values). Therefore the reflection-free complex absorbing potentials which were obtained by the use of the smooth-exterior-scaling transformation are efficient for the period of time for which the slow-moving Fourier components of the propagated wavepacket have not yet reached to the edge of the grid which has been used in the numerical propagation calculations. One may extend the time where the RF-CAPs are efficient without increasing the number of grid points or basis functions which were used in the numerical propagation calculations by adding a weak static electric field in the edge of the grid in order to accelerate the slow-moving Fourier components of the propagated wavepacket as they get close to the edge of the grid and thereby make them decay faster to zero and avoid the artificial reflections from the edge of the grid.

Exercise 5.17

Assume that the solution of the time-independent Schrödinger equation with an outgoing boundary condition is $\Psi(x)$. It can be either a bound or a resonance state. Discuss under what conditions numerical instabilities resulting from the complex scaling procedure can be avoided by the use of the exterior-scaling or the smooth-exterior-scaling similarity transformations (i.e., by the introducing the RF-CAPs).

5.9 Solutions to the exercises

Answer to Exercise 5.1

In order to show that an eigenfunction Ψ of an Hermitian and real Hamiltonian $\hat{H}$ is real, let us assume first that Ψ is a function with complex values,

$$\hat{H}\Psi = E\Psi\,, \tag{5.102}$$

where E gets real values only due to the Hermitian property of the Hamiltonian. By taking the complex conjugate of this equation we get that

$$\hat{H}\Psi^* = E\Psi^*\,. \tag{5.103}$$

Therefore, by adding the two equations one gets that the real part of Ψ, $\phi = \mathrm{Re}[\Psi]$, is an eigenfunction of the Hamiltonian,

$$\hat{H}\phi = E\phi\,. \tag{5.104}$$

Similarly, also the imaginary part of function Ψ, $\chi = \mathrm{Im}\Psi$, is a real eigenfunction of the Hamiltonian as well,

$$\hat{H}\chi = E\chi\,. \tag{5.105}$$

Thus, if there is no degeneracy in E, ϕ and χ are equivalent up to a constant normalization factor. This is equivalent to the freedom of defining Ψ up to a constant phase factor. If there is a degeneracy in E it means that we could always choose a linear combination of the eigenfunctions with energy E that will be real.

Answer to Exercise 5.2

Let us define the 1D Hamiltonian as

$$\hat{H} = -\frac{\hbar^2}{2M}\frac{\mathrm{d}^2}{\mathrm{d}x^2} + V(x)\,, \tag{5.106}$$

where

$$\hat{H}\Psi_{\mathrm{res}}(x) = E_{\mathrm{res}}\Psi_{\mathrm{res}}(x)\,, \tag{5.107}$$

and $E_{\mathrm{res}} = E - \mathrm{i}/2\Gamma$. Since $(\hbar k)^2/(2M) = E_{\mathrm{res}}$ we get that the resonance wavefunction diverges asymptotically, $\lim_{x\to\infty}\Psi_{\mathrm{res}}(x) = \gamma\exp(+\mathrm{i}kx) \to \infty$.

It is clear that

$$\hat{H}_S\Psi_S = [\mathrm{e}^{-\epsilon x^2}\hat{H}\mathrm{e}^{+\epsilon x^2}]\mathrm{e}^{-\epsilon x^2}\Psi_{\mathrm{res}} = E_{\mathrm{res}}\mathrm{e}^{-\epsilon x^2}\Psi_{\mathrm{res}} = E_{\mathrm{res}}\Psi_S\,. \tag{5.108}$$

In order to observe the effect of the transformation on the kinetic term in the Hamiltonian we need to find the effect of the transformation on the operator

d^2/dx^2,

$$e^{-\epsilon x^2}\frac{d^2}{dx^2}e^{+\epsilon x^2} = 4\epsilon^2 x^2 + 2\epsilon + 4\epsilon x\frac{d}{dx} + \frac{d^2}{dx^2}\,. \tag{5.109}$$

Now since we will take ϵ to be infinitely small we can neglect the small term $4\epsilon^2 x^2$, and by using the operator equality

$$\frac{d}{dx}x = 1 + x\frac{d}{dx} \tag{5.110}$$

we get that

$$\hat{H}_S = \hat{H} - \frac{\hbar^2\epsilon}{M}\left[x\frac{d}{dx} + \frac{d}{dx}x\right] = \hat{H} + \hat{V}_{\text{zel}}\,. \tag{5.111}$$

The complex absorbing potential (CAP) term added to the Hamiltonian, which can be termed as the Zel'dovich CAP, can be recast in the form:

$$\hat{V}_{\text{zel}}(x) = \lim_{\epsilon\to 0}\left[-\frac{\hbar i\epsilon}{M}(\hat{x}\cdot\hat{p}_x + \hat{p}_x\cdot\hat{x})\right]. \tag{5.112}$$

It is clearly evident that due to the i factor in $\hat{V}_{\text{zel}}$ it is an anti-Hermitian operator. Thus the transformed Hamiltonian, $\hat{H}_S$, is a non-Hermitian operator. The normalization of the resonance functions implies that

$$\lim_{\epsilon\to 0}\int_{-\infty}^{+\infty}\Psi_S^2(x)dx = 1\,. \tag{5.113}$$

The fact that indeed Ψ_S is a normalizable function will be proved in Ex. 5.3.

Answer to Exercise 5.3

We denote the normalization factor of the resonance wavefunction by $\mathcal{N}$. The asymptotes of the resonance wavefunctions are considered here to be linearly proportional to outgoing plane waves with complex wave vectors k_{res}. This is the case in 1D problems and also for s-waves in 3D problems with spherical symmetric potentials when we use the transformation for which the volume element is dr rather than r^2dr. In such a case the asymptotes of the resonance wavefunctions are exponentially divergent functions and

$$\int_0^\infty dr\,\Psi_{\text{res}}^2(r) = \int_0^\infty dr\,\Phi_{\text{res}}^2(r)e^{+2ik_{\text{res}}r}dr = \infty\,, \tag{5.114}$$

where $\lim_{r\to\infty}\Phi_{\text{res}}^2(r) = 1$ and $k_{\text{res}} = |k_{\text{res}}|\exp(-i\alpha_{\text{res}})$. Note that here we use the c-product and not the scalar product as used in the standard (Hermitian) formalism of quantum mechanics.

Following the Zel'dovich inner product definition, Ψ_{res} is a normalizable function if

$$\mathcal{N}^2 \lim_{\epsilon \to 0} \int_0^\infty \mathrm{e}^{-\epsilon r^2} \Phi^2_{\text{res}}(r) \mathrm{e}^{+2\mathrm{i}k_{\text{res}} r} \mathrm{d}r = 1 \,. \tag{5.115}$$

In order to show that by using the Zel'dovich inner product definition Ψ_{res} is indeed a normalizable function, we take here the case where $\Phi^2_{\text{res}}(r) = 1$, i.e., $\Psi_{\text{res}}(x) = \exp(+\mathrm{i}k_{\text{res}} r)$ is an eigenfunction of the kinetic energy operator with complex wave vector $k = k_{\text{res}}$. Then the integral given in Eq. (5.115) is associated with the error functions[12]

$$\int_0^\infty \mathrm{e}^{-\epsilon r^2 + 2\mathrm{i}k_{\text{res}} r} \mathrm{d}r = \frac{1}{2}\sqrt{\frac{\pi}{\epsilon}} \mathrm{e}^{-k^2_{\text{res}}/\epsilon} \operatorname{erfc}\left(-\frac{\mathrm{i}k_{\text{res}}}{\sqrt{\epsilon}}\right) = 1 \,. \tag{5.116}$$

It is known (see Eq. 7.4.2 in M. Abramowitz and I. A. Stegun, *Handbook of Mathematical Functions*) that for the complex variable $Z = |Z| \exp(-\mathrm{i}\phi)$, where

$$\phi < 3\pi/4 \,, \tag{5.117}$$

we have

$$\lim_{Z \to \infty} \sqrt{\pi} Z \mathrm{e}^{+Z^2} \operatorname{erfc}(Z) = 1 + \sum_{m=1} (-1)^m \frac{1 \cdot 2 \cdot 3 \cdots (2m-1)}{(2Z^2)^m} \,. \tag{5.118}$$

By substituting

$$Z = -\frac{\mathrm{i}k_{\text{res}}}{\sqrt{\epsilon}} \tag{5.119}$$

into Eq. (5.118) one gets that as $\epsilon \to 0$,

$$-\mathrm{i}k_{\text{res}} \sqrt{\frac{\pi}{\epsilon}} \mathrm{e}^{-k^2_{\text{res}}/\epsilon} \operatorname{erfc}\left(-\frac{\mathrm{i}k_{\text{res}}}{\sqrt{\epsilon}}\right) \to 1 + \frac{\epsilon}{2k^2_{\text{res}}} \,. \tag{5.120}$$

By substituting Eqs. (5.120) and (5.116) into Eq. (5.115) the normalization factor is found to be equal to

$$\mathcal{N}^2 = -2\mathrm{i}k_{\text{res}} \,, \tag{5.121}$$

provided that the phase of k_{res} (using the condition given in Eq. (5.117))

$$\alpha_{\text{res}} < \frac{\pi}{4} \,. \tag{5.122}$$

---

[12] See, for example, Eq. 7.1.23 in M. Abramowitz and I. A. Stegun, *Handbook of Mathematical Functions*, New York, Dover Publications, Inc, 1972.

For anti-bound states $\alpha = \pi/2$ and for resonances which are embedded below the threshold energy, $\alpha_{\text{res}} > \frac{\pi}{4}$ and therefore they can not be normalized by the Zel'dovich inner product approach.

For resonances, $2\alpha_{\text{res}} = -\text{Im}(E_{\text{res}})/\text{Re}(E_{\text{res}})$. The resonance rate of decay is $\Gamma = -2\text{Im}(E_{\text{res}})$, where the resonance position is $E = \text{Re}(E_{\text{res}})$ (the threshold energy is taken here as a reference point which is equal to zero). Therefore the norm can be calculated only for resonances for which

$$\frac{\Gamma}{E} \leq \frac{\pi}{8} . \tag{5.123}$$

It is a point of interest that the result for the norm presented in Eq. (5.121) is obtained by calculating the indefinite integral $\int \exp(+2\mathrm{i}k_{\text{res}}r)\mathrm{d}r$ and substitute only the lower limit of $r = 0$.

Answer to Exercise 5.4

Upon complex scaling $x \to x\exp(\mathrm{i}\theta)$. Therefore in the asymptote the functional form will be

$$\Psi^{\theta}_{\text{res}}(x \to \infty) = \gamma \mathrm{e}^{+\mathrm{i}k_{\text{res}}x\mathrm{e}^{\mathrm{i}\theta}} = \gamma \mathrm{e}^{\mathrm{i}|k_{\text{res}}|\cos(\theta-\phi_{\text{res}})x}\mathrm{e}^{-|k_{\text{res}}|\sin(\theta-\phi_{\text{res}})x} , \tag{5.124}$$

where ϕ_{res} is as defined in Eq. (5.12). The scaled resonance wavefunction decays to zero as $x \to \infty$ when the following condition is satisfied:

$$\theta \geq \phi_{\text{res}} . \tag{5.125}$$

There are, however, limitations on the maximal value of θ which will be discussed later in the text. The complex scaled resonance wavefunction $\Psi_{\text{res}}(z)$ can be normalized to unity when we take the contour $\zeta = x\exp(\mathrm{i}\theta)$ in the complex z plane, where x is the real part of z,

$$\int_{\zeta} \Psi^2_{\text{res}}(z)\mathrm{d}z = 1 . \tag{5.126}$$

When Ψ_{res} is non-singular at any point inside an area in the complex coordinate plane bounded by the line $x = \text{Re}(z)$ and the line $\zeta = x\exp(\mathrm{i}\theta)$, then the contour of integration can be changed to be along the real axis such that

$$\int_{\zeta} \Psi^2_{\text{res}}(z)\mathrm{d}z = \mathrm{e}^{\mathrm{i}\theta}\int_{-\infty}^{+\infty} \Psi^2_{\text{res}}(x\mathrm{e}^{\mathrm{i}\theta})\mathrm{d}x = 1 . \tag{5.127}$$

This normalization condition holds when Ψ_{res} is an analytical function. This result is a hint of the difficulty in applying the complex scaling transformation to cases where the potential is not an analytical function and therefore the resonance wavefunctions are non-analytical functions as well. Note that when the potential is not an analytical function we require the eigenfunctions and their first derivatives to be continuous. However, the higher order derivatives are not necessarily continuous.

Answer to Exercise 5.5

A general scaling operator is defined in Eq. (5.14) and is given by

$$\hat{S} = \sqrt{\eta}\mathrm{e}^{\hat{A}} , \tag{5.128}$$

where

$$\hat{A} = \alpha x \frac{\partial}{\partial x} \tag{5.129}$$

and $\alpha = \ln \eta$. We begin by noting that the eigenfunctions and corresponding eigenvalues of the operator $\hat{A}$ are given by

$$\hat{A}x^n = nx^n . \tag{5.130}$$

We now assume that $\Psi(x)$ is an analytical function which can be described in terms of the Taylor series expansion, $\Psi(x) = \sum_{n=0}^{\infty} C_n x^n$. By expanding also the operator $\hat{S}$ in powers of $\hat{A}$ we get that

$$\hat{S}\Psi(x) = \sqrt{\eta} \sum_{k=0}^{\infty} \frac{(\alpha\hat{A})^k}{k!} \sum_{n=0}^{\infty} C_n x^n . \tag{5.131}$$

By applying Eq. (5.130) and changing the order of summation we get that

$$\hat{S}\Psi(x) = \sqrt{\eta} \sum_{n=0}^{\infty} C_n x^n \sum_{k=0}^{\infty} \frac{(\alpha n)^k}{k!} = \sqrt{\eta} \sum_{n=0}^{\infty} C_n (\mathrm{e}^{\alpha} x)^n = \sqrt{\eta}\Psi(\eta x) . \tag{5.132}$$

Answer to Exercise 5.6

Within the framework of the Born–Oppenheimer approximation only the electronic coordinates are complex scaled while the nuclear coordinates remain unscaled. Therefore, within the framework of the Born–Oppenheimer approximation the complex scaled electron–nuclei potential energy terms are given by

$$\hat{V}^{\theta}_{\mathrm{eN}} = \sum_{\alpha,j} - \frac{z_\alpha e^2}{\sqrt{\mathbf{Q}^{\mathrm{T}}_{j,\alpha} \cdot \mathbf{Q}_{j,\alpha}}} , \tag{5.133}$$

where α and j run over all nuclei and electrons respectively and

$$\mathbf{Q}_{j,\alpha} = \mathrm{e}^{\mathrm{i}\theta}\mathbf{r}_j - \mathbf{R}_\alpha . \tag{5.134}$$

Therefore,

$$\mathbf{Q}_{j,\alpha}^{\mathrm{T}} \cdot \mathbf{Q}_{j,\alpha} = \mathrm{e}^{\mathrm{i}\theta}(\mathbf{r}_j - \mathbf{R}_\alpha^{-\theta})^{\mathrm{T}} \cdot (\mathbf{r}_j - \mathbf{R}_\alpha^{-\theta}), \tag{5.135}$$

where

$$\mathbf{R}_\alpha^{-\theta} = \mathrm{e}^{-\mathrm{i}\theta}\mathbf{R}_\alpha . \tag{5.136}$$

Consequently, one obtains that the electrons–nuclei potential energy terms are singular at the complex rotated nuclei positions $\mathbf{R}_\alpha^{-\theta}$. At these points the resonance functions do not vanish as opposed to the nuclei positions $\mathbf{R}_\alpha$ where the wavefunctions do vanish. The singular point of a function determines the radius of convergence of the Taylor series expansion of the function. Therefore, the complex scaled electron–nuclei potential energy terms are analytical functions only inside a circle in the complex electronic coordinate plane where its center is the molecular center of mass and its radius is the distance of the nuclei position from it, $|\mathbf{R}_\alpha|$. Outside this circle $\hat{V}_{\mathrm{eN}}^{\theta}$ is not an analytical function of the electronic coordinates. This explains why within the framework of the Born–Oppenheimer approximation the electron–nuclei potential energy terms are non-analytical operators.

Answer to Exercise 5.7

The function $F(x)$ should be singular at $x = x_0 < 2$. Therefore,

$$F(x) = \frac{a}{x_0 - x} . \tag{5.137}$$

We know from the first term in the Taylor series expansion that $F(0) = 1$. Therefore, $a = x_0$. The other terms in the series Taylor expansion should satisfy the following condition:

$$\frac{1}{n!}\left[\frac{\mathrm{d}^n F}{\mathrm{d}x^n}\right]_{x=0} x^n = x^n \tag{5.138}$$

and therefore $x_0 = 1$. Consequently, the non-analytical function is given by

$$F(x) = \frac{1}{1 - x} . \tag{5.139}$$

This function is an analytical function only for complex values of x inside a circle with the radius $R = |x_0| = 1$, which is centered at $x = 0$. Outside this circle the function $F(x)$ is not an analytical function and its Taylor series expansion (around $x = 0$) does not converge. Since the application of the complex scaling operator to the function $F(x)$ requires it to be an analytical function which has a converging Taylor series expansion for any value of x, it is clear that this function is not dilation analytic (i.e., a function that can be analytically continued into the complex plane for any value of x).

Answer to Exercise 5.8

The solution of this problem is based on the work of Moiseyev and Katriel.[13] We examine here a bound Hamiltonian (i.e., the spectrum is discrete) of the form

$$\hat{H} = -\frac{1}{2}\frac{d^2}{dr^2} + r^n \,. \tag{5.140}$$

Since for large values of r we solve the problem $\hat{H}\Psi_\pm(r) = 0$, the asymptotic behavior of the eigenfunctions can be easily shown to be

$$\lim_{r\to\infty} \Psi_\pm(r) = r^{-n/4} e^{\pm 2^{3/2}(n+2)^{-1} r^{n/2+1}} \,. \tag{5.141}$$

Here Ψ_- are square integrable functions but Ψ_+ are not. Note that the square integrable functions Ψ_- are associated with the discrete bound states, whereas the non-square integrable function are not associated with resonances (which do not exist in the case of bound potentials) and are known in scattering theory as anti-bound or virtual states (see Chapter 3). Upon complex scaling, $r \to r\exp(i\theta)$, $\Psi_+(re^{i\theta})$ and $\Psi_-(re^{i\theta})$ are respectively square integrable when the expression

$$\mathrm{Re}[e^{i\theta(n/2+1)}] = \cos[(n/2+1)\theta] \tag{5.142}$$

attains negative values for Ψ_+ and positive values for Ψ_-. At the critical values of $\theta = \theta_c$ for which $\cos((n/2+1)\theta_c) = 0$ the eigenfunctions "jumps" from one type of boundary condition (i.e. $\Psi_+ \to 0$) to the other type ($\Psi_- \to 0$). These critical angles are given by

$$\theta_c^{(j)} = \frac{\pi(2j+1)}{n+2}\,, \quad j = 0, 1, 2, \ldots \tag{5.143}$$

Writing the complex scaled Hamiltonian in the form

$$\hat{H} = e^{-2i\theta}\left[-\frac{1}{2}\frac{d^2}{dr^2} + e^{i\theta(n+2)} r^n\right], \tag{5.144}$$

we note that for

$$\theta \equiv \theta_j = \frac{\pi(j+1)}{n+2};\ j = 0, 1, \ldots, \tag{5.145}$$

$\exp(i\theta(n+2)) = 1$ and therefore

$$\hat{H}(\theta_j) = e^{-2i\theta_j}\hat{H}(\theta = 0) \,. \tag{5.146}$$

---

[13] N. Moiseyev and J. Katriel, *Chem. Phys. Lett.* **105**, 194 (1984).

Consequently, the eigenvalues of the complex scaled *bound* Hamiltonian when $\theta = \theta_j$ are given by

$$E_m^{(j)} = \mathrm{e}^{-\mathrm{i}\pi j(n+2)} E_m(\theta = 0)\,, \tag{5.147}$$

where $E_m(\theta = 0)$ are the discrete real eigenvalues of the unscaled Hamiltonian associated with the real square integrable eigenfunctions.

Here we show that, for the bound $V(r) = r^n$ potential, the bound states remain square integrable and remain on the real energy axis when $r \to r\exp(\mathrm{i}\theta)$, only when

$$0 \le \theta \le \frac{\pi}{n+2}\,. \tag{5.148}$$

Note that, within the range

$$\theta_{\mathrm{c}}^{(j)} < \theta \le \theta_{\mathrm{c}}^{(j+1)}\,, \quad j \ge 1\,, \tag{5.149}$$

the spurious eigenvalues as defined by Eq. (5.147) are θ-dependent. The changes in the phase factors of the eigenvalues occur abruptly at the critical angles $\theta_{\mathrm{c}}^{(j)}$. It is a point of interest that the spurious eigenvalues of bound systems in very special cases were associated with measurable quantities.[14]

Answer to Exercise 5.9

Since the potential is not spherical symmetric we should modify the exterior scaling operator, Eq. (5.29). The potential is dilation analytic for $x > x_0$, $|y| > y_0$ and $|z| > z_0$. Since z is not a dissociative coordinate we can keep z unscaled and scale only the dissociative coordinates x and y. Therefore, for $x < x_0$ we keep x as before, $x \to x$, while for $x \ge x_0$ we scale $x \to (x - x_0)\exp(\mathrm{i}\theta) + x_0$. Similarly, for $-y_0 < y < +y_0$ we keep $y \to y$ while for $|y| \ge y_0$, $y \to (y \mp y_0)\exp(\mathrm{i}\theta) \pm y_0$. Consequently, the Hamiltonian after the exterior complex scaling transformation is given by

$$\hat{H}_{\mathrm{ES}} = \hat{S}_{\mathrm{ES}}\hat{H}\hat{S}_{\mathrm{ES}}^{-1} = -\frac{\hbar^2}{2M}\left(\frac{\partial^2}{\partial x^2} + \frac{\partial^2}{\partial y^2} + \frac{\partial^2}{\partial z^2}\right) + V_{\mathrm{ES}}(x, y, z)\,, \tag{5.150}$$

where $V_{\mathrm{ES}}(x, y, z) = V(u, v, z)$ with $u = x$ if $x < x_0$ and $u = (x - x_0)\exp(\mathrm{i}\theta) + x_0$ when $x \ge x_0$; $v = y$ when $-y_0 < y < +y_0$; $v = (y - y_0)\exp(\mathrm{i}\theta) + y_0$ when $y \ge y_0$ and $v = (y + y_0)\exp(\mathrm{i}\theta) - y_0$ when $y \le y_0$.

---

[14] R. Lefebvre and N. Moiseyev, Automerization of cyclobutadiene, *J. Am. Chem. Soc.* **112**, 5052–5054 (1990); R. Lefebvre and N. Moiseyev, Artificial resonance procedure for the determination of quantum mechanical rate constants in the tunneling regime, *J. Chem. Phys.* **93**, 7173–7178 (1990); N. Rom, V. Ryaboy and N. Moiseyev, Thermal rate constants of multi-mode systems for the price of one: aziridine, *Chem. Phys. Lett.* **204**, 175–182 (1993).

Answer to Exercise 5.10

As we have shown in Chapter 3, the transcendental equations for the resonance complex eigenvalues are obtained by requiring the continuity of Ψ and $\mathrm{d}\Psi/\mathrm{d}x$. Inside the potential well, $0 < x < a$, the solutions remain unscaled,

$$\Psi_{\text{in}} = A\mathrm{e}^{+\mathrm{i}kx} + B\mathrm{e}^{-\mathrm{i}kx} \,, \tag{5.151}$$

where $k = \sqrt{2M(E + V_0)}/\hbar$. Outside the potential well the solutions are scaled from the edges of the well. For $x > a$,

$$x \to z_{\mathrm{R}} \equiv (x - a)\mathrm{e}^{\mathrm{i}\theta} + a \,, \tag{5.152}$$

while for $x < 0$,

$$x \to z_{\mathrm{L}} \equiv x\mathrm{e}^{\mathrm{i}\theta} \,. \tag{5.153}$$

Accordingly, for $x > a$ and for $x < 0$ one gets that

$$\Psi_{\text{out}} = C \exp(\pm \mathrm{i}k_0 z_{\mathrm{L,R}}) \,, \tag{5.154}$$

where $k_0 = \sqrt{2ME}/\hbar$. The continuity conditions for Ψ imply that

$$\begin{aligned} \Psi_{\text{in}}(x = a) &= \Psi_{\text{out}}(z_{\mathrm{R}} = a) = C \exp(+\mathrm{i}k_0 a) \,, \\ \Psi_{\text{in}}(x = 0) &= \Psi_{\text{out}}(z_{\mathrm{L}} = 0) = C \,. \end{aligned} \tag{5.155}$$

Therefore, the continuity conditions for Ψ are identical to those obtained before without the the use of the exterior complex scaling transformation. Similarly, the continuity conditions for the first derivative of Ψ imply that

$$\begin{aligned} \left.\frac{\partial \Psi_{\text{in}}}{\partial x}\right|_{x=a} &= \left.\frac{\partial \Psi_{\text{out}}}{\partial x}\right|_{z_{\mathrm{R}}=a} = \mathrm{i}k_0 C \exp(+\mathrm{i}k_0 a) \,, \\ \left.\frac{\partial \Psi_{\text{in}}}{\partial x}\right|_{x=0} &= \left.\frac{\partial \Psi_{\text{out}}}{\partial x}\right|_{z_{\mathrm{L}}=0} = \mathrm{i}k_0 C. \end{aligned} \tag{5.156}$$

Therefore, also the continuity conditions for the first derivative of Ψ are identical to those obtained without, exterior complex scaling transformation.

Consequently, we have shown here that for a rectangular potential well the transcendental equations for the resonance complex eigenvalues are invariant under the exterior scaling transformation. The only net effect of this transformation is in the behavior of the asymptotes of the corresponding wavefunctions which now become square-integrable.

Answer to Exercise 5.11

The exterior complex scaling transformation implies that the complex path in the complex coordinate plane, $z = F_{\mathrm{ES}}(x)$, is defined as

$$z = F_{\mathrm{ES}}(x) = \begin{cases} x & \text{if } x < x_0 \,, \\ (x - x_0)\mathrm{e}^{\mathrm{i}\theta} + x_0 & \text{if } x \geq x_0 \,. \end{cases} \tag{5.157}$$

Since

$$\frac{\mathrm{d}}{\mathrm{d}z} = f_{\mathrm{ES}}(x)\frac{\mathrm{d}}{\mathrm{d}x} \,, \tag{5.158}$$

where

$$f_{\mathrm{ES}}(x) \equiv \frac{\mathrm{d}x}{\mathrm{d}z} = \begin{cases} 1 & \text{if } x < x_0 \,, \\ \mathrm{e}^{-\mathrm{i}\theta} & \text{if } x \geq x_0 \,, \end{cases} \tag{5.159}$$

then

$$\frac{\mathrm{d}f_{\mathrm{ES}}}{\mathrm{d}x} = (\mathrm{e}^{-\mathrm{i}\theta} - 1)\delta(x - x_0) \tag{5.160}$$

and therefore

$$\begin{aligned} \frac{\mathrm{d}^2}{\mathrm{d}z^2} &= f_{\mathrm{ES}}^2(x)\frac{\mathrm{d}^2}{\mathrm{d}x^2} + \frac{\mathrm{d}f_{\mathrm{ES}}}{\mathrm{d}x} f_{\mathrm{ES}}(x)\frac{\mathrm{d}}{\mathrm{d}x} \\ &= f_{\mathrm{ES}}^2(x)\frac{\mathrm{d}^2}{\mathrm{d}x^2} + (\mathrm{e}^{-\mathrm{i}\theta} - 1)\delta(x - x_0) f_{\mathrm{ES}}(x)\frac{\mathrm{d}}{\mathrm{d}x} \,. \end{aligned} \tag{5.161}$$

Since the exterior complex scaled kinetic energy operator is defined as $-[\hbar^2/2M]\mathrm{d}^2/\mathrm{d}z^2$, the proof of Eq. (5.32) from Eq. (5.31) has been completed. On the basis of this proof the partial integrator exterior scaling method has been derived.[15]

Answer to Exercise 5.12

The proof presented here is based on the derivation of reflection-free complex absorbing potentials.[16]

We define the complex path in the one-dimensional coordinate space by $\rho = F(x)$ such that

$$\rho = F(x) \to x \exp(\mathrm{i}\theta) \tag{5.162}$$

---

[15] N. Rom and N. Moiseyev, *J. Chem. Phys.* **99**, 7703 (1993).

[16] N. Moiseyev, *J. Phys. B* **31**, 1431 (1998).

as $x \to \infty$. In order for the transition to be smooth, the path should be as close as one wishes to the real axis for $-x_0 < x < +x_0$, and therefore we choose

$$f(x) = \frac{\partial F}{\partial x} = 1 + g(x)(\mathrm{e}^{\mathrm{i}\theta} - 1)\,, \tag{5.163}$$

where $g(x)$ varies smoothly but fast from 0 to 1 around the point $x = x_0$. Since

$$\frac{\partial}{\partial \rho} = f^{-1}(x)\frac{\partial}{\partial x}\,, \tag{5.164}$$

we have

$$\frac{\partial^2}{\partial \rho^2} = -f^{-3}(x)\frac{\partial f(x)}{\partial x}\frac{\partial}{\partial x} + f^{-2}(x)\frac{\partial^2}{\partial x^2}\,. \tag{5.165}$$

Therefore the smooth exterior scaling Hamiltonian is given by

$$\hat{H}_{\mathrm{SES}} = -\frac{\hbar^2}{2M}\frac{\partial^2}{\partial \rho^2} + V(\rho) = -\frac{\hbar^2}{2M}\frac{\partial^2}{\partial x^2} + V(x) + \hat{V}_{\mathrm{SES}}(x) = \hat{H} + \hat{V}_{\text{RF-CAP}}(x)\,, \tag{5.166}$$

where

$$\hat{V}_{\text{RF-CAP}}(x) = \Delta V_{\mathrm{SES}}(x) + \hat{V}^{\mathrm{SES}}_{\mathrm{CAP}}\,, \tag{5.167}$$

$$\Delta V_{\mathrm{SES}}(x) = V(F(x)) - V(x) \tag{5.168}$$

and the reflection-free complex absorbing potential (RF-CAP) is given by

$$\hat{V}^{\mathrm{SES}}_{\mathrm{CAP}} = V_1(x)\frac{\partial}{\partial x} + V_2(x)\frac{\partial^2}{\partial x^2}\,, \tag{5.169}$$

where

$$V_1(x) = \frac{\hbar^2}{2M} f^{-3}(x)\frac{\partial f}{\partial x}\,, \tag{5.170}$$

$$V_2(x) = \frac{\hbar^2}{2M}[1 - f^{-2}(x)]\,. \tag{5.171}$$

In order to simplify the volume element, $\mathrm{d}\rho = f(x)\mathrm{d}x$, the eigenfunctions of the SES Hamiltonian as defined in Eq. (5.166) are transformed, $\Psi_{\mathrm{SES}}(\rho) = f^{-1/2}\Phi_{\mathrm{SES}}(x)$, such that $\Phi_{\mathrm{SES}}(x)$ is an eigenfunction of the transformed Hamiltonian,

$$\hat{H}^{\mathrm{trans}}_{\mathrm{SES}} = -\frac{\hbar^2}{2M} f^{+\frac{1}{2}}(x)\frac{\partial^2}{\partial z^2} f^{-\frac{1}{2}}(x) + V(\rho)\,. \tag{5.172}$$

After some algebraic derivations, $\hat{H}^{\text{trans}}_{\text{SES}}$ can be rewritten as

$$\hat{H}^{\text{trans}}_{\text{SES}} = \hat{H} + \hat{V}^{\text{trans}}_{\text{RF-CAP}}(x)\,, \tag{5.173}$$

where the transformed RF-CAP is defined as

$$\hat{V}^{\text{trans}}_{\text{RF-CAP}}(x) = \Delta V_{\text{SES}}(x) + V_0(x) + \hat{V}^{\text{SES}}_{\text{CAP}} \tag{5.174}$$

and $V_0(x)$ is defined as

$$V_0(x) = \frac{\hbar^2}{4M} f^{-3}(x) \frac{\partial^2 f}{\partial x^2} - \frac{5\hbar^2}{8M} f^{-4}(x) \left(\frac{\partial f}{\partial x}\right)^2 . \tag{5.175}$$

In the text we omit the label trans from the transformed RF-CAP and $\hat{V}^{\text{SES}}_{\text{CAP}}$ is defined to include the $V_0(x)$ term. The extra $V_0(x)$ term has been obtained due to the simplification of the expression of the volume element.

As an example we define a specific family of SES paths in the complex coordinate space which are associated with $g(x)$, given by

$$g(x) = 1 + 0.5[\tanh(\lambda(x - x_0)) - \tanh(\lambda(x + x_0))]\,. \tag{5.176}$$

By integrating over $g(x)$, the complex paths, $F(x)$, are obtained:

$$F(x) = x + (\mathrm{e}^{\mathrm{i}\theta} - 1)\left[x + \frac{1}{2\lambda} \ln\left(\frac{\cosh[\lambda(x - x_0)]}{\cosh[\lambda(x + x_0)]}\right)\right] . \tag{5.177}$$

Illustrative examples for different possible SES paths are given in Fig. 5.1 for $\lambda = 5$ when $x_0 = 0$ and when $x_0 = 6$. For $x_0 = 0$ (i.e. $\lambda = 0$) the usual complex scaling path $\rho = \exp(\mathrm{i}\theta)$ is obtained. In Fig. 5.2 the corresponding $V_0(x)$, $V_1(x)$ and $V_2(x)$ are presented. Note that when it is possible to define an SES path such that $\Delta V_{\text{SES}}(x) = 0$ the RF-CAP becomes a *universal (problem-independent) energy-independent operator*.

Answer to Exercise 5.13

The solution here is based on Shemer *et al.* studies of optimal reflection-free complex absorbing potentials for quantum propagation of wave packets.[17]

The propagated wavepacket obtained when the RF-CAP has been added to the original Hamiltonian is give by

$$\Psi^{\text{WP}}_{\text{RF-CAP}}(r, t) = \Psi^{\text{WP}}_{\text{exact}}(F(r), t)\,. \tag{5.178}$$

---

[17] O. Shemer, D. Brisker and N. Moiseyev, *Phys. Rev. A* **71**, 032716 (2005).

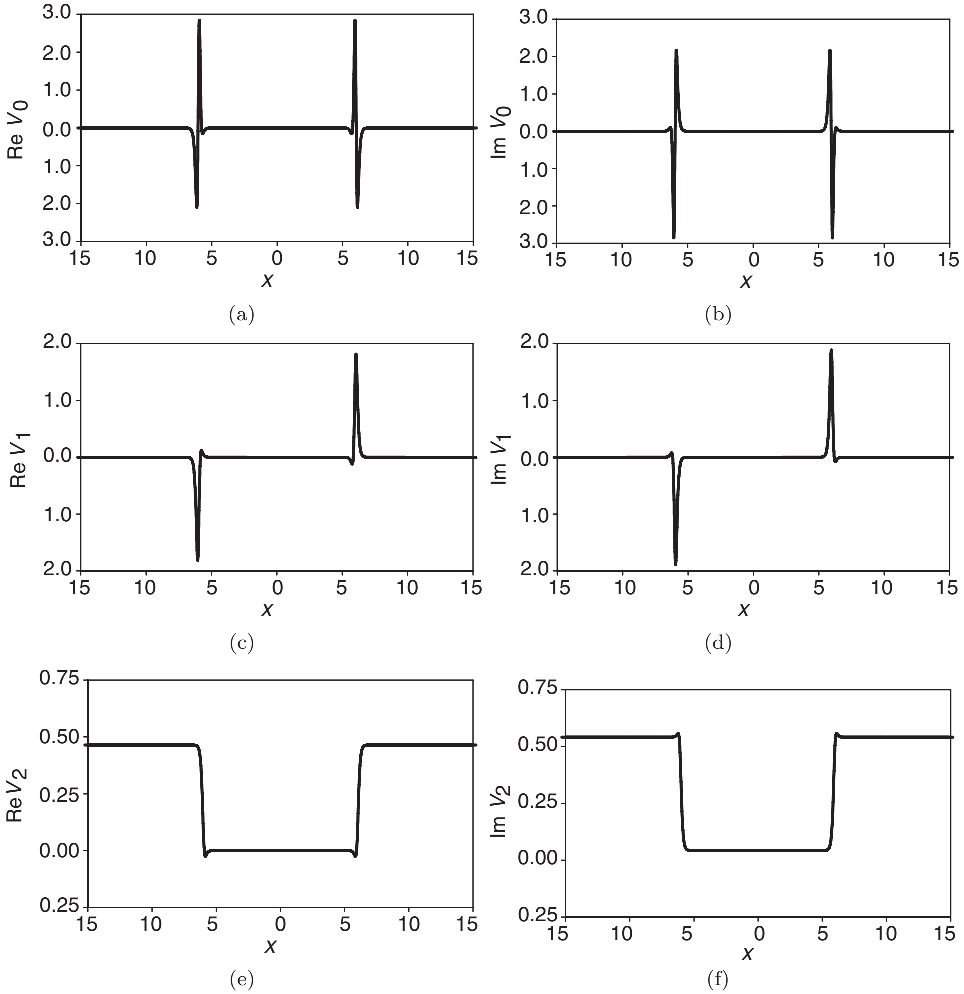

Figure 5.2 The different parts of the complex, energy-independent, problem-independent RF-CAP which is associated with the smooth-exterior-scaling path in the complex coordinate plane, $F(x) = x\mathrm{e}^{\mathrm{i}\theta}$, with $\lambda = 5$, $x_0 = 6$ and $\theta = 0.75$ rad.

Since $F(r) = r$ for $r \leq L \leq r_0$ then from a comparison between Eq. (5.178) and Eq. (5.47) one gets that in the relevant region of interest where $r < L$ at any given time t,

$$\Psi^{\mathrm{WP}}_{\text{RF-CAP}}(r \leq L, t) = \Psi^{\mathrm{WP}}_{\mathrm{exact}}(r \leq L, t)\,. \tag{5.179}$$

Using the fact that in the asymptote $F(r) \to r\exp(\mathrm{i}\theta)$ we get from Eq. (5.178) that

$$\Psi^{\mathrm{WP}}_{\text{RF-CAP}}(r \gg L, t) = \Psi^{\mathrm{WP}}_{\mathrm{exact}}(r\mathrm{e}^{\mathrm{i}\theta}, t)\,. \tag{5.180}$$

The asymptote of the propagated exact wavepacket can be described as a linear combination of outgoing waves only, since the asymptote of a propagated WP describes outgoing particles with momentum that can be measured by a detector (no source of incoming waves at infinity and therefore there is no incoming flux of particles arriving from infinity):

$$\lim_{r\to\infty} \Psi^{\mathrm{WP}}_{\mathrm{exact}}(r,t) = \int_0^\infty \mathrm{d}k C(k)\mathrm{e}^{\mathrm{i}kr} \,. \tag{5.181}$$

By scaling the asymptote of the propagated WP one gets that

$$\lim_{r\to\infty} \Psi^{\mathrm{WP}}_{\mathrm{exact}}(r\mathrm{e}^{\mathrm{i}\theta},t) = \int_0^\infty \mathrm{d}k C(k)\mathrm{e}^{\mathrm{i}k\cos(\theta)r}\mathrm{e}^{-k\sin(\theta)r} \,. \tag{5.182}$$

As one can see from Eq. (5.182) for sufficiently large value of r

$$\Psi_{\mathrm{exact}}(r\mathrm{e}^{\mathrm{i}\theta},t) \cong 0 \,, \tag{5.183}$$

although $\Psi_{\mathrm{exact}}(r,t)$ might have a large positive or negative amplitude. On the basis of Eq. (5.180) one gets that for $r \gg L$, $\Psi^{\mathrm{WP}}_{\mathrm{RF\text{-}CAP}}(r\mathrm{e}^{\mathrm{i}\theta},t) \cong 0$.

Answer to Exercise 5.14

The solution of this problem is given by Moiseyev and Corcoran.[18]

The matrix element for s-type Gaussians is of the form[19]

$$V_{n,n'}(\eta R) \sim \mathrm{e}^{-(\gamma_n+\gamma_{n'})(\mathbf{R}_n-\vec{R}_{n'})} F_0[(\gamma_n+\gamma_{n'})(\mathbf{P}-\eta\mathbf{R}^2] \,, \tag{5.184}$$

where $\eta = \alpha\exp(-\mathrm{i}\theta)$, $\mathbf{P}$ is the weighted center of the two functions with orbital exponents γ_n and $\gamma_{n'}$ and positions $\vec{R}_n$ and $\mathbf{R}_{n'}$, respectively, $\mathbf{R}$ is the position of the nucleus and F_0 is the incoming γ function. The simplest example of the problem occurs for $\gamma_n = \gamma_{n'} \equiv \gamma$ and $R_n = R_{n'} \equiv R \neq 0$. In this case we have

$$V_{n,n'}(\eta R) \sim F_0[2\gamma R^2(1-\eta)^2] \equiv F_0(\zeta) \,. \tag{5.185}$$

The series expansion for $F_0(\zeta)$ has a pre-factor of $\exp(-\zeta)$. Near $|\eta| = 1$ (i.e., $\alpha = 1$), one may have $\mathrm{Re}(1-\eta)^2 < 0$, and therefore $V_{n,n'}(\eta R)$ may become large for large values of the non-linear Gaussian's parameter, γ. When ζ has positive values then the pre-factor $\exp(-\zeta)$ of the function F_0 can become very large and thereby introduces numerical instabilities for large values of θ. To overcome this numerical instability one should keep $\alpha\cos\theta$ larger than unity. Since usually the

---

[18] N. Moiseyev and C. T. Corcoran, *Phys. Rev. A* **20**, 814 (1979).

[19] I. Shavit, *Method in Computational Physics* (New York, Academic Press, 1963), Vol. 2.

resonances of interest are embedded close enough to the real axis, the rotational angle θ, which is required to transform the exponentially divergent resonance wavefunction to the generalized Hilbert space, gets sufficiently small. In such a case α does not have to get very large to satisfy the numerical stability condition, $\alpha\cos(\theta) > 1$, and it might be sufficient to keep α only slightly larger than unity.

Answer to Exercise 5.15

(a) The solution of this problem has been given by Alon and Moiseyev.[20] The basis functions are given by

$$\varphi_n(x) = \sqrt{\frac{2}{A_{\text{box}}}}\sin\left(\frac{n\pi x}{A_{\text{box}}}\right), \tag{5.186}$$

where $n = 1, 2, \ldots, N$. The Hamiltonian matrix elements are accordingly

$$\begin{aligned} H_{n',n} &= \langle\varphi_{n'}|\hat{H}|\varphi_n\rangle \qquad (5.187)\\ &= \frac{2}{A_{\text{box}}}\int_0^{A_{\text{box}}} \sin\left(\frac{n'\pi x}{A_{\text{box}}}\right)\left[\frac{-\hbar^2}{2M}\frac{\mathrm{d}^2}{\mathrm{d}x^2} - V_0\Theta(x-L)\right]\sin\left(\frac{n\pi x}{A_{\text{box}}}\right)\mathrm{d}x\,. \end{aligned}$$

After performing the integration this translates to the following matrix elements

$$\begin{aligned} H_{n,n} &= \frac{\hbar^2}{2M}\left(\frac{n\pi}{A_{\text{box}}}\right)^2 - V_0\left(\frac{\sin(2n\pi L/A_{\text{box}})}{2\pi n} + \frac{A_{\text{box}} - L}{A_{\text{box}}}\right),\\ H_{n',n} &= -V_0\left(\frac{\sin[(n+n')\pi L/A_{\text{box}}]}{\pi(n+n')} - \frac{\sin[(n-n')\pi L/A_{\text{box}}]}{\pi(n-n')}\right), \end{aligned} \tag{5.188}$$

where

$$A_{\text{box}} = |A_{\text{box}}|\mathrm{e}^{\mathrm{i}\theta}\,. \tag{5.189}$$

For the parameters of $\theta = 0.05$, $N = 1000$, $L = 1$, $A_{\text{box}} = 150$ and $V_0 = 100$ the eigenvalues of the Hamiltonian matrix $\mathbf{H}$ presented in Fig. 5.3 are associated with the resonances and the rotated continuum.

(b) The N grid points are given by $\{x_i = \Delta(i-1)\}_{i=1,\ldots,N}$. The calculation of resonances by analytical continuation of Hamiltonian matrix elements is based on the assumption that the spectrum of the original non-dilation analytic potential can often be well-approximated by the spectrum of another potential which is dilation analytic and therefore the complex scaling transformation is applicable. Note that for dilation analytical potentials the Hamiltonian matrix elements obtained by analytical continuation of the scaling parameter of the basis functions by $\mathrm{e}^{-\mathrm{i}\theta}$

---

[20] O. E. Alon and N. Moiseyev, *Phys. Rev. A* **46**, 3807 (1992).

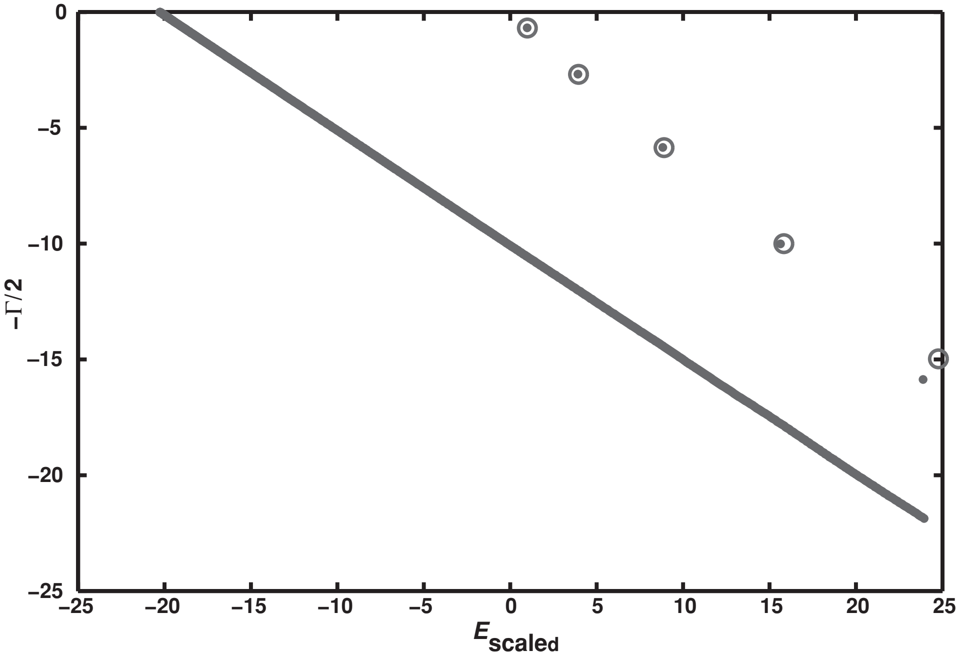

Figure 5.3 The complex eigenvalues, $E - \mathrm{i}/2\Gamma$ obtained by the diagonalization of the Hamiltonian matrix defined in Eqs. (5.188). In the plot the scaled energies $\tilde{E} = 2ML^2E/(\pi^2\hbar^2)$ are presented. The open circles stand for the exact values obtained by solving the corresponding transcendental equations (see Tables 4.1 and 4.2). The continua are rotated into the complex energy plane by the angle $2\theta = 0.1$. The deviations of the calculated resonances from the exact values are partially due to the truncation of the basis set and the artificial truncation of space at $|A_{\mathrm{box}}|$. However, as explained in Ex. 5.5, the calculation of resonances of the piecewise potential is limited to narrow resonances only.

where the Hamiltonian is unscaled are identical to the matrix elements which are calculated by using complex scaled Hamiltonian (where $x \to x\mathrm{e}^{\mathrm{i}\theta}$) and unscaled basis functions (see Eq. (5.51) where $F(x) = x\mathrm{e}^{\mathrm{i}\theta}$ and Eq. (5.53)). We assume that the dilation analytical function is such that $V(x \leq L) \simeq 0$ and $V(x > L) \simeq -V_0$. For example, we can chose a smooth potential

$$V(x) = -\frac{V_0}{\mathrm{e}^{\alpha(L-x)} + 1}\,, \tag{5.190}$$

then

$$V(x = L - \Delta/2) = -\frac{V_0}{1 + \mathrm{e}^{+\alpha\Delta/2}} \tag{5.191}$$

and

$$V(x = L + \Delta/2) = -\frac{V_0}{1 + \mathrm{e}^{-\alpha\Delta/2}}\,. \tag{5.192}$$

The accuracy of our calculations depends on the value of α. As $\alpha\Delta$ gets larger the deviation of the dilation analytical potential from the piecewise potential is smaller. This implies that for a given accuracy of the calculations

$$\alpha\Delta = C\,, \tag{5.193}$$

where C determines the deviation of the smooth potential from the original discontinuous potential. However, the smooth potential has poles at $x = x_{\mathrm{p}}$ when

$$\mathrm{e}^{\alpha(L - x_{\mathrm{p}})} + 1 = 0\,. \tag{5.194}$$

Eq. (5.194) is satisfied when

$$\alpha(x_{\mathrm{p}} - L) = \pm \mathrm{i}\pi \tag{5.195}$$

and therefore

$$x_{\mathrm{p}} = L \pm \mathrm{i}\frac{\pi}{\alpha} = |x_{\mathrm{p}}|\mathrm{e}^{\mathrm{i}\theta_{\mathrm{p}}}\,. \tag{5.196}$$

Consequently, the Taylor series expansion of the potential given in Eq. (5.192) converges *only* when

$$|x| < |x_{\mathrm{p}}|\,, \tag{5.197}$$

and only within a circle in the complex coordinate plane which is centered at $x = 0$ and with radius is $|x_{\mathrm{p}}|$ is this potential dilation analytic. The conclusion is clear. If the complex scaled resonance wavefunctions are practically equal to zero for $x \geq |x_{\mathrm{p}}| - \Delta$ then we can estimate the resonance positions and widths of the piecewise potential by carrying out analytical continuation of the Hamiltonian matrix elements into the complex plane (which is equivalent to complex scaling if the potential is dilation analytic). As we will show here, by this complex scaling method we can never obtain the exact values of the resonance positions and widths and therefore it is preferable to calculate the resonances for non-dilation analytic potentials by the exterior complex scaling or by the smooth exterior scaling methods.

Let us assume, for example, that $\psi_{\mathrm{res}}(x\mathrm{e}^{\mathrm{i}\theta})|_{x=|x_{\mathrm{p}}|-\Delta} = 10^{-8}$, which within the accuracy of the numerical calculations can be taken as equal to zero. We can estimate the resonances for which this condition is satisfied since we know that the asymptotic behavior of $\psi_{\mathrm{res}}(x\mathrm{e}^{\mathrm{i}\theta})$ is

$$\psi_{\mathrm{res}}(x\mathrm{e}^{\mathrm{i}\theta} \to \infty) \propto \mathrm{e}^{+\mathrm{i}|k_{\mathrm{res}}|\mathrm{e}^{\mathrm{i}(\theta - \phi_{\mathrm{res}})}x}\,, \tag{5.198}$$

where (in au) $\frac{1}{2}|k_{\text{res}}|^2 \mathrm{e}^{-2i\phi_{\text{res}}} = E_{\text{res}} + V_0$ and $-2\mathrm{Im}(E_{\text{res}}) = \Gamma$ while the threshold energy in our case is $-V_0$. As Γ gets larger ϕ_{res} also becomes larger and therefore the rotational angle θ should be significantly larger to insure that the condition of $\psi_{\text{res}}(x\mathrm{e}^{\mathrm{i}\theta})|_{x=|x_{\text{p}}|-\Delta} \approx 0$ is satisfied. However, as will be shown below, the complex scaling transformation is limited to $\theta < \theta_{\text{c}}$. In order to estimate the critical angle θ_{c} we can look at the dominant term: in the expansion of the exponential potential term:

$$\mathrm{e}^{\alpha(L-x)} = \sum_{n=0}^{\infty} \frac{(\alpha(L-x))^n}{n!} \,. \tag{5.199}$$

It is simpler to approximate at any given point x_0 the logarithm of this term and find the value n_{max} for which it is maximal.

$$\frac{\partial \ln[\alpha(L-x_0)^n/n!]}{\partial n}\bigg|_{n_{\text{max}}} \approx \ln[\alpha(L-x_0)] - \ln n = 0 \,. \tag{5.200}$$

This means that the most dominant contribution in the expansion at x_0 is

$$n_{\text{max}} \approx \alpha(L-x_0) \,. \tag{5.201}$$

Let x_0 be just beyond the edge of the potential barrier, i.e. $L - x_0 = \Delta$. Consequently, just beyond the edge of the potential barrier the potential can be approximated by

$$V \propto -\frac{V_0}{x^{\alpha\Delta} + 1} \,, \tag{5.202}$$

where $C = \alpha\Delta$ defines the accuracy of our numerical calculations (see Eq. (5.193)). Writing the complex scaled Hamiltonian we note that

$$\theta C < \pi \tag{5.203}$$

in order to avoid the change of the phase of x^{C}. Therefore,

$$\theta < \theta_{\text{c}} \equiv \frac{\pi}{C} \,. \tag{5.204}$$

However, in order to expose the resonance state $E_{\text{r}} - \frac{\mathrm{i}}{2}\Gamma$ we must have

$$2\theta \geq \arctan \frac{\Gamma}{2E_{\text{r}}} \,. \tag{5.205}$$

This means that the resonances calculated by the analytical continuation of Hamiltonian matrix elements can serve as adequate estimates for the resonance values obtained by solving the original problem with outgoing boundary conditions if and only if

$$\frac{2\pi}{C} > \arctan\frac{\Gamma}{2E_\mathrm{r}}\,. \tag{5.206}$$

Thus the resonance widths must be sufficiently narrow to satisfy

$$\Gamma \ll 2E_\mathrm{r}\tan\left[\frac{2\pi}{C}\right]. \tag{5.207}$$

It is clear that as C is increased and the smooth potential approaches the shape of a piecewise potential barrier the ability of calculating resonance positions and widths by the analytical continuation of Hamiltonian matrix elements is reduced. The only motivation for using this approach for estimating the resonances for non-dilation analytic potentials is to reduce the computational effort by using a small number of grid points or basis functions and limiting the numerical calculations to the interaction region of the potential under study.

Answer to Exercise 5.16

We will prove here that by increasing the laser field intensity, $I = c\epsilon_0^2/(8\pi)$, the rate of decay (e.g., ionization of the atom or a dissociation of a molecule) due to the absorption of n photons oscillates with the quiver length $\alpha_0 = e\epsilon_0/(M\omega^2)$. This behavior is due to the interference between the phase modulation induced by the ac field of the electron that occupies a bound state in one Floquet channel with the phase modulation of the electron when it occupies the continuum states of other Floquet channels which are open for decay (see discussion in Chapter 2).

The interaction potential between the atom/molecule and a linearly polarized cw laser field within the framework of the acceleration representation is given in the Fourier basis set expansion by

$$V_\mathrm{ACC}(\mathbf{r} + \mathbf{e}_z\alpha_0\cos(\omega t)) = \int_{-\infty}^{+\infty} \mathrm{d}k v(x, y, k)\mathrm{e}^{\mathrm{i}kz}\mathrm{e}^{\mathrm{i}k\alpha_0\cos(\omega t)}\,. \tag{5.208}$$

The coupling between the eigenstates of the n'-th dressed potential (so-called n-Floquet channel or n-th Brillouin zone) and the eigenstates of the n-th dressed potential is thus given by an interaction potential of the form

$$V_\mathrm{ACC}(n, n') = \frac{1}{T}\int_0^T \mathrm{d}t\mathrm{e}^{-\mathrm{i}(n-n')\omega t}V_\mathrm{ACC}(\mathbf{r} + \mathbf{e}_z\alpha_0\cos(\omega t))\,. \tag{5.209}$$

Therefore, the Fourier basis set expansion of the interaction potential in the acceleration presentation yields

$$[V_{\mathrm{ACC}}(\mathbf{r})]_{n',n} = \int_{-\infty}^{+\infty} \mathrm{d}k v(x, y, k) \mathrm{e}^{\mathrm{i}kz} \frac{1}{T} \int_0^T \mathrm{d}t \mathrm{e}^{\mathrm{i}k\alpha_0 \cos(\omega t) - \mathrm{i}(n-n')\omega t}$$
$$= \int_{-\infty}^{+\infty} \mathrm{d}k v(x, y, k) \mathrm{e}^{\mathrm{i}kz} \mathrm{e}^{\mathrm{i}\frac{(n-n')\pi}{2}} J_{n-n'}(\alpha_0 k) \,. \tag{5.210}$$

If $n - n' > 0$ the coupling matrix element includes the coupling of the bound states of the n-th dressed potential with the continuum states of the n'-th dressed potentials that have the *same* energy as the bound states, $\{E_\mathrm{b}\}$.

Following the Fermi golden rule, the partial width, Γ_n, which results from the coupling of a bound state in the $n' = 0$ dressed potential, $|E_\mathrm{b}(0)\rangle$, with the continuum of the $n > 0$ dressed potential, $|E_\mathrm{c}(n)\rangle$, which is approximately described as a spatial function multiplied by $\delta(k - k_n) \exp(\mathrm{i}kr)$, where $k_n = \sqrt{2M(E_b + \hbar\omega n)}/\hbar$, is given by the matrix element,

$$\Gamma_n(\alpha_0, E_\mathrm{b}) \propto |\langle E_\mathrm{b}(0)|[V_{\mathrm{ACC}}(\mathbf{r})]_{0,n}|E_\mathrm{c}(n)\rangle|^2 = |a_n J_n(\alpha_0 k_n)|^2 \,, \tag{5.211}$$

where $J_n(\alpha_0 k_n)$ is the n-th Bessel function with the argument $\zeta = \alpha_0 k_n$. Since the Bessel functions oscillate with ζ it is clear that the partial widths oscillate with the variation of $\alpha_0 = e\epsilon_0/(M\omega^2)$ as well.

The branching ratio $\Gamma_n(\alpha_0, E_\mathrm{b}) / \sum_n \Gamma_n(\alpha_0, E_\mathrm{b})$ provides the probability of observing ionized electrons or fragmented particles with the kinetic energy $(\hbar k_n)^2/(2M)$ as a result absorbing n-photons. Therefore, the kinetic energy distribution of the ionized electron or of the fragmented particle in the case of molecular photo-dissociation is proportional to $|J_n(\alpha_0 k)|^2$, where $(\hbar k_n)^2/(2M)$ and $k_n = \sqrt{2M(E_\mathrm{b} + \hbar\omega n)}/\hbar$ is the kinetic energy of the fragmented particles.

Therefore, if the dynamics are described by an n-photon process the kinetic energy distribution of the fragmented particles will show an oscillatory behavior determined by the zeroes of the n-th Bessel function. The effect of the variation of the laser parameters (frequency and intensity) on the structure of the kinetic energy distribution (i.e., the energy gaps between the fragmented particles) is similar to the effect of the variation of α_0 on the locations of the zeroes of the n-th Bessel function.

Answer to Exercise 5.17

In order to address numerical effects of the complex scaling technique on the resonance or bound states wavefunctions we expand $\Psi(x)$ in the Fourier basis set,

$$\Psi(x) = \int_{-\infty}^{+\infty} \mathrm{d}k C(k) \mathrm{e}^{\mathrm{i}kx} \,, \tag{5.212}$$

where the wave vector k is related to the momentum of the wavefunction by $p = \hbar k$.

Complex scaling implies that

$$\Psi_\theta(x) = \int_{-\infty}^{+\infty} \mathrm{d}k C(k) \mathrm{e}^{\mathrm{i}k\cos\theta x} \mathrm{e}^{-\sin\theta k x} \,. \tag{5.213}$$

The probability of finding the quantum particle in a given point of the classical phase space of $\{x_0, p_0\}$ can be obtained from the Husimi distribution of Ψ,

$$\Xi(x_0, p_0) = (\pi\hbar)^{-1/4} \int_{-\infty}^{+\infty} \mathrm{d}x \Psi(x) \mathrm{e}^{-\frac{(x-x_0)^2}{2\hbar} + \mathrm{i}\frac{p_0 x}{\hbar}} \,. \tag{5.214}$$

From the Husimi distribution of the unscaled function, $\Psi(x)$, one can learn at what point in phase space the product $p_0 x_0 < 0$ associated with the contribution of incoming waves to the Fourier expansion of Ψ gets the maximal value of $\Xi(x_0, p_0 < 0)$.

From Eq. (5.213) it is clear that when $\mathrm{e}^{-\sin\theta x_0 k_0}$ gets very large the numerical calculations of the complex scaled function Ψ_θ will be very unstable. It is, therefore, quite clear that it will be hard to compute the highly excited bound or resonance complex scaled states due to the large amplitude far from the bottom of the potential well which usually is chosen as the origin of the coordinates. This numerical instability should be more pronounced in the calculations of molecular resonances within the Born–Oppenheimer approximation where the molecular wavefunctions might have large amplitudes far from the center of mass of the molecule. Therefore, this kind of numerical instability is avoided when the exterior scaling method or the smooth exterior scaling method (as for example by introducing the RF-CAPs into the Hamiltonian) are applied and only the outgoing asymptote of Ψ is complex scaled (i.e., $x_0 p_0 > 0$).

5.10 Further reading

Resonances, diverging wavefunctions and complex scaling for analytical potentials

G. Gamow, Zur Quantentheorie des Atomkernes, *Z. Phys. A* **51**, 204–212 (1928).

A. J. F. Siegert, On the derivation of the dispersion formula for nuclear reactions, *Phys. Rev.* **56**, 750–752 (1939).

J. Aguilar and J. M. Combes, A class of analytic perturbations for one-body Schrödinger Hamiltonians, *Commun. Math. Phys.* **22**, 269–279 (1971).

E. Balslev and J. M. Combes, Spectral properties of many-body Schrödinger operators with dilatation-analytic interactions, *Comm. Math. Phys.* **22**, 280–294 (1971).

B. Simon, Quadratic form techniques and the Balslev–Combes theorem, *Commun. Math. Phys.* **27**, 1–9 (1972).

B. Simon, Resonances in *n*-body quantum systems with dilatation analytic potentials and the foundations of time-dependent perturbation theory, *Ann. Math.* **97**, 247–274 (1973).

N. Moiseyev and J. O. Hirschfelder, Representation of several complex coordinate methods by similarity transformation operators, *J. Chem. Phys.* **88**, 1063–1065 (1988).

Zel'dovich transformation

Ya. B. Zel'dovich, On the theory of unstable states, *Sov. Phys. JETP* **12**, 542–548 (1961).

I. Baz', Ya. B. Zel'dovich and A. M. Perelomov, *Scattering, Reactions and Decay in Nonrelativistic Quantum Mechanics*, Moskva, Fiziko-Matematicheskoi Literatury, 1966 and translation from Russian by the Israel Program for Scientific Translations, Jerusalem 1969.

Complex scaling transformation for Coulomb potentials in electric fields

S.-I. Chu and D. A. Telnov, Beyond the Floquet theorem: generalized Floquet formalisms and quasienergy methods for atomic and molecular multiphoton processes in intense laser fields, *Phys. Rep.* **390(1–2)**, 1–131 (2004).

A. Maquet, S.-I. Chu and W. P. Reinhardt, Stark ionization in dc and ac fields: an L2 complex-coordinate approach, *Phys. Rev. A* **27**, 2946–2970 (1983).

C. Cerjan, W. P. Reinhardt and J. E. Avron, Spectra of atomic Hamiltonians in DC fields: use of the numerical range to investigate the effect of a dilatation transformation, *J. Phys. B* **11**, L201–L205 (1978).

Resonance wavefunctions by analytical continuation of Hamiltonian matrix elements to the complex plane

N. Moiseyev and C. T. Corcoran, Autoionizing states of H_2 and H_2^- using the complex scaling method, *Phys. Rev. A* **20**, 814–817 (1979).

N. Lipkin, N. Moiseyev and C. Leforestier, Resonance positions and widths by a similarity transformation of a Hermitian Hamiltonian matrix, *J. Chem. Phys.* **92**, 227–230 (1990).

Exterior complex scaling

B. Gyarmati and R. T. Vertse, Normalization of Gamow functions, *Nucl. Phys. A* **160**, 523–528 (1971).

C. A. Nicolaides and D. R. Beck, The variational calculation of energies and widths of resonances, *Phys. Lett. A* **65**, 11–12 (1978).

B. Simon, The definition of molecular resonance curves by the method of exterior complex scaling, *Phys. Lett. A* **71**, 211–214 (1979).

J. Simons, The complex coordinate rotation method and exterior scaling: a simple example, *Int. J. Quant. Chem. Symp.* **14**, 113–121 (1980).

N. Lipkin, N. Moiseyev and E. Brändas, Resonances by the exterior-scaling method within the framework of the finite-basis-set approximation, *Phys. Rev. A* **40**, 549–553 (1989).

Smooth exterior scaling transformation

N. Rom, N. Lipkin and N. Moiseyev, Optical potentials by the complex coordinate method, *Chem. Phys.* **151**, 199–204 (1991).

N. Moiseyev, Derivations of universal exact complex absorption potentials by the generalized complex coordinate method, *J. Phys. B: At. Mol. Opt. Phys.* **31**, 1431–1441 (1998).

R. Zavin, I. Vorobeichik and N. Moiseyev, Motion of wave-packets using the smooth-exterior-scaling complex potential, *Chem. Phys. Letts.* **288**, 413–417 (1998).

S. Klaiman, I. Gilary and N. Moiseyev, Resonances for Coulombic potentials by complex scaling and free-reflection complex-absorbing potentials, *Phys. Rev. A* **70**, 012709/1–012709/6 (2004).

O. Shemer, D. Brisker and N. Moiseyev, Optimal reflection-free complex absorbing potentials for quantum propagation of wave packets, *Phys. Rev. A* **71**, 032716/1–032716/8 (2005).

Y. Sajeev, M. Sindelka and N. Moiseyev, Reflection-free complex absorbing potential for electronic structure calculations: Feshbach type autoionization resonance of helium, *J. Chem. Phys.* **329**, 307–312 (2006).

Complex scaling of piecewise analytical potentials

O. E. Alon and N. Moiseyev, Balslev–Combes Theorem within the framework of the finite-matrix element approximation, *Phys. Rev. A* **46**, 3807–3811 (1992).

V. Mandelshtam and N. Moiseyev, Complex scaling of ab-initio molecular potential surfaces, *J. Chem. Phys.* **104**, 6192–6195 (1996).

R. Zavin and N. Moiseyev, One-dimensional symmetric rectangular well: from bound to resonance via self-orthogonal virtual state, *J. Phys. A* **37**, 4619–4628 (2004).

A. Emmannouilidou and N. Moiseyev, Stark and field-born resonances of an open square well in a static external electric field, *J. Chem. Phys.* **122**, 194101/1–194101/9 (2005).

Resonances by non-similarity transformations and by using the Padé approximation

R. Lefebvre and N. Moiseyev, Artificial resonance procedure for the determination of quantum mechanical rate constants in the tunneling regime, *J. Chem. Phys.* **93**, 7173–7178 (1990).

N. Rom, N. Lipkin and N. Moiseyev, Optical potentials by the complex coordinate method, *Chem. Phys.* **151**, 199–204 (1991).

N. Lipkin, R. Lefebvre and N. Moiseyev, Resonances by complex nonsimilarity transformations of the Hamiltonian, *Phys. Rev. A* **45**, 4553–4564 (1992).

V. A. Mandelshtam, H. S. Taylor, V. Ryaboy and N. Moiseyev, Stabilization theory for computing energies and widths of resonances, *Phys. Rev. A* **50**, 2764–2766 (1994).

R. Lefebvre, M. Sindelka and N. Moisesev, Resonance positions and lifetimes for flexible complex absorbing potentials, *Phys. Rev. A* **72**, 052704/1–052704/6 (2005).

M. Gluck, A. R. Kolovsky, H. J. Korsch and N. Moiseyev, Calculation of Wannier–Bloch and Wannier–Stark states, *Euro. Phys. J. D* **4**, 239–246 (1998).

N. Moiseyev, M. Gluck and H. J. Korsch, Stark resonances in dc fields from short time propagation of the field-free Hamiltonian, *Chem. Phys. Letts.* **303**, 22–26 (1999).

Resonances by filter diagonalization methods

E. Narevicius, D. Neuhauser, H. J. Korsch and N. Moiseyev, Resonances from short time complex-scaled cross-correlation probability amplitudes by the filter-diagonalization method, *Chem. Phys. Letts.* **276**, 250–254 (1997).

P. Jungwirth, B. Schmidt and N. Moiseyev, Vibrationally resolved spectra from short-time quantum molecular dynamics by the filter-diagonalization method, *Chem. Phys. Letts.* **280**, 177–184 (1997).

M. Gluck, H. J. Korsch and N. Moiseyev, Selective quasi-energies from short time cross-correlation probability amplitudes by the filter-diagonalization method, *Phys. Rev. E.* **58**, 376–381 (1998).

M. Alacid, C. Leforestier and N. Moiseyev, Bound and resonance states by a time-independent filter diagonalization method for large Hamiltonian systems, *Chem. Phys. Letts.* **305**, 258–262 (1999).

Computational methods with complex basis sets

N. Moiseyev, P. R. Certain and F. Weinhold, Complex-coordinate calculations with complex basis sets, *Phys. Rev. A* **24**, 1254–1259 (1981).

P. Zdanska and N. Moiseyev, Hartree–Fock orbitals for complex-scaled configuration interaction calculation of highly excited Feshbach resonances, *J. Chem. Phys.* **123**, 194105/1–194105/8 (2005).

Complex scaling by the Lanczos method

K. F. Milfeld and N. Moiseyev, Complex resonance eigenvalues by the Lanczos recursion method, *Chem. Phys. Lett.* **130**, 145–151 (1986).

O. Kolin, C. Leforestier and N. Moiseyev, Resonance transition probabilities by the complex Lanczos recursion method, *J. Chem. Phys.* **89**, 6836–6840 (1988).

Resonances by complex scaling applied to the non-linear Schrödinger equation

N. Moiseyev, L. D. Carr, B. A. Malomed and Y. B. Band, Transition from resonances to bound states in nonlinear systems: application to Bose–Einstein condensates, *J. Phys. B* **37**, L193–L200 (2004).

N. Moiseyev and L. S. Cederbaun, Resonance solutions of the nonlinear Schrödinger equation: tunneling lifetime and fragmentation of trapped condensates, *Phys. Rev. A* **72**, 033605/1–033605/8 (2005).

Partial widths from the analysis of the tail of the complex scaled resonance wavefunction

U. Peskin, N. Moiseyev and R. Lefebvre, Partial widths by asymptotic analysis of the complex scaled resonance wave function, *J. Chem. Phys.* **92**, 2902–2909 (1990).

N. Moiseyev and U. Peskin, Partial widths obtained by the complex resonance-scattering theory, *Phys. Rev. A* **42**, 255–260 (1990).

H. Masui, S. Aoyama, T. Myo and K. Kato, Partial decay widths in coupled-channel systems with the complex-scaled Jost function method, *Prog. Theor. Phys.* **102**, 1119–1130 (2008).

Properties of resonance wavefunctions

N. Moiseyev, P. R. Certain and F. Weinhold, Resonance properties of complex-rotated Hamiltonians, *Mol. Phys.* **36**, 1613–1630 (1978).

N. Hatano, K. Sasada, H. Nakamura and T. Petrosky, Some properties of the resonant state in quantum mechanics and its computation, *Prog. Theor. Phys.* **119**, 187–222 (2008).

6

Bi-orthogonal product (c-product)

This chapter is divided into several sections which together represent one of the fundamental concepts in the non-Hermitian formalism of quantum mechanics (NH QM). First we discuss the need to replace the inner product used in the standard (Hermitian) formalism of quantum mechanics by another construct which was termed the c-product by Moiseyev, Certain and Weinhold[1] in 1978. Unlike the standard situation where the eigenfunctions (eigenvectors) of an Hermitian operator (matrix) form a complete set which can be used to expand a wavepacket which describes the system at a given time, in NH QM it might happen that the eigenfunctions make up an incomplete set since several (usually two) eigenfunctions (eigenvectors) coalesce to generate a self-orthogonal state. We need completeness and closure relations in order to develop, for example, perturbation theory and scattering theories for non-Hermitian Hamiltonians and in order to be able to solve the Schrödinger equation by numerical methods. Therefore, the second section of this chapter is devoted to the completeness of the spectrum in NH QM. Other aspects of the non-Hermitian formalism which stem from this issue deal with the advantages of using a non-Hermitian formalism for a time-dependent description of a decaying system as well as its application to time-periodic systems. Accordingly, the discussion in one of the sections will encompass the propagation of wavepackets in non-Hermitian quantum mechanics whereas another will elaborate on the benefits of the formalism for the description of the interaction of matter with intense laser radiation.

6.1 The c-product

One of the basic postulates of quantum mechanics is that a solution of the time-dependent Schrödinger equation describes the studied system at any given time

---

[1] N. Moiseyev, P. R. Certain and F. Weinhold, Resonance properties of complex-rotated Hamiltonians, *Mol. Phys.* **36**, 1613–1630 (1978).

and any measurable dynamical quantity can be evaluated from $|\Psi(t)\rangle$. A dynamical property O, such as momentum, kinetic energy, total energy etc. is represented by the corresponding operator $\hat{O}$. In the standard (Hermitian) formalism of quantum mechanics the projection of $|\Psi(t)\rangle$ on a specific eigenstate of an operator $\hat{O}$, which is denoted by $|n\rangle$, provides the information on the probability of measuring in a specific experiment the corresponding eigenvalue of $\hat{O}$, labelled by O_n. The projection of $|\Psi(t)\rangle$ on $|n\rangle$ is carried out by using the scalar product (often referred to as the inner product) between any two square integrable analytical functions. The mean value of the quantity $\bar{O}$ that will be measured in a series of identical experiments is given by the expectation value,

$$\bar{O} = \frac{\langle\Psi(t)|\hat{O}|\Psi(t)\rangle}{\langle\Psi(t)|\Psi(t)\rangle} . \tag{6.1}$$

The questions we address in this chapter are:

(1) how the information on a specific measurable quantity can be extracted from the solution of the time-dependent Schrödinger equation within the framework of the non-Hermitian formalism of quantum mechanics;
(2) what the advantages are of using the non-Hermitian formalism rather than the standard quantum mechanical treatment of a given problem.

Since expectation values are evaluated through the inner product we briefly review the relevant properties of such a functional between functions in the L^2 space of square-integrable functions. If for simplicity we look at any one-dimensional square integrable functions $f(x)$, $g(x)$ and $h(x)$ when α and β are scalars, then the inner product is defined by

$$\begin{aligned}
&\langle f|g\rangle = \int_{-\infty}^{+\infty} f^*(x)g(x)\mathrm{d}x\,, \\
&\langle h(x)|\alpha f(x) + \beta g(x)\rangle = \alpha\langle h|f\rangle + \beta\langle h|g\rangle\,, \\
&\langle f|g\rangle = \langle g|f\rangle^* = \text{scalar}\,, \\
&\langle f|f\rangle \geq 0\,,
\end{aligned} \tag{6.2}$$

where $\langle f|f\rangle = 0$ if and only if $f(x) = 0$.

Using this definition one can prove that all non-degenerate eigenfunctions of a Hermitian operator $\hat{O}$ are orthogonal. To simplify our discussion but without lost of generality we can assume that the box quantization condition, i.e., $\{\psi(x = \pm L)\} = 0$, is applied and therefore the continuum part of the spectrum of $\hat{O}$ (if it exists) is a discrete quasi-continuum that becomes denser as the box size is increased. If a system is initially prepared as a wavepacket $|\Psi(0)\rangle$

then the probability of measuring the quantity O_n at any given time is

$$|a_n(t)|^2 = |\langle n|\Psi(t)\rangle|^2 , \tag{6.3}$$

where $\hat{O}|n\rangle = O_n|n\rangle$. The fact that the eigenstates of a Hermitian operator form a complete set and thus one can write the resolution of the identity by

$$\sum_n |n\rangle\langle n| = \hat{1} \tag{6.4}$$

plays a key role in the calculations of measurable quantities within the standard formalism of quantum mechanics. Equation (6.4) is also known as the closure relation.

Due to the importance of matrix representations for practical calculations in quantum mechanics and since they serve here as a convenient tool for the presentation of the theory in this chapter, we now review several properties of matrix representations in the following exercises.

Exercise 6.1

Show how by using the closure relation in Eq. (6.4) the complex scaled Hamiltonian, $\hat{H}_\theta$, can be represented by an infinitely large general complex matrix (i.e., a matrix of dimensions $N \times N$ where $N \to \infty$).

Exercise 6.2

Prove that for a general complex matrix $\mathbf{H}$ which represents a linear operator $\hat{H}$ (which is not necessarily a Hermitian operator), $\mathbf{H}^\dagger = (\mathbf{H}^{\mathrm{T}})^*$.

Exercise 6.3

Prove that if $\hat{H}$ is a Hermitian operator with a spectrum bounded from below, then the eigenvalues of the $N \times N$ truncated Hamiltonian matrix, $\mathbf{H} = (\mathbf{H}^{\mathrm{T}})^*$, are upper bounds to the exact eigenvalues of $\hat{H}$. This property is also known as the Hylleraas–Undheim–McDonald linear variational theorem.

Similarly to the situation in the standard (Hermitian) formalism of quantum mechanics, the definition of an equivalent to the inner product for eigenfunctions of non-Hermitian operators, which is the subject of the present chapter, is essential for the derivation of the formalism of non-Hermitian quantum mechanics. The properties we wish to keep in the non-Hermitian formalism of quantum mechanics are the orthogonality of the non-degenerate eigenfunctions of the non-Hermitian Hamiltonian and the closure relations. These properties are necessary for projecting from a wavepacket that describes the system the information which provides the probability of measuring a specific dynamical quantity. Besides the necessity for deriving quantum theory, these properties are essential for deriving new analytical and numerical computational methods. For example, in Chapter 7 we will use these properties to derive perturbation theory for non-Hermitian operators, while in Chapter 8 we will use them in the derivation of non-Hermitian scattering theory.

An answer to the question of what is the equivalent to the inner product for eigenfunctions of a non-Hermitian operator is obtained by using linear algebra arguments (see, for example, Wilkinson[2] on the use of linear operators in standard (Hermitian) quantum mechanics and on the representation of any linear operator by a matrix see Dirac[3]). In order to differentiate between the conventional scalar product $\langle\cdot\cdot\,|\,\cdot\cdot\rangle$ we will label the functional we define below as the c-product by $(\cdot\cdot\,|\,\cdot\cdot)$. Let us associate the eigenstates of the non-Hermitian operator $\hat{O}_\theta$ as $|\psi_n^\theta)$, with the eigenfunctions of the differential eigenvalue problem

$$\hat{O}_\theta|\psi_n^\theta) = \lambda_n^\theta|\psi_n^\theta)\,. \tag{6.5}$$

We require the c-product to satisfy the orthogonality condition for the eigenstates of $\hat{O}$,

$$(\psi_{n'}^\theta|\psi_n^\theta) = \delta_{n',n}\,. \tag{6.6}$$

It is straightforward to define the c-product $(\psi_{n'}^\theta|\psi_n^\theta)$ through the definition of left and right eigenvectors of the matrix $\mathbf{O}$ representing the operator in some complete set of orthonormal basis functions $\{f_j\}_{j=1,2,\ldots}$. The matrix elements of $\mathbf{O}$ are given by

$$[\mathbf{O}_\theta]_{j',j} = \langle f_{j'}|\hat{O}_\theta|f_j\rangle\,. \tag{6.7}$$

The key point in our definition of the c-product is the realization that the differential eigenvalue problem can be transformed into a matrix eigenvalue problem,

$$\begin{aligned}
\mathbf{O}_\theta\mathbf{C}_n^\theta &= \lambda_n^\theta\mathbf{C}_n^\theta\,,\\
[\mathbf{D}_m^\theta]^{\mathrm{T}}\mathbf{O}_\theta &= \lambda_m^\theta[\mathbf{D}_m^\theta]^{\mathrm{T}}\,,\\
[\mathbf{D}_{m\neq n}^\theta]^{\mathrm{T}}\mathbf{C}_n^\theta &= 0\,,
\end{aligned} \tag{6.8}$$

---

[2] J. H. Wilkinson,*The Algebraic Eigenvalue Problem*, Oxford, Clarendon Press, 1965.

[3] P. A. M. Dirac, *The Principle of Quantum Mechanics*, London, Oxford University Press, fourth edition, 1967.

where $\mathbf{C}_n$ and $[\mathbf{D}_m^\theta]^{\mathrm{T}}$ are respectively the right and left eigenvectors of the matrix $\mathbf{O}_\theta$. Since

$$\left[[\mathbf{D}_m^\theta]^{\mathrm{T}}\mathbf{O}_\theta\right]^{\mathrm{T}} = \mathbf{O}_\theta^{\mathrm{T}}\mathbf{D}_m^\theta\,, \tag{6.9}$$

the left eigenvectors of the matrix $\mathbf{O}$ are the right eigenvectors of $\mathbf{O}^{\mathrm{T}}$ (the transpose of the matrix $\mathbf{O}$) and

$$\mathbf{O}_\theta^{\mathrm{T}}\mathbf{D}_m^\theta = \lambda_m^\theta\mathbf{D}_m^\theta\,. \tag{6.10}$$

Using the left and right eigenvectors we define the bra and ket eigenstates of the operator $\hat{O}_\theta$,

$$\begin{aligned}(x|\psi_n^\theta) &\equiv \sum_j C_{j,n} f_j(x)\,,\\ (\psi_m^\theta|x) &\equiv \sum_j D_{j,m} f_j^*(x)\,.\end{aligned} \tag{6.11}$$

A matrix and its transpose support the same eigenvalue spectrum and therefore the column eigenvector of $\mathbf{O}$, which is denoted by $\mathbf{C}_n^\theta$, and the column eigenvector of $\mathbf{O}^{\mathrm{T}}$, which is denoted by $\mathbf{D}_n^\theta$, are associated with the *same* eigenvalue λ_n^θ. Therefore, except for very special situations where two or more eigenvalues and eigenfunctions of $\hat{O}_\theta$ coalesce (this special situation which is referred to as the self-orthogonality phenomena will be discussed separately in Chapter 9) then **the c-product** is defined by

$$(\psi_m^\theta|\psi_n^\theta) = \sum_j D_{j,m}C_{j,n} = \delta_{m,n}\,, \tag{6.12}$$

where the bra and ket states are defined in Eq. (6.11). When real basis functions $\{f_j(x)\}_{j=1,2\ldots}$ are used and the unscaled matrix $\mathbf{O}_{\theta=0}$ is represented by a real symmetric matrix, the complex scaled matrix $\mathbf{O}_\theta$ is a complex and symmetric matrix and therefore (note that $\mathbf{D}_j$ and $\mathbf{C}_j$ are respectively columns vectors of the eigenvector matrices $\mathbf{C}$ and $\mathbf{D}$),

$$\begin{aligned}\mathbf{D}_j &= \mathbf{C}_j\,,\\ \mathbf{C}^T\mathbf{C} &= \mathbf{I}\,.\end{aligned} \tag{6.13}$$

Consequently, when the unscaled operator is Hermitian and real (i.e., represented by a real and symmetric matrix) then the non-degenerate eigenfunctions of the complex scaled operator $\hat{O}_\theta$ are orthonormal using the c-product rather than the usual scalar product,

$$(\psi_m^\theta|\psi_n^\theta) = \int_{-\infty}^{+\infty} \psi_m^\theta(x)\psi_n^\theta(x)\mathrm{d}x = \delta_{m,n} \tag{6.14}$$

and the closure relations for non-Hermitian operators implies that

$$\sum_n |\psi_n^\theta)(\psi_n^\theta| = \hat{1}\,. \tag{6.15}$$

Exercise 6.4

(a) Prove that for *any* general complex matrix **H** the left and right eigenvectors which are associated with different eigenvalues are orthogonal.
(b) What are the number of degrees of freedom in the normalization of the N linearly independent eigenvectors of an $N \times N$ non-Hermitian matrix?

As an example of the use of the c-product as first proposed by Moiseyev, Certain and Weinhold let us return to our model problem of a one-dimensional potential barrier described in Fig. 3.1. The potential barrier depends on two parameters, the height of the potential barrier V_0 and its width L. The resonances are the solutions of the time-independent Schrödinger equation with outgoing asymptotes (see Chapter 4),

$$\Psi_n(x \geq L) = B(q_n)\mathrm{e}^{+\mathrm{i}q_n(x-L)} \to \infty\,, \tag{6.16}$$

where $n = 1, 2, \ldots$ denotes the discrete resonance states, $E_\mathrm{t} = -V_0$ is the threshold energy and therefore the outgoing complex wave-vector, q_n, is given by

$$q_n = \sqrt{2M(E_n + V_0)} = |q_n|\exp(-\mathrm{i}\alpha_n)\,. \tag{6.17}$$

The complex resonance eigenvalue is defined as usual by

$$E_n = \varepsilon_n - \mathrm{i}/2\Gamma_n\,, \tag{6.18}$$

where ε_n is the resonance energy and Γ_n is the resonance width. Up to a normalization factor the coefficient of the outgoing wave is given by

$$B(k_n) = \frac{1}{2}[\sin(k_n L) - \frac{\mathrm{i}k_n}{q_n}\cos(k_n L)]\,, \tag{6.19}$$

where the wave vector, k_n, of the resonance in the interaction region is given by

$$k_n = \sqrt{2ME_n}\,. \tag{6.20}$$

The resonance functions can be seen to decay to zero by carrying out any of the similarity transformations described in Chapter 5. Using, for example, the exterior complex scaling transformation $x \to (x-L)\mathrm{e}^{\mathrm{i}\theta} + L$ the transformed resonance wavefunction reads

$$\Psi_n(x > L;\theta) = B(q_n)\mathrm{e}^{+\mathrm{i}|q_n|\mathrm{e}^{\mathrm{i}(\theta-\alpha_n)}(x-L)} \to 0\,. \tag{6.21}$$

Now we return to Eq. (6.12) and substitute for the two transformed resonance wavefunctions,

$$\begin{aligned}\left(\Psi_n^\theta|\Psi_{n'}^\theta\right) &= \int_0^\infty \Psi_n(x;\theta)\Psi_{n'}(x;\theta)\mathrm{d}x = \int_0^L \Psi_n(x)\Psi_{n'}(x)\mathrm{d}x \\ &\quad + B(q_n)B(q_{n'})\int_L^\infty \mathrm{e}^{+\mathrm{i}|q_n|x\mathrm{e}^{\mathrm{i}(\theta-\alpha_n)}}\mathrm{e}^{+\mathrm{i}|q_{n'}|x\mathrm{e}^{\mathrm{i}(\theta-\alpha_{n'})}}\mathrm{e}^{\mathrm{i}\theta}\mathrm{d}x\,,\end{aligned} \tag{6.22}$$

where

$$\Psi_n(x < L) = \sin(k_n x)\,. \tag{6.23}$$

Since the value of the integral at $x = \infty$ is equal to zero we may define the contour of integration in the second integral as $x' = x\exp(\mathrm{i}\theta)$ and substitute only the lower bound of the integral. That is,

$$\begin{aligned}\left(\Psi_n^\theta|\Psi_{n'}^\theta\right) &= \int_0^L \sin(k_n x)\sin(k_{n'}x)\mathrm{d}x + B(q_n)B(q_{n'})\int_0^\infty \mathrm{d}x'\mathrm{e}^{+\mathrm{i}(q_n+q_{n'})x'} \\ &= \frac{\sin[(k_n-k_{n'})L]}{2(k_n-k_{n'})} - \frac{\sin[(k_n+k_{n'})L]}{2(k_n+k_{n'})} + \frac{\mathrm{i}B(q_n)B(q_{n'})}{q_n+q_{n'}}\mathrm{e}^{\mathrm{i}(q_n+q_{n'})L}\,.\end{aligned} \tag{6.24}$$

Exercise 6.5

(a) By using the c-product in Eq. (6.24) prove that any two decay resonances of the the one-dimensional potential barrier in Fig. 3.1 are orthogonal i.e., show that $(\Psi_n|\Psi_{n'}) = 0$.

(b) Calculate the normalization factor for the n-th resonance state.

(c) Find out what conditions should be satisfied in order for the "length" of a resonance vector to be zero. That is, show under what conditions using the c-product we get that $(\Psi_n|\Psi_n) = 0$. Later we will refer to such a vector with zero "length" as a self-orthogonal vector.

The proof in Ex. 6.5 that the decay resonances for the one-dimensional potential barrier are orthogonal under the c-product is just an illustrative example of a more general property. *Using the c-product, non-degenerate resonances are always orthogonal*. This theorem has been proved above (see Eq. (6.12)) by representing the eigenfunctions of the non-Hermitian operator in a finite sized basis set which contains square-integrable orthonormal (using the scalar product) basis functions. However, Eq. (6.12) can be proved in an analogous manner to the proof in conventional Hermitian quantum mechanics. Let Ψ_n and Ψ_m be two resonance eigenfunctions of the Hamiltonian, $\hat{H}$, associated with different complex eigenvalues. That is,

$$\begin{aligned} \hat{H}\Psi_n &= E_n\Psi_n \,, \\ \hat{H}\Psi_m &= E_m\Psi_m \,, \end{aligned} \tag{6.25}$$

The resonance functions Ψ_n and Ψ_m diverge exponentially. However, as explained above and in Chapter 5, they exponentially decay to zero under the proper transformation, $\vec{r} \to F(\vec{r})$. Using these two equations we immediately obtain that

$$\begin{aligned} (\Psi_m|\hat{H}|\Psi_n) &= \int \Psi_m \hat{H}\Psi_n \mathrm{d}[F(\vec{r})] \\ &= E_n \int \Psi_m\Psi_n \mathrm{d}[F(\vec{r})] \equiv E_n(\Psi_m|\Psi_n)\,. \end{aligned} \tag{6.26}$$

Alternatively, we can look at the effect of $\hat{H}$ on Ψ_m through the following equation:

$$\begin{aligned} (\Psi_n|\hat{H}|\Psi_m) &= \int \Psi_n \hat{H}\Psi_m \mathrm{d}[F(\vec{r})] \\ &= E_m \int \Psi_n\Psi_m \mathrm{d}[F(\vec{r})] \equiv E_m(\Psi_m|\Psi_n)\,. \end{aligned} \tag{6.27}$$

The Hamiltonian $\hat{H} = \hat{T} + \hat{V}$ consists of a kinetic energy operator $\hat{T}$ and a potential energy operator $\hat{V}$. It is clear that $(\Psi_n|\hat{V}|\Psi_m) = (\Psi_m|\hat{V}|\Psi_n)$ since the product of any two functions is a commutative operation. Integration by parts shows that, since the two transformed complex resonance wavefunctions decay exponentially, $(\Psi_n|\hat{T}|\Psi_m) = (\Psi_m|\hat{T}|\Psi_n)$ and therefore $(\Psi_n|\hat{H}|\Psi_m) = (\Psi_m|\hat{H}|\Psi_n)$. This equality implies that

$$E_n\,(\Psi_m|\Psi_n) = E_m\,(\Psi_n|\Psi_m)\ . \tag{6.28}$$

Since $(\Psi_n|\Psi_m) = (\Psi_m|\Psi_n)$ we get that

$$(E_n - E_m)(\Psi_m|\Psi_n) = 0\,. \tag{6.29}$$

When the two resonances are non-degenerate states (i.e., $E_n \neq E_m$), then they must be orthogonal, under the c-product,

$$\left(\Psi_m | \Psi_{n \neq m}\right) = 0\,. \tag{6.30}$$

The c-product implies that the complex conjugation is applied *only* to the terms in the "bra" state which are complex regardless of any complex scaling transformation. This definition is in the spirit of the usual understanding of analytical continuation in complex analysis. *One does not take the complex conjugate of the terms in the wavefunction which become complex only due to the rotating of the coordinate into the complex plane.* If, for example, $\langle x | f \rangle = \mathrm{e}^{+\mathrm{i}kx}$ when k is real, then the "bra" state is $\langle f | x \rangle = \mathrm{e}^{-\mathrm{i}kx}$. The complex scaled "ket" state is $\langle x | f(\theta)\rangle = \mathrm{e}^{+\mathrm{i}kx\mathrm{e}^{\mathrm{i}\theta}}$, whereas the complex scaled "bra" state is given by $\langle f(-\theta)|x\rangle = \mathrm{e}^{-\mathrm{i}kx\mathrm{e}^{\mathrm{i}\theta}}$. Therefore, if

$$\langle f(\theta = 0)| f(\theta = 0)\rangle_x = 1\,, \tag{6.31}$$

also

$$(f(\theta)|f(\theta))_{x\mathrm{e}^{\mathrm{i}\theta}} = \mathrm{e}^{\mathrm{i}\theta}\langle f(-\theta)|f(\theta)\rangle_x = 1\,. \tag{6.32}$$

In the above definitions of "*bra*" and "*ket*" states the wave vector k has real values only. However, the asymptote of a resonance state is associated with an outgoing wave with a complex wave vector k_{res}, such that $\lim_{x\to\infty}\langle x|\Psi_{\mathrm{res}}(\theta)\rangle \propto \langle x | f_{\mathrm{res}}(\theta)\rangle \equiv \mathrm{e}^{+\mathrm{i}k_{\mathrm{res}}x\mathrm{e}^{\mathrm{i}\theta}}$. One may conclude that by carrying analytical continuation of the wave vector k to the complex plane then $\langle f(-\theta)|x\rangle = \mathrm{e}^{-\mathrm{i}kx\mathrm{e}^{\mathrm{i}\theta}} \to \langle f_{\mathrm{res}}(-\theta)|x\rangle = \mathrm{e}^{-\mathrm{i}k_{\mathrm{res}}x\mathrm{e}^{\mathrm{i}\theta}}$. This conclusion, however, is wrong. $\langle f_{\mathrm{res}}(-\theta)|x\rangle \neq \mathrm{e}^{-\mathrm{i}k_{\mathrm{res}}x\mathrm{e}^{\mathrm{i}\theta}}$ but $\langle f_{\mathrm{res}}(-\theta)|x\rangle = \mathrm{e}^{+\mathrm{i}k_{\mathrm{res}}x e^{\mathrm{i}\theta}}$. The mistake we have made is in our assumption that the asymptote of a resonance state is an analytical continuation of the wave vector k of an outgoing wave to the complex wave vector plane. The *square integrable* complex scaled resonance wavefunctions are **not** associated with analytical continuation of continuum functions (with outgoing wave components only) to the complex plane **but** with analytical continuation of *bound states* (which are also square integrable functions) or anti-bound states into the complex plane. If the asymptote of a complex scaled bound state is given by $\lim_{x\to\infty}\langle x|\Psi_{\mathrm{bound}}(\theta)\rangle \propto \langle x|f_{\mathrm{bound}}(\theta)\rangle \equiv \mathrm{e}^{-ax\mathrm{e}^{\mathrm{i}\theta}}$, where a takes real and positive values only, then $\langle f_{\mathrm{bound}}(-\theta)|x\rangle = \mathrm{e}^{-ax\mathrm{e}^{\mathrm{i}\theta}} \to \langle f_{\mathrm{res}}(-\theta)|x\rangle = \mathrm{e}^{-a_{\mathrm{res}}x\mathrm{e}^{\mathrm{i}\theta}}$ when $x > 0$ and where $a_{\mathrm{res}} = \mathrm{i}k_{\mathrm{res}}$. This association of resonances with bound states is understandable in view of the fact that by imposing outgoing boundary conditions on the solutions of the time-independent Schrödinger equation *only* the bound and resonance poles of the scattering matrix (and not the continuum part of the spectrum) are obtained.

The connection between bound and resonance states is natural if we look at dependence of the analytical solutions of the time-independent Schrödinger equation on some potential parameter. For example, the exponential coefficient a in e^{-ax^2} for 1D problems or in e^{-ar} for 3D problems would be a function of the potential parameters denoted here by λ (e.g., depth of the 1D potential well or the charge of the nuclei in a 3D Coulomb potential). By reducing the value of λ the n-th bound state will turn to be a resonance state. In such a case a will become complex. Note that for the special case of a rectangular potential well the resonances are created from the coalescence of anti-bound states which have the same structure as bound states with $a < 0$. However, even in this case the resonances are not associated with the analytical continuation of continuum states.

Exercise 6.6

The kinetic energy operator in one dimension in atomic units is $\hat{T} = -\frac{1}{2}\frac{\mathrm{d}^2}{\mathrm{d}z^2}$, where $z = F(x)$ is a complex contour in the coordinate space. Prove that when real basis sets are used the matrix which represents $\hat{T}$ is a complex symmetric matrix. In other words show that $\int_z \mathrm{d}z\phi(x)\frac{\mathrm{d}^2}{\mathrm{d}z^2}\chi(x) = \int_z \mathrm{d}z\chi(x)\frac{\mathrm{d}^2}{\mathrm{d}z^2}\phi(x)$.

6.2 Completeness of the spectrum

The eigenfunctions of a Hermitian operator form a complete set which satisfies the closure relation (see the discussion on Hermitian matrices in the introductory part of this chapter). Similarly, in non-Hermitian quantum mechanics the eigenfunctions of the non-Hermitian Hamiltonian form a complete set, assuming that the c-product is used and assuming that there are no degenerate eigenfunctions which we refer to in this book as self-orthogonal states. The situation where the spectrum is not complete is discussed separately in Chapter 9 where the self-orthogonality phenomenon is discussed. Here we wish to discuss the possibility that the poles of the scattering matrix serve as a complete set, and more specifically the possibility and the conditions for which the decay resonance states serve as an almost complete basis in the calculations of wave packet dynamics.

As an illustrative numerical example we studied the problem of a step barrier potential which is presented in Fig. 3.1. The width of the potential barrier is L and its height is V_0. The resonance eigenvalues, $E_{\mathrm{res}} = k_{\mathrm{res}}^2/2$, and eigenfunctions were calculated for this problem in Chapter 4 (see Eq. (4.15) and Fig. 4.1). The interaction region is taken as $0 \leq x \leq L$. Following our above discussion, a wavepacket which is localized in the interaction region can be expanded to a very high accuracy by the decay resonance eigenfunctions. For the sake of simplicity of the analytical calculations we have chosen a non-normalized wavepacket given by

$$\Phi(x) = \sum_n C_n \sin(n\pi x/L) , \tag{6.33}$$

where

$$C_n = \mathrm{e}^{-(n-10)^2/\sigma} . \tag{6.34}$$

As a criterion for completeness of the resonance eigenfunctions expansion for $\Phi(x)$ we define $S(\sigma)$, given by

$$S(\sigma) = \left| \sum_{k_{\text{res}}} (\psi_{k_{\text{res}}} | \Phi)^2 \right| , \tag{6.35}$$

such that

$$S(\sigma) \cong 1 \tag{6.36}$$

when

$$\sum_{k_{\text{res}}} |\psi_{k_{\text{res}}})(\psi_{k_{\text{res}}}| \cong 1 . \tag{6.37}$$

When $S(\sigma)$ approaches unity then we can describe the whole wavepacket by the overlap with the resonance eigenfunctions. In our case $S(\sigma)$ can be calculated analytically (when the resonance wavevectors k_{res} and the resonance wavefunction normalization factors $\mathcal{N}_{\text{res}}$ were calculated as described in Chapter 5):

$$S(\sigma) = \frac{L}{2} \left| \sum_{k_{\text{res}}} \frac{\mathcal{N}_{\text{res}}}{2} \left(\sum_n C_n \left[\frac{\sin(n\pi/L - k_{\text{res}})}{2(n\pi/L - k_{\text{res}})} - \frac{\sin(n\pi/L + k_{\text{res}})}{2(n\pi/L + k_{\text{res}})} \right] \right)^2 \right| . \tag{6.38}$$

In Fig. 6.1 the deviations of $S(\sigma)$ from unity as function of σ for different values of the height of the potential barrier V_0 are presented. The parameter σ determines the degree of localization of the initial wavepacket in the interaction region. As σ increases the initial wavepacket is more localized in the interaction region. Note that the results presented in Fig. 6.1 were calculated for the case where the width of the potential barrier is $L = 1$. Therefore $V_0 = V_0/L$ measures the ratio between the height of the potential barrier and its width.

The deviation of $S(\sigma)$ from unity for small values of σ is due to the fact that exponential localization of the wavepacket in the interaction region is not satisfied in our case when σ does not get sufficiently large. The deviation of $S(\sigma)$ from unity for large values of σ results from the fact that for large values of σ

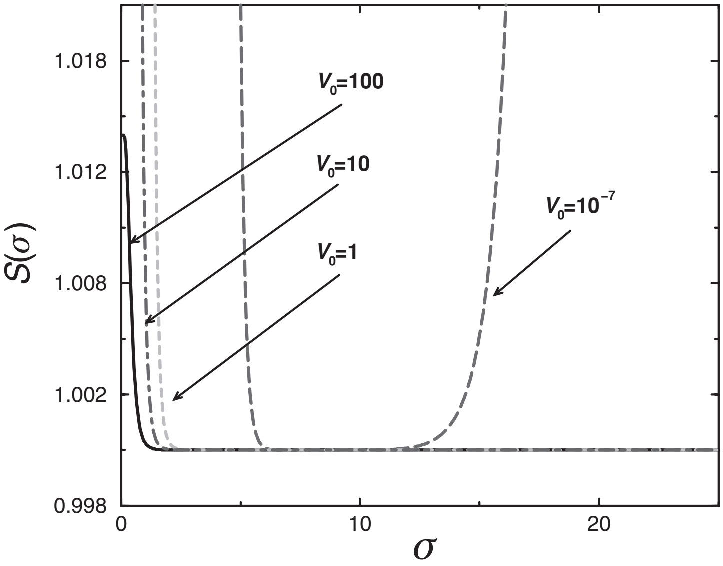

Figure 6.1 σ-trajectory calculations of $S(\sigma) = |\sum_{k_{\text{res}}}(\psi_{k_{\text{res}}}|\Phi(\sigma))^2|$, where a wavepacket, Φ, which is defined in Eqs. (6.33)–(6.34), is projected on the 500 decay resonance eigenstates (poles of the scattering matrix) which were calculated for a one-dimensional Hamiltonian with a step-like potential barrier. The width of the potential barrier is $L = 1$ and its height is V_0. When the resonance wavefunctions serve as an almost complete basis set, $S(\sigma) \simeq 1$.

the standard deviation for the energy is large (following the uncertainty relations $\Delta E_{\text{WP}} = 1/(8\sigma^2)$ when we consider $\Delta x = \sigma$) and the 500 resonance decay poles which have been used for the calculations are not enough to get converged results. The fact that even for the case where $V_0/L = 10^{-7}$ the 500 resonance poles we have used as a basis set serve as a complete set for a broad interval of values of σ is a quite remarkable result and provides an illustrative numerical support to our claim that the decay resonances serve as a complete basis set in the expansion of an wavepacket which is localized in the interaction region.

Exercise 6.7

From the results presented in Fig. 6.1 for the case where the ratio between the height of the potential barrier and its width is equal to 10^{-7} it seems that a continuum can be described as a collective of broad and overlapping resonances. Show how under this approximation a Feshbach resonance is generated. Show also that this resonance can be associated with a Lorenzian peak in the cross section. This peak is centered at the position of the Feshbach resonance and its width is the Feshbach resonance width.

6.3 Advantages of calculating survival probabilities by c-product

The use of the c-product as presented above within the framework of the non-Hermitian formalism of quantum mechanics enables one to study the dynamics of systems which at times are technically extremely hard (and even impossible using finite sources of computational facilities) to study within the framework of the standard formalism of quantum mechanics. As an example we wish to study a system in which an initially prepared wavepacket, $\Phi(x, t = 0)$ is localized in the interaction region (e.g., a well embedded between two potential barriers). The lifetime of the initial wave packet can be very long and therefore the survival probability $S(t) = |\langle\Phi(0)|\Phi(t)\rangle|^2$ might decay very slowly in time. This decay can be in fact so slow that even for a one-particle problem in one dimension the wave packet propagation is too difficult for numerical reasons due to the long propagation time. If the propagated wave packet is expanded in the basis of the eigenfunctions of the Hermitian Hamiltonian (using the finite-box approximation only discrete eigenstates are obtained)

$$\Phi(x, t) = \mathrm{e}^{-\mathrm{i}\hat{H}t/\hbar}\Phi(x, 0) = \sum_n \langle\psi_n|\Phi(0)\rangle \mathrm{e}^{-\mathrm{i}E_n t/\hbar}\psi_n(x)\,, \tag{6.39}$$

then the calculation of the survival probability

$$\begin{aligned} S(t) &\\ = \sum_n |\langle\psi_n|\Phi(0)\rangle|^4 + 2\sum_{n'}\sum_{n<n'} |\langle\Phi(0)|\psi_{n'}\rangle|^2 |\langle\psi_n|\Phi(0)\rangle|^2 \cos\left(\frac{(E_n - E_{n'})t}{\hbar}\right) \end{aligned} \tag{6.40}$$

requires the use of a very large box in the numerical calculations for which $\Delta E \Delta t > 1$, where Δt is the duration of the time propagation and $\Delta E = \min|E_n - E_{n'}|$ for the values of n and n' for which $|\langle\psi_n|\Phi(0)\rangle|^2 > 0$ and $|\langle\psi_{n'}|\Phi(0)\rangle|^2 > 0$. The requirement of $\Delta E \Delta t > 1$ in order to avoid artificial interference effects between the outgoing components of the propagated wave and the incoming wave components which are produced by the reflections of the tail of the propagated wavepacket from the edges of the box is a tough numerical task within the framework of the Hermitian formalism of quantum mechanics, even for simple problems where the rate of decay of $S(t)$ is sufficiently small. However, when the overlap integral of the complex scaled initial wavepacket with a single (or several) narrow long-living resonance state is large, then the calculation of the decay of $S(t)$ is straightforward and requires relatively simple numerical calculations. Let us explain this claim in some more detail. Within the framework of the non-Hermitian formalism of quantum mechanics we use as a basis set the eigenfunctions of the complex scaled Hamiltonian which contains resonance states and rotated continuum states (we assume that the initial wavepacket does not populate the bound states, but even if they are populated the arguments will be similar) and therefore

$$\Phi_\theta(x,t) = \mathrm{e}^{-\mathrm{i}\hat{H}_\theta t/\hbar}\Phi(x,0) = \sum_n (\psi_n^\theta|\Phi_\theta(0))\mathrm{e}^{-\mathrm{i}E_n^\theta t/\hbar}\psi_n^\theta(x)\,, \tag{6.41}$$

where $\hat{H}_\theta \psi_n^\theta(x) = E_n^\theta \psi_n^\theta(x)$, $(\psi_{n'}^\theta|\psi_n^\theta) = \delta_{n',n}$, and the complex scaled initial wavepacket is defined as $\Phi_\theta(x,0) = \mathrm{e}^{-\mathrm{i}\theta/2}\Phi(x\mathrm{e}^{\mathrm{i}\theta},0)$. The multiplication by the factor of $\mathrm{e}^{-\mathrm{i}\theta/2}$ is in order to maintain normalization, $\langle\Phi(0)|\Phi(0)\rangle = (\Phi_\theta(0)|\Phi_\theta(0)) \equiv \langle\Phi_{-\theta}(0)|\Phi_\theta(0)\rangle$.

Therefore, the survival probability is given by

$$\begin{aligned} S(t) = {} & \sum_n |(\psi_n^\theta|\Phi_\theta(0))|^4 \mathrm{e}^{-2\mathrm{Im}E_n^\theta t/\hbar} \\ & +2\sum_{n'}\sum_{n<n'} \mathrm{e}^{-2\mathrm{Im}(E_n^\theta+E_{n'}^\theta)t/\hbar}\mathrm{Re}[(\Phi_\theta(0)|\psi_{n'}^\theta)(\psi_n^\theta|\Phi_\theta(0))]^2 \cos\left(\frac{(E_n^\theta-E_{n'}^\theta)t}{\hbar}\right) \\ & -2\sum_{n'}\sum_{n<n'} \mathrm{e}^{-2\mathrm{Im}(E_n^\theta+E_{n'}^\theta)t/\hbar}\mathrm{Im}[(\Phi_\theta(0)|\psi_{n'}^\theta)(\psi_n^\theta|\Phi_\theta(0))]^2 \sin\left(\frac{(E_n^\theta-E_{n'}^\theta)t}{\hbar}\right). \end{aligned} \tag{6.42}$$

Note that

$$(\psi_n^\theta|\Phi_\theta(0)) = \langle\psi_n^{-\theta}|\Phi_\theta(0)\rangle\,. \tag{6.43}$$

When the unscaled Hamiltonian is real and real basis functions are used then $(\psi_n^\theta|\Phi_\theta(0)) = \langle\psi_n^{-\theta}|\Phi_\theta(0)\rangle = ([\Phi_{-\theta}(0)]^*|\psi_n^\theta) = \langle\Phi_{-\theta}(0)|\psi_n^\theta\rangle$. When the complex scaled initial wavepacket populates mainly a single resonance state denoted by $n = n_{\mathrm{res}}$ (i.e., $|(\psi_{n_{\mathrm{res}}}^\theta|\Phi_\theta(0))|^4 \simeq 1$), for which $-2\mathrm{Im}E_{n_{\mathrm{res}}}^\theta \equiv \Gamma_{n_{\mathrm{res}}}$, then

$$S(t) \simeq \mathrm{e}^{-\Gamma_{n_{\mathrm{res}}}t/\hbar}\,. \tag{6.44}$$

The analysis of the decay in terms of the resonance state enables us to understand the dynamics based on the different decay times of the resonances even when the wavepacket survives inside the interaction region for a very long time. The survival probability of a given wavepacket will be determined by the interference between resonances which decay at different rates. At long times we usually have one state which survives. This analysis is not possible within the realms of Hermitian quantum mechanics where the resonance states are not given as eigenstates of the Hamiltonian and we need to propagate the wavepacket to extremely long times which is numerically cumbersome.

Exercise 6.8

Consider a general complex matrix **H** which has a complete spectrum. The amplitude of the survival probability of an initial vector $\mathbf{v}_0$ is given by $A(t) = \mathbf{v}_0^{\mathrm{T}} \cdot \mathbf{U}(t)\mathbf{v_0}$, where $\mathbf{U}(t) = \mathrm{e}^{-\mathrm{i}\mathbf{H}t}$. Evaluate $A(t)$ in terms of the right and left eigenvector matrices and the corresponding eigenvalues of **H**.

6.4 The c-product for non-Hermitian time-periodic Hamiltonians

In Section 5.6 we described the photo-induced resonances as complex eigenvalues of a Floquet type operator,

$$\mathcal{H} \; = \; -\mathrm{i}\hbar \, \frac{\partial}{\partial t'} \; + \; \hat{H}(t') \, . \tag{6.45}$$

The Hamiltonian is time-dependent. For example, see in Chapter 2 the presentation of the time-dependent Hamiltonian, $\hat{H}(t')$, which describes the interaction of atoms or molecules or mesoscopic systems with a linearly polarized laser field. Here we use t' rather than t in order to stress that t' is an additional coordinate and not a parameter (time) as in the conventional representations of the solutions of the time-dependent Schrödinger equation.

In the case of time-periodic Hamiltonians, $\hat{H}(t') = \hat{H}(t' + T)$, the eigenstates of $\mathcal{H}$ are known as the Floquet quasi-energy states. Therefore one can choose $T_{\mathrm{p}} = NT$, where $N \geq 1$. For pulsed lasers T_{p} is taken as any given time which is equal to or larger than the duration of the laser pulse. As discussed in Chapter 5, the complex quasi-energy eigenvalues of the complex scaled Floquet-type operator,

$$[-\mathrm{i}\hbar \frac{\partial}{\partial t'} + \hat{H}_\theta(t')] f_\alpha^\theta \mathbf{r}, t') = \mathcal{E}_\alpha f_\alpha^\theta(\mathbf{r}, t') \tag{6.46}$$

are associated with the photo-induced resonance phenomenon. That is,

$$\mathcal{E}_\alpha = E_\alpha - \frac{\mathrm{i}}{2}\Gamma_\alpha \, , \tag{6.47}$$

where Γ_α provides the rate of the photo-induced decay of the particles (e.g. electrons) at the energy $E_\alpha + 2\pi\hbar n/T_{\mathrm{p}}$ where n attains integer values associated with the $n = 0, \pm 1, \pm 2, \ldots$ Floquet/Brillouin channels. Note that $\mathcal{E}_\alpha$ for the non-resonance solutions (associated with the rotated continua) are θ-dependent eigenvalues. The "*ket*" resonance eigenstate

$$(\mathbf{r}|f_\alpha^\theta) = f_\alpha^\theta(\mathbf{r}, t') \tag{6.48}$$

is a function of t' that serves here as a coordinate and the internal degrees of freedom of the Hamiltonian, **r** (such as electronic, inter-molecular and nuclear coordinates and in case of laser cooling also the center of mass coordinates). The *left* resonance eigenfunctions of $\mathcal{H}$ are the eigenfunctions of $\mathcal{H}^{\dagger *}$,

$$\mathcal{H}^{\dagger *} = +\mathrm{i}\hbar \frac{\partial}{\partial t'} + \hat{H}_\theta(t') \, . \tag{6.49}$$

In order to define the "bra" quasi-energy resonance states we first should carry out the Fourier series expansion of the "ket" resonance quasi-energy eigenfunction, which is given by

$$f_\alpha^\theta(\mathbf{r}, t') = \sum_{n=-\infty}^{+\infty} \phi_{\alpha,n}^\theta(\mathbf{r}) \mathrm{e}^{+\mathrm{i}\omega n t'} \, , \tag{6.50}$$

where

$$\omega = \frac{2\pi}{T_\mathrm{p}} \, . \tag{6.51}$$

For cw lasers ω is the laser frequency. The Fourier components are square integrable (i.e., their asymptotes decay exponentially to zero). Moreover, the norm $|(\phi_{\alpha,n}^\theta|\phi_{\alpha,n}^\theta)|$ is usually exponentially localized around the chosen $n = 0$ Floquet/Brillouin zone and therefore even in strong laser fields the summation in Eq. (6.50) can be truncated to a finite number of Fourier channels.

On the basis of Eq. (6.49) the "bra" quasi-energy resonance states are defined by

$$(f_\alpha^\theta|\mathbf{r}) = g_\alpha^\theta(\mathbf{r}, t') \, , \tag{6.52}$$

where

$$g_\alpha^\theta(\mathbf{r}, t') = \sum_{n=-\infty}^{+\infty} \phi_{\alpha,n}^\theta(\mathbf{r}) \mathrm{e}^{-i\omega n t'} \, . \tag{6.53}$$

The c-product implies that

$$\begin{aligned}(f_{\alpha'}^\theta|f_\alpha^\theta) &= \frac{1}{T_p}\int_0^{T_\mathrm{p}} \mathrm{d}t' \int_{-\infty}^{+\infty} \mathrm{d}\mathbf{r}\, g_{\alpha'}^\theta(\mathbf{r}, t') f_\alpha^\theta(\mathbf{r}, t') \\ &= \delta_{\alpha',\alpha} \sum_{n=-\infty}^{+\infty} \int_{-\infty}^{+\infty} \mathrm{d}\mathbf{r}\, [\phi_{\alpha,n}^\theta(\mathbf{r})]^2 \, .\end{aligned} \tag{6.54}$$

Therefore, the quasi-energy resonance states are a bi-orthonormal set of solutions (normalization implies multiplication of the Fourier components by a factor such that $(f_\alpha^\theta|f_\alpha^\theta) = 1$).

■

6.5 The F-product for time propagated wavepackets

The F-product is the generalization of the c-product which was derived for eigenstates of non-Hermitian operators to wavepackets which are the solutions of the time-dependent Schrödinger equation in order to enable the calculations of time-dependent expectation values. The name F-product indicates that the generalization of the c-product as introduced above for eigenfunctions of the complex scaled Hamiltonian (or for the complex scaled Floquet operator) takes into consideration the decay of the propagated wavepacket from a finite region in space (where the particles do not move freely). This finite region in space can be taken as large as one wishes. The motivation which lies behind this definition is the desire to describe the dynamics of the decaying system through the evolution of the resonance states. If we expand any initial state in the eigenstates of the non-Hermitian Hamiltonian the contributions of the resonances (as well as the bound states) will dominate the evolution of the wavepacket in time. In many cases quite accurate results are obtained by using a relatively small number of resonance eigenfunctions as a basis set. In Chapter 8 we will show how such-treatment of time-dependent problems can be beneficiary for studying phenomena resulting from the interaction of high intensity radiation with matter. For example, by using a single resonance eigenfunction of the complex scaled Floquet operator one can explain the spectrum of high harmonics generated from atoms (or molecules).

In this spirit, if a single resonance has a distinctively longer lifetime than all others then in the long time limit we get that the "norm" of the propagated wavepacket decays exponentially to zero as time passes (here without loss of generality we assume that the complex scaled Hamiltonian is represented by a complex and symmetric matrix),

$$(\Phi_\theta(t)|\Phi_\theta(t)) \rightarrow \langle \mathrm{e}^{-\mathrm{i}E_{n_\mathrm{res}}t/\hbar}\phi_{n_\mathrm{res}}^{-\theta}|\mathrm{e}^{-\mathrm{i}E_{n_\mathrm{res}}t/\hbar)}\phi_{n_\mathrm{res}}^{\theta}\rangle = \mathrm{e}^{-\Gamma_{n_\mathrm{res}}t/\hbar} . \tag{6.55}$$

In contrast to the Hermitian formalism of quantum mechanics where the norm of the propagated wavepacket is conserved, here the number of the particles in the interaction region, given by

$$\mathcal{N}(t) = (\Phi_\theta(t)|\Phi_\theta(t)) , \tag{6.56}$$

is not conserved.

Within the framework of the standard (Hermitian) formalism of quantum mechanics the number of particles in the interaction region requires long time propagations and the use of many basis functions (or grid points)

$$\mathcal{N}(t) = \lim_{V\to\infty}\int_V |\Phi_{\theta=0}(\mathbf{r},t)|^2 \mathrm{d}V , \tag{6.57}$$

where V is some finite volume in space which encloses the region of interaction. It is important to compare the exponential decay of the survival probability $S(t)$ given in Eq. (6.44) with the exponential decay of the "norm" as defined in Eq. (6.55). The decay of $S(t) = |(\Phi_\theta(0)|\Phi_\theta(t))|^2$ as shown in Eq. (6.44) would be obtained even in Hermitian quantum mechanics when the "norm" of the resonance state is conserved and $(\Phi_\theta(t)|\Phi_\theta(t)) = 1$ at any given time. On the other hand, the requirement of the exponential decay of the "norm" of the wavepacket is the key point behind the generalization of the c-product for wavepackets. *It implies that we take the approach where the decay of the wavepacket is from a finite region in space which can be taken as large as one wishes.* The notation for the definition of the "inner" product for wave packets as F(finite-space)-inner product is motivated by our wish to emphasize on the fact that the integration over all space in non-Hermitian quantum mechanics represents the expectation values of the localized part of the wavepacket in standard quantum mechanics. This means that the average physical properties of the particles which remain in the interaction region will be given in the standard (Hermitian) formalism of quantum mechanics by

$$\bar{O}(t) = |\bar{O}(t)|\mathrm{e}^{\mathrm{i}\phi_O(t)} \equiv \mathcal{N}^{-1}(t) \lim_{V\to\infty} \int_V \mathrm{d}V [\Phi_\theta^*(\mathbf{r},t)\hat{O}_\theta \Phi_\theta(\mathbf{r},t)]_{\theta=0}\,, \tag{6.58}$$

while in non-Hermitian quantum mechanics it will be

$$\bar{O}(t) = |\bar{O}(t)|\mathrm{e}^{\mathrm{i}\phi_O(t)} \equiv \mathcal{N}^{-1}(t)(\Phi_\theta(t)|\hat{O}_\theta|\Phi_\theta(t))\,. \tag{6.59}$$

Note that sometimes the quantity which is relevant to the experiment at hand is not the expectation value $\bar{O}$ itself but rather $\mathcal{N}(t)\bar{O}(t)$ which represents an extensive property of the system depending on the number of the particles which are yet to decay.

As example is when the intensity of emitted radiation from an atom in a strong laser field is measured. In such a case the intensity depends on the number of atoms which have not been ionized. The frequency of the emitted radiation from an atom in a strong laser field is the Fourier transform of the expectation value of the acceleration operator $\hat{O} = \partial\hat{V}/\partial x$, where $\hat{V}$ is the atomic electronic potential which is exposed to a laser that induced an ac field which oscillates along the x-direction. However, the intensity of the radiation depends on $\mathcal{N}(t)$ which provides in this case the number of electrons which have not been ionized and are still temporarily bound to the atom. Therefore the high-order harmonic generation spectra is obtained by the Fourier transform of $\mathcal{N}(t)\bar{O}(t)$ and not of $\bar{O}(t)$.

Exercise 6.9

(a) Prove that within the c-product formalism the expectation values of a given wavepacket are the same as those obtained within the conventional Hermitian propagation.

(b) In non-Hermitian numerical calculations we expand any wavepacket in a finite number of eigenfunctions of a complex scaled Hamiltonian which are associated with bound, resonance and rotated continuum states. Explain why numerical errors are introduced in the non-Hermitian calculations of time-dependent expectation values using the c-product formalism.

(c) Explain under what conditions these numerical difficulties are avoided when the *same* calculations are carried out within the framework of the F-product formalism. Explain the difference between the expectation values obtained by the c-product and F-product formalisms.

A key point in the extension of the c-product to time-dependent calculations is in understanding the role of the decay and capture resonances in the propagation of wavepackets. The time-dependent state which is associated with the forward time propagation of an initial state can be described using the Fourier representation of the time evolution operator,

$$\begin{aligned}\Phi_\theta(\mathbf{r}, t > 0) = \mathrm{e}^{-\mathrm{i}\hat{H}_\theta t/\hbar}\Phi_\theta(\mathbf{r}, t = 0) &= \int_0^\infty \mathrm{d}E\mathrm{e}^{-\mathrm{i}Et/\hbar}\Phi_\theta(\mathbf{r}, E)\\ &= +\mathrm{i}\hbar\int_0^\infty \mathrm{d}E\mathrm{e}^{+\mathrm{i}Et/\hbar}\hat{G}_\theta(E)\Phi_\theta(\mathbf{r}, 0)\,,\end{aligned} \tag{6.60}$$

where, using the spectral representation of the Green's operator,

$$\hat{G}_\theta(E) = \frac{1}{E - \hat{H}_\theta} = \sum_n \frac{|\psi_n^\theta)(\psi_n^\theta|}{E - E_n^\theta} \tag{6.61}$$

and E_n^θ and ψ_n^θ are correspondingly the eigenvalues and eigenfunctions of $\hat{H}_\theta = \hat{S}_{+\theta}\hat{H}\hat{S}_{-\theta}$. Note that the spectrum of $\hat{H}_\theta$ includes the *decay* resonances and the continuum states which are rotated into the fourth quadrant in the complex energy plane.

The time-dependent state which is associated with the backward time propagation of an initial state is given by

$$\Phi_\theta(\mathbf{r}, t < 0) = [\Phi_\theta(\mathbf{r}, t > 0)]^* = -\mathrm{i}\hbar\int_0^\infty \mathrm{d}E\mathrm{e}^{+\mathrm{i}Et/\hbar}\hat{G}_{-\theta}(E)[\Phi_\theta(\mathbf{r}, 0)]^*\,. \tag{6.62}$$

where

$$\hat{G}_{-\theta}(E) = \frac{1}{E - \hat{H}_{-\theta}} = \sum_n \frac{|[\psi_n^\theta]^*)([\psi_n^\theta]^*|}{E - (E_n^\theta)^*} \tag{6.63}$$

and $[E_n^\theta]^*$ and $[\psi_n^\theta]^*$ are correspondingly the eigenvalues and eigenfunctions of $\hat{H}_{-\theta} = \hat{S}_{-\theta}\hat{H}\hat{S}_\theta$. Note that the spectrum of $\hat{H}_{-\theta}$ includes the *capture* resonances and the continuum states which are rotated into the first quadrant in the complex energy plane and *not* to the fourth quadrant as before.

Can we associate the forward and backward time-propagated initial states respectively with the time-dependent "ket" states (i.e., right states) and "bra" states (i.e., left states)?

For the case where $\theta = 0$ we know the answer since $\hat{H}_{\theta=0}$ is a Hermitian Hamiltonian. The "ket"-right time-dependent state is defined by

$$\Phi_\mathrm{R}(\mathbf{r}, t \geq 0) = \Phi_{\theta=0}(\mathbf{r}, t > 0) \tag{6.64}$$

whereas the "bra"-left time dependent state is defined as

$$\Phi_\mathrm{L}(\mathbf{r}, t \geq 0) = \Phi_{\theta=0}(\mathbf{r}, t < 0)\,. \tag{6.65}$$

One may wonder whether we can generalize these definitions for the non-Hermitian case. Let us postulate that the right-"ket" time-dependent state is the solution of the time-dependent Schrödinger equation with the non-Hermitian Hamiltonian,

$$\Phi_\mathrm{R}^\theta(\mathbf{r}, t \geq 0) = \Phi_\theta(\mathbf{r}, t > 0)\,. \tag{6.66}$$

Can we define for non-Hermitian Hamiltonians the left-"bra" time-dependent state as

$$\Phi_\mathrm{L}^\theta(\mathbf{r}, t \geq 0) \overset{?}{=} \Phi_\theta(\mathbf{r}, t < 0)\,. \tag{6.67}$$

The answer to this question is no. We can't describe the "ket"-right states and the "bra"-left states by using entirely different complex poles of the scattering matrix. The "ket"-right states are associated with the poles of the scattering matrix which are embedded in the fourth quadrant of the complex energy plane (where the decay resonances are located), whereas the "bra"-left states as proposed above are associated with the poles of the scattering matrix which are embedded in the first quadrant of the complex energy plane (where the capture resonances are located). We have to describe the "ket"-right states and the "bra"-left states by using the same complex poles of the scattering matrix. How can we carry out the transformation from one type of pole to the other?

We propose that in order to transform from capture poles (C) to decay poles (D) we use the following operator:

$$\hat{O}_{\mathrm{D}\leftarrow\mathrm{C}} = \sum_n |\psi_n^\theta)([\psi_n^\theta]^*|\,, \tag{6.68}$$

whereas in order to transform from decay poles (D) to capture poles (C) we use the operator

$$\hat{O}_{\mathrm{C}\leftarrow\mathrm{D}} = \sum_n |[\psi_n^\theta]^*)(\psi_n^\theta|\,. \tag{6.69}$$

Here ψ_n^θ and $[\psi_n^\theta]^*$ are the eigenfunctions of $\hat{H}_\theta$ and $\hat{H}_{-\theta}$ correspondingly. Therefore, the "bra"-left propagated wavepacket is given by

$$\begin{aligned}\Phi_{\mathrm{L}}^\theta(\mathbf{r}, t \geq 0) &= \hat{O}_{\mathrm{D}\leftarrow\mathrm{C}}[\mathrm{e}^{-\mathrm{i}\hat{H}_\theta t/\hbar}]^* \hat{O}_{\mathrm{C}\leftarrow\mathrm{D}}[\Phi_{-\theta}(0)]^* \\ &= \sum_{n'n} |\psi_{n'}^\theta)([\psi_{n'}^\theta]^*|\mathrm{e}^{+\mathrm{i}\hat{H}_{-\theta} t/\hbar}|[\psi_n^\theta]^*)(\psi_n^\theta|\Phi_{-\theta}^*(0)) \\ &= \sum_n a_n^{\mathrm{L}} \mathrm{e}^{+\mathrm{i}(E_n^\theta)^* t/\hbar} a_n^{\mathrm{L}} |\psi_n^\theta) = \sum_n a_n^{\mathrm{L}} \mathrm{e}^{+\mathrm{i}E_n^{-\theta} t/\hbar} \psi_n^\theta(\mathbf{r})\,, \end{aligned} \tag{6.70}$$

where

$$a_n^{\mathrm{L}} = (\psi_n^\theta|\Phi_{-\theta}^*(0))\,; \tag{6.71}$$

whereas the ket-right propagated wavepacket is defined as usual:

$$\Phi_{\mathrm{R}}^\theta(\mathbf{r}, t \geq 0) = \mathrm{e}^{-\mathrm{i}\hat{H}_\theta t/\hbar} \Phi_\theta(x, 0) = \sum_n a_n^{\mathrm{R}} \mathrm{e}^{-\mathrm{i}E_n^\theta t/\hbar} \cdot \psi_n^\theta(\mathbf{r})\,, \tag{6.72}$$

where

$$a_n^{\mathrm{R}} = (\psi_n^\theta|\Phi_\theta(0))\,. \tag{6.73}$$

This establishes a formal ground for evaluating observables using the non-Hermitian formalism. The "norm" of a time-dependent wavepacket for the most general case is given by

$$\mathcal{N}(t) \equiv (\Phi_{\mathrm{L}}^\theta(t \geq 0)|\Phi_{\mathrm{R}}^\theta(t \geq 0)) = \sum_n a_n^{\mathrm{L}} a_n^{\mathrm{R}} \mathrm{e}^{-2\mathrm{Im}[E_n^\theta]t/\hbar}\,. \tag{6.74}$$

The time-dependent expectation value of any complex scaled operator $\hat{O}_\theta$ is accordingly given by

$$\begin{aligned}\bar{O}(t) &= \frac{1}{\mathcal{N}(t)} \sum_{n',n} a^{\mathrm{L}}_{n'} a^{\mathrm{R}}_{n} \mathrm{e}^{-\mathrm{i}(E^{\theta}_{n} - E^{-\theta}_{n'})t/\hbar} (\psi^{\theta}_{n'} | \hat{O}_\theta | \psi^{\theta}_{n}) \\ &= \frac{1}{\mathcal{N}(t)} \sum_{n',n} a^{\mathrm{L}}_{n'} a^{\mathrm{R}}_{n} \mathrm{e}^{-\mathrm{i}\mathrm{Re}(E^{\theta}_{n} - E^{\theta}_{n'})t/\hbar} \mathrm{e}^{-\mathrm{Im}(E^{\theta}_{n} + E^{\theta}_{n'})t/\hbar} (\psi^{\theta}_{n'} | \hat{O}_\theta | \psi^{\theta}_{n}) \,. \qquad (6.75)\end{aligned}$$

6.6 The F-product and the conservation of the number of particles

Using the F-product formalism the number of particles is not conserved, as a result of the fact that the limits of $t \to \infty$ and $x \to \infty$ are taken independently from one another. In the spirit of the discussion given in Section 4.7 we argue here that by using the F-product the number of particles is conserved when the limits of $t \to \infty$ and $x \to \infty$ are coupled through the velocity of the ionized (dissociated or radiated) electron (atom or α-particle). If we think of the decaying particle as a freely moving particle, this velocity depends on the ratio between the position of the particle x and the time of propagation t and is given by

$$v = \frac{p}{M} = \sqrt{\frac{2\mathrm{Re}(E_{\mathrm{res}})}{M}} = \sqrt{\frac{2\epsilon}{M}} \,. \qquad (6.76)$$

The idea of coupling time and space results from two facts which are closely related:

(1) the eigenvalue of the Hamiltonian which is associated with the resonance state has a complex eigenvalue, E_{res}, only due to the requirement of the outgoing boundary condition, i.e., restriction on the spatial behavior of the corresponding resonance eigenfunction;

(2) the inverse of -2Im$(E_{\mathrm{res}})/\hbar = \Gamma/\hbar$ is the resonance lifetime.

The asymptote of the complex scaled resonance wavefunction is given by

$$\Psi_\theta(x \to \infty, t \to \infty) = \gamma_{\mathrm{res}} \hat{S}_\theta \mathrm{e}^{-\mathrm{i}E_{\mathrm{res}}t/\hbar} \mathrm{e}^{+\mathrm{i}k_{\mathrm{res}}x} \,, \qquad (6.77)$$

where for sufficiently narrow resonances the resonance wave vector can be approximated by the first leading term as

$$k_{\mathrm{res}} = \sqrt{2ME_{\mathrm{res}}}/\hbar \simeq [\sqrt{2M\epsilon}/\hbar] \left(1 - \frac{\mathrm{i}\Gamma}{4\epsilon}\right) . \qquad (6.78)$$

Using the F-product formalism for the time-dependent inner product, the asymptote of the complex scaled probability density is defined as

$$\rho_\theta(x \to \infty, t \to \infty) = \gamma_{\text{res}}^2 \hat{S}_\theta \mathrm{e}^{-\mathrm{i}\Gamma t/\hbar} \mathrm{e}^{+2\mathrm{i}k_{\text{res}}x} \,. \tag{6.79}$$

Therefore, by using Eq. (6.78) one gets that

$$\rho_\theta(x \to \infty, t \to \infty) \simeq \gamma_{\text{res}}^2 \hat{S}_\theta \left[\mathrm{e}^{+\Gamma(x/v-t)/\hbar}\right] \left[\mathrm{e}^{+2\mathrm{i}xMv/\hbar}\right] \,. \tag{6.80}$$

By keeping the ratio $x/t = v$ and using the identity $Mv = p$, Eq. (6.80) reduces to

$$\rho_\theta(x \to \infty, t \to \infty) \simeq \gamma_{\text{res}}^2 \lim_{x\to\infty} \mathrm{e}^{+2\mathrm{i}xp\cos\theta/\hbar} \mathrm{e}^{-2xp\sin\theta/\hbar} = 0 \tag{6.81}$$

and consequently the integral of $\rho_\theta(x, t)$ over the entire space and time converges and the number of particles in the generalized space is conserved. The F-product formalism conserves the number of particles under the assumption that a free particle with velocity v is obtained at long times, and provided that we apply the scaling operator after inserting the condition $x = vt$ and not before. The exponential decay of the particles from a finite region in space, which can be taken as large as one wishes, results from the application of the scaling operator without imposing the requirement of $x = vt$ as $x \to \infty$.

6.7 Concluding remarks

(1) Although in this chapter non-Hermitian operators were associated with complex scaled operators, the c-product and the F-product presented here are applicable for more general cases, as for example when one uses complex potentials in waveguide propagations or in the studies of the $\mathcal{PT}$ symmetry properties of complex Hamiltonians.

(2) Quantum mechanics deals with linear operators and any linear operator can be represented by a matrix. The unscaled operators in quantum mechanics are represented by Hermitian matrices where $\mathbf{H} = \mathbf{H}^{*\mathrm{T}}$. In the case of real and Hermitian operators (e. g., in the absence of magnetic fields atomic and molecular Hamiltonians are real) they can be represented by real symmetric matrices. Complex scaled operators are represented by non-Hermitian matrices where $\mathbf{H}_\theta \neq \mathbf{H}_\theta{}^{*\mathrm{T}}$. In the cases where the unscaled operators are represented by real symmetric matrices, upon complex scaling they are represented by complex symmetric matrices where $\mathbf{H}_\theta = \mathbf{H}_\theta^{\mathrm{T}}$.

(3) The left and right eigenvectors of a non-Hermitian matrix which are associated with different eigenvalues, $E_{j'} \neq E_j$, are orthogonal, $\mathbf{d}_{j'}^{\mathrm{T}} \cdot \mathbf{c}_j = 0$. Note that even in the case of degenerate states one can always choose linear combinations of the degenerate states which will be orthogonal to one another, as stated above.

(4) In this chapter we introduced the c-product which can be considered as a replacement for the scalar-product used in standard (Hermitian) quantum mechanics. The c-product enables one to use the orthonormal eigenfunctions of the non-Hermitian Hamiltonian (as, for example, the complex scaled Hamiltonian) as a basis set in the expansion

of a given function. As we will see in Chapter 8, the use of the c-product enables us to derive a non-Hermitian scattering theory (also for time-dependent problems). Moreover, in experiments where the projectiles are temporarily trapped by the target, the wavepacket which describes the scattering process of the projectiles from the target has very small number of dominant terms in the series expansion of the wavepacket when the eigenfunctions of the non-Hermitian Hamiltonian are used as a basis set. This is in contradiction to the situation when the eigenfunctions of the Hermitian Hamiltonian (i.e., when the rotational scaling angle is zero) are used as a basis functions. The compact expansion of the wavepacket that describes the studied system in terms of the eigenfunctions of the complex scaled Hamiltonian is not limited to scattering experiments but also to the half-collision process where, for example, the system is excited to a resonance (metastable) state by a laser (read more on the above threshold ionization and the high harmonic generation phenomena in Chapter 8).

(5) The F-product presented in this chapter is an extension of the c-product to propagated wavepackets, emphasizing the desire to reduce the number of eigenfunctions of the non-Hermitian (e.g., complex scaled) Hamiltonian as a basis set in the expansion of the propagated wavepacket. The postulate which stands behind the F-product formalism is that $(\Psi_{\text{res}}(t)|\Psi_{\text{res}}(t))$ decays exponentially as time passes. The F-product plays a key role in the derivation of a theory for the high-order harmonic and the above threshold ionization and dissociation phenomenon, as will be shown in detail in Chapter 8.

6.8 Solutions to the exercises

Answer to Exercise 6.1

The orthonormal basis functions denoted by $\{j\}$ satisfy Eq. (6.4). The eigenfunctions of the complex scaled Hamiltonian can be expanded in this basis set,

$$|\Psi_n(\theta)\rangle = \sum_j C_{j,n}(\theta)|j\rangle \,. \tag{6.82}$$

By substituting Eq. (6.82) into the time-independent Schrödinger equation,

$$\hat{H}_\theta|\Psi_n(\theta)\rangle = E_n|\Psi_n(\theta)\rangle \,, \tag{6.83}$$

and multiplying from the left by $\langle j'|$, where $j' = 1, 2, \ldots,$ one gets a set of coupled equations of the form

$$\sum_j \langle j'|\hat{H}_\theta|j\rangle C_{j,n} = E_n C_{j',n} \,. \tag{6.84}$$

This set of equations can be condensed to a matrix eigenvalue problem,

$$\mathbf{H}_\theta \mathbf{C_n}(\theta) = \mathbf{E_n}\mathbf{C_n}(\theta) \,, \tag{6.85}$$

where

$$[\mathbf{H}_\theta]_{j',j} = \langle j'|\hat{H}_\theta|j\rangle \,. \tag{6.86}$$

Here we showed that the operator $\hat{H}_\theta$ can be represented by a matrix with infinite dimension. However, it is also possible to take a finite $N \times N$ matrix as an approximation which will converge to the exact solution when $N \to \infty$.

Answer to Exercise 6.2

The elements of a general complex matrix $\mathbf{H}$ are given by $H_{i,j} = \langle i|\hat{H}|j\rangle$. Similarly, $H^{\dagger}_{i,j} = \langle i|\hat{H}^{\dagger}|j\rangle$. Since by definition $\langle i|\hat{H}^{\dagger}|j\rangle = [\langle j|\hat{H}|i\rangle]^*$ one immediately obtains that $\mathbf{H}^{\dagger} = \mathbf{H}^{\mathrm{T}*}$. Note that, only when the orthonormal basis functions are real functions, the matrix elements of $\mathbf{H}^{\mathrm{T}}$ can also be expressed as $\langle j|\hat{H}|i\rangle = \langle i|H^{\dagger *}|j\rangle$.

Answer to Exercise 6.3

By setting $\theta = 0$ in the solution to Ex. 6.1, and by realizing that $\hat{H}(\theta = 0)$ is a Hermitian Hamiltonian denoted by $\hat{H}$, one gets that for a finite number of basis functions N,

$$\mathbf{H}\mathbf{C}_n = E_n(N)\mathbf{C}_n \,, \tag{6.87}$$

where $n = 1, 2, \ldots, N$. In a more compact way we can write

$$\mathbf{H}\mathbf{C} = \mathbf{C}\mathbf{E}^{(\mathrm{diag})}(N) \,, \tag{6.88}$$

where $[\mathbf{E}^{(\mathrm{diag})}(N)]_{n',n} = \delta_{n',n}E_n(N)$. Therefore,

$$(\mathbf{C}^{\mathrm{T}})^*\mathbf{H}\mathbf{C} = \mathbf{E}^{(\mathrm{diag})}(N) \,. \tag{6.89}$$

Here $\mathbf{H}$ is an $N \times N$ Hermitian matrix in the orthonormal basis functions for $i = 1, 2, \ldots, N$. We now increase the dimension of our Hamiltonian matrix by one. The basis set we will use is N eigenvectors given in Eq. (6.87) and the $(i + 1)$th original basis functions. The eigenvalues of the new matrix, $\mathbf{M}$, are denoted by $E(N + 1)$. These eigenvalues are the solutions of secular equations for which

$$\det[E(N + 1) \cdot \mathbf{I} - \mathbf{M}] = 0 \,, \tag{6.90}$$

where $\mathbf{I}$ is an $(N + 1) \times (N + 1)$ unit matrix, and $\mathbf{M}$ is an $(N + 1) \times (N + 1)$ matrix with the following structure:

$$\begin{aligned}
M(1, 1) &= \langle N + 1|\hat{H}|N + 1\rangle \,, \\
M(1, i + 1) &= \langle N + 1|\hat{H}|i\rangle \,; \; i = 1, 2, \ldots, N \,, \\
M(i + 1, 1) &= [M(1, i + 1)]^* \,; \; i = 1, 2, \ldots, N \,, \\
M(i + 1, j + 1) &= E_i(N)\delta_{i,j} \,; \; \{i, j\} = 1, 2, \ldots, N \,.
\end{aligned} \tag{6.91}$$

We denote the elements of the $1 \times N$ row $M(1, i+1); i = 1, \dots N$ by $\mathbf{M}_1^{\mathrm{T}}$. The 1, 1 element will be labelled A and the $N \times N$ diagonal block following A will be denoted by $\mathbf{B}$, while the $1 \times N$ off-diagonal block matrices will be given the labels $\mathbf{G}^{\mathrm{T}}$ and $\mathbf{G}^{\dagger}$.

From the equality $[E \cdot \mathbf{I} - \mathbf{M}][E \cdot \mathbf{I} - \mathbf{M}]^{-1} = \mathbf{I}$, i.e.,

$$\begin{pmatrix} E - M(1,1) & \mathbf{M}_1^{\mathrm{T}} \\ \mathbf{M}_1^{*} & E\mathbf{I} - \mathbf{H} \end{pmatrix} \begin{pmatrix} A & \mathbf{G}^{\mathrm{T}} \\ \mathbf{G}^{\dagger} & \mathbf{B} \end{pmatrix} = \mathbf{I}\,, \tag{6.92}$$

one immediately gets

$$\begin{aligned} [E - M(1,1)]A + \mathbf{M}_1^{\mathrm{T}}\mathbf{G}^{\dagger} &= \mathbf{I}\,, \\ \mathbf{M}_1^{*}A + [E \cdot \mathbf{I} - \mathbf{H}]\mathbf{G}^{\dagger} &= 0\,. \end{aligned} \tag{6.93}$$

Since $E \cdot \mathbf{I} - \mathbf{H}$ is a square matrix,

$$\mathbf{G}^{\dagger} = -[E \cdot \mathbf{I} - \mathbf{H}]^{-1}\mathbf{M}_1{}^{*}A\,, \tag{6.94}$$

and therefore

$$\left[E - M(1,1) - \mathbf{M}_1^{\mathrm{T}}[E \cdot \mathbf{I} - \mathbf{H}]^{-1}\mathbf{M}_1{}^{*}\right] A = 1\,. \tag{6.95}$$

Consequently,

$$A = [E - M(1,1) - \mathbf{M}_1^{\mathrm{T}}[E \cdot \mathbf{I} - \mathbf{H}]^{-1}\mathbf{M}_1{}^{*}]^{-1}\,. \tag{6.96}$$

The eigenvalues of the extended matrix $\mathbf{M}$ are obtained from the poles of

$$[E(N+1) - M(1,1) - \mathbf{M}_1^{\mathrm{T}}\mathbf{H}^{-1}\mathbf{M}_1{}^{*}]^{-1}\,. \tag{6.97}$$

Thus we proved here that the eigenvalues of $\mathbf{M}$ satisfy the following equation:

$$E - M(1,1) = \mathbf{M}_1^{\mathrm{T}}[E \cdot \mathbf{I} - \mathbf{H}]^{-1}\mathbf{M}_1{}^{*}\,. \tag{6.98}$$

By introducing Eq. (6.89) into Eq. (6.98) one gets that

$$E - H(1,1) = \mathbf{D}^{\mathrm{T}*}[E \cdot \mathbf{I} - \mathbf{E}^{(\mathrm{diag})}]^{-1}\mathbf{D}\,, \tag{6.99}$$

where

$$\mathbf{D} = \mathbf{C}\mathbf{M}_{\mathbf{1}}^{*}\,. \tag{6.100}$$

The left-hand side of Eq. (6.99) is a straight line in E. The right-hand side of Eq. (6.99) has poles when $E = E_n(N)$. Therefore, the intersection points between the straight line and the curve obtained when the right-hand side of Eq. (6.99) is plotted as function of E are the solutions we are looking for, $E_n(N+1)$, such that

$$E_{n-1}(N) < E_n(N+1) < E_n(N)\,. \tag{6.101}$$

Answer to Exercise 6.4

(a) The multiplication of $\mathbf{H}\mathbf{c}_j = E_j\mathbf{c}_j$ from the left by the vector $\mathbf{d}_{j'}^{\mathrm{T}}$ and multiplication of $\mathbf{d}_{j'}^{\mathrm{T}}\mathbf{H} = W_{j'}\mathbf{d}_{j'}^{\mathrm{T}}$ from the right by $\mathbf{c}_j$ provide the following two equations:

$$\begin{aligned}\mathbf{d}_{j'}^{\mathrm{T}}\mathbf{H}\mathbf{c}_j &= E_j\mathbf{d}_{j'}^{\mathrm{T}}\mathbf{c}_j\,,\\ \mathbf{d}_{j'}^{\mathrm{T}}\mathbf{H}\mathbf{c}_j &= W_{j'}\mathbf{d}_{j'}^{\mathrm{T}}\mathbf{c}_j\,.\end{aligned} \tag{6.102}$$

By subtracting the two equations one gets that

$$(E_j - W_{j'})\mathbf{d}_{j'}^{\mathrm{T}}\mathbf{c}_j = 0 \tag{6.103}$$

whenever

$$E_j - W_{j'} \neq 0\,. \tag{6.104}$$

This condition is satisfied only when

$$\mathbf{d}_{j'}^{\mathrm{T}}\mathbf{c}_j = 0\,. \tag{6.105}$$

Thus we established that the left and right eigenvectors are orthogonal.

The fact that this is not an inner product in the usual sense is illustrated by the possibility (though quite a rare one) that even when $W_{j'} = E_j$ (of course one can reorder the eigenvalues and the eigenvectors such the $W_{j'} = E_j$ for $j' = j$) it may happen that $\mathbf{d}_j^{\mathrm{T}}\mathbf{c}_j = 0$. We entitle these special eigenvectors as "self-orthogonal" eigenvectors.

(b) The fact that a non-Hermitian $N \times N$ matrix has N linearly independent vectors implies that $\mathbf{H} = \mathbf{C}\mathbf{E}_N^{\mathrm{diag}}\mathbf{D}^{\mathrm{T}}$, where $[\mathbf{E}_N^{\mathrm{diag}}]_{i,j} = \delta_{i,j}E_j$ and therefore

$$\mathbf{d}_j^{\mathrm{T}}\mathbf{c}_j = N_j = \rho_j \mathrm{e}^{\mathrm{i}\alpha_j} \neq 0\,. \tag{6.106}$$

As we will show below, there is some freedom in the definition of the normalized right and left eigenvectors. The normalized right and left eigenvectors, $\tilde{\mathbf{c}}_j$ and $\tilde{\mathbf{d}}_j$, are respectively given by

$$\tilde{\mathbf{c}}_j = N_j^{\mathrm{R}}\mathbf{c}_j = \rho_j^{\mathrm{R}}\mathrm{e}^{\mathrm{i}\alpha_j^{\mathrm{R}}}\mathbf{c}_j\,. \tag{6.107}$$

$$\tilde{\mathbf{d}}_j = N_j^{\mathrm{L}}\mathbf{d}_j = \rho_j^{\mathrm{L}}\mathrm{e}^{\mathrm{i}\alpha_j^{\mathrm{L}}}\mathbf{d}_j\,, \tag{6.108}$$

where

$$N_j^{\mathrm{L}}N_j^{\mathrm{R}} = N_j\,. \tag{6.109}$$

Therefore,

$$\rho_j^{\mathrm{L}} \rho_j^{\mathrm{R}} = \rho_j \,. \tag{6.110}$$

$$\alpha_j^{\mathrm{L}} + \alpha_j^{\mathrm{R}} = \alpha_j \,. \tag{6.111}$$

There are three degrees of freedom in the normalization of every set of left and right eigenvectors of the non-Hermitian matrix. Two free parameters are the length and the phase of one of the two normalization factors which can be chosen arbitrarily and still keep the vectors normalized to unity. The third one is the global ± phase. Note that for complex symmetric matrices one may wish to keep $\tilde{\mathbf{c}}_j = \tilde{\mathbf{d}}_j$ and therefore only one degree of freedom remains (the ± global phase).

Answer to Exercise 6.5

By substituting the coefficient of the out-going waves $B(q_n)$ and $B(q_{n'})$ as calculated in Chapter 4 (see Eq. (6.19)) in Eq. (6.24) one gets

$$\begin{aligned}(\Psi_n|\Psi_{n'}) = {} & \frac{1}{2}\left(\frac{\sin[(k_n - k_{n'})L]}{k_n - k_{n'}} - \frac{\sin[(k_n + k_{n'})L]}{k_n + k_{n'}}\right) \\ & + \frac{\mathrm{i}}{4(q_n + q_{n'})}\left[\sin(k_n L) - \mathrm{i}\frac{k_n}{q_n}\cos(k_n L)\right]\left[\sin(k_{n'} L) - \mathrm{i}\frac{k_{n'}}{q_{n'}}\cos(k_{n'} L)\right] .\end{aligned} \tag{6.112}$$

Note that when $n' = n$,

$$\lim_{n' \to n} \frac{\sin[(k_n - k_{n'})L]}{k_n - k_{n'}} = L \,, \tag{6.113}$$

and therefore the normalization factor of the n-th resonance state according to the c-product is given by

$$N_n(k_n, q_n) = \left[\frac{1}{2}\left(L - \frac{\sin(2k_n L)}{2k_n}\right) + \frac{\mathrm{i}}{8q_n}\left[\sin(k_n L) - \mathrm{i}\frac{k_n}{q_n}\cos(k_n L)\right]^2\right]^{-1/2} . \tag{6.114}$$

Since the functions $\Psi_n(x)$ and $\Psi_{n'}(x)$ are two decay resonances of the one-dimensional potential barrier problem, the wave vectors associated with the n-th resonance state should satisfy the following condition:

$$k_n = n\pi - \mathrm{i}\frac{L}{2}\ln\left[\frac{q_n + k_n}{q_n - k_n}\right] . \tag{6.115}$$

The self-orthogonality condition is

$$N_n(k_n, q_n) = 0 \,, \tag{6.116}$$

where k_n and q_n satisfy Eq. (6.115). By varying the potential parameters, L and V_0, accidental degeneracy can be obtained (provided there is a solution to Eq. (6.116)). By substituting Eq. (6.115) for n and n' in Eq. (6.112) one gets that for $\Psi_n(x) \neq \Psi_{n'}(x)$

$$(\Psi_n|\Psi_{n'\neq n}) = 0\,, \tag{6.117}$$

and for the normalizable resonance wavefunctions

$$(\tilde{\Psi}_n|\tilde{\Psi}_{n'}) = \delta_{n,n'}\,. \tag{6.118}$$

Answer to Exercise 6.6

Since the real basis functions $\phi(x)$ and $\chi(x)$ decay exponentially to zero as $x \to \pm\infty$, also the asymptotes of the transformed functions,

$$\tilde{\phi}(z) = \phi(x)|_{x=F^{-1}(z)} \tag{6.119}$$

and

$$\tilde{\chi}(z) = \chi(x)|_{x=F^{-1}(z)} \tag{6.120}$$

vanish at $z = \pm\infty$. Therefore the complex scaled kinetic energy matrix elements we need to calculate are given by

$$\int_{-\infty}^{+\infty} \mathrm{d}z\tilde{\phi}(z)\frac{\mathrm{d}^2}{\mathrm{d}z^2}\tilde{\chi}(z)\,. \tag{6.121}$$

By carrying out integration by parts one gets

$$\int_{-\infty}^{+\infty} \mathrm{d}z\tilde{\phi}(z)\frac{\mathrm{d}^2}{\mathrm{d}z^2}\tilde{\chi}(z) = \int_{-\infty}^{+\infty} \mathrm{d}z\tilde{\chi}(z)\frac{\mathrm{d}^2}{\mathrm{d}z^2}\tilde{\phi}(z) + \left[\frac{\mathrm{d}\tilde{\phi}}{\mathrm{d}z}\tilde{\chi}(z) - \frac{\mathrm{d}\tilde{\chi}}{\mathrm{d}z}\tilde{\phi}(z)\right]_{-\infty}^{+\infty}\,. \tag{6.122}$$

Since, as explained above, $\tilde{\phi}(z) \to 0$ and $\tilde{\chi}(z) \to 0$ as $|z| \to \infty$, we get that

$$\int_{-\infty}^{+\infty} \mathrm{d}z\tilde{\phi}(z)\frac{\mathrm{d}^2}{\mathrm{d}z^2}\tilde{\chi}(z) = \int_{-\infty}^{+\infty} \mathrm{d}z\tilde{\chi}(z)\frac{\mathrm{d}^2}{\mathrm{d}z^2}\tilde{\phi}(z)\,. \tag{6.123}$$

Answer to Exercise 6.7

Let us consider a case where one bound state in a closed channel interacts with the continuum of an open channel. We assume that the continuum can be represented by broad decay resonance states only, $\{\Gamma_{n_c}\}_{n_c=1,2,\ldots}$. Note that even for a very shallow finite square potential well or a barrier there are an infinite number of broad overlapping resonances. These decay resonances which are associated with the open channel are very broad ones and are assigned a good quantum number n_c. As we will show below, the widths of these broad decay resonances play the role of density of continuum states in the open channel in the calculations of the width of the Feshbach resonance state which is "born" due to the interaction of the bound state in the closed channel with the continuum state in the open channel. Even when the open channel does not support any decay resonances one might modify the potential of the open channel by adding a shallow rectangular potential well/barrier with a depth/height denoted by v_0. The resonance width $\Gamma_{n_\mathrm{c}} \to \infty$ as $v_0 \to 0$. As we will show below, our conclusions do not dependent on the value of v_0 (or Γ_{n_c}).

The Hamiltonian in this case is given by

$$\begin{aligned}\hat{H} = E_b|b\rangle\langle b| &+ \sum_{n_\mathrm{c}}\left(E_{n_\mathrm{c}} - \frac{\mathrm{i}}{2}\Gamma_{n_\mathrm{c}}\right)|[n_\mathrm{c}]^*\rangle\langle n_\mathrm{c}| \\ &+ \sum_{n_\mathrm{c}} V_{b,n_\mathrm{c}}(|[n_\mathrm{c}]^*\rangle\langle b| + |b\rangle\langle n_\mathrm{c}|)\,. \qquad (6.124)\end{aligned}$$

The bound state is represented by a real function. When the coupling between the two channels is sufficiently weak it is reasonable to consider the case where the bound state is mainly coupled to a single decay resonance state, $|c\rangle$, and Eq. (6.124) reduces to

$$\hat{H} = E_b|b\rangle\langle b| + \left(E_c - \frac{\mathrm{i}}{2}\Gamma_c\right)|[c]^*\rangle\langle c| + V_{b,c}(|[c]^*\rangle\langle b| + |b\rangle\langle c|)\,, \qquad (6.125)$$

where

$$E_c = E_b + \Delta\,. \qquad (6.126)$$

It is convenient to define the strength of the coupling parameter between the two channels as

$$V_{b,c} = \frac{\sqrt{g\Gamma_c}}{2}\,. \qquad (6.127)$$

As will be shown below, when $g \ll \Gamma_c$, g is the width of *the Feshbach resonance state which is created due to the interaction of the bound state in the closed channel with the continuum of the open channel*. The strength of the coupling between the closed and open channels is increased as Γ_c is increased. This result might be expected since, within the framework of the standard formalism of quantum mechanics, the bound state in the closed channel is mainly coupled to the continuum states in the open channel within the energy interval $E_b \pm \Gamma_c/2$.

The time-independent Schrödinger equation we should solve is given by

$$\mathbf{H}|\psi\rangle = E|\psi\rangle\,, \qquad (6.128)$$

where

$$\mathbf{H} = \begin{pmatrix} E_b & \sqrt{g\Gamma_c}/2 \\ \sqrt{g\Gamma_c}/2 & E_b + \Delta - \frac{\mathrm{i}}{2}\Gamma_c \end{pmatrix} \tag{6.129}$$

and

$$|\psi\rangle = \begin{pmatrix} |b\rangle \\ |c\rangle \end{pmatrix} . \tag{6.130}$$

The two eigenvalues of the 2 × 2 matrix **H** are given by

$$E_\pm = \frac{2E_b + \Delta - \mathrm{i}/2\Gamma_c}{2} \pm \frac{1}{2}\sqrt{(\Delta - \mathrm{i}/2\Gamma_c)^2 + g\Gamma_c} \, . \tag{6.131}$$

For the sake of simplicity, without loss of generality, we set here the shift in the resonance position equal to zero, $\Delta = 0$. The two eigenvalues are reduced to

$$E_\pm = E_b - \frac{\mathrm{i}}{4}\Gamma_c \mp \frac{\mathrm{i}}{4}\Gamma_c\sqrt{1 - \frac{4g}{\Gamma_c}} \tag{6.132}$$

and for $4g/\Gamma_c \ll 1$ we get the first-order approximated values for the Feshbach resonance state resulting from the interaction of the bound state in the open channel with the continuum of the open channel (presented here by a broad resonance state) and for the shifted continuum state of the open channel,

$$E_{\mathrm{res}} = E_b - \frac{\mathrm{i}}{2}\Gamma_{\mathrm{res}} \, , \tag{6.133}$$

where

$$\Gamma_{\mathrm{res}} = g \tag{6.134}$$

and

$$E_c^{\mathrm{shifted}} = E_b - \frac{\mathrm{i}}{2}(\Gamma_c + g) \, . \tag{6.135}$$

Let us consider now a situation where our 2 × 2 Hamiltonian describes a quantum dot which is attached to two leads through the open channel in our Hamiltonian. Using the results presented above, we can calculate the probability amplitude of a transition from one lead to the second one through the quantum dot. Using the Lippmann–Schwinger equation (the extension of the time-independent quantum scattering theory to non-Hermitian Hamiltonians is presented in Chapter 8), the probability amplitude for the scattering event where the final state is exactly as the initial state

$$\begin{pmatrix} 0 \\ |c\rangle \end{pmatrix} \to \begin{pmatrix} 0 \\ |c\rangle \end{pmatrix} \tag{6.136}$$

is approximately given by

$$t(\epsilon) = 1 + (\,0 \quad 1\,)\begin{pmatrix} 0 & \sqrt{g\Gamma_c}/2 \\ \sqrt{g\Gamma_c}/2 & 0 \end{pmatrix}$$
$$\cdot \begin{pmatrix} \epsilon & -\sqrt{g\Gamma_c}/2 \\ -\sqrt{g\Gamma_c}/2 & \epsilon + \frac{i}{2}\Gamma_c \end{pmatrix}^{-1} \begin{pmatrix} 0 & \sqrt{g\Gamma_c}/2 \\ \sqrt{g\Gamma_c}/2 & 0 \end{pmatrix} \begin{pmatrix} 0 \\ 1 \end{pmatrix}, \tag{6.137}$$

where $\epsilon = E - E_b$ is the deviation from the resonance condition where E is the energy of the incoming particle in the open channel. After some algebraic manipulation one gets that

$$t(\epsilon) = 1 - \frac{\Gamma_{\text{res}}\Gamma_c(2\epsilon + \Gamma_c \text{i})}{2\Gamma_{\text{res}}\Gamma_c - 8\epsilon^2 - 4\text{i}\epsilon\Gamma_c}\,. \tag{6.138}$$

For $\Gamma_c \gg \Gamma_{\text{res}}$ (as in our case) one gets that the transition probability in the scattering experiment has a Lorenzian peak at $\epsilon = 0$ (i.e., at the Feshbach resonance position),

$$|t(\epsilon)|^2 \simeq \left(\frac{\Gamma_c}{2}\right)^2 \left[1 + (2\epsilon/\Gamma_{\text{res}})^2\right]^{-1} \tag{6.139}$$

with a width at half-height of $\Gamma_{\text{res}} = g$, where g is defined above as the potential interaction between the closed and open channels divided by the density of states in the open channels as presented here by Γ_c.

Answer to Exercise 6.8

The Taylor series expansion of the matrix $\mathbf{U}(t)$ is given by

$$\mathbf{U}(t) = \text{e}^{-\text{i}\mathbf{H}t} = \sum_n \frac{(-\text{i}t)^n}{n!}\mathbf{H}^n\,. \tag{6.140}$$

Using the closure relations and the fact that $\mathbf{d}_j$ and $\mathbf{c}_j$ are correspondingly the left and right eigenvectors of $\mathbf{H}$ that are associated with the same eigenvalue E_j, Eq. (6.140) can be re-written in the spectral representation as

$$\mathbf{U}(t) = \mathbf{C}\mathbf{D}^{\text{T}}\text{e}^{-\text{i}\mathbf{H}t}\mathbf{C}\mathbf{D}^{\text{T}} = \sum_j \sum_n \frac{(-\text{i}t)^n}{n!} E_j^n \mathbf{c}_j \cdot \mathbf{d}_j^{\text{T}} = \sum_j \text{e}^{-\text{i}E_j t}\mathbf{c}_j \cdot \mathbf{d}_j^{\text{T}}\,. \tag{6.141}$$

Using Eq. (6.141), the survival probability amplitude of the initial vector $\mathbf{v_0}$ is obtained,

$$A(t) = \mathbf{v}_0^{\text{T}} \cdot \mathbf{U}(t)\mathbf{v}_0 = \sum_j \text{e}^{-\text{i}E_j t}(\mathbf{v}_0^{\text{T}} \cdot \mathbf{c}_j)(\mathbf{d}_j^{\text{T}} \cdot \mathbf{v}_0)\,. \tag{6.142}$$

For Hermitian matrices $\{E_j\}$ are real. For non-Hermitian matrices which represent the complex scaled Hamiltonians $\text{Im}\{E_j\} \leq 0$ and therefore $A(t)$ decays to zero as time passes whenever the initial state vector populates eigenvectors which are associated with the resonance states. This is essentially the F-product formalism which was discussed in detail in this chapter.

Answer to Exercise 6.9

(a) For the sake of simplicity we assume that the Hamiltonian is real and Hermitian within the framework of standard QM. The time-dependent expectation values of a given operator $\hat{O}$ are given by

$$\bar{O}(t) = \frac{\int_{\text{all-space}} d\mathbf{r}\Phi^{\mathrm{L}}(\mathbf{r},t)\hat{O}\Phi^{\mathrm{R}}(\mathbf{r},t)}{\int_{\text{all-space}} d\mathbf{r}\Phi^{\mathrm{L}}(\mathbf{r},t)\Phi^{\mathrm{R}}(\mathbf{r},t)}\,, \tag{6.143}$$

where

$$\Phi^{\mathrm{R}}(\mathbf{r},t) = \mathrm{e}^{-\mathrm{i}\hat{H}t/\hbar}\Phi_{\mathrm{WP}}(\mathbf{r})\,,$$
$$\Phi^{\mathrm{L}}(\mathbf{r},t) = \mathrm{e}^{+\mathrm{i}\hat{H}t/\hbar}\Phi^{*}_{\mathrm{WP}}(\mathbf{r})\,. \tag{6.144}$$

Since the initial wave packet $\Phi_{\mathrm{WP}}(\mathbf{r})$ is a square integrable function, also the time-propagated WP is a square integrable function at any given time t. Consequently, one can use orthonormal square integrable functions $\{g_n\}_{n=1,2,\ldots}$ (e.g., 3D harmonic oscillators) as a basis set. In such a case

$$\Psi^{\mathrm{R}}_{\mathrm{WP}}(\mathbf{r},t) = \sum_n C_n(t)g_n(\mathbf{r})\,,$$
$$\Psi^{\mathrm{L}}_{\mathrm{WP}}(\mathbf{r},t) = \sum_n C^{*}_n(t)g^{*}_n(\mathbf{r})\,,$$
$$C_n(t) = \langle g_n|\Psi^{\mathrm{R}}_{\mathrm{WP}}(t)\rangle \tag{6.145}$$

and

$$\bar{O}(t) = \sum_{n',n} C^{*}_{n'}(t)C_n(t)\int g^{*}_{n'}(\mathbf{r})\hat{O}g_n(\mathbf{r})\mathrm{d}\mathbf{r}\,. \tag{6.146}$$

Here we use the normalization condition that $\sum_{n',n} C^{*}_{n'}(t)C_n(t) = \delta_{n',n}$. We now use the complex scaling transformation $\mathbf{r} \to \mathbf{r}\mathrm{e}^{\mathrm{i}\theta}$ (see Chapter 5) for calculating the time-dependent expectation values:

$$\int \Psi^{\mathrm{L}}_{\mathrm{WP}}(\mathbf{r}\mathrm{e}^{+\mathrm{i}\theta},t)\hat{O}_\theta\Psi^{\mathrm{R}}_{\mathrm{WP}}(\mathbf{r}\mathrm{e}^{+\mathrm{i}\theta},t)\mathrm{e}^{+3\mathrm{i}\theta}\mathrm{d}\mathbf{r}$$
$$= \sum_{n',n} C^{*}_{n'}(t)C_n(t)\int [g_{n'}(\mathbf{r}\mathrm{e}^{-\mathrm{i}\theta})]^{*}\hat{O}_\theta g_n(\mathbf{r}\mathrm{e}^{+\mathrm{i}\theta})\mathrm{e}^{+3\mathrm{i}\theta}\mathrm{d}\mathbf{r}\,, \tag{6.147}$$

where the complex scaled operator $\hat{O}$ is denoted by $\hat{O}_\theta$. Since the square integrable basis functions are analytical functions and $\hat{O} g_n(\mathbf{r})$ is an analytical function,

$$\int g^*_{n'}(\mathbf{r})\hat{O} g_n(\mathbf{r})\mathrm{d}\mathbf{r} = \int [g_{n'}(\mathbf{r}\mathrm{e}^{-\mathrm{i}\theta})]^* \hat{O}_\theta g_n(\mathbf{r}\mathrm{e}^{+\mathrm{i}\theta})\mathrm{e}^{+3\mathrm{i}\theta}\mathrm{d}\mathbf{r}\,. \tag{6.148}$$

Using this result we get that

$$\begin{aligned}&\int \Psi^{\mathrm{L}}_{\mathrm{WP}}(\mathbf{r}\mathrm{e}^{+\mathrm{i}\theta}, t)\hat{O}_\theta \Psi^{\mathrm{R}}_{\mathrm{WP}}(\mathbf{r}\mathrm{e}^{+\mathrm{i}\theta}, t)\mathrm{e}^{+3\mathrm{i}\theta}\mathrm{d}\mathbf{r}\\ &\quad = \sum_{n',n} C^*_{n'}(t)C_n(t)\int g^*_{n'}(\mathbf{r})\hat{O} g_n(\mathbf{r})\mathrm{d}\mathbf{r} = \bar{O}(t)\end{aligned} \tag{6.149}$$

and the *same* expectation value is obtained as in standard QM. Note that in the calculations of the l.h.s. of Eq. (6.149) we have used the c-product formalism. The c-product is applicable since square integrable functions remain square integrable upon complex scaling.

(b) We now discuss the situation where the use of the c-product as derived for eigenstates of non-Hermitian operators in calculations of the time-dependent expectation values might introduce numerical difficulties, while the use of the F-product formalism simplifies the calculations. This happens when one wishes to use the eigenfunctions of the complex scaled Hamiltonian as a basis set in numerical calculations of the complex scaled time evolution operator. Thus any state can be expressed in terms of the solutions of the complex scaled TISE,

$$\hat{H}_\theta \psi^\theta_n(\mathbf{r}) = E^\theta_n \psi^\theta_n(\mathbf{r})\,, \tag{6.150}$$

where n is the index of the complex scaled bound states (if they exist), rotated continuum states and the resonance states. Only for the bound states $\psi^\theta_n(\mathbf{r}) = \psi_n(\mathbf{r}\mathrm{e}^{\mathrm{i}\theta})$ (up to a normalization factor). For the rotated continuum and resonance sates $\psi^\theta_n(\mathbf{r}) \neq \psi_n(\mathbf{r}\mathrm{e}^{\mathrm{i}\theta})$, which implies that the rotated continuum eigenfunctions of the complex scaled Hamiltonian are *not* equal to the complex scaled eigenfunctions of the unscaled Hermitian Hamiltonian. Using a finite-box quantization condition, the spectrum of the complex scaled Hamiltonian is discrete and as the size of the box is increased the density of the quasi-continuum states is increased as well.

The time-dependent expectation value $\bar{O}(t)$ is calculated using the c-product for the calculations of time-dependent expectation values, which yields

$$\bar{O}(t) = \sum_{n',n}[\mathcal{D}^{-\theta}_{n'}]^*[\mathcal{D}^\theta_n]\mathrm{e}^{-\mathrm{i}(E^\theta_n - E^\theta_{n'})t/\hbar}\int \psi^\theta_{n'}(\mathbf{r})\hat{O}_\theta \psi^\theta_n(\mathbf{r})\mathrm{d}\mathbf{r}\,, \tag{6.151}$$

where here we assume that for $\theta = 0$ the eigenfunctions of the Hamiltonian are real functions (i.e., become complex upon the complex scaling) and therefore $\langle [\psi_{n'}^{-\theta}]^* | \psi_n^\theta \rangle = (\psi_{n'}^\theta | \psi_n^\theta) = \delta_{n',n}$. The linear coefficients are given by

$$\mathcal{D}_n^\theta = \langle \psi_n^{-\theta} | \Phi_{\mathrm{WP}}^\theta \rangle = (\psi_n^\theta | \Phi_{\mathrm{WP}}^\theta) , \tag{6.152}$$

where $\sum_n [\mathcal{D}_n^{-\theta}]^* [\mathcal{D}_n^\theta] = 1$. The complex scaled initial wave packet is $|\Phi_{\mathrm{WP}}^\theta\rangle$ and the integration is carried out over $\mathrm{e}^{+3\mathrm{i}\theta} d\mathbf{r}$. The motivation for using the orthonormal eigenfunctions of the complex scaled Hamiltonian as a basis set results from the fact that in many physical situation the dynamics is controlled by a single or by several resonance states. A simple case is when the initial state is already mostly populated by a single resonance state,

$$|\mathcal{D}_{n_{\mathrm{res}}}^\theta|^2 \sim 1 . \tag{6.153}$$

In such a case it might be necessary to carry out the time-propagation calculations for a very long period of time (longer than the lifetime of the narrowest resonance state which is populated by the initial wavepacket). Even in the case where the dominant contribution to the basis set expansion of the initial state is a resonance state there are other non-vanishing contributions of other basis functions (resonances or rotated continuum states). Therefore, as one can see from Eq. (6.151), due to the fact that there are always pairs of complex eigenvalues for which $\mathrm{Im}[E_n^\theta - E_{n'}^\theta] > 0$,

$$\lim_{t \to \infty} \mathrm{e}^{-\mathrm{i}(E_n^\theta - E_{n'}^\theta)t/\hbar} = \infty . \tag{6.154}$$

The n-th and n'-th states can be two resonances states that do not have the same widths or one resonance state (or a bound state) and one rotated continuum state (note that the initial wave packet can never populate exclusively one resonance state only). This time asymmetry problem in non-Hermitian quantum mechanics limits the ability to propagate a resonance wavefunction from the initial time $t = 0$ to $t = -\infty$. However, as has been proved above, the time-dependent expectation value $\bar{O}(t)$ which is calculated within the framework of the c-product formalism is equal to to the value which is obtained within the framework of the standard formalism of QM. Therefore, the summation over the *entire* eigenstates of the complex scaled Hamiltonian introduces quantum interferences which compensate the diverging and decaying nature of different individual terms in the basis set expansion of the time-dependent expectation value of the operator $\hat{O}$. However, the truncation of the number of basis functions which are used in the calculations of $\bar{O}(t)$ might introduce numerical difficulties which require special attention.

The same analysis presented above for a time-independent Hamiltonian can be implemented for a time-periodic Hamiltonian where the time-independent Hamiltonian $\hat{H}$ and $\hat{H}_\theta$ are replaced respectively by the Floquet operators

$$\mathcal{H}_{\mathrm{F}}(\mathbf{r}, t) = -\mathrm{i}\hbar\partial_t + \hat{H} \tag{6.155}$$

and

$$\mathcal{H}^{\theta}_{\mathrm{F}}(\mathbf{r}, t) = -\mathrm{i}\hbar\partial_t + \hat{H}_\theta \tag{6.156}$$

and t serves as an additional coordinate. Similarly E_n and E_n^θ are replaced by the eigenvalues of the Floquet and complex scaled Floquet operators. Therefore, the same time-asymmetry problem exists also in the calculations of time-dependent expectation values by using the quasi-energy solutions of the TDSE when the time-dependent Hamiltonian is complex scaled.

(c) We now have motivation for applying the F-product formalism. There are two conditions which should be satisfied in order to justify replacing the c-product by the F-product:

(1) the operator $\hat{O}$ gets non-zero values at the interaction region and vanishes elsewhere (e.g., the acceleration operator $-(1/m)\partial V/\partial r$);
(2) as time passes the propagated wavepacket populates a single or several resonance states.

Under such conditions we wish to normalize the resonance wavefunctions such that they decay exponentially as time passes, and therefore Eq. (6.151) is replaced by

$$\bar{O}(t) = \frac{\sum_{n',n}[\mathcal{D}^{-\theta}_{n'}]^*[\mathcal{D}^{\theta}_{n}]\mathrm{e}^{-\mathrm{i}(E^\theta_n - [E^\theta_{n'}]^*)t/\hbar}\int \psi^\theta_{n'}(\mathbf{r})\hat{O}_\theta\psi^\theta_n(\mathbf{r})\mathrm{d}\mathbf{r}}{\sum_n[\mathcal{D}^{-\theta}_{n}]^*[\mathcal{D}^{\theta}_{n}]\mathrm{e}^{-2\mathrm{Im}[E^\theta_n]t/\hbar}}\,. \tag{6.157}$$

If, for example, the initial wavepacket populates mostly the lowest (i.e., long-living) resonance state which is denoted by $n = n_{\mathrm{res}}$ then the complex expectation value is time-independent,

$$\bar{O} = [\mathcal{D}^{-\theta}_{n_{\mathrm{res}}}]^*[\mathcal{D}^{\theta}_{\mathrm{res}}]\int \psi^\theta_{n_{\mathrm{res}}}(\mathbf{r})\hat{O}_\theta\psi^\theta_{n_{\mathrm{res}}}(\mathbf{r})\mathrm{d}\mathbf{r}\,. \tag{6.158}$$

Note, however, that in the case that $\psi^\theta_{n_{\mathrm{res}}}$ are the resonance eigenfunctions of the complex scaled Floquet operator which describes the interaction of our system with a cw laser, then $\psi^\theta_{n_{\mathrm{res}}}$ are time-periodic functions with the period $T = 2\pi/\omega_{\mathrm{L}}$, where ω_L is the laser frequency and therefore the expectation values $\bar{O}$ are time-dependent even when the initial wavepacket populates mostly the lowest (i.e., long-living) resonance state (i.e., Eq. (6.158) becomes a time-periodic function).

The conclusion is that there is no contradiction between the c-product and the F-product. The F-product is an extension of the c-product which has been derived for eigenstates of non-Hermitian operators as an equivalent to the inner product which is used in the standard (Hermitian) formalism of quantum mechanics to wavepackets that are involved in time and are the solutions of the time-dependent Schrödinger equation (for time-independent Hamiltonians and also for time-dependent ones). In this exercise we compare two different possible extension of the c-product to wavepackets. One possibility is discussed in (b) and it is shown to be numerical unstable, whereas the second possibility which is referred to as the F-product (decay from a finite volume in space which can be as large as pleased) is discussed in (c) and is the preferable approach when the dynamics is controlled by the resonance states.

6.9 Further reading

Reviews

W. P. Reinhardt, Complex coordinates in the theory of atomic and molecular structure and dynamics, *Ann. Rev. Phys. Chem.* **33**, 223–255 (1982).

B. R. Junker, Recent computational developments in the use of complex scaling in resonance phenomena, *Adv. At. Mol. Phys.* **18**, 207–263 (1982).

Y. K. Ho, The method of complex coordinate rotation and its applications to atomic collision processes, *Phys. Rep. C* **99**, 1–68 (1983).

N. Moiseyev, Quantum theory of resonances: calculating energies, widths and cross-sections by complex scaling, *Phys. Rep.* **302**, 211–293 (1998).

I. Rotter, A non-Hermitian Hamilton operator and the physics of open quantum systems, *J. Phys. A* **42**, 153001–153051 (2009).

On completeness

J. von Neumann, *Mathematical Foundation of Quantum Mechanics*, Princeton, Princeton University Press, 1955.

R. G. Newton, Analytic properties of radial wave functions, *J. Math. Phys.* **1**, 319–347 (1960); *Scattering Theory of Waves and Particles*, New York, McGraw-Hill Book Co. Inc., 1966.

T. Berggren, On the use of resonant states in eigenfunction expansions of scattering and reaction amplitudes, *Nucl. Phys.* **109**, 265–278 (1968).

N. Michel, Direct demonstration of the completeness of the eigenstates of the Schrödinger equation with local and nonlocal potentials bearing a Coulomb tail, *J. Math. Phys.* **49**, 022109–022136 (2008).

7

The properties of the non-Hermitian Hamiltonian

The focus of this chapter is on the complex analogs to basic theorems and principles in the standard (Hermitian) formalism of quantum mechanics. These theorems are the basis for a formalism analogous to the standard (Hermitian) formalism of quantum mechanics. This will allow us to construct theoretical methods and tools similar to those used to solve problems in conventional quantum mechanics, and enable us to establish, for instance, a non-Hermitian time-independent scattering theory for time-independent Hamiltonians which is presented in Chapter 8. Moreover, on the basis of the theorems presented in this chapter, one can observe novel phenomena which are hard to predict or explain by using the standard formalism of quantum mechanics. This chapter sets the ground for the derivation of computational algorithms and their applications to different problems and to study different types of physical phenomenon.

7.1 The turn-over rule

As discussed in Chapter 4, the complex scaled Hamiltonian is defined by

$$\hat{H}_\theta = \hat{S}_\theta \hat{H} \hat{S}_\theta^{-1}\,, \tag{7.1}$$

where

$$\tilde{\Psi}(r_\theta) = \hat{S}_\theta \Psi(r) = \mathrm{e}^{\mathrm{i}\theta/2}\Psi(r\mathrm{e}^{\mathrm{i}\theta}) \tag{7.2}$$

and the complex scaled coordinate is given by

$$\rho_\theta = r\mathrm{e}^{\mathrm{i}\theta}\,. \tag{7.3}$$

Since

$$\hat{S}_\theta^{-1}\hat{S}_\theta = \hat{1}\,, \tag{7.4}$$

it is clear that

$$\hat{S}_\theta^{-1} = \hat{S}_{-\theta} = [\hat{S}_\theta]^* . \tag{7.5}$$

What is $\hat{S}_\theta^\dagger$? If $f(r)$ and $g(r)$ are two functions in the Hilbert space then

$$\int_{\text{all space}} f(r)\hat{S}_\theta^\dagger g(r)\mathrm{d}r = \int_{\text{all space}} g(r)[\hat{S}_\theta]^* f(r)\mathrm{d}r . \tag{7.6}$$

Therefore,

$$\begin{aligned}\int_{\text{all space}} f(r)\hat{S}_\theta^\dagger g(r)\mathrm{d}r &= \int_{\text{all space}} g(r)\mathrm{e}^{-\mathrm{i}\theta/2} f(r\mathrm{e}^{-\mathrm{i}\theta})\mathrm{d}r \\ &= \int_{\text{all space}} \mathrm{e}^{\mathrm{i}\theta/2} g(\rho_{-\theta}\mathrm{e}^{\mathrm{i}\theta}) f(\rho_{-\theta})\mathrm{d}\rho_{-\theta} .\end{aligned} \tag{7.7}$$

Since the functions in the Hilbert space are analytical functions we can change the contour of integration to be a real contour, $\rho_{-\theta} \to r$, and consequently,

$$\begin{aligned}\int_{\text{all space}} f(r)\hat{S}_\theta^\dagger g(r)\mathrm{d}r &= \int_{\text{all space}} \mathrm{e}^{\mathrm{i}\theta/2} g(r\mathrm{e}^{\mathrm{i}\theta}) f(r)\mathrm{d}r \\ &= \int_{\text{all space}} f(r)[\mathrm{e}^{\mathrm{i}\theta/2} g(r\mathrm{e}^{\mathrm{i}\theta})]\mathrm{d}r .\end{aligned} \tag{7.8}$$

Therefore,

$$\int_{\text{all space}} f(r)\hat{S}_\theta^\dagger g(r)\mathrm{d}r = \int_{\text{all space}} f(r)\hat{S}_\theta g(r)\mathrm{d}r . \tag{7.9}$$

Thus we have shown here that

$$\hat{S}_\theta^\dagger = \hat{S}_\theta , \tag{7.10}$$

and consequently (using Eq. (7.1)),

$$\hat{H}_\theta^\dagger = \hat{H}_{-\theta}. \tag{7.11}$$

The turn-over rule implies that for any two square integrable functions in the Hilbert space (which may be complex functions *regardless* of the complex scaling),

$$\int_{\text{all space}} g\hat{H}_\theta^\dagger f\mathrm{d}r = \int_{\text{all space}} f\hat{H}_\theta^* g\mathrm{d}r . \tag{7.12}$$

Using the Dirac notation Eq. (7.12) can be written as

$$\langle g^*|\hat{H}_\theta^\dagger|f\rangle = \langle f^*|\hat{H}_\theta^*|g\rangle . \tag{7.13}$$

When $\hat{H}_{\theta=0}$ is a real Hermitian operator, then for the case where $\theta \neq 0$, $\hat{H}^*_\theta = \hat{H}_{-\theta}$ and therefore (using Eq. (7.11)) one gets that

$$\langle g^* | \hat{H}_{-\theta} | f \rangle = \langle f^* | \hat{H}_{-\theta} | g \rangle \, . \tag{7.14}$$

By making the simple transformation $\theta \rightarrow -\theta$ one gets the turn-over rule for the complex scaled Hamiltonians which operate on functions in the Hilbert space,

$$\langle g^* | \hat{H}_{\theta} | f \rangle = \langle f^* | \hat{H}_{\theta} | g \rangle . \tag{7.15}$$

Note that in principle the functions f and g can also be eigenfunctions of any complex scaled Hamiltonian, provided that their asymptotes decay exponentially to zero. Specifically, they may be associated with the bound and/or resonance states of a complex scaled Hamiltonian. Moreover, one may choose g to be the complex conjugate of the resonance eigenfunction of a complex scaled Hamiltonian since its asymptote also decays exponentially to zero.

It is clear from the turn-over rule that for $\theta \neq 0$, unlike the situation in the Hermitian case, *the complex scaled Hamiltonian is not a self-adjoint operator*. We should stress again that in Eq. (7.15) the square integrable functions are in the Hilbert space and, for example, can be associated with the eigenfunctions of the Hermitian Hamiltonian using the box-quantization condition.

Exercise 7.1

Prove that non-degenerate states of a real Hermitian Hamiltonian are real functions. Also show that degenerate states can always be transformed to be real functions as well. What would be the properties of the matrix which represents the complex scaled Hamiltonian which is constructed from real basis functions?

7.2 The complex analog of the variational principle

The complex analog of the variational principle (the so-called c-variational method) provides the *formal justification for the use of computational techniques that originally were developed for bound states* in the calculation of the resonance position and widths by the complex coordinate method.

As discussed in Chapter 5, one can assume that the eigenfunctions of $\hat{\mathrm{H}}(\theta)$ form a complete c-normalizable set. The possibility of an incomplete spectrum is extensively discussed in Chapter 9. However, even in the case where the exact spectrum is incomplete due to round-off errors in numerical calculations, the spectrum turns to be a complete one. From now on in the discussions in this chapter we assume that the spectrum is complete.

$$\bar{E} = \frac{(\phi|\hat{\mathrm{H}}_\theta|\phi)}{(\phi|\phi)} \tag{7.16}$$

provides a stationary approximation to the true complex eigenvalue E_k when ϕ is a c-normalizable (i.e. $(\phi|\phi) = 1$) approximation that is close to the eigenfunction ψ_k of $\hat{\mathrm{H}}_\theta$. In other words

$$\phi = \psi_k + \partial(\epsilon) \quad \text{implies} \quad E = E_k + \partial(\epsilon^2)\,. \tag{7.17}$$

This complex *variational principle* is, however, a stationary principle rather than an upper or lower bound for either the real or imaginary part of the complex eigenvalue. As noted above, even this stationary property fails if the eigenfunctions are not c-normalizeable (i.e. c-normalization implies that $(\psi_k|\psi_k) \neq 0$ for any value of k).

7.2.1 Linear c-variational calculations

Let us expand the trial functions ϕ by N orthonormal basis functions, $\{\chi_i\}$; $i = 1, \ldots, N$,

$$|\phi) = \sum_{j=1}^{N} C_j^{\mathrm{R}} |\chi_j\rangle\,,$$

$$(\phi| = \sum_{i=1}^{N} C_i^{\mathrm{L}} \langle\chi_i|\,. \tag{7.18}$$

By substituting Eqs. (7.18) into Eq. (7.16) one obtains

$$\sum_{i,\,j} C_i^{\mathrm{L}} C_j^{\mathrm{R}} (H_{ij}(\theta) - \bar{E}\delta_{ij}) = 0\,, \tag{7.19}$$

where

$$H_{ij}(\theta) = \langle\chi_i|\hat{\mathrm{H}}_\theta|\chi_j\rangle\,. \tag{7.20}$$

On the basis of the c-variational principle given in Eqs. (7.16) and (7.17) we require that

$$\frac{\partial\bar{E}}{\partial C_i^{\mathrm{L}}} = 0 \quad \text{for} \quad i = 1,\, 2, \ldots, N\,. \tag{7.21}$$

Consequently,

$$\sum_{j=1}^{N} C_j^{\mathrm{R}} \left(H_{ij}(\theta) - \bar{E}\delta_{ij} \right) = 0 \,, \tag{7.22}$$

which can be recast in matrix form as

$$\mathbf{H}(\theta)\mathbf{C}^{\mathrm{R}} = \mathbf{C}^{\mathrm{R}}\bar{\mathbf{E}} \,, \tag{7.23}$$

where $\bar{\mathbf{E}}$ is a diagonal matrix. Here we proved that the solutions of the matrix eigenvalue problem in Eq. (7.23) are stationary solutions in the complex variational space, and as $N \to \infty$ the exact solution of the time-independent complex scaled Schrödinger equation would be obtained. This theorem sets the ground for c-variational calculations by which auto-ionization, predissociation and other types of resonance positions and widths can be obtained.

Exercise 7.2

This exercise is based on the Milfeld and Moiseyev application of the Lanczos algorithm to complex and symmetric Hamiltonian matrices.[1] Using N complex orthonormal basis functions the non-Hermitian Hamiltonian is represented by an N-dimensional *non*-symmetric matrix, $\mathbf{H}_\theta$. The eigenvalues of $\mathbf{H}_\theta$ are the complex variational solutions of our problem. Derive the Lanczos recursion equations by which $\mathbf{H}_\theta$ is transformed to a tri-diagonal matrix $\mathbf{T}_\theta$. Explain why the matrix $\mathbf{T}_\theta$ can always be made symmetric.

The c-variational principle has been derived here for a time-independent non-Hermitian Hamiltonian. The c-variational solutions can be used for the calculations of time-dependent expectation values when the initial state is a wavepacket which can be described as a linear combination of the variational solutions.

7.2.2 Non-linear variational approaches

We will focus here on two different types of non-linear variational calculation. The first type of non-linear c-variational calculation is associated with the use of non-orthogonal basis functions where in addition to the linear variational parameters, $\{\mathbf{C}\}$, a set of non-linear parameters, $\{\gamma\}$, are also optimized. The second type of non-linear variational calculation is considered when mean field approximations are applied. This usually occurs when self-consistent-field (SCF) methods are used to solve the set of pseudo-coupled variational equations.

---

[1] K. Milfeld and N. Moiseyev, Complex resonance eigenvalues by the Lanczos recursion method, *Chem. Phys. Lett.* **130**, 145 (1986).

Optimization of non-linear variational parameters

A simple example of the first type of non-linear variational calculation is the case where the trial function ϕ is defined similarly to Eqs. (7.18) as

$$|\phi) = \sum_{j=1}^{N} C_j^{\mathrm{R}} |\chi_j(\gamma_j)\rangle \,,$$

$$(\phi| = \sum_{j=1}^{N} C_j^{\mathrm{L}} \langle\chi_j(\gamma_j^*)| \,, \tag{7.24}$$

where $\{\gamma_j\}$ $j = 1, \ldots, N$ are the scaling parameters of the basis functions. These non-linear parameters might get complex values when the variational energy $\bar{E} = (\phi|\hat{H}|\phi)/(\phi|\phi)$ is optimized to satisfy the following secular equations:

$$\left[\mathbf{H}(\gamma) - \bar{E}(\gamma)\mathbf{S}(\gamma)\right] \mathbf{C}^{\mathrm{R}}(\gamma) = 0 \,, \tag{7.25}$$

$$\left[[\mathbf{H}(\gamma)]^{\mathrm{T}} - \bar{E}(\gamma)[\mathbf{S}(\gamma)]^{\mathrm{T}}\right] \mathbf{C}^{\mathrm{L}}(\gamma) = 0 \,, \tag{7.26}$$

where

$$[\mathbf{H}(\gamma)]_{i,j} = \langle\chi_i(\gamma_i^*)|\hat{H}|\chi_j(\gamma_j)\rangle \,,$$

$$[\mathbf{S}(\gamma)]_{i,j} = \langle\chi_i(\gamma_i^*)|\chi_j(\gamma_j)\rangle \tag{7.27}$$

and

$$\frac{\partial \bar{E}}{\partial \gamma_j} = 0 \;\; j = 1, \ldots, N \,. \tag{7.28}$$

The stationary solutions of Eq. (7.28) in complex variational space are associated with resonances. This is the generalized complex variational method as derived by Moiseyev.[2] A very special case is when one uses only a single non-linear variational scaling parameter such that $\gamma_j = \eta = \alpha e^{i\theta}$. The requirement for the potential to be an analytical function of the scaling parameter results from the fact that there is an equivalence between the dilation of the Hamiltonian and the scaling of the basis,

$$\frac{(\phi(\mathbf{r})|H(\mathbf{r}/\eta)|\phi(\mathbf{r}))_{\mathbf{r}}}{(\phi(\mathbf{r})|\phi(\mathbf{r}))_{\mathbf{r}}} = \frac{(\phi(\eta\mathbf{r})|H(\mathbf{r})|\phi(\eta\mathbf{r}))_{\mathbf{r}}}{(\phi(\eta\mathbf{r})|\phi(\eta\mathbf{r}))_{\mathbf{r}}} \,. \tag{7.29}$$

This equality holds for any complex value of η only when $H(\mathbf{r})$ is a dilation analytic operator. Therefore, in such a situation the generalized variational method is reduced to the linear c-variational method where one requires a stationary condition with respect to the variation of the rotation angle θ. Equation (7.29) can be

---

[2] N. Moiseyev, *Mol. Phys.* **47**, 585 (1982).

extended to the cases where several non-linear variational parameters are optimized when the potential is an analytical function. In such cases $\langle \chi_i(\gamma_i^*)|\hat{H}|\chi_j(\gamma_j)\rangle = \langle \chi_i(\alpha)|\hat{H}_\theta|\chi_j(\alpha)\rangle$.

What about the cases where the potentials are not dilation analytic operators? As discussed in Chapter 5, the complex scaling transformation is not applicable and one should use another method for calculating the resonances, such as the exterior scaling, smooth exterior methods, or carry out analytical continuation of the Hamiltonian matrix elements rather than dilation of the Hamiltonian. The generalized variational principle (in the non-linear variational approach) enables the calculation of resonances also for non-dilation analytic operators. See, for example, Ex. 5.15 or the use of this method for the calculation of energies and lifetimes of auto-ionization resonances of molecules within the framework of the Born–Oppenheimer approximation where the Coulombic electron–nuclear attraction potential is not an analytical function of the electronic coordinates.

Derivation of non-Hermitian mean field theory for Bose–Einstein condensates

The non-Hermitian mean field theory which leads to a non-Hermitian non-linear Schrödinger equation which can be solved by an iterative self-consistent-field method was formulated by Moiseyev and Cederbaum.[3]

Assuming a contact interaction between N atoms in a condensate, the full complex scaled Hamiltonian is given by

$$\left(-\frac{\hbar^2}{2M}\mathrm{e}^{-2\mathrm{i}\theta}\sum_{j=1}^{N}\nabla_j^2+\sum_{j=1}^{N}V_{\mathrm{ext}}(\mathrm{e}^{\mathrm{i}\theta}\mathbf{r}_j)+U_0\sum_{j=1}^{N}\sum_{j'\neq j}\delta_\theta(\mathbf{r}_j-\mathbf{r}_{\mathbf{j}'})\right)\Psi_\theta=\mathcal{E}\Psi_\theta \tag{7.30}$$

when the δ-function is taken as a Gaussian with vanishing width and its complex scaled version takes on the following appearance:

$$\delta_\theta(\mathbf{r}_j-\mathbf{r}_{j'})=\lim_{\sigma\to 0}\left(\frac{1}{\sigma\pi}\right)^{\frac{D}{2}}\mathrm{e}^{-\frac{\mathrm{e}^{\mathrm{i}2\theta}}{\sigma}(\mathbf{r}_j-\mathbf{r}_{j'})^2}. \tag{7.31}$$

$D = 1, 2, 3$ is the dimensionality of the BEC. Note that, in order to avoid the mathematical complications which result from the high singularity of a multi-dimensional δ-function, the limit of $\sigma \to 0$ is taken only after the application of the Hartree approximation which leads to the Gross–Pitaevskii (GP) non-linear equation. See, for example, the review of Pitaevskii and co-authors.[4] Equation (10.27)

---

[3] N. Moiseyev and L. S. Cederbaum, *Phys. Rev. A* **72**, 033605 (2005).

[4] F. Dalfovo, S. Giorgini and L. P. Pitaevskii, *Rev. Mod. Phys.* **71**, 463 (1999).

can be rewritten as

$$\delta_\theta(\mathbf{r}_j - \mathbf{r}_{j'}) = \mathrm{e}^{-\mathrm{i}\theta D} \lim_{\tilde{\sigma}\to 0} (\frac{1}{\tilde{\sigma}\pi})^{\frac{D}{2}} \mathrm{e}^{-\frac{(\mathbf{r}_j - \mathbf{r}_{j'})^2}{\tilde{\sigma}}} , \tag{7.32}$$

where

$$\tilde{\sigma} = \mathrm{e}^{-\mathrm{i}2\theta}\sigma \tag{7.33}$$

and

$$0 \le \theta < \frac{\pi}{4} . \tag{7.34}$$

The latter relation leads to $\mathrm{Re}(\tilde{\sigma}) > 0$. Here we have shown that under the constrains given in Eq. (7.34) the complex scaled δ_θ function is equal to

$$\delta_\theta(\mathbf{r}_j - \mathbf{r}_{j'}) = \mathrm{e}^{-\mathrm{i}\theta D}\delta(\mathbf{r}_j - \mathbf{r}_{j'}) . \tag{7.35}$$

The Hermitian (i.e. $\theta = 0$) GP non-linear equation is obtained from the full Hamiltonian of the system by assuming that all atoms occupy the same orbital. In analogy, a non-linear Schrödinger equation can be derived starting from the complex scaled full Hamiltonian in Eq. (7.30) by assuming that the *c-variational* solution is given by

$$\Psi_\theta(\mathbf{r}_1, \ldots, \mathbf{r}_j, \ldots, \mathbf{r}_N) = \prod_{j=1}^{N} \phi_\theta(\mathbf{r}_j) . \tag{7.36}$$

The complex variational solution of the time-independent Schrödinger equation implies that for $j = 1, 2, \ldots, N$,

$$\frac{\delta \mathcal{E}}{\delta \phi_\theta(\mathbf{r}_j)} = 0 . \tag{7.37}$$

Equation (7.37) is satisfied when for any value of $j = 1, 2, \ldots, N$,

$$\mathcal{H}_{\mathrm{eff}}(\mathbf{r}_j)\phi_\theta(\mathbf{r}_j) = \mu(N)\phi_\theta(\mathbf{r}_j) , \tag{7.38}$$

where

$$\mathcal{H}_{\mathrm{eff}}(\mathbf{r}_j) = -\frac{\hbar^2}{2M}\mathrm{e}^{-2\mathrm{i}\theta}\nabla_j^2 + V_{\mathrm{ext}}(\mathrm{e}^{\mathrm{i}\theta}\mathbf{r}_j) + V_{\mathrm{eff}}^{\theta}(\mathbf{r}_j) \tag{7.39}$$

and

$$\begin{aligned} V_{\mathrm{eff}}^{\theta}(\mathbf{r}_j) &= U_0(\Pi_{j'\neq j}\phi_\theta(\mathbf{r}_{j'})| \sum_{j'\neq j} \delta_\theta(\mathbf{r}_j - \mathbf{r}_{j'})|\Pi_{j'\neq j}\phi_\theta(\mathbf{r}_{j'})) \\ &= U_0(N-1)\mathrm{e}^{-\mathrm{i}\theta D}\phi_\theta^2(\mathbf{r}_j) . \end{aligned} \tag{7.40}$$

The chemical potential $\mu(N)$ is given by

$$\mu(N) = \mathcal{E} + \frac{U_0(N-1)}{2} e^{-i\theta D} \int \phi_\theta^4(\mathbf{r}_j) d\mathbf{r}_j \, . \tag{7.41}$$

Note that since all atoms occupy the *same* orbital ϕ_θ it is possible to drop the subscript j from the vector position of the j-th atom when the non-linear GP Schrödinger equation is solved.

The complex energy, $\mathcal{E}$, of the BEC is the expectation value,

$$\mathcal{E} = (\Psi_\theta | H_\theta | \Psi_\theta) \equiv \left\langle \Psi_\theta^* \right| H_\theta \left| \Psi_\theta \right\rangle \, . \tag{7.42}$$

Here we use the c-product rather the conventional scalar product since Ψ_θ is a complex function only due to the rotation of the internal coordinates of the Hamiltonian into the complex coordinate plane (see Chapter 4). $\mathcal{E}$ is associated with the complex chemical potential as follows:

$$\frac{\mathcal{E}}{N} \equiv E(N) - \frac{i}{2}\Gamma(N) = \mu(N) - \frac{U(N)}{2} e^{-i\theta D} \int \phi_\theta^4 d\mathbf{r} \, . \tag{7.43}$$

The complex chemical potential μ is defined by Eq. (7.38). The quantity $\mathcal{E}$ in Eq. (7.43) provides the GP complex mean-field energy of the condensate. Of course, this quantity is only an approximation to the exact energy in Eq. (7.30) which is associated with a complex eigenvalue of the full Hamiltonian (i.e. beyond the GP approximation).

Exercise 7.3

Explain why the complex scaled non-linear Schrödinger equation given in Eq. (7.38) differs from the direct application of the complex scaling transformation, $\mathbf{r} \to e^{iD\theta}\mathbf{r}$, to the D-dimensional GP equation which results in

$$\left(-\frac{\hbar^2}{2M} e^{-2i\theta} \nabla^2 + V_{\text{ext}}(e^{i\theta}\mathbf{r}) + U_0(N-1)\phi_\theta^2 \right) \phi_\theta = \mu(N)\phi_\theta \, . \tag{7.44}$$

The non-Hermitian mean field theory for fermions: the Hartree–Fock method

Let us first discuss the non-Hermitian mean field theory for a system of N electrons. The corresponding wavefunction is $\Psi(\mathbf{r}_1, \ldots, \mathbf{r}_N)$ with $\mathbf{r}_j \in \mathcal{R}^3$. According to the Pauli exclusion principle, $\Psi(\mathbf{r}_1, \ldots, \mathbf{r}_N)$ must switch its sign whenever an interchange of coordinates $\mathbf{r}_j \leftrightarrow \mathbf{r}_{j'}$ (and also an analogical interchange of spins) is made for any pair (j, j') of electrons. The simplest mean field wavefunction ansatz satisfying this basic anti-symmetry requirement is given by the so-called

Slater determinant,

$$\Psi_{\mathrm{HF}}(\mathbf{r}_1, \ldots, \mathbf{r}_N) = \mathcal{A} \prod_{j=1}^{N} \phi_j(\mathbf{r}_j)$$

$$= \frac{1}{\sqrt{N!}} \begin{vmatrix} \phi_1(\mathbf{r}_1) & \phi_2(\mathbf{r}_1) & \cdots & \phi_N(\mathbf{r}_1) \\ \phi_1(\mathbf{r}_2) & \phi_2(\mathbf{r}_2) & \cdots & \phi_N(\mathbf{r}_2) \\ \cdots & \cdots & \cdots & \cdots \\ \phi_1(\mathbf{r}_N) & \phi_2(\mathbf{r}_N) & \cdots & \phi_N(\mathbf{r}_N) \end{vmatrix} . \tag{7.45}$$

Here, the one-electron orbitals $\{\phi_j(\mathbf{r})\}_{j=1}^{N}$ are functions of the electron positions and their spins and therefore they are called spin-orbitals. Specifically, $\phi_j(\mathbf{r}) = \varphi_j(\mathbf{r})s_j$, where φ_j is a spatial function and s_j is a spin function α or β. The spin-orbitals are required to be linearly independent to guarantee that the determinant in Eq. (7.45) is non-zero. The symbol $\mathcal{A}$ stands for the anti-symmetrizer, which converts an ordinary product

$$\Phi_{\mathrm{HF}}(\mathbf{r}_1, \ldots, \mathbf{r}_N) = \prod_{j=1}^{N} \phi_j(\mathbf{r}_j) \tag{7.46}$$

into the corresponding determinant (Eq. (7.45)). Clearly,

$$\mathcal{A} = (1/\sqrt{N!}) \sum_{\wp} \varepsilon_{\wp} \, \wp \, , \tag{7.47}$$

where $\wp$ determines a particular permutation of spins and spatial variables $(\mathbf{r}_1, \ldots, \mathbf{r}_N)$, and $\varepsilon_{\wp}$ stands for parity of the permutation $\wp$ (equal to ±1 for even and odd permutations, respectively). We recall that the number of such distinct permutations equals $N!$.

Variational optimization of Eq. (7.45) forms the basis for the well-known Hartree–Fock–Roothaan method. Let us briefly describe the underlying theoretical formulation for the case when the studied N-electron system is either an atom or a quantum dot described by a scaled Hamiltonian

$$\hat{H}_{\eta} = \sum_{j=1}^{N} \left(-\frac{\hbar^2}{2m_e} \eta^{-2} \nabla_j^2 + V(\eta \mathbf{r}_j) \right) + \sum_{j<j'} \frac{e^2 \eta^{-1}}{|\mathbf{r}_j - \mathbf{r}_{j'}|} . \tag{7.48}$$

where η represents for now a real scaling parameter. For an atom or ion $V(\mathbf{r}_j \eta) = -\eta^{-1} e^2 \mathcal{Z}/|\mathbf{r}_j|$, where $e\mathcal{Z}$ is the positive charge of the nucleus. For a molecular system or an array of multiple center quantum dots the scaled Hamiltonian is given by

$$\hat{H}_\eta = \sum_{j=1}^{N}\left(-\frac{\hbar^2}{2m_e}\eta^{-2}\nabla_j^2 + \sum_{\alpha=1}^{M} V_\alpha(\mathbf{r}_j\eta)\right) + \sum_{j<j'}\frac{e^2\eta^{-1}}{|\mathbf{r}_j-\mathbf{r}_{j'}|} + \sum_{\alpha>\alpha'} V_{\alpha,\alpha'}^{\mathrm{MOL}}\,, \tag{7.49}$$

where $V_{\alpha,\alpha'}^{\mathrm{MOL}} = 0$ for quantum dots and $V_{\alpha,\alpha'}^{\mathrm{MOL}} = +e^2\mathcal{Z}_\alpha\mathcal{Z}_{\alpha'}/|\mathbf{R}_\alpha - \mathbf{R}_{\alpha'}|$ for molecules, where $e\{\mathcal{Z}_\alpha\}_{\alpha=1}^{M}$ are the charges of the M nuclei in the molecule. For molecules $V_\alpha(\mathbf{r}_j\eta) = -e^2\mathcal{Z}_\alpha/|\eta\mathbf{r}_j - \mathbf{R}_\alpha|$.

An implementation of the variational method is similar in spirit to the bosonic theory treated in the previous section. Again, we shall search for a stationary point of the energy functional, which is given by the standard formula

$$\overline{E}[\Psi_{\mathrm{HF}}] = \frac{\langle\Psi_{\mathrm{HF}}|\hat{H}_\eta|\Psi_{\mathrm{HF}}\rangle}{\langle\Psi_{\mathrm{HF}}|\Psi_{\mathrm{HF}}\rangle}\,. \tag{7.50}$$

For the sake of clarity, we recall in this context that we use the Hermitian scalar product since the scaling factor is treated as a real parameter. We also note in passing that not only the spatial coordinates, but also the discrete spin variables of the electrons are integrated over.

Importantly, the Hamiltonian in Eq. (7.48) treats all the electrons on a symmetric equal footing, hence $\hat{H}_\eta\,\mathcal{A}\,\Phi_{\mathrm{HF}} = \mathcal{A}\,\hat{H}_\eta\,\Phi_{\mathrm{HF}}$. Moreover, for any two square integrable N-electron functions $\psi_1(\mathbf{r}_1,\ldots,\mathbf{r}_N)$ and $\psi_2(\mathbf{r}_1,\ldots,\mathbf{r}_N)$, be they permutationally anti-symmetric or not, one has $\langle\mathcal{A}\psi_1|\mathcal{A}\psi_2\rangle = \langle\psi_1|\mathcal{A}\psi_2\rangle$. The just-mentioned properties may be exploited to express the energy functional (7.50) as

$$\overline{E}[\Psi_{\mathrm{HF}}] = \frac{\langle\mathcal{A}\Phi_{\mathrm{HF}}|\hat{H}_\eta|\mathcal{A}\Phi_{\mathrm{HF}}\rangle}{\langle\mathcal{A}\Phi_{\mathrm{HF}}|\mathcal{A}\Phi_{\mathrm{HF}}\rangle} = \frac{\langle\Phi_{\mathrm{HF}}|\hat{H}_\eta|\mathcal{A}\Phi_{\mathrm{HF}}\rangle}{\langle\Phi_{\mathrm{HF}}|\mathcal{A}\Phi_{\mathrm{HF}}\rangle}\,. \tag{7.51}$$

Consequently, one may substitute Eq. (7.46) and express $\overline{E}[\Psi_{\mathrm{HF}}]$ directly in terms of the one-electron spin-orbitals.

After this is done, we are ready to carry out the variational optimization of $\overline{E}[\Psi_{\mathrm{HF}}]$. Specifically, we wish to find such linearly independent spin-orbitals $\{\phi_j(\mathbf{r})\}_{j=1}^{N}$ for which the energy functional $\overline{E}[\Psi_{\mathrm{HF}}]$ is stable relative to infinitesimal changes $\phi_j(\mathbf{r}) \to \phi_j(\mathbf{r}) + \delta\phi_j(\mathbf{r})$. Let us expand the spatial orbital functions in a square integrable one-electron basis set, $\{\chi_k(\mathbf{r})\}_{k=1}^{N_{\mathrm{b}}}$ such that the $j = 1, 2, \ldots, N$ spin-orbitals are given by

$$\phi_j(\mathbf{r};\eta) = \sum_{k=1}^{N_{\mathrm{b}}} c_{k,j}(\eta)\chi_k(\mathbf{r})s_j\,. \tag{7.52}$$

By substituting Eq. (7.52) into Eq. (7.46) and afterwards into Eq. (7.51), the energy functional is converted into an ordinary function of variables $\{c_{k,j};\ k = 1,\ldots,N_{\mathrm{b}};\ j = 1,\ldots,N\}$.

The optimized variational coefficients are obtained by solving the following set of coupled equations:

$$\left[\frac{\partial \overline{E}_{\mathrm{HF}}(\mathbf{c})}{\partial c_{k,j}}\right]_{\mathbf{c}^{\mathrm{opt}}} = 0\,, \tag{7.53}$$

where $j = 1,\ldots,N$ and $k = 1,\ldots,N_{\mathrm{b}}$. The coefficients for which the set of the coupled equations presented in Eq. (7.53) are satisfied are functions of the scaling parameter η. Therefore the Hartree–Fock orbitals and the variational energy are also functions of the scaling parameter η.

Here we come to a delicate point in our derivation. So far η was treated as a real parameter. When the Hamiltonian matrix elements are analytical functions of η (e.g. when one uses the Gaussian basis functions) we can carry out an analytical continuation of the energy functional as defined in Eq. (7.51) into the complex plane by making a substitution $\eta \to |\eta|\mathrm{e}^{\mathrm{i}\theta}$. In the case of atoms or single center quantum dots, such an analytical continuation is equivalent to the basis set representation of the energy functional of the complex scaled Hamiltonian. However, for molecules the electron–nuclei attractive potential energy operators are not dilation analytic operators and therefore the molecular Hamiltonian can not be scaled by a complex factor. The "trick" we use here is to scale the molecular Hamiltonian matrix elements as explained above rather than the Hamiltonian itself. The resonances are the stationary solutions in the non-linear complex variational space for which

$$\begin{aligned}\left[\frac{\partial \overline{E}_{\mathrm{HF}}(\mathbf{c}(\eta))}{\partial |\eta|}\right]_{\eta=\eta_{\mathrm{opt}}} &= 0\,,\\ \left[\frac{\partial \overline{E}_{\mathrm{HF}}(\mathbf{c}(\eta))}{\partial \theta}\right]_{\eta=\eta_{\mathrm{opt}}} &= 0\,,\end{aligned} \tag{7.54}$$

where $\eta_{\mathrm{opt}} = |\eta_{\mathrm{opt}}|\mathrm{e}^{\mathrm{i}\theta_{\mathrm{opt}}}$.

We address the reader to Section 5.5 where we describe in more detail how resonances can be calculated by carrying out analytical continuation of the Hamiltonian matrix elements into the complex plane.

The requirement of linear independence of the spin-orbitals is usually incorporated by imposing a set of orthonormality constraints,

$$(\phi_j|\phi_{j'}) = \delta_{jj'}\,. \tag{7.55}$$

We note in this context that the rows or columns of any Slater determinant (Eq. (7.45)) can be linearly combined without affecting the overall outcome Ψ_{HF}. Hence, the orthonormality constraints in Eq. (7.55) can always be assumed to apply for any Hartree–Fock ansatz Ψ_{HF}, without loss of generality. Due to the presence of the aforementioned constraints, the problem of stationarity of $\overline{E}[\Psi_{\mathrm{HF}}]$ becomes more involved, and must be treated using the method of Lagrange multipliers. However, in order to simplify the representation of the non-Hermitian mean field theory for fermions we take here another approach where we do not use the method of Lagrange multipliers.[5] Let us briefly explain this non-traditional approach. We assume that at the beginning of the calculation we have an initial guess for all the coefficients $c_{k,j}$ appearing in Eq. (7.52) for $j = 1, 2, \ldots, N$. We wish to systematically correct this initial guess in an iterative fashion. Consider an iteration aimed at improving a given orbital j (where j can be any one of the N spin-orbitals). We substitute the basis set expansion in Eq. (7.52) of this particular spin orbital j (and not for other spin-orbitals $j' \neq j$) into Eq. (7.51). After straightforward manipulations one arrives at a set of coupled equations,

$$\sum_{k'=1}^{N_{\mathrm{b}}} c_{k',j}(\eta) \sum_{k=1}^{N_{\mathrm{b}}} c_{k,j}(\eta) \left(H^{(j)}_{k',k}(\eta) - \bar{E}_{\mathrm{HF}}(\eta) S^{(j)}_{k',k}(\eta) \right) = 0\,. \tag{7.56}$$

Here,

$$H^{(j)}_{k',k}(\eta) = \left[\left(\Phi^{(j)}_{k'}(\eta) \middle| \hat{H}_\eta \middle| \mathcal{A}\Phi^{(j)}_{k}(\eta) \right) \right]_{\eta=|\eta|\mathrm{e}^{\mathrm{i}\theta}}\,, \tag{7.57}$$

$$S^{(j)}_{k',k}(\eta) = \left[\left(\Phi^{(j)}_{k'}(\eta) \middle| \mathcal{A}\Phi^{(j)}_{k}(\eta) \right) \right]_{\eta=|\eta|\mathrm{e}^{\mathrm{i}\theta}}\,, \tag{7.58}$$

where

$$\Phi^{(j)}_{k}(\mathbf{r}_1, \ldots, \mathbf{r}_N\,;\,\eta) = \prod_{i=1}^{j-1} \phi_i(\mathbf{r}_i, \eta)[\chi_k(\mathbf{r}_j) s_j] \prod_{i=j+1}^{N} \phi_i(\mathbf{r}_i, \eta)\,. \tag{7.59}$$

Next, we take a derivative of Eq. (7.56) with respect to $c_{k',j}$ (k' fixed but arbitrary), and consequently incorporate the variational requirement of Eq. (7.53). This yields a set of coupled secular equations,

$$\sum_{k=1}^{N_{\mathrm{b}}} c_{k,j}(\eta) \left(H^{(j)}_{k',k}(\eta) - \bar{E}_{\mathrm{HF}}(\eta) S^{(j)}_{k',k}(\eta) \right) = 0\,; \quad k' = 1, \ldots, N_{\mathrm{b}}\,, \tag{7.60}$$

---

[5] N. Moiseyev and J. Katriel, The continuity dilemma and Hartree–Fock instabilities. *Chem. Phys. Lett.* **29**, 69 (1974).

which can be summarized in a matrix form as

$$\left[\mathbf{H}^{(j)}(\eta) - \bar{E}_{\mathrm{HF}}(\eta)\mathbf{S}^{(j)}(\eta)\right]\mathbf{c}_j(\eta) = 0\,. \tag{7.61}$$

This equation should be solved numerically in order to get an improved guess for the considered spin-orbital j. After this is done, we proceed along similar lines further and correct iteratively all the other spin-orbitals. This procedure is repeated until convergence is achieved.

So far we did not specify which particular eigensolution of Eq. (7.61) should be taken as an outcome of a given iteration. For the sake of simplicity let us explain this point for the case when one wishes to calculate the lowest lying electronic state (which can be either a bound state or a resonance). The complex eigenvalues obtained in each of the diagonalizations, $\{\bar{E}_\nu^{\mathrm{HF}}(\eta)\}_{\nu=1}^{N}$ are ordered such that $|\bar{E}_1^{\mathrm{HF}}(\eta)| \leq |\bar{E}_2^{\mathrm{HF}}(\eta)| \leq |\bar{E}_3^{\mathrm{HF}}(\eta)| \leq \cdots \leq |\bar{E}_N^{\mathrm{HF}}(\eta)|$. The approach is based upon the requirement that each spin orbital may accommodate either one electron or two electrons with opposite spins.

Therefore, if we order the eigenvalues obtained by solving the general eigenvalue problems given in Eq. (7.61) from the highest to the highest absolute value of the eigenvalues then the $j = 1, 3, \ldots = 2\nu - 1; \nu = 1, 2, 3 \ldots$ orbitals are obtained by solving the following eigenvalue problems:

$$\left[\mathbf{H}^{(j=2\nu-1)}(\eta) - \bar{E}_\nu^{\mathrm{HF}}(\eta)\mathbf{S}^{(j)}(\eta)\right]\mathbf{c}_{j,\nu}(\eta) = 0\,; \tag{7.62}$$

and similarly the $\{\phi_j\,; j = 2, 4, \ldots = 2\nu; \nu = 1, 2, 3, \ldots\}$ orbitals are associated with the solutions of the set of general eigenvalue problems given by

$$\left[\mathbf{H}^{(j=2\nu)}(\eta) - \bar{E}_\nu^{\mathrm{HF}}(\eta)\mathbf{S}^{(j)}(\eta)\right]\mathbf{c}_{j,\nu}(\eta) = 0\,. \tag{7.63}$$

For example, the most inner spatial orbital $\varphi_{j=1}$ is associated with the eigenvector $\mathbf{c}_{j,\nu=1}(\eta)$, where $j = 1$ (spin α) and also $j = 2$(spin β). Generally speaking, the $\{\varphi_{j=2\nu-1}; \nu = 1, 2, \ldots\}$ and the $\{\varphi_{j=2\nu}; \alpha = 1, 2, \ldots\}$ spin-orbitals are associated with the ν lowest absolute values of the complex eigenvalues. Note that upon convergence

$$\epsilon_{\mathrm{HF}} - \frac{\mathrm{i}}{2}\Gamma_{\mathrm{HF}} \equiv \bar{E}_1^{\mathrm{HF}}(\eta) = \bar{E}_2^{\mathrm{HF}}(\eta) = \cdots = \bar{E}_\nu^{\mathrm{HF}}(\eta) = \cdots \tag{7.64}$$

The resonance width as obtained within the framework of the non-Hermitian mean field theory, Γ_{HF}, is expected to be a good approximation to the exact value when the resonances are shape-type resonances (as for example in N_2^-) and less accurate when they are Feshbach-type resonances (as for example in He $(2s)^2$).

Exercise 7.4

Derive the set of coupled equations that provide the solution for the singlet and triplet spin adapted resonance functions for a two-electron system within the framework of the non-Hermitian mean field theory. Explain why in this case the energies and lifetimes of auto-ionization, Auger and ICD type resonances can be calculated.

7.3 The complex analogs of the virial and hypervirial theorem

From the turn-over rule for the complex-scaled Hamiltonian, it follows immediately that commutators of $\hat{\mathrm{H}}_\theta$ and any given operator $\hat{\Lambda}$ have vanishing c-expectation values in any eigenstate ψ_k,

$$\big(\psi_k|\big[\hat{\mathrm{H}}_\theta,\ \hat{\Lambda}\big]|\psi_k\big) = 0\,. \tag{7.65}$$

This complex analog of the *hypervirial theorem* holds for a wide class of operators $\hat{\Lambda}$, whether Hermitian or not. In particular, if $\hat{\Lambda}$ is chosen to be $\mathbf{r} \cdot \nabla$ (or a sum of such terms in a many-particle system), and if the potential V is a homogeneous function of coordinates of degree m, Eq. (7.65) reduces to the complex *virial theorem* where $\hat{\mathrm{T}}_\theta$ is the scaled kinetic energy operator,

$$\big(\psi_k|\hat{\mathrm{T}}_\theta|\psi_k\big) = \frac{m}{2}\big(\psi_k|\hat{\mathrm{V}}_\theta|\psi_k\big)\,. \tag{7.66}$$

Thus we have a relation between the average (complex) kinetic and potential energies.

Exercise 7.5

Consider the scattering of particles by a central field potential, $V(r)$. The l-th partial wave satisfies

$$\int_0^\infty \psi_{l,k}(r)\,[2V(r) + r\mathrm{d}V/\mathrm{d}r]\,\psi_{l,k}(r)\mathrm{d}r = E\frac{\mathrm{d}\eta_l}{\mathrm{d}k}\,, \tag{7.67}$$

where $E = k^2/2$ is the eigenvalue of the radial Schrödinger equation and η_l is the corresponding phase shift. Derive the bound, virtual and resonance states on the basis of the virial theorem for the l-th partial wave. A delicate point here lies in the fact that in our derivation for the virial theorem for the poles of the scattering matrix we do not take the complex conjugate of the scattering function, assuming that it is a real function for real values of E.

7.4 The complex analog of the Hellmann–Feynman theorem

In quantum mechanics, the Hellmann–Feynman theorem relates the derivative of the total energy with respect to a given parameter to the expectation value of the derivative of the Hamiltonian with respect to that same parameter. That is,

$$\frac{\mathrm{d}E}{\mathrm{d}\lambda} = \langle \Psi(\lambda)|\frac{\partial \hat{H}}{\partial \lambda}|\Psi(\lambda)\rangle\,, \tag{7.68}$$

where $\Psi(\lambda)$ is the normalized eigenfunction of the Hamiltonian and λ is a parameter in the Hamiltonian (e.g., a potential parameter or a mass of one of the particles).

The proof is extended below for a non-Hermitian Hamiltonian and shows that the Hellmann–Feynman theorem holds (both for Hermitian and non-Hermitian Hamiltonians) either for the eigenfunctions of the Hamiltonian or for the linear variational solutions. Suppose a trial function Φ depends on a set of variational parameters $\{C_i\}$. Variationally optimal values of these parameters must satisfy the relation

$$\frac{\partial \bar{E}}{\partial C_i} = 0, \quad i = 1,\, 2, \ldots, N\,, \tag{7.69}$$

where

$$\bar{E} = \frac{(\Phi|\hat{\mathrm{H}}_\theta|\Phi)}{(\Phi|\Phi)} \tag{7.70}$$

and H_θ contains an embedded parameter ζ,

$$H_\theta = H_\theta(\zeta)\,. \tag{7.71}$$

For example, ζ can be the scaling factor, $\eta = \mathrm{e}^{\mathrm{i}\theta}$, or a physical parameter such as a nuclear charge, intra-molecular distance in the Born–Oppenheimer Hamiltonian, etc. However, for c-normalized Φ (i.e. $(\Phi|\Phi) = 1$),

$$\frac{\mathrm{d}\bar{E}}{\mathrm{d}\zeta} = \left(\Phi|\frac{\partial H_\theta}{\partial \zeta}|\Phi\right) + \sum_{j=1}^{M}\left(\frac{\partial \bar{E}}{\partial C_j}\right)\left(\frac{\partial C_j}{\partial \zeta}\right)\,. \tag{7.72}$$

Thus, if Φ is variationally optimal for any given value of ζ, Eq. (7.69) is satisfied and therefore Eq. (7.72) reduces to

$$\frac{\mathrm{d}\bar{E}}{\mathrm{d}\zeta} = \left(\Phi|\frac{\partial H_\theta}{\partial \zeta}|\Phi\right)\,. \tag{7.73}$$

Equation (7.73) is the complex form of the Hellmann–Feynman theorem. When $\zeta = \mathrm{e}^{\mathrm{i}\theta}$ the requirement of $\mathrm{d}\bar{E}/\mathrm{d}\theta = 0$ (the resonance solution satisfies this condition following the Balslev–Combes theorem) leads to another derivation of the virial theorem in Eq. (7.66). Within the framework of the finite basis set approximation ($\{C_i\}$ are the linear variational parameters) the resonance stationary condition

$$\left.\frac{\mathrm{d}\bar{E}}{\mathrm{d}\theta}\right|_{\theta_{\mathrm{opt}}} = 0 \tag{7.74}$$

($\zeta \equiv \theta$ in Eq. 7.73) leads to an iterative procedure for calculating the resonances.

In order to describe the iterative procedure for calculating the resonances by the Hellmann–Feynman theorem let us first assume without loss of generality that the non-Hermitian Hamiltonian is given by

$$\mathbf{H}_\theta = \mathrm{e}^{-2\mathrm{i}\theta}\mathbf{T} + \mathbf{V}_\theta; \quad [\mathbf{H}_\theta]_{ij} = \langle \chi_i | \hat{H}(\mathbf{r}\mathrm{e}^{\mathrm{i}\theta}) | \chi_j \rangle \,, \tag{7.75}$$

where $\{\chi_j\}$ are orthonormal basis functions and the resonances are associated with specific eigenvalues of the complex scaled Hamiltonian matrix (or of its transpose),

$$\begin{aligned} \mathbf{H}_\theta \mathbf{C}_k^{\mathrm{R}} &= \bar{E}_k \mathbf{C}_k^{\mathrm{R}} \,, \\ \mathbf{H}_\theta^{\mathrm{T}} \mathbf{C}_k^{\mathrm{L}} &= \bar{E}_k \mathbf{C}_k^{\mathrm{L}} \,. \end{aligned} \tag{7.76}$$

On the basis of the complex analog of the Hellmann–Feynman theorem we proved above one gets that

$$\mathrm{e}^{-2\mathrm{i}\theta} = \frac{\left(\mathbf{C}_k^{\mathrm{L}}\right)^{\mathrm{T}} \dfrac{\partial \mathbf{V}_\theta}{\partial \theta} \mathbf{C}_k^{\mathrm{R}}}{2\mathrm{i} \left(\mathbf{C}_k^{\mathrm{L}}\right)^{\mathrm{T}} \mathbf{T} \mathbf{C}_k^{\mathrm{R}}} \,. \tag{7.77}$$

Note that following the Cauchy–Riemann conditions the θ_{opt} for which Eqs. (7.73)–(7.77) are satisfied will usually be complex The imaginary part of (θ_{opt}) can be either negative or positive, that is, the absolute value of the complex scaling parameter, $\eta = \mathrm{e}^{\mathrm{i}\theta_{\mathrm{opt}}}$, can be either smaller or larger than unity. For atomic Coulombic potentials Eq. (7.73) reduces to the c-virial theorem. This iterative algorithm enables the calculations of energies and lifetimes of resonances. In some cases, as in the calculations of molecular auto-ionization within the framework of the Born–Oppenheimer approximation, numerical difficulties can be avoided by enabling θ to be complex (see the solution of Ex. 5.15).

7.5 Cusps and θ-trajectories

A graphical method of solving Eq. 7.72 is known as θ-trajectory. In this method $\bar{E}(\theta)$ is plotted as function of Re(θ), holding Im(θ) fixed. The stationary points along the trajectories which provide the *minimal* (not necessarily zero value) of $|\mathrm{d}\bar{E}/\mathrm{d}\theta|$ give us estimates for the resonance positions and widths. As proved by

Moiseyev, Friedland and Certain,[6] the stationary solutions where $\mathrm{d}\bar{E}/\mathrm{d}\theta = 0$ at $\theta = \theta_0$ are associated with a cusp in the θ-trajectory plot. This can be shown by considering the neighborhood of a stationary point of the complex energy, $\bar{E}$, where it can be expanded in powers of $(\eta - \eta_0)^\mu$ (Puiseux expansion). The first two terms are

$$\bar{E} = E_0 + a(\eta - \eta_0)^\mu + \cdots \,, \tag{7.78}$$

where

$$\begin{aligned} \eta &= \mathrm{e}^{\mathrm{i}\theta} = \alpha \mathrm{e}^{\mathrm{i}\theta_\mathrm{R}}\,; &\quad \eta_0 &= \mathrm{e}^{\mathrm{i}\theta_0} = \alpha_0 \mathrm{e}^{\mathrm{i}\theta_\mathrm{R}^{(0)}}\,; \\ \theta &= \theta_\mathrm{R} + \mathrm{i}\theta_\mathrm{I}\,; &\quad \theta_0 &= \theta_\mathrm{R}^{(0)} + \mathrm{i}\theta_\mathrm{I}^{(0)}\,; \\ \alpha &= \mathrm{e}^{-\theta_\mathrm{I}}\,; &\quad \alpha_0 &= \mathrm{e}^{-\theta_\mathrm{I}^{(0)}} \end{aligned} \tag{7.79}$$

and μ is a positive rational number. For small enough $(\eta - \eta_0)$ along the θ-trajectory,

$$\eta = \alpha_0 \mathrm{e}^{\mathrm{i}\theta_\mathrm{R}} \tag{7.80}$$

and therefore we can write

$$\eta - \eta_0 = \mathrm{i}\eta_0 x \,, \tag{7.81}$$

where

$$x = \theta_\mathrm{R} - \theta_\mathrm{R}^{(0)} \,. \tag{7.82}$$

Consequently, for $x \geq 0$ (i.e. approaching the cusp from "above")

$$\bar{E}_+ = E_0 + a(\mathrm{i}\eta_0)^\mu |x|^\mu + \cdots \,, \tag{7.83}$$

while for $x \leq 0$ (i.e. approaching the cusp from "below")

$$x = -|x| = |x|\mathrm{e}^{\mathrm{i}\pi} \tag{7.84}$$

and

$$\bar{E}_- = E_0 + a(\mathrm{i}\eta_0)^\mu |x|^\mu \mathrm{e}^{\mathrm{i}\pi\mu} \ldots \tag{7.85}$$

Thus, one observes that a cusp exists between the two branches $\bar{E}_+$ and $\bar{E}_-$ at the stationary point, $\theta = \theta_0$, with a cusp angle $\pi\mu$. A smooth curve (cusp angle $= \pi$) will be observed at the stationary point when μ is an odd integer (3, 5, 7, ...).

A schematic representation of such an example is given in Fig. 7.1(a), where we see that the θ_R-trajectory "slows down" at the stationary point, but no cusp is apparent. It should be remembered, however, that the θ_R-trajectories for non-optimum $|\eta_0|$ (i.e. non-optimal value of $\mathrm{Im}(\theta_0)$) are also smooth. A zero cusp angle

---

[6] N. Moiseyev, S. Friedland and P. R. Certain, *J. Chem. Phys.* **74**, 4739 (1981).

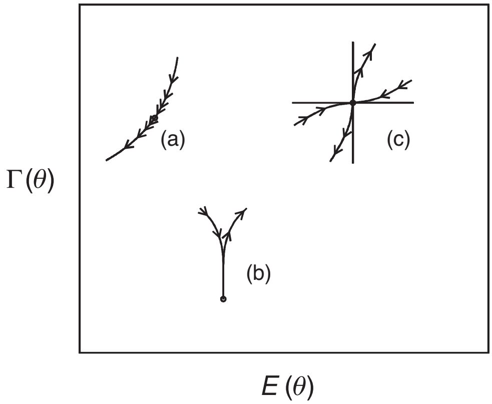

Figure 7.1 θ_{R} trajectory when α is held fixed at $\alpha = \alpha_0$. The arrows show the motion of complex "energies" as θ is varied. The open circles denote the stationary solutions which are obtained for $\eta = \theta_{\mathrm{R}} = \theta_{\mathrm{R}}^{(0)}$, see Eqs. (7.78)–(7.80), (a) $\mu = 3, 5, 7, \ldots$ (b) $\mu = 2, 4, 6, \ldots$ (c) $\mu = \frac{3}{2}, \frac{7}{2}, \ldots$

will be observed at the stationary point when μ is an even integer $(2, 4, 6, \ldots)$. This case, which is shown schematically in Fig. 7.1(b), is the most common case.

An interesting case occurs for rational $\mu = n/m > 1$, where n and m are prime numbers, since here the cusp angle is neither zero nor π. A fractional π angle in the cusp is the result of the coalescence of at least m eigenvalues (and also their corresponding eigenvectors!) of the complex Hamiltonian **matrix** at the stationary point $\theta = \theta_0$. As discussed in Chapter 9, $\bar{E}(\theta_0)$ in such a case is a defective eigenvalue (so-called exceptional point in the spectrum of the complex scaled Hamiltonian). This case, which is shown schematically in Fig. 7.1(c), for $\mu = 3/2$, apparently has not been observed so far in resonance calculations. Presumably, this is due to the very special conditions at which a defective eigenvalue is obtained.

These cusp conditions can be generalized for other cases where stationary solutions of complex variables are calculated. After all, any physical measurable quantity should be θ-independent! For example, when one uses complex absorbing potentials (even non-formally justified ones) for calculating resonances the resonance energy should be associated with the stationary solutions in the potential's parameter space. Another example is the calculation of the optimal scattering transition probability amplitude, $T_{\mathrm{scatt}}(\theta)$.[7] The optimal condition

$$\left.\frac{\partial T_{\mathrm{scatt}}}{\partial \theta}\right|_{\theta_{\mathrm{opt}}} = 0 \tag{7.86}$$

---

[7] U. Peskin and N. Moiseyev, *J. Chem. Phys.* **97**, 6443 (1992).

has been found to be the key point in the successful application of the complex-coordinate scattering theory (see Chapter 8) to long-range potentials.

7.6 Upper and lower bounds of the resonance positions and widths

One of the most important results of the linear variational principle in the standard formalism of quantum mechanics is that the n-th eigenvalue of the Hamiltonian matrix (when they are ordered from the smallest value to the largest one) is an upper bound to the exact eigenvalue. When the Hamiltonian is non-Hermitian and the eigenvalues are complex numbers the conventional theorems for upper and lower bounds of the energy levels are not applicable. The c-variational principle presented above is a stationary principle rather than an upper or lower bound for either the real or imaginary part of the complex eigenvalue. In this section, however, we will show how one can calculate upper and lower bounds of the real and imaginary parts of the complex eigenvalues of the non-Hermitian Hamiltonian from the calculations of complex expectation values of the non-Hermitian Hamiltonian. In the following derivation we will outline regions in the complex energy plane where the exact complex eigenvalues lie based on the Hermitian representation of the solutions of the non-Hermitian time-independent Schrödinger equation.

7.6.1 The Hermitian representation of the solutions of the non-Hermitian time-independent Schrödinger equation

Even though the complex coordinate method (as well as other methods discussed in this book) involves the solution of the Schrödinger equation with a non-Hermitian Hamiltonian, one can still represent the problem in Hermitian form and show that[8]

$$|E_{\mathrm{ex}} - \bar{E}| \geq \lambda \,, \tag{7.87}$$

where E_{ex} is the exact eigenvalue, $\bar{E}$ is the variational energy and λ^2 is the lowest real and positive eigenvalue of the complex, yet Hermitian, operator $\hat{\mathcal{H}}^2$, given by

$$\mathcal{H}^2(\bar{E},\ \bar{E}^*)\Phi = \lambda^2\Phi \,, \tag{7.88}$$

$$\mathcal{H}^2 \equiv \left(\hat{H}_\theta - \bar{E}\right)^* \left(\hat{H}_\theta - \bar{E}\right) \tag{7.89}$$

and

$$\bar{E} \equiv \bar{\epsilon} - \frac{\mathrm{i}}{2}\bar{\Gamma} \,. \tag{7.90}$$

---

[8] N. Moiseyev, *J. Chem. Phys.* (Lett.) **99**, 364 (1983).

Here $\hat{H}_\theta$ stands for any non-Hermitian Hamiltonian and not necessarily for the complex scaled Hamiltonian (the subscript θ is used here as a symbolic notation for "non-Hermitian").

Proof of Eq. (7.87) $|E_{\mathrm{ex}} - \bar{E}| \geq \lambda$ The exact resonance eigenfunction ψ_{ex} and the its energy E_{ex} satisfy the following eigenvalue problem for $\hat{H}_\theta$,

$$\hat{H}_\theta \psi_{\mathrm{ex}} = E_{\mathrm{ex}} \psi_{\mathrm{ex}} \,. \tag{7.91}$$

$\mathcal{H}^2(\bar{E},\ \bar{E}^*)$ is a Hermitian operator and λ^2 is its lowest, real, and positive eigenvalue. Therefore, following the conventional variational principle,

$$\frac{\langle \psi_{\mathrm{ex}} | \mathcal{H}^2(\bar{E},\ \bar{E}^*) | \psi_{\mathrm{ex}} \rangle}{\langle \psi_{\mathrm{ex}} | \psi_{\mathrm{ex}} \rangle} \geq \lambda^2 \,. \tag{7.92}$$

Since

$$\langle \psi_{\mathrm{ex}} | \mathcal{H}^2 | \psi_{\mathrm{ex}} \rangle = \langle \chi | \chi \rangle, \tag{7.93}$$

where

$$\chi = \left(H_\theta - \bar{E} \right) \psi_{\mathrm{ex}} = (E_{\mathrm{ex}} - \bar{E}) \psi_{\mathrm{ex}} \,, \tag{7.94}$$

therefore,

$$\langle \psi_{\mathrm{ex}} | \mathcal{H}^2 | \psi_{\mathrm{ex}} \rangle = |E_{\mathrm{ex}} - \bar{E}|^2 \langle \psi_{\mathrm{ex}} | \psi_{\mathrm{ex}} \rangle \,. \tag{7.95}$$

By substituting Eq. (7.95) into Eq. (7.92) one gets that

$$|E_{\mathrm{ex}} - \bar{E}|^2 \geq \lambda^2 \,. \tag{7.96}$$

$\lambda^2 = 0$ if and only if the function Φ is the exact eigenfunction of the non-Hermitian Hamiltonian with the eigenvalue $\bar{E}$. If Φ is a given trial function, then by using the Hellman–Feynman theorem we get that

$$\frac{\mathrm{d}\lambda}{\mathrm{d}\bar{E}^*} = 0 \tag{7.97}$$

when

$$\bar{E} = \frac{\langle \Phi | \hat{H}_\theta | \Phi \rangle}{\langle \Phi | \Phi \rangle} \tag{7.98}$$

and Φ is the conventional variational solution of the time-independent Schrödinger equation with the Hermitian Hamiltonian $\mathcal{H}^2$.

By carrying out an iterative calculation, $\bar{E}$ obtained from Eq. (7.98) is substituted in Eq. (7.88) to get a new estimate for Φ. Here we assume that the ground state of the Hermitian operator $\mathcal{H}^2$ can be accurately evaluated from numerical computations. Equation (7.87) can be used as an error estimate for $\bar{E}$ obtained from c-variational calculations,

$$\bar{E} = \frac{(\Phi|H_\theta|\Phi)}{(\Phi|\Phi)} \equiv \frac{\langle\Phi^*|H_\theta|\Phi\rangle}{\langle\Phi^*|\Phi\rangle} \,. \tag{7.99}$$

Note that in Eq. (7.99) the c-product is used rather than the scalar product which was used in Eq. (7.98). In such a case, by combining Eq. (7.87) with the bounds to resonance eigenvalues evaluated by Davidson, Engdahl and Moiseyev we get that E_{ex} *is embedded in an annular ring centered at* $\bar{E}$*, where the inner and outer radii are respectively the lowest eigenvalue of* $\mathcal{H}^2(\bar{E},\ \bar{E}^*)$ *and the complex-variance of* $\mathcal{H}^2(\bar{E},\ \bar{E}^*)$,

$$|\sigma_{\text{C}}| \geq |E_{\text{ex}} - \bar{E}| \geq \lambda \,, \tag{7.100}$$

where

$$\sigma_{\text{C}}^2 = \frac{\big(\Phi|(H_\theta - \bar{E})^2|\Phi\big)}{(\Phi|\Phi)} \,. \tag{7.101}$$

It is interesting to mention that

$$|\sigma_{\text{C}}| \leq \sigma_H |\langle\Phi|\Phi\rangle|^{1/2} \,, \tag{7.102}$$

where

$$\sigma_H^2 = \frac{\langle\Phi|\mathcal{H}^2(\bar{E},\ \bar{E}^*)|\Phi\rangle}{\langle\Phi|\Phi\rangle} \,, \tag{7.103}$$

provided $|\langle\Phi|\psi_{\text{ex}}\rangle|^2 > \frac{1}{2}$, and $\langle\Phi|\Phi\rangle = 1$. Note that Φ is a complex normalized function, $(\Phi|\Phi) = 1$, and therefore $\langle\Phi|\Phi\rangle > 1$. An illustrative numerical example for a 1D model Hamiltonian used in previous chapters is given in Fig. 7.2.

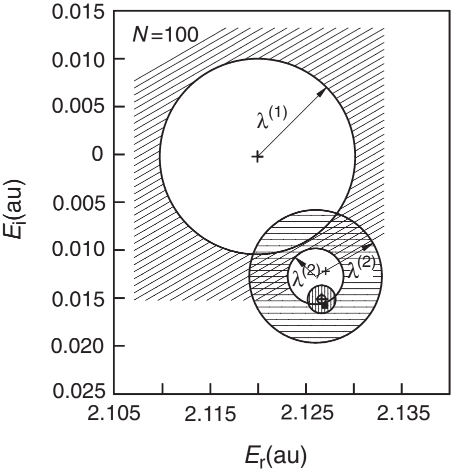

Figure 7.2 Bounds on the estimated complex resonance eigenvalues $\bar{E}$, for $\hat{H} = -0.5\mathrm{d}^2/\mathrm{d}x^2 + (\frac{x^2}{2} - 0.8)\exp(-0.1x^2) + 0.8$ obtained for N even-parity harmonic oscillator basis functions. $\bar{E}$ are indicated by the signs "+" and the exact value of E by a dot. The dashed areas give an optimal estimate of the resonance location. The upper and lower bounds (as calculated by using Eq. (7.100)) of the estimated shape-type complex-coordinate resonance eigenvalue were obtained for $N = 2,\ 3,\ 4$ even-parity harmonic oscillator basis functions. See N. Moiseyev, P. Froelich and E. Watkins, *J. Chem. Phys.* **80**, 3623 (1985).

Proof of Eq. (7.100) $|E_{\text{ex}} - \bar{E}| \le |\sigma_{\text{C}}|$ Here we shall use the Lanczos recursion procedure to construct a three-diagonal complex-scaled Hamiltonian matrix,

$$\mathbf{H}_\theta = \begin{pmatrix} \alpha_0 & \beta_0 & & & \\ \beta_0 & \alpha_1 & \beta_1 & & \\ & \beta_1 & \alpha_2 & \beta_2 & \\ & & \ddots & \ddots & \ddots \end{pmatrix}, \tag{7.104}$$

where $\chi_0 \equiv \Phi$ is a given wavefunction which describes well enough the exact eigenfunction ψ, and

$$\begin{aligned} \alpha_0 &\equiv \bar{E} = \left(\Phi|\hat{H}_\theta|\Phi\right) , \\ \beta_0 &\equiv \sigma_{\text{C}}^2 = (\chi_1|\chi_1)^{1/2} , \\ \chi_1 &= \left(\hat{H}_\theta - \alpha_0\right)\Phi_0 . \end{aligned} \tag{7.105}$$

Similarly for $n \geq 1$,

$$\begin{aligned} \alpha_n &= \left(\chi_n|\hat{H}_\theta|\chi_n\right) , \\ \beta_n &= (\chi_{n+1}|\chi_{n+1})^{1/2} , \\ \chi_{n+1} &= \left(\hat{H}_\theta - \alpha_n\right)\chi_n - \beta_{n-1}\chi_{n-1} . \end{aligned} \tag{7.106}$$

By diagonalizing the three-diagonal Hamiltonian matrix $\mathbf{H}_\theta$, the exact eigenfunction is obtained:

$$\psi = \sum_{n=0}^{\infty} C_n \chi_n(x) , \tag{7.107}$$

where $\mathbf{C}$ is an eigenvector of $\mathbf{H}_\theta$ satisfying

$$\mathbf{H}_\theta \mathbf{C} = E_{\text{ex}} \mathbf{C} \tag{7.108}$$

and χ_n are the Lanczos recursive functions

$$(\chi_n|\chi_{n'}) = \delta_{n,n'} \tag{7.109}$$

defined in Eq. (7.106). By substituting Eq. (7.104) into Eq. (7.108) one gets

$$\alpha_0 C_0 + \beta_0 C_1 = E_{\text{ex}} C_0 . \tag{7.110}$$

Since $\alpha_0 = \bar{E}$ (see Eq. (7.105)) and $\beta_0 = \sigma_{\text{C}}^2$ (Eq. (7.105)) then from Eq. (7.110) one immediately obtains that

$$|E_{\text{ex}} - \bar{E}|^2 = |\sigma_{\text{C}}|^2 \left|\frac{C_1}{C_0}\right|^2 . \tag{7.111}$$

If $\chi_0 = \Phi$ is the dominant function in the Lanczos basis set expansion such that

$$\left|\frac{C_1}{C_0}\right|^2 < 1 , \tag{7.112}$$

then from Eq. (7.111) we obtain the following inequality:

$$|E_{\text{ex}} - \bar{E}|^2 \leq |\sigma_{\text{C}}|^2 . \tag{7.113}$$

Exercise 7.6

Explain under what conditions the resonance position (energy) and width (inverse lifetime) can be estimated by solving the following equation system:

$$\frac{\lambda_1}{|E - \bar{E}_1|} = \frac{\lambda_2}{|E - \bar{E}_2|} = \frac{\lambda_3}{|E - \bar{E}_3|} , \tag{7.114}$$

where $\{\lambda_n\}_{n=1,2,3}$ are the lowest eigenvalues of $(\hat{H}_\theta - \bar{E}_n)^*(\hat{H}_\theta - \bar{E}_n)$ and $\{\bar{E}_n\}_{n=1,2,3}$ are estimated values for the complex resonance eigenvalues. One may estimate the position of the resonances from stabilization calculations for $\theta = 0$ (see Chapter 3). The imaginary parts of $\{\bar{E}_n\}_{n=1,2,3}$ can be set equal to zero or can be estimated by one of the methods described in Chapter 3.

7.7 Perturbation theory for non-Hermitian Hamiltonians

The application of time-independent perturbation theory to non-Hermitian Hamiltonians is straightforward provided that the zero-order non-Hermitian Hamiltonian, $\hat{H}_0^\theta$, and the full Hamiltonian, $\hat{H}^\theta$, have a complete spectrum. Here we assign the label θ to the non-Hermitian operators although the zero-order and full Hamiltonians can be non-Hermitian, not only due to one of the complex scaling transformations described in Chapter 5. On the possibility of having a non-complete spectrum and using the algebraic expansion in the perturbation strength parameter, λ, of the eigenvalues and eigenfunctions, read Chapter 9. For the sake of clarity we will briefly sketch here how the the n-th order corrections to the eigenvalues and eigenfunctions of $\hat{H}^\theta$ can be calculated. Following the $(2n + 1)$ rule of Wigner, $E_j^{(2n+1)}$, the n-th correction terms to the eigenvalues of $\hat{H}^\theta$, can be calculated from the corrections to the eigenfunctions up to the n-th order, $\{\psi_j^{(k)}\}_{k=0,1,\ldots,n}$.

The scheme presented here holds also when the full non-Hermitian Hamiltonian and the non-Hermitian zero-order Hamiltonian are represented by matrices (using a finite number of orthonormal basis functions). In such a case the zero-order eigenvalues are the c-variational solutions of $\hat{H}_0^\theta$. The j-th c-variational eigenfunction of the full Hamiltonian is given by

$$\psi_j^\theta = \sum_{i=1}^{M} C_{ij}^\theta \psi_i^{(0)} = \sum_{n=0}^{\infty} \lambda^n \psi_j^{(n)}, \tag{7.115}$$

where $\mathbf{C}_j^\theta$ are the variational linear parameters and $\{\psi_i^{(0)}\}_{i=1,\ldots,M}$ are the eigenfunctions of $\hat{H}_0^\theta$ ordered by the $\mathrm{Re}[E_i^{(0)}]$. Using these states as a basis set the n-th order correction to variational function is given by

$$\psi_j^{(n)} = \sum_{i=1}^{M} C_{ij}^{(n)} \psi_i^{(0)} \tag{7.116}$$

and the n-th order correction to the variational j-th energy level is given by

$$E_j^{(n)} = \sum_{k=1}^{M} H_{jk}^\theta C_{kj}^{(n-1)}, \tag{7.117}$$

where

$$H^{\theta}_{jk} = \left(\psi^{(0)}_j \left| \hat{H}^{\theta} - \hat{H}^{\theta}_0 \right| \psi^{(0)}_k\right) \equiv \langle[\psi^{(0)}_j]^{*}|\hat{H}^{\theta} - \hat{H}^{\theta}_0|\psi^{(0)}_k\rangle \,. \tag{7.118}$$

Following the $(2n+1)$ rule of Wigner, when the zero-order and full Hamiltonians are represented by finite complex symmetric matrices and $\mathbf{C}^{(n)}_j$ are the n-th order components of the j-th exact eigenvector such that

$$\mathbf{C}^{\theta}_j = \sum_{n=0}^{\infty} \lambda^n \mathbf{C}^{(n)}_j \,, \tag{7.119}$$

then

$$E^{(2n+1)}_j = [\mathbf{C}^{(n)}_j]^{\mathrm{T}} \mathbf{V}^{\theta} [\mathbf{C}^{(n)}_j] \,, \tag{7.120}$$

where

$$\mathbf{V}^{\theta} = [\mathbf{H}^{\theta} - \mathbf{H}^{\theta}_0] \,. \tag{7.121}$$

Note that we do not take the complex conjugates of $[\mathbf{C}^{(n)}_j]^{\mathrm{T}}$ since we use here the c-product rather than the standard scalar product. In order to simplify the calculations we do not use the $(2n+1)$ rule of Wigner for the calculations of $\mathbf{C}^{(n)}_j$. From the Rayleigh–Schrödinger perturbation theory we get that for $k = 1, 2, \ldots, M$,

$$\left[\left(E^{(0)}_k - E^{(0)}_j\right) C^{(n)}_{kj} + \sum_{i=0}^{M} C^{(n-1)}_{ij}\left(H^{\theta}_{ki} - E^{(1)}_j \delta_{ki}\right)\right] = \sum_{m=2}^{n} E^{(m)}_j C^{(n-m)}_{kj} \tag{7.122}$$

and

$$E^{(n)}_j = H^{\theta}_{jj} \,, \tag{7.123}$$

$$C^{(n)}_{jj} = \delta_{n0} \,. \tag{7.124}$$

By re-ordering the summation on the l.h.s. of Eq. (7.122) (using as a running index $n-m$ rather than m) and using the fact that for $j \neq k$, $C^{(0)}_{kj} = 0$ one gets that the components of $\mathbf{C}^{(n)}_j$ are given by

$$C^{(n)}_{k,j\neq k} = \frac{\sum_{i=0}^{M} C^{(n-1)}_{ij}\left(H^{\theta}_{ki} - E^{(1)}_j \delta_{ki}\right) - \sum_{m=1}^{n-2} E^{(n-m)}_j C^{(m)}_{kj}}{E^{(0)}_j - E^{(0)}_k} \,. \tag{7.125}$$

The values of $E^{(n)}_j$ are used for the calculations of the radius of convergence as described in Chapter 9. Also, in Ex. 9.4 we show how one gets Eq. (7.125) from

Eq. (7.122). It is possible, however, to increase the radius of convergence by redefining $\mathbf{H}_0^\theta$. Let us define the new zero-order matrix Hamiltonian as

$$[\mathbf{H}_0^\theta]_{ij} = \delta_{ij} E_j^{(0)} \,\{i, j = 1, \ldots, N < M\}\,, \tag{7.126}$$

$$[\mathbf{H}_0^\theta]_{ij} = \delta_{ij} [\mathbf{H}^\theta]_{ii} \;\{i, j = N+1, \ldots, M\}\,, \tag{7.127}$$

where M is the dimension of the square, complex and symmetric matrix $\mathbf{H}^\theta$ and $\{E_j^{(0)}\}_{j=1,\ldots,N}$ are the eigenvalues of $[\mathbf{H}^\theta]_{ij}$ $\{i, j = 1, \ldots, N < M\}$, associated with the complex c-normalized eigenvectors $\{\mathbf{D}_j\}_{j=1,\ldots,N}$ (the $N \times N$ eigenvector matrix is denoted by $\mathbf{D}$). The perturbation matrix is given by

$$[\mathbf{V}^\theta]_{ij} = 0\,\{i, j = 1, \ldots, N\}\,, \tag{7.128}$$

$$[\mathbf{V}^\theta]_{ij} = [\mathbf{H}^\theta]_{ij} - \delta_{ij} [\mathbf{H}^\theta]_{ii} \;\{i, j = N+1, N+2, \ldots, M\}\,, \tag{7.129}$$

$$[\mathbf{V}^\theta]_{ij} = \sum_{k=1}^{N} D_{ki} [\mathbf{H}^\theta]_{kj} \;\{i = 1, \ldots, N\,;\; j = N+1, N+2, \ldots, M\}\,. \tag{7.130}$$

The full Hamiltonian matrix is given here as $\mathbf{H}^\theta = \mathbf{H}_0^\theta + \lambda \mathbf{V}^\theta$.

Exercise 7.7

Using the $1/Z$ perturbation theory for an atom with nuclear charge Z where the zero-order Hamiltonian is a separable complex scaled hydrogen-like Hamiltonian, show that the resonance position and width $E = \varepsilon - \mathrm{i}/2\Gamma$ are respectively given by

$$\begin{aligned} \varepsilon &= Z^2 E^{(0)} + Z E^{(1)} + \mathrm{Re}(E^{(2)}) + Z^{-1} \mathrm{Re}(E^{(3)}) + O(Z^{-2})\,, \\ \Gamma &= -2\mathrm{Im}(E^{(2)}) - 2Z^{-1} \mathrm{Im}(E^{(3)}) + O(Z^{-2})\,, \end{aligned} \tag{7.131}$$

where $E^{(n)}$ are the coefficients in the $1/Z$ expansion of $Z^{-2}E$.

7.8 Concluding remarks

(1) The complex analog of the variational principle provides a powerful tool for the numerical calculations of resonances of problems for which the analytical solutions are not known. In principle, by extending the number of basis functions in linear variational calculations numerically exact resonance solutions can be obtained. The c-variational method enables the calculations of resonances for many body systems. The variational solutions are stationary solutions in the complex variational space. However, it is possible to evaluate the upper and lower bounds of the resonance position and widths which were obtained from variational calculations. The c-virial theorem

and the complex analog to the Hellmann–Feynman theorem aid the calculations of resonances and their dependence on the physical parameters of the studied problem.

(2) Perturbation theory for non-Hermitian Hamiltonians is quite a straight-forward extension from the Hermitian case but one should be aware of the importance of using the correct inner product. In the non-Hermitian case we use the c-product rather than the scalar product used in the standard formalism of quantum mechanics. In many-body problems the mean field theory simplifies the numerical calculations of the eigenvalues (including resonances). However, when resonance phenomena result from the electronic correlation often one needs to go beyond the mean field approach. Nevertheless, even in such cases, the Hartree–Fock orbitals can be used as a basis set just as in the standard configuration interaction calculations of bound states. We described here the application of the mean field approach to Bose–Einstein condensates which leads to the Gross–Pitaevskii equation. The derivation of mean field theories and beyond for such systems enables the calculations of resonances associated with the fragmentation of the condensate.

(3) The proofs which were given in this chapter for time-independent non-Hermitian Hamiltonians can be extended to time-dependent problems by using the (t,t') method where a Floquet-type operator replaces the Hamiltonian and t' serves as an additional coordinate. Most of the complex analogs presented in this chapter were proved by Moiseyev, Certain and Weinhold.[9] The extension of perturbation theory and almost degenerate perturbation to non-Hermitian formalism of QM is based on the work of Moiseyev and Certain.[10] The upper and lower bounds of the resonance positions and widths were proved on the basis of the Hermitian representation of the complex coordinate method (complex scaling)[11] and on the non-Hermitian Lanczos recursion method.[12] The application of these properties of the non-Hermitian Hamiltonians and the methods presented in this chapter enable the study the resonance phenomena in very different fields in atomic, molecular, mesoscopic and optical sciences.

7.9 Solutions to the exercises

Answer to Exercise 7.1

The eigenvalues of a Hermitian Hamiltonian are real. Therefore, $[\hat{H}\Psi]^* = [E\Psi]^* = E\Psi^*$. If $\hat{H}$ is a real Hamiltonian then $\hat{H}\Psi^* = E\Psi^*$. In the absence of degeneracy this means that $\Psi^* = \Psi$ and Ψ must be a real function. In the case of degeneracy any linear combination of the degenerate states, Ψ and Ψ^*, is also an eigenfunction of $\hat{H}$. Therefore $\mathrm{Re}(\Psi) = (\Psi + \Psi^*)/2$ and $\mathrm{Im}(\Psi) = (\Psi - \Psi^*)/(2\mathrm{i})$ are two real degenerate eigenfunctions of $\hat{H}$. Following Eq. (7.15) it is clear that

---

[9] N. Moiseyev, P. R. Certain and F. Weinhold, *Mol. Phys.* **36**, 1613 (1978).

[10] N. Moiseyev and P. R. Certain, *Mol. Phys.* **37**, 1621 (1979).

[11] N. Moiseyev, *Chem. Phys. Lett.* **99**, 364 (1983).

[12] E. Davidson, E. Engdahl and N. Moiseyev, *Phys. Rev. A* **33**, 2436 (1985).

the matrix which represents the complex scaled Hamiltonian (when the unscaled Hamiltonian is a real Hermitian operator) is a complex symmetric matrix.

Answer to Exercise 7.2

The given matrix $\mathbf{H}_\theta$ can be a general complex matrix. We are looking for a transformation $\mathbf{U}_\theta$ (for which $\tilde{\mathbf{U}}_\theta^{\mathrm{T}}\mathbf{U}_\theta = \mathbf{I}$) such that

$$\begin{aligned}\tilde{\mathbf{U}}_\theta^{\mathrm{T}}\mathbf{H}_\theta\mathbf{U}_\theta &= \mathbf{T}_\theta\ ,\\ \mathbf{H}_\theta\mathbf{U}_\theta &= \mathbf{U}_\theta\mathbf{T}_\theta\ .\end{aligned} \tag{7.132}$$

$\mathbf{U}_\theta$ can be described as a matrix of column vectors $\{\mathbf{\Phi}_i\}_{i=1,\ldots,n}$ such that

$$\mathbf{H}_\theta\mathbf{U}_\theta = (\mathbf{\Phi}_1, \mathbf{\Phi}_2, \Phi_3, \ldots, \mathbf{\Phi}_n)\begin{pmatrix}\alpha_1 & \beta_1 & & & & 0\\ \beta_1 & \alpha_2 & \beta_2 & & & \\ & \beta_2 & \alpha_3 & \ddots & & \\ & & \ddots & \ddots & \beta_{n-2} & \\ & & & \beta_{n-2} & \alpha_{n-1} & \beta_{n-1}\\ 0 & & & & \beta_{n-1} & \alpha_n\end{pmatrix}, \tag{7.133}$$

where $\{\alpha_i;\beta_i\}_{i=1,\ldots,n}$ are the elements of the tri-diagonal matrix $\mathbf{T}_\theta$. Since the eigenvalues of a tri-diagonal matrix are obtained by solving a polynomial equation where the coefficients contain only the diagonal T_{ii} elements and the *product* of the off-diagonal elements $[T_{i,i+1}T_{i+1,i}]$, it is clear that the most general representation of $\mathbf{T}$ is when

$$T_{i,i+1} = T_{i+1,i} \equiv \beta_i\ . \tag{7.134}$$

Since any matrix can be transformed to a tri-diagonal matrix, it implies that any matrix can be transformed into a symmetric matrix. For any value of n that is not on the extreme we get that

$$\begin{aligned}\mathbf{H}_\theta\mathbf{\Phi}_n &= \beta_{n-1}\mathbf{\Phi}_{n-1} + \alpha_n\mathbf{\Phi}_n + \beta_n\mathbf{\Phi}_{n+1},\\ (\mathbf{H}_\theta - \alpha_n\mathbf{I})\,\mathbf{\Phi}_n - \beta_{n-1}\mathbf{\Phi}_{n-1} &= \beta_n\mathbf{\Phi}_{n+1}\ .\end{aligned} \tag{7.135}$$

and similarly

$$\begin{aligned}\mathbf{H}_\theta^{\mathrm{T}}\tilde{\mathbf{\Phi}}_n &= \beta_{n-1}\tilde{\mathbf{\Phi}}_{n-1} + \alpha_n\tilde{\mathbf{\Phi}}_n + \beta_n\tilde{\mathbf{\Phi}}_{n+1}\ ,\\ \left(\mathbf{H}_\theta^{\mathrm{T}} - \alpha_n\mathbf{I}\right)\tilde{\mathbf{\Phi}}_n - \beta_{n-1}\tilde{\mathbf{\Phi}}_{n-1} &= \beta_n\tilde{\mathbf{\Phi}}_{n+1}\ .\end{aligned} \tag{7.136}$$

Let us now define

$$\begin{aligned}\boldsymbol{\Psi}_{n+1} &\equiv (\mathbf{H}_\theta - \alpha_n \mathbf{I})\, \boldsymbol{\Phi}_n - \beta_{n-1}\boldsymbol{\Phi}_{n-1}\,,\\ \tilde{\boldsymbol{\Psi}}_{n+1} &\equiv \left(\mathbf{H}_\theta^{\mathrm{T}} - \alpha_n \mathbf{I}\right) \tilde{\boldsymbol{\Phi}}_n - \beta_{n-1}\tilde{\boldsymbol{\Phi}}_{n-1}\,,\end{aligned} \tag{7.137}$$

and therefore

$$\begin{aligned}&\beta_n^2 = \tilde{\boldsymbol{\Psi}}_{n+1}^{\mathrm{T}}\boldsymbol{\Psi}_{n+1}\,;\\ &\boldsymbol{\Phi}_{n+1} = \frac{\boldsymbol{\Psi}_{n+1}}{\beta_n}\,; \quad \tilde{\boldsymbol{\Phi}}_{n+1} = \frac{\tilde{\boldsymbol{\Psi}}_{n+1}}{\beta_n}\,.\end{aligned} \tag{7.138}$$

To start the Lanczos recursion procedure one should define the first Lanczos recursion state $\boldsymbol{\Phi}_1 = \tilde{\boldsymbol{\Phi}}_1$. For the calculations of the scattering matrix (see Chapter 8) it is recommended to carry out the Lanczos recursions twice, first when $\boldsymbol{\Phi}_1$ is the *initial* state in the scattering process multiplied by the complex scaled potential and a second time when $\boldsymbol{\Phi}_1$ is the complex scaled *final* state multiplied by the complex scaled potential. For the calculations of a specific resonance state one can choose a crude guess for the resonance wavefunction as obtained from stabilization calculations within the framework of the standard (Hermitian) formalism of quantum mechanics. In principle one can take $\boldsymbol{\Phi}_1$ to be a random c-normalized vector.

Another point we wish to emphasize is that β_1 is the complex standard deviation of the expectation of the energy as obtained from the first Lanczos recursion function(vector), $\boldsymbol{\Phi}_1$. That is,

$$\beta_1^2 = \left[\tilde{\boldsymbol{\Phi}}_1^{\mathrm{T}}\mathbf{H}_\theta^2\boldsymbol{\Phi}_1\right] - \left[\boldsymbol{\Phi}_1^{\mathrm{T}}\mathbf{H}_\theta\boldsymbol{\Phi}_1\right]^2. \tag{7.139}$$

The proof is based on the fact that $\sum_n \boldsymbol{\Phi}_n\tilde{\boldsymbol{\Phi}}_n^{\mathrm{T}} = \mathbf{I}$. This leads to

$$\begin{aligned}\boldsymbol{\Phi}_1^{\mathrm{T}}\mathbf{H}_\theta^2\boldsymbol{\Phi}_1 &= \sum_n \left[\boldsymbol{\Phi}_1^{\mathrm{T}}\mathbf{H}_\theta^2\boldsymbol{\Phi}_n\right]\left[\tilde{\boldsymbol{\Phi}}_n^{\mathrm{T}}\mathbf{H}_\theta^2\boldsymbol{\Phi}_1\right]\\ &= \left[\boldsymbol{\Phi}_1^{\mathrm{T}}\mathbf{H}_\theta\boldsymbol{\Phi}_1\right]^2 + \left[\boldsymbol{\Phi}_1^{\mathrm{T}}\mathbf{H}_\theta\boldsymbol{\Phi}_2\right]\left[\tilde{\boldsymbol{\Phi}}_2^{\mathrm{T}}\mathbf{H}_\theta^2\boldsymbol{\Phi}_1\right]\\ &= \left[\boldsymbol{\Phi}_1^{\mathrm{T}}\mathbf{H}_\theta\boldsymbol{\Phi}_1\right]^2 + \beta_1^2\,.\end{aligned} \tag{7.140}$$

Note that although the Lanczos vectors are supposed to be c-orthogonal in numerical calculations they fail to be so due to round-off errors. There are three types of Lanczos eigenvector: “good”, “bad” and “ghost” eigenvectors. The “bad” ones are those for which the first components of the corresponding eigenvectors are equal to zero. These solutions are not related to the spectrum of **T** since the projection of the initial (first) Lanczos vector on the exact eigenvector of **T** is equal to zero. The “ghost” eigenvectors are degenerate eigenvalues within the numerical accuracy of the computer. The rest are the “good” ones. The j-th eigenvector of $\mathbf{H}$ is defined as $\mathbf{\Psi}_j = \sum_n C_{nj}\mathbf{\Phi}_n$ where $\mathbf{C}_j$ is the “good” j-th eigenvector of $\mathbf{T}$, and

$$\mathbf{C}_j = \left(\sum_{k\in G}[\tilde{\mathbf{C}}_k]^{\mathrm{T}}[\mathbf{C}_k]\right)^{1/2}, \tag{7.141}$$

where the summation is over the ghost eigenvectors of $\mathbf{T}$.

Answer to Exercise 7.3

The difference between the complex scaled non-linear GP equations given in Eq. (7.38) and Eq. (7.44) results from different normalization conditions. In the derivation of Eq. (7.38) the c-product has been used to normalize the complex scaled Hartree function,

$$\int \mathrm{d}\mathbf{r}[\phi_\theta(\mathbf{r})]^2 = 1\,, \tag{7.142}$$

while in the direct application of the complex scaling transformation to the D-dimensional GP equation the following normalization condition is applied:

$$\int \mathrm{d}(\mathrm{e}^{\mathrm{i}D\theta}\mathbf{r})[\tilde{\phi}_\theta(\mathbf{r})]^2 = 1\,. \tag{7.143}$$

From a comparison between Eq. (7.142) and Eq. (7.143) one gets

$$\tilde{\phi}_\theta(\mathbf{r}) = \mathrm{e}^{-\mathrm{i}D\theta/2}\phi_\theta(\mathbf{r})\,. \tag{7.144}$$

By substituting Eq. (7.144) into Eq. (7.44) the non-Hermitian non-linear Schrödinger equation in Eq. (7.38) is obtained.

Answer to Exercise 7.4

The solution of this problem is an extension of the derivation[13] to non-Hermitian Hamiltonians. For a two-electron system the complex scaled Hamiltonian is

$$\hat{H}_\theta = \hat{h}_1^\theta + \hat{h}_2^\theta + \frac{\mathrm{e}^{-\mathrm{i}\theta}}{r_{12}} \tag{7.145}$$

and the open-shell spin adapted Hartree–Fock function can be expressed as

$${}^{1,3}\Psi^\theta(1,2) = [{}^{1,3}\phi_1^\theta(1)][{}^{1,3}\phi_2^\theta(2)] \pm [{}^{1,3}\phi_2^\theta(1)][{}^{1,3}\phi_1^\theta(2)]\,, \tag{7.146}$$

---

[13] N. Moiseyev and J. Katriel, *Chem. Phys. Lett.* **29**, 69 (1974).

where the plus and minus signs refer to the singlet and triplet states respectively. Note that, while the triplet state is associated with a single determinant, the singlet spin state is a linear combination of two determinants. In the case of open-shell excited state calculations two different orbitals can be obtained by the spin-adapted mean field computations such that the electronic correlation which is needed for the Auger and interatomic Coulombic decay (ICD) resonance phenomena is partially included in the mean field calculations. The one-electron Hamiltonians $\hat{h}_1$ and $\hat{h}_2$ consist of the complex scaled kinetic operator and the complex scaled one-electron potential which is problem dependent (i.e. for atoms and molecules it is the Coulomb electron–nuclei attractive potential and for quantum dots it is an effective potential that can often be described by a Gaussian potential well). The two orbitals are expanded in a primitive basis set (usually Gaussians for which the Hamiltonian matrix elements can be calculated analytically)

$$ {}^{1,3}\phi_i^\theta(j) = \sum_{\alpha=1}^{N_i} [{}^{1,3}C_{\alpha i}^\theta] \chi_{\alpha i}(j) \,, \tag{7.147} $$

where the two orbitals are denoted by $i = 1, 2$ and $j = 1, 2$ is the index of the electronic coordinates. For different orbitals different basis functions can be used, but this is not a necessary condition. The variational energy is given by

$$ {}^{1,3}\bar{E}^\theta = \frac{\sum_{\alpha\alpha'} \sum_{\beta\beta'} [{}^{1,3}C_{\alpha 1}^\theta][{}^{1,3}C_{\alpha' 1}^\theta][{}^{1,3}H_{\alpha\alpha'\beta\beta'}^\theta][{}^{1,3}C_{\beta 2}^\theta][{}^{1,3}C_{\beta' 2}^\theta]}{\sum_{\alpha\alpha'} \sum_{\beta\beta'} [{}^{1,3}C_{\alpha 1}^\theta][{}^{1,3}C_{\alpha' 1}^\theta][{}^{1,3}S_{\alpha\alpha'\beta\beta'}^\theta][{}^{1,3}C_{\beta 2}^\theta][{}^{1,3}C_{\beta' 2}^\theta]} \tag{7.148} $$

and is obtained under the requirements that

$$ \left[\frac{\partial [{}^{1,3}\bar{E}^\theta]}{\partial [{}^{1,3}C_{\alpha i}^\theta]} \right]_{\alpha=1,\ldots,N_i;\, i=1,2} = 0 \,, \tag{7.149} $$

where

$$ {}^{1,3}H_{\alpha\alpha'\beta\beta'}^\theta = \langle \chi_{\alpha 1}(1)\chi_{\beta 2}(2) | \hat{H}_\theta | \chi_{\alpha' 1}(1)\chi_{\beta' 2}(2) \pm \chi_{\beta' 2}(1)\chi_{\alpha' 1}(2) \rangle \tag{7.150} $$

and

$$ {}^{1,3}S_{\alpha\alpha'\beta\beta'}^\theta = \langle \chi_{\alpha 1}(1)\chi_{\beta 2}(2) | \chi_{\alpha' 1}(1)\chi_{\beta' 2}(2) \pm \chi_{\beta' 2}(1)\chi_{\alpha' 1}(2) \rangle \,. \tag{7.151} $$

Equation (7.149) is satisfied when the two coupled sets of pseudo-secular equations are solved:

$$ \left([{}^{1,3}\mathbf{H}_1^\theta] - [{}^{1,3}\bar{E}^\theta][{}^{1,3}\mathbf{S}_1^\theta] \right) = 0 \,, \tag{7.152} $$

$$ \left([{}^{1,3}\mathbf{H}_2^\theta] - [{}^{1,3}\bar{E}^\theta][{}^{1,3}\mathbf{S}_2^\theta] \right) = 0 \,, \tag{7.153} $$

where

$$[{}^{1,3}\mathbf{H}_1^\theta]_{\alpha\alpha'} = \sum_{\beta\beta'} [{}^{1,3}H^\theta_{\alpha\alpha'\beta\beta'}][{}^{1,3}C^\theta_{\beta 2}][{}^{1,3}C^\theta_{\beta' 2}]\,, \tag{7.154}$$

$$[{}^{1,3}\mathbf{H}_2^\theta]_{\beta\beta'} = \sum_{\alpha\alpha'} [{}^{1,3}H^\theta_{\alpha\alpha'\beta\beta'}][{}^{1,3}C^\theta_{\alpha 1}][{}^{1,3}C^\theta_{\alpha' 1}]\,, \tag{7.155}$$

$$[{}^{1,3}\mathbf{S}_1^\theta]_{\alpha\alpha'} = \sum_{\beta\beta'} [{}^{1,3}S^\theta_{\alpha\alpha'\beta\beta'}][{}^{1,3}C^\theta_{\beta 2}][{}^{1,3}C^\theta_{\beta' 2}]\,, \tag{7.156}$$

$$[{}^{1,3}\mathbf{S}_2^\theta]_{\beta\beta'} = \sum_{\alpha\alpha'} [{}^{1,3}S^\theta_{\alpha\alpha'\beta\beta'}][{}^{1,3}C^\theta_{\alpha 1}][{}^{1,3}C^\theta_{\alpha' 1}]\,. \tag{7.157}$$

The coupled equations in Eq. (7.152) and Eq. (7.153) can be solved by an iterative self-consistent-field (SCF) method. For the calculations of atomic and molecular auto-ioniozation and Auger resonances the two electrons should be in excited states. Therefore, during the iterative procedure the n-th excited state is calculated in the solution of Eq. (7.152), whereas the m-th excited state is calculated in the solution of Eq. (7.153). Therefore, in the spin adapted mean field approach the resonances are assigned two good quantum numbers (n, m). By choosing different types of symmetry basis functions one can calculate different types of resonance with the same good quantum numbers (n, m). For example, in the calculations of the ${}^1S$ resonances of helium during the iterative SCF calculations one should keep $n = m = 1$ (first excited state) and the basis functions for the two orbitals are spherically symmetric. Different resonances can be calculated by replacing the spherically symmetric basis functions with other type of symmetry functions (for example p-type orbitals) while keeping $n = m = 1$ in the SCF calculations. In ICD calculations (see Chapter 2) the most common situation is where $n = 0$ (ground state) when Eq. (7.152) is solved, but $m = 1$ when Eq. (7.153) is solved. For sufficiently narrow quantum-dot effective potentials the repulsion between the two electrons can be large enough to render the ground state metastable and the resonance energy and lifetime of the ground state of the two-electron quantum dot is obtained when in the SCF calculations $n = m = 0$.

The resonance solutions are obtained for the optimal scaling angle for which

$$\left[\frac{\partial[{}^{1,3}\bar{E}^\theta]}{\partial\theta}\right]_{\theta_{\text{opt}}} = 0\,. \tag{7.158}$$

Answer to Exercise 7.5

The solution of this exercise is based on Moiseyev.[14] From scattering theory we can relate the derivative of the phase shift η_l to the eigenfunction $\psi_{l,k}$

---

[14] N. Moiseyev, *Phys. Rev. A* **24**, 2824 (1981).

through

$$\frac{\mathrm{d}\eta_l}{\mathrm{d}k} = \frac{1}{k^2} \lim_{r\to\infty} W[\psi_{l,k}, \Phi] , \tag{7.159}$$

where W stands for the Wronskian of two functions, $W[\psi_{l,k}, \Phi] = \psi_{l,k}\partial\Phi/\partial r - \Phi\partial\psi_{l,k}/\partial r$, and Φ is

$$\Phi(r) = r\frac{\partial\psi_{l,k}}{\partial r} - k\frac{\partial\psi_{l,k}}{\partial k} . \tag{7.160}$$

We can express the scattering eigenfunction $\psi_{l,k}(r)$ by

$$\psi_{l,k}(r) = \frac{\mathrm{i}}{2}\left[f_l(k)\chi^-_{l,k} - f_l(-k)\chi^+_{l,k}(r)\right] , \tag{7.161}$$

in which $f_l(k)$ is the amplitude of the scattering state and $\chi^\pm_{l,k}(r)$ satisfy the condition

$$\lim_{r\to\infty} \chi^\pm_{l,k}(r) = h^\pm_l(kr) = n_l(kr) \pm \mathrm{i}\, j_l(kr) , \tag{7.162}$$

where $n_l(kr)$ and $j_l(kr)$ are respectively the Neumann and Bessel functions. Note that since for real values of E the scattering functions are real, the amplitudes $f_l(k)$ might have complex values since $\chi^\pm_{l,k}(r)$ are complex functions when k has real values. By substituting Eq. (7.161) into Eq. (7.160) one obtains

$$\Phi(r) = \frac{k}{4}\left(\frac{\partial_l f(+k)}{\partial k}\chi^-_{l,k}(r) + \frac{\partial_l f(-k)}{\partial k}\chi^+_{l,k}(r)\right) \tag{7.163}$$

and consequent substitution of Eqs. (7.162) and (7.163) into Eq. (7.159) yields

$$E\frac{\partial\eta_l}{\partial k} = \frac{k}{8}W[h^+_l(kr), h^-_l(kr)]\left(f_l(k)\frac{\partial f_l(-k)}{\partial k} + f_l(-k)\frac{\partial f_l(+k)}{\partial k}\right) . \tag{7.164}$$

From conventional scattering theory we know that $W[j_l, n_l] = -k$ and consequently $W[h^+_l, h^-_l] = -2\mathrm{i}k$. It is also well established that the bound, resonance and virtual states are associated the zeros of the amplitude of the scattering wavefunction (which are the poles of the scattering matrix). In other words we are looking for the solution for which

$$f_l(k_0) = 0 \tag{7.165}$$

and therefore

$$\psi_{l,k_0}(r) = -\frac{\mathrm{i}}{2}f_l(-k)\chi^+_{l,k_0}(r) . \tag{7.166}$$

We will now prove that at the poles of the S-matrix where $E_0 = k_0^2/2$

$$E_0 \frac{\mathrm{d}\eta_l}{\mathrm{d}k}|_{k_0} = -2\mathrm{i}E_0 f_l(-k_0) \frac{\mathrm{d}f_l(k)}{\mathrm{d}k}|_{k_0} \,. \tag{7.167}$$

The derivative of the amplitude of the scattering eigenfunction at the poles of the S-matrix is given by

$$\frac{\mathrm{d}f_l(k)}{\mathrm{d}k} = -2\int_0^\infty \chi_{l,k_0}^+(r)\psi_{l,k_0}(r)\mathrm{d}r = \mathrm{i}\int_0^\infty \psi_{l,k_0}(r)\psi_{l,k_0}(r)\mathrm{d}r \,. \tag{7.168}$$

It is a point of interest that here the c-product is obtained from our derivation. At the poles of the S-matrix Eq. (7.167) reduces to

$$E_0 \frac{\mathrm{d}\eta_l}{\mathrm{d}k}|_{k_0} = 2E_0 \int_0^\infty \psi_{l,k_0}(r)\psi_{l,k_0}(r)\mathrm{d}r \tag{7.169}$$

and from the virial theorem for the scattering of particles by a central field potential, $\int_0^\infty \psi_{l,k}(r)\,(2V(r) + r\mathrm{d}V/\mathrm{d}r)\,\psi_{l,k}(r)\mathrm{d}r = E\mathrm{d}\eta_l/\mathrm{d}k$, we get the following *virial theorem for the resonance, virtual, and bound states*:

$$E_0 = \frac{\int_0^\infty \psi_{l,k_0}(r)\left(V(r) + \frac{r}{2}\frac{\mathrm{d}V}{\mathrm{d}r}\right)\psi_{l,k_0}(r)\mathrm{d}r}{\int_0^\infty \psi_{l,k_0}(r)\psi_{l,k_0}(r)\mathrm{d}r} \,, \tag{7.170}$$

where $E_0 = k_0^2/2$. For bound states E_0 attains real values (k_0 are pure imaginary numbers) and ψ_{l,k_0} are square integrable functions. For the resonance and the virtual states, $\mathrm{Im}(E_0) < 0$ and $\psi_{l,k_0}(r)$ diverges in the asymptotic limit. As discussed in Chapter 5, upon complex scaling the resonance eigenfunctions become square integrable and

$$\lim_{r\to\infty} \psi_{l,k_0}(r\mathrm{e}^{\mathrm{i}\theta}) = h_l^+(kr\mathrm{e}^{\mathrm{i}\theta}) \in L_2 \,, \tag{7.171}$$

where now

$$k_0^2/2 \equiv E_{\mathrm{res}} = k_{\mathrm{res}}^2/2 \,. \tag{7.172}$$

Therefore, by complex scaling of the radial Schrödinger equation, similarly to Eq. (7.169), the complex virial theorem is obtained,

$$E_{\mathrm{res}} = \frac{\int_0^\infty \psi_{l,k_{\mathrm{res}}}^\theta(r)\left(V(r) + \frac{r}{2}\frac{\mathrm{d}V}{\mathrm{d}r}\right)\psi_{l,k_{\mathrm{res}}}^\theta(r)\mathrm{d}r}{\int_0^\infty [\psi_{l,k_{\mathrm{res}}}^\theta(r)]^2\mathrm{d}r} \,, \tag{7.173}$$

where

$$\psi^{\theta}_{l,k_{\mathrm{res}}}(r) = \psi_{l,k_{\mathrm{res}}}(r\mathrm{e}^{\mathrm{i}\theta}) \in L_2 \,. \tag{7.174}$$

Answer to Exercise 7.6

The solution of this exercise is based on Engdahl and Moiseyev.[15] Assuming existence of "perfect" correlation between the error estimate of the resonance position and width, $|E_n - \bar{E}_n|$, and the corresponding λ_n which is defined as the lowest eigenvalue of $(\hat{H}_\theta - \bar{E}_n)^*(\hat{H}_\theta - \bar{E}_n)$,

$$\lambda_n(\theta) = C(\theta) \cdot |E_n - \bar{E}_n| \tag{7.175}$$

for $n = 1, 2, 3$.

Since the constant $C(\theta)$ depends only on the value of the rotational angle (or more generally speaking on the parameters of the contour of integration in the complex plane or of the used complex absorbing potential) and *not* on the chosen trial energy $\bar{E}_n$, the unknowns $\mathrm{Re}[E_n]$, $\mathrm{Im}[E_n]$ and $C(\theta)$ can be obtained by solving the equation system given in Eq. (7.114). Therefore the answer to this problem is that the proposed procedure for calculating an accurate value for the resonance position and width holds under the following assumptions:

(1) we have a "perfect" correlation between the error estimate of the resonance position and the error estimate of the width;
(2) the proportionality factor C depends on θ only and not on the differnet trial energies $\{\bar{E}_n\}_{n=1,2,3}$.

Answer to Exercise 7.7

The resonance position ε and width Γ of an auto-ionizing state is associated with a complex energy $E = \varepsilon - \mathrm{i}/2\Gamma$ of the complex scaled Hamiltonain $\hat{H}_\theta(\mathbf{r}) = \hat{H}(\mathbf{r}\mathrm{e}^{\mathrm{i}\theta})$,

$$\hat{H}_\theta(\mathbf{r})\psi_\theta(\mathbf{r}) = E\psi_\theta(\mathbf{r}) \tag{7.176}$$

with square integrable eigenfunction ψ_θ. By scaling $\mathbf{r}$ in Eq. (7.176) by $1/Z$, where Z is the atom's nuclear charge, one gets that

$$\hat{H}_\theta(\mathbf{r}/Z)\psi_\theta(\mathbf{r}/Z) = E\psi_\theta(\mathbf{r}/Z)\,. \tag{7.177}$$

We can express the scaled Hamiltonian $\hat{H}_\theta(\mathbf{r}/Z)$ as

$$Z^{-2}\hat{H}_\theta(\mathbf{r}/Z) = \hat{H}^{(0)}_\theta(\mathbf{r}) + Z^{-1}\hat{H}^{(1)}_\theta(\mathbf{r})\,, \tag{7.178}$$

---

[15] E. Engdahl and N. Moiseyev, *J. Chem. Phys.* **84**, 1379 (1986).

where

$$\hat{H}_\theta^{(0)}(\mathbf{r}) = \mathrm{e}^{-2\mathrm{i}\theta} \sum_i \left(-\frac{1}{2}\nabla_i^2\right) - \mathrm{e}^{-\mathrm{i}\theta} \sum_i \frac{1}{r_i}\,,$$
$$\hat{H}_\theta^{(1)}(\mathbf{r}) = \mathrm{e}^{-\mathrm{i}\theta} \sum_{i<j} \frac{1}{|\mathbf{r}_\mathrm{i} - \mathbf{r}_\mathrm{j}|}\,. \tag{7.179}$$

The perturbed complex eigenvalue up to the order N is

$$[\varepsilon - \mathrm{i}/2\Gamma]^{(N)} = Z^2 \sum_{n=0}^{N} \frac{E^{(n)}}{Z^n}\,, \tag{7.180}$$

where $E^{(n)}$ are the n-th order perturbation correction terms of the eigenvalue of $\hat{H}_\theta^{(0)}(\mathbf{r}) + \lambda \hat{H}_\theta^{(1)}(\mathbf{r})$, which can be calculated by Eq. (7.117). Since $\hat{H}_\theta^{(0)}(\mathbf{r})$ is separable into hydrogen-like Hamiltonians both $E^{(0)}$ (bound states of $\hat{H}_\theta^{(0)}(\mathbf{r})$) and the first order correction terms $E^{(1)}$ are real and therefore

$$\varepsilon = Z^2 E^{(0)} + Z E^{(1)} + \mathrm{Re}(E^{(2)}) + Z^{-1}\mathrm{Re}(E^{(3)}) + O(Z^{-2})\,,$$
$$\Gamma = -2\mathrm{Im}(E^{(2)}) - 2Z^{-1}\mathrm{Im}(E^{(3)}) + O(Z^{-2})\,. \tag{7.181}$$

The first-order correction to the energy is real, although the perturbation is the complex scaled electronic repulsion potential term since the zero-order functions are bound states, and one can carry out a back rotational transformation such that the contour of integration becomes $\mathrm{d}\mathbf{r}_1 \mathrm{d}\mathbf{r}_2$ rather than the complex scaled one. Thus the integral is over a real function which gives only real-valued correction to the the energy.

This approach has been used by Moiseyev and Weinhold for calculations of electron-correlation effects in positions and widths of two-electron auto-ionizing resonances.[16]

7.10 Further reading

Reviews

J. M. Combes, Complex scaling transformations in stationary and scattering problems, *Int. J. Quantum. Chem.* **14**, 353–359 (1978).

B. Simon, Resonances and complex scaling: a rigorous overview, *Int. J. Quantum Chem.* **14**, 529–542 (1978).

W. P. Reinhardt, Complex coordinate in the theory of atomic and molecular structure and dynamics, *Ann. Phys. Chem.* **33**, 223–146 (1982).

---

[16] N. Moiseyev and F. Weinhold, *Phys. Rev. A* **20**, 27 (1979).

B. R. Junker, Recent developments in the use of complex scaling in resonance phenomena, *Adv. At. Mol. Phys.* **18**, 208–263 (1982).

Y. K. Ho, The method of complex coordinate rotation and its application to atomic collision processes, *Phys. Rep.* **99**, 1–68 (1983).

N. Moiseyev, Quantum theory of resonances: calculating energies, widths and cross-sections by complex scaling, *Physics Reports* **302**, 211–293 (1998).

E. Narevivius and N. Moiseyev, Review on: Non-Hermitian quantum mechanics: theory and experiments not amenable to conventional quantum mechanics, *Prog. Theor. Chem. Phys.* **12**, 311–338 (2003).

E. Narevivius and N. Moiseyev, Review on: Non-Hermitian quantum mechanics: formalism and applications, *Fundamental World of Quantum Chemistry* **2**, 1–31 (2003).

S.-I. Chu and D. A. Telnov, Beyond the Floquet theorem: generalized Floquet formalisms and quasienergy methods for atomic and molecular multiphoton processes in intense laser fields, *Phys. Rep.* **390**, 1–131 (2004).

K. Kato, Resonances and continuum states in the complex scaling method, *J. Phys.: Conference Series* **49**, 73–78 (2006).

Complex analogs to fundamental theorems in quantum mechanics

E. Brandas and P. Proelich, Continuum orbitals, complex scaling problem, and the extended virial theorem, *Phys. Rev. A* **16**, 2207–2210 (1977).

N. Moiseyev, P. R. Certain and F. Weinhold, Resonance Properties of complex-rotated Hamiltonians, *Mol. Phys.* **36**, 1613–1630 (1978).

N. Moiseyev, Virial theorem for bound and resonance states as a special case of the scattering virial theorem. *Phys. Rev. A* **24**, 2824–2825 (1981).

N. Moiseyev, Resonance states by the generalized complex variational method, *Mol. Phys.* **47**, 582–598 (1982).

M. Garcia-Sucre, Complex scaling for subsets of coordinates and associated virial-type relations, *Int. J. Quantum Chem.* **43**, 209–214 (1992).

H. Barkay and N. Moiseyev, Complex density probability in non-Hermitian quantum mechanics: interpretation and a formula for resonant tunneling probability amplitude. *Phys. Rev. A* **64**, 044702–044705 (2001).

Perturbation theory for non-Hermitian Hamiltonians

B. Simon, Resonances in n-body quantum systems with dilation analytic potentials and the foundations of time-dependent perturbation theory, *Ann. Math.* **97**, 247–274 (1973).

N. Moiseyev and P. R. Certain, Perturbation approach to the complex-coordinate method. *Mol. Phys.* **37**, 1621–1632 (1979).

S. Graffi, V. Grecchi and H. J. Silverstone, Resonances and convergence of perturbation theory for N-body atomic systems in external AC-electric field, *Annales de l'institut Henri Poincarè* **42**, 215–234 (1985).

E. Engdahl and N. Moiseyev, Perturbation analysis of gas-surface diffractive selective adsorption resonance states, *Mol. Phys.* **66**, 465–478 (1989).

The Hermitian representation of non-Hermitian Hamiltonians and bounds of the resonance positions and widths

N. Moiseyev, Resonances by the complex coordinate method with Hermitian Hamiltonian, *Chem. Phys. Lett.* **99**, 364–366 (1983).

N. Moiseyev, P. Froelich and E. Watkins, Resonances by the complex coordinate method with Hermitian Hamiltonian II: error estimates, *J. Chem. Phys.* **80**, 3623–3628 (1984).

P. Froelich and N. Moiseyev, Resonances by the complex coordinate method with Hermitian Hamiltonian III: autoionization, *J. Chem. Phys.* **81**, 1352–1354 (1984).

E. Engdahl and N. Moiseyev, Resonances by the complex coordinate method with Hermitian Hamiltonian IV: the linear correlation procedure, *J. Chem. Phys.* **84**, 1379–1384 (1986).

E. Davidson, E. Engdahl and N. Moiseyev, New bounds to resonance eigenvalues, *Phys. Rev. A* **33**, 2436–2439 (1986).

8

Non-Hermitian scattering theory

We begin by considering the following scattering experiment. A projectile, e.g., an atom A in a given electronic state, collides with a target which we will take as a diatomic molecule BC in its ground electronic, vibrational and rotational state. For a short period of time an activated complex $[ABC]^{\#}$ is generated. As time passes the activated complex can break into different products. For instance, in our example these products will be $A + BC$, $B + AC$, $C + AB$ and $A + B + C$. Each one of the possible products can be in different electronic, vibrational and rotational quantum states. The total energy which is originally the sum of the electronic and translational energies of the projectile A and the electronic, vibrational, rotational and translational energies of target BC is conserved during the scattering process.

Time-independent scattering theory enables one to calculate the probability of obtaining the specific products in given quantum states and the kinetic energy distribution of the products as a function of the total energy of the system without the need to solve the time-dependent Schrödinger equation. The time-independent formulation of scattering theory is based on the ability to propagate *analytically* an initial given wavepacket, $\Phi(0)$, to infinite times. That is, we need to get a closed-form expression for $\lim_{t\to\pm\infty} \mathrm{e}^{-\mathrm{i}\hat{H}t/\hbar}|\Phi(t = 0)\rangle$. To quote from the introduction of the excellent book on scattering theory written by Taylor:[1] "The most important experimental technique in quantum physics is the scattering experiment. That this is so is clear from even the briefest review of modern physics." The rational behind this statement is that one of the best ways to extract information on the structure of matter is via scattering experiments.

Calculations based on time-independent scattering theory within the Hermitian formalism of quantum mechanics require the ability to obtain quite accurately the continuum of a given Hamiltonian. For instance, in the above example it is the continuum of all possible dissociation products of the Hamiltonian of the ABC

---

[1] J. R. Taylor, *Scattering Theory*, New York, John Wiley & Sons, Inc., 1972.

complex. This is quite often a tough computational task since the density of states in the continuum does not vary monotonically with the energy (read about the calculations of resonances in the continuum by the standard formalism of quantum mechanics in Chapter 3).

The non-Hermitian formalism of quantum mechanics enables us to split the continuum into two parts. One part contains the resonances which are represented by square integrable functions[2] whereas the other part of the spectrum contains a continuum of functions with monotonically varying density of states (so-called "white" continuum). The use of non-Hermitian scattering theory simplifies the calculations of cross sections, transition probabilities and the probability of obtaining specific products since often one can disregard the "white" continuum and consider only the contribution of the resonances to the process under study.[3]

The complex coordinate (i.e., non-Hermitian) time-independent scattering theory enables one to calculate cross sections, partial widths and state-to-state transition probabilities even for time-dependent Hamiltonians. The transition from some initial state, ϕ_{i}, to a final state, ϕ_{f}, is given by the matrix element (known as the Lippmann–Schwinger equation).

$$T(E) = \langle \phi_{\mathrm{f}} | \hat{V} + \hat{V}\hat{G}(E)\hat{V}) | \phi_{\mathrm{i}} \rangle \,, \tag{8.1}$$

where ϕ_{i} and ϕ_{f} are two eigenfunctions with the same energy E of the unperturbed Hamiltonian $\hat{H}_0 = \hat{H} - \hat{V}$ and $\hat{G}(E)$ is the outgoing Green's operator given by

$$\hat{G}(E) = \lim_{\epsilon \to 0^+} \frac{1}{E - \hat{H} + \mathrm{i}\epsilon} \,. \tag{8.2}$$

The initial and final states are embedded in the continuum of the unperturbed Hamiltonian and therefore are energy normalized functions. The interacting potential $\hat{V}$ vanishes as the projectiles move far from the target. It should be stressed here that $T(E)$ is *not* the probability of getting the final state (i.e., product) from the initial state (i.e., reactants) in a scattering collision experiment. We will address this point later in this chapter.

The motivation for deriving a complex-coordinate scattering theory has been explained above. The manner in which it is implemented is by evaluating the state-to-state transition probability amplitude by integration along a complex contour in coordinate space.

For example, the complex spatial contour can be obtained by scaling the cartesian coordinates by a complex factor $\mathrm{e}^{\mathrm{i}\theta}$. Conversely, it may be numerically advantageous to scale only the "reaction coordinate" by a complex factor, while all

---

[2] See the different types of complex scaled transformations presented in Chapter 5 which should be used to associate the resonances with square integrable functions.

[3] Note that even if there is a need to include the "white" continuum in the calculations one can replace it with quasi-continuum functions which are obtained by applying the finite box approximation.

other coordinates will remain unscaled. The "reaction coordinate" may be considered as the distance between the center of mass of the scattered particle and the center of mass of the target. Therefore, as $\mathbf{x} \to \mathbf{x}e^{i\theta}$, $\langle \phi_f(\mathbf{x})| \to \langle \phi_f(\mathbf{x}e^{-i\theta}|$ and $|\phi_i(\mathbf{x})\rangle \to |\phi_i(\mathbf{x}e^{i\theta}\rangle$. The interaction potential is also scaled by the same factor, $V(\mathbf{x}) \to V(\mathbf{x}e^{i\theta})$, and so is the Green's operator, $\hat{G}(E) \to \hat{G}_\theta(E)$. In principle one can use any one of the complex scaling transformations which were introduced and discussed in Chapter 5. More generally speaking, any transformation $\mathbf{x} \to F(\mathbf{x}, \theta)$ for which $F(\mathbf{x}, \theta) \to \mathbf{x}e^{i\theta}$ as $|\mathbf{x}| \to \infty$ will be encompassed by the derivation which follows below.

The complex scaled Green's operator, $\hat{G}_\theta(E)$, is defined by

$$\hat{G}_\theta(E) = \frac{1}{E - \hat{H}_\theta}\,, \tag{8.3}$$

where $\hat{H}_\theta$ is the complex scaled Hamiltonian of the system. Since the outgoing boundary conditions are already embedded in the complex scaled Hamiltonian there is no need now to introduce the $+i\epsilon$ factor which appears in the Green's operator in Eq. (8.2). Consequently, the energy contour of integration becomes complex when $\hat{G}$ is in the spectral representation. Since this is a crucial point in the derivation of the complex coordinate scattering method, we shall discuss it in some more detail. First we discuss the spectral representation of the Green's operator within the framework of the standard (Hermitian) formalism of quantum mechanics (i.e., the Hamiltonian is Hermitian since $\theta = 0$). The Green's function provides us with the probability amplitude to get from $\mathbf{x}$ to $\mathbf{x}'$ at a given energy E. In the spectral representation $G_E^{\theta=0}$ is given by

$$G_E^{\theta=0}\left(\mathbf{x}', \mathbf{x}\right) = \langle \mathbf{x}'|\hat{G}_{\theta=0}(E)|\mathbf{x}\rangle = \sum\!\!\!\!\!\!\!\int \mathrm{d}E' \frac{\psi_{E'}(\mathbf{x}')\psi_{E'}(\mathbf{x})}{E - E'}\,, \tag{8.4}$$

where $\sum\!\!\!\!\!\!\!\int$ stands for summation over the bound states of the unscaled Hamiltonian $\hat{H}$ and integration over the energy normalized continuum eigenfunctions, i.e., $\langle \psi_{E'}|\psi_E\rangle = \delta(E - E')$. Note that the non-degenerate eigenfunctions of a Hermitian and real Hamiltonian have to be real, and that degenerate eigenfunctions can always be transformed to be real, and therefore we do not take here the complex conjugate of $\psi_{E'}(\mathbf{x}')$.

As one can see from Eq. (8.4), $G_E^{\theta=0}$ has a branch cut along the real energy axis. Consequently, large numerical errors are expected in a brute force application of Eq. (8.4), due to the vanishing of the energy denominator. This is a very serious technical problem which is taken care of in the Hermitian formalism of quantum mechanics by adding $-i\epsilon$ to the Hamiltonian where in the final step of the calculations the limit of $\epsilon \to 0$ is taken. However, this technical problem is avoided in the non-Hermitian formalism of quantum mechanics by rotating the energy contour of integration from the real axis into the complex plane. The energy contour of integration becomes complex when the relevant spatial contour is rotated into the complex plane, as discussed in Chapter 5. The wavefunctions $\psi_{E'}$ and the energy E' in Eq. (8.4) are replaced by the eigenfunctions and eigenvalues of the complex scaled Hamiltonian H_θ. The eigenfunctions of the complex scaled Hamiltonian are associated with the discrete spectrum of real bound state energies, E_n(bound), and with the complex resonance spectrum, $E_n(\mathrm{res}) = \varepsilon_n - \frac{\mathrm{i}}{2}\Gamma_n$, where $\psi_{n_{\mathrm{res}}}$, $n_{\mathrm{res}} = 1, 2, \ldots,$ are square integrable functions. The spectrum consists also of a rotated continua, $\psi_{E_\theta^j}$ where $E_\theta^j = \epsilon \mathrm{e}^{-2\mathrm{i}\theta} + E_j^{\mathrm{th}}$, and ϵ varies from 0 to ∞ while E_j^{th}, $j = 1, 2, \ldots,$ are the (real) threshold energies. The complex scaled Green's function in the spectral representation is given by

$$G_E^\theta(\mathbf{x}', \mathbf{x}) = \sum_n \frac{\psi_n(\mathbf{x}')\psi_n(\mathbf{x})}{E - E_n} + \sum_j \int \mathrm{d}E_\theta^j \frac{\psi_{E_\theta^{(j)}}(\mathbf{x}')\psi_{E_\theta^{(j)}}(\mathbf{x})}{E - E_\theta^{(j)}} . \tag{8.5}$$

Here we assume that the wavefunctions are complex only due to the complex scaling. When the eigenfunctions of the complex scaled Hamiltonian are variationally obtained with complex basis functions one should use the left and right eigenstates of H_θ as defined in Chapter 5.

Usually we can describe two main types of scattering event. In full collision scattering experiments using the non-Hermitian formalism the transition probability amplitude, $T(E)$, is calculated, whereas in half collision experiments (i.e., the system is initially prepared in a state where it has enough energy to ionize or dissociate) $T(E)$ represents the amplitude of probability of obtaining a given set of products resulting from an ionization and/or dissociation process. $T(E)$ either in a full scattering experiment or in a half collision process is complex. Being a measurable quantity, $T(E)$ is in principle θ-independent. In the numerical calculations when finite grid or finite basis set methods are used $T(E)$ is θ-dependent. The optimal values of T are associated with the stationary solutions for which $\mathrm{d}T/\mathrm{d}\theta = 0$. Since T is complex, θ should be allowed to have complex values and to be optimized to satisfy the two Cauchy–Riemann conditions:

$$\left.\frac{\partial \mathrm{Re} T(\theta)}{\partial \mathrm{Re}\theta}\right|_{\theta_{\mathrm{opt}}} = 0 \quad \text{and} \quad \left.\frac{\partial \mathrm{Im} T(\theta)}{\partial \mathrm{Re}\theta}\right|_{\theta_{\mathrm{opt}}} = 0$$

or

$$\left.\frac{\partial \mathrm{Re} T(\theta)}{\partial \mathrm{Im}(\theta)}\right|_{\theta_{\mathrm{opt}}} = 0 \quad \text{and} \quad \left.\frac{\partial \mathrm{Im} T(\theta)}{\partial \mathrm{Im}\theta}\right|_{\theta_{\mathrm{opt}}} = 0 . \tag{8.6}$$

The fact that the optimal rotational angle θ_{opt} may have complex values can be introduced as the result of using a complex scaling factor

$$\eta = \mathrm{e}^{\mathrm{i}\theta} = \alpha \mathrm{e}^{\mathrm{i}\theta'}, \tag{8.7}$$

where α and θ' are real. The optimal values of α and θ' are those for which $\partial T/\partial\alpha = 0$ and $\partial T/\partial\theta' = 0$. The optimization of the complex scaling factor η (i.e. $\theta' = \theta_{\text{opt}}$, $\alpha = \alpha_{\text{opt}}$) enables the application of the complex coordinate scattering theory to long-range potentials, and avoids the serious singularities and convergence problems due to the exponential asymptotic divergence of the complex scaled incoming ($|\phi_{\mathrm{i}}\rangle$) or outgoing ($\langle\phi_{\mathrm{f}}|$) states.

8.1 Full collision processes for time-independent systems

Full collision processes cover the types of experiment described in the introduction to this chapter. Examples include electron scattering from atoms and molecules where the electron is temporarily trapped by the atom/molecule and scattering of atoms and molecules from solid surfaces where the projectiles are temporarily trapped by the solid. These types of scattering experiment can be described by $p + T \to [p - T]^{\#} \to p + T^*$, where p is the projectile and T is the target (an atom, a molecule or a solid surface in our examples) where $[p - T]^{\#}$ stands for the so-called activated complex produced during the scattering process. This activated complex has a finite lifetime and will eventually break up and decay. T^* stands for the final quantum state of the target which is not necessarily equal to the initial quantum state. The theory presented in this section is applicable to more complicated situations where, for example, the products obtained as $[p - T]^{\#}$ breaks apart and can also include fragments of the target or new molecular ions and radicals. Of course, our association of the projectiles, the target and the products with electrons, atoms, molecules and solids is for illustration purposes only, and the theory presented here is applicable to other fields in physics and not necessarily to molecular or surface physics.

The probability of getting from an initial state ϕ_{i} to a final state ϕ_{f} is given by the corresponding S-matrix element,

$$P_{\mathrm{f}\leftarrow\mathrm{i}} = |S_{\mathrm{i,f}}|^2\,, \tag{8.8}$$

where the scattering matrix element is given by

$$S_{\mathrm{f,i}} = \delta_{\mathrm{f,i}} - \mathrm{i}T_{\mathrm{f,i}}\,. \tag{8.9}$$

$T_{\mathrm{f,\,i}}$ is the complex scaled T-matrix element (the asymptotic plane waves in the T-matrix elements are re-normalized such that the flux along the scattering coordinate is independent of the initial wavevector, as mentioned above). When the initial and final states are energy normalized the T-matrix elements are given by

$$T_{\mathrm{f,\,i}}(E) = (\phi_{\mathrm{f}}|V + V\hat{G}_E V|\phi_{\mathrm{i}})\,, \tag{8.10}$$

where $(\cdot\cdot\,|\,\cdot\cdot)$ stands for the complex inner product discussed in detail in Chapter 6. $\hat{G}_E = (E - H)^{-1}$ and $\hat{V}(\mathbf{x},\, r) = V$ describes the interaction potential of the scattered particle and the target where $\{\mathbf{x}\}$ are the internal (or target) coordinates and r is the reaction coordinate. In general three-dimensional problems r should be considered as a vector, however, for the scattering of S-waves this becomes a one-dimensional coordinate which varies from 0 to ∞. This is in contrast to one-dimensional scattering problems where the scattering coordinate varies from $-\infty$ to $+\infty$. The Hamiltonian $\hat{H}$ is given by

$$\hat{H} = \hat{H}_0 + \hat{V}\,, \tag{8.11}$$

where

$$\hat{H}_0 = -\frac{\hbar^2}{2\mu}\,\Delta_r + \hat{h}(\mathbf{x})\,. \tag{8.12}$$

Δ_r stands for the Laplacian operator with respect to the coordinates of the scattered particle and $\hat{h}(\mathbf{x})$ is the Hamiltonian of the target. In this stage of the representation we will carry out an analytical continuation of $H,\ V,\ \phi_{\mathrm{i}},\ \phi_{\mathrm{f}},\ H_0$ and $\hat{G}$ by scaling the reaction coordinate by a complex factor. That is,

$$r \to r\mathrm{e}^{\mathrm{i}\theta}\,, \tag{8.13}$$

where r has real values only and

$$\begin{aligned} V_\theta &= V\left(\mathbf{x},\, r\mathrm{e}^{\mathrm{i}\theta}\right), \\ H_\theta &= \hat{H}\left(\mathbf{x},\, r\mathrm{e}^{\mathrm{i}\theta}\right), \\ \hat{G}_\theta(E) &= \frac{1}{E - \hat{H}_\theta}\,. \end{aligned} \tag{8.14}$$

The energy normalized initial and final states are eigenfunctions of the complex scaled H_0^θ Hamiltonian,

$$\phi_{\mathrm{i}}(\mathbf{x}, r) = \sqrt{\frac{\mu}{\hbar^2|k_{m_{\mathrm{i}}}|\mathrm{e}^{\mathrm{i}\theta}}}\mathrm{e}^{+\mathrm{i}k_{m_{\mathrm{i}}}\mathrm{e}^{\mathrm{i}\theta}r} \cdot \chi_{m_{\mathrm{i}}}(\mathbf{x}) \tag{8.15}$$

and

$$\phi_{\mathrm{f}}(\mathbf{x}, r) = \sqrt{\frac{\mu}{\hbar^2|k_{m_{\mathrm{f}}}|\mathrm{e}^{\mathrm{i}\theta}}}\mathrm{e}^{-\mathrm{i}k_{m_{\mathrm{f}}}\mathrm{e}^{\mathrm{i}\theta}r} \cdot \chi^*_{m_{\mathrm{f}}}(\mathbf{x})\,, \tag{8.16}$$

where χ_m are solutions of the Hamiltonian of the target given by

$$\begin{aligned}\hat{h}(\mathbf{x})\chi_{m_\mathrm{i}}(\mathbf{x}) &= E^\mathrm{th}_{m_\mathrm{i}}\chi_{m_\mathrm{i}}(\mathbf{x})\,,\\ \hat{h}(\mathbf{x})\chi_{m_\mathrm{f}}(\mathbf{x}) &= E^\mathrm{th}_{m_\mathrm{f}}\chi_{m_\mathrm{f}}(\mathbf{x})\,.\end{aligned}\tag{8.17}$$

The complex scaling of the flux normalization factor results from the standpoint of numerical convenience where we wish to keep the integration volume as dr rather than dr $\mathrm{e}^{\mathrm{i}\theta}$. If the reaction coordinate is radial, $-2\mathrm{i}\sin(k\mathrm{e}^{\theta}r)$ replaces the $\mathrm{e}^{-\mathrm{i}k\mathrm{e}^{\mathrm{i}\theta}r}$ in Eqs. (8.15) and (8.16). The initial and final wave vectors are defined such that the total energy of the “particle-target” system is conserved:

$$E = \frac{\hbar^2 k^2_{m_\mathrm{i}}}{2\mu} + E^\mathrm{th}_{m_\mathrm{i}} = \frac{\hbar^2 k^2_{m_\mathrm{f}}}{2\mu} + E^\mathrm{th}_{m_\mathrm{f}}\,.\tag{8.18}$$

Upon complex scaling both the initial state $\phi_{m_\mathrm{i}}(r\mathrm{e}^{\theta}, \mathbf{x})$ and the final state $\phi_{m_\mathrm{f}}(\mathbf{x}, r\mathrm{e}^{\theta})$ are *not* eigenfunctions of $\mathbf{H}^{\theta}_0 = \mathbf{H}_\theta - \mathbf{V}_\theta$ since the initial k_i and the final k_f are real wave vectors.

In the calculation of the complex scaled T-matrix element we first evaluate the right and left eigenfunctions of the full complex scaled Hamiltonian, $\hat{H}_\theta$.

The right and left eigenfunctions of the complex scaled Hamiltonian can be obtained by the diagonalization of the Hamiltonian matrix $\mathbf{H}_\theta$ when $\{\chi_m\}$ are used as a basis function:

$$\psi^\mathrm{R}_n = \sum_m \varphi^\mathrm{R}_{m,\,n}(r)\chi_m(\mathbf{x})\,,\tag{8.19}$$

$$\psi^\mathrm{L}_n = \sum_m \varphi^\mathrm{L}_{m,\,n}(r)\chi_m(\mathbf{x})\,,\tag{8.20}$$

where

$$\begin{aligned}\mathbf{H}_\theta\varphi^\mathrm{R}_n &= E_n\varphi^\mathrm{R}_n\,,\\ \mathbf{H}^\mathrm{T}_\theta\varphi^\mathrm{L}_n &= E_n\varphi^\mathrm{L}_n\,,\\ [H_\theta]_{m',m} &= (\chi_{m'}|\hat{H}(\mathbf{x}, r\mathrm{e}^{\mathrm{i}\theta})|\chi_m)\,.\end{aligned}\tag{8.21}$$

Note that when the Hermitian unscaled full Hamiltonian $\hat{H}$ is real then $\mathbf{H}^\mathrm{T}_\theta = \mathbf{H}_\theta$ and the left-states (labeled by L) and the right-states (labeled by R) are equal. By using the complex eigenvalues and eigenfunctions given in Eqs. (8.20)–(8.21) to construct the complex scaled Green’s operator (see Eq. (8.5)), the complex scaled T-matrix element is obtained by substituting in Eq. (8.10), leading to

$$T_{\mathrm{f,\,i}}(E) = T^\mathrm{direct}_\mathrm{f,\,i} + T^\mathrm{indirect}_\mathrm{f,\,i}\,,\tag{8.22}$$

where the direct part is due to a single scattering event and the indirect part is due to multiple scattering processes. These scattering matrix elements are given by

$$T^{\text{direct}}_{\mathrm{f,i}} = \frac{\mu}{\hbar^2\sqrt{|k_{\mathrm{i}}||k_{\mathrm{f}}|}} \int\int \mathrm{d}r\, \mathrm{d}\mathbf{x}\, \chi^*_{m_{\mathrm{f}}}(\mathbf{x})\, \mathrm{e}^{-\mathrm{i}k_{\mathrm{f}}r}\, V(\mathbf{x}, r)\, \chi_{m_{\mathrm{i}}}(\mathbf{x})\, \mathrm{e}^{+\mathrm{i}k_{\mathrm{i}}r}\,,$$

$$T^{\text{indirect}}_{\mathrm{f,i}} = \mathrm{e}^{\mathrm{i}\theta} \sum_n \frac{a^{\mathrm{L}}(k_{\mathrm{f}})\, a^{\mathrm{R}}(k_{\mathrm{i}})}{E - E_n}\,. \tag{8.23}$$

The summation over n in the indirect term runs over all bound, resonance and rotated continua solutions which are associated with a discrete spectrum due to the use of a finite number of basis functions. E_n are the eigenvalues of the non-Hermitian Hamiltonian which are real for bound states and complex for resonances and rotated continuum states. The multiple scattering coefficients $a^{\mathrm{L}}(k_{\mathrm{f}})$ and $a^{\mathrm{R}}(k_{\mathrm{i}})$ are defined by

$$a^{\mathrm{L}}(k_{\mathrm{f}}) = \int\int \mathrm{d}r\, \mathrm{d}\mathbf{x}\, \chi^*_{m_{\mathrm{f}}}(\mathbf{x})\, \mathrm{e}^{-\mathrm{i}k_{\mathrm{f}}\mathrm{e}^{\mathrm{i}\theta}r}\, V(\mathbf{x}, \mathrm{e}^{\mathrm{i}\theta}r)\, \psi^{\mathrm{R}}_n(r, \mathbf{x})\,,$$

$$a^{\mathrm{R}}(k_{\mathrm{i}}) = \int\int \mathrm{d}r\, \mathrm{d}\mathbf{x}\, \chi_{m_{\mathrm{i}}}(\mathbf{x})\, \mathrm{e}^{+\mathrm{i}k_{\mathrm{i}}\mathrm{e}^{\mathrm{i}\theta}r}\, V(\mathbf{x}, \mathrm{e}^{\mathrm{i}\theta}r)\, \psi^{\mathrm{L}}_n(r, \mathbf{x})\,. \tag{8.24}$$

The following paragraph with some more technical detail is addressed to the readers who wish to carry out scattering calculations within the framework of the non-Hermitian formalism of quantum mechanics. The indirect (multiple scattering) term in Eq. (8.22) is multiplied by the complex factor $\mathrm{e}^{\mathrm{i}\theta}$ since the integration in the Lippmann–Schwinger equation along a complex contour requires maintaining the normalization of the eigenfunctions of the complex scaled Hamiltonian,

$$\int\int \mathrm{d}\mathbf{x}\mathrm{e}^{\mathrm{i}\theta}\mathrm{d}r\, \psi^{\mathrm{L}}_n(\mathbf{x}, r)\psi^{\mathrm{R}}_n(r, \mathbf{x}) = 1\,, \tag{8.25}$$

whereas we required instead that

$$\int\int \mathrm{d}\mathbf{x}\, \mathrm{d}r\, \psi^{\mathrm{L}}_n(\mathbf{x}, r)\psi^{\mathrm{R}}_n(r, \mathbf{x}) = 1 \tag{8.26}$$

and therefore the second term in Eq. (8.22) should be multiplied by $\mathrm{e}^{\mathrm{i}\theta}$ in order to keep the contour of integration as $\mathbf{x}\mathrm{e}^{\mathrm{i}\theta}$. Note that the 2π in the energy normalization factor of the continuum functions cancels out when the T-matrix elements are multiplied by $-2\pi\mathrm{i}$ in the calculations of the scattering matrix elements.

Since the integral in the first term of Eq. (8.22) is unaffected by the value of θ (provided $V(r, \mathbf{x})$ is an analytical function) we choose here to carry this integral along the real r axis.

Note in passing that Eq. (8.22) can be simplified if the exterior scaling procedure is used rather than the commonly used uniform complex scaling. If $r = r$ when

$r \leq r_0$; $r \to (r - r_0)\mathrm{e}^{\mathrm{i}\theta} + r_0$ when $r > r_0$ and $V(\mathbf{x}, r > r_0) = 0$, then the initial and final states and the interaction potential V remain *unscaled*. The only complex functions used in this case in Eq. (8.22) are the left and right eigenfunctions of the exterior-complex-scaled Hamiltonian $\mathbf{H}_\theta$, and the only complex numbers in Eq. (8.22) are the corresponding complex eigenvalues of $\mathbf{H}_\theta$.

Equation (8.22) provides an expression for the T-matrix element that does not suffer from the numerical disadvantages of $T(\theta = 0)$. The continuous spectrum of $\hat{H}$ is discretizised and the complex eigenvalues, E_n^θ, avoid the vanishing of the energy denominators in the Green's operator (see Eq. (8.4)), such that the energy integral in Eq. (8.5) for summation in Eq. (8.22) converges. Another benefit is the inclusion of the resonance states (poles of the S-matrix) in the spectrum of $\hat{H}$, where one resonance eigenstate represents a large number of scattering eigenstates of the non-scaled Hamiltonian. The price we pay for these benefits is the need to confirm the stability of the calculated *complex* T-matrix in terms of the size of the basis set and the need to look for the optimal value of the scaling parameter $\eta = \mathrm{e}^{\mathrm{i}\theta}$, for which Eq. (8.6) is satisfied.

8.1.1 The complex coordinate scattering theory and the Kohn variational principle

On the basis of the c-variational principle proved in Chapter 7, the eigenfunctions of the complex scaled Hamiltonian can be expanded in terms of N square integrable basis functions, Φ_n,

$$|\psi_\alpha) = \sum_{n=1}^{N} C_{n,\alpha}|\Phi_n)\,; \qquad (\psi_\alpha| = \sum_{n=1}^{N} D_{n,\alpha}(\Phi_n|\,. \tag{8.27}$$

The linear variational parameters $\mathbf{C}_\alpha$ and $\mathbf{D}_\alpha$ are respectively the right and left eigenvectors of the complex scaled Hamiltonian matrix H_θ, corresponding to the eigenvalue E_α (real for bound states and complex for resonances and rotated continua).

$$\begin{aligned} \mathbf{H}_\theta \mathbf{C}_\alpha &= E_\alpha \mathbf{C}_\alpha\,, \\ \mathbf{H}_\theta^{\mathrm{T}} \mathbf{D}_\alpha &= E_\alpha \mathbf{D}_\alpha\,, \end{aligned} \tag{8.28}$$

where

$$\left[H_\theta^\theta\right]_{n',n} = (\Phi_{n'}|\hat{H}_\theta|\Phi_n) \tag{8.29}$$

and

$$\hat{H}_\theta = \hat{H}(\mathbf{x}, r\mathrm{e}^{\mathrm{i}\theta})\,. \tag{8.30}$$

Since the Hamiltonian is non-Hermitian (due to the complex scaling) the c-product should be used as an inner product rather than the usual scalar product. Consequently,

$$\mathbf{D}^{\mathrm{T}}\mathbf{C} = 1\,. \tag{8.31}$$

The spectral representation of the Green's operator in terms of the variational eigenfunctions of the complex scaled Hamiltonian matrix

$$\hat{G}_\theta(E) = \sum_\alpha \frac{|\psi_\alpha)\,(\psi_\alpha|}{E - E_\alpha} \tag{8.32}$$

is valid if and only if the eigenfunctions of $\hat{H}_\theta$ form a complete set. As discussed in Chapter 6, for any given finite number of basis functions, N, one can always find well-defined complex values of θ for which the spectrum is incomplete. In such cases the number of non-linear dependent (i.e. "orthogonal") eigenvectors of H_θ is smaller than N. However, under very small variation of θ the spectrum becomes complete (see the relevant discussion on the generalized inner product for non-Hermitian Hamiltonians and the self-orthogonality phenomenon in Chapter 9).

By substituting Eqs. (8.27)–(8.32) into Eq. (8.10) one can get that

$$T = (\phi_{\mathrm{f}}|\hat{V}|\phi_{\mathrm{i}}) + \mathrm{e}^{+2\mathrm{i}\theta}\boldsymbol{\nu}_f^{\mathrm{T}}(\mathbf{C}\mathbf{A}^{-1}\mathbf{D}^T)\boldsymbol{\nu}_{\mathrm{i}}, \tag{8.33}$$

where $\mathbf{A}$ is a diagonal matrix defined by

$$\mathbf{A}_{\alpha,\,\alpha'} = (E - E_\alpha)\,\delta_{\alpha,\,\alpha'} \tag{8.34}$$

and the elements of the vectors $\boldsymbol{\nu}_{\mathrm{f}}$ and $\boldsymbol{\nu}_{\mathrm{i}}$ are given by

$$\begin{aligned} [\boldsymbol{\nu}_{\mathrm{f}}]_n &= (\phi_{\mathrm{f}}|\hat{V}_\theta|\Phi_n)\,,\\ [\boldsymbol{\nu}_{\mathrm{i}}]_n &= (\Phi_n|\hat{\mathbf{V}}_\theta|\phi_{\mathrm{i}})\,, \end{aligned} \tag{8.35}$$

where

$$\hat{V}_\theta = \hat{\mathbf{V}}(\mathbf{x}, r\,\mathrm{e}^{\mathrm{i}\theta})\,. \tag{8.36}$$

Since

$$\mathbf{A} = \mathbf{D}^{\mathrm{T}}[E - \mathbf{H}(\theta)]\mathbf{C}\,, \tag{8.37}$$

by using Eqs. (8.32), (8.33) and (8.37), we get that

$$T = (\phi_{\mathrm{f}}|\hat{V}|\phi_{\mathrm{i}}) + \mathrm{e}^{+2\mathrm{i}\theta}\boldsymbol{\nu}_f^{\mathrm{T}}\mathbf{G}_\theta(E)\boldsymbol{\nu}_{\mathrm{i}}\,, \tag{8.38}$$

where

$$\mathbf{G}_\theta(E) = \frac{1}{E - \mathbf{H}_\theta} . \tag{8.39}$$

This is exactly the result obtained from the Kohn T-matrix variational principle by Nuttall and Cohen.[4]

8.1.2 Resonance scattering: partial widths

Partial widths represent the probability per unit time of obtaining a specific reaction product in a well-defined quantum state in full scattering or half-collision experiments. Resonance scattering theory enables the calculations of partial widths from the "tail" (i.e. asymptote) of a single, time-independent, square integrable resonance wavefunction. This method has been used, so far, in the calculations of the rotational distribution of a diatom in specular and non-specular scattering of the diatom from a solid surface; the rotational distribution of a diatom obtained in a photodissociation of a van der Waals complex; and the probability of ionizing an atom or dissociating a diatom resulting from the absorption of n photons in the presence of very strong electromagnetic fields.

Within the framework of the resonance-scattering-theory, as developed by Moiseyev and Peskin,[5] one assumes that the dynamics of the studied system is controlled by a single intermediate isolated narrow resonance state (i.e., Γ is much smaller than the gap between the resonance position, E_r, and the position of any other resonance state). Under this condition the transition probability from the initial state to the final state is given by

$$P_{\mathrm{f}\leftarrow\mathrm{i}} = |T^\theta_{\mathrm{f,i}}(E)|^2 , \tag{8.40}$$

where the direct transition probability amplitude is zero. By using Eq. (8.22) the complex scaled T-matrix element is approximately given by

$$T_{\mathrm{f,i}}(E) = (\phi_\mathrm{f}|V_\theta + V_\theta \hat{G}_\theta(E) V_\theta|\phi_\mathrm{i}) \simeq \frac{(\phi_\mathrm{f}|V_\theta|\psi_\mathrm{res})(\psi_\mathrm{res}|V_\theta|\phi_\mathrm{i})}{E - E_\mathrm{res}} , \tag{8.41}$$

where

$$\begin{aligned} |\psi_\mathrm{res}) &\sim [1 + \hat{G}_\theta(E) V_\theta]|\phi_\mathrm{i}) , \\ H_\theta|\psi_\mathrm{res}) &= E_\mathrm{res}|\psi_\mathrm{res}) , \\ E_\mathrm{res} &= E_\mathrm{r} - \frac{\mathrm{i}}{2}\Gamma , \\ E_\mathrm{r} - \Delta \le E &\le E_\mathrm{r} + \Delta \end{aligned} \tag{8.42}$$

---

[4] J. Nuttall and H. L. Cohen, *Phys. Rev.* **188**, 1542 (1969).

[5] N. Moiseyev and U. Peskin, *Phys. Rev. A* **42**, 255 (1990).

and Δ should be smaller than the difference between the real part of E_{res} and the nearest resonance position. Note that when $E = E_{\mathrm{res}}$ the denominator in the term on the left-hand side of Eq. (8.41) gets very small (as the resonance width is smaller and the resonance lifetime is larger the denominator gets smaller) and the contribution of the single resonance term to calculated T-matrix elements becomes more dominant.

It is important to notice that the initial state $\phi_{\mathrm{i}}^{\theta}$ and the final state $\phi_{\mathrm{f}}^{\theta}$ in Eq. (8.41) are the complex scaled degenerate eigenfunctions of the *unscaled*, unperturbed $\hat{H}_0$ Hamiltonian which are associated with the real energy E and therefore they are *not* eigenfunctions of the complex scaled unperturbed Hamiltonian

$$\hat{H}_0^{\theta} = \hat{H}_{\theta} - \hat{V}_{\theta}\,. \tag{8.43}$$

The approximation given in Eq. (8.41) holds provided that the contribution of the direct scattering event to the cross section is small relative to the contribution of the multiple-scattering events. In other words, the $\hat{V}_{\theta}\hat{G}(E)\hat{V}_{\theta}$ term is associated with the multiple-scattering events through the Born series expansion where $\hat{G}_{\theta}(E) = \hat{G}_0^{\theta}(E) + \hat{G}_0^{\theta}(E)\,\hat{V}_{\theta}\,\hat{G}_0^{\theta}(E) + \hat{G}_0^{\theta}(E)\,\hat{V}_{\theta}\,\hat{G}_0^{\theta}(E)\,\hat{V}_{\theta}\,\hat{G}_0^{\theta}(E) + \cdots$ and $\hat{G}_0^{\theta}(E) = (E - \hat{H}_0^{\theta})^{-1}$. To avoid interference with the rotated continuum, θ should be large enough to satisfy the following condition:

$$2\left(E_{\mathrm{r}} - E_m^{\mathrm{th}}\right)\tan(2\theta) \gg \Gamma\,, \tag{8.44}$$

where E_m^{th} is the m-th threshold energy which is defined as the discrete m-th real bound state energy of the $\hat{H}_0^{\theta}$ Hamiltonian given in Eq. (8.12). The index m can stand for the initial or one of the possible final states which are all degenerate states of $\hat{H}_0^{\theta}$. This is one of the main advantages of the non-Hermitian formalism of quantum mechanics which enables us to split the contribution of the "white" continuum (by "white" we mean without any specific information that characterizes the studied system and the interaction between the projectiles and the target).

Since the denominator in Eq. (8.41) varies with E much more slowly than the numerator we may keep the energy of the initial and final states (which appear in the calculation of the numerator) fixed at the value of $E = \mathrm{Re}(E_{\mathrm{res}}) = E_{\mathrm{r}}$. This implies that the initial state is associated with a free particle with the *real* wave vector

$$k_{\mathrm{i}} = \frac{\sqrt{2\mu(E_{\mathrm{r}} - E_{\mathrm{i}}^{\mathrm{th}})}}{\hbar} \tag{8.45}$$

whereas the final state is a free particle associated with the *real* wave vector

$$k_{\mathrm{f}} = \frac{\sqrt{2\mu(E_{\mathrm{r}} - E_{\mathrm{f}}^{\mathrm{th}})}}{\hbar}\,. \tag{8.46}$$

However, in order to get analytical closed-form expressions for the resonance partial widths we make another approximation. We assume that the resonance widths are sufficiently small to enable us to replace the real initial and final values of the wave-vectors by *complex* values. Specifically, rather than imposing the conservation condition in Eq. (8.18) the initial and final state complex wave-vectors are obtained under the requirement that *in the complex-coordinate resonance scattering theory the complex energy is conserved* and therefore

$$E_{\mathrm{res}} = E_{\mathrm{r}} - \frac{\mathrm{i}}{2}\Gamma = \frac{(\hbar k_{\mathrm{i}})^2}{2\mu} + E_{\mathrm{i}}^{\mathrm{thres}} = \frac{(\hbar k_{\mathrm{f}})^2}{2\mu} + E_{\mathrm{f}}^{\mathrm{thres}} \,. \tag{8.47}$$

There is no physical justification for the requirement of complex energy conservation! It is an approximation which holds only for sufficiently narrow resonances which provides a simple expression for the transition probability of a particle through a resonance state. The simple formula which will be derived on the basis of this approximation explains the amazing phenomenon of resonance tunneling where a particle passes through a potential barrier at almost 100% probability even though it possesses a much smaller energy than necessary to penetrate the barrier. Consequently, under the approximation that the complex energy is conserved, the *initial complex wave vector* is defined by

$$k_{\mathrm{i}}^{\mathrm{res}} = \frac{\sqrt{2\mu(E_{\mathrm{r}} - E_{\mathrm{i}}^{\mathrm{th}} - \mathrm{i}\Gamma/2)}}{\hbar} \tag{8.48}$$

such that the original energy normalized physical initial state is replaced by

$$(\mathbf{x}, r|\phi_{\mathrm{i}}) = \chi_{\mathrm{i}}^{*}(\mathbf{x})\sqrt{\frac{\mu}{\hbar^2 k_{\mathrm{i}}^{\mathrm{res}} \mathrm{e}^{\mathrm{i}\theta}}}\ \mathrm{e}^{-\mathrm{i}k_{\mathrm{i}}^{\mathrm{res}} r \mathrm{e}^{\mathrm{i}\theta}} \,. \tag{8.49}$$

where $\chi_{\mathrm{i}}(\mathbf{x})$ is an eigenfunction of the target while the incoming plane wave describes the projectile before it hits the target (under the approximation that the real wave vector is replaced by the complex resonance wave-vector). Similarly, the *final complex wave vector* is defined by

$$k_{\mathrm{f}}^{\mathrm{res}} = \frac{\sqrt{2\mu(E_{\mathrm{r}} - E_{\mathrm{f}}^{\mathrm{th}} - \mathrm{i}\Gamma/2)}}{\hbar} \tag{8.50}$$

such that the original energy normalized physical final state is replaced by

$$(\phi_{\mathrm{f}}|\mathbf{x}, r) = \chi_{\mathrm{f}}(\mathbf{x})\sqrt{\frac{\mu}{\hbar^2 k_{\mathrm{f}}^{\mathrm{res}} \mathrm{e}^{\mathrm{i}\theta}}}\ \mathrm{e}^{-\mathrm{i}k_{\mathrm{f}}^{\mathrm{res}} r \mathrm{e}^{\mathrm{i}\theta}} \,. \tag{8.51}$$

The complex scaling parameter $e^{i\theta}$ appears in the denominators of the energy normalized factors since we keep the integration contour on r rather than $e^{i\theta}r$ as we should.

In the radial case where $r \in [0, \infty]$ the functions $\phi_{i,f}(\mathbf{x}, re^{i\theta})$ vanish at $r = 0$ and therefore the exponent $e^{+ik_i re^{i\theta}}$ in Eq. (8.49) is replaced by $2i\sin(k_i re^{i\theta})$. Similarly, the exponent in Eq. (8.51) is replaced by $-2i\sin(k_f re^{i\theta})$.

The conservation of the complex energy implies that the initial and final states and *also* the asymptotes of the resonance states are all eigenfunctions of the complex scaled non-interacting Hamiltonian H_0^θ which is defined in Eq. (8.43). The asymptotes of the resonance eigenfunctions of the complex scaled full Hamiltonian are eigenfunctions of H_0^θ since the interaction potential $\hat{V}$ vanishes when the projectiles are at an infinitely large distance from the target. For example, the target can be a diatomic molecule and the projectile could be an atom or an electron. In another type of experiment the target can be an atom, a molecule or a mesoscopic system like nanotubes where the incoming "particles" could be low-energy photons and the scattered particles are high-energy photons. Following this reasoning, let us consider a case where a resonance state has a several open channels to decay (in more than one dimension it is possible to have more open channels for decay and therefore the number of degenerate states would be larger than two). For example,

$$|\psi^{\text{res}}) \to \begin{cases} |\phi_i) \\ |\phi_f) \\ |\phi_{f'}) \\ |\phi_{f''}) \end{cases} . \tag{8.52}$$

The conservation of complex energy implies that we get that:

$$\begin{aligned}
(E_{\text{res}} - \hat{H}_0^\theta)|\phi_i) &= 0 \, , \\
(E_{\text{res}} - \hat{H}_0^\theta)|\phi_f) &= 0 \, , \\
(E_{\text{res}} - \hat{H}_0^\theta)|\phi_{f'}) &= 0 \, , \\
(E_{\text{res}} - \hat{H}_0^\theta)|\phi_{f''}) &= 0 \, , \\
(E_{\text{res}} - \hat{H}^\theta)|\psi_{\text{res}}) &= 0 \, ,
\end{aligned} \tag{8.53}$$

where the energy-normalized incoming particles are associated with ϕ_i and the outgoing scattered particles with $\phi_f, \phi_{f'}, \phi_{f''}, \ldots$ It should be stressed that all the eigenfunctions of H_0^θ in Eq. (8.53) are associated with complex-scaled free-particle functions with complex wavevectors, and therefore by rotating the contour of integration backward by θ one gets that the outgoing exponentially diverging unscaled functions are the eigenfunctions of the unscaled H_0 Hamiltonian. This is a proof that the complex scaled free particle functions with complex wave vectors are *not* in the Hermitian sector of the domain of the complex scaled Hamiltonian, *unlike* the rotated continuum of the complex scaled non-interacting Hamiltonian H_0^θ given by $|E - E_{\text{th}}|e^{-i2\theta}$ for $E_{\text{th}} \leq |E| \leq \infty$ which are associated with bounded continuum functions that are exactly equal (up to a factor which depends of the normalization conditions) to the solutions of the unscaled non-interacting Hamiltonian H_0 (see Chapter 5).

Under the assumption that the dynamics are controlled by a single complex-scaled resonance state, and under the approximation made above where the initial and the final states are associated with the complex wave-vectors which conserve the complex resonance energy $E_{\text{res}} = E_{\text{r}} - i\Gamma/2$ we will calculate the different probabilities of getting from the *same* initial state to different final states. We will prove that the probability of transition from the initial state to one of the possible final states at the resonance condition where $E = E_{\text{r}}$ is approximately given by

$$P_{\text{f}\leftarrow\text{i}} \simeq 4\frac{\Gamma_{\text{f}}\Gamma_{\text{i}}}{\Gamma^2}\,, \tag{8.54}$$

where $\Gamma = -2\text{Im}(E_{\text{res}})$ is the total rate of decay of the resonance state whereas the partial widths Γ_{f} and Γ_{i} are respectively the rate of decay of the resonance state into the *entrance open channel* i and into the *exit open channel* f. Note these are only two open channels out of many others that might exist. The sum of *all* partial widths (i.e., partial decay rates) is equal to the total resonance width (i.e., total decay rate). That is, $\Gamma = \Gamma_{\text{i}} + \Gamma_{\text{f}} + \Gamma_{\text{f}'} + \Gamma_{f''} + \cdots$. From this we can infer that when the resonance state that controls the dynamics of the scattering process has *more than two* open channels to decay it is not possible to design a simple scattering experiment where $P_{\text{f}\leftarrow\text{i}} = 1$, and the deviation of $P_{\text{f}\leftarrow\text{i}}$ from unity will be very large when the sum of the partial widths associated with the entrance and the exit channels is much smaller than the total rate of decay Γ. When there are two open channels for decay where one of them serves as the entrance channel and the second one as the exit channel, then when the energy E of projectiles is in the interval $E_{\text{r}} - \Gamma < E < E_{\text{r}} + \Gamma$ it is possible to get very close to $P_{\text{f}\leftarrow\text{i}} = 1$ when the total rate of decay is sufficiently small (the resonance state has a long lifetime).

The probability of obtaining from a given initial state which is on the resonance energy condition two different products (i.e., to get from the same entrance open channel into two different exit channels) one should calculate the branching ratio given by

$$\frac{P_{\text{f}\leftarrow\text{i}}}{P_{\text{f}'\leftarrow\text{i}}} = \left|\frac{(\phi_{\text{f}}|\hat{V}_\theta|\psi_{\text{res}})}{(\phi_{\text{f}'}|\hat{V}_\theta|\psi_{\text{res}})}\right|^2 = \frac{\Gamma_{\text{f}}}{\Gamma_{\text{f}'}}\,. \tag{8.55}$$

This is done by evaluating the matrix elements $(\phi_m|\hat{V}_\theta|\psi_{\text{res}})$ where m stands for f, f′, f″, ... for all the open channels. Integration of these matrix elements by parts leads leads to

$$(\phi_m|\hat{V}_\theta|\psi_{\mathrm{res}}) = (\phi_m|\hat{H}_\theta - \hat{H}_0^\theta|\psi_{\mathrm{res}}) = (\phi_m|E_{\mathrm{res}} - \hat{H}_0^\theta|\psi_{\mathrm{res}}) . \tag{8.56}$$

Since by integration by parts $fg'' = gf'' + [fg']' - [gf']'$, where in our case $f = \psi_{\mathrm{res}}$ (right eigenstate of $\hat{H}_\theta$) and $g = \phi_m$ (left eigenstate of $\hat{H}_0^\theta$), one gets that

$$\begin{aligned}&(\phi_m|E_{\mathrm{res}} - \hat{H}_0^\theta|\psi_{\mathrm{res}})\\ &\quad = (\psi_{\mathrm{res}}|E_{\mathrm{res}} - \hat{H}_0^\theta|\phi_m) - \frac{\hbar^2 \mathrm{e}^{-2\mathrm{i}\theta}}{2\mu} \lim_{r\to\infty} \int_{-\infty}^{+\infty} \mathrm{d}\mathbf{x} \left[\frac{\mathrm{d}\phi_m^{\mathrm{L}}}{\mathrm{d}r} \psi_{\mathrm{res}}^{\mathrm{R}} - \frac{\mathrm{d}\psi_{\mathrm{res}}^{\mathrm{R}}}{\mathrm{d}r} \phi_m^{\mathrm{L}} \right] .\end{aligned} \tag{8.57}$$

Assuming that for sufficiently narrow resonances we can take $\hat{H}_0^\theta|\phi_m) = E_{\mathrm{res}}|\phi_m)$, one obtains

$$(\phi_m|\hat{V}_\theta|\psi_{\mathrm{res}}) = -\frac{\hbar^2 \mathrm{e}^{-2\mathrm{i}\theta}}{2\mu} \lim_{r\to\infty} \int_{-\infty}^{+\infty} \mathrm{d}\mathbf{x} \left[\frac{\mathrm{d}\phi_m^{\mathrm{L}}}{\mathrm{d}r} \psi_{\mathrm{res}}^{\mathrm{R}} - \frac{\mathrm{d}\psi_{\mathrm{res}}^{\mathrm{R}}}{\mathrm{d}r} \phi_m^{\mathrm{L}} \right] . \tag{8.58}$$

Note that only the upper limit has to been taken in Eq. (8.58) for two reasons. The first is that in 3D problems the eigenfunctions of the full Hamiltonian and of the non-interacting Hamiltonian vanish at the origin. The second reason is that when r stands for the "reaction" coordinate (e.g., the distance of the projectile from the center of mass of the target) the flux-like term oscillates very rapidly when $r \to -\infty$ and vanishes upon local averaging. In such a case where the flux is oscillating, $\lim_{r\to-\infty}$ is replaced by $\lim_{r''\to-\infty} \int_{r''-\Delta r}^{r''+\Delta r} \mathrm{d}r$. We now get to the final part of the proof of Eq. (8.55). The asymptote of the "ket" resonance state (eigenfunction of $\hat{H}_\theta$) is a linear combination of the products of target eigenstates with the outgoing waves of the projectile which possess complex resonance wave vectors,

$$\lim_{r\to\infty} \psi_{\mathrm{res}}^{\mathrm{R}}(\mathbf{x}, r) = \sum_{m'} \gamma_{m'}^{\mathrm{res}} \phi_{m'}(\mathbf{x}, r) = \sum_{m'} \gamma_{m'}^{\mathrm{res}} \chi_{m'}(\mathbf{x}) \sqrt{\frac{\mu}{\hbar^2 k_{m'} \mathrm{e}^{\mathrm{i}\theta}}}\, \mathrm{e}^{+\mathrm{i}k_{m'} r \mathrm{e}^{\mathrm{i}\theta}} , \tag{8.59}$$

where the coefficients $\gamma_{m'}^{\mathrm{res}}$ have energy units and m' stands for the different open channels for decay (one of them serves as the incoming channel and all the others as outgoing open channels).

By substituting Eq. (8.59) into Eq. (8.58) while using the orthonormality condition

$$(\chi_{m'}|\chi_m) = \delta_{m',m} , \tag{8.60}$$

one gets that

$$(\phi_m|\hat{V}_\theta|\psi_{\mathrm{res}}) = \mathrm{i}\gamma_m^{\mathrm{res}} . \tag{8.61}$$

Therefore by defining the m-th partial width as

$$\Gamma_m = |\gamma_m^{\mathrm{res}}|^2 . \tag{8.62}$$

we proved that

$$|(\phi_m|\hat{V}_\theta|\psi_{\mathrm{res}})|^2 = \Gamma_m \tag{8.63}$$

and we arrived at Eq. (8.55). Accordingly, if we sum over all possible channels we get that

$$-2\mathrm{Im}(E_{\mathrm{res}}) \equiv \Gamma = \sum_m \Gamma_m . \tag{8.64}$$

It is interesting to point out that using our proof that the coefficients $\{\gamma_{m'}^{\mathrm{res}}\}$ are the partial width amplitudes one can calculate the partial widths from the tail of the complex scaled square integrable resonance wavefunction from the following ratio as function of r:

$$\gamma_m^{\mathrm{res}} = \frac{\int \mathrm{d}\mathbf{x}\chi_m^*(\mathbf{x})\psi_{\mathrm{res}}^\theta(\mathbf{x}, r)}{\sqrt{\frac{\mu}{\hbar^2 k_m \mathrm{e}^{\mathrm{i}\theta}}}\ \mathrm{e}^{+\mathrm{i}k_m r \mathrm{e}^{\mathrm{i}\theta}}} . \tag{8.65}$$

The complex value of this ratio which is invariant to the variation of r is the partial width amplitude γ_m^{res}.[6] Formally, this should happen in the limit of $r \to \infty$, while in numerical calculations this is true at the tail of the complex scaled resonance wavefunction.

Exercise 8.1

Using Eq. (8.41) and Eq. (8.61) derive the conditions under which a particle that is almost completely reflected from a single potential barrier will transfer almost completely through two potential barriers. Specifically, by adding another identical potential barrier along the scattering direction the reflection is almost entirely suppressed. This resonance tunneling phenomenon is used in the construction of resonance tunneling diodes and transistors.

8.2 Half collision processes for time-independent systems

In the introduction to this chapter we described the scattering of an atom A from a diatomic molecule BC where an activated complex $[ABC]^\#$ which has a finite lifetime is generated. As time passes this complex breaks apart into the final

---

[6] Recently it has been proved by T. Goldzak, I. Gilary and N. Moiseyev, *Phys. Rev. A* **82**, 05215 (2010), that the complex momentum $\hbar k_m$ in the flux normalization coefficient should be replaced by $\mathrm{Re}(\hbar k_m)$.

products. As discussed above, in many physical situations the scattering process is controlled by a single resonance state of the metastable complex $[ABC]^{\#}$. In such a case we may consider the dynamical process as a half collision process where the system has been initially prepared at the resonance state without the need to discuss how this situation has occurred. Here we will extend this approach to the situation where a bound system such as an ABC molecule is suddenly exposed to an external perturbation. Such a scenario creates a wavepacket $|\Phi_0)$ which may populate several resonance states,

$$|\Phi_0) = \sum_{n(\mathrm{res})} c_n |\psi_n^{\mathrm{res}}) \,. \tag{8.66}$$

Using the c-product discussed in Chapter 6, the coefficients c_n can be calculated by their overlap with the original bound state, ϕ_{i}, (usually the ground state) of the unperturbed Hamiltonian (i.e., the Hamiltonian of the stable ABC molecule).

$$c_n = (\psi_n^{\mathrm{res}}|\phi_{\mathrm{i}}) \,. \tag{8.67}$$

The products obtained from the decay of the perturbed system in this so-called half collision process can be obtained through analytical time propagation of $|\Phi_0)$ to infinite time. The physical situation where a system is exposed to an external perturbation where energy is suddenly "pumped" into it can occur for instance when a molecule is suddenly exposed to a source of high power radiation (such as high intensity lasers) or when it suddenly collides with high energy particles.

First we will focus here on the calculation of the kinetic energy distribution of an ionized electron obtained from an electronically excited molecule, i.e. the result of the process $M^* \to M^+ + \mathrm{e}$. This ionization might be due to an auto-ionization process, Auger process or inter-Coulombic decay (ICD) process. Often the electronic and nuclear motions are strongly coupled and therefore within the framework of the standard (Hermitian) formalism of quantum mechanics the Born–Oppenheimer approximation is not applicable. A clear-cut situation where the adiabatic approximation in the standard formalism of quantum mechanics breaks down is when the ionization is accompanied by molecular dissociation. This situation may arise when a molecular ion is exposed to a high-power external source of energy (e.g., accelerators or free electron lasers) such that $M^+ \to [M^+]^{\#}$ where the molecular positive charged ion $[M^+]^{\#}$ has enough energy to ionize to $[M^{++}] + \mathrm{e}^-$, then the ionization process occurs along with a Coulombic explosion of the doubly positive charged molecular ion $[M^{++}] \to [M_1^+] + [M_2^+]$. For example, $[M^{++}]$ could be Na_2^{++} and the Coulombic explosion results in $2\mathrm{Na}^+$. Unlike the situation when the standard formalism of quantum mechanics is applied, within the framework of the non-Hermitian formalism of quantum mechanics the complex adiabatic approach (i.e., the Born–Oppenheimer approximation) holds and takes into consideration the coupling between the ionization and dissociation processes. In the first step of such calculations the complex eigenvalues of the adiabatic molecular electronic Hamiltonian are evaluated as functions of the geometry of the molecule. The imaginary part of the complex eigenvalues of the non-Hermitian electronic Hamiltonian provides the ionization rate of decay as a function of the geometry of the molecule. In the second step of the calculations the nuclear time-independent Schrödinger equation is solved where one of the complex energies of the non-Hermitian electronic Hamiltonian serves as a complex potential term.

The ability to maintain such an adiabatic picture even when a conventional quantum treatment of this type breaks down leads us towards deriving the non-Hermitian scattering theory for half collision processes within the adiabatic approximation. We begin with a molecular system containing N electrons for which the full Hamiltonian is described by

$$H = T_{\mathrm{nuc}}(R) + H_{\mathrm{elec}}(\{\mathbf{r}_j \ ; j = 1, 2, \ldots, N\}, R)\,, \tag{8.68}$$

where R stands for the nuclear coordinates and $\{\mathbf{r}_j\}$ for coordinates of the N electrons. The electronic Hamiltonian is defined as

$$H_{\mathrm{elec}}(\mathbf{r}_1, \ldots, \mathbf{r}_N, R) \equiv H^{(N)}_{\mathrm{elec}} = H^{\mathrm{f}}_{\mathrm{elec}}(\mathbf{r}_1, \ldots, \mathbf{r}_N, R) + V\,, \tag{8.69}$$

where V is defined such that H^{f} is the Hamiltonian for a molecular ion consisting of $N-1$ electrons and a free electron. Specifically, H^{f} describes the molecular Hamiltonian after ionization has been completed. That is,

$$H^{\mathrm{f}}_{\mathrm{elec}}(\mathbf{r}_1, \ldots, \mathbf{r}_N, R) = H_{\mathrm{elec}}(\mathbf{r}_1, \ldots, \mathbf{r}_{N-1}, R) + \hat{T}_N\,. \tag{8.70}$$

Within the framework of the Born–Oppenheimer approximation

$$\begin{aligned}
&H^{(N)}_{\mathrm{elec}}\varphi_n(\mathbf{r}_1, \ldots, \mathbf{r}_N, R) = E^{(N)}_n(R)\varphi_n(\mathbf{r}_1, \ldots, \mathbf{r}_N, R)\,,\\
&[T_{\mathrm{nuc}} + E^{(N)}_n(R)]\chi_{n,\alpha}(R) = \epsilon^{(N)}_{n,\alpha}\chi_{n,\alpha}(R)\,,\\
&\psi_{n,\alpha}(\mathbf{r}_1, \ldots, \mathbf{r}_N, R) = \varphi_n(\mathbf{r}_1, \ldots, \mathbf{r}_N, R)\chi_{n,\alpha}(R)\,,
\end{aligned} \tag{8.71}$$

where discrete bound states of the N-electron molecule are obtained when

$$E^{(N)}_n(R) < E^{(N)}_{\mathrm{th}}(R) \tag{8.72}$$

and $E^{(N)}_{\mathrm{th}}(R)$ is the threshold energy which depends on the nuclear coordinate. Quasi-continuum states are obtained when

$$E^{(N)}_n(R) > E^{(N)}_{\mathrm{th}}(R)\,. \tag{8.73}$$

In such a case, by imposing outgoing boundary conditions on the solutions of the electronic Hamiltonian within the framework of the Born–Oppenheimer approximation and by using one of the complex scaling transformations described in Chapter 5, one renders the molecular resonance eigenstates square integrable. These state are associated with complex potential energy surfaces (CPES). The imaginary part of the CPES describes the rate of ionization (auto-ionization, Auger or ICD) as a function of the geometry of the molecule.

We are interested in the situation where the molecule has enough energy to ionize. The final state $\psi^{\mathrm{f}}_{n_0,\alpha_0}(\mathbf{r}_1, \ldots, \mathbf{r}_N, R)$ is given by

$$\psi^{\mathrm{f}}_{n_0,\alpha_0}(\mathbf{r}_1, \ldots, \mathbf{r}_N, R) = f_{n_0}(\mathbf{r}_1, \ldots, \mathbf{r}_N, R; \mathbf{k})\chi^{\mathrm{f}}_{n_0,\alpha_0}(R)\,, \tag{8.74}$$

where

$$f_{n_0}(\mathbf{r}_1, \ldots, \mathbf{r}_N, R; \mathbf{k}) = \mathcal{A}\varphi_{n_0}(\mathbf{r}_1, \ldots, \mathbf{r}_{N-1}, R)\phi^{\mathrm{f}}(\mathbf{r}_N) \tag{8.75}$$

and $\mathcal{A}$ is the anti-symmetrizer operator and $\phi^{\mathrm{f}}(\mathbf{r}_N)$ is the flux-normalized wavefunction of the free electron. Within the framework of the mean field approximation, the Coulombic potential is replaced by a Yukawa-like potential and then

$$\phi^{\mathrm{f}}(\mathbf{r}_N) = \sqrt{\frac{m_{\mathrm{e}}}{\hbar k}}[\mathrm{e}^{\mathrm{i}\mathbf{k}\mathbf{r}_N} + \mathcal{R}\mathrm{e}^{-\mathrm{i}\mathbf{k}\mathbf{r}_N}]\,, \tag{8.76}$$

where $\mathcal{R}$ is the reflection coefficient and $\varphi_{n_0}(\mathbf{r}_1, \ldots, \mathbf{r}_{N-1}, R)$ is a bound state of the $(N-1)$-electron molecular ion Hamiltonian, $H^{(N-1)}_{\mathrm{elec}}$ and $f_{n_0}(\mathbf{r}_1, \ldots, \mathbf{r}_N, R; \mathbf{k})$ is the eigenfunction of the "final" Hamiltonian $H^{\mathrm{f}}_{\mathrm{elec}}$ defined in Eq. (8.70),

$$\begin{aligned}&[T_{\mathrm{e}}(\mathbf{r}_N) + H_{\mathrm{elec}}(\mathbf{r}_1, \ldots, \mathbf{r}_{N-1}, R)]f_{n_0}(\mathbf{r}_1, \ldots, \mathbf{r}_N, R; \mathbf{k})\\ &\quad = [E^{(N-1)}_{n_0}(R) + E_{\mathrm{kin}}]f_{n_0}(\mathbf{r}_1, \ldots, \mathbf{r}_N, R; \mathbf{k})\,,\end{aligned} \tag{8.77}$$

where the kinetic energy of the ionized electron is given by

$$E_{\mathrm{kin}} = \frac{\hbar^2|\mathbf{k}|^2}{2m_{\mathrm{e}}}\,. \tag{8.78}$$

The nuclear wavefunction of the molecular ion is given by

$$[T_{\mathrm{nuc}} + E^{(N-1)}_{n_0}(R)]\chi^{\mathrm{f}}_{n_0,\alpha_0}(R) = \epsilon^{(N-1)}_{n_0,\alpha_0}\chi^{\mathrm{f}}_{n_0,\alpha_0}(R)\,. \tag{8.79}$$

Note that $E^{(N-1)}_{n_0}(R)$ can be a repulsive potential energy surface while, for example, $E^{(N)}_{n_0}(R)$ supports a potential well.

Following the Lippmann–Schwinger derivation, an eigenfunction of H that has the asymptote of $|\psi^{\mathrm{f}}_{n_0,\alpha_0})$ with energy $E = \epsilon^{(N-1)}_{n_0,\alpha_0} + E_{\mathrm{kin}}$ is given by

$$\begin{aligned}|\Phi_{n_0,\alpha_0}) &= [1 + G(E)V]|\psi^{\mathrm{f}}_{n_0,\alpha_0}) \\ &= |\psi^{\mathrm{f}}_{n_0,\alpha_0}) + \lim_{\eta\to 0^+} \sum_{n,\alpha} \frac{(\psi_{n,\alpha}|V|\psi^{\mathrm{f}}_{n_0,\alpha_0})}{\epsilon^{(N-1)}_{n_0,\alpha_0} + E_{\mathrm{kin}} - \epsilon^{(N)}_{n,\alpha} + \mathrm{i}\eta}|\psi_{n,\alpha})\,. \qquad (8.80)\end{aligned}$$

Exercise 8.2

The Hamiltonian of a given system is defined as $\hat{H} = \hat{H}_0 + V(\mathbf{r})$ where $\lim_{r\to\infty} V(\mathbf{r}) = 0$. Prove that if $\hat{H}_0\phi = E\phi$ and $\hat{H}\Psi = E\Psi$ then $\Psi = (1 + \hat{G}(E)V)\phi$, where the Green's operator is defined as $\hat{G}(E) = \lim_{\eta\to 0^+}(E - \hat{H} + \mathrm{i}\eta)^{-1}$. Explain why for the most general case both Ψ and ϕ are respectively embedded in the continuum parts of the spectra of $\hat{H}$ and $\hat{H}_0$.

In the derivation of Eq. (8.80) we have used the spectral representation of the Green's operator in the Born–Oppenheimer approximation and by using the box-quantization condition as mentioned above. We also assume that the ionized electron is described by an s-wave function where $\mathbf{k}\cdot\mathbf{r} = kr$.

Equation (8.80) can be rewritten since the inner product involves integration over both the electronic and nuclear coordinates and thus

$$(\psi_{n,\alpha}|V|\psi^{\mathrm{f}}_{n_0,\alpha_0})_{\mathbf{r}_1,\ldots,\mathbf{r}_N,R} = (\chi_{n,\alpha}|\gamma_{n,n_0}(R;k)|\chi^{\mathrm{f}}_{n_0,\alpha_0})_R\,, \qquad (8.81)$$

where

$$\gamma_{n,n_0}(R;k) = (\varphi_n(R)|V|f_{n_0}(R;k))_{\mathbf{r}_1,\ldots,\mathbf{r}_N}\,. \qquad (8.82)$$

Accordingly, Eq. (8.80) rearranges to

$$|\Phi_{n_0,\alpha_0}) = |\psi^{\mathrm{f}}_{n_0,\alpha_0}) + \lim_{\eta\to 0^+} \sum_{n,\alpha} \frac{(\chi_{n,\alpha}|\gamma_{n,n_0}(R;k)|\chi^{\mathrm{f}}_{n_0,\alpha_0})_R}{\epsilon^{(N-1)}_{n_0,\alpha_0} + E_{\mathrm{kin}} - \epsilon^{(N)}_{n,\alpha} + \mathrm{i}\eta}|\psi_{n,\alpha})\,. \qquad (8.83)$$

Now in Eq. (8.83) the integration is taken only over the nuclear coordinates. Using this derivation we can tackle the problem of the kinetic energy distribution of the ionized electron. This distribution results from the preparation of the system at a reference time $t = 0$ in an initial wavepacket which is mainly localized on the $\alpha_\#$-th electronic potential energy surface. That is,

$$|\Phi_0(t = 0)) = \sum_n \xi_n(t = 0, R)|\varphi_n(R))\,, \qquad (8.84)$$

where $\xi_n(t = 0, R)$ are obtained by projecting the initial wavepacket (determined by the experiment) on the eigenfunctions of the non-Hermitian adiabatic electronic Hamiltonian, $\{\varphi_n(\mathbf{r}, R)\}$. Since the adiabatic molecular electronic eigenfunctions are c-normalized, $\sum_n (\xi_n(t = 0)|\xi_n(t = 0)) = 1$. The situation we considered is that the dominant contribution to this expansion is of the $n_\#$-th term such that $(\xi_{n_\#}(t = 0)|\xi_{n_\#}(t = 0)) \simeq 1$.

The kinetic energy distribution of the ionized electron can be evaluated by projecting the initial state of the electronically excited molecular system $|\Phi_0(t = 0))$ on the eigenfunctions of the full Hamiltonian $|\Phi_{n_0,\alpha_0})$ which are associated with the final states $\psi^{\mathrm{f}}_{n_0,\alpha_0}$ that describe a free electron with the kinetic energy E_{kin}. That is,

$$\sigma(E_{\mathrm{kin}}) = \sum_{n_0,\alpha_0} |(\Phi(t = 0)|\Phi_{n_0,\alpha_0})|^2$$

$$\simeq \sum_{n_0,\alpha_0} |\lim_{\eta\to 0} \sum_{n,\alpha} \frac{(\chi_{n,\alpha}|\gamma_{n,n_0}(R;k)|\chi^{\mathrm{f}}_{n_0,\alpha_0})}{\epsilon^{(N-1)}_{n_0,\alpha_0} + E_{\mathrm{kin}} - \epsilon^{(N)}_{n,\alpha} + \mathrm{i}\eta} (\xi_n(t = 0)|\chi_{n,\alpha})|^2 . \quad (8.85)$$

We are now in a position to repeat the derivation presented above when we carry out the integration along a complex contour in the spatial electronic space, $\mathbf{r}_j = F_\theta(\mathbf{r}'_j)$ for $j = 1, 2, \ldots, N$, where $\mathbf{r}'_j$ is a real vector and as $\mathbf{r}_j \to \infty$, $\mathbf{r}_j \to \mathrm{e}^{\mathrm{i}\theta}\mathbf{r}'_j$. In our derivation we use the smooth exterior complex scaling transformation and we do not label the real vectors by $\mathbf{r}'_j$ but keep using the notation of $\mathbf{r}_j$. It is a crucial point in our derivation to carry out this transformation *before* the use of the spectral representation of the Green's operator. That is, $\psi_{n_0,\alpha}$ are the eigenfunctions of the *complex scaled full Hamiltonian* and $E^{(N)}_{n,\alpha}$ are the corresponding eigenvalues of the scaled Hamiltonian. If the eigenfunctions $\psi_{n,\alpha}$ get complex values, *only* because of use of the smooth exterior complex scaling transformation, then the scalar product should be replaced by the c-product, as explained in Chapter 6. However, $f_{n_0}(\mathbf{r}_1, \ldots, \mathbf{r}_N; R, k, \theta)$ are obtained by applying the smooth exterior complex scaling transformation on the unscaled functions which were labeled above as $f_{n_0}(\mathbf{r}_1, \ldots, \mathbf{r}_N; R, k)$, where k has real values. Consequently, after the application of the smooth-exterior complex scaling transformation Eq. (8.100), that was derived within the standard (Hermitian) formalism of quantum mechanics, is replaced by

$$\sigma(E_{\mathrm{kin}}) \simeq \sum_{n_0,\alpha_0} |\sum_{n,\alpha} \frac{(\chi^*_{n,\alpha}|\gamma_{n,n_0}(R;k)|\chi^{\mathrm{f}}_{n_0,\alpha_0})}{\epsilon^{(N-1)}_{n_0,\alpha_0} + E_{\mathrm{kin}} - \epsilon^{(N)}_{n,\alpha}} (\xi_n(t = 0)|\chi_{n,\alpha})|^2 , \quad (8.86)$$

where $\epsilon^{(N-1)}_{n_0,\alpha_0}$ is a *real* eigenvalue of the molecular ionic Hamiltonian H^{f} and $\epsilon^{(N)}_{n_0,\alpha}$ is a *complex* eigenvalue of the smooth-exterior complex scaled neutral molecular

Hamiltonian $\hat{H}$. Within the Born–Oppenheimer approximation $\epsilon^{(N-1)}_{n_0,\alpha_0}$ is an eigenvalue of $T_{\text{nuc}} + E^{(N-1)}_{n_0}(R)$, where $E^{(N-1)}_{n_0}(R)$ is a real eigenvalue of the molecular ion of the complex scaled electronic molecular ionic Hamiltonian associated with a complex scaled bound electronic state, $\varphi^{\text{f}}_{n_0}(\vec{r}_1, \ldots, \vec{r}_{N-1}, R; \theta)$. $E^{(N-1)}_{n_0}(R)$ serves as a potential energy surface (PES) in the nuclear equation of motion of the molecular ion. Similarly, within the Born–Oppenheimer approximation $\epsilon^{(N)}_{n,\alpha}$ is a complex eigenvalue of $T_{\text{nuc}} + E^{(N)}_n(R)$, where $E^{(N)}_n(R)$ is a complex eigenvalue associated with an electronic eigenfunction of the complex scaled electronic molecular Hamiltonian, $\varphi_n(\mathbf{r}_1, \ldots, \mathbf{r}_N; R, \theta)$. $E^{(N)}_n(R)$ serves as a *complex* PES in the molecular dynamics calculations. The complex valued function $\gamma_{n_0}^{\text{complex}}(R; k)$ in Eq. (8.86) is defined as

$$\gamma_{n,n_0}(R;k) = \sum_{j\neq N} \int d\mathbf{r}_1, \ldots, d\mathbf{r}_N \varphi_n(\mathbf{r}_1, \ldots, \mathbf{r}_N; R, \theta) \frac{\mathrm{e}^{-\mathrm{i}\theta}}{|\mathbf{r}_j - \mathbf{r}_N|} f_{n_0}(\mathbf{r}_1, \ldots, \mathbf{r}_N, R; k, \theta), \tag{8.87}$$

where (assuming a Yukawa-like potential)

$$f_{n_0}(\mathbf{r}_1, \ldots, \mathbf{r}_N, R; k, \theta) = \mathcal{A}\varphi^{f}_{n_0}(\mathbf{r}_1, \ldots, \mathbf{r}_{N-1}, R; \theta)\sqrt{\frac{m_{\text{e}}}{\hbar k}} \left(\mathrm{e}^{\mathrm{i}kr_N \mathrm{e}^{\mathrm{i}\theta}} + \mathcal{R}\mathrm{e}^{-\mathrm{i}kr_N \mathrm{e}^{\mathrm{i}\theta}}\right). \tag{8.88}$$

The next step in the derivation is to distinguish between the localized square-integrable resonance states which are associated with θ-independent eigenvalues of the smooth-exterior complex scaled molecular Hamiltonian, and the non-localized quasi-continuum states which are square-integrable only due to the use of the box-quantization condition and are associated with θ-dependent eigenvalues of the smooth exterior complex scaled molecular Hamiltonian. The narrow resonances are embedded close to the real axis and the θ-independent rate of decay $\Gamma_n(R) = -2\text{Im}[E^{(N)}_n(R)]$ is much smaller than $|\text{Re}[E^{(N)}_n(R) - E^{(N)}_{n'}(R)]|$ for any value of $n' \neq n$ and for any value of R. In such a case the resonances are isolated.

Since, due to the initial setup, $\max|(\xi_n(t=0)|\chi_{n,\alpha})|$ is the largest for $n = n_\#$ and since the $n_\#$-th electronic resonance state is an isolated one Eq. (8.86) is reduced to

$$\sigma(E_{\text{kin}}) \simeq \sum_{n_0,\alpha_0} \left| \sum_{\alpha} \frac{(\chi^*_{n_\#,\alpha}|\gamma_{n_\#,n_0}(R;k)|\chi^{\text{f}}_{n_0,\alpha_0})}{\epsilon^{(N-1)}_{n_0,\alpha_0} + E_{\text{kin}} - \epsilon^{(N)}_{n_\#,\alpha}} (\xi_{n_\#}(0)|\chi_{n_\#,\alpha}) \right|^2. \tag{8.89}$$

Another simplification of the calculation of the kinetic energy distribution of the ionized electron can be achieved by making use of the fact that $\gamma_{n_\#,n_0}(R; k = \sqrt{2m_{\text{e}}E_{\text{kin}}})$ varies much slower with E_{kin} in comparison with $[\epsilon^{(N-1)}_{n_0,\alpha_0} + E_{\text{kin}} - \epsilon^{(N)}_{n_\#,\alpha}]^{-1}$. Therefore, one can ignore the dependence of $\gamma_{n_\#,n_0}(R; k = \sqrt{2m_{\text{e}}E_{\text{kin}}})$

on $E_{\rm kin}$ in the calculation of $\sigma(E_{\rm kin})$ by substituting in $\gamma_{n_\#,n_0}$ the *complex* wave vector,

$$k^{\rm res} = \sqrt{2m_{\rm e}[E^{(N)}_{n_\#}(R) - E^{(N-1)}_{n_0}(R)]}. \tag{8.90}$$

Using this approximation for Yukawa-like potentials (the extension to Coulombic potential is possible but is avoided here in order to keep the derivation as simple as possible), we get that

$$\gamma_{n_\#,n_0}(R,k) \to \gamma^{\rm res}_{n_\#,n_0}(R) \equiv \int {\rm d}\mathbf{r}_1 \ldots {\rm d}\mathbf{r}_N \varphi_{n_\#}(R) V(F_\theta(\mathbf{r}_1), \ldots, F_\theta(\mathbf{r}_N))$$

$$\cdot [\mathcal{A}\varphi_{n_0}(F_\theta(\mathbf{r}_1), \ldots, F_\theta(\mathbf{r}_{N-1}), R)\sqrt{\frac{m_{\rm e}}{\hbar k^{\rm res}}}{\rm e}^{+{\rm i}k^{\rm res}{\rm e}^{{\rm i}\theta} r_N}]\,. \tag{8.91}$$

Note that in Eq. (8.91) we set the reflection coefficient $\mathcal{R}$ to zero since the resonance state is associated with outgoing boundary conditions. In Eq. (8.62) we have shown that $|\gamma^{\rm res}_{n_\#,n_0}(R)|$ is the partial width for the ionization of an electron from the $n_\#$-th molecular resonance state to the n_0 open channel and therefore

$$\Gamma_{n_\#}(R) = \sum_{n_0} |\gamma^{\rm res}_{n_\#,n_0}(R)|^2\,. \tag{8.92}$$

Consequently, under the condition that the ionization process is controlled by a single narrow isolated resonance state and there is only one open channel for ionization (i.e., $n_0 = 0$), then the kinetic energy distribution of the ionized electron can be calculated by

$$\sigma_{n_\#}(E_{\rm kin}) \simeq \sum_{\alpha_0} \left| \sum_{\alpha} \frac{(\xi_{n_\#}(t=0)|\chi_{n_\#,\alpha})(\chi^*_{n_\#,\alpha}|\sqrt{\Gamma_{n_\#}(R)}|\chi^{\rm f}_{0,\alpha_0})}{\epsilon^{(N-1)}_{0,\alpha_0} + E_{\rm kin} - \epsilon^{(N)}_{n_\#,\alpha}} \right|^2 . \tag{8.93}$$

A short summary

In the above derivation we have shown that when the ionization process is controlled by a single narrow electronic resonance state the kinetic energy distribution of the ionized electron from an electronic excited molecular system can be obtained when we know the following properties.

(1) A complex potential energy surface, $E_{n_\#}(R)$ which is associated with a molecule in an electronic metastable(resonance) state. The ionization rate of decay as a function of the nuclear coordinates is given by, $\Gamma_{n_\#}(R) = -2{\rm Im}[E_{n_\#}(R)]$.

(2) The initial wavepacket in the nuclear coordinate which is localized on the $n_\#$-th metastable electronic state is given and defined as $\xi_{n_\#}(t=0,R)$.

(3) The potential energy surface of the molecular ion in its ground electronic state, $E_{n_0=0}(R)$.

(4) The solution of the nuclear equation of motion for the complex potential energy surface which is associated with the $n_\#$-th molecular electronic resonance state,

$$\begin{aligned} \hat{H}^{\#}\chi_{n_\#,\alpha}(R) &= \epsilon_{n_\#,\alpha}\chi_{n_\#,\alpha}(R)\,, \\ \hat{H}^{\#} &= T_{\mathrm{nuc}} + E_{n_\#}^{(N)}(R)\,. \end{aligned} \tag{8.94}$$

(5) The solution of the nuclear equation of motion for the real potential energy surface which is associated with the ground state of the molecular ion (i.e, final product),

$$\begin{aligned} \hat{H}^{\mathrm{f}}\chi_{0,\alpha_0}(R) &= \epsilon_{0,\alpha_0}\chi_{0,\alpha_0}(R)\,, \\ \hat{H}^{\mathrm{f}} &= T_{\mathrm{nuc}} + E_{0}^{(N-1)}(R)\,. \end{aligned} \tag{8.95}$$

The spectrum of $\hat{H}^{\mathrm{f}}$ is discrete not only for the bound states but also for the continuum states due to the use of the box-quantization boundary condition.

8.2.1 Wave packet propagation on complex potential energy surfaces

The calculation of the kinetic energy distribution of the ionized electron by the expression given in Eq. (8.93) is equivalent to the result obtained from solving the following time-dependent Schrödinger equation (for a proof see Moiseyev *et al.*[7] or see the solution of Ex. 8.3):

$$\begin{pmatrix} |\xi^{\#}(t)) \\ |\xi^{f}(t)) \end{pmatrix} = \mathrm{e}^{-\mathrm{i}\mathcal{H}t/\hbar} \begin{pmatrix} |\xi^{\#}(0)) \\ 0 \end{pmatrix}, \tag{8.96}$$

where

$$\mathcal{H} = \begin{pmatrix} \hat{H}^{\#} & 0 \\ \sqrt{\Gamma(R)} & \hat{H}^{\mathrm{f}} + E_{\mathrm{kin}} \end{pmatrix}. \tag{8.97}$$

In the formulation of Eq. (8.96) we assume that at $t = 0$ the excitation creates an initial wavepacket, $\xi^{\#}(R, 0)$, which propagates via $\hat{H}^{\#}$ on the intermediate complex potential surface of the decaying state

$$\xi^{\#}(R,t) = \mathrm{e}^{-\mathrm{i}\hat{H}^{\#}t/\hbar}\xi^{\#}(R,0)\,. \tag{8.98}$$

Note that in order to simplify the notation we replace the subscript $n_\#$ that appears in the expressions presented in the pervious section by the super script #. Another assumption in the formulation of Eq. (8.96) is that at every small time step dt the initial wavepacket loses a part which decays to the final state and adds to its wave packet $\xi^{\mathrm{f}}(R,t)$. $\Gamma(R)$ is the rate of decay and $-\mathrm{i}\Gamma(R)/2$ is the imaginary part of the complex potential as it appears in the Hamiltonian $\hat{H}^{\#}$. E_{kin} is the energy

---

[7] N. Moiseyev, S. Scheit and L. S Cederbaum, *J. Chem. Phys.* **121**, 722 (2004).

carried away by the emitted particle (electron) when it arrives on the final potential energy surfaces such that

$$\left(-\mathrm{i}\frac{\partial}{\partial t}+\hat{H}^{\mathrm{f}}+E_{\mathrm{kin}}\right)\xi^{\mathrm{f}}(R,t)=-\sqrt{\Gamma(R)}\xi^{\#}(R,t)\,. \tag{8.99}$$

The resulting electron kinetic energy distribution is given by the norm of the final state, $\xi^{\mathrm{f}}(R,t)$, at the limit of $t\to\infty$:

$$\sigma(E_{\mathrm{kin}})=\lim_{t\to\infty}(\xi^{\mathrm{f}}(t)|\xi^{\mathrm{f}}(t))\,. \tag{8.100}$$

Exercise 8.3

Prove that Eq. (8.100) reduces to Eq. (8.93) when the wavepacket which propagates on the final potential energy surface of the molecular ion is expanded in terms of the eigenfunctions of $\hat{H}^{\mathrm{f}}+E_{\mathrm{kin}}$.

8.3 Time-independent scattering theory for time-dependent systems

The interaction of photons with an atom, molecule or nanostructure can be described either as a photo-ionization process,

$$n\hbar\omega+A\to A^{+m}+m\mathrm{e}^{-}\,, \tag{8.101}$$

where n is the number of absorbed photons, or as a full collision process where the atom/molecule serves as a catalyst. That is,

$$n\hbar\omega+A\to[A/\mathrm{photons}]^{\#}\to A+m\hbar\Omega\,;m=1,2,\ldots,n \tag{8.102}$$

and

$$\Omega=\frac{n}{m}\omega\,. \tag{8.103}$$

When the field intensity is very large (i.e., the flux of photons is very large) rather than using quantum electrodynamics to describe the interaction of the system with the photons one can describe the quantum system which interacts with the classical electromagnetic field which is produced by the laser. In such a case the Hamiltonian is time-dependent. For the sake of coherence of the representation of the time-independent scattering theory for time-dependent Hamiltonians, let us remind the reader that within the dipole approximation the interaction of the (continuous wave) cw laser with the system under study (atom, molecule etc.) is given by $\hat{H}(t) = \hat{H}_{\text{system}} + \epsilon_0 \sum_j \mathbf{e}_x^{\mathrm{T}} \mathbf{r}_j \cos(\omega t)$, where the polarization direction is x and ϵ_0 and ω are respectively the maximum field amplitude and the frequency of the cw laser. In such a case the quasi-stationary solutions of the time-dependent Schrödinger equation are $\Psi(t) = \mathrm{e}^{-\mathrm{i}E^{\mathrm{QE}}t/\hbar}\Phi(t)$, where the quasi-energies E^{QE} and the corresponding time-periodic quasi-energy states $\Phi(t) = \Phi(t + 2\pi/\omega)$ are respectively the eigenvalues and eigenfunctions of the Floquet operator $\hat{\mathcal{H}}(t) = -\mathrm{i}\hbar\partial_t + \hat{H}(t)$, where t serves as an additional coordinate rather than a parameter. The (t, t') method enables us to use a similar formalism for pulsed lasers where $f(t)$ is the envelope of the laser pulse and the time-dependent Hamiltonian is $\hat{H}(t) = \hat{H}_{\text{system}} + \epsilon_0 f(t) \sum_j \mathbf{e}_x^{\mathrm{T}} \mathbf{r}_j \cos(\omega t)$ (see Section 4.6). Following the (t, t') method rather than solving the time-dependent Schrödinger equation, $\Psi(t) = \hat{U}(t \leftarrow 0)\Psi(t = 0)$, where the time evolution operator for time-dependent Hamiltonians is

$$\hat{U}(t \leftarrow 0) = \hat{\mathcal{T}}\mathrm{e}^{-\mathrm{i}\int_0^t \mathrm{d}t' \hat{H}(t')/\hbar} \tag{8.104}$$

and $\hat{\mathcal{T}}$ is a time ordering operator which orders the terms in the Taylor series expansion of the exponents chronologically[8], we use as the time evolution operator

$$\hat{U}(t', t \leftarrow 0) = \mathrm{e}^{-\mathrm{i}\hat{\mathcal{H}}(t')t/\hbar}\,, \tag{8.105}$$

where

$$\hat{\mathcal{H}}(t') = -\mathrm{i}\hbar\partial_{t'} + \hat{H}(t') \tag{8.106}$$

and the Hamiltonian does not have to be time periodic, and in the case where the duration of the laser pulse is T one can impose t' periodic boundary conditions of $\Psi(t', t) = \Psi(t' + mT, t)$ (where $m \geq 1$). The reason we can impose this t' periodic behavior results from the fact that the energy operator of the additional coordinate t' is a first-order derivative rather than a second-order derivative. The only reason there are reflections in a scattering process from the potential barriers and wells is the fact that the kinetic energy operator is a second-order derivative operator where the incoming and outgoing plane waves are degenerate solutions. Since the additional energy term is $-\mathrm{i}\hbar\partial_{t'}$ there are no reflections from the t' potential $f(t')\cos(\omega t')$ and therefore we can impose periodic boundary conditions on the propagated wavepacket. We may say that we apply a train of laser pulses rather than a single pulse where the time interval between the laser pulses is determined by the value of mT. It was proved by Peskin and Moiseyev that the propagated wavepacket obtained by the (t, t') method reduces to the solution of the

---

[8] See, for example, the discussion in section 9.3 of *Introduction to Quantum Mechanics – a Time Dependent Perspective* by David J. Tannor, Sausalito, CA, University Science Books (2007).

time-dependent Schrödinger equation with time-dependent Hamiltonian when we take the cut $t' = t$, i.e. $\Psi(t) = [\hat{U}(t', t \leftarrow 0)\Psi(t = 0)]_{t'=t}$. The fact that the (t, t') evolution operator is as in the cases where the Hamiltonian is a time (t) independent operator enables us to derive here a time-dependent scattering theory for a time-dependent Hamiltonian. The advantage of using the non-Hermitian formalism in the cases where the Hamiltonian is time-dependent is similar to the advantages in the cases where the Hamiltonian is time-independent. The light induced process is often described by a single or small number of Feshbach-type resonances that are all square integrable functions and can be calculated by well-established computational methods that originally were developed for the calculations of bound states. Moreover, even in the cases that in the calculations of cross sections we need to take into consideration the interference of the resonances with the rotated continuum, it does not require heavy numerical calculations as in the standard formalism since the rotated continuum is a "white continuum" which has a monotonic variation in the density of states and therefore can be represented as standing waves calculated within the framework of the finite-box quantization approximation.

Before getting into the derivation of the non-Hermitian time-independent scattering theory for time-dependent systems, we wish to emphasize two points. The first is a technical one. $\mathcal{H}$ is the Floquet operator when the Hamiltonian is time-periodic and its use simplifies the calculations based on our theory, and for this reason we will discuss the properties of the Floquet operator, although as stressed above the use of the (t, t') formalism enables us to derive time-independent scattering theory even for the cases where pulsed lasers are used. The second point we wish to emphasize here is the ability to use the theory presented in this chapter to derive simple expressions for the high-harmonic generation (HHG) spectra and above-threshold ionization (ATI) spectra (both briefly described in Chapter 2). These expressions can be used to explain and to predict different features and properties in the HHG and ATI spectra even without the need to carry out numerical calculations. Yet, they also simplify the numerical calculations of the HHG and ATI spectra in comparison to any other ab-initio method within the standard formalism of quantum mechanics.

The study of photo-induced dynamics in strong laser fields within the framework of the standard (Hermitian) formalism of quantum mechanics requires the time-dependent propagation of an initial given wavepacket. Wavepacket propagation calculations are carried out by solving the time-dependent Schrödinger equation (TDSE) with a time-dependent Hamiltonian $\hat{H}(t)$ which describes the field-free system (atom, molecule, cluster, solid or nano-structured material) which interacts with strong laser fields. When the strong field induces ionization then, even when $\hat{H}(t)$ is a time-periodic operator, as in the case of a system which interacts with a cw laser, one cannot describe the photo-induced dynamics by calculating a *single* Floquet state since the spectrum of the Floquet operator, $\hat{\mathcal{H}} = -i\hbar\partial_t + \hat{H}(t)$, is continuous. This limitation is removed when the time-dependent Schrödinger equation is solved with the restriction of outgoing boundary conditions which do not conserve the flux of the electrons and result in a non-Hermitian Floquet-type operator. By applying one of the complex scaling transformations $\mathbf{r} \to F_\theta(\mathbf{r})$ which are described in Chapter 5, the photo-induced resonance eigenstates of the complex scaled Floquet operator become square integrable and are in the generalized Hilbert space.

This approach holds many benefits. Beside the numerical advantages due to the fact that the solution of the complex scaled TDSE is often dominated by a single resonance Floquet state, analytical expressions can be derived for many observable quantities. These include, for example, the cross sections, the coherent high-frequency emitted radiation and the kinetic energy distributions of the photo-induced ionized electrons (read about the high-harmonic generation (HHG) phenomenon and the above-threshold-ionization phenomenon in Chapter 2). These analytical expressions for the cross sections provide insight into the photo-induced process without the need to carry out heavy numerical calculations. For example, it enables one to derive selection rules for the HHG spectra, design experiments by which the HHG and ATI processes can be controlled and explain other experimental observations which are often hard to explain by standard QM formalism. One such example is the observation of odd-order harmonics in the high-harmonics spectra generated from an atom under intense laser radiation even when the duration of the laser pulse is short and supports a very small number of optical cycles (an optical cycle is defined as $T = 2\pi/\omega$, where ω is the fundamental laser frequency).

8.3.1 Resonance photo-induced ionization decay rates by the non-Hermitian formalism of quantum mechanics

As explained above, the derivation of time-independent scattering theory for time-periodic Hamiltonians is based on Floquet theory. More specifically, on the non-Hermitian (complex scaled) Floquet theory and its extension by the (t, t') method to general time-dependent problems (read about (t, t') in Chapter 4). Since the spectral representation of the complex scaled Green's operator is carried out when the eigenfunctions of the complex scaled Floquet operator are used as a basis set, we will devote this subsection to the eigenvalues of the non-Hermitian complex scaled Floquet operator which are associated with the photo-induced resonance phenomenon. In what follows we will prove that the complex scaled photo-induced resonance wave functions are square integrable.

The time-dependent Hamiltonian of the atom or molecule interacting with the electromagnetic field consists of two terms. The first term is of the field-free Hamiltonian which describes the system under study, $\hat{H}_S$. The second term describes the interaction of the system which consists of N charged particles (electrons and nuclei) with the strong electromagnetic field. Within the framework of the dipole approximation this interaction is given by

$$\hat{V}(t) = \sum_{j=1}^{N} q_j \mathbf{r}_j \cdot \mathbf{E}(t)\,, \tag{8.107}$$

where q_j is the charge of the j-th particle, $\mathbf{r}_j$ is its position in the atomic/molecular center of mass frame and the electric field vector is given by $\mathbf{E}(t) = (E_x(t), E_y(t), E_z(t))$. When z is taken as the light propagation axis then $E_z(t) = 0$. For circularly polarized light $E_x^2(t) + E_y^2(t) = \epsilon_0^2$, where ϵ_0 is a time-independent maximum field amplitude. The interaction of a linearly polarized field with an atom can be written within the dipole approximation as

$$\hat{V}(t) = \epsilon_0 e \sum_j x_j^{\text{elec}} f(t) \cos(\omega_{\text{L}} t - k_{\text{L}} Z)\,, \tag{8.108}$$

where ϵ_0 is the maximum field amplitude of the ac field which oscillates along the x-axis, e is the charge of the electrons which interact with the laser field, ω_{L} is the laser field frequency, $k_{\text{L}} = \omega_{\text{L}}/c$ is the wave vector, Z is the center of mass coordinate of the particle and $f(t)$ is the envelope of the laser field. Often it is approximated as $f(t) = \sin(\omega_{\text{L}} t/N_{\text{opt}}) = \sin(2\pi t/(N_{\text{opt}} T))$, where $0 \leq t \leq T$ and the duration of the laser field is about equal to N_{opt} optical cycles. The duration of one optical cycle is given by $T = 2\pi/\omega_{\text{L}}$.

The complex scaled Floquet-type operator is denoted here by $\hat{H}_{\text{F}} = -\mathrm{i}\hbar\partial_t + \hat{H}_{\text{S}} + \hat{V}(t)$, where the coordinates of the charged particles which can ionize (electrons) and/or are dissociate (nuclei), $\mathbf{r}_j$, are transformed to $\mathbf{F}_\theta(\mathbf{r}_j)$, where $\mathbf{F}$ is a complex vector in three-dimensional space which depends on the selected contour of integration. Following the non-Hermitian variational principle derived in Chapter 7, the eigenvalues of the complex scaled Floquet-type operator can be obtained by calculating the eigenvalues of the Floquet matrix which is constructed by using a direct product of spatial basis functions denoted by $\phi_k(\mathbf{r})$, where $k = 1, 2, \ldots, N_r$ (these can be, for example, the eigenfunctions of the field-free Hamiltonian) and a periodic time-dependent basis set. A convenient basis for this analysis is a Fourier basis set $\mathrm{e}^{\mathrm{i}\omega n t}$, where $n = 0, \pm 1, \pm 2, \ldots, N_t$ and $\omega = 2\pi/T$. The value of T is a problem-dependent parameter. In the case of cw lasers where the field is time periodic, i.e., $\mathbf{E}(t) = \mathbf{E}(t + T)$ then, as stated above, $T = 2\pi/\omega_{\text{L}}$ and ω_{L} is the cw laser frequency. In this case T is the period of one oscillation of the electromagnetic field (see the relevant discussion and Fig. 2.3). When the setup of the problem involves multiple color cw lasers with frequencies ωq, where $q = 1, 2, \ldots,$ then we use for the construction of the basis functions $T = 2\pi/\omega$.

The resonance eigenvalues of the complex scaled Floquet matrix (which do not have to be complex and symmetric) are the θ-independent eigenvalues which are assigned two quantum numbers since the real parts of the Floquet operator are defined up to modulo $\hbar\omega$, where ω is the frequency used in the construction of the time-dependent Fourier basis functions. That is, the resonance quasi-energy eigenvalue of the Floquet-type operator is given by

$$E_{\alpha,n} = [\epsilon_\alpha + \hbar\omega n] - \frac{\mathrm{i}}{2}\Gamma_\alpha\,, \tag{8.109}$$

where $\alpha = 1, 2\ldots,\ n = 0, \pm 1, \pm 2, \ldots$ and Γ_α is the photo-induced ionization decay rate of the α-th resonance state. It is clear from this discussion that the α-th quasi-energy resonance state is associated with multi-copies of the same eigenvalues defined modulo $\hbar\omega$. Therefore, it is more reasonable to calculate the eigenvalues of the time-evolution Floquet-type operator $U(T \leftarrow 0) = \mathrm{e}^{-\mathrm{i}\hat{\mathcal{H}}(x,t')T/\hbar}$ which are defined as λ_α, rather than the eigenvalues of the Floquet-type matrix. The relationship between the eigenvalues of the time-evolution operator and the eigenvalues of the Floquet-type operator is given by

$$\lambda_\alpha = \mathrm{e}^{-\mathrm{i}\frac{E_{\alpha,n}T}{\hbar}}\,, \tag{8.110}$$

exactly like the relationship between the eigenvalues of $\mathrm{e}^{-\mathrm{i}\hat{H}t/\hbar}$ and the eigenvalues of the time-independent Hamiltonian $\hat{H}$. The eigenstates of the time-evolution operator in the (t, t') representation $\mathrm{e}^{-\mathrm{i}\hat{\mathcal{H}}T/\hbar}$ are the eigenfunctions of the complex-scaled non-Hermitian Floquet operator at $t = 0$ (note that the eigenfunctions of $\hat{H}_\mathrm{F}$ are time-periodic functions). The rate of photo-ionization decay associated with the α-th QE resonance state is obtained from Eq. (8.110),

$$\Gamma_\alpha = -\frac{2\hbar}{T}\ln|\lambda_\alpha|\,. \tag{8.111}$$

In variational calculations where a finite Floquet matrix is diagonalized the dependence of the resonance eigenvalues on θ decreases as the basis set becomes more complete (for the use of the cusp condition to obtain stationary variational complex resonance eigenvalues see Chapter 7).

Exercise 8.4

Consider a system which interacts with a linearly polarized cw laser with frequency ω_L. Derive an expression for the complex scaled time-evolution operator,

$$U(0 \to T) = \exp(-\mathrm{i}\hat{\mathcal{H}}(t')T/\hbar)\,, \tag{8.112}$$

by using as basis functions the direct product of the field-free eigenstates of the system and t'-dependent Fourier functions, where $\hat{\mathcal{H}}(t')$ is the Floquet operator. Note that here,

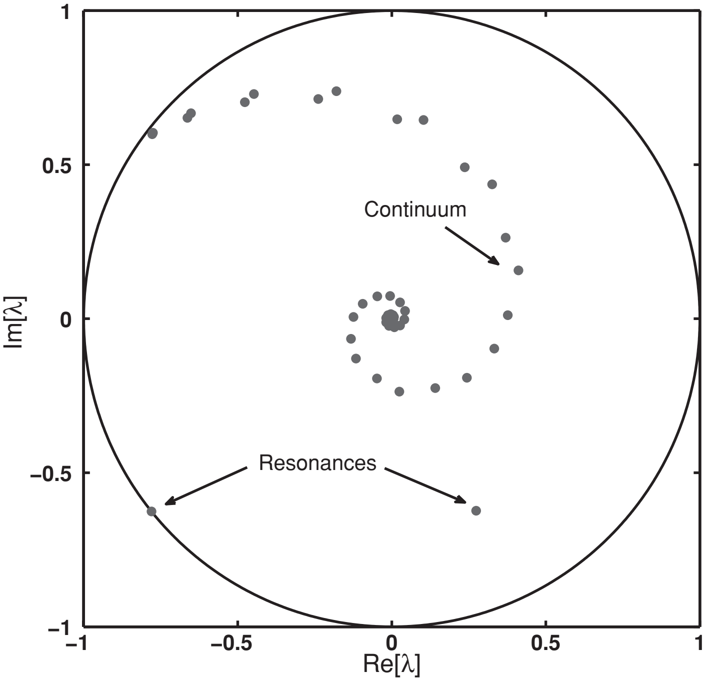

Figure 8.1 The real vs. the imaginary parts of the eigenvalues, E_α, of the complex time-evolution matrix as obtained by the (t, t') method (see Eq. (8.245)) applied to a 1D model Hamiltonian of a xenon atom which interacts with a linear polarized laser field. All quantities are given in au.

in order to distinguish between time in the complex scaled Floquet operator, which is used as an additional coordinate, and the physical time appearing in the time evolution operator we have used the (t, t') notation as originally defined by Peskin and Moiseyev. Derive the expression for $U(0 \to T)$ on a grid of points for t. Explain the numerical advantage of calculating the photo-induced resonances when the laser field is strong by the diagonalization of the complex time-evolution matrix over the calculation of the resonance positions and widths by the diagonalization of the Floquet Hamiltonian matrix.

In Fig. 8.1 we show the complex eigenvalues, E_α, of the complex scaled time-evolution matrix for the same 1D model Hamiltonian of a xenon atom in a strong laser field which was used for the calculations of the resonances by the diagonalization of the complex scaled Floquet Hamiltonian matrix. The resonances are associated with the isolated points inside the unit circle in the complex E_α plane. As the resonance solution is located closer to the center of the circle its lifetime is smaller. The rotated continuum is represented by a spiral where the threshold energy is located close to the edge of the unit circle. Since there are two open channels for decay for a symmetric 1D potential the spiral of rotated continuum appears twice (i.e., degenerate rotated continua). Any deviation from a complete degeneracy results from the use of a non-complete basis set in the numerical calculations and the use of box quantization.

8.3.2 The complex-scaled resonance wave functions of atoms/molecules in intense time-periodic laser fields

For the sake of simplicity we will associate the field-free system (e.g., an atom or a molecule) which interacts with an intense time-periodic electromagnetic field with an effective one-dimensional, single electron model Hamiltonian,

$$\hat{H}_{\mathrm{FF}} = \frac{\hat{p}_x^2}{2\mu} + \hat{V}(x)\,. \tag{8.113}$$

The extension of the derivations given below to many-electron systems is quite straightforward and we avoid it here in order to simplify the notation. We assume that the field-free potential vanishes asymptotically,

$$\lim_{x\to\infty} \hat{V}(x) = 0\,, \tag{8.114}$$

and thus as $x \to \infty$ a free particle is obtained. This means that we refer to short-range potentials and exclude the case of the "pure Coulombic" potential. However, on the basis of the works of Balslev–Combes and Simon[9] the conclusions will hold also for a "pure Coulombic" potential.

The most direct proof that the photo-induced complex scaled resonance functions are square integrable is when one uses the acceleration representation, since only in this representation, even for cw lasers, the ionized electrons are free outgoing particles.

In this representation the origin of the coordinates oscillates with the same frequency, ω_{L}, as the electromagnetic field, $E(t) = E(t+T)$, where $T = 2\pi/\omega_{\mathrm{L}}$. From the "point of view" of the oscillating electron(s) the field-free potential oscillates in time. The time-dependent complex scaled Hamiltonian in the *acceleration gauge* is given by

$$\hat{H}^{\mathrm{ac}}(t) = \mathrm{e}^{-2\mathrm{i}\theta}\frac{\hat{p}_x^2}{2\mu} + V\left(x\mathrm{e}^{\mathrm{i}\theta} - \frac{1}{\mu}\int_0^t A(t')\mathrm{d}t'\right)\,, \tag{8.115}$$

---

[9] E. Balslev and J. M. Combes, Spectral properties of many-body Schrödinger operators with dilatation-analytic interactions, *Comm. Math. Phys.* **22**, 280–294 (1971); B. Simon, Resonances in n-body quantum systems with dilatation analytic potentials and the foundation of time-dependent perturbation theory. *Ann. Math.* **97**, 247–274 (1973).

where, following Maxwell's equations, the time average of the periodic electromagnetic vector potential $A(t)$ has to vanish, i.e., $\int_0^T A(t)\mathrm{d}t = 0$. The time-oscillating electric field, $E(t)$, is defined by

$$E(t) = -\frac{\mathrm{d}}{\mathrm{d}t}A(t)\,. \tag{8.116}$$

In Gaussian units $E(t) = -\frac{1}{c}\frac{\mathrm{d}}{\mathrm{d}t}A(t)$, where c is the speed of light in vacuum. For the sake of clarity let us assume here that the field-free Hamiltonian does not support any resonance states and that the eigenvalues of the non-Hermitian field-free Hamiltonian $\hat{H}_{\mathrm{FF}}(x\mathrm{e}^{\mathrm{i}\theta})$ consist of discrete *real* bound state energy levels and *complex* continuous eigenvalues which are associated with the rotated continuum, $E_{\mathrm{c}} = |E_{\mathrm{c}}|\mathrm{e}^{-2\mathrm{i}\theta}$, where $0 \le |E_{\mathrm{c}}| \le \infty$. The photo-induced resonances are associated with the discrete solutions of the time-dependent complex-scaled Schrödinger equation (to simplify the notation we drop the θ dependence from the complex scaled Hamiltonian, complex scaled Floquet operator etc.),

$$\hat{H}^{\mathrm{ac}}(x,t)\Psi_j^{\mathrm{res}}(x,t) = \mathrm{i}\hbar\frac{\partial}{\partial t}\Psi_j^{\mathrm{res}}(x,t)\,, \tag{8.117}$$

which are often referred to as the quasi-energy solutions such that

$$\Psi_j^{\mathrm{res}}(x,t) = \mathrm{e}^{-\mathrm{i}E_j^{\mathrm{res}}t/\hbar}\Phi_j^{\mathrm{res}}(x,t)\,, \tag{8.118}$$

where $\Phi_j^{\mathrm{res}}(x,t) = \Phi_j^{\mathrm{res}}(x,t+T,\theta)$ are the time-periodic eigenfunctions of the complex scaled Floquet operator in the acceleration gauge,

$$\hat{\mathcal{H}}^{\text{ac-gauge}}(x,t) = -\mathrm{i}\hbar\partial_t + \hat{H}^{\mathrm{ac}}(x,t) \tag{8.119}$$

associated with the resonance complex quasi-energy eigenvalues

$$E_j^{\mathrm{res}} = \epsilon_j - \frac{\mathrm{i}}{2}\Gamma_j\,, \tag{8.120}$$

such that

$$\hat{\mathcal{H}}^{\text{ac-gauge}}(x,t)[\mathrm{e}^{\mathrm{i}\omega_{\mathrm{L}}nt}\Phi_j^{\mathrm{res}}(x,t)] = [(\epsilon_j + \hbar\omega_{\mathrm{L}}n) - \frac{\mathrm{i}}{2}\Gamma_j][\mathrm{e}^{\mathrm{i}\omega_{\mathrm{L}}nt}\Phi_j^{\mathrm{res}}(x,t)]\,, \tag{8.121}$$

where

$$n = 0, \pm1, \pm2, \pm3, \ldots \tag{8.122}$$

The resonance positions, $(\epsilon_j + \hbar\omega_{\mathrm{L}}n)$, and widths, Γ_k, are θ-invariant values when θ exceeds certain values for which the corresponding resonance eigenfunctions, $\Phi_j^{\mathrm{res}}(x,t)$, are square integrable functions. This becomes evident by analyzing the asymptotes of $\Phi_j^{\mathrm{res}}(x,t)$ which possess outgoing boundary conditions and are solutions of the potential-free Floquet Hamiltonian,

$$\hat{\mathcal{H}}^{\text{ac-gauge}}(x \to \infty, t) = -\mathrm{i}\hbar\partial_t + \mathrm{e}^{-2\mathrm{i}\theta}\frac{\hat{p}_x^2}{2\mu}, \tag{8.123}$$

since $V(x\mathrm{e}^{\mathrm{i}\theta} - \mu^{-1}\int_0^t A(t')\mathrm{d}t') \to 0$ as $x \to \infty$. Therefore, the asymptotes of $\Phi_j^{\text{res}}(x, t)$ are given by

$$\lim_{x\to\infty} \Phi_j^{\text{res}}(x, t) = A_j \mathrm{e}^{\mathrm{i}k_j^{\text{res}}\mathrm{e}^{\mathrm{i}\theta}x}, \tag{8.124}$$

where the complex discrete values of the momentum $\hbar k_j$ (when $j = 1, 2, \ldots$) are associated with the complex resonance eigenvalues of the complex scaled Floquet operator,

$$\hbar k_j = \sqrt{2\mu\left(\epsilon_j - \frac{\mathrm{i}}{2}\Gamma_j\right)}. \tag{8.125}$$

Note that in the calculation of the complex momentum of the resonance we have taken into consideration the fact that the threshold energies are $\hbar\omega_{\mathrm{L}}n$. By substituting the polar representation of the complex momentum, $\hbar k_j^{\text{res}} = \hbar|k_j^{\text{res}}|\mathrm{e}^{-\mathrm{i}\alpha_j^{\text{res}}}$, where

$$\alpha_j^{\text{res}} = \arctan\left(\frac{\Gamma_j}{2\epsilon_j}\right), \tag{8.126}$$

into Eq. (8.124) one gets that the asymptotes of $\Phi_j^{\text{res}}(x, t)$ can be expressed by

$$\lim_{x\to\infty} \Phi_j^{\text{res}}(x, t) = A_j \mathrm{e}^{\mathrm{i}|k_j^{\text{res}}|\mathrm{e}^{\mathrm{i}(\theta-\alpha_j^{\text{res}})}x} = A_j \mathrm{e}^{\mathrm{i}|k_j^{\text{res}}|\cos(\theta-\alpha_j^{\text{res}})x}\mathrm{e}^{-|k_j^{\text{res}}|\sin(\theta-\alpha_j^{\text{res}})x}, \tag{8.127}$$

From the second exponent in this expression it is clear that as $x \to \infty$ the function vanishes provided that $\theta - \alpha_j^{\text{res}} \geq 0$. Thus we can safely assume that the periodic resonance eigenfunctions of the complex scaled Floquet operator (in the acceleration gauge) are square integrable. This proof is very similar to the proof given in Chapter 5 for the resonances associated with a time-independent Hamiltonian. However, it is not self-evident that such a proof holds for a time-dependent Hamiltonian. As we will show below, on the basis of the proof presented above for the acceleration representation of the time-dependent Hamiltonian we will prove that the complex scaled photo-induced resonances are square integrable functions when other representations are used (such as the momentum (velocity) and the length gauges). First we will transform the square integrable complex scaled photo-induced resonance function as obtained above for the acceleration presentation of the time-periodic Hamiltonian, to another function which will be proved below to be the square integrable complex scaled photo-induced resonance function obtained in the momentum (velocity) gauge. The proof is as follows.

By carrying out the Krammers–Henneberger transformation $\Phi_j^{\mathrm{res}}(x,t)$ can be expressed as

$$\Phi_j^{\mathrm{res}}(x,t) = \exp\left[-\frac{\mathrm{i}}{\hbar}\int_0^t \mathrm{d}t'\left(\mathrm{e}^{-\mathrm{i}\theta}\hat{p}_x\frac{A(t')}{\mu} - \frac{A^2(t')-C}{2\mu}\right)\right]\phi_j^{\mathrm{res}}(x,t)\,, \tag{8.128}$$

where

$$C = \frac{1}{T}\int_0^T \mathrm{d}t' A^2(t')\,. \tag{8.129}$$

The insertion of the parameter C into the transformation is necessary in order to ensure the periodicity of $\phi_j^{\mathrm{res}}(x,t)$.

The transformed resonance function $\phi_j^{\mathrm{res}}(x,t)$ is a square integrable function since

$$\lim_{x\to\infty}\phi_j^{\mathrm{res}}(x,t) = \exp\left[-\frac{\mathrm{i}}{\hbar}\int_0^t \mathrm{d}t'\left(\mathrm{e}^{-\mathrm{i}\alpha_j}|k_j|\frac{A(t')}{\mu} - \frac{A^2(t')-C}{2\mu}\right)\right]\cdot$$
$$\cdot A_j \lim_{x\to\infty}\mathrm{e}^{\mathrm{i}|k_j^{\mathrm{res}}|\cos(\theta-\alpha_j^{\mathrm{res}})x}\cdot\mathrm{e}^{-|k_j^{\mathrm{res}}|\sin(\theta-\alpha_j^{\mathrm{res}})x} = 0\,. \tag{8.130}$$

By substituting Eq. (8.128) into Eq. (8.121) one gets that the *square integrable* resonance functions $\phi_j^{\mathrm{res}}(x,t)$, where $j = 1, 2, \ldots$ are the eigenfunctions of the complex scaled p-gauge Floquet operator,

$$\hat{\mathcal{H}}^{\text{p-gauge}}(x,t)[\mathrm{e}^{\mathrm{i}\omega_{\mathrm{L}}nt}\phi_j^{\mathrm{res}}(x,t)] = \left[(\epsilon_j + \hbar\omega_{\mathrm{L}}n) - \frac{\mathrm{i}}{2}\Gamma_j\right][\mathrm{e}^{\mathrm{i}\omega_{\mathrm{L}}nt}\phi_j^{\mathrm{res}}(x,t)]\,, \tag{8.131}$$

where

$$\hat{\mathcal{H}}^{\text{p-gauge}}(x,t) = -\mathrm{i}\hbar\partial_t + \hat{H}^{\mathrm{p}}(x,t) \tag{8.132}$$

and the complex scaled time-dependent Hamiltonian in the *momentum gauge* is given by

$$\hat{H}^{\mathrm{p}}(x,t) = \frac{[\mathrm{e}^{-\mathrm{i}\theta}\hat{p}_x - A(t)]^2}{2\mu} + V(x\mathrm{e}^{\mathrm{i}\theta})\,. \tag{8.133}$$

By carrying out another time-periodic transformation we will obtain the resonance eigenfunctions of the complex scaled Floquet operator in the length gauge which we will show are also square integrable functions. This will be accomplished by expressing $\phi_j^{\mathrm{res}}(x,t)$ as

$$\varphi_j^{\mathrm{res}}(x,t) = \mathrm{e}^{-\frac{\mathrm{i}}{\hbar}x\mathrm{e}^{\mathrm{i}\theta}A(t)}\phi_j^{\mathrm{res}}(x,t)\,. \tag{8.134}$$

Since $\phi_j^{\mathrm{res}}(x,t) \to 0$ and $\mathrm{e}^{-\frac{\mathrm{i}}{\hbar}x\mathrm{e}^{\mathrm{i}\theta}A(t)} \to 0$ as $x \to \infty$ it is clear that for any value of j, $\varphi_j^{\mathrm{res}}(x,t)$ decays to zero at the asymptotes. By substituting Eq. (8.134) into Eq. (8.131) one gets that the square integrable resonance functions $\varphi_j^{\mathrm{res}}(x,t)$ are eigenfunctions of the complex scaled Floquet operator in the length gauge,

$$\hat{\mathcal{H}}^{\text{l-gauge}}(x,t)[\mathrm{e}^{\mathrm{i}\omega_{\mathrm{L}}nt}\varphi_j^{\mathrm{res}}(x,t)] = [(\epsilon_j + \hbar\omega_{\mathrm{L}}n) - \frac{\mathrm{i}}{2}\Gamma_j][\mathrm{e}^{\mathrm{i}\omega_{\mathrm{L}}nt}\varphi_j^{\mathrm{res}}(x,t)]\,, \tag{8.135}$$

where

$$\hat{\mathcal{H}}^{\text{l-gauge}}(x,t) = -\mathrm{i}\hbar\partial_t + \hat{H}^l(x,t) \tag{8.136}$$

and the complex scaled time-dependent Hamiltonian in the *length gauge* is given by

$$\hat{H}^{\mathrm{l}}(x,t) = \mathrm{e}^{-\mathrm{i}2\theta}\frac{\hat{p}_x^2}{2\mu} + V(x\mathrm{e}^{\mathrm{i}\theta}) + \left[\frac{\mathrm{d}}{\mathrm{d}t}A(t)\right]x\mathrm{e}^{\mathrm{i}\theta}\,. \tag{8.137}$$

This completes the proof that the complex scaled photo-induced resonance wavefunctions are square integrable regardless of the gauge which is used.

Exercise 8.5

(1) Derive an expression for the resonance quasi-energy position and widths for a many-electron atom which interacts with a cw laser within the framework of non-Hermitian perturbation theory up to second order. Use the time-dependent Hamiltonian in the acceleration gauge as a basis for the analysis and explain why the first-order correction term vanishes.

(2) The zero-order resonance quasi-energies obtained in (1) depend on the amplitude of the quiver motion of the free electron which is given by $\alpha_0 = \frac{e\epsilon_0}{\mu\omega_{\mathrm{L}}^2}$. Find a transformation for which the eigenvalues of the zero-order transformed Floquet operator depends explicitly on two parameters, the laser frequency ω_{L} and the maximum field amplitude ϵ_0. This is in contrast to (1) where only one parameter α_0 effects the zero-order Hamiltonian. Such a transformation was first introduced by Gilary and Moiseyev.[10]

8.3.3 The non-Hermitian adiabatic theorem for time-dependent open systems

The question we address here is whether the adiabatic theorem can apply to the cases where the Hamiltonian is time-dependent. In particular, when the laser field amplitude is described as $e\,f(t)\cos(\omega_{\mathrm{L}}t)$, where e is the electron charge, $f(t)$ is

---

[10] I. Gilary and M. Moiseyev, *Phys. Rev. A* **66**, 063415 (2002).

the envelope of the laser field which describes the on and off switching of the laser and ω_{L} is the fundamental laser frequency. When the field-free system is bound the applicability of adiabatic theory to time-dependent systems can be studied in a very similar manner to that used in applying adiabatic theory to bound eigenstates of time-independent Hamiltonians. The situation is very different for the case that the field-free Hamiltonian has, besides bound states, also a continuous energy spectrum. For such an open system the adiabatic theorem is not applicable within the framework of the standard (Hermitian) formalism of quantum mechanics (see the work of Kohn and co-workers from 1997[11]). However, within the framework of the non-Hermitian formalism of quantum mechanics the photo-induced resonance eigenfunctions of the complex scaled Floquet operator are square integrable and therefore the adiabatic theorem is applicable. The non-Hermitian adiabatic theorem is based on the assumption that $f(t)$ varies sufficiently slowly in time in order to justify the assumption that the photo-induced resonance solutions adiabatically follow the variation of $f(t)$. This variation in the envelope is in fact equivalent to variation of the maximum field amplitude as the laser is turned on and off. As we see, there are two different characteristic time scales in our problem. The slow time scale is associated with the change of $f(t)$ in time, whereas the fast time scale is the oscillations of the field amplitude with time which is given by $\cos(\omega_{\mathrm{L}}t)$. Therefore, we will derive the non-Hermitian adiabatic theorem when the interaction of the open system with the laser is described as $e\, f(t')\cos(\omega_{\mathrm{L}}t'')$.

We will now proceed to present a derivation of the adiabatic theorem for general time-dependent open systems given by Fleischer and Moiseyev.[12] In this derivation there are no bound states and the resonances aren't necessarily narrow. We will use the non-Hermitian Floquet formalism which allows us to describe the dynamics in term of resonance quasi-energy eigenfunctions of the non-Hermitian complex scaled Floquet-type operator. The non-Hermitian derivation of the adiabatic theorem will show us that often the photo-induced dynamics is controlled by a *single* resonance quasi-energy state even when the laser field intensity is high and the duration of the laser pulse is short and supports a small number of optical cycles.

The derivation of the adiabatic theorem for time-dependent open systems is based on the the extended (t, t') formalism. Therefore the reader is advised to refresh his knowledge by reading the brief review of the (t, t') method which is given in Chapter 4. On the physical motivation for using two different characteristic time scales for this problem see the introduction to this subsection.

---

[11] D. W. Hone, R. Ketzmerik and W. Kohn, Time-dependent Floquet theory and absence of an adiabatic limit, *Phys. Rev. A* **56**, 4045–4054 (1997).

[12] A. Fleischer and N. Moiseyev, Adiabatic theorem for non-Hermitian time-dependent open systems. *Phys. Rev. A* **72**, 032103 (2005).

By the term "extended" (t, t') formalism we mean that, in the same manner presented, one may add any number of time "coordinates" to the Schrödinger equation as one wishes, if by this a better understanding or an easier solution of the problem is achieved. Here we will show that by addition of two time "coordinates" to the time-dependent Schrödinger equation (TDSE) the derivation of the adiabaticity criteria for photo-induced dynamical systems is simplified. In this sense, we are using here a (t, t', t'') formalism.

For the sake of simplicity and without loss of generality, the dynamics of a single active electron in an atom or molecule subjected to a pulse of strong monochromatic linearly polarized laser radiation is studied here. The Hamiltonian is given by

$$\hat{\mathcal{H}}(\mathbf{r}, t)\Psi^{\mathrm{R}}(\mathbf{r}, t) = \mathrm{i}\hbar\frac{\partial}{\partial t}\Psi^{\mathrm{R}}(\mathbf{r}, t)\,, \tag{8.138}$$

where

$$\hat{\mathcal{H}}(\mathbf{r}, t) = H_0(\mathbf{r}) - e\mathbf{r}\cdot\mathbf{f}(t)\cos(\omega_{\mathrm{L}}t) \tag{8.139}$$

and

$$\mathbf{f}(t) \equiv \varepsilon_0\mathbf{e}_k f(t)\,. \tag{8.140}$$

Here $f(t)$ is the function which describes the envelope of the laser pulse and $\mathbf{f}(t)$ is a vector as defined in Eq. (8.140); ε_0 is the laser's amplitude, $\mathbf{e}_k$ is a unit vector in the direction of the electric component of the laser field, ω_{L} is the laser's frequency, with $T = 2\pi/\omega_{\mathrm{L}}$ the optical period. $H_0(\mathbf{r})$ is the field-free Hamiltonian and the vector operator $\mathbf{r}$ describes the internal degrees of freedom (the coordinates are complex-scaled throughout).

Since $\mathrm{d}F(t)/\mathrm{d}t = [\partial_t G(t, t', t'') + \partial_{t'} G(t, t', t'') + \partial_{t''} G(t, t', t'')]_{t'=t''=t}$, where $G(t, t' = t, t'' = t) = F(t)$,

$$\hat{\mathcal{H}}(\mathbf{r}, t', t'') \equiv \widetilde{H}(\mathbf{r}, t', t'') - \mathrm{i}\hbar\frac{\partial}{\partial t'} - \mathrm{i}\hbar\frac{\partial}{\partial t''}\,, \tag{8.141}$$

where

$$\widetilde{H}(\mathbf{r}, t', t'') \equiv H_0(\mathbf{r}) - e\mathbf{r}\cdot\mathbf{f}(t'')\cos(\omega_{\mathrm{L}}t') \tag{8.142}$$

and t', t'' should be regarded as additional *coordinates*. The t'' coordinate is associated with the envelope function which describes how fast the laser field is turned on and off while the t' coordinate is associated with the oscillating electric field which is induced by the running laser waves.

Upon complex scaling of the spatial coordinates $\hat{\mathcal{H}}(\mathbf{r}, t', t'')$ becomes non-Hermitian. Therefore the inner c-product should be used. The quasi-energy solutions of this complex-scaled Floquet-type operator are:

$$\hat{\mathcal{H}}(\mathbf{r}, t', t'')\psi_k^{\mathrm{R}}(\mathbf{r}, t', t'') = E_k\psi_k^{\mathrm{R}}(\mathbf{r}, t', t''), \tag{8.143}$$

$$\hat{\mathcal{H}}^{\dagger *}(\mathbf{r}, t', t'')\psi_k^{\mathrm{L}}(\mathbf{r}, t', t'') = E_k\psi_k^{\mathrm{L}}(\mathbf{r}, t', t''), \tag{8.144}$$

where the symbol $\hat{\mathcal{H}}^{\dagger *}$ doesn't stand for an operator but for the transpose of the matrix representing the operator $\hat{\mathcal{H}}$. The eigenfunctions form a complete set in the extended Hilbert space of functions in $\mathbf{r}, t', t''$.

Say we want to solve the following TDSE with the initial state $\widetilde{\Psi}(\mathbf{r}, t', t'', t = 0)$:

$$\hat{\mathcal{H}}(\mathbf{r}, t', t'')\widetilde{\Psi}^{\mathrm{R}}(\mathbf{r}, t', t'', t) = \mathrm{i}\hbar\frac{\partial}{\partial t}\widetilde{\Psi}^{\mathrm{R}}(\mathbf{r}, t', t'', t). \tag{8.145}$$

The solution to this equation is

$$\widetilde{\Psi}^{\mathrm{R}}(\mathbf{r}, t', t'', t) = \mathrm{e}^{-\frac{\mathrm{i}}{\hbar}\hat{\mathcal{H}}(\mathbf{r},t',t'')t}\widetilde{\Psi}^{\mathrm{R}}(\mathbf{r}, t', t'', t = 0) = \sum_k c_k\mathrm{e}^{-\frac{\mathrm{i}}{\hbar}E_k t}\psi_k^{\mathrm{R}}(\mathbf{r}, t', t''). \tag{8.146}$$

This solution has a corresponding function $\widetilde{\Psi}^{\mathrm{L}}(\mathbf{r}, t', t'', t)$, which is *not* a solution of any Schrödinger equation, which is defined by

$$\widetilde{\Psi}^{\mathrm{L}}(\mathbf{r}, t', t'', t) = \sum_k c_k\mathrm{e}^{+\frac{\mathrm{i}}{\hbar}E_k^* t}\psi_k^{\mathrm{L}}(\mathbf{r}, t', t''). \tag{8.147}$$

By taking the cut $t' = t'' = t = 0$ on Eq. (8.146) it is immediately evident that we have a solution of the original TDSE where the expansion coefficients are

$$c_k = (\psi_k^{\mathrm{L}}(\mathbf{r}, t', t'')|_{t'=t''=0}|\widetilde{\Psi}^{\mathrm{R}}(\mathbf{r}, t', t'', t)|_{t'=t''=t=0})_{\mathbf{r}}. \tag{8.148}$$

This is true since any of the eigenstates of Eq. (8.143) on the cut $t' = t'' = t$, (i.e. $\mathrm{e}^{-\frac{\mathrm{i}}{\hbar}E_k t}\psi_k^{\mathrm{R}}(\mathbf{r}, t', t'')|_{t'=t''=t}$) is a solution of the original time-dependent Schrödinger equation and therefore any linear combination of these solutions is also a solution.

We now return to the derivation of the adiabatic theorem for non-Hermitian open systems. We would like to treat t'' as an adiabatic coordinate. This is the "coordinate" associated with the envelope of the pulse which usually varies much slower than the carrier frequency of the field. This would be done in the same way that the electronic motion is separated from the nuclear one in the treatment of molecules within the Born–Oppenheimer approximation. First we define the following operator:

$$H_{\mathrm{ad}}(\mathbf{r}, t', t'') \equiv \widetilde{H}(\mathbf{r}, t', t'') - \mathrm{i}\hbar\frac{\partial}{\partial t'}, \tag{8.149}$$

where t'' should be regarded as a parameter for now. This means that this Hamiltonian is a Floquet Hamiltonian describing the interaction of the atom with a cw laser of strength ε_1, where, following Eq. (8.140),

$$\varepsilon_1 = |\mathbf{f}(t)| = \varepsilon_0 f(t)\,. \tag{8.150}$$

The eigenstates of this operator form a complete basis (in the $\mathbf{r} - t'$ function space) for every value of the parameter t'':

$$H_{\mathrm{ad}}(\mathbf{r}, t', t'')\psi_\alpha^{\mathrm{ad,R}}(\mathbf{r}, t', t'') = \varepsilon_\alpha^{\mathrm{ad}}(t'')\psi_\alpha^{\mathrm{ad,R}}(\mathbf{r}, t', t'')\,. \tag{8.151}$$

Notice that, due to the complex scaling, E_k and $\varepsilon_\alpha^{\mathrm{ad}}(t'')$ are complex.

We can now expand each eigenstate of the complete problem (Eq. (8.143)) in this basis:

$$\psi_k^{\mathrm{R}}(\mathbf{r}, t', t'') = \sum_{\alpha'} \psi_{\alpha'}^{\mathrm{ad,R}}(\mathbf{r}, t', t'')\chi_{\alpha',k}(t'')\,. \tag{8.152}$$

By substituting Eq. (8.152) into Eq. (8.143), multiplying the obtained equation from the left-hand side by $\psi_{\alpha'}^{\mathrm{ad,L}}(\mathbf{r}, t', t'')$ and integrating over $\mathbf{r}$ and t', one gets the following equality in matrix notation,

$$\left[-\mathrm{i}\hbar\frac{\partial}{\partial t''}\mathbf{I} + (\mathbf{E}^{\mathrm{ad}}(t'') + \mathbf{V}(t''))\right]\chi_k(t'') = E_k\chi_k(t'')\,, \tag{8.153}$$

where

$$\begin{aligned}
[\mathbf{E}^{\mathrm{ad}}(t'')]_{\alpha,\alpha'} &= \varepsilon_\alpha^{\mathrm{ad}}(t'')\delta_{\alpha,\alpha'}\,,\\
\left[\mathbf{V}(t'')\right]_{\alpha,\alpha'} &= ((\psi_\alpha^{\mathrm{ad,L}}(\mathbf{r}, t', t'')| - \mathrm{i}\hbar\frac{\partial}{\partial t''}|\psi_{\alpha'}^{\mathrm{ad,R}}(\mathbf{r}, t', t'')))_{\mathbf{r},t'}\,,\\
\left[\chi_k(t'')\right]_\alpha &= \chi_{\alpha,k}(t'')\,.
\end{aligned} \tag{8.154}$$

Notice that in the case that the matrix on the left-hand side of Eq. (8.153) is diagonal, a homogeneous systems of uncoupled equations is obtained. In such a case one should solve each equation separately. Therefore, the sum in Eq. (8.152) reduces to a single product. This is exactly analogous to the adiabatic approximation in the context of the Born–Oppenheimer approximation. The next step in our derivation is to represent the matrix $(\mathbf{E}^{\mathrm{ad}}(t'') + \mathbf{V}(t''))$ by its spectral decomposition,

$$[\mathbf{E}^{\mathrm{ad}}(t'') + \mathbf{V}(t'')]\mathbf{D}^{\mathrm{R}}(t'') = \mathbf{D}^{R}(t'')\mathbf{W}(t'')\,, \tag{8.155}$$

$$[\mathbf{E}^{\mathrm{ad}}(t'') + \mathbf{V}(t'')]^t\mathbf{D}^{\mathrm{L}}(t'') = \mathbf{D}^{\mathrm{L}}(t'')\mathbf{W}(t'')\,, \tag{8.156}$$

The matrix of eigenvalues $\mathbf{W}(t'')$ is diagonal and the right and left eigenvectors are normalized with respect to each other in order to maintain the correct inner product:

$$[\mathbf{D}^{\mathrm{L}}(t'')]^{t}\mathbf{D}^{\mathrm{R}}(t'') = \mathbf{I}\,. \tag{8.157}$$

In the case that the matrix $(\mathbf{E}^{\mathrm{ad}}(t'') + \mathbf{V}(t''))$ is not strictly diagonal we can use first-order perturbation theory to find the first-order deviation from diagonal. If we treat the matrix $\mathbf{V}(t'')$ as perturbation, we get that

$$[\mathbf{D}^{\mathrm{R}}(t'')]_{\alpha',\alpha} = \delta_{\alpha',\alpha} + \frac{[\mathbf{V}(t'')]_{\alpha',\alpha}}{\varepsilon^{\mathrm{ad}}_{\alpha}(t'') - \varepsilon^{\mathrm{ad}}_{\alpha'}(t'')}\,. \tag{8.158}$$

This matrix will be diagonal to a good approximation if

$$A_\alpha(t'') \equiv \sum_{\alpha'\neq\alpha} |[\mathbf{D}^{\mathrm{R}}(t'')]_{\alpha',\alpha}| \ll 1\,, \tag{8.159}$$

which produces the following adiabaticity criterion:

$$A_\alpha(t'') \equiv \sum_{\alpha'\neq\alpha} \left| \frac{((\psi^{\mathrm{ad}}_{\alpha}(\mathbf{r},t',t'')| - \mathrm{i}\hbar\frac{\partial}{\partial t''}|\psi^{\mathrm{ad}}_{\alpha'}(\mathbf{r},t',t'')))_{\mathbf{r},t'}}{\varepsilon^{\mathrm{ad}}_{\alpha'}(t'') - \varepsilon^{\mathrm{ad}}_{\alpha}(t'')} \right| \ll 1\,. \tag{8.160}$$

Using the specific form of the Hamiltonian of the problem given in Eq. (8.139) and the Hellman–Feynman theorem one gets the adiabatic condition for time-dependent open systems:

$$|e|\hbar\varepsilon_0 \left|\frac{\mathrm{d}f(t'')}{\mathrm{d}t''}\right| \sum_{\alpha'\neq\alpha} \left| \frac{((\psi^{\mathrm{ad,L}}_{\alpha}(\mathbf{r},t',t'')|\mathbf{r}\cdot\mathbf{e}_k\cos(\omega_{\mathrm{L}}t')|\psi^{\mathrm{ad,R}}_{\alpha'}(\mathbf{r},t',t'')))_{\mathbf{r},t'}}{(\varepsilon^{\mathrm{ad}}_{\alpha'}(t'') - \varepsilon^{\mathrm{ad}}_{\alpha}(t''))^2} \right| \ll 1\,. \tag{8.161}$$

The index α is a super-index since in Eq. (8.151) it is easily seen that not only is $\psi^{\mathrm{ad,L/R}}_{\alpha}(\mathbf{r},t',t'')$ a solution of the eigenvalue equation, with eigenvalue $\varepsilon^{\mathrm{ad}}_{\alpha}(t'')$, but also $\mathrm{e}^{\mathrm{i}\omega_{\mathrm{L}}mt'}\psi^{\mathrm{ad,L/R}}_{\alpha}(\mathbf{r},t',t'')$ is a solution, with the eigenvalue $\varepsilon^{\mathrm{ad}}_{\alpha}(t'') + \hbar\omega_{\mathrm{L}}m$, for any integer m. Let us take all the states whose corresponding eigenvalues lie in the interval $[0,\hbar\omega_{\mathrm{L}}]$ (the first Brillouin zone) and define them to have an index $m=0$; we call these states $\phi^{\mathrm{ad,L}}_{j}(\mathbf{r},t',t'')$, $\phi^{\mathrm{ad,R}}_{j}(\mathbf{r},t',t'')$, and the corresponding eigenvalues $E^{\mathrm{ad}}_{j}(t'')$, and accordingly all of the solutions are given by:

$$\psi^{\mathrm{ad,R}}_{\alpha}(\mathbf{r},t',t'') \equiv \phi^{\mathrm{ad,R}}_{j}(\mathbf{r},t',t'')\mathrm{e}^{\mathrm{i}\omega_{\mathrm{L}}mt'}\,, \tag{8.162}$$

$$\psi^{\mathrm{ad,L}}_{\alpha}(\mathbf{r},t',t'') \equiv \phi^{\mathrm{ad,L}}_{j}(\mathbf{r},t',t'')\mathrm{e}^{\mathrm{i}\omega_{\mathrm{L}}mt'}\,, \tag{8.163}$$

$$\varepsilon^{\mathrm{ad}}_{\alpha}(t'') \equiv E^{\mathrm{ad}}_{j}(t'') + \hbar\omega_{\mathrm{L}}m\,, \tag{8.164}$$

where

$$0 \le E^{\mathrm{ad}}_{j}(t'') \le \hbar\omega_{\mathrm{L}}\,. \tag{8.165}$$

Thus, the index α actually counts both the position of the quasi-energy within the first Brillouin zone (the index j) and the Brillouin zone itself (the index m). With respect to the generalized inner product, two states with one or more of the indices (j, m) different are orthogonal.

Going back to Eq. (8.161) now, it is evident that the probability of coupling an initial adiabatic state $\psi^{\mathrm{ad}}_{\alpha=(j,0)}(\mathbf{r}, t', t'')$ to any other adiabatic state $\psi^{\mathrm{ad}}_{\alpha'=(j',m')}(\mathbf{r}, t', t'')$ is given by

$$A_{(j,0)}(t'') = F(t'') \cdot \sum_{j' \neq j} a^{(j)}_{(j')}(t'') \,, \tag{8.166}$$

where

$$F(t'') = |e|\hbar\varepsilon_0 \left| \frac{\mathrm{d}f(t'')}{\mathrm{d}t''} \right| \tag{8.167}$$

and

$$a^{(j)}_{(j')}(t'') = \sum_{m \neq 0} |c^{(j,0)}_{(j',m)}(t'')| \,. \tag{8.168}$$

The functions $c^{(j,0)}_{(j',m)}(t'')$, that will be termed here from now on as *"adiabatic cross terms"*, are given by

$$c^{(j,0)}_{(j',m)}(t'') = \frac{((\phi^{\mathrm{ad,L}}_{j}(\mathbf{r}, t', t'')|\mathbf{r} \cdot \mathbf{e}_k \cos(\omega_{\mathrm{L}} t') \mathrm{e}^{\mathrm{i}\omega_{\mathrm{L}} m t'} |\phi^{\mathrm{ad,R}}_{j'}(\mathbf{r}, t', t'')))_{\mathbf{r},t'}}{(E^{\mathrm{ad}}_{j'}(t'') - E^{\mathrm{ad}}_{j}(t'') + \hbar\omega_{\mathrm{L}} m)^2} \,. \tag{8.169}$$

Since the energies $E^{\mathrm{ad}}_{j'}(t'')$ are complex (the Hamiltonian is non-Hermitian) then for $j \neq j'$ it is most unlikely that $E^{\mathrm{ad}}_{j'} = E^{\mathrm{ad}}_{j}$. It is clear that the denominator hardly ever vanishes even when $m = 0$. This holds true even when $j = j'$ but $m \neq 0$.

Therefore, the criterion for a pulse to be considered adiabatic is that the following condition will be fulfilled:

$$A_{(j,0)}(t'') \ll 1 \,. \tag{8.170}$$

Which is the adiabatic state $\psi^{\mathrm{ad}}_{\alpha=(j,0)}(\mathbf{r}, t', t'')$ whose couplings to all other states $\psi^{\mathrm{ad}}_{\alpha'=(j',m')}(\mathbf{r}, t', t'')$ should remain small in the adiabatic limit? Assuming that before the action of the field the system is initially in a stationary state of the field-free problem $\varphi_j(\mathbf{r})$ (relying on the superposition principle of the solutions of the TDSE that generality is not lost by this assumption) and provided that the field is switched on and off adiabatically, this Floquet resonanace state $\psi^{\mathrm{ad}}_{\alpha=(j,0)}(\mathbf{r}, t', t'')$ is the state which is "born" from the stationary state $\varphi_j(\mathbf{r})$ as the field is switched on. If the process is not done adiabatically many Floquet resonance states will be populated, resulting in considerable couplings with $\psi^{\mathrm{ad}}_{\alpha=(j,0)}(\mathbf{r}, t', t'')$ leading to the collapse of the adiabatic condition in Eq. (8.170). The only adiabatic criteria which is physically meaningful is one in which α *denotes a resonance state*. However, α' *stands for both resonances and rotated continuum states*.

One should notice that the derivation of the adiabatic theorem presented above holds even for many-electron systems where the symbol $\mathbf{r}$ can stand for the coordinates of all electrons. The same arguments will also hold for a polychromatic radiation, where the cw field is a collection of monochromatic fields with different frequencies ω_i and phases φ_i.

Notice that for a given problem (given spectral profile of the cw field and a given field-free potential), the sum over the absolute value of the adiabatic cross terms should be calculated as a function of the effective cw-field intensity (which is characterized here through t'') *only once*. The adiabatic cross terms should then be converted to some functions of time, through the explicit time-dependence of the pulse envelope, and then the sum of their absolute values should be multiplied by the slope of the pulse envelope and by the maximal field intensity to obtain the final expression which indicates whether the adiabatic criteria are fulfilled or not.

It is easily seen in Eq. (8.167) that for a given system, the shape and intensity of the laser pulse determine its adiabaticity since these parameters influence the shape-derivative term. Accordingly, a short pulse which is switched on and off abruptly and has a high maximal intensity will most likely be not adiabatic.

In the case that the adiabaticity criteria are fulfilled, the sum over different channels in Eq. (8.152) can be reduced to a single product:

$$\psi^{\mathrm{R}}_{k,j}(\mathbf{r}, t', t'') \cong \phi^{\mathrm{ad,R}}_{j}(\mathbf{r}, t', t'')\chi_{j,k}(t'') \tag{8.171}$$

and the adiabatic states are assigned two good quantum numbers k and j. The solution to the eigenvalue equation of Eq. (8.153) is now ($[\mathbf{V}(t'')]_{\alpha,\alpha'} \approx 0$):

$$\chi_{j,k}(t'') = \mathrm{e}^{+\frac{\mathrm{i}}{\hbar}E_k t''}\mathrm{e}^{-\frac{\mathrm{i}}{\hbar}\int^{t''}\mathrm{d}\tau E^{\mathrm{ad}}_{j}(\tau)}\,. \tag{8.172}$$

By using Eq. (8.146), Eq. (8.171) and Eq. (8.172) we get that the adiabatic solution, in the (t, t', t'') formalism, is given by

$$\widetilde{\Psi}^{\mathrm{R}}(\mathbf{r}, t', t'', t) = \left[\sum_{k} c_k \mathrm{e}^{-\frac{\mathrm{i}}{\hbar}E_k(t-t'')}\right]\phi^{\mathrm{ad,R}}_{j}(\mathbf{r}, t', t'')\mathrm{e}^{-\frac{\mathrm{i}}{\hbar}\int^{t''}\mathrm{d}\tau E^{\mathrm{ad}}_{j}(\tau)}\,. \tag{8.173}$$

Now, applying the cut $t'' = t$ while eliminating the phase factor $\sum_k c_k$ in order to obtain the physical solution of Eq. (8.138) one gets:

$$\Psi^{\mathrm{R}}(\mathbf{r}, t) = \widetilde{\Psi}^{\mathrm{R}}(\mathbf{r}, t', t'', t)|_{t''=t'=t} = \mathrm{e}^{-\frac{\mathrm{i}}{\hbar}\int^{t}\mathrm{d}\tau E^{\mathrm{ad}}_{j}(\tau)}\phi^{\mathrm{ad,R}}_{j}(\mathbf{r}, t', t'')|_{t''=t'=t}\,. \tag{8.174}$$

This is the adiabatic solution of the TDSE associated with an initial state $\varphi_j(\mathbf{r})$.

Let us recap and clarify the procedure which determines if a given pulse is adiabatic or not. This determination relies on the calculation of the factors $A_{(j,0)}(t)$ which sum over the adiabatic cross terms. The steps in procedure are as follows.

(1) Perform a non-Hermitian adiabatic Floquet calculation (via Eq. (8.151)) with a cw field, for a range of intensities ε_1 which covers all intensities between zero and the maximal intensity ε_0 of the pulse. The adiabatic Floquet Hamiltonian for this purpose is

$$H_{\text{ad}}(\mathbf{r}, t', \varepsilon_1) \equiv H_0(\mathbf{r}) - e\mathbf{r} \cdot \varepsilon_1 \cos(\omega_{\text{L}} t') - \text{i}\hbar \frac{\partial}{\partial t'} \,. \tag{8.175}$$

From the corresponding eigenvalue equation,

$$H_{\text{ad}}(\mathbf{r}, t', \varepsilon_1)\phi_j^{\text{ad,R}}(\mathbf{r}, t', \varepsilon_1) = E_j^{\text{ad}}(\varepsilon_1)\phi_j^{\text{ad,R}}(\mathbf{r}, t', \varepsilon_1) \tag{8.176}$$

obtain the quasi-energy spectrum $E_j^{\text{ad}}(\varepsilon_1)$ and all the adiabatic cross terms $c_{(j',m)}^{(j,0)}(\varepsilon_1)$ as a function of the intensities based on Eq. (8.169) and Eq. (8.176). This step is done only once, for a given system under study.

(2) For a given laser pulse $f(t)$ with a maximal intensity ε_0, evaluate the effective cw-field intensity as function of time, $\varepsilon_0 f(t)$ (Eq. (8.140)). Then, convert the adiabatic cross terms to time-dependent functions through the equality $\varepsilon_1 = \varepsilon_0 f(t)$ (Eq. (8.150) while using $c_{(j',m)}^{(j,0)}(\varepsilon_1)$ obtained in the first step of the procedure). Consequently the time-dependent adiabatic cross terms are given by $c_{(j',m)}^{(j,0)}(t) = c_{(j',m)}^{(j,0)}(\varepsilon_0 f(t))$).

(3) For each resonance state $\alpha = (j, 0)$ calculate

$$A_{(j,0)}(t) = F(t) \cdot \sum_{j' \neq j} \sum_{m \neq 0} |c_{(j',m)}^{(j,0)}(t)| \tag{8.177}$$

using the time-dependent adiabatic cross terms from the previous step. Notice that here t'' in Eqs. (8.166)–(8.169) is replaced by t. If for a given resonance state $\alpha = (j, 0)$ the corresponding expression $A_{(j,0)}(t)$ is much smaller than unity at every time instant, it is guaranteed that the system, initially at the corresponding bound state, will evolve adiabatically to that specific resonance state. In this case the high-order harmonic generation spectra that will be discussed in detail in the next section will show only odd harmonics as for the cw case.

8.3.4 Non-Hermitian quantum mechanical theory of high order harmonic generation

High-order harmonic generation spectra of atoms and molecules in intense laser fields usually show a wide plateau of *odd* harmonics, with photon energies high up to the soft X-ray regime. The phenomenon can be treated using the standard (Hermitian) formalism of quantum mechanics through the solution of the time-dependent

Schrödinger equation when the initial state at $t = 0$ is the field-free ground state. The probability of obtaining high-energy photons can be obtained from the time-dependent solution of the Schrödinger equation by studying the acceleration of the driven electrons. In other words we need to evaluate the time-dependent expectation of the electronic acceleration operator, $a(t)$. The Fourier transform of $a(t)$ provides the amplitudes of the probabilities of high-harmonic generation process and thereby the intensity of the high-frequency emitted radiation. This will give the probability that an atomic or molecular system which interacts with a laser with a fundamental frequency ω_{L} will emit frequencies $\Omega \gg \omega_{\mathrm{L}}$. Besides the heavy numerical task of the involved calculations which require the solution of the time-dependent Schrödinger equation of a many-electron atomic or molecular system, there are difficulties in qualitatively analyzing the expression for the amplitude of the probability of emitting high frequency, $\sigma(\Omega)$. In order to get, for example, the conditions where only odd harmonics are obtained or under what condition also hyper-Raman lines (side bands for which $\Omega/\omega_{\mathrm{L}}$ is not an integer) would be observed in the experiments we must be able to analyze $\sigma(\Omega)$ based on some perturbative analysis or by using some symmetry considerations. The main difficulty in applying perturbation theory in the conventional formalism of quantum mechanics is in the fact that the spectrum of a Hermitian Floquet operator is not discrete, as well as the fact that the laser field is too strong for any perturbational analysis of $\sigma(\Omega)$ to be effective. This, however, is not the case when $\sigma(\Omega)$ is derived by the non-Hermitian formalism of quantum mechanics. The spectrum of the non-Hermitian complex scaled Floquet operators consists of a discrete resonance spectrum associated with square-integrable states and often $\sigma(\Omega)$ is dominated by the contribution of a single resonance eigenfunction of the non-Hermitian complex-scaled Floquet operator.

When the evolution is controlled by resonance states, then the integration over energy (or summation over the discrete continuum energy terms) is replaced by the summation over the resonance poles of the Floquet operator which upon complex scaling are associated with square-integrable functions. The interference effects with the rotated continuum states can be neglected since the photo-induced dynamics is dominated by the narrow quasi-energy resonances. As already discussed in this chapter, this possibility to separate between resonances and "white" continuum states does not exist in conventional (Hermitian) quantum mechanics. Unlike the situation in non-Hermitian quantum mechanics, in conventional quantum mechanics, a resonance state is *not* associated with a single eigenstate of the Hamiltonian, so that we cannot distinguish between the contribution to the photo-emission cross section of resonance states and the contribution of other states in the continuum.

Let us briefly discuss this situation where we do not take the "bra" state as the complex conjugate of the "ket" state when we calculate expectation values in non-Hermitian quantum mechanics, and the so-called left eigenstates are equal to the right eigenstates of the Floquet matrix. The QE states $|\Phi_k(t))$ are time-periodic functions. We expand them in the Fourier basis set $f_n(t) \equiv e^{i\omega_L nt}$, where $n = 0, \pm1, \pm2, \ldots,$ i.e. $|\Phi_k(t)) = \sum_n f_n(t)|\phi_{n,k})$. The Fourier components are spatial functions. They are the components of the right eigenvector of the Floquet Hamiltonian matrix,

$$\mathcal{H}_{n',n} = \frac{1}{T}\int_0^T dt (f_{n'}(t))^* \left[-i\hbar\frac{\partial}{\partial t} + \hat{H}(\hat{\mathbf{r}}_j e^{i\theta}, t)\right] f_n(t)\,. \tag{8.178}$$

Here, $\hat{H}(\hat{\mathbf{r}}_j e^{i\theta}, t) = \hat{H}_0^\theta + eF_0 e^{+i\theta}\sum_j \hat{z}_j \cos(\omega_L t)$. Note that in the calculation of the Floquet matrix elements we used the usual scalar product. From linear algebra we know that the most general representation of a matrix is a complex and symmetric one. Therefore, without loss of generality we consider the case where the Floquet matrix is equal to its transpose (i.e., $\mathcal{H}$ is a complex symmetric matrix). In such a case the "left" eigenvectors of $\mathcal{H}$ are equal to the "right" eigenvectors. Therefore, we should *not* take the complex conjugate of the spatial Fourier components when we calculate expectation values. This means that the inner product is defined such that, for example, $\left(\phi_{n',k'}|\sum_j \hat{z}_j|\phi_{n,k}\right) = \langle\phi^*_{n',k'}|\sum_j \hat{z}_j|\phi_{n,k}\rangle$, where $\langle\cdots\rangle$ stands for the usual definition of the scalar product. This inner product, which is known as the c-product, has been discussed extensively in Chapter 6. Consequently, the Floquet eigenstates are orthonormal functions under the definition

$$\frac{1}{T}\int_0^T dt \left(\sum_{n'} f_{n'}(t)\,\phi_{n',k'}|\sum_n f_n(t)\,\phi_{n,k}\right) = \delta_{k',k}\,. \tag{8.179}$$

The time period is $T = 2\pi/\omega_L$. In other words, we calculate the inner product as an integral over the spatial coordinates and over time where we do not take the complex conjugate of quantities that are complex merely due to complex scaling. This means that we conjugate the time-dependent functions f_n but not the spatial functions $\phi_{n,k}$. From Eq. (8.179), it follows that $\sum_n(\phi_{n,k'}|\phi_{n,k}) = \delta_{k',k}$. Furthermore, when we take into account the fact that the states $|\Phi_k)$ and $e^{iN\omega t}|\Phi_k)$ are orthogonal eigenstates of the Floquet operator for $N \neq 0$, we find that $\sum_n(\phi_{n+N,k}|\phi_{n,k}) = \delta_{N,0}$ and finally $(\sum_{n'} f_{n'}(t)\,\phi_{n',k}|\sum_n f_n(t)\,\phi_{n,k}) = 1$ for all times.

The probability of detecting an electron *somewhere* in space is equal to *one* at any given time since the number of particles in the entire space is conserved. However, the high-energy photons are generated only due to the interaction of the electrons with the nuclei. Free electrons oscillating in the presence of the electromagnetic field do not emit high-energy photons. Therefore, the high harmonics are generated only within the lifetime of the resonance state. On the basis of this physical argument, we conclude that the number of electrons should *not* be conserved inside a finite box where the electrons interact with the nuclei. As time passes, the electrons escape from the finite box. Outside the box, we assume that the electron–nuclei interaction is equal to zero. The size of the box can be as large as one wishes. Within the framework of this box-quantization formalism, the number of electrons inside the box decays exponentially to zero as time passes. The norm of the decaying wavepacket is reduced in time due to the "loss" of electrons. This is the main motivation behind the derivation of the F-product introduced in Chapter 6. However, since we use this definition for the norm of a wavepacket in the derivation of the non-Hermitian expressions for the probability of getting high-harmonic when an atom or a molecule interacts with a strong laser field, we will briefly repeat it in this context.

We impose this time-dependent normalization on the quasi-energy resonance solutions by introducing the following complex phase factors:

$$\mathrm{e}^{-\mathrm{i}E_{k_{\mathrm{res}}}t/\hbar} = \mathrm{e}^{-\mathrm{i}\mathcal{E}_{k_{\mathrm{res}}}t/\hbar}\mathrm{e}^{-\frac{1}{2}\Gamma_{k_{\mathrm{res}}}t/\hbar} \tag{8.180}$$

for the "ket" Floquet states, and

$$\mathrm{e}^{+\mathrm{i}E^*_{k_{\mathrm{res}}}t/\hbar} = \mathrm{e}^{+\mathrm{i}\mathcal{E}_{k_{\mathrm{res}}}t/\hbar}\mathrm{e}^{-\frac{1}{2}\Gamma_{k_{\mathrm{res}}}t/\hbar} \tag{8.181}$$

for the "bra" states. Thus, within the framework of the box quantization, we obtain for the state $|\Psi(t)) = \mathrm{e}^{-\mathrm{i}E_{k_{\mathrm{res}}}t/\hbar}|\Phi_{k_{\mathrm{res}}}(t))$ the normalization

$$\begin{aligned}(\Psi(t)|\Psi(t)) &= \left(\mathrm{e}^{-\mathrm{i}E_{k_{\mathrm{res}}}t/\hbar}\sum_{n'} f_{n'}(t)\,\phi_{n',k_{\mathrm{res}}}\middle|\mathrm{e}^{-\mathrm{i}E_{k_{\mathrm{res}}}t/\hbar}\sum_{n} f_{n}(t)\,\phi_{n,k_{\mathrm{res}}}\right)\\ &= \mathrm{e}^{-\Gamma_{k_{\mathrm{res}}}t/\hbar}.\end{aligned} \tag{8.182}$$

This means that the probability of detecting the system in a given atomic/molecular quasi-energy resonance state decays exponentially in time with the decay rate $\Gamma_{k_{\mathrm{res}}}/\hbar$. To obtain this result we used the norm conservation for the states $|\Phi_{k_{\mathrm{res}}}(t))$ (i.e., $(\Phi^{\mathrm{L}}_{k_{\mathrm{res}}}(t)\Phi^{\mathrm{R}}_{k_{\mathrm{res}}}(t)) = \sum_{n=-\infty}^{+\infty}(\phi_{n,k_{\mathrm{res}}}|\phi_{n,k_{\mathrm{res}}}) = 1$).

Following this discussion, in non-Hermitian quantum mechanics, Eq. (8.100) is replaced by the following expression:

$$\sigma(\Omega) = |t_{\mathrm{res}}(\Omega) + t_{\text{non-res}}(\Omega)|^2\,. \tag{8.183}$$

This means that we have two contributions to $\sigma(\Omega)$. The main contribution is that of the resonant states and an additional contribution from the background continuum.

The resonance contribution to the photo-emission cross section is given by

$$t_{\mathrm{res}}(\Omega) = \sum_{k'_{\mathrm{res}},k_{\mathrm{res}}} C^{\mathrm{L}}_{k'_{\mathrm{res}}} C^{\mathrm{R}}_{k_{\mathrm{res}}} \sum_{n=-\infty}^{+\infty} \sum_{n'=-\infty}^{+\infty} \frac{[(E_{k_{\mathrm{res}}} - E^*_{k'_{\mathrm{res}}})/\hbar + \omega(n'-n))]^2}{\Omega - [(E_{k_{\mathrm{res}}} - E^*_{k'_{\mathrm{res}}})/\hbar + \omega(n'-n)]}$$
$$\times \left(\phi_{n',k'_{\mathrm{res}}} \middle| \sum_j \hat{z}_j \middle| \phi_{n,k_{\mathrm{res}}}\right), \tag{8.184}$$

where the resonance Fourier components $\phi_{n,k_{\mathrm{res}}}$ are θ-dependent spatial functions, whereas the resonance complex quasi-energies are invariant with respect to θ.

An important point in the derivation of Eq. (8.184) is the time integration over the range $0 < t < \infty$. Physically, this is reasonable for laser pulses which are switched on at $t = 0$ and last longer than the lifetimes of the QE states. The correction for short pulses will be given below.

In order to calculate the complex coefficients C^{R}_k and C^{L}_k in the expansions of the right and left wave functions

$$\Psi^{\mathrm{R}}_0(t=0) = \sum_{n,k} C^{\mathrm{R}}_k \phi_{n,k}\,, \tag{8.185}$$

$$\Psi^{\mathrm{L}}_0(t=0) = \sum_{n,k} C^{\mathrm{L}}_k \phi_{n,k}\,, \tag{8.186}$$

we should first explain how the complex-scaled initial state is projected on these resonances. Here we consider the general case that the atom, before being exposed to the external laser field, is not in an eigenstate but in a linear combination of the field-free eigenstates. The unscaled initial wave packet is denoted by $\Phi^{\mathrm{FF}}_0(\mathbf{r}_j)$. If the field is suddenly turned on to its maximal field amplitude (the envelope of the laser field amplitude is a Heavyside function), then

$$C^{\mathrm{R}}_{k_{\mathrm{res}}} = \sum_n (\phi_{n,k_{\mathrm{res}}} | \Phi^{\mathrm{FF},\theta}_0)\,, \tag{8.187}$$

$$C^{\mathrm{L}}_{k_{\mathrm{res}}} = \sum_n ([\Phi^{\mathrm{FF},-\theta}_0]^* | \phi_{n,k}), \tag{8.188}$$

where $\Phi^{\mathrm{FF},\theta}_0(\mathbf{r}_j) = \Phi^{\mathrm{FF}}_0(\mathbf{r}_j \mathrm{e}^{\mathrm{i}\theta})$. The other possibility is to turn the field on during several optical cycles. Let us assume that this time is equal to MT, where M is an integer and an optical cycle is $T = 2\pi/\omega$. The wavepacket is propagated by solving the conventional time-dependent Schrödinger equation from $t = -MT$ to $t = 0$, yielding $\Phi_0(\mathbf{r}_j, t=0)$, which is different from $\Phi^{\mathrm{FF}}_0(\mathbf{r}_j)$. The coefficients follow by projection of the complex-scaled wave function $\Phi^{\theta}_0(\mathbf{r}_j, t = 0)$ on the complex QE

Floquet solutions, i.e.,

$$C^{\rm R}_{k_{\rm res}} = \sum_n (\phi_{n,k}|\Phi_0^{\theta}(t=0))\,, \tag{8.189}$$

$$C^{\rm R}_{k_{\rm res}} = \sum_n \left([\Phi_0^{-\theta}(t=0)]^*\middle|\phi_{n,k}\right). \tag{8.190}$$

If the laser is turned on adiabatically, then the coefficients are given by

$$C^{\rm R}_{k_{\rm res}} = {\rm e}^{-{\rm i}\int_{-MT}^{0} E^{\rm ad}_{k_{\rm res}}(t'){\rm d}t'/\hbar} C^{\rm FF}_{k_{\rm res}}, \tag{8.191}$$

$$C^{\rm L}_{k_{\rm res}} = {\rm e}^{+{\rm i}\int_{-MT}^{0} (E^{\rm ad}_{k_{\rm res}}(t'))^*{\rm d}t'/\hbar} (C^{\rm FF}_{k_{\rm res}})^*, \tag{8.192}$$

where the coefficients $C^{\rm FF}_{k_{\rm res}}$ are obtained by projection of $\Phi_0^{\rm FF}$ on the field-free eigenstates, and $E^{\rm ad}_{k_{\rm res}}$ are the adiabatic quasi-energies. Clearly, this approach is valid only as long as there is no significant ionization during the turn-on period, i.e., as long as the peak intensity is below the saturation intensity.

By substituting these coefficients into Eq. (8.184) we obtain the spectrum for emission of high harmonics. When the interference between different populated QE states is ignored, the double summation over $k'_{\rm res}$ and $k_{\rm res}$ in Eq. (8.184) is replaced by a single sum over $k_{\rm res}$. Then, following the dynamical symmetry properties of the Floquet Hamiltonian for atoms,

$$\left(\phi_{n',k_{\rm res}}\middle|\sum_j \hat{z}_j\middle|\phi_{n,k_{\rm res}}\right) = 0 \tag{8.193}$$

if

$$n' - n \neq 2m + 1\,, \tag{8.194}$$

where m is an integer, i.e. only odd $N_{\rm o} = 2m+1$ harmonics are generated. The intensity of the high-order harmonic lines is then given by

$$\sigma\left(\Omega = N_{\rm o}\omega_{\rm L}\right) \simeq \left|\sum_{k_{\rm res}} C^{\rm L}_{k_{\rm res}} C^{\rm R}_{k_{\rm res}} \frac{(\Omega - {\rm i}\Gamma_{k_{\rm res}}/\hbar)^2}{\Gamma_{k_{\rm res}}/\hbar} \sum_{n=-\infty}^{+\infty} \left(\phi_{n+N_{\rm o},k_{\rm res}}\middle|\sum_j \hat{z}_j\middle|\phi_{n,k_{\rm res}}\right)\right|^2 . \tag{8.195}$$

Equation (8.196) suggests that the odd high-order harmonic generation spectrum is controlled by the narrowest populated QE resonance state. Let us explain this important result for the simple case where only one resonance QE state is populated, i.e., we have no summation over $k_{\rm res}$ in Eq. (8.196). In such a case, if $\hbar\Omega \gg \Gamma_{k_{\rm res}}$, then

$$\frac{(\Omega - \mathrm{i}\Gamma_{k_{\mathrm{res}}}/\hbar)^2}{\Gamma_{k_{\mathrm{res}}}/\hbar} \simeq \frac{\Omega^2}{\Gamma_{k_{\mathrm{res}}}/\hbar} \tag{8.196}$$

and, consequently, the signal from state k_{res},

$$\sigma\big(\Omega = N_{\mathrm{o}}\omega_{\mathrm{L}}\big) \simeq \left(\frac{\Omega^2}{\Gamma_{k_{\mathrm{res}}}/\hbar}\right)^2 \left|\sum_{n=-\infty}^{+\infty} \left(\phi_{n+N_{\mathrm{o}},k_{\mathrm{res}}}\middle|\sum_j \hat{z}_j\middle|\phi_{n,k_{\mathrm{res}}}\right)\right|^2, \tag{8.197}$$

is proportional to $1/(\Gamma_{k_{\mathrm{res}}})^2$. The assumption that only the narrowest (i.e, longest-lived) quasi-energy (QE) resonance state controls the photo-induced dynamics probably holds when one QE resonance state (usually associated with the field-free ground state) is narrower than all other resonance states by several orders of magnitude. Perhaps this is the reason why, for example, the experimental high-order harmonic generation spectra of helium fit so well with the results obtained from complex-scaling *ab-initio* calculations carried out by Moiseyev and Weinhold.[13] In that study it was assumed that $\sigma(\Omega = N_{\mathrm{o}}\omega) \sim \left|\sum_{n=-\infty}^{+\infty} \Omega^2(\phi_{n+N_{\mathrm{o}},k_0}|\sum_j \hat{z}_j|\phi_{n,k_0})\right|^2$ although the short high-intensity laser pulses used in the experiments should populate more than one quasi-energy state. Note in passing that in their *ab-initio* calculations the electronic correlations were taken into consideration, which provided the first indication that the odd high-harmonic generation spectrum is produced by the photo-induced resonance state of the neutral atom in the strong laser field and not by the helium ion as one might think. However, one should be aware of the fact that the value of $\sigma(\Omega = N_{\mathrm{o}}\omega)$ does not only depend on the resonance width but also on the matrix elements $(\phi_{n+N_{\mathrm{o}},k_{\mathrm{res}}}|\sum_j \hat{z}_j|\phi_{n,k_{\mathrm{res}}})$. Due to this dependence, it may happen that although $\Gamma_{k_{\mathrm{res}}} < \Gamma_{k'_{\mathrm{res}}}$, the contribution of a state k_{res} will be smaller than the contribution of a state k'_{res}. This is possible when the difference between the resonance widths is not large, and when the two resonance wavefunctions have very different "lengths of localization" in Fourier space. Let us explain the last statement more carefully. The Fourier components satisfy the normalization condition $\sum_n(\phi_{n,k_{\mathrm{res}}}|\phi_{n,k_{\mathrm{res}}}) = 1$. The localization length measures the number of dominant components in the Fourier expansion of the resonance complex-scaled wavefunction. By plotting the value of $(\phi_{n,k_{\mathrm{res}}}|\phi_{n,k_{\mathrm{res}}})$ versus n, the localization length in Fourier space can be obtained. It is clear that higher harmonic orders are obtained for a resonance state with a longer localization length. We note in passing that quasi-energy states that are associated with classical chaotic dynamics are less localized in Fourier space than the quasi-energy states

---

[13] N. Moiseyev and F. Weinhold, *Phys. Rev. Lett.* **78**, 2100 (1997).

which are associated with a quasi-periodic regular classical photo-induced dynamics.[14] Without going too deep into this matter we can conclude that a situation can arise where a quasi-energy state with a short lifetime will generate high-order harmonics more efficiently than another, longer-lived, resonance state. Yet, we still may expect that if a populated resonance quasi-energy state is narrower by several orders of magnitude than the other resonances, this narrow resonance quasi-energy state will control the photo-induced dynamics.

So far we have discussed the harmonic generation spectra for cw lasers or for the case where the duration of the laser pulse supports many optical cycles, which justifies the use of Floquet theory. Before proceeding to discuss the conditions for the appearance of side-bands, let us generalize the derivation of Eqs. (8.196) and (8.197) to the case of short laser pulses. Using the (t, t') formalism, the derivation of of the high-harmonic generation spectrum presented above holds also for non-periodic time-dependent Hamiltonians.

In such instances, ω_{L} is not the cw laser frequency. Instead we replace ω_{L} in the above expressions by the frequency $\omega = 2\pi/\tau$, where τ, is any finite time which is larger than the duration of the pulse. However, when the dominant Fourier component of the laser pulse is the fundamental frequency of the laser, we may use the Floquet QE states as a basis set in the calculations of the time-dependent dipole moment, $d_{\mathrm{res}}(t)$. In such a case, ω in our expansion is the laser frequency as before.

Under the assumption that the high-order harmonics are generated only during the period of time that the laser field is turned on (the possibility that the laser field generates an electronic wavepacket which generates the high harmonics long after the laser has been turned on is excluded here) then the the Fourier transform of $d_{\mathrm{res}}(t)$ should be taken from 0 to τ_{p} rather than 0 to ∞, where τ_{p} is the duration of the laser pulse. Therefore, when short laser pulses are applied, the term $1/\Gamma_{k_{\mathrm{res}}}$ in Eqs. (8.196) and (8.197) should be replaced by $(1 - \mathrm{e}^{-\Gamma_{k_{\mathrm{res}}}\tau_{\mathrm{p}}/\hbar})/\Gamma_{k_{\mathrm{res}}}$. For sufficiently short pulses, $(1 - \mathrm{e}^{-\Gamma_{k_{\mathrm{res}}}\tau_{\mathrm{p}}/\hbar})/\Gamma_{k_{\mathrm{res}}} \simeq \tau_{\mathrm{p}}/\hbar$. This shows that for ultrashort pulses, the generation of high-order harmonics does not depend directly on the resonance width but rather on the matrix elements $\sum_{n=-\infty}^{+\infty}(\phi^*_{n+2m+1,k_{\mathrm{res}}}|\sum_j \hat{z}_j|\phi_{n,k_{\mathrm{res}}})$ which appear in Eqs. (8.196) and (8.197). *Thus, when short laser pulses are applied, the resonance QE state making the dominant contribution to the HG spectrum will not necessarily be the one with the longest lifetime*. Clearly, in this case, the matrix elements must be evaluated for the system of interest in order to make a prediction of which QE states are dominant. In this respect, our general analysis is only the

---

[14] V. Averbukh and N. Moiseyev, Cutoff in molecular harmonic-generation spectra resulting from classical chaotic dynamics, *Phys. Rev. A.* **51**, 3911–3915 (1995); V. Averbukh, N. Moiseyev, B. Mirbach and H. J. Korsch, Dynamical tunneling through a chaotic region – a continuously driven rigid rotor. *Z. Physik D – Atoms, Moleculers and clusters* **35**, 247–256 (1995).

first step. We should stress again that this discussion holds for the cases where there is a dominant contribution of a single resonance state to the photo-induced dynamics. When an electronic wavepacket is generated one should calculate the complex time-dependent expectation value of the acceleration and use it as a source term in the Maxwell equation in order to calculate the emitted high-frequency radiation.

We return now to discussion on the conditions which are required for the observation of side-bands (hyper-Raman lines). From Eq. (8.184), it follows that the hyper-Raman lines in the emission spectra are obtained at

$$\Omega = \mathrm{Re}[(E_{k_{\mathrm{res}}} - E^*_{k'_{\mathrm{res}}})/\hbar] + \omega(n' - n) = (\mathcal{E}_{k_{\mathrm{res}}} - \mathcal{E}_{k'_{\mathrm{res}}})/\hbar + \omega(n' - n), \tag{8.198}$$

where $n' - n = 2m + 1$ (i.e. odd values) or $n' - n = 2m$ (i.e. even values), and $k_{\mathrm{res}} \neq k'_{\mathrm{res}}$. The result of even or odd values of $n' - n$ depends on the dynamical symmetry properties of the complex-scaled QE resonance states. Let us explain this point. For atoms (the potential is spherical symmetric) in a time-periodic field within the dipole approximation, the Floquet operator satisfies the symmetry condition $\hat{\mathcal{H}}(\mathbf{r}, t) = \hat{\mathcal{H}}(-\mathbf{r}, t + T/2)$, where $T = 2\pi/\omega_{\mathrm{L}}$. Therefore, the right and left eigenfunctions of the Floquet operator are also eigenfunctions of this dynamical symmetry operator, $\Phi^{\mathrm{R,L}}(-\mathbf{r}, t + T/2) = \pm\Phi^{\mathrm{R,L}}(-\mathbf{r}, t + T/2)$. This symmetry property of the eigenfunctions holds for Hermitian Floquet operators and for non-Hermitian ones. However, *only* within the framework of the non-Hermitian formalism where outgoing boundary conditions are imposed, the photo-induced resonance Floquet eigenfunctions are obtained. Only within this framework can we assume that the photo-induced dynamics is controlled solely by a single resonance Floquet state that becomes square integrable by complex scaling. Consequently, the high-harmonic generation spectra can be associated with the Fourier transform of the acceleration,

$$\sigma_{\mathrm{HG}}(N\omega_{\mathrm{L}}) \simeq |T^{-1} \int_0^T \mathrm{d}t \int \mathrm{d}\mathbf{r}\; a(\mathbf{r}, t)|^2\,, \tag{8.199}$$

where

$$a(\mathbf{r}, t) = \Phi^{\mathrm{L}}(\mathbf{r}, t)\hat{O}_N(\mathbf{r}, t)\Phi^{\mathrm{R}}(\mathbf{r}, t) \tag{8.200}$$

and

$$\hat{O}_N(\mathbf{r}, t) = \mathrm{e}^{\mathrm{i}N\omega_{\mathrm{L}}t}[-\partial_x V_{\mathrm{atom}}/m_{\mathrm{e}}]\,. \tag{8.201}$$

The integration over the two coordinates, $\mathbf{r}$ and t, is not equal to zero if and only if

$$\hat{O}(\mathbf{r}, t) = \hat{O}_N(-\mathbf{r}, t + T/2)\,, \tag{8.202}$$

which implies that

$$e^{iN\omega_L T/2} = -1\,. \tag{8.203}$$

Therefore, for $m = 0, 1, 2, \ldots,$

$$\begin{aligned} N\omega_L T/2 &= (2m+1)\pi, \\ N &= 2m+1, \end{aligned} \tag{8.204}$$

only odd harmonics should be obtained.

Note that even orders are allowed when the parity with respect to the dynamical symmetry of the two resonances is different. *Here we showed that the hyper-Raman lines in the emission spectra are comprised of a series of shifted odd and even high-order harmonics.* The intensity of the hyper-Raman lines at frequencies $\Omega = (\mathcal{E}_{k_{\text{res}}} - \mathcal{E}_{k'_{\text{res}}})/\hbar + N\omega_L$, resulting from the interference between two different resonance QE states $k_{\text{res}} \neq k'_{\text{res}}$, is given by

$$\sigma(\Omega) \simeq \left| C^{L}_{k'_{\text{res}}} C^{R}_{k_{\text{res}}} \frac{[\Omega - \frac{i}{2\hbar}(\Gamma_{k_{\text{res}}} + \Gamma_{k'_{\text{res}}})]^2}{(\Gamma_{k_{\text{res}}} + \Gamma_{k'_{\text{res}}})/\hbar} \sum_{n=-\infty}^{+\infty} \left(\phi_{n+N,k'_{\text{res}}} \middle| \sum_j \hat{z}_j \middle| \phi_{n,k_{\text{res}}} \right) \right|^2 . \tag{8.205}$$

We now apply the dynamical symmetry properties of the Floquet operator to Eq. (8.205). When the two QE states have the same parity with respect to the dynamical symmetry operator the matrix elements vanish unless $N_o = 2m+1$ This means that the hyper-Raman lines are shifted odd harmonics. When the two QE states have different generalized parity then the matrix elements vanish unless $N_e = 2m$. If these two resonance QE states are degenerate eigenstates of the Floquet operator, even high-order harmonics will be obtained. If they are non-degenerate eigenstates of the Floquet operator, shifted even harmonics will be generated.

As one can see from Eq. (8.205), the intensity of the hyper-Raman lines in the emission spectra depends on the probability of populating two QE resonance states which can have different energies but should possess *similar* narrow widths.

This is a crucial point for possible experiments that would show the fingerprints of the hyper-Raman lines in the emission spectra: if $\Gamma_{k'_{\text{res}}} \gg \Gamma_{k_{\text{res}}}$, the cross terms in Eq. (8.205) are negligible compared to the direct term in Eq. (8.196) associated with state k_{res}, and only significant odd harmonics will be observed. The hyper-Raman lines will be obtained only when $\Gamma_{k'_{\text{res}}} \sim \Gamma_{k_{\text{res}}}$.

As discussed above for the direct terms, the situation is drastically different for very short pulses. Then, the harmonic intensities are not directly controlled by the widths of the resonance states. In this case, hyper-Raman lines may even be obtained when the populated QE states have significantly different lifetimes.

8.3.5 Non-Hermitian theory of above threshold ionization (ATI) spectra

Due to the interaction of an atom or a molecule with the induced electromagnetic field, ionization or dissociation may occur. In the former case, the measurement of the kinetic energy of the photo-induced ionized electron is known as ATI (above-threshold-ionization) spectroscopy. In the latter case the measurement of the relative kinetic energy of the dissociated particles due to the molecule–field interaction is known as ATD (above-threshold-dissociation) spectroscopy. In both cases the spectrum shows a series of isolated peaks separated by the integer multiples of photon energy $\hbar\omega$. These peaks are observed due to multi-photon absorption processes.

In the description below, in order to simplify the notation we assume that the field-free Hamiltonian is an effective single electron Hamiltonian. The extension to many-electron systems is quite straightforward as we indicate below. The one-electron coordinate x stands for the complex scaled coordinate, for example, the function $\psi_b(x)$ stands for the complex scaled bound state of the field-free complex scaled Hamiltonian, similarly $\varphi_{\mathrm{f}}(x)$ is the complex scaled outgoing plane wave which describes the ionized electron of the system when it interacts with a time-periodic electromagnetic field. As a reference frame we choose here the acceleration gauge. The reason is simple. Only in this representation the time-periodic Hamiltonian reduces in the asymptote to the Hamiltonian of free electrons which is essential for the derivation of non-Hermitian time-independent scattering theory for a time-dependent Hamiltonian.

In the case of a many-electron system $\varphi_{\mathrm{f}}(x)$ represents a many-electron wavefunction which is anti-symmetric with respect to permutation and consists of a product of the complex scaled ground state of the atomic (molecular) ion with the outgoing complex scaled waves which describes the single ionized electron. The *initial* state which describes a system which is suddenly exposed to a cw laser is given by

$$\Psi(x,\ t',\ t=0) = \psi_{\mathrm{b}}(x)\delta(t') = \sum_n \mathrm{e}^{\mathrm{i}wnt'}\psi_{\mathrm{b}}(x)\,, \tag{8.206}$$

where $\psi_{\mathrm{b}}(x)$ is a complex scaled bound-state eigenfunction of the field-free Hamiltonian. Therefore, the initial state $\Psi(x,\ t',\ t=0)$ in the Fourier basis set is defined as

$$|\boldsymbol{\psi}_0) = \begin{pmatrix} \vdots \\ \psi_{\mathrm{b}}(x) \\ \psi_{\mathrm{b}}(x) \\ \vdots \end{pmatrix}. \tag{8.207}$$

The complex scaled final state obtained when the Hamiltonian is represented in *the acceleration gauge* and $\mathrm{Re}(x) \to \infty$ is given by

$$\psi(x,\, t',\, t_\mathrm{f}) = \sqrt{\frac{\mu}{\hbar^2 k}}\mathrm{e}^{\mathrm{i}kx} \equiv \varphi_\mathrm{f}(x)\,, \tag{8.208}$$

where

$$E_\mathrm{f} = \frac{(\hbar k)^2}{2\mu} \tag{8.209}$$

is the real kinetic energy of the photo-ionized electron. Therefore, when Fourier basis functions, $\mathrm{e}^{\mathrm{i}\omega_\mathrm{L} n t'}$, where $n = \ldots, 1, 0, -1, \ldots$ are used as a basis set then $n = 0$ is the only non-zero component,

$$|\boldsymbol{\psi}_\mathrm{f}(t = 0)) = \begin{pmatrix} \vdots \\ 0 \\ \varphi_f(x) \\ 0 \\ \vdots \end{pmatrix}. \tag{8.210}$$

The free electron propagation is given by

$$\boldsymbol{\psi}_\mathrm{f}(t) = \mathrm{e}^{-\,\mathrm{i}E_\mathrm{f}t/\hbar}\varphi_\mathrm{f}(x) = \mathrm{e}^{-\mathrm{i}\hat{\mathbf{H}}_\mathrm{F}^\mathrm{final}t/\hbar}\boldsymbol{\psi}_\mathrm{f}(0)\,, \tag{8.211}$$

where $\mathbf{H}_\mathrm{F}^\mathrm{final}$ is a matrix representation of the complex scaled Floquet operator for the final state where a free electron is obtained (i.e, the Floquet operator for the final state is obtained by taking the limit of $\mathrm{Re}(x) \to \infty$ where the interacting potential vanishes).

In a similar fashion the propagation of the initial states is given by

$$\boldsymbol{\psi}_0(t) = \mathrm{e}^{-\mathrm{i}\hat{\mathbf{H}}_\mathrm{F}t/\hbar}\boldsymbol{\psi}_0(0)\,, \tag{8.212}$$

where $\hat{\mathbf{H}}_\mathrm{F}$ is the complex scaled Floquet matrix obtained by using the time-dependent Fourier functions as a basis set.

The transition probability from a bound state of the field-free Hamiltonian to a free electron with the kinetic energy E_f is obtained by evaluating the overlap integral,

$$P(E_\mathrm{f}) = |\lim_{t\to\infty}(\boldsymbol{\psi}_\mathrm{f}(t)|\boldsymbol{\psi}_0(t))|^2\,, \tag{8.213}$$

where $(\ldots)$ stands for the c-product in the generalized Hilbert space where in the Floquet operator time is used as an additional coordinate.

By using the fact that the limit of $t \to \infty$ can be analytically carried out, the closed-form expression for the state-to-state transition in a half-collision process is obtained (here we used the Lippmann–Schwinger equation for the Floquet operator):

$$P(E_{\mathrm{f}}) = \left|(\boldsymbol{\psi}_0(0)\middle|1 + \boldsymbol{G}^{+}(E_{\mathrm{f}})\boldsymbol{V}\middle|\boldsymbol{\psi}_f(0))\right|^2, \tag{8.214}$$

where

$$\mathbf{V} \equiv \hat{\mathbf{H}}_{\mathrm{F}} - \hat{\mathbf{H}}_{\mathrm{F}}^{\mathrm{final}}. \tag{8.215}$$

Here $\hat{\mathbf{H}}_{\mathrm{F}}^{\mathrm{final}}$ is obtained by eliminating from $\hat{\mathbf{H}}_{\mathrm{F}}$ the matrix Fourier matrix elements of the interaction potential term $V(x + \alpha_0 \cos \omega_{\mathrm{L}} t')$ and the complex scaled Green's operator is defined as

$$\hat{\boldsymbol{G}}^{+}(E_{\mathrm{f}}) = \frac{1}{E\mathbf{I} - \hat{\mathbf{H}}_{\mathrm{F}}(x,\, t')}. \tag{8.216}$$

Similarly to the notation in the standard (Hermitian) scattering theory (where $-\mathrm{i}\epsilon$ is added to the Hamiltonian where $\epsilon > 0$ to impose outgoing boundary conditions on the propagated wavepacket) also in the non-Hermitian formalism of scattering theory the "+" sign on the Green's operator indicates the fact that the imaginary part of the eigenvalues of the complex scaled Floquet matrix are negative and thus

$$\frac{1}{E\mathbf{I} - \hat{\mathbf{H}}_{\mathrm{F}}(x, t')} = \frac{1}{E\mathbf{I} - \mathrm{Re}[\hat{\mathbf{H}}_{\mathrm{F}}(x, t')] + \mathrm{i}\mathrm{Im}[\hat{\mathbf{H}}_{\mathrm{F}}(x, t')]}. \tag{8.217}$$

An important non-trivial fact is that only the $n = 0$ Fourier component of ψ_{f} (i.e. the $n = 0$ component in the vector $\boldsymbol{\psi}_{\mathrm{f}}(0)(t = 0)$) is non-zero, whereas all the Fourier components of the initial state $\boldsymbol{\psi}_0$ are identical and equal to the bound state of the field-free Hamiltonian.

Using Eq. (8.214) under the assumption that the photo-induced dynamics is controlled by a single QE resonance state we will prove that the peaks in the ATI spectra have the same width. The relative height of these peaks can be associated with the ratios of the partial widths of the resonance state. On the basis of the analysis of the expression we will obtain for the ATI spectra it is possible to explain, without the need to carry out any numerical calculations, why as the lifetime of the QE resonance state which controls the photo-induced process increases, the height of the peaks in the ATI spectra decreases and the peaks become narrower.

In the first step of the derivation we use the spectral representation of the Green's operator associated with the complex scaled Floquet operator. Using the Fourier functions $\mathrm{e}^{\mathrm{i}\omega_{\mathrm{L}} n t'}$, where $n = 0, \pm 1, \pm 2, \ldots$ (ordered from the smallest value to the largest one) as a basis set, the eigenvectors of the complex-scaled Floquet matrix (i.e., the spatial components of the eigenfunctions of the complex scaled Floquet operator) are given by

$$|\boldsymbol{\Psi}_\alpha) = \begin{pmatrix} \vdots \\ \varphi_{n+1,\alpha}(x) \\ \varphi_{n,\alpha}(x) \\ \varphi_{n-1,\alpha}(x) \\ \vdots \end{pmatrix}, \tag{8.218}$$

where $\alpha = 0$ is assigned to the longest-living resonance state associated with the quasi-energy eigenvalue $\epsilon_0 - \mathrm{i}\Gamma_0/2$. This is the state which usually has the largest overlap with the complex-scaled field-free ground state ψ_b. Let us denote the complex overlap integral by $S_\alpha = \sum_n (\psi_\mathrm{b}|\Psi_{n,\alpha})$. As already discussed, the quasi-energies are defined modulo $\hbar\omega_\mathrm{L}$. Therefore we have QE solutions which are associated with the complex eigenvalues, $\epsilon_0 + \hbar\omega_\mathrm{L} m - \mathrm{i}\Gamma_0/2$, where the spatial Fourier components of the corresponding QE eigenvectors are shifted by m.

That is, $\Psi_{n,\alpha}(x) \to \Psi_{n+m,\alpha}(x) \equiv \Psi^m_{n,\alpha}(x)$. Since we assume that $|S_0| \gg |S_{\alpha\neq 0}|$, Eq. (8.214) reduces to

$$P(E_\mathrm{f}) \sim \left| S_0 \sum_{m=1}^{\infty} \frac{(\boldsymbol{\Psi}^m_0|\mathbf{V}|\boldsymbol{\psi}_\mathrm{f}(t=0))}{(E_\mathrm{f} - \epsilon_0 - \hbar\omega_\mathrm{L} m) + (\mathrm{i}/2)\Gamma_0} \right|^2, \tag{8.219}$$

where here we assume that the system can be ionized even by absorbing one photon ($m = 1$). Our result shows that in principle when a cw laser is used there are an infinitely large number of peaks in the ATI spectra. When the absorption of m_p photons is required to ionize the system then the summation in Eq. (8.219) starts at $m = m_\mathrm{p}$. Note that the resonance position has a negative value since it is associated with the $m = 0$ Floquet channel. It is closely related to the ground bound state of the field-free Hamiltonian which has a negative energy value. Due to the interaction of the atom/molecule with the laser field this state becomes a resonance state. From Eq. (8.219) it is evident that the peaks in the ATI spectra are obtained when

$$E_\mathrm{f} = \hbar\omega_\mathrm{L} m - |\epsilon_0|\,. \tag{8.220}$$

Therefore the kinetic energy of the photo-ionized electron is quantized. The shape of the Lorenzian m-th ATI peak is given by

$$P(E_\mathrm{f} = \hbar\omega_\mathrm{L} m - |\epsilon_0| + \Delta E_\mathrm{f}) \sim \left| S_0 \frac{(\boldsymbol{\Psi}^m_0|\mathbf{V}|\boldsymbol{\psi}_\mathrm{f}(t=0))}{\Delta E_\mathrm{f} + (\mathrm{i}/2)\Gamma_0} \right|^2. \tag{8.221}$$

Since the nominator varies slowly with E_f we can make another approximation by associating the final state $\boldsymbol{\psi}_\mathrm{f}(t=0) = \varphi_\mathrm{f}(x)$ with free electrons which possess the kinetic energy in the m-th peak in the ATI spectrum. As a result of this approximation *all the ATI peaks have about the same width which is equal to the* *photo-induced resonance width* Γ_0. Moreover, since even for strong laser fields and in particular when the system can ionize even by absorbing a single photon, the dominant Fourier spatial component of the resonance quasi-energy state $\left|\boldsymbol{\Psi}_0^m\right)$ is the one associated with the m-th Floquet channel. Moreover, $(\varphi_{m\pm n,0}\middle|\varphi_{m\pm n,0})$ increases with n. Bearing in mind that the integral in the numerator is dominated by the lowest m-th Fourier components of $[\mathbf{V}]_{m,0}$, then the typical situation where $|\varphi_{m,0})$ is the dominant spatial Fourier component of the QE resonance state explains why usually (but not necessarily always) the height of the ATI peaks decreases as m increases.

It is possible to associate the nominator in Eq. (8.221) with the amplitudes of the partial widths $\gamma_{n,0}$, where $|\gamma_{m,0}|^2 = \Gamma_{m,0}$ are the partial widths which sum up to the photo-induced resonance width Γ_0. The ratio of $\Gamma_{m,0}/\,\Gamma_0$ provides the probability of ionizing the atomic or molecular system by absorbing m-photons. The replacement of $\left|(\boldsymbol{\Psi}_0^m|\mathbf{V}|\boldsymbol{\psi}_\mathrm{f}(t=0))\right|^2$ in Eq. (8.221) by $\Gamma_{m,0}$ is justified by carrying out an analytical continuation of the momentum of the final state appearing in the nominator to the complex momentum space, $\hbar k = \sqrt{2\mu E_\mathrm{f}} \to \sqrt{2\mu(E_\mathrm{f} - (\mathrm{i}/2)\Gamma_0)}$. By this analytical continuation, which is similar to the derivation of the Lippmann–Schwinger equation in Section 9.1, one gets that

$$\left|(\boldsymbol{\Psi}_0^m|\mathbf{V}|\boldsymbol{\psi}_\mathrm{f}(t=0))\right|^2 = \left|(\boldsymbol{\Psi}_0^m|\hat{\mathbf{H}}_\mathrm{F} - \hat{\mathbf{H}}_\mathrm{F}^\mathrm{final}|\boldsymbol{\psi}_\mathrm{f}(t=0))\right|^2. \tag{8.222}$$

Since $|\boldsymbol{\psi}_\mathrm{f}(t=0))$ is an eigenfunction of $\hat{\mathbf{H}}_\mathrm{F}^\mathrm{final}$, and $|\boldsymbol{\Psi}_0^m)$ is an eigenfunction of $\hat{\mathbf{H}}_\mathrm{F}$, and since both of them are associated with the *same* complex eigenvalue $E_\mathrm{f} - (\mathrm{i}/2)\Gamma_0$, where $E_\mathrm{f} = \hbar\omega_\mathrm{L} m - |\epsilon_0|$,

$$\left|\frac{\hbar^2}{2\mu} W[\boldsymbol{\psi}_\mathrm{f}(t=0),\, \boldsymbol{\Psi}_0^m]\right|^2 = \hbar\Gamma_{m,0}/2\,, \tag{8.223}$$

where W stands for the Wronskian defined by

$$W[g,f] = g\frac{\mathrm{d}f}{\mathrm{d}x} - f\frac{\mathrm{d}g}{\mathrm{d}x}\,. \tag{8.224}$$

The result of $\Gamma_{m,0}/2$ in Eq. (8.223) is due to the fact that the Coulombic potential is symmetric and therefore electrons can equally ionize to the $+|\mathrm{Re}(x)|$ direction and the $-|\mathrm{Re}(x)|$ direction. By substituting Eq. (8.223) into Eq. (8.221) one gets a simple approximate expression for the ATI spectra:

$$P(E_\mathrm{f}) \simeq |S_0|^2 \sum_m \frac{\hbar\Gamma_{m,0}/2}{|E_\mathrm{f} - (\hbar\omega_\mathrm{L} m - |\epsilon_0|) + (\mathrm{i}/2)\Gamma_0|^2}. \tag{8.225}$$

The ratio between the maximum heights of the m-th peak and the m'-th ATI peak is the branching ratio $\Gamma_{m,0}/\,\Gamma_{m',0}$. Since $\sum_m \Gamma_{m,0} = \Gamma_0$ it is clear that as $\Gamma_0 \to 0$ the widths of the ATI peaks reduces to zero while the heights of the ATI peaks depend on the ratios between the partial widths and the total width.

Note that since the resonance position is slightly below the ground bound state energy of the field-free system, as $\theta \to 0$ the resonance state is rotated backward to the real axis. That is, $\epsilon_0 = E_\mathrm{b} - \Delta$, where Δ is the shift of the resonance position from the ground bound state energy of the field-free system. Therefore, the maximum of the Lorenzian ATI peaks are at the resonance positions which are red shifts with respect to the bound state energy of the field free Hamiltonian.

8.4 Solutions to the exercises

Answer to Exercise 8.1

A potential V that consists of two potential barriers separated by a potential well supports shape-type resonances which are localized inside the potential well and decay through the potential barriers. Let us denote the resonance complex "energy" by $E_n^{\mathrm{res}} = \epsilon_n - \mathrm{i}/2\Gamma_n$, where $n = 1, 2, \ldots$ are ordered according to their energy position ϵ_n. When the barriers are sufficiently large the resonances which lie deep below the top of the barriers are narrow and isolated and consequently $|\epsilon_n - \epsilon_{n\pm1}| \gg \Gamma_n$. In one-dimensional problems with two potential barriers separated by a potential well there are two open channels to decay. One open channel to decay is tunneling through the left potential barrier where the second open channel to decay is tunneling out through the right potential barrier. In two- and three-dimensional problems there are more open channels to decay.

Let us denote the partial widths associated with the rate of decay through two possible open channels as $\Gamma_{n,i} = |\gamma_{n,i}^{\mathrm{res}}|^2$ and $\Gamma_{n,j} = |\gamma_{n,j}^{\mathrm{res}}|^2$. In 1D problems $\Gamma_n = \Gamma_{n,i} + \Gamma_{n,j}$, whereas in 2D and 3D problems $\Gamma_n < \Gamma_{n,i} + \Gamma_{n,j}$. When the mean energy of the particles which are scattered from the potential V is equal to one of the resonance positions, e.g., $E = \epsilon_{n_0}$, and the standard deviation of the energy of the incoming particles is less than Γ_{n_0}, the transition probability through the potential V is controlled by the single resonance tunneling mechanism and the transition probability amplitude in Eq. (8.41). Following Eqs. (8.41)–(8.61) the transition probability from the initial (i = initial) to the final (f = final) state through a resonance state then is given by

$$T_{\mathrm{i}\to\mathrm{f}} = \left|\frac{\gamma_{n_0,\mathrm{i}}\gamma_{n_0,\mathrm{f}}}{+\mathrm{i}\Gamma_{n_0}/2}\right|^2 = \frac{4\Gamma_{n_0,\mathrm{i}}\Gamma_{n_0,\mathrm{f}}}{\Gamma_{n_0}^2} \,. \tag{8.226}$$

Without loss of generality we now proceed to discuss here the situation of a 1D problem where there are only two open channels to decay and therefore

$$\Gamma_{n_0} = \Gamma_{n_0,\mathrm{i}} + \Gamma_{n_0,\mathrm{f}} \,. \tag{8.227}$$

By substituting Eq. (8.227) into Eq. (8.226) one gets that the transition probability on resonance is equal to

$$T_{\mathrm{i}\to\mathrm{f}} = \frac{4}{2+\mathcal{R}^{-1}+\mathcal{R}}\,, \tag{8.228}$$

where $\mathcal{R}$ is the branching ratio given by

$$\mathcal{R} = \frac{\Gamma_{n_0,\mathrm{f}}}{\Gamma_{n_0,\mathrm{i}}}\,. \tag{8.229}$$

When the two partial widths are equal (e.g., when the two potential barriers are identical) then the branching ratio is equal to one and $T_{\mathrm{i}\to\mathrm{f}} = 1$. It is obvious that when there are more than two open channels, as in the 2D and 3D cases, the transmission is smaller than unity since the sum of the two partial widths is smaller than the total width.

Answer to Exercise 8.2

Let us define $\Psi = \phi + \chi$ and use the fact that Ψ is an eigenfunction of $\hat{H} = \hat{H}_0 + \hat{V}$ and ϕ is eigenfunction of $\hat{H}_0$. This leads to the following results:

$$\begin{aligned}
&[\hat{H}_0 + \hat{V}](\phi+\chi) = E(\phi+\chi)\,,\\
&[\hat{H}_0 - E]\phi + \hat{V}\phi + [\hat{H}_0+\hat{V}]\chi = E\chi\,,\\
&\hat{V}\phi + [\hat{H}_0+\hat{V}]\chi = E\chi\,,\\
&(E-\hat{H})\chi = \hat{V}\phi\,,\\
&\chi = \hat{G}(E)\hat{V}\phi\,,\\
&\psi = \phi+\chi = [1+\hat{G}(E)\hat{V}]\phi\,.
\end{aligned} \tag{8.230}$$

For a given $\hat{H}_0$ and $\hat{H}$ it might happen that ψ and ϕ are associated with the same eigenvalue. For example, by adding a constant to $\hat{H}$ we can always shift the spectrum of $\hat{H}$ such that at least one of the discrete eigenvalues will be equal to a discrete eigenvalue of $\hat{H}_0$. However, it is very unlikely that the constant is equal to zero for our original Hamiltonians. The use of the Gel'fand–Levitan equation makes possible an easy evaluation of a perturbation V such that two *different* Hamiltonians support the *same* discrete energy spectrum.[15] For example, when

$$V = -2\frac{\mathrm{d}^2}{\mathrm{d}x^2}\ln\left(1-\int_{-\infty}^{x}\psi_n^2(z)\mathrm{d}z\right) \tag{8.231}$$

---

[15] I. M. Gel'fand and B. M. Levitan, *Am. Math. Soc. Transl.* **1**, 253 (1951).

$\hat{H}_0$ will have the same energy spectrum of $\hat{H}$ except for one eigenvalue of $\hat{H}$ which is associated with ψ_n. For the use of this method to "remove" one resonance state from the original spectrum see Moiseyev and Goscinski.[16] This example shows how special the perturbation should be in order for two different Hamiltonians to share the same discrete spectrum. *Only when both ψ and ϕ are continuum functions is it possible to satisfy the condition that $\hat{H}_0\phi = E\phi$ and $\hat{H}\Psi = E\Psi$ for the most general case.*

Answer to Exercise 8.3

The eigenfunctions and eigenvalues of $\hat{H}^{\mathrm{f}}$ are defined in Eq. (8.95). Here we omit the index $n = 0$ to simplify the notation. The time-dependent wavepacket which propagates onto the final potential energy surface of the molecular ion is expanded in the basis set of the eigenfunctions of $\hat{H}^{\mathrm{f}} + E_{\mathrm{kin}}$,

$$\xi^{\mathrm{f}}(R, t) = \sum_{\alpha} C_{\alpha_0}(t) \mathrm{e}^{-\mathrm{i}(\epsilon^{\mathrm{f}}_{\alpha_0} + E_{\mathrm{kin}})t/\hbar} \chi^{\mathrm{f}}_{\alpha_0}(R) , \tag{8.232}$$

where $(\chi^{\mathrm{f}}_{\alpha}|\chi^{\mathrm{f}}_{\alpha_0}) = \delta_{\alpha,\alpha_0}$ and $C_{\alpha_0}(0) = 0$ satisfies the initial condition. Therefore,

$$\sigma(E_{\mathrm{kin}}) = \lim_{t\to\infty} (\xi^{\mathrm{f}}(t)|\xi^{\mathrm{f}}(t)) = \sum_{\alpha_0} |C_{\alpha_0}(\infty)|^2 . \tag{8.233}$$

By substituting Eq. (8.232) and Eq. (8.98) into Eq. (8.99) and multiplying from the left by $(\chi^{\mathrm{f}}_{\alpha_0}|$, one gets

$$\frac{\partial C_{\alpha_0}(t)}{\partial t} = \mathrm{i}(\chi^{\mathrm{f}}_{\alpha_0}|\sqrt{\Gamma(R)}|\mathrm{e}^{+\mathrm{i}(E_{\mathrm{kin}} + E^{\mathrm{f}}_{\alpha_0} - \hat{H}^{\#})t/\hbar} \xi^{\#}(0)) . \tag{8.234}$$

Using the c-product, the orthonormal eigenfunctions of $\hat{H}^{\#}$ form a complete set. That is,

$$\sum_{\alpha} |\chi^{\#}_{\alpha})(\chi^{\#}_{\alpha}| = 1 . \tag{8.235}$$

The self-orthogonality phenomenon is excluded here since it is an ill-condition situation which can be removed in numerical calculations due to the infinitesimally small round-off errors when $\hat{H}^{\#}$ is represented by a finite matrix. By using Eq. (8.235) the time evolution operator is described as

$$\mathrm{e}^{+\mathrm{i}(E_{\mathrm{kin}} + E^{\mathrm{f}}_{\alpha_0} - \hat{H}^{\#})t/\hbar} = \sum_{\alpha} \mathrm{e}^{+\mathrm{i}(E_{\mathrm{kin}} + \epsilon^{\mathrm{f}}_{\alpha_0} - \epsilon^{\#}_{\alpha})t/\hbar} |\chi^{\#}_{\alpha})(\chi^{\#}_{\alpha}| \tag{8.236}$$

---

[16] N. Moiseyev and O. Goscinski, *Chem. Phys. Lett.* **120**, 520 (1985).

and consequently,

$$\frac{\partial C_{\alpha_0}(t)}{\partial t} = \mathrm{i}\sum_{\alpha}(\chi^{\mathrm{f}}_{\alpha_0}|\sqrt{\Gamma(R)}|\chi^{\#}_{\alpha})(\chi^{\#}_{\alpha}|\xi^{\#}(0))\mathrm{e}^{+\mathrm{i}(E_{\mathrm{kin}}+\epsilon^{\mathrm{f}}_{\alpha_0}-\epsilon^{\#}_{\alpha})t/\hbar}. \tag{8.237}$$

By integrating over time (while keeping in mind that $\epsilon^{\mathrm{f}}_{\alpha_0}$ is real and $\mathrm{Im}[\epsilon^{\#}_{\alpha}] < 0$ and the initial condition of $C_\alpha(0) = 0$) one gets that

$$C_\alpha(\infty) = \sum_{\alpha}\frac{(\chi^{\mathrm{f}}_{\alpha_0}|\sqrt{\Gamma(R)}|\chi^{\#}_{\alpha})(\chi^{\#}_{\alpha}|\xi^{\#}(0))}{E_{\mathrm{kin}}+\epsilon^{\mathrm{f}}_{\alpha_0}-\epsilon^{\#}_{\alpha}}. \tag{8.238}$$

By substituting Eq. (8.238) in Eq. (8.233) one gets the *same expression as obtained from non-Hermitian scattering theory which is given in Eq. (8.93).*

Answer to Exercise 8.4

The field-free (FF) electronic eigenfunctions are denoted here by $|\psi_j)$. The associated eigenvalues are E^{FF}_j. The t' periodic basis functions are denoted by $|n)$, where $(t'|n) = (1/T)\,\mathrm{e}^{\mathrm{i}\omega n t'}$. The basis functions of the full problem are thus denoted by $|j, n)$, where $j = 1, \ldots, N_{\mathrm{FF}}$, $n = 0, \pm 1, \pm 2, \ldots, \pm(N_{\mathrm{f}} - 1)/2$ and the number of the Fourier channels of the field is $N_{\mathrm{f}} \geq 3$. The notation ([...]) stands for the calculation of the scalar product (when the field-free Hamiltonian is an unscaled Hermitian operator) where the integration is over the electronic coordinates and over the the t' coordinate (from $t' = 0$ to $t' = T$). When the field-free Hamiltonian is complex-scaled then one should use the c-product rather than the scalar product for the integration over the spatial coordinates, while there is no effect in the integration over the t' coordinate. For the sake of simplicity we assume here that the spatial basis functions are the eigenfunctions of the complex scaled non-Hermitian Hamiltonian and therefore the c-product is used in the calculations of the Floquet Hamiltonian matrix. Note that in order to further simplify the notation here we assume that the eigenfunctions of the field-free non-Hermitian Hamiltonian, $\hat{H}^{\theta}_{\mathrm{S}}$, are complex functions *only* due to the complex similarity transformation which has been used for the construction of $\hat{H}^{\theta}_{\mathrm{S}}$. Here we assume that the electronic coordinates were scaled by $\mathrm{e}^{\mathrm{i}\theta}$. The elements of the Floquet matrix are given accordingly by

$$\begin{aligned}\mathbf{H}_{\mathrm{F}}(jn, j'n') &= \frac{1}{T}\int_0^T \mathrm{d}t'\mathrm{e}^{-\mathrm{i}\omega_{\mathrm{L}}nt'}(\psi_j| - \mathrm{i}\hbar\partial_{t'} + \hat{H}^{\theta}_{\mathrm{S}} + \hat{V}_{\theta}(t')|\psi_{j'})\mathrm{e}^{+\mathrm{i}\omega_{\mathrm{L}}n't'}\\ &= [E^{\mathrm{FF}}_j + \hbar\omega_{\mathrm{L}}]\delta_{n,n'}\delta_{j,j'} + \frac{1}{T}\int_0^T \mathrm{d}t'\mathrm{e}^{+\mathrm{i}\omega_{\mathrm{L}}(n'-n)t'}(\psi_j|\hat{V}_{\theta}(t')|\psi_{j'})\end{aligned} \tag{8.239}$$

The eigenvalues E_j^{FF} are real for the energies which are associated with the bound states of the field-free complex-scaled Hamiltonian. On the other hand the eigenvalues are complex *θ-independent* values for the shape or Feshbach resonances of the field-free system (e.g., auto-ionization or Auger or ICD resonances), and complex θ-dependent eigenvalues which are associated with the rotated continua. The rotated continua become discrete due to the use of a finite number of field-free basis functions.

For a cw linearly polarized laser

$$\hat{V}_\theta(t') = e\epsilon_0 \mathrm{e}^{\mathrm{i}\theta} \sum_i x_i^{\mathrm{elec}} \cos(\omega_{\mathrm{L}} t') \tag{8.240}$$

and therefore

$$\mathbf{H}_{\mathrm{F}}^{\theta}(jn, j'n') = [E_j^{\mathrm{FF}} + \hbar\omega_{\mathrm{L}}]\delta_{n,n'}\delta_{j,j'} + \frac{\epsilon_0}{2} d_{j,j'}\delta_{n\pm 1,n'}\,, \tag{8.241}$$

where the electronic dipole transition matrix elements are given by

$$d_{j,j'} = \mathrm{e}^{\mathrm{i}\theta}(\psi_j|e\sum_i x_i^{\mathrm{elec}}|\psi_{j'})\,. \tag{8.242}$$

The complex non-unitary time evolution operator $\hat{U}(t \leftarrow 0)$ is defined as

$$\begin{aligned}\hat{U}(t \leftarrow 0) &= \sum_{j,j'}\sum_{n,n'} |j,n)(j,n|\mathrm{e}^{-\mathrm{i}\hat{H}_{\mathrm{F}}t/\hbar}|j',n')(j',n'| \\ &= \sum_{j,j'}\sum_{n,n'} [\mathrm{e}^{-\mathrm{i}\mathbf{H}_{\mathrm{F}}^{\theta}t/\hbar}]_{jn,j'n'}|j,n)(j',n'|\,. \end{aligned} \tag{8.243}$$

Since the initial state is a time-independent function we may choose it to be also a t'-independent function for which the only non-vanishing Fourier component is associated with the $n' = 0$ Fourier component. Therefore the time evolution operator can be rewritten as

$$\hat{U}(t \leftarrow 0) = \sum_n \sum_{j,j'} [\mathrm{e}^{-\mathrm{i}\mathbf{H}_{\mathrm{F}}^{\theta}t/\hbar}]_{jn,j'0}|j,n)(j',0|\,. \tag{8.244}$$

By using the field-free eigenfunctions of the complex-scaled non-Hermitian Hamiltonian as a basis set, the eigenfunctions of the time evolution complex scaled non-Hermitian Floquet operator at $t = nT$, where $n = 0, 1, \ldots,$ are associated with the eigenvectors of the time-evolution matrix $\mathbf{U}(T \leftarrow 0)$ which can be decomposed to many small time steps $\mathrm{d}t$:

$$\mathbf{U}(T \leftarrow 0) = \mathbf{U}(T \leftarrow T - \mathrm{d}t)\mathbf{U}(T - \mathrm{d}t \leftarrow T - 2\mathrm{d}t)\ldots\mathbf{U}(2\mathrm{d}t \leftarrow \mathrm{d}t)\mathbf{U}(\mathrm{d}t \leftarrow 0), \tag{8.245}$$

where $T = N_t \mathrm{d}t$ and N_t is the number of time steps during the propagation from $t = 0$ to $t = T$. The dimension of the complex time-evolution matrix is $N_{\mathrm{FF}} \times N_{\mathrm{FF}}$, where N_{FF} is the number of eigenfunctions of the complex scaled field-free Hamiltonian which have been used as a basis set in our calculations. Note that for molecules we may not use the complex scaling transformation but must apply the smooth-exterior-scaling (SES) transformation instead since the attraction Coulombic potential energy of an electron j and a nuclei α is inversely proportional to $|\mathbf{r}_j - \mathbf{R}_\alpha|$, which is not a dilation analytic function and complex scaling is not applicable. However, by using the SES transformation or the exterior scaling transformation, as described in Chapter 5, the transformation into the complex coordinate plane takes place when the electron–nuclei attractive potential term attains a sufficiently small value which within the accuracy of the numerical calculations can be regarded as zero. The propagator for a short time interval is calculated by

$$\begin{aligned}[\mathbf{U}(t_0 + \mathrm{d}t \leftarrow t_0)]_{j,j'} &= \sum_{n,n'} \mathrm{e}^{+\mathrm{i}\omega_{\mathrm{L}} n(t_0+\mathrm{d}t)} [\mathrm{e}^{-\mathrm{i}\mathbf{H}_{\mathrm{F}}^{\theta}\mathrm{d}t/\hbar}]_{jn,j'n'} \mathrm{e}^{-\mathrm{i}\omega_{\mathrm{L}} n't'} \delta_{n',0} \\ &= \sum_{n} \mathrm{e}^{-\mathrm{i}\omega_{\mathrm{L}} n(t_0+\mathrm{d}t)} [\mathrm{e}^{-\mathrm{i}\mathbf{H}_{\mathrm{F}}^{\theta}\mathrm{d}t/\hbar}]_{jn,j'0}\,, \end{aligned} \tag{8.246}$$

where $t_0 = k\mathrm{d}t$ and $k = 0, 1, 2, \ldots, (N_t - 1)$. Here we use the fact that within the framework of the (t, t') formalism the Floquet operator is t-independent (t' serves as additional coordinate) and therefore the time evolution operator has an analytical expression just like the time-independent Hamiltonian. We see that the evolution relies on the matrix $\mathbf{A} = [\mathrm{e}^{-\mathrm{i}\mathbf{H}_{\mathrm{F}}^{\theta}\mathrm{d}t/\hbar}]$ which has dimensions which depend on the number of eigenfunctions of the field-free Hamiltonian that are used as a basis set and the number of Fourier channels accounted for. For small values of dt the matrix $\mathbf{A} = [\mathrm{e}^{-\mathrm{i}\mathbf{H}_{\mathrm{F}}^{\theta}\mathrm{d}t/\hbar}]$ can be calculated using a Taylor series expansion. For a sufficiently small value of dt an expansion up to the linear term will be enough and thus $\mathbf{A} \simeq 1 - \mathrm{i}\mathbf{H}_{\mathrm{F}}^{\theta}\mathrm{d}t/\hbar$. In the case of linearly polarized light the Floquet Hamiltonian matrix is a tridiagonal matrix and therefore

$$[\mathbf{A}]_{jn,j'0} = [1 - \mathrm{i}\mathrm{d}t(E_j^{\mathrm{FF}}/\hbar + \omega_{\mathrm{L}})]\delta_{n,0}\delta_{j',j} + \frac{\epsilon_0}{2} d_{j',j}\delta_{n,\pm 1} \tag{8.247}$$

and it is sufficient to construct the Floquet Hamiltonian matrix from just *three* Fourier basis functions $\mathrm{e}^{-\omega_{\mathrm{L}} nt'}; n = -1, 0, +1$ even for a very strong laser field. This is quite a surprising result. For strong laser fields the photo-ionized (dissociated) resonance positions (energies) and widths (inverse lifetimes) can be obtained from a direct diagonalization of the complex scaled Floquet matrix $\mathbf{H}_{\mathrm{F}}^{\theta}$ only when a very large number of Fourier components is used (i.e., $\mathrm{e}^{\mathrm{i}\omega_{\mathrm{L}} nt'}; n = 0, \pm 1, \pm 2, \ldots, \pm(N_{\mathrm{f}} - 1)/2$, where N_{f} should become very large). See, for example, the results presented in Fig. 8.2 which were obtained from the diagonalization

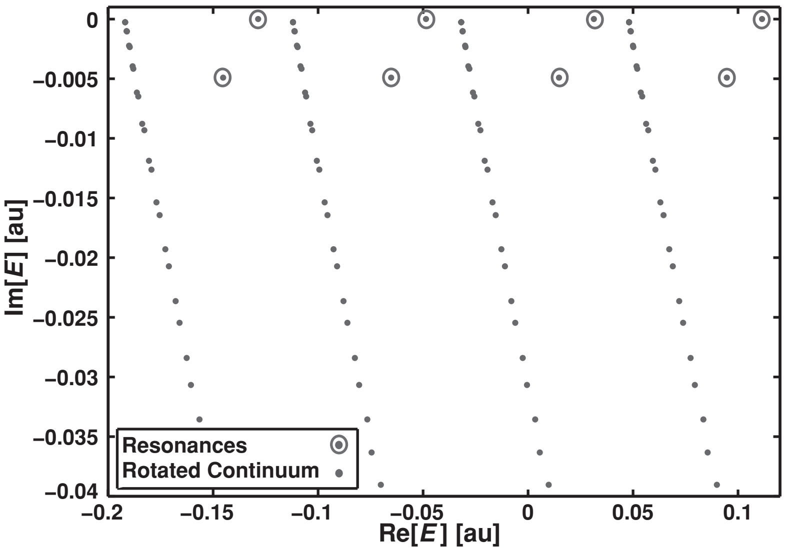

Figure 8.2 The real (energy) vs. the imaginary (inverse lifetime) parts of the eigenvalues of the complex scaled Floquet matrix which has been calculated for a 1D model Hamiltonian of xenon (a Gaussian potential that supports three bound states where the two lowest ones provide respectively the ionization energies of xenon in its ground and first excited electronic states) which interacts with a linear polarized laser field. All quantities are given in au.

of the complex scaled Floquet matrix for a 1D model Hamiltonian of xenon in a strong laser field.

The resonances are associated with cusps in the θ-trajectory calculations and become less and less affected by the rotational angle as the basis set approaches completeness. The resonances appear as isolated points in the complex energy plane. The non-resonance solutions are the rotated continua that are affected by θ. As the basis set is increased the solutions which are associated with the continua become more dense since the continuous spectrum is discretizised by the use of a finite number of basis functions. As the basis set is increased the eigenvalues of the complex Floquet Hamiltonian matrix which are associated with the rotated continuum fall onto straight lines with a slope of $\tan 2\theta$. The same results where obtained by a much smaller computational effort by the diagonalization of the time-evolution complex matrix (the relations between the complex eigenvalues of the complex scaled Floquet matrix and the eigenvalues of the complex scaled time-evolution matrix are presented in Eq. (8.110). The reason for the reduction of the computational efforts when we diagonalize the complex time-evolution matrix rather than the complex Floquet matrix is as follows: although only three t'-Fourier basis functions might be sufficient for the construction of $\mathbf{A}$ and of

$[\mathbf{U}(t_0 + \mathrm{d}t \leftarrow t_0)]$ the construction of the full time-evolution matrix $[\mathbf{U}(T \leftarrow 0)]$ is by using $3N_t$ Fourier basis set. Specifically, in every time step of propagation from t to $t + \mathrm{d}t$ we use only three Fourier basis functions, but due to Eq. (8.245) the number of Fourier basis functions which construct the propagated function is $3N_t$, and this is the "secret" which stands behind the astonishing ability of the (t, t') method to calculate very accurately the photo-induced resonance positions and widths from the diagonalization of $[\mathbf{U}(T \leftarrow 0)]$ despite of the fact that the Floquet matrix has been constructed from three t'-Fourier basis functions only.

Answer to Exercise 8.5

(1) An electric field of a linearly polarized cw laser is given by

$$E(t) = e \sum_{j=1}^{N} x_j \epsilon_0 \cos \omega_{\mathrm{L}} t \,, \tag{8.248}$$

where ϵ_0 is the maximum field amplitude, ω_{L} is the laser frequency, e is the charge of an electron and $\{x_j\}$ are the x-components of the vector positions of the N electrons in the system. Therefore, the complex scaled Floquet operator in the acceleration gauge is given by

$$\hat{\mathcal{H}}^{\mathrm{ac}}(\{\mathbf{r}_j\}, t; \theta) = -\mathrm{i}\hbar\partial_t - \mathrm{e}^{-2\mathrm{i}\theta} T_{\mathrm{e}} + \hat{V}_{\mathrm{eN}}(\{\mathrm{e}^{\mathrm{i}\theta}\mathbf{r}_{\boldsymbol{j}} + \alpha_0 \cos \omega_{\mathrm{L}} t \mathbf{e}_x\}) + \mathrm{e}^{-\mathrm{i}\theta} \hat{V}_{\mathrm{ee}} \,. \tag{8.249}$$

Here $\{\mathbf{r}_j\}$ represent the coordinates of all electrons, where $j = 1, 2, \ldots, N$. $\hat{T}_{\mathrm{e}}$ is the *unscaled* kinetic energy operator of all the electrons, $\hat{V}_{\mathrm{eN}}$ is the *complex scaled* electron–nuclei attractive Coulombic potential term in the acceleration representation and $\hat{V}_{\mathrm{ee}}$ is the *unscaled* electron–electron repulsion term between all electrons. $\alpha_0 = e\epsilon_0/(\mu\omega_{\mathrm{L}}^2)$ is the free-electron quiver motion amplitude and $\mathbf{e}_x$ is a unit vector along the polarization axis. The n-th order of the resonance quasi-energies (eigenvalues of $\hat{\mathcal{H}}^{\mathrm{ac}}$) can be evaluated using time-independent perturbation theory (extended to the non-Hermitian case) when time is treated as a additional coordinate. The zero-order complex scaled Floquet operator in this case is defined by

$$\hat{\mathcal{H}}^{(0)}_{\mathrm{ac}}(\{\mathbf{r}_j\}; \theta) = -\mathrm{i}\hbar\partial_t + \mathrm{e}^{-2\mathrm{i}\theta} \hat{T}_{\mathrm{e}} + V_0^{\mathrm{ac}}(\{\mathbf{r}_j\}; \theta) + \mathrm{e}^{-\mathrm{i}\theta} \hat{V}_{\mathrm{ee}} \,, \tag{8.250}$$

where V_0^{ac} is the temporal average over one optical cycle of the electron–nuclei potential energy operator,

$$V_0^{\mathrm{ac}}(\{\mathbf{r}_j\}; \theta) = \frac{1}{T} \int_0^T \mathrm{d}t \, \hat{V}_{\mathrm{eN}}(\{\mathrm{e}^{\mathrm{i}\theta}\mathbf{r}_j + \alpha_0 \cos \omega_{\mathrm{L}} t \mathbf{e}_x\}) \,. \tag{8.251}$$

This leaves the rest of the potential as a time-dependent perturbation given by

$$\begin{aligned}\hat{V}^{\mathrm{ac}}_{\mathrm{pert}}(\{\mathbf{r}_j\},t;\theta) &= \hat{V}_{\mathrm{eN}}(\{\mathrm{e}^{\mathrm{i}\theta}r_j+\alpha_0\cos\omega_{\mathrm{L}}t\mathbf{e}_x\})-V^{\mathrm{ac}}_0(\{\mathbf{r}_j\};\theta)\\ &=\sum_{m\neq 0}V^{\mathrm{ac}}_m(\{\mathbf{r}_j\};\theta)\mathrm{e}^{im\omega_{\mathrm{L}}t}\,,\end{aligned}\tag{8.252}$$

where

$$V^{\mathrm{ac}}_m(\{\mathbf{r}_j\};\theta)=\frac{1}{T}\int_0^T \mathrm{d}t\mathrm{e}^{-\mathrm{i}m\omega_{\mathrm{L}}t}\hat{V}_{\mathrm{eN}}(\{\mathrm{e}^{\mathrm{i}\theta}\mathbf{r}_j+\alpha_0\cos\omega_{\mathrm{L}}t\mathbf{e}_x\})\,.\tag{8.253}$$

Note that the zeroth Fourier component is subtracted from the perturbation since it is included in the zero-order Hamiltonian. The zero-order photo-induced resonance positions and widths are associated with the θ-independent eigenvalues of $\hat{\mathcal{H}}^{(0)}_{\mathrm{ac}}(\{\mathbf{r}_j\},t;\theta)$,

$$\hat{\mathcal{H}}^{(0)}_{\mathrm{ac}}[\mathrm{e}^{\mathrm{i}\omega_{\mathrm{L}}nt}\Phi^{(0)}_j(\{\mathbf{r}_j\};\theta)]=\left[(\epsilon^{(0)}_j+\hbar\omega_{\mathrm{L}}n)-\frac{\mathrm{i}}{2}\Gamma^{(0)}_j\right][\mathrm{e}^{\mathrm{i}\omega_{\mathrm{L}}nt}\Phi^{(0)}_j(\{\mathbf{r}_j\};\theta)]\,.\tag{8.254}$$

It is important to notice that $\Phi^{(0)}_j(\{\mathbf{r}_j\};\theta)$, where $j=1,2,\ldots,N$, are the *time-independent* eigenfunctions of the *time-independent* operator,

$$\hat{H}^{(0)}_{\mathrm{ac}}(\{\mathbf{r}_j\};\theta)=\mathrm{e}^{-2\mathrm{i}\theta}\hat{T}_{\mathrm{e}}+V^{\mathrm{ac}}_0(\{\mathbf{r}_j\};\theta)+\mathrm{e}^{-\mathrm{i}\theta}\hat{V}_{\mathrm{ee}}\,,\tag{8.255}$$

which satisfy

$$\hat{H}^{(0)}_{\mathrm{ac}}\Phi^{(0)}_j(\{\mathbf{r}_j\};\theta)=\left[\epsilon^{(0)}_j-\frac{\mathrm{i}}{2}\Gamma^{(0)}_j\right]\Phi^{(0)}_j(\{\mathbf{r}_j\};\theta)\,.\tag{8.256}$$

The zero-order photo-induced resonance positions and widths depend only on *one* field parameter, α_0, which is the free-electron quiver motion amplitude.

The first-order corrections to the resonance quasi-energies eigenvalues of the complex scaled Floquet operator vanish because of the integration over the additional "time" coordinate,

$$\begin{aligned}\epsilon^{(1)}_j-\frac{\mathrm{i}}{2}\Gamma^{(1)}_j &= \frac{1}{T}\int_0^T \mathrm{d}t\int\prod_{j=1}^{N}\mathrm{d}\mathbf{r}_j\Phi^{(0)}_j(\{\mathbf{r}_j\};\theta)\hat{V}^{\mathrm{ac}}_{\mathrm{pert}}(\{\mathbf{r}_j\},t;\theta)\Phi^{(0)}_j(\{\mathbf{r}_j\};\theta)\\ &=\sum_{m\neq 0}\Big[\frac{1}{T}\int_0^T \mathrm{d}t\,\mathrm{e}^{\mathrm{i}m\omega_{\mathrm{L}}t}\Big]\int\prod_{j=1}^{N}\mathrm{d}\mathbf{r}_j[\Phi^{(0)}_j(\{\mathbf{r}_j\};\theta)]^2V^{\mathrm{ac}}_m(\{\mathbf{r}_j\};\theta)\\ &=\sum_{m\neq 0}\Big[\frac{1}{T}\int_0^T \mathrm{d}t\mathrm{e}^{\mathrm{i}m\omega_{\mathrm{L}}t}\Big](\Phi^{(0)}_j(\theta)|V^{\mathrm{ac}}_m(\theta)|\Phi^{(0)}_j(\theta))=0\,,\end{aligned}\tag{8.257}$$

since $[\frac{1}{T}\int_0^T \mathrm{d}t \mathrm{e}^{\mathrm{i}m\omega_{\mathrm{L}}t}] = 0$ for $m \neq 0$. Note that in the integration over space we have used here the c-product. The second-order corrections to the resonance quasi-energies for a many-electron system are given by

$$\epsilon_j^{(2)} - \frac{\mathrm{i}}{2}\Gamma_j^{(2)} = \sum_{m\neq 0}\sum_k \frac{((\Phi_k^{(0)\text{-res}}(\theta)|V_m^{\mathrm{ac}}(\theta)|\Phi_j^{(0)\text{-res}}(\theta)))^2}{[\epsilon_j^{(0)} - \frac{\mathrm{i}}{2}\Gamma_j^{(0)}] - [\epsilon_k^{(0)} + \hbar\omega_{\mathrm{L}}m - \frac{\mathrm{i}}{2}\Gamma_k^{(0)}]}\,. \tag{8.258}$$

(2) The Gilary–Moiseyev (GM) transformation implies that the eigenfunctions of the complex scaled Floquet operator in the acceleration gauge can be written as

$$\Phi_j^{\mathrm{res}}(\{\mathbf{r}_j\}, t;\theta) = \mathrm{e}^{\frac{\mathrm{i}}{\hbar}\int_0^t \mathrm{d}t' \hat{V}_{\mathrm{pert}}^{\mathrm{ac}}(\{\mathbf{r}_j\};\theta)}\chi_j^{\mathrm{res}}(\{\mathbf{r}_j\};\theta)\,. \tag{8.259}$$

By substituting Eq. (8.259) into

$$\hat{\mathcal{H}}^{\mathrm{ac}}\Phi_j^{\mathrm{res}}(\{\mathbf{r}_j\}, t;\theta) = \left[\epsilon_j - \frac{\mathrm{i}}{2}\Gamma_j\right]\Phi_j^{\mathrm{res}}(\{\mathbf{r}_j\};\theta)\,, \tag{8.260}$$

where $\hat{\mathcal{H}}^{\mathrm{ac}}$ is defined in Eq. (8.249) one gets that the transformed square integrable resonance wavefunctions, $\chi_j^{\mathrm{res}}(\{\mathbf{r}_j\};\theta)$, are eigenfunctions of the transformed complex scaled Floquet operator,

$$\hat{\mathcal{H}}^{\mathrm{GM}} = \hat{\mathcal{H}}_{\mathrm{ac}}^{(0)} + \hat{V}_{\mathrm{pert}}^{\mathrm{GM}}\,, \tag{8.261}$$

where

$$\hat{V}_{\mathrm{pert}}^{\mathrm{GM}} = -\frac{1}{2\mu\omega_{\mathrm{L}}^2}\left(\sum_{n\neq 0}\frac{f_n}{n}\mathrm{e}^{\mathrm{i}\omega_{\mathrm{L}}nt}\right)^2$$

$$-\,\mathrm{e}^{-\mathrm{i}\theta}\frac{\hbar}{2\mu\omega_{\mathrm{L}}}\sum_{n\neq 0}\frac{1}{n}\frac{\partial f_n}{\partial \mathbf{x}}\mathrm{e}^{\mathrm{i}n\omega_{\mathrm{L}}t} - \mathrm{e}^{-\mathrm{i}\theta}\frac{\hbar}{\mu\omega_{\mathrm{L}}}\sum_{n\neq 0}\frac{f_n}{n}\mathrm{e}^{\mathrm{i}n\omega_{\mathrm{L}}t}\sum_{j=1}^{N}\frac{\partial}{\partial x_j} \tag{8.262}$$

and $f_n(\{\mathbf{r}_j\};\theta)$, where $n = \pm 1, \pm 2, \ldots$, are the Fourier components of the complex scaled force:

$$f_n(\{\mathbf{r}_j\};\theta) = -\mathrm{e}^{-\mathrm{i}\theta}\sum_{j=1}^{N}\frac{\partial}{\partial x_j}V_n^{\mathrm{ac}}(\{\mathbf{r}_j\};\theta)\,. \tag{8.263}$$

8.5 Further reading

Useful references not necessarily related to NHQM

U. Peskin, O. E. Alon and N. Moiseyev, The solution of the time-dependent Schrödinger equation by the (t, t') method: multiphoton ionization/dissociation probabilities in different gauges of the electromagnetic potentials, *J. Chem. Phys.* **100**, 7310 (1994).

J. W. Pang, D. Neuhauser and N. Moiseyev, Photoabsorption probability for a system governed by a time-dependent Hamiltonian through the (t, t') formalism, *J. Chem. Phys.* **106**, 6839–6847 (1997).

D. W. Hone, R. Ketzmerik and W. Kohn, Time-dependent Floquet theory and absence of an adiabatic limit, *Phys. Rev. A* **56**, 4045–4054 (1997).

K. Drese and M. Holthaus, Floquet theory for short laser pulses, *Eur. Phys. J. D.* **5**, 119–134 (1999).

D. Barash, A. E. Orel and R. Baer, Laser-induced resonance states as dynamic suppressors of ionization in high-frequency short pulses, *Phys. Rev. A* **61**, 013402/1–013402/5 (1999).

Partial widths and cross sections for time-independent Hamiltonians

J. Nuttal and H. L. Cohen, Method of complex coordinates for three-body calculations above the breakup threshold, *Phys. Rev.* **188**, 1542–1544 (1969).

T. Noro and H. S. Taylor, Resonance partial widths and partial photodetachment rate using the rotated-coordinate method, *J. Phys. B* **13**, L377–L381 (1980).

B. R. Johnson and W. P. Reinhardt, L2 discretization and complex coordinates in the calculation of bound-free amplitudes in the presence of long-range forces", *Phys. Rev. A* **28**, 1930–1944 (1983).

T. N. Rescigno and C. W. McCurdy, Locally complex distortions of the energy spectrum in the calculation of scattering amplitudes and photoionization cross sections, *Phys. Rev. A* **31**, 624–633 (1985).

P. Froelich, A. Flores-Riveros and W. Wegric, Nonrelativistic Compton scattering in Furry's picture. II. Bethe surface by means of the complex-coordinate method, *J. Chem. Phys.* **82**, 2305–2312 (1985).

N. Moiseyev and U. Peskin, Partial widths obtained by the complex resonance-scattering theory, *Phys. Rev. A* **42**, 255–260 (1990).

U. Peskin and N. Moiseyev, The complex coordinate scattering theory and the Kohn variational method: a general formulation and application to long range potentials, *J. Chem. Phys.* **97**, 6443–6450 (1992).

E. Narevicius and N. Moiseyev, Trapping of an electron due to molecular vibrations, *Phys. Rev. Lett.* **84**, 1681–1684 (2000).

N. Moiseyev, R. Santra, J. Zobeley and L. S. Cederbaum, Fingerprints of the nodal structure of autoionizing vibrational wave functions in clasters: interatomic Coulombic decay in Ne dimer, *J. Chem. Phys*, **114**, 7351–7360 (2001).

E. Narevicius, P. Serra and N. Moiseyev, Critical phenomena associated with self-orthogonality in non-Hermitian quantum mechanics, *Europhys. Lett.* **62**, 789–794 (2003).

E. Narevicius and N. Moiseyev, Non-Hermitian quantum mechanics: formalism and applications, *Fundamental World of Quantum Chemistry* **2**, 1–32 (2003).

P. Zdanska, H. R. Sadeghpour, N. Moiseyev, Non-Hermitian diabatic formulation of antiproton collision: protonium formation, *J. Phys. B: At. Mol. Opt. Phys.* **37**, L35–L41 (2004).

E. Narevicius, N. Moiseyev, H. R. Sadeghpour and L. S. Cederbaum, Extremely narrow peaks in predissociation of sodium dimer due to rovibronic coupling, *J. Chem. Phys*, **121**, 3527–3532 (2004).

Cross sections for scattering of atoms and molecules from solid surfaces

N. Moiseyev, T. Maniv, R. Elber and R. B. Gerber, Lifetimes of rotational resonances in molecule-surface scattering: quantum versus classical results, *Mol. Phys.* **55**, 1369–1381 (1985).

T. Maniv, E. Engdahl and N. Moiseyev, Application of the complex rotation method to the study of resonance states of atoms at a corrugated surface, *J. Chem. Phys.* **86**, 1048–1054 (1987).

E. Engdahl, T. Maniv and N. Moiseyev, Complex quasiprobability for atoms trapped on surfaces: a novel application of the complex coordinate method, *J. Chem. Phys.* **88**, 5864–5870 (1988).

A. Ben-Ephraim, M. Folman, J. Heidberg and N. Moiseyev, Predesorption of CO from the sodium chloride (100) surface: study by the complex coordinate method, *J. Chem. Phys.* **89**, 3840–3846 (1988).

N. Moiseyev, Complex scaling applied to trapping of atoms and molecules on solid surfaces, in E. Brändas and N. Elander, eds. Resonances, the Unifying Route Towards the Formulation of Dynamical Processes. *Lecture Notes in Physics*, Berlin, Springer-Verlag, 1989.

E. Engdahl and N. Moiseyev, Perturbation analysis of gas-surface diffractive selective adsorption resonance states, *Mol. Phys.* **66**, 465–478 (1989).

E. Engdahl, T. Maniv and N. Moiseyev, Gas-surface scattering cross section by the complex coordinate method, *J. Chem. Phys.* **94**, 6330–6333 (1991).

U. Peskin and N. Moiseyev, Gas/surface complex coordinate scattering theory: HD/Ag(111), HD/Pt(111) rotationally inelastic transition intensities, *J. Chem. Phys.* **96**, 2347–2355 (1992).

U. Peskin and N. Moiseyev, The complex coordinate scattering theory: broken inversion symmetry of corrugated surfaces in helium diffraction from Cu(115), *J. Chem. Phys.* **97**, 2804–2808 (1992).

U. Peskin and N. Moiseyev, The complex coordinate scattering theory and its application to the study of the surface asymmetry effect in helium diffraction from copper, *Int. J. Quantum. Chem.* **46**, 343–363 (1993).

A. K. Gupta and N. Moiseyev, Trapping of molecules by highly rotational excitations, *Chem. Phys.* **338**, 113–120 (2007).

Resonances, partial widths and cross sections for time-dependent Hamiltonians

N. Moiseyev, F. Bensch and H. J. Korsch, Multiphoton dissociation or ionization partial widths and branching ratios for time-periodic systems, *Phys. Rev. A* **42**, 4045–4049 (1990).

F. Bensch, H. J. Korsch and N. Moiseyev, Decay dynamics of a time-periodic quantum system, *J. Phys. B* **24**, 1321–1341 (1991).

N. Ben-Tal, N. Moiseyev, C. Leforestier and R. Kosloff, Positions, lifetimes, and partial widths of metastable quasienergy states by solving the time-dependent complex-scaled Schrödinger equation, *J. Chem. Phys.* **94**, 1636–1642 (1991).

F. Bensch, H. J. Korsch and N. Moiseyev, Simple method for constructing the ionization spectra of driven time-periodic Hamiltonians, *Phys. Rev. A* **43**, 5145–5148 (1991).

U. Peskin and N. Moiseyev, The solution of the time-dependent Schrödinger equation by the (t, t') method: theory, computational algorithm and applications, *J. Chem. Phys.* **99**, 4590–4596 (1993).

N. Moiseyev, The solution of the time-dependent Schrödinger equation by the (t, t') method: complex scaled multiphoton ionization/dissociation resonance wave functions are square integrable, *J. Chem. Phys.* **101**, 9716–9718 (1994).

I. Vorobeichik and N. Moiseyev, State-to-state transition probabilities for time-dependent Hamiltonians using complex absorbing potentials, *J. Phys. B* **31**, 645–656 (1998).

I. Gilary, A. Fleischer and N. Moiseyev, Calculations of time-dependent observables in non-Hermitian quantum mechanics: the problem and a possible solution, *Phys. Rev. A* **72**, 012117/1–012117/8 (2005).

A. Fleischer and N. Moiseyev, Adiabatic theorem for non-Hermitian time-dependent open systems. *Phys. Rev. A* **72**, 032103/1–032103/11 (2005).

High harmonic generation (HHG) and above threshold ionization (ATI) by NHQM

N. Ben-Tal, N. Moiseyev, R. Kosloff and C. Cerjan, Harmonic generation in ionizing systems by the time-dependent complex coordinate Floquet Method, *J. Phys. B* **26**, 1445–1461 (1993).

U. Peskin and N. Moiseyev, Time-independent scattering theory for time-periodic hamiltonians: formulation and complex scaling calculations of above-threshold -ionization spectra, *Phys. Rev. A* **49**, 3712–7318 (1994).

N. Moiseyev, M. Chrysos, O. Atabek and R. Lefebvre, harmonic generation in molecular systems: application to H2+ in intense laser fields, *J. Phys. B* **28**, 2007–2019 (1995).

N. Moiseyev and F. Weinhold, High harmonic generation spectra of neutral helium by the complex-scaled (t, t') method: role of dynamical electron correlation, *Phys. Rev. Lett.,* **78**, 2100–2103 (1997).

P. Zdanska, V. Averbukh and N. Moiseyev, High harmonic generation spectra of aligned benzene in circular polarized laser field, *J. Chem. Phys.* **118**, 8726–8738 (2003).

N. Moiseyev and M. Lein, Non-Hermitian quantum mechanics for high-order harmonic generation spectra, *J. Phys. Chem. A* **107**, 7181–7188 (2003).

A. Fleischer, V. Averbukh and N. Moiseyev, Non-Hermitian quantum mechanics versus the conventional quantum mechanics: effect of the relative phasing of bichromatic fields on high-order harmonic generation, *Phys. Rev. A* **69**, 043404/1–043404/8 (2004).

I. Gilary, P. Zdanska and N. Moiseyev, Ab initio calculation of harmonic generation spectra of helium using a time-dependent non-Hermitian formalism. *Phys Rev. A* **74**, 052505/1–052505/8 (2006).

A. Fleischer and N. Moiseyev, Attosecond laser pulse synthesis using bichromatic high-order harmonic generation, *Phys. Rev. A* **74**, 053806/1–053806/7(2006).

A. Fleischer and N. Moiseyev, Amplification of high-order harmonics using weak perturbative high-frequency radiation, *Phys. Rev. A* **77**, 010102/1(R)–010102/4(R) (2008).

A. Fleischer, A. K. Gupta and N. Moiseyev, Dynamical symmetry analysis of ionization and harmonic generation of atoms in bichromatic laser pulses, *Int. J. Quantum Chem.* **103**, 824–840 (2005).

Calculations of leaking modes by NHQM methods

I. Vorobeichik, U. Peskin and N. Moiseyev, Modal losses and design of modal irradiance patterns in an optical fiber by the complex (t,t′) method, *J. Opt. Soc. An. B* **12**, 1133–1141 (1995).

A. M. Kenis, I. Vorobeichik and N. Moiseyev, Analysis of an intermediate-mode-assisted optical directional coupler using Bloch theory, *IEEE J. Quant. Electron.* **36**, 563–573 (2000).

Resonances for the non-linear Schrödinger equation

N. Moiseyev and L. S. Cederbaum, Resonance solutions of the nonlinear Schrödinger equation: tunneling lifetime and fragmentation of trapped condensates, *Phys. Rev. A* **72**, 033605/1–033605/8 (2005).

N. Moiseyev, L. D. Carr, B. A. Malomed and Y. B. Band. Transition from resonances to bound states in nonlinear systems: application to BEC, *J. Phys. B* **37**, L193–L200 (2004).

Dynamics on complex potential energy surfaces: kinetic energy distribution of ionized electrons from electronically excited molecules

E. Narevicius and N. Moiseyev, Non-Hermitian formulation of interference effect in scattering experiments, *J. Chem. Phys.* **113**, 6088–6095.

(2000); Structured photo-absorbtion spectra of ArHCl: fingerprints of overlapping broad resonances, *Chem. Phys. Lett.* **287**, 250–254 (1998).

N. Moiseyev, R. Santra, J. Zobeley and L. S. Cederbaum, Fingerprints of the nodal structure of autoionizing vibrational wave functions in clusters: interatomic coulombic decay in Ne dimer, *J. Chem. Phys.* **114**, 7351–7360 (2001).

S. Scheit, L. S. Cederbaum and H.-D. Meyer, Time-dependent interplay between electron emission and fragmentation in the interatomic Coulombic decay, *J. Chem. Phys.* **118**, 2092–2107 (2003).

N. Moiseyev, S. Scheit and L. S. Cederbaum, Non-Hermitian quantum mechanics: wave packet propagation on autoionizing potential energy surfaces, *J. Chem. Phys.* **121**, 722–725 (2004).

9

The self-orthogonality phenomenon

In the standard (Hermitian) formalism of quantum mechanics, usually when a potential parameter is varied the crossing of energy levels with the same symmetry is avoided. However, within the framework of the non-Hermitian formalism it is possible that two (or even more) complex eigenvalues with the same symmetry will cross. At the crossing point the eigenvalues are degenerate and this is accompanied by the coalescence of the eigenfunctions (or eigenvectors). Therefore, we may term this special situation as a non-Hermitian degeneracy. This special situation is associated with a branch point in the complex energy plane which is commonly termed an "exceptional point" in the spectrum of the non-Hermitian Hamiltonian. With respect to the c-product defined for non-Hermitian operators (matrices) in Chapter 6, the degenerate eigenstate is self-orthogonal. Since a branch point in the spectrum is removed by any infinitesimally small external perturbation, it seems to be inaccessible experimentally and may be considered just as a mathematical object rather than a physical one. However, as we will show here, by varying the potential parameters the existence of a branch point is reflected in the measurement of the geometrical phases also known as Berry phases. It should be stressed here that while in our case the geometrical phase results from a coalescence of eigenfunctions of a non-Hermitian Hamiltonian, the so-called Berry phase phenomenon occurs also within the Hermitian formalism of quantum mechanics when the eigenvalues of the molecular Hamiltonian in the Born–Oppenheimer approximation are degenerate for specific geometry of the poly-atomic molecule.[1] Moreover, sufficiently close to the branch point the eigenfunctions of the coalescing eigenvalues are nearly self-orthogonal. By normalizing these nearly degenerate states to unity the amplitudes of the wavefunction might attain enormously large values. This is due to the use of the c-product rather than the scalar product as in the standard formalism of quantum

---

[1] See, for example, W. Domcke, D. R. Yarkony and H. Koppel, *Conical Intersections: Electronic Structure, Dynamics and Spectroscopy*, Singapore, World Scientific, 2004.

mechanics. Of course, in the cases when the potentials are complex, as, for example, when the scalar Maxwell equation is solved in the paraxial approximation for a light beam that is propagated in a wave guide with complex index of refraction, it is a must to use the c-product, and the enormously large amplitude of the two modes which are almost coalesced can be observed in principle in the lab, as we have first predicted.[2] However, when the Hamiltonian is non-Hermitian only due to the requirement of the eigenfunctions of the Hamiltonian to have outgoing asymptotes, then one may use the conventional scalar product and not the c-product, and the normalized almost-degenerate eigenfunctions (i.e., the functions that are almost coalesced) would not get a very large amplitude. We advise the reader to read again Section 3.9 where we describe the propagation of a wavepacket $\phi(x, t)$ such that for a certain period of time (which is problem-dependent) in the interaction region $-L \leq x \leq +L$ where the potential is not equal to zero the propagated wavepacket can be described as $\phi(x, t) \simeq \mathrm{e}^{-\mathrm{i}E_{\mathrm{res}}t/\hbar}\psi_{\mathrm{res}}(x)$, where E_{res} and $\psi_{\mathrm{res}}(x)$ are correspondingly the complex eigenvalue and eigenfunction of the unscaled Hamiltonian, which are obtained under the requirement of an outgoing boundary condition (the so-called Siegert boundary condition[3]). We should stress here that since the propagation is carried out within the framework of the Hermitian formalism of quantum mechanics (although often a complex absorbing potential is introduced in the non-interacting region in order to simplify the numerical calculations) the time-dependent expectation values of operators which are localized in the interaction region (e.g., the acceleration operator $-(1/m)\mathrm{d}V/\mathrm{d}x$) are calculated by using the scalar product and not by the c- or F-product as described in Chapter 6. Yet, regardless of the reason why the Hamiltonian is non-Hermitian, the situation where two or more eigenfunctions of a non-Hermitian Hamiltonian are coalesced can have a strong effect on measurable quantities such as, for instance, the appearance of unexpected sharp peaks in the cross section of scattering experiments.

9.1 The phenomenon of self-orthogonality

When we introduced the c-product in Chapter 6 we proved that any two non-degenerate decay resonances are orthogonal provided we apply the proper transformation which brings them into the generalized Hilbert space where they decay asymptotically to zero. It is easy to extend this proof to the eigenstates of the non-Hermitian time-dependent Hamiltonians (using Floquet for time-periodic problems or the (t, t') method for general time-dependent problems). Specifically, for the

---

[2] S. Klaiman, U. Gunther and N. Moiseyev, *Phys. Rev. Lett.* **101**, 080402-4 (2008).

[3] A. F. J. Siegert, *Phys. Rev.* **56**, 750–752 (1939).

eigenfunctions of the non-Hermitian Hamiltonian, e.g., Ψ_n and Ψ_m,

$$\big(\Psi_m|\hat{H}|\Psi_n\big) = \big(\Psi_n|\hat{H}|\Psi_m\big) \tag{9.1}$$

and therefore when $(E_n - E_m) \neq 0$,

$$\big(\Psi_m|\Psi_{n\neq m}\big) = 0\,. \tag{9.2}$$

As we will show in this chapter, for very special parameters in the Hamiltonian denoted by $\boldsymbol{\lambda}$ (e.g., mass or potential parameter) at least two of the orthogonal eigenfunctions of the non-Hermitian Hamiltonian coalesce. For reasons which will be clarified later we do not normalize these two functions to unity via the c-product. Instead we choose some other normalization condition. For example, if we assign the labels Ψ_1 and Ψ_2 to the two orthogonal eigenfunctions which coalesce when $\boldsymbol{\lambda} = \boldsymbol{\lambda}_{\text{bp}}$ where the label "bp" stands for a branch point, we can choose the condition that $|\Psi_1|^2 = 1$ and $|\Psi_2|^2 = 1$ at the points where they attain their maximal values (when the two functions are square integrable). When we vary $\boldsymbol{\lambda}$ inside a sphere with a radius of $\rho = |\boldsymbol{\lambda}_{\text{bp}}|$ then the eigenfunctions vary analytically with the parameters and therefore

$$\begin{aligned} &\lim_{\boldsymbol{\lambda}\to\boldsymbol{\lambda}_{\text{bp}}} [E_1(\boldsymbol{\lambda}) - E_2(\boldsymbol{\lambda})] = 0\,,\\ &\lim_{\boldsymbol{\lambda}\to\boldsymbol{\lambda}_{\text{bp}}} [\Psi_1(\mathbf{r};\boldsymbol{\lambda}) - \Psi_2(\mathbf{r};\boldsymbol{\lambda})] = 0\,. \end{aligned} \tag{9.3}$$

At the coalescence point (a branch point in the complex energy plane)

$$\begin{aligned} &\Psi_1(\mathbf{r};\boldsymbol{\lambda}_{\text{bp}}) = \Psi_2(\mathbf{r};\boldsymbol{\lambda}_{\text{bp}}) \equiv \Psi_{\text{bp}}(\mathbf{r})\,,\\ &\big(\Psi_{\text{bp}}|\Psi_{\text{bp}}\big) = 0\,. \end{aligned} \tag{9.4}$$

The eigenfunction $\Psi_1(\mathbf{r};\lambda_{\text{bp}})$ for which Eq. (9.4) is satisfied is referred to by us as a *self-orthogonal* state. Often this coalescence phenomenon, which can occur only in non-Hermitian quantum mechanics, is also termed an exceptional point (EP) in the spectrum of the non-Hermitian Hamiltonian. We should re-emphasize here that self-orthogonality (SO) and EPs are different names for the same phenomenon. The term EP emphasizes the appearance of a branch point in the complex eigenvalue (complex "energy") plane where the spectrum becomes incomplete. The term SO emphasizes the coalescence of two (or more) orthogonal eigenfunctions of the non-Hermitian Hamiltonian such that Eq. (9.4) is satisfied.

An infinitesimal change in one of the parameters in the Hamiltonian will remove this degeneracy and Eq. (9.4) will not be satisfied. However, when one gets sufficiently close to the values of the parameters in the Hamiltonian for which Eq. (9.4) is satisfied then

$$\begin{aligned}(\Psi_1|\Psi_1) &= \epsilon_1\,,\\ (\Psi_2|\Psi_2) &= \epsilon_2\,,\end{aligned}\tag{9.5}$$

where ϵ_1 and ϵ_2 vanish as $\lambda \to \lambda_{\mathrm{bp}}$. Now we reach the point in our discussion where we require the eigenfunctions of the non-Hermitian Hamiltonian to be square integrable. We do so only when the non-Hermitian Hamiltonian has a complete spectrum and we are *not* at the situation where two (or more) eigenfunctions coalesce. The normalization of the eigenfunctions (see Chapter 5) is necessary to the definition of the closure relations which we use, for example, in the spectral representation of the Green's operator. By normalizing the two almost degenerate functions,

$$\begin{aligned}\Phi_1(\mathbf{r};\lambda) &= \epsilon_1^{-1/2}\Psi_1(\mathbf{r};\lambda)\,,\\ \Phi_2(\mathbf{r};\lambda) &= \epsilon_2^{-1/2}\Psi_2(\mathbf{r};\lambda)\,,\end{aligned}\tag{9.6}$$

then

$$\begin{aligned}(\Phi_1|\Phi_1) &= 1\,,\\ (\Phi_2|\Phi_2) &= 1\,.\end{aligned}\tag{9.7}$$

It is clear from Eq. (9.6) that upon this kind of normalization the amplitudes of the wavefunctions Φ_1 and Φ_2 become extremely large as the system's parameters approach the SO-EP situation. We will show in this chapter that this situation is not rare. Moreover, it has dramatic effects on the experimental measurements that so far have not been predicted by using the standard (Hermitian) formalism of quantum mechanics.

9.1.1 The self-orthogonal eigenvectors of non-Hermitian matrices

In the case of Hermitian matrices the two eigenvalues can attain the same value by varying the Hamiltonian parameters, but the corresponding eigenvectors are *different* and *orthogonal* vectors. These two eigenvectors are referred to as degenerate vectors. For Hermitian matrices degeneracy can occur only when the matrix can be transformed to diagonal blocks which are decoupled from each other. Crossing of two eigenvalues as a parameter in the Hamiltonian matrix is varied implies that there is a "hidden" symmetry and at the crossing point the Hamiltonian splits to decoupled subspaces. Note, however, that although the eigenvalue structures of Hermitian and non-Hermitian degeneracies are very different – conical ("diabolic") points versus branch points – the degree of accidentalness is exactly the same. For real Hermitian matrices which are symmetric and for non-Hermitian matrices (symmetric or non-symmetric), two parameters are required to capture a degeneracy. However, for complex Hermitian matrices (i.e., non-symmetric), three parameters are necessary.[4]

Exercise 9.1

The possible *accidental* crossing of two levels of the same symmetry is not excluded by the non-crossing rule, as proved by von Neumann, Wigner, Teller, Longuet-Higgins and others.[5] However, this is a very rare phenomenon and unlikely event in Hermitian quantum mechanics. As an illustrative example we can consider the following matrix:

$$\mathbf{H}(x) = \begin{pmatrix} a & (1-a)/2 & 1/4 \\ (1-a)/2 & x & -(1+a)/2 \\ 1/4 & -(1+a)/2 & -a \end{pmatrix}, \tag{9.8}$$

where $a = 1/\sqrt{2}$. Solve for the eigenvalues of this matrix as a function of x and discuss the following points.

1. At what value of x is a crossing of two eigenvalues obtained and what are the corresponding eigenvalues, $E_i\,; i = 1, 2, 3$ at the crossing point?
2. What is the behavior of $|E_3 - E_2|$ as function of x?
3. What is the difference in the behavior of $|E_3(x) - E_2(x)|$ when we change a slightly to $a = 1/\sqrt{2.001}$?
4. Show that the crossing at $a = 1/\sqrt{2}$ is an accidental one due to a hidden symmetry in the problem, and under a unitary transformation $\mathbf{U}$ the Hermitian Hamiltonian matrix, $\mathbf{H}$(x), shifted by 0.25 $\mathbf{I}$, can be transformed to the matrix

$$\mathbf{M} = \begin{pmatrix} 0 & 1 & 0 \\ 1 & 0 & 0 \\ 0 & 0 & 1 \end{pmatrix}, \tag{9.9}$$

which has eigenvalues $-1,\ 1,\ 1$. Here we wish to emphasize the fact that eigenvalue crossing for a Hermitian matrix is an accidental phenomenon which is associated with a hidden symmetry in the problem that is often hard to discover. Moreover, they are usually symmetries in a merely formal sense, with no physical significance. See, for example, the non-symmetric triangular billiards with degenerate eigenvalue.[6]

For the sake of clarity and before continuing the discussion for general finite sized matrices we wish to give an illustrative simple example. In our example the matrix is complex and symmetric since *any* matrix, including non-diagonalizable

---

[4] M. V. Berry, Czech. *J. Phys.* **54** 1039–1047 (2004).

[5] J. von Neumann and E. P. Wigner, *Z. Physik* **30**, 467 (1929); F. Hund, *Z. Physik* **40**, 742 (1927); E. Teller, *J. Phys. Chem.* **41**, 109–116 (1937); H. C. Longuet-Higgins, *Proc. R. Soc. Lond. Ser. A* **344**, 147–156 (1975).

[6] M. V. Berry and M. Wilkinson, *Proc. R. Soc. A* **392**, 15–43, (1984).

matrices (e.g., $H_{11} = H_{22} = 0\,;\ H_{12} = 1;\ H_{21} = 0$), can be transformed to be symmetric.[7] Therefore, although we will discuss symmetric matrices in our examples we do not restrict ourselves to symmetric matrices. On the definition of inner products for symmetric and non-symmetric matrices see Chapter 6. It should be mentioned here that for quantum problems where the Hamiltonian is non-Hermitian when we impose outgoing boundary conditions and real and Hermitian otherwise (i.e., when the eigenfunctions are in the Hilbert space), there is no physical motivation to represent the non-Hermitian operator (usually complex scaled as explained in Chapter 5) by non-symmetric matrices. However, there are other cases where the non-symmetric non-Hermitian matrices are important in applications. For example, the Hamiltonian of an atom in a uniform magnetic field (leading to the so-called Zeeman effect) is presented by a Hermitian complex matrix, i.e., $\mathbf{H}^{\mathrm{T}} = \mathbf{H}^{*}$. Therefore, by studying the resonance phenomenon for atoms in electromagnetic fields one of the complex scaling transformations presented in Chapter 5 is applied, yielding a non-Hermitian non-symmetric matrix. Another example for a case where non-symmetric non-Hermitian matrices are important is in optics of absorbing chiral anisotropic crystals.[8]

Exercise 9.2

Calculate the Lanczos recursion vectors which transform a diagonalizable $N \times N$ non-symmetric matrix to a symmetric tri-diagonal matrix. A key point in the derivation is that the eigenvalues of a tri-diagonal matrix $\mathbf{T}$ are the roots of a polynomial with coefficients which depend only on $T_{n,n}$ and on the product of the off-diagonal matrix elements $T_{n,n+1}T_{n+1,n}$. Therefore, any tri-diagonal matrix where the product of the off-diagonal matrix elements results in the same vector $\{\beta_n = \sqrt{T_{n,n+1}T_{n+1,n}}\}_{n=1,\ldots,N-1}$ has the same eigenvalue spectrum.

Let us consider the complex symmetric 2×2 Hamiltonian matrix

$$\mathbf{H} = \begin{pmatrix} 1 & \lambda \\ \lambda & -1 \end{pmatrix}. \tag{9.10}$$

The two eigenvalues of this matrix are given by

$$E_{\pm} = \pm\sqrt{1+\lambda^2}\,. \tag{9.11}$$

---

[7] R. Santra, L. S. Cederbaum, *Phys. Rep.* **368**, 1 (2002) and references therein.

[8] M. V. Berry and M. R. Dennis, *Proc. R. Soc. Lond. A* **459**, 1261–1292 (2003). For an early appreciation of non-Hermitian phenomena associated with crystal singular axes see S. Pancharatnam, *Proc. Ind. Natl. Sci. Acad.* **42**, 86–109, (1955); and 235–248, (1955); M. V. Berry, Pancharatnam, virtuoso of the Poincaré sphere: an appreciation, *Current Sci.* **67**, 220–223 (1994).

The corresponding eigenvectors are given by

$$\mathbf{c}_{\pm} = \begin{pmatrix} \frac{\lambda}{E_{\pm}-1} \\ 1 \end{pmatrix} . \tag{9.12}$$

These two eigenvectors are *orthogonal* for *any* value of λ provided we use the c-product,

$$\mathbf{c}_{\mp}^{\mathrm{T}} \cdot \mathbf{c}_{\pm} = \left(\frac{\lambda}{E_{\mp}-1} \ , \quad 1 \right) \cdot \begin{pmatrix} \frac{\lambda}{E_{\pm}-1} \\ 1 \end{pmatrix} = 0 \, . \tag{9.13}$$

From Eq. (9.11) we get that the two eigenvalues converge when $1 + \lambda^2 = 0$. Specifically, coalescence occurs for $\lambda = \pm \mathrm{i}$. Here λ is a branch point in the complex λ-plane and therefore it is also denoted often by λ_{bp}.

From Eq. (9.12) one immediately gets that in our case *the coalescence is not only a coalescence of the eigenvalues but* **also** *a coalescence of the corresponding eigenvectors.* The two orthogonal vectors $\mathbf{c}_{\pm}$ which are associated with two eigenvalues $E_{\pm}$ coalesce at $\lambda = \pm\,\mathrm{i}$ (i.e., the coalescence of the eigenvalues and of the corresponding eigenvectors happens either when $\lambda = \mathrm{i}$ or when $\lambda = -\mathrm{i}$). This implies that, by definition, upon this kind of coalescence a self-orthogonal eigenvector is obtained at a branch point,

$$E_{\mathrm{bp}} \equiv E_{+}(\lambda = \pm\,\mathrm{i}) = E_{-}(\lambda = \pm\,\mathrm{i}) = 0 \, , \tag{9.14}$$

and the corresponding eigenvector is equal to

$$\mathbf{c}_{\mathrm{bp}} \equiv \mathbf{c}_{+} = \mathbf{c}_{-} = \begin{pmatrix} \mp\,\mathrm{i} \\ 1 \end{pmatrix} . \tag{9.15}$$

The self-orthogonality can be easily verified,

$$\mathbf{c}_{\mathrm{bp}}^{\mathrm{T}} \cdot \mathbf{c}_{\mathrm{bp}} = (\mp\,\mathrm{i} \ , \quad 1) \cdot \begin{pmatrix} \mp\,\mathrm{i} \\ 1 \end{pmatrix} = 0 \, . \tag{9.16}$$

In numerical calculations, due to round off errors the eigenvectors are normalized and the closure relations can always be satisfied. This implies that in numerical calculations the zero value in Eq. (9.16) is replaced by a small number ϵ which depends on the accuracy of the machine we use for the diagonalization. In order to normalize the eigenvectors to unity, the components of the so-called defective vectors associated with $\mathbf{c}_{\mathrm{bp}}$ are divided by $\sqrt{\epsilon}$ and thus get extremely large. This is easily seen in our simple case of a 2 × 2 matrix. The two eigenvectors given in Eq. (9.12) can be c-normalized. The normalized eigenvectors are given by

$$\mathbf{c}_{\pm} = \pm \frac{1}{\sqrt{2(\lambda^2 + 1 - E_{\pm})}} \begin{pmatrix} \lambda \\ E_{\pm} - 1 \end{pmatrix} . \tag{9.17}$$

From Eq. (9.17) one can see that when λ is at its critical value the two eigenvalues merge into the value of $E_{\pm} = 0$, and then the components of the normalized vector $\mathbf{c}_{\pm}$ get infinitely large. In numerical diagaonalization calculations two normalized eigenvectors with extremely large components will be obtained. Specifically, the coalescence of the eigenvectors when two degenerate eigenvalues are obtained is reflected by two c-product normalized eigenvectors, $\mathbf{c}_{\pm}^{\mathrm{T}} \cdot \mathbf{c}_{\pm} = 1$, whereas the conventional scalar product between these two vectors becomes extremely large, $\mathbf{c}_{\pm}^{\mathrm{T}*} \cdot \mathbf{c}_{\pm} = 1/\epsilon$ where $\epsilon \to 0$ as the accuracy of the calculation improves.

The self-orthogonality phenomenon occurs whenever there is no similarity transformation which reduces a given non-Hermitian matrix to diagonal form, i.e., there is no invertible matrix $\mathbf{A}$ which gives a diagonal matrix $\mathbf{A}^{-1}\mathbf{HA}$. An $N \times N$ ($N \geq 2$) matrix which cannot be reduced to diagonal form must include at least one submatrix called *a simple Jordan matrix of order* r, where $N \geq r \geq 2$. Note that $\mathbf{A}^{-1}\mathbf{HA}$ is the direct sum of the simple Jordan submatrices. A simple Jordan matrix of order $r > 1$ is a matrix which is composed of 0 elements everywhere except for the diagonal where all the elements have the same value λ and the super-diagonal (second upper diagonal) where all the values are 1.[9]

Exercise 9.3

Show that by an appropriate similarity transformation of the complex symmetric matrix

$$\mathbf{H} = \begin{pmatrix} 1 & \mathrm{i} \\ \mathrm{i} & -1 \end{pmatrix} \tag{9.18}$$

$\mathbf{H}$ can be reduced to a simple Jordan block.

The fact that self-orthogonality only occurs for specific parameters of a given Hamiltonian might lead us to wonder whether it is an accidental phenomenon in non-Hermitian quantum mechanics which is very specific to a limited number of problems which are of no general interest? The answer to this question is negative. If, for example, $\mathbf{A}$ and $\mathbf{B}$ are two Hermitian matrices which do not commute, i.e., $[\mathbf{A}\,,\ \mathbf{B}] \neq \mathbf{0}$, then the matrix $\mathbf{H}$,

$$\mathbf{H} = \mathbf{A} + \lambda\mathbf{B}\,, \tag{9.19}$$

has an incomplete spectrum for at least one critical value of λ for which as least one self-orthogonal eigenvector (so-called defective eigenvector) is obtained.[10] If $\mathbf{H}$ stands for the complex symmetric matrix which represents the complex scaled Hamiltonian, $\hat{H}(\theta)$, then $\mathbf{A} = \mathrm{Re}[\mathbf{H}(\theta)]$ and $\mathbf{B} = \mathrm{Im}[\mathbf{H}(\theta)]$.

---

[9] J. H. Wilkinson,*The Algebraic Eigenvalue Problem*, Oxford, Oxford University Press, 1965.

[10] For a proof see N. Moiseyev and S. Friedland, *Phys. Rev. A* **22**, 618 (1980).

The critical values of λ for which $p \geq 2$ eigenvalues and also the p corresponding eigenvectors merge ($p = 2$ in our studied problem), are *branch points* for these eigenvalues. This implies that for these eigenvalues there is no Taylor expansion in $(\lambda - \lambda_{\mathrm{bp}})$ around the branch points, λ_{bp}. This is an important point which explains the validity of perturbation theory in quantum mechanics within the framework of the standard (Hermitian) formalism as well.

The Rayleigh–Schrödinger perturbation expansion of **H** in Eq. (9.19) converges for $\lambda < |\lambda_{\mathrm{bp}}|$. Here **A** serves as the zero-order self-adjoint Hamiltonian (i.e. Hermitian Hamiltonian), λ is the perturbational strength parameters and **B** is the perturbation. The radius of convergence is $|\lambda_{\mathrm{bp}}|$ where λ_{bp} is a branch point in the complex λ plane which has the minimal distance to the origin at $\lambda = 0$ (i.e. $|\lambda_{\mathrm{bp}}|$ has a minimal value among all branch points). Let us illustrate it for our model problem, Eq. (9.10). The branch points are $\lambda_{\mathrm{bp}} = \pm\mathrm{i}$. Therefore, the eigenvalues of **H** can be expanded in the Taylor series expansion around $\lambda = 0$,

$$E_{\pm}(\lambda) = \pm\sqrt{1+\lambda^2} = \pm\left[1 + \frac{\lambda^2}{2} - \frac{\lambda^4}{8} + \frac{\lambda^6}{32} + \cdots\right] \tag{9.20}$$

only inside a circle in the complex plane where $|\lambda| < 1$.

Although $E_{\pm}(\lambda) = \pm\sqrt{1+\lambda^2}$ do not have Taylor expansions around the branch points $\lambda_{\mathrm{bp}} = \pm\mathrm{i}$, it is possible to make algebraic expansions in $(\lambda - \lambda_{\mathrm{bp}})^{1/2}$. In the more general case when p eigenvalues $E_j(\lambda)$, $j = 1, \ldots, p$ and eigenvectors coalesce they can be expanded in $(\lambda - \lambda_{\mathrm{bp}})^{1/p}$ (the so-called Puiseux series):

$$E_j(\lambda) = \sum_{k=0}^{\infty} \alpha_{jk}(\lambda - \lambda_{\mathrm{bp}})^{\frac{k}{p}}\,. \tag{9.21}$$

In the case where λ^*_{bp} is also a branch point (such is the case of decay resonances and capture resonances) then

$$E_j(\lambda) = \sum_{k=0}^{\infty} \alpha_{jk}[(\lambda - \lambda_{\mathrm{bp}})(\lambda - \lambda^*_{\mathrm{bp}})]^{\frac{k}{p}}\,. \tag{9.22}$$

In our model problem around $\lambda = \pm\mathrm{i}$ Eq. (9.22) is immediately satisfied,

$$E_{\pm}(\lambda) = \pm\sqrt{1+\lambda^2} = \pm\sqrt{(\lambda - \mathrm{i})(\lambda + \mathrm{i})} = \pm[(\lambda - \lambda_{\mathrm{bp}})(\lambda - \lambda^*_{\mathrm{bp}})]^{1/2}\,. \tag{9.23}$$

How can one find the branch points for an $N \times N$ Hamiltonian matrix **H** in Eq. (9.19)?

We introduce here a method proposed by Byers Brown.[11] In the neighborhood of the branch point,

$$\lambda_{\mathrm{bp}} = \rho_{\mathrm{c}} \mathrm{e}^{-\mathrm{i}\phi_{\mathrm{c}}}\,, \tag{9.24}$$

the eigenvalue, E_j, of the matrix $\mathbf{H}$ can be expanded in the algebraic series of Eq. (9.22). Let us concentrate on the leading term of this expansion (for the sake of simplicity we omit the subscript "j" and denote the eigenvalue by E): when $|\lambda - \lambda_{\mathrm{bp}}|$ gets sufficiently small while $|\lambda| < |\lambda_{\mathrm{bp}}|$,

$$E(\lambda) = \alpha_1 [(\lambda - \lambda_{\mathrm{bp}})(\lambda - \lambda^*_{\mathrm{bp}})]^{1/2} + W(\lambda)\,. \tag{9.25}$$

On one hand, the singularity which determines the radius of convergence of the Rayleigh–Schrödinger perturabtion theory,

$$E(\lambda) = \sum_{n=0} \lambda^n E^{(n)}\,, \tag{9.26}$$

determines the behavior of the *high-order* perturbation eigenvalues, $E^{(n)}$. This perturbational series expansion converges for values of λ for which $|\lambda| < |\lambda_{\mathrm{bp}}|$. As λ attains values which are closer to the critical value λ_{bp} the rate of the convergence of the perturbational series expansion becomes slower and one should calculate higher-order terms (i.e., n is large) in order to get converged result to a given accuracy. On the other hand, when λ is close to the critical value λ_{bp} then

$$\begin{aligned}
[(\lambda - \lambda_{\mathrm{bp}})(\lambda - \lambda^*_{\mathrm{bp}})]^{\gamma} &= [\rho_{\mathrm{c}}^2 - 2\lambda\rho_{\mathrm{c}}\cos\phi_{\mathrm{c}} + \lambda^2]^{\gamma} \\
&= \rho_{\mathrm{c}}^{2\gamma} \sum_{n=0} \left(\frac{\lambda}{\rho_{\mathrm{c}}}\right)^n C_n^{(-\gamma)}(\cos\phi_{\mathrm{c}}),\ \ |\lambda| < \rho_{\mathrm{c}}\,,
\end{aligned} \tag{9.27}$$

where the coefficients $C_n^{(-\gamma)}(\cos\phi_{\mathrm{c}})$ are the Gegenbauer (or ultraspherical) polynomials and for $\gamma = 1/2$,

$$C_n^{(-1/2)}(\cos\phi_{\mathrm{c}}) = [P_{n-2}(\cos\phi_{\mathrm{c}}) - P_n(\cos\phi_{\mathrm{c}})]/(2n-1)\,, \tag{9.28}$$

where $P_n(\cos\phi_{\mathrm{c}})$ are Legendre polynomials. Therefore, for sufficiently large values of n (under the assumption that the branch point results from the coalescence of two eigenstates),

$$E^{(n)} = [P_{n-2}(\cos\phi_{\mathrm{c}}) - P_n(\cos\phi_{\mathrm{c}})]/[(2n-1)\rho_{\mathrm{c}}^{n-1}] + R^{(n)}\,, \tag{9.29}$$

where $R^{(n)}$ is a remainder term which we assume is negligible in the calculations of the high-order perturbation eigenvalues. Now the Gegenbauer polynomials satisfy

---

[11] W. Byers Brown, published in 1971 as a technical report of TCI-University of Wisconsin at Madison and briefly described in N. Moiseyev and P. R. Certain, *Mol. Phys.* **37**, 1621 (1979).

a three-term recurrence relation for all values of γ:

$$C_n^{(-\gamma)}(\cos\phi_{\mathrm{c}}) = 2(n-1-\gamma)\cos\phi_{\mathrm{c}} C_{n-1}^{(-\gamma)}(\cos\phi_{\mathrm{c}}) - (n-2-2\gamma)C_{n-2}^{(-\gamma)}(\cos\phi_{\mathrm{c}})\,, \tag{9.30}$$

where $C_0^{(-\gamma)}(\cos\phi_{\mathrm{c}}) = 1$ and polynomials of negative degree vanish. This three-term recurrence relation reduces for $\gamma = 1/2$ to the recurrence relations of the Legendre polynomials, and by putting them to use one gets that $E^{(n)}$ satisfy

$$\rho_{\mathrm{c}}^2 E^{(n)} - 2\rho_{\mathrm{c}}\cos\phi_{\mathrm{c}}\left(1-\frac{3}{2n}\right)E^{(n-1)} + \left(1-\frac{3}{n}\right)E^{(n-2)} = 0\,. \tag{9.31}$$

Introducing the ratio between consecutive corrections,

$$r_n \equiv \frac{E^{(n)}}{E^{(n-1)}}\,, \tag{9.32}$$

we solve Eq. (9.31) for $\cos\phi_{\mathrm{c}}(n \to \infty)$,

$$\cos\phi_{\mathrm{c}} = \left[\frac{n}{2n-3}\right](\rho_{\mathrm{c}} r_n) + \left[\frac{n-3}{2n-3}\right](\rho_{\mathrm{c}} r_{n-1})^{-1}\,. \tag{9.33}$$

Eliminating $\cos\phi_{\mathrm{c}}$ by substituting in this equation for two successive values of n gives

$$\rho_{\mathrm{c}}^2 = \lim_{n\to\infty} \frac{(n-4)(2n-3)r_{n-2}^{-1} - (n-3)(2n-5)r_{n-1}^{-1}}{n(2n-5)r_n - (n-1)(2n-3)r_{n-1}}\,. \tag{9.34}$$

If the three ratios r_n, r_{n-1}, r_{n-2} are consistent with this analysis, Eq. (9.34) will be positive and lead to a real value of ρ_{c}. By substituting ρ_{c} back into Eq. (9.33) a value for $\cos\phi_{\mathrm{c}}$ can be found, and should be in the range between -1 and $+1$.

Exercise 9.4

For a given Hamiltonian matrix $\mathbf{H} = \mathbf{H_0} + \lambda\mathbf{V}$, where $\mathbf{H_0}$ is a diagonal matrix with values $E_k^{(0)}; k = 1, \ldots, N$, calculate the values of the matrix elements of $\mathbf{C^{(n)}}$ for which the n-th order terms in the perturbation expansion of the eigenvalues are given for $n \geq 2$ by $E_k^{(n)} = [\mathbf{V}(\mathbf{C^{(n-1)}})^{\mathrm{T}}]_{k,k}$.

Exercise 9.5

Show that the Hamiltonian of an atom/molecule in a combination of strong and weak linearly polarized laser pulses,

$$\hat{H}(\mathbf{r},t) = \hat{H}_{\mathrm{system}}(\mathbf{r}) + f(t)\mathbf{e}_x \cdot \mathbf{r}[\epsilon_0\cos(\omega_0 t) + \epsilon_1\cos(\omega_1 t)]\,, \tag{9.35}$$

can be represented by the Hamiltonian matrix as described in Section 2.2 with a real value of ϵ_1^{bp} when the intensity $I_0 = \epsilon_0^2 \gg \epsilon_1^2$. Here we assume that the duration time of the laser pulse, $f(t)$, is $\tau > N_0 T_0$, where $T_0 = 2\pi/\omega_0$ and N_0 is a *large* number of optical cycles of the strong laser supported by the envelope of the laser pulse. Similarly, $\tau > N_1 T_1$, where $T_1 = 2\pi/\omega_1$ and N_1 is the number of optical cycles of the weak laser which is supported by $f(t)$. Use the rotating wave approximation in order to derive conditions under which two photo-induced resonance states can coalesce and a self-orthogonal resonance state is obtained. The derivation will be simplified by the use of the (t, t') formalism which was briefly presented in Chapter 4.

9.2 On self-orthogonality and the closure relations

The spectrum of an $N \times N$ complex symmetric matrix $\mathbf{H}(\lambda)$ is complete when the closure relation is satisfied. λ is a real or complex parameter and it is given that for $\lambda \neq \lambda_{\mathrm{bp}}$, N orthonormal eigenvectors are obtained,

$$\mathbf{H}(\lambda)\mathbf{c}_j(\lambda) = E_j \mathbf{c}_j(\lambda) \tag{9.36}$$

such that

$$[\mathbf{C}(\lambda)\mathbf{C}^{\mathrm{T}}(\lambda)]_{N\times N} = \sum_{j=1}^{N} |\mathbf{c}_j)(\mathbf{c}_j| = \mathbf{I}_{N\times N}\,, \tag{9.37}$$

where $\mathbf{C}(\lambda) = (\mathbf{c}_1(\lambda), \mathbf{c}_2(\lambda), \ldots, \mathbf{c}_j(\lambda)\ldots, \mathbf{c}_N(\lambda))$ is the eigenvector matrix of $\mathbf{H}(\lambda)$. *At the critical value of $\lambda = \lambda_{\mathrm{bp}}$ the spectrum is not complete since at least two linearly independent eigenvectors reduce to one.* Let us assume that N_{bp} eigenvectors of $\mathbf{H}(\lambda)$ coalesce at $\lambda = \lambda_{\mathrm{bp}}$. The number of linearly independent eigenvectors of the $N \times N$ matrix $\mathbf{H}(\lambda_{\mathrm{bp}})$ is

$$M = N - N_{\mathrm{bp}}\,, \tag{9.38}$$

such that for the $\{\mathbf{c}_{i=1,2,\ldots,M}\}$ eigenvectors that are associated with the eigenvalues $\{E_i(\lambda_{\mathrm{bp}})\}_{i=1,\ldots,M}$,

$$(\mathbf{c}_i|\mathbf{c}_i) = \mathbf{c}_i(\lambda_{\mathrm{bp}})^{\mathrm{T}}\mathbf{c}_i(\lambda_{\mathrm{bp}}) = 1\,, \tag{9.39}$$

while for the $[M = N - N_{\mathrm{bp}}]$ self-orthogonal eigenvector which is associated with the eigenvalue E_{bp},

$$(\mathbf{c}_{M+1}|\mathbf{c}_{M+1}) = [\mathbf{c}_{M+1}(\lambda_{\mathrm{bp}})]^{\mathrm{T}}[\mathbf{c}_{M+1}(\lambda_{\mathrm{bp}})] = 0\,. \tag{9.40}$$

In order to emphasize the fact that $\mathbf{c}_{M+1}(\lambda_{\text{bp}})$ is a self-orthogonal vector we may re-label it as

$$\mathbf{c}_{\text{bp}}(\lambda_{\text{bp}}) \equiv \mathbf{c}_{M+1}(\lambda_{\text{bp}})\,. \tag{9.41}$$

It is clear that for $\lambda = \lambda_{\text{bp}}$ Eq. (9.37) is not satisfied and

$$\mathbf{C}(\lambda_{\text{bp}})\mathbf{C}^{\text{T}}(\lambda_{\text{bp}}) \neq \mathbf{I}_{N\times N}\,. \tag{9.42}$$

As we will show below, it is possible to construct the closure relations by adding $N_{\text{bp}} - 1$ vectors $\{\mathbf{c}_i(\lambda_{\text{bp}})\}_{i=M+2,\ldots,N}$ to the $M + 1$ eigenvectors of $\mathbf{H}(\lambda_{\text{bp}})$. Let us first explain how these additional $N_{\text{bp}} - 1$ vectors can be computed and only afterwards we will explain why these vectors enable the calculations of the closure relations.

The desired N vectors construct an $N \times N$ matrix

$$\mathbf{B}_{N\times N} = (\mathbf{c}_1(\lambda_{\text{bp}}), \ldots, \mathbf{c}_M(\lambda_{\text{bp}}), \mathbf{c}_{\text{bp}}(\lambda_{\text{bp}}), \mathbf{c}_{M+2}(\lambda_{\text{bp}}), \ldots, \mathbf{c}_N(\lambda_{\text{bp}})) \tag{9.43}$$

which can be used to decompose $\mathbf{H}(\lambda_{\text{bp}})$ into two blocks, $\mathbf{A}_{M\times M}$ and $\mathbf{J}_{N_{\text{bp}}\times N_{\text{bp}}}$. The first matrix is a diagonal matrix whereas the second matrix is non-diagonalizable. That is,

$$\mathbf{B}\mathbf{H}(\lambda_{\text{bp}})\mathbf{B}^{-1} = \begin{pmatrix} \mathbf{A} & \mathbf{0} \\ \mathbf{0} & \mathbf{J} \end{pmatrix}. \tag{9.44}$$

The diagonal matrix $\mathbf{A}$ contains the eigenvalues of $\mathbf{H}$ while the non-diagonalizable matrix $\mathbf{J}$ has only two non-zero diagonals. The main diagonal $J_{i,i} = E_{\text{bp}}$ and the elements on the upper-diagonal are equal to 1, $J_{i,i+1} = 1$. The closure relations for the whole N-dimensional space are given by

$$\mathbf{I}_{N\times N} = \mathbf{B}[\mathbf{B}^{\text{T}}\mathbf{B}]^{-1}\mathbf{B}^{\text{T}} = (\mathbf{c}_1, \ldots, \mathbf{c}_N)\mathbf{U}(\mathbf{c}_1, \ldots, \mathbf{c}_N)^{\text{T}} = \sum_{i,j=1}^{N} U_{i,j}|\mathbf{c}_i)(\mathbf{c}_j|\,. \tag{9.45}$$

Note that for the Hermitian case $\mathbf{B}^{\text{T}} = \mathbf{B}^{-1}$.

The question now is: how can we calculate the additional $N_{\text{bp}} - 1$ vectors $\{\mathbf{c}_{M+r}(\lambda_{\text{bp}})\}_{r=2,\ldots,N_{\text{bp}}}$? This can be done by solving the following linear set of equations:

$$\begin{aligned}
&[\mathbf{H}(\lambda_{\text{bp}}) - E_{\text{bp}}\mathbf{I}]\mathbf{c}_{M+2}(\lambda_{\text{bp}}) = \mathbf{c}_{\text{bp}}(\lambda_{\text{bp}})\,,\\
&[\mathbf{H}(\lambda_{\text{bp}}) - E_{\text{bp}}\mathbf{I}]\mathbf{c}_{M+3}(\lambda_{\text{bp}}) = \mathbf{c}_{M+2}(\lambda_{\text{bp}})\,,\\
&\vdots\\
&[\mathbf{H}(\lambda_{\text{bp}}) - E_{\text{bp}}\mathbf{I}]\mathbf{c}_{N-1}(\lambda_{\text{bp}}) = \mathbf{c}_N(\lambda_{\text{bp}})
\end{aligned} \tag{9.46}$$

such that *all* the N_{bp} vectors $\{\mathbf{c}_{M+r}(\lambda_{\mathrm{bp}})\}_{r=1,\ldots,N_{\mathrm{bp}}}$ are degenerate eigenvectors of the same $N \times N$ matrix,

$$[\mathbf{H}(\lambda_{\mathrm{bp}}) - E_{\mathrm{bp}}\mathbf{I}]^{N_{\mathrm{bp}}}\mathbf{c}_{M+r}(\lambda_{\mathrm{bp}}) = 0 \cdot \mathbf{c}_{M+r}(\lambda_{\mathrm{bp}})\,, \tag{9.47}$$

where

$$r = 1, 2, \ldots, N_{\mathrm{bp}}\,. \tag{9.48}$$

Note that for the block associated with the almost self-orthogonal vectors $\lim_{\lambda\to\lambda_{\mathrm{bp}}}[\mathbf{H}(\lambda_{\mathrm{bp}}) - E_{\mathrm{bp}}\mathbf{I}]^{N_{\mathrm{bp}}} = 0$ and therefore we should multiply the $[\mathbf{H}(\lambda_{\mathrm{bp}}) - E_{\mathrm{bp}}\mathbf{I}]$ matrices one by one by the vectors $\mathbf{c}_{M+r}(\lambda_{\mathrm{bp}})$.

The orthonormal eigenvectors of $\mathbf{H}(\lambda_{\mathrm{bp}})$, denoted above as $\{\mathbf{c}_{i=1,2,\ldots,M}\}$, are also eigenvectors of the $N \times N$ matrix $[\mathbf{H}(\lambda_{\mathrm{bp}}) - E_{\mathrm{bp}}\mathbf{I}]^{N_{\mathrm{bp}}}$,

$$[\mathbf{H}(\lambda_{\mathrm{bp}}) - E_{\mathrm{bp}}\mathbf{I}]^{N_{\mathrm{bp}}}\mathbf{c}_i(\lambda_{\mathrm{bp}}) = [E_i - E_{\mathrm{bp}}]^{N_{\mathrm{bp}}} \cdot \mathbf{c}_i(\lambda_{\mathrm{bp}})\,, \tag{9.49}$$

where

$$i = 1, 2, \ldots, N\,. \tag{9.50}$$

We show here that $\mathbf{B} = (\mathbf{c}_1(\lambda_{\mathrm{bp}}), \ldots, \mathbf{c}_N(\lambda_{\mathrm{bp}}))$ is an $N \times N$ eigenvector matrix of the $N \times N$ matrix $[\mathbf{H}(\lambda_{\mathrm{bp}}) - E_{\mathrm{bp}}\mathbf{I}]^{N_{\mathrm{bp}}}$. Since the non-degenerate eigenvectors of the matrix are orthogonal it is clear that the additional vectors $\{\mathbf{c}_{M+r}(\lambda_{\mathrm{bp}})\}_{r=2,\ldots,N_{\mathrm{bp}}}$ are orthogonal to $\{\mathbf{c}_i(\lambda_{\mathrm{bp}})\}_{i=1,\ldots,M}$. Therefore, if we prove that $\{\mathbf{c}_{M+r}(\lambda_{\mathrm{bp}})\}_{r=2,\ldots,N_{\mathrm{bp}}}$ are linearly independent it implies that the spectrum of $[\mathbf{H}(\lambda_{\mathrm{bp}}) - E_{\mathrm{bp}}\mathbf{I}]^{N_{\mathrm{bp}}}$ is complete while the spectrum of $\mathbf{H}(\lambda_{\mathrm{bp}})$ is not. The proof is simple. If $\mathbf{c}_{M+2} = \alpha\mathbf{c}_{\mathrm{bp}}$ then from the first linear equation in Eq. (9.46) one gets the impossible result that $\mathbf{c}_{\mathrm{bp}} = 0$. So, $\mathbf{c}_{M+2}$ and $\mathbf{c}_{\mathrm{bp}}$ are two linearly independent vectors. Moreover, we can conclude also that $\mathbf{c}_{M+2}$ is *not* an eigenvector of $[\mathbf{H}(\lambda_{\mathrm{bp}}) - E_{\mathrm{bp}}\mathbf{I}]$. This conclusion together with the second linear equation in Eq. (9.46) leads us to another conclusion that $\mathbf{c}_{M+3} \neq \alpha\mathbf{c}_{M+2}$. From similar arguments one can reach the conclusion that indeed $\{\mathbf{c}_{M+r}(\lambda_{\mathrm{bp}})\}_{r=2,\ldots,N_{\mathrm{bp}}}$ are linearly independent and therefore one can use the eigenvectors of $[\mathbf{H}(\lambda_{\mathrm{bp}}) - E_{\mathrm{bp}}\mathbf{I}]^{N_{\mathrm{bp}}}$ to construct the closure relations (identity operator when the operator is represented by a finite matrix). On the basis of the derivation given above the closure relations in the N_{bp}-dimensional subspace of the self-orthogonal vectors are given by

$$\mathbf{I}_{N_{\mathrm{bp}}\times N_{\mathrm{bp}}} = \sum_{i=M+1}^{N} \frac{|\mathbf{c}_{i+1}(\lambda_{\mathrm{bp}}))(\mathbf{c}_i(\lambda_{\mathrm{bp}})|}{(\mathbf{c}_{i+1}(\lambda_{\mathrm{bp}})|\mathbf{c}_i(\lambda_{\mathrm{bp}}))}\,. \tag{9.51}$$

For the case where two eigenstates coalesce as $\lambda \to \lambda_{\rm bp}$ it is easy to see that for $N_{\rm bp} = 2$,

$$\mathbf{I}_{N_{\rm bp}\times N_{\rm bp}} = \frac{|\mathbf{c}_{\rm bp})(\mathbf{c}^*_{\rm bp}| + |\mathbf{c}^*_{\rm bp})(\mathbf{c}_{\rm bp}|}{(\mathbf{c}^*_{\rm bp}|\mathbf{c}_{\rm bp})} \tag{9.52}$$

since $\mathbf{c}_{\rm bp}$ is an eigenvector of a Hermitian matrix

$$\mathcal{H} = (\mathbf{H}(\lambda_{\rm bp}) - E_{\rm bp}\mathbf{I})^*(\mathbf{H}(\lambda_{\rm bp}) - E_{\rm bp}\mathbf{I}) \tag{9.53}$$

and therefore the scalar product should be used. Specifically,

$$\begin{aligned} \mathcal{H}|\mathbf{c}_{\rm bp}) &= 0|\mathbf{c}_{\rm bp})\,, \\ (\mathbf{c}^*_{\rm bp}|\mathcal{H} &= 0(\mathbf{c}^*_{\rm bp}|\,. \end{aligned} \tag{9.54}$$

Exercise 9.6

(a) Show how the eigenvectors of the 2 × 2 matrix given in Eq. (9.10) which has an incomplete spectrum when $\lambda = i$, can be used to construct the identity matrix $\mathbf{I}_{2\times 2}$.
(b) Similarly, show how the two linearly independent eigenvectors of the 3 × 3 matrix

$$\mathbf{H} = \begin{pmatrix} 6 & i & -1 \\ i & 5 & 2i \\ -1 & 2i & 1 \end{pmatrix} \tag{9.55}$$

can be used to construct the identity matrix $\mathbf{I}_{3\times 3}$.

It should be mentioned here that in numerical diagonalization calculations, due to round-off errors, the eigenvectors obtained are only nearly degenerate and can always be normalized to unity. Thus the spectrum of the matrix is always complete and there is no need to use the special closure relations given in Eq. (9.46) even when two or more eigenvectors coalesce. The same derivations and formulas which are given above for the closure relations hold for operators and are not limited to linear algebra where the operators are represented by finite matrices.

9.2.1 On self-orthogonality for complex potentials

Let us continue our discussion here by using a simple illustrative analytically soluble problem of a particle in a one-dimensional box with length L, where within the interval $0 < x < a$, $(a < L)$ a complex potential V_0 is introduced. That is,

$$V(R) = \begin{cases} V_0 = v_0 - \mathrm{i}\Gamma\,, & 0 < R \le a\,, \\ 0\,, & a < R \le L\,, \\ \infty\,, & \textit{otherwise}\,. \end{cases} \tag{9.56}$$

v_0 and Γ are real parameters that model the electronic resonance's position and width. In this model the eigenvalues of the complex Hamiltonian are a function of three parameters, $E_\nu(a, v_0, \Gamma)$.

This simple 1D model potential shows how the original n-th particle-in-a-box wavefunction is deformed to be a self-orthogonal state when the complex V_0 potential parameter is varied. We will show here how the values of $V_0 = v_0 - \mathrm{i}\Gamma$ for which a self-orthogonal state is obtained vary with the potential parameter a. It is a point of interest that this simple model problem can be associated with the propagation of light in a waveguide with a complex index of refraction. Last but not least, we will show here how the existence of a self-orthognal state effects different measurable quantities.

In Chapter 3 we solved this problem for real V_0. However, for the sake of coherence we remind the reader that due to the continuity condition at $x = a$,

$$\sin(ka) = A\sin(q(a - L))\,, \tag{9.57}$$

and the flux continuity condition at $x = a$,

$$k\cos(ka) = Aq\cos(q(a - L))\,, \tag{9.58}$$

where

$$\frac{(\hbar k)^2}{2M} = E - v_0 + \mathrm{i}\Gamma \tag{9.59}$$

and

$$\frac{(\hbar q)^2}{2M} = E\,. \tag{9.60}$$

Let us prove that for given potential parameters a, L and v_0, when we change Γ from zero to ∞ then the spectrum of the one-dimensional particle in a box of length L transforms to a linear combination of two independent spectra associated with a particle in a box with length $L - a$ and a particle in another box with length a. That is, as Γ changes from 0 to ∞ then the energies

$$E_n = \frac{1}{2M}\left(\frac{\hbar n\pi}{L}\right)^2; \quad n = 1, 2, \ldots \tag{9.61}$$

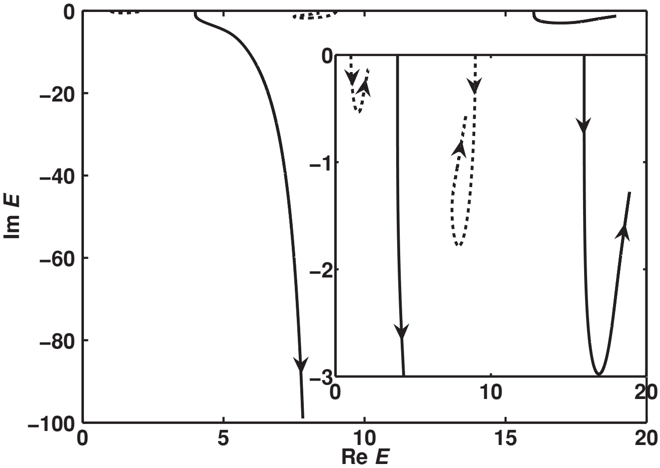

Figure 9.1 The Γ-trajectory of the first four eigenvalues of the model potential (solutions of Eq. (9.63)) with $L = \pi/\sqrt{2}$ and $a = L/\sqrt{3}$. Atomic units are used throughout.

change to

$$E_{n',n''} = \frac{1}{2M}\left(\frac{\hbar n'\pi}{L-a}\right)^2 + \frac{1}{2M}\left(\frac{\hbar n''\pi}{a}\right)^2 + v_0 - \mathrm{i}\Gamma\,; \quad n', n'' = 1, 2, \ldots \tag{9.62}$$

This can be easily shown by substituting Eqs. (9.59) and (9.60) into the following transcendental equation:

$$\frac{q}{k}\tan(ka) = \tan(q(a-L)) \tag{9.63}$$

and taking the limit $\Gamma \to \infty$, which yields the equality

$$\mathrm{e}^{-\mathrm{i}\pi/4}\sqrt{\frac{E}{\Gamma}}\tan(ka) = \tan(q(a-L))\,. \tag{9.64}$$

As $\Gamma \to \infty$ the left-hand side of Eq. (9.64) vanishes (assuming that $ka \neq \pi(n+1/2)$, where $n = 0, 1, 2, \ldots$) and therefore $\tan(q(a-L)) = 0$. Consequently, $q(L-a) = n''\pi$ and $E_{n'} = (\hbar q)^2/(2M) = [(\hbar n')/(L-a)]^2/[2M]$. By substituting this result into Eq. (9.57) one gets that $\sin(ka) = 0$ and therefore $ka = n''\pi$. Consequently, $E_{n''} = (\hbar k)^2/(2M) = (\hbar n'')^2/(2Ma^2) + v_0 - \mathrm{i}\Gamma$ and we have the two contributions in Eq. (9.64).

Let us visualize this result by solving Eq. (9.63) for the case where $a = L/\sqrt{3}$ and $v_0 = 0$. Figure 9.1 shows the changes in the complex eigenvalues with the variation in Γ obtained for $L = \pi/\sqrt{2}$. For $\Gamma = 0$ the eigenvalues of our model Hamiltonian are the energies of a particle in a box of size L. As Γ is increased the

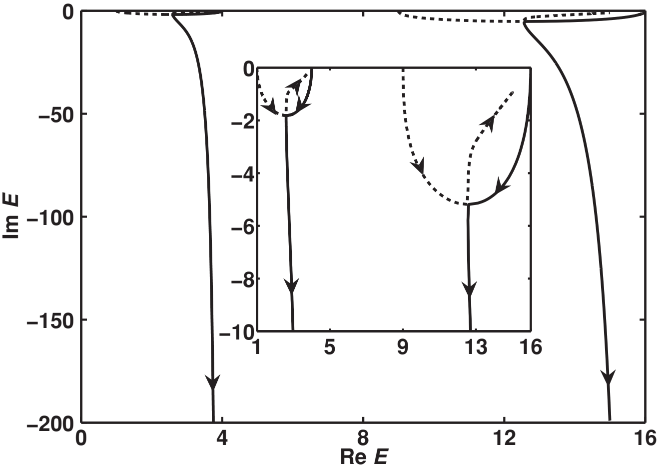

Figure 9.2 The Γ-trajectory of the first four eigenvalues of the model potential (solutions of Eq. (9.63)) with $L = \pi/\sqrt{2}$ and $a = L/2$. Atomic units are used throughout. The inset shows the formation of branch points as Γ is varied.

eigenvalues depart from the real axis and penetrate into the complex energy plane. For sufficiently large values of Γ some of the eigenvalues form a loop and return to the real axis, while others move almost tangentially to straight lines parallel to the imaginary axis. In complete agreement with the analysis given above, in the limit of $\Gamma \to \infty$ the spectrum of our model Hamiltonian is a superposition of two spectra where each of them is associated with a different problem. One spectra is that of a Hamiltonian of a particle in a box of size a, which is shifted into the complex energy plane by an imaginary constant $-\mathrm{i}\Gamma$. The corresponding eigenfunctions are given by

$$\Psi_n(x) = \mathrm{e}^{-\frac{\Gamma t}{\hbar}} \mathrm{e}^{-\frac{\mathrm{i}}{\hbar}\left[\frac{(\hbar n\pi)^2}{2Ma^2} - v_0\right] t} \sqrt{\frac{2}{a}} \sin\left(\frac{n\pi x}{a}\right) . \tag{9.65}$$

The eigenfunctions have a nodal structure and their amplitudes decay to zero with the same rate as time passes. The other spectrum is that of a particle in a box of size $L - a$. Specifically, $E_m = (\hbar m\pi/(L-a))^2/(2M)$ and the corresponding eigenfunctions are stationary solutions given by

$$\Psi_m(x) = \mathrm{e}^{-\frac{\mathrm{i}}{\hbar}\left[\frac{(\hbar m\pi)^2}{2M(L-a)^2}\right] t} \sqrt{\frac{2}{L-a}} \sin\left(\frac{m\pi x}{L-a}\right) . \tag{9.66}$$

In Fig. 9.2 we present the result of Γ-trajectory calculations for the case where $a = L/2$ and $v_0 = 0$. In this special case each pair of initial eigenvalues (obtained for $\Gamma = 0$) associated with the quantum numbers $(n, n+1)$, where $n = 1, 3, 5, \ldots$, coalesce in the complex energy plane as Γ is increased. Each pair of eigenstates merges at a different critical value of $\Gamma^{\mathrm{bp}}_{(n,n+1)}$. Each time Γ exceeds such a critical value a new pair of solutions is obtained. One of every pair of the new-born eigenvalues returns to the real energy axis as $\Gamma \to \infty$ whereas the other solution approaches a complex value with the same real part and an imaginary part which approaches $-\mathrm{i}\Gamma$. In the more general case where $a \neq L/2$ branch points are not obtained for $v_0 = 0$ and only for very critical values of v_0 (and Γ) the spectrum become incomplete and two eigenvalues and their corresponding eigenfunctions coalesce. The values of $v_0 = v_0^{\mathrm{bp}}$ for which branch points are obtained due to the coalescence of two eigenfunctions were calculated by using the method of Byers Brown presented in the solution of Ex. 9.4 and in Section 9.1.1. Let us re-emphasize that, as $\Gamma \to \Gamma_{\mathrm{bp}}$,

$$\|E_1 - E_2\| \to 0 \tag{9.67}$$

and also

$$\|\Psi_1(x) - \Psi_2(x)\| \to 0\,, \tag{9.68}$$

where E_1 and E_2 are the solutions of Eq. (9.63) obtained by using the definitions for k and q as given respectively in Eqs. (9.59) and (9.60). The wavefunctions $\Psi_1(x)$ and $\Psi_2(x)$ are obtained from Eq. (9.71).

In Fig. 9.3 we show how the two eigenfunctions change with the increase in Γ. At the branch point the two orthogonal eigenfunctions become equal to one another and they reduced to a single self-orthogonal state. We can use this property, i.e.,

$$(\Psi_{\mathrm{bp}}|\Psi_{\mathrm{bp}}) = \int_0^L \mathrm{d}x\,\Psi^2(x; E = E_{\mathrm{bp}}) = 0\,, \tag{9.69}$$

to derive a condition which must be satisfied at the branch points. By substituting the eigenfunctions of our model Hamiltonian which are given by (see Chapter 3)

$$\begin{aligned}
\Psi(0 \le x < a) &= \sin(\sqrt{2M(E - v_0 + \mathrm{i}\Gamma)}x)\,,\\
\Psi(a \le x \le L) &= \left[\frac{\sin(\sqrt{2M(E - v_0 + \mathrm{i}\Gamma)}a)}{\sin(\sqrt{2ME}(a - L))}\right]\sin(\sqrt{2ME}(x - L))
\end{aligned} \tag{9.70}$$

into Eq. (9.69) and using the value of A^2 given in Eq. (9.57), one gets that self-orthogonal states which are associated with a branch point in the complex energy plane are the solutions of the following equation:

$$\begin{aligned}
&(\Psi_{\mathrm{bp}}|\Psi_{\mathrm{bp}})\\
&= \left[\frac{L - a}{2} - \frac{\sin(2q(L - a))}{4q}\right]\left(\frac{k}{q}\right)^2\left(\frac{\cos^2(ka)}{\cos^2(q(L - a))}\right) + \frac{a}{2} - \frac{\sin(2ka)}{4k} = 0\,.
\end{aligned} \tag{9.71}$$

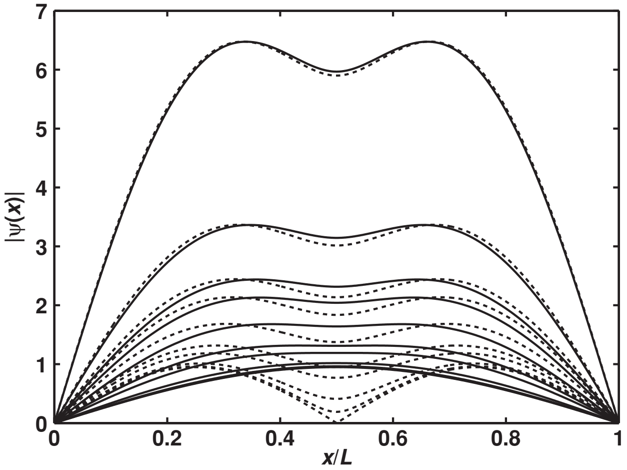

Figure 9.3 The absolute value of the first two eigenfunctions of the model potential, Ψ_1 (full line) and Ψ_2 (dashed line) as a function of $\Gamma = 0, 1, 2, 3, 3.25, 3.5, 3.58, 3.6, 3.62$ and 3.627. $\Gamma_{\mathrm{bp}} = 3.627\,586\,692\,482\,452\ldots$ Note how the functions start to resemble one another as Γ approaches Γ_{bp}. Note that as $\Gamma \to \Gamma_{\mathrm{bp}}$, $\Psi_1 \to \Psi_2$ and a self-orthogonal state is obtained (see how the dashed and the full lines, which are very different when $\Gamma \ll \Gamma_{\mathrm{bp}}$, become almost identical in the limit of $\Gamma \to \Gamma_{\mathrm{bp}}$).

This equation can be simplified by taking the value of A^2 from a combination of Eq. (9.57) and Eq. (9.58) and substituting into Eq. (9.72), yielding the following equation:

$$(\Psi_{\mathrm{bp}}|\Psi_{\mathrm{bp}}) = q^2\left[\frac{1-\mathrm{sinc}(2ak)}{\mathrm{sinc}(2ak)}\right] - k^2\left[\frac{1-\mathrm{sinc}(2(L-a)q)}{\mathrm{sinc}(2(L-a)q)}\right] = 0\,, \quad (9.72)$$

where $\mathrm{sinc}(\zeta) = \sin(\zeta)/\zeta$.

What kind of information can be obtained from the calculations of the branch points in the complex energy plane? Below we list several consequences of the self-orthogonality phenomenon.

9.3 Calculations of the radius of convergence of perturbational expansion of the eigenvalues in V_0

Although we have already briefly mentioned in this chapter the relevance of self-orthogonality to the radius of convergence of the Taylor series expansion of a given function, for the sake of coherence and clarity let us extend our discussion on this subject. In the case that the eigenvalues and eigenfunctions of the full problem are calculated by the Rayleigh–Schrödinger perturbation theory where

V_0 is the perturbational expansion parameter, the radius of convergence, R_c, is the smallest value of the absolute value of $V_0(\mathrm{bp})$ at which branch points in the complex energy plane are obtained. Note that this is also the radius of convergence of perturbational expansion of the eigenvalues within the framework of standard quantum mechanics when V_0 is real and the Hamiltonian is Hermitian. The Taylor expansions of the eigenvalues and eigenfunctions in V_0 are converged for the real and complex values of V_0 which are inside a circle of radius R_c around $V_0 = 0$.

9.4 The effect of self-orthogonality on c-expectation values

The potential parameters of a non-Hermitian Hamiltonian are denoted by the vector $\boldsymbol{\lambda}$. The square integrable eigenfunctions are associated with complex non-degenerate eigenvalues. Without loss of generality we assume that the non-Hermitian Hamiltonian is a complex scaled Hamiltonian and that the square integrable non-degenerate eigenfunctions are the resonance wavefunctions,

$$\begin{aligned} \hat{H}_\theta(\boldsymbol{\lambda})|\Psi_j(\boldsymbol{\lambda})) &= E_j(\boldsymbol{\lambda})|\Psi_j(\boldsymbol{\lambda}))\,, \\ (\Psi_{j'}(\boldsymbol{\lambda})|\Psi_j(\boldsymbol{\lambda})) &= \delta_{j',j}\,. \end{aligned} \tag{9.73}$$

The vector of potential parameters can include, for example, the laser parameters (intensity and frequency) when the interaction with a laser field is taken into consideration. In such a case $\hat{H}_\theta(\lambda)$ stands for the complex scaled Floquet type operator (one should used the (t, t') method when the laser field is not time-periodic).

For specific values of the real potential parameters, $\boldsymbol{\lambda} = \boldsymbol{\lambda}_{\mathrm{bp}}$, a branch point in the complex energy plane is obtained where the two corresponding eigenfunctions coalesce,

$$\begin{aligned} E_1(\boldsymbol{\lambda}_{\mathrm{bp}}) &= E_2(\boldsymbol{\lambda}_{\mathrm{bp}}) \equiv E_{\mathrm{bp}}\,, \\ |\Psi_1(\boldsymbol{\lambda})) &= |\Psi_2(\boldsymbol{\lambda})) \equiv |\Psi_{\mathrm{bp}})\,. \end{aligned} \tag{9.74}$$

The degeneracy of the two c-orthogonal functions implies that at the branch point a self-c-orthogonal (SO) state is obtained,

$$(\Psi_{\mathrm{bp}}|\Psi_{\mathrm{bp}}) = 0\,. \tag{9.75}$$

We assume that the eigenfunctions of the Hermitian Hamiltonian $\hat{H}_{\theta=0}$ are real and therefore for $\theta \neq 0$ the c-product implies in this case that $(\Psi_{j'}(\boldsymbol{\lambda})|\Psi_j(\boldsymbol{\lambda})) = \langle[\Psi_{j'}(\boldsymbol{\lambda})]^*|\Psi_j(\boldsymbol{\lambda})\rangle$ and $(\Psi_{\mathrm{bp}}|\Psi_{\mathrm{bp}}) = \langle[\Psi_{\mathrm{bp}}]^*|\Psi_{\mathrm{bp}}\rangle$.

By varying one of the potential parameters when all the others are held fixed at $\boldsymbol{\lambda} = \boldsymbol{\lambda}_{\mathrm{bp}}$, the degeneracy is removed from the spectrum and so is the SO phenomenon. Being sufficiently close to the SO conditions (i.e., $|(\lambda - \lambda_{\mathrm{bp}})/\lambda_{\mathrm{bp}}| \ll 1$),

$$\begin{aligned} E_1(\lambda) &= E_{\mathrm{bp}} + \alpha\sqrt{\lambda - \lambda_{\mathrm{bp}}} + \beta(\lambda - \lambda_{\mathrm{bp}}) + \cdots \\ E_2(\lambda) &= E_{\mathrm{bp}} - \alpha\sqrt{\lambda - \lambda_{\mathrm{bp}}} + \beta(\lambda - \lambda_{\mathrm{bp}}) + \cdots , \end{aligned} \tag{9.76}$$

where

$$\begin{aligned} |\Psi_1(\lambda)) &= \mathcal{N}_1[\,|\Psi_{\mathrm{bp}}) + \sqrt{\lambda - \lambda_{\mathrm{bp}}}\,|\chi) + (\lambda - \lambda_{\mathrm{bp}})|\xi) + \cdots] \\ |\Psi_2(\lambda)) &= \mathcal{N}_2[\,|\Psi_{\mathrm{bp}}) - \sqrt{\lambda - \lambda_{\mathrm{bp}}}\,|\chi) + (\lambda - \lambda_{\mathrm{bp}})|\xi) + \cdots]\,. \end{aligned} \tag{9.77}$$

It is important to realize that in the above algebraic expansion the coefficient α and the function $|\chi)$ are correspondingly a λ-independent parameter and function. Let us give a graphic representation of the coalescence of the two almost degenerate eigenvalues $E_1(\lambda)$ and $E_2(\lambda)$ defined in Eq. (9.76), assuming that the coefficient α is complex. Sufficiently close to the branch point (the so-called exceptional point) the two complex almost-degenerate eigenvalues are

$$\begin{aligned} E_1(\lambda) &\simeq E_{\mathrm{bp}} + \alpha\sqrt{\lambda - \lambda_{\mathrm{bp}}}\,, \\ E_2(\lambda) &\simeq E_{\mathrm{bp}} - \alpha\sqrt{\lambda - \lambda_{\mathrm{bp}}}\,. \end{aligned} \tag{9.78}$$

Assuming that the coefficient α is complex and both λ and λ_{bp} are real parameters, for a specific value of $\lambda = \lambda_0$ which satisfies $\lambda_0 - \lambda_{\mathrm{bp}} > 0$ we get that $E_1(\lambda_0)$ and $E_2(\lambda_0)$ are two points on a line in the complex energy plane where the branch point, E_{bp}, lies on the mid-point (see Fig. 9.4). As λ is increased the two eigenvalues move along the straight line towards the mid-point E_{bp} and at the value of $\lambda = \lambda_{\mathrm{bp}}$ the two coalesce. When $\lambda - \lambda_{\mathrm{bp}} < 0$ the coefficient α is multiplied by $\mathrm{i} = \exp(\mathrm{i}\pi/2)$ and therefore as λ is further reduced below λ_{bp} the two almost-degenerate eigenvalues move along a line which is perpendicular to the previous line (see Fig. 9.4). We now move to examine the behavior of the corresponding eigenfunctions. Since the two almost-degenerate eigenfunctions are orthogonal,

$$(\Psi_1(\lambda))|\Psi_2(\lambda)) \cong \mathcal{N}_1\mathcal{N}_2[\,\lambda - \lambda_{\mathrm{bp}}][(\chi|\chi) + 2(\Psi_{\mathrm{bp}}|\xi)] \;=\; 0\,, \tag{9.79}$$

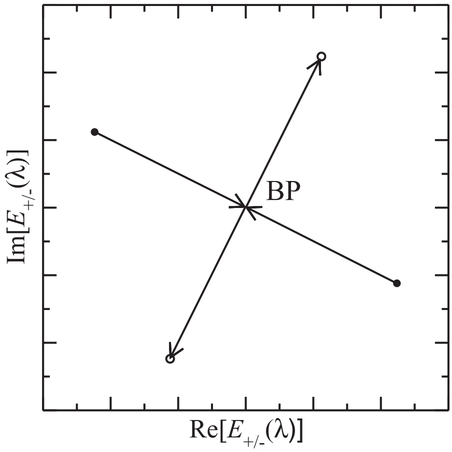

Figure 9.4 A schematic representation of the coalescence of two almost-degenerate eigenvalues given in Eq. (9.78) as a real parameter in the Hamiltonian λ is varied. The full circles stand for $E_{\pm}(\lambda_0) = \lambda_{\rm bp} + \delta$, the open circles for $E_{\pm}(\lambda_0) = \lambda_{\rm bp} - \delta$, where $\delta > 0$, and the meeting-point of the arrows stands for $E_{\rm bp}$. Note that for a real or imaginary value of the coefficient α the two almost-degenerate eigenvalues move along the two perpendicular lines such that for one of them $\mathrm{Re}(E_1(\lambda)) = \mathrm{Re}(E_2(\lambda))$ whereas for the second line $\mathrm{Im}(E_1(\lambda)) = \mathrm{Im}(E_2(\lambda))$.

which implies that $(\chi|\chi) \cong -2(\Psi_{\rm bp}|\xi)$. For sufficiently small values of $|\lambda - \lambda_{\rm bp}|$ the complex normalization factors are chosen to be

$$\mathcal{N}_1^2 \cong [2(\lambda - \lambda_{\rm bp})^{1/2}(\chi|\Psi_{\rm bp})]^{-1} ,$$
$$\mathcal{N}_2^2 = -\mathcal{N}_1^2 , \tag{9.80}$$

such that

$$(\Psi_1(\lambda)|\Psi_1(\lambda)) = 1 ,$$
$$(\Psi_1(\lambda)|\Psi_1(\lambda)) = 1 . \tag{9.81}$$

Therefore, as $(\lambda - \lambda_{\rm bp}) \to 0, \mathcal{N}_1 = i\mathcal{N}_2 \to \infty$. As we will see later, this fact plays an important role in the large sensitivity of expectation values (using the c-product) to the potential parameters as the system approaches the SO conditions.

It is straightforward to see from Eq. (9.76)–(9.77) that the first derivatives of the resonance energy and the resonance widths which are associated with the almost-degenerate states $\Psi_1(\lambda)$ and $\Psi_2(\lambda)$ get infinitely large as $\lambda \to \lambda_{\rm bp}$. It is of particular interest to realize that sufficiently close to the SO conditions the decay rates of the resonance $\Gamma_1 = -2\mathrm{Im}(E_1)$ and $\Gamma_2 = -2\mathrm{Im}(E_2)$ associated with these states will show contrasting cusp-like behavior with respect to variation in λ. Γ_1 will exhibit a sharp peak whereas Γ_2 will show a dip near the branch point.

It is also clear that the c-product expectation value of a complex scaled operator $\hat{O}_\theta$ which does not commute with the non-Hermitian Hamiltonian in one of the almost SO states will be very large, such that

$$\begin{aligned}\bar{O}_1 &= \frac{(\Psi_1(\lambda)|\hat{O}_\theta|\Psi_1(\lambda))}{(\Psi_1(\lambda)|\Psi_1(\lambda))} \to \infty\,,\\ \bar{O}_2 &= \frac{(\Psi_2(\lambda)|\hat{O}_\theta|\Psi_2(\lambda))}{(\Psi_2(\lambda)|\Psi_2(\lambda))} \to \infty \end{aligned} \tag{9.82}$$

as $\lambda \to \lambda_{\text{bp}}$.

The conclusion is that by **adiabatically** varying the potential parameters $\boldsymbol{\lambda}$, one can keep the system in one eigenstate and remain sufficiently close to the SO situation such that the expectation values of any operator that does not commute with the Hamiltonian will be very large. It implies, for example, that the standard deviation of any property which is represented by such an operator would be extremely large under these conditions. This means that one must vary the potential parameters sufficiently slowly to maintain the propagated wavepacket at a large overlap with one of the almost-SO states but almost orthogonal to the other SO state. Of course, at the branch point the adiabatic approach breaks down regardless of how slowly the potential parameters are varied.

Note, however, that although the resonance width has a finite value $\Gamma_{\text{bp}} = -2\text{Im}(E_{\text{bp}})$, when $\boldsymbol{\lambda} = \boldsymbol{\lambda}_{\text{bp}}$ the first derivative of the resonance width, which is obtained by adiabatically varying the potential parameters, is increased as one gets closer the SO conditions since from Eq. (9.76) one gets that

$$\left|\frac{\partial \Gamma_{1,2}}{\partial \lambda}\right|_{\lambda=\lambda_{\text{bp}}} = \left|\frac{\partial(\Gamma_{\text{bp}} \mp 2\text{Im}[\alpha\sqrt{\lambda-\lambda_{\text{bp}}}])}{\partial\lambda}\right|_{\lambda=\lambda_{\text{bp}}} = \infty\,. \tag{9.83}$$

Here we vary only one real parameter λ out of many potential parameters which are the components of $\boldsymbol{\lambda}$, where all other parameters are held fixed at the values at which the two eigenfunctions coalesce. This approach simplifies the representation and the analysis of the effects of being near the SO situation on measurable quantities.

Since near the branch point the two nearly degenerate states have similar wavefunctions, an important question is what the effect will be of the SO phenomenon on measurable quantities when the system is prepared in a wavepacket that populates both of them. That is, we what to see what happens if instead of populating one state we study a an initial complex scaled wavepacket, $|\Phi_0)$, of the form:

$$|\Phi_0) = \sum_{j=1} a_j |\Psi_j(\lambda)) \,,$$
$$a_j = (\Psi_j(\lambda)|\Phi_0) \,. \tag{9.84}$$

We use here the closure relation $\sum_{j=1} |\Psi_j(\lambda))(\Psi_j(\lambda)|$ which holds even when λ is very close to λ_{bp} where the spectrum is incomplete. When the complex scaled initial state is normalized to unity, $(\Phi_0|\Phi_0) = 1$, then $\sum_{j=1} a_j^2 = 1$ although both a_1 and a_2 have very large complex values which increase as $|\lambda - \lambda_{\mathrm{bp}}|$ decreases. Indeed, using Eqs. (9.76) and (9.80) one can see that

$$a_1^2 + a_2^2 = 2\frac{(\Psi_{\mathrm{bp}}|\Phi_0)(\chi|\Phi_0)}{(\chi|\Psi_{\mathrm{bp}})} \tag{9.85}$$

is a λ-independent parameter. With the help of Eq. (9.89) we see that the leading term in the expansion of the expectation value of the mean energy of the wavepacket (WP) in $(\lambda - \lambda_{\mathrm{bp}})$ is given by

$$\begin{aligned}\bar{E}_{\mathrm{WP}}(\lambda) = (\Phi_0|\hat{H}_\theta|\Phi_0) &= \sum_{j=1} (\Psi_j(\lambda)|\Phi_0)^2 E_j(\lambda) \\ \simeq \frac{2(\Psi_{\mathrm{bp}}|\Phi_0)(\chi|\Phi_0)}{(\chi|\Psi_{\mathrm{bp}})} E_{\mathrm{bp}} &+ \frac{\alpha(\Psi_{\mathrm{bp}}|\Phi_0)^2}{(\chi|\Psi_{\mathrm{bp}})} + \frac{\alpha(\lambda - \lambda_{\mathrm{bp}})(\Psi_{\mathrm{bp}}|\Phi_0)^2}{(\chi|\Psi_{\mathrm{bp}})} \\ + \sum_{j\neq 1,\neq 2} (\Psi_j(\lambda)|\Phi_0)^2 E_j(\lambda) \,. \end{aligned} \tag{9.86}$$

Here $\hat{H}_\theta$ stands for any non-Hermitian Hamiltonian and not necessarily for the complex scaled Hamiltonian. Note that, even when the last term in Eq. (9.86) can be neglected the third term in Eq. (9.86) is explicitly λ-dependent for any case which is close to the SO situation, while the rest of the terms in the last expression can be λ-independent. From Eq. (9.86) we conclude that the value of the complex mean energy is **not** very sensitive to the value of the potential parameters even when the system is very close to the SO situation. It is important to stress that here we assume that the initial state Φ_0 is λ-independent. The situation, of course, is very different when Φ_0 changes adiabatically with λ, as explained above.

The effect of the SO phenomenon on time-dependent measureable quantities. The discussion below is restricted to the cases where the time-dependent Schrödinger equation is solved for a complex potential (the situation where the physical potential is real and complex absorbing potentials are introduced to simplify the numerical calculations is excluded from this discussion).

The evolution in time of the complex scaled initial wavepacket, Φ_0, is given by

$$|\Phi_0(t)) = \sum_{j=1} a_j \mathrm{e}^{-\mathrm{i}E_j(\lambda)t/\hbar} |\Psi_j(\lambda)), \tag{9.87}$$

where the coefficients $\{a_j\}_{j=1,2,\ldots}$ are given in Eq. (9.84). Using the F-product formalism presented in Chapter 6 we can calculate the probability of observing particles in the interaction region (in any finite volume in space) as a function of time,

$$\rho(t) = \left| \sum_{j=1} a_j^2 \mathrm{e}^{-\Gamma_j t/\hbar} \right|, \tag{9.88}$$

where $\Gamma_j = -2\mathrm{Im}(E_j)$. When $|\lambda - \lambda_{\mathrm{bp}}|$ is sufficiently large such that the system is far from the SO situation, then it is expected that the envelope of $\rho(t)$ will decay to zero, and when the initial WP mainly populates the longest living resonance state, Γ_1, then $\mathrm{d}[\ln \rho(t)]/\mathrm{d}t \simeq \Gamma_1$. As we will see below, the situation is very different when $|\lambda - \lambda_{\mathrm{bp}}|$ is small so the system is very close to the SO situation. When λ gets sufficiently close to λ_{bp} then E_1 and E_2 are two almost-degenerate states (see Eq. (9.76)). Then Ψ_1 and Ψ_2 are orthonormal functions which have the form given in Eq. (9.77). Using Eqs. (9.76) and (9.80) one can see that

$$\begin{aligned} &a_1^2 \mathrm{e}^{-\Gamma_1 t/\hbar} + a_2^2 \mathrm{e}^{-\Gamma_2 t/\hbar} \\ &\quad = F_-(t) \left[\frac{(\Psi_{\mathrm{bp}}|\Phi_0)^2}{2\sqrt{\lambda - \lambda_{\mathrm{bp}}}(\chi|\Psi_{\mathrm{bp}})} + \frac{(\lambda - \lambda_{\mathrm{bp}})(\chi|\Phi_0)^2}{2(\chi|\Psi_{\mathrm{bp}})} \right] + F_+(t) \frac{(\Psi_{\mathrm{bp}}|\Phi_0)(\chi|\Phi_0)}{(\chi|\Psi_{\mathrm{bp}})}, \end{aligned} \tag{9.89}$$

where

$$F_\pm(t) = \mathrm{e}^{-\Gamma_{\mathrm{bp}} t/\hbar} \left[\mathrm{e}^{-\mathrm{Im}(\alpha\sqrt{\lambda - \lambda_{\mathrm{bp}}})t/\hbar} \pm \mathrm{e}^{+\mathrm{Im}(\alpha\sqrt{\lambda - \lambda_{\mathrm{bp}}})t/\hbar} \right]. \tag{9.90}$$

At $t = 0$ a $[\lambda - \lambda_{\mathrm{bp}}]$-independent result as given in Eq. (9.89) is obtained. As time passes more terms are involved in the dynamics and the dominant one is

$$\frac{(\Psi_{\mathrm{bp}}|\Phi_0)^2}{2(\chi|\Psi_{\mathrm{bp}})\sqrt{\lambda - \lambda_{\mathrm{bp}}}} \left[\mathrm{e}^{-\Gamma_1 t/\hbar} - \mathrm{e}^{-\Gamma_2 t/\hbar} \right]. \tag{9.91}$$

It is quite clear that as the system is closer to the SO situation, although $\lim_{t\to\infty} \rho(t) = 0$ there is a time interval $T_1 < t < T_2$ for which

$$\rho(t) \gg \rho(t = 0) \tag{9.92}$$

and therefore as time passes presumably more particles have been created than initially introduced into the interaction region. How is it possible that when the system is close to the branch point the number of particles embedded inside the interaction region is increased? The answer to this question depends on the answer to another question. Are $\rho(t)$ and $|\Psi_j)$ observable quantities? When the problem we solve is the scalar Maxwell equation within the paraxial approximation, where t in the time-dependent Schrödinger equation plays the role of the propagation axis Z of light in a waveguide and the potential energy term plays the role of the square of the spatial dependent index of refraction of the material, then $\rho(t = Z)$ is the power of the propagated light as function of Z. In such a case the 2×2 matrix

$$\mathbf{H} = \begin{pmatrix} \epsilon - \mathrm{i} & 1 \\ 1 & +\mathrm{i} \end{pmatrix} \tag{9.93}$$

(which is equal to the matrix which has an incomplete spectrum and is given in Eq. (9.18) at time $-\mathrm{i}$ when $\epsilon = 0$ in Eq. (9.93)) is a model Hamiltonian of two coupled single-mode waveguides. One waveguide is constructed from a material which absorbs the propagated light and the rate of the **loss** of light power is $+2 = -2\mathrm{Im}(\epsilon - \mathrm{i})$, whereas in the second waveguide there is a **gain** of power of the propagated light beam with a rate which is equal to $-2 = -2\mathrm{Im}(+\mathrm{i})$. The off-diagonal Hamiltonian matrix elements stand for the couplings between the two optical modes. The calculations of $\rho(t)$ for an initial vector $(1, 1)$ will show that for sufficiently small values of ϵ where two almost SO states are obtained one can find a time interval $T_1 < t < T_2$ for which $\rho(t = Z) > \rho(0)$.

However, when the time-dependent Schrödinger equation is solved both $\rho(t)$ and $|\Psi_j)$ are **not** measurable quantities. Only expectation values stand for measurable quantities. Let us assume we wish to find the probability of detecting particles inside a box of volume L^3 as a function of time. When the initial (complex scaled) wavepacket is Φ_0, by using the F-product formalism this measurable quantity, which we denote by $P_\mathrm{L}(t)$, is given by

$$\begin{aligned} P_\mathrm{L}(t) &= \left| \frac{\sum_{j',j} a_{j'} a_j \mathrm{e}^{-\mathrm{i}(E_j - [E_{j'}]^*)t/\hbar} \int_{-L/2}^{+L/2} \mathrm{d}\mathbf{r} \Psi_{j'}(\mathbf{r}) \Psi_j(\mathbf{r})}{\sum_{j',j} a_{j'} a_j \mathrm{e}^{-\mathrm{i}(E_j - [E_{j'}]^*)t/\hbar} \int_{-\infty}^{+\infty} \mathrm{d}\mathbf{r} \Psi_{j'}(\mathbf{r}) \Psi_j(\mathbf{r})} \right| \\ &= \left| \frac{\sum_{j',j} a_{j'} a_j \mathrm{e}^{-\mathrm{i}(E_j - [E_{j'}]^*)t/\hbar} \int_{-L/2}^{+L/2} \mathrm{d}\mathbf{r} \Psi_{j'}(\mathbf{r}) \Psi_j(\mathbf{r})}{\sum_j a_j^2 \mathrm{e}^{-2\mathrm{Im}(E_j)t/\hbar}} \right|, \end{aligned} \tag{9.94}$$

where $\{a_j\}_{j=1,2,\ldots}$ are defined in Eq. (9.84) and the non-measurable quantity $\rho(t)$ is given by

$$\rho(t) = \left| \sum_j a_j^2 \mathrm{e}^{-2\mathrm{Im}(E_j)t/\hbar} \right|. \tag{9.95}$$

Although $\rho(t)$ may grow in time, $P_L(t = 0) > P_L(t > 0)$ and the probability of finding the particles inside the box decays at all times, as it should.

9.5 Zero resonance contribution to the cross section

From the time-independent scattering theory presented in Chapter 8 we see that when a single resonance state controls the dynamics, the probability of a projectile with an energy E in an initial state denoted by $|\mathrm{i}\rangle$ passing through a target to a specific final state denoted by $|\mathrm{f}\rangle$ is approximately given by

$$T_{\mathrm{f,i}}(E) \simeq \left| \frac{\gamma_{\mathrm{i}}^{\mathrm{res}} \gamma_{\mathrm{f}}^{\mathrm{res}}}{E - E^{\mathrm{res}} + \mathrm{i}\Gamma/2} \right|^2 , \tag{9.96}$$

where up to phase factors, $\mathrm{e}^{\mathrm{i}\alpha_{\mathrm{i}}}$ and $\mathrm{e}^{\mathrm{i}\alpha_{\mathrm{f}}}$, the coefficients $\gamma_{\mathrm{i}}^{\mathrm{res}}$ and $\gamma_{\mathrm{f}}^{\mathrm{res}}$ are the square roots of the partial widths. For the sake of simplicity let us discuss here the case where the system has two open channels for the decay and both of them have the same threshold energies. In such a case the two partial widths are identical,

$$\gamma_{\mathrm{i}}^{\mathrm{res}} = \gamma_{\mathrm{f}}^{\mathrm{res}} = \mathrm{e}^{\mathrm{i}\varphi/2} \sqrt{\Gamma/2} . \tag{9.97}$$

On the basis of the full transmission at resonance when $E = E^{\mathrm{res}}$, i.e., $T(E^{\mathrm{res}}) = 1$, resonance tunneling diodes and transistors are produced. When the system is close to the condition for self-orthogonality, two resonances are nearly degenerate and thus, unlike the single resonance case, we get that

$$\begin{aligned} T(E) &\simeq \left| \frac{\gamma_+^2}{E - E_+^{\mathrm{res}} + \mathrm{i}\Gamma_+/2} + \frac{\gamma_-^2}{E - E_+^{\mathrm{res}} + \mathrm{i}\Gamma_-/2} \right|^2 \\ &= \frac{1}{2} \left| \frac{\Gamma_+/2}{E - E_-^{\mathrm{res}} + \mathrm{i}\Gamma_+/2} + \mathrm{e}^{\mathrm{i}(\varphi_- - \varphi_+)} \frac{\Gamma_-/2}{E - E_+^{\mathrm{res}} + \mathrm{i}\Gamma_-/2} \right|^2 . \end{aligned} \tag{9.98}$$

The two resonance eigenvalues are given according to Eq. (9.76) by

$$\begin{aligned} E_\pm^{\mathrm{res}} &= \mathrm{Re}[E_{\mathrm{bp}}] \pm \mathrm{Re}[\alpha\sqrt{\lambda - \lambda_{\mathrm{bp}}}] , \\ \Gamma_\pm &= -2\mathrm{Im}[E_{\mathrm{bp}}] \mp 2\mathrm{Im}[\alpha\sqrt{\lambda - \lambda_{\mathrm{bp}}}] , \end{aligned} \tag{9.99}$$

where E_{bp} is the exceptional point in the spectrum which is associated with a branch point where two resonances coalesce with the change in the potential parameter λ up to λ_{bp}. A crucial point in our derivation is that the value of the relative phase factor $\mathrm{e}^{\mathrm{i}(\varphi_- - \varphi_+)}$ is equal to -1. Another crucial point in our derivation is approaching the limit of $\lambda \to \lambda_{\mathrm{bp}}$ when $\lambda \leq \lambda_{\mathrm{bp}}$, which is within the radius of convergence of the perturbational expansion in λ. The reason for it is as follows. The partial width amplitudes, $\gamma_\pm^2 = \exp(\mathrm{i}\varphi_\pm)\Gamma_\pm/2$, can be obtained by calculating the expectation values of the flux operator, $\gamma_{\pm}^2 = (\Psi_{\pm}|\hat{\mathcal{F}}|\Psi_{\pm})$, where the two nearly degenerate functions are given as in Eq. (9.77). That is, $\Psi_+ \equiv \Psi_1(\lambda)$ and similarly $\Psi_- \equiv \Psi_2(\lambda)$. From Eq. (9.77) one can see that as $\lambda \to \lambda_{\mathrm{bp}}$, $\Psi_- \to \mathrm{i}\Psi_+$ and therefore $\gamma_-^2 = -\gamma_+^2$, which implies that indeed $\mathrm{e}^{\mathrm{i}(\varphi_- - \varphi_+)} = -1$. By substituting this result and Eqs. (9.99) into Eq. (9.98) one gets that

$$T(E,\epsilon) \simeq \left| \frac{\mathrm{Im}(E_{\mathrm{bp}}+\epsilon)}{E - \mathrm{Re}(E_{\mathrm{bp}}+\epsilon) - \mathrm{i}\mathrm{Im}(E_{\mathrm{bp}}+\epsilon)} - \frac{\mathrm{Im}(E_{\mathrm{bp}}-\epsilon)}{E - \mathrm{Re}(E_{\mathrm{bp}}-\epsilon) - \mathrm{i}\mathrm{Im}(E_{\mathrm{bp}}-\epsilon)} \right|^2, \tag{9.100}$$

where $\epsilon = \alpha\sqrt{\lambda - \lambda_{\mathrm{bp}}}$. From Eq. (9.100) one gets that the transition probability vanishes, $T(E,\epsilon) = 0$, when $E = E_0(\epsilon)$, which is given by

$$\begin{aligned} E_0(\epsilon) &= \frac{\mathrm{Im}(E_{\mathrm{bp}}+\epsilon)\mathrm{Re}(E_{\mathrm{bp}}-\epsilon) - \mathrm{Im}(E_{\mathrm{bp}}-\epsilon)\mathrm{Re}(E_{\mathrm{bp}}+\epsilon)}{\mathrm{Im}(E_{\mathrm{bp}}+\epsilon) - \mathrm{Im}(E_{\mathrm{bp}}-\epsilon)} \\ &= \mathrm{Re}(E_{\mathrm{bp}}) - \mathrm{Im}(E_{\mathrm{bp}})\frac{\mathrm{Re}(\epsilon)}{\mathrm{Im}(\epsilon)}\,. \end{aligned} \tag{9.101}$$

Since the limit of $\epsilon \to 0$ is obtained by taking the limit of $\lambda - \lambda_{\mathrm{bp}} \le 0$, $\lim_{\epsilon\to 0} E_0(\epsilon) = \mathrm{Re}(E_{\mathrm{bp}}) - \mathrm{Im}(E_{\mathrm{bp}})\mathrm{Im}(\alpha)/\mathrm{Re}(\alpha)$ and consequently, for the cases where $\mathrm{Im}(\alpha)$ (without loss of generality we assume here that λ and λ_{bp} get real values only) or $\mathrm{Im}(E_{\mathrm{bp}})$ gets sufficiently small,

$$T(E = \mathrm{Re}(E_{\mathrm{bp}}), \lambda \simeq \lambda_{\mathrm{bp}}) \simeq 0\,. \tag{9.102}$$

For the special cases where α is real, $\mathrm{Re}(\epsilon) = \mathrm{Im}(\alpha) = 0$ and the transition probability vanishes at the branch point.

9.6 Geometric phases (Berry phases)

The fact that for a certain set of potential parameters two (in principle it can be more than two) eigenfunctions coalesce is associated with a branch point in the complex energy plane (which is also known as an exceptional point). As discussed above, by holding fixed all the potential parameters except one (denoted by λ) the branch point is obtained at $\lambda = \lambda_{\mathrm{bp}}$, such that $E_\pm = E_{\mathrm{bp}} \pm \alpha\sqrt{\lambda - \lambda_{\mathrm{bp}}}$ for a real value of λ_{bp} or $E_\pm = E_{\mathrm{bp}} \pm \alpha\sqrt{(\lambda - \lambda_{\mathrm{bp}})(\lambda - \lambda_{\mathrm{bp}}^*)}$ when λ_{bp} is complex. Note that we can always extend the $\boldsymbol{\lambda}$-space to include the real and imaginary parts of the potential parameters separately (i.e., rather than N complex parameters in the vector $\boldsymbol{\lambda}$ there can be $2N$ real parameters) so that without lost of generality we can study here the case where $\boldsymbol{\lambda}_{\mathrm{bp}}$ is a set of real parameters. We vary one parameter in the complex parameter space in a circle with radius R which is centered around $\lambda = \lambda_{\mathrm{bp}}$. That is, we change λ such that

$$\lambda - \lambda_{\mathrm{bp}} = R\mathrm{e}^{\mathrm{i}\phi} . \tag{9.103}$$

We now wish to study how the energy and the corresponding eigenfunction change when ϕ is adiabatically varied from $\phi = 0$ to $\phi = 2n\pi$, where $n = 1, 2, \ldots$ If the circle is centered such that there are no branch points inside the circle then $E_{\pm}(\phi = 0) = E_{\pm}(\phi = 2n\pi)$ and $\Psi_{\pm}(\phi = 0) = \Psi_{\pm}(\phi = 2n\pi)$. As we will see, the situation is very different when the path we choose encircles a branch point. By substituting Eq. (9.103) into Eqs. (9.76), (9.77) and (9.80) one gets that the energies are given by

$$E_{\pm}(\phi) \equiv E_{\pm}(\lambda_{\mathrm{bp}} + R\mathrm{e}^{\mathrm{i}\phi}) = E_{\mathrm{bp}} \pm \alpha R^{1/2}\mathrm{e}^{\mathrm{i}\phi/2} \tag{9.104}$$

and the wavefunctions (assuming that the matrix is symmetric and therefore $(\Psi_{\mathrm{bp}}|\Psi_{\mathrm{bp}}) = \langle\Psi^*_{\mathrm{bp}}|\Psi_{\mathrm{bp}}\rangle = 0$) are

$$\begin{aligned} |\Psi_+(\phi)) &\equiv |\Psi_+(\lambda_{\mathrm{bp}} + R\mathrm{e}^{\mathrm{i}\phi})) \\ &= R^{-1/4}\mathrm{e}^{-\mathrm{i}\phi/4}[2(\chi|\Psi_{\mathrm{bp}})]^{-1/2}[\,|\Psi_{\mathrm{bp}}) + R^{1/2}\mathrm{e}^{\mathrm{i}\phi/2}|\chi)\,] , \\ |\Psi_-(\phi)) &\equiv |\Psi_-(\lambda_{\mathrm{bp}} + R\mathrm{e}^{\mathrm{i}\phi})) \\ &= \mathrm{i}R^{-1/4}\mathrm{e}^{-\mathrm{i}\phi/4}[2(\chi|\Psi_{\mathrm{bp}})]^{-1/2}[\,|\Psi_{\mathrm{bp}}) - R^{1/2}\mathrm{e}^{\mathrm{i}\phi/2}|\chi)\,] . \end{aligned} \tag{9.105}$$

From Eqs. (9.104) and (9.105) one can see that after one loop of 2π there is an exchange between the two almost-SO states,

$$\begin{aligned} E_{\pm}(2\pi) &= E_{\mp}(0) , \\ |\Psi_{\pm}(2\pi)) &= \mp|\Psi_{\mp}(0)) , \end{aligned} \tag{9.106}$$

while after two loops the energy returns to its original value while the corresponding almost-degenerate eigenfunction accumulates a phase of π,

$$\begin{aligned} E_{\pm}(4\pi) &= E_{\pm}(0) , \\ |\Psi_{\pm}(4\pi)) &= -|\Psi_{\pm}(=0)) . \end{aligned} \tag{9.107}$$

Only after four loops do both the energy and the corresponding almost-SO eigenfunctions return to the initial energy and eigenfunction,

$$\begin{aligned} E_{\pm}(8\pi) &= E_{\pm}(0) , \\ |\Psi_{\pm}(8\pi)) &= |\Psi_{\pm}(=0)) . \end{aligned} \tag{9.108}$$

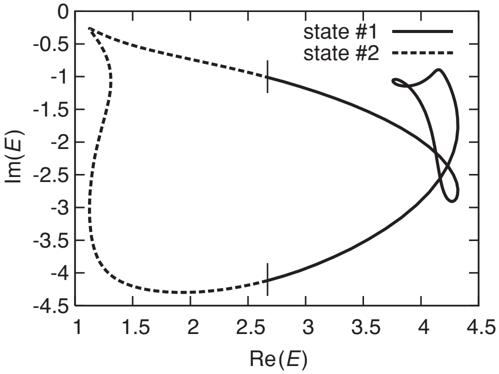

Figure 9.5 Adiabatic ϕ-trajectory in the parameter space (Γ, a) for the complex eigenvalue of our model problem which is defined in Eq. (9.56) ($v_0 = 0$). The trajectory starts at $\phi = 0$ and ends at $\phi = 2\pi$. The loop (Γ, a) is parameterized by the angle ϕ, where $\Gamma = \Gamma_{\text{bp}} + R_\Gamma \cos\phi$ and $a = a_{\text{bp}} + R_a \sin\phi$. $R_\Gamma = 1.5$, the branch point is at $\Gamma_{\text{bp}} = 3.627\,586\,69\ldots$ and $a_{\text{bp}} = L/2$; $R_a = L/4$. As one can see, the loop around the branch point shows a transition from one state to another. This happens when we are quite far from the branch point (the so-called exceptional point, EP).

The geometrical phases (known also as Berry phases) are the signs in Eqs. (9.107) and (9.108). Note that the situation is the same in the non-symmetric case since the transition from the symmetric to the non-symmetric is possible by carrying out the proper transformation (see, for example, the use of the Lanczos recursion method as described in Ex. 9.2). Note also that we discuss here the non-Hermitian degeneracy (i.e., self-orthogonality) which occurs when exploring *one complex parameter*, while in many cases (i.e., optics and laser physics) the non-Hermitian degeneracy typically occur when exploring *two real parameters*.

This important result can be verified for the illustrative model potential given in Eq. (9.56) without the need for R to be small.

In Fig. 9.5 we show the adiabatic ϕ-trajectory for the complex eigenvalue of our model problem.

Figure 9.6 shows the projection of $\Psi_+(x; R, \phi)$ for $0 \leq \phi \leq 4\pi$ on the initial state $\Psi_+(x; R, 0)$ (one of the almost self-orthogonal eigenfunctions). The projection has been carried out by the c-product where $(\Psi_+(x; R, 0)|\Psi_+(x; R, \phi) = \langle \Psi_+^*(x; R, 0)|\Psi_+(x; R, \phi)\rangle$. As one can see, after one-loop the projection is equal to zero. It implies that after one-loop $\Psi_+ \to \Psi_-$. After two loops $\Psi_+ \to -\Psi_+$ as we obtained from our analytical analysis. Only after four loops does $\Psi_+ \to \Psi +$.

Let us consider a closed loop in the space of complex V_0. This is to be distinguished from the previous calculations presented above for a loop in the parameter space (Γ, a).

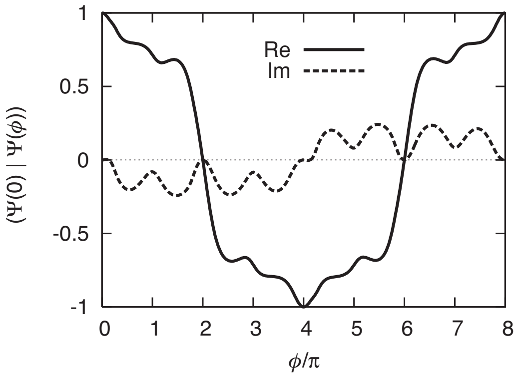

Figure 9.6 The projection of an eigenfunction where ϕ varies adiabatically (in (Γ, a) parameter space) on the initial eigenfunction (obtained at $\phi = 0$) of our model potential which is defined in Eq. (9.56). The trajectory starts at $\phi = 0$ and ends at $\phi = 8\pi$. As one can see, after one-loop the projection is equal to zero. It implies that after one-loop $\Psi_+ \to \Psi_-$. After two loops $\Psi_+ \to -\Psi_+$ as we obtained from our analytical analysis. Only after four loops does $\Psi_+ \to \Psi+$.

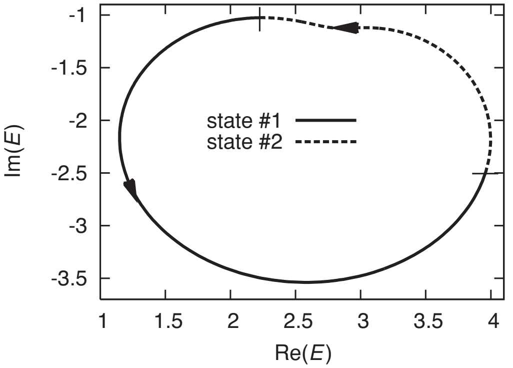

Figure 9.7 Adiabatic ϕ-trajectory in V_0 complex parameter space for the complex eigenvalue of our model problem. The trajectory starts at $\phi = 0$ and ends at $\phi = 2\pi$. As one can see, the loop around the branch point shows a transition from one state to another. This happens when we are quite far from the branch point.

In Fig. 9.7 we portray the variation of the eigenvalues in a loop $V_0(\phi) = V_{\mathrm{bp}} + R\exp(\mathrm{i}\phi)$, where a is constant. The transition from a solid to a dashed line reflects the adiabatic transition from one eigenvalue to another as we complete the loop around the branch point at $V_0 = V_{\mathrm{bp}}$.

Similarly, we show in Fig. 9.8 the variation of the eigenfunction, which corresponds to the eigenvalue in Fig. 9.7, as the phase ϕ is varied such that $V_0(\phi)$ forms a loop around the branch point Γ_{bp}. The purpose of Fig. 9.7 and Fig. 9.8 is to show

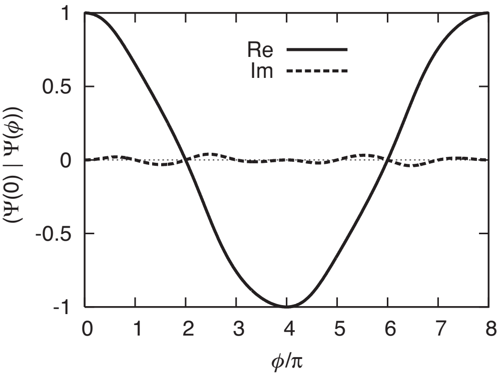

Figure 9.8 The projection of the eigenfunction on the initial eigenfunction of our model potential which is defined in Eq. (9.56), obtained for $\phi = 0$ where ϕ is varied adiabatically (in V_0 complex parameter space). The trajectory starts at $\phi = 0$ and ends at $\phi = 8\pi$.

that the transition from one eigenstate to another takes place whenever an adiabatic variation in parameter space occurs in a closed loop around a branch point. This is regardless of the parameter space where the adiabatic variation calculations were performed.

Can we get an estimate for the SO state from the two states we obtain near the branch point? From Eqs. (9.80) and (9.77) we get that when $|\lambda - \lambda_{\rm bp}|$ is sufficiently small

$$|\Psi_1) - \mathrm{i}|\Psi_2) = 2\mathcal{N}_1|\Psi_{\rm bp}) \equiv |\tilde{\Psi}_{\rm bp}) \,. \tag{9.109}$$

Since $\Psi_{\rm bp}$ is a self-orthogonal state of the Hamiltonian $\hat{H}(\boldsymbol{\lambda}_{\rm bp})$ then so is $|\tilde{\Psi}_{\rm bp})$ and $(\tilde{\Psi}_{\rm bp}|\tilde{\Psi}_{\rm bp}) = 0$. Note that one can use different normalization conditions for the almost-SO states. For example, when the calculations are carried out by using a finite number of basis functions (based on the c-linear variational principle in Chapter 7) then $|\Psi_1)$ and $|\Psi_2)$ are normalized such that the largest dominant component in the basis set expansion is equal to unity. In such a case,

$$|\Psi_1) - |\Psi_2) = |\tilde{\Psi}_{\rm bp}) \tag{9.110}$$

such that

$$(\tilde{\Psi}_{\rm bp}|\tilde{\Psi}_{\rm bp}) = 0 \,. \tag{9.111}$$

The conclusion is that a linear superposition of the two c-normalizable almost-SO eigenstates that are obtained for $\lambda \neq \lambda_{\rm bp}$ converges to the SO state as $\lambda \to \lambda_{\rm bp}$ faster than each of these states. Consider the situation when two parameters, λ_1

and λ_2, should be varied in order to obtain an SO situation. For example, when an atom, a molecule or a nanostructure system interacts with a laser field the two parameters can be the laser field intensity and frequency. There are many ways to find the branch point (if it exists). Here we describe one method which is simple to implement and requires the calculations of the eigenvalues of the non-Hermitian Hamiltonian only. First carry out adiabatic calculations when the two parameters are varied along a circle with radius R centered at λ_1^{c} and λ_2^{c}. That is,

$$\begin{aligned}\lambda_1 &= \lambda_1^{c} + R\sin\varphi\,,\\ \lambda_2 &= \lambda_2^{c} + R\cos\varphi\,,\end{aligned} \tag{9.112}$$

where $0 \le \varphi \le 2\pi$. Let us assume that for a sufficiently large value of R only a single branch point is embedded somewhere inside this circle. In such a case, when the adiabatic variation of φ starts with the almost-degenerate eigenvalue $E_1(\varphi_0)$ then by the end of the loop the second almost-degenerate eigenvalue will be obtained,

$$E_1(\varphi_0) = E_2(\varphi_0 + 2\pi)\,, \tag{9.113}$$

and similarly,

$$E_2(\varphi_0) = E_1(\varphi_0 + 2\pi)\,. \tag{9.114}$$

The next step in the calculations of λ_1^{bp} and λ_2^{bp} is to gradually reduce the radius such that for $R > R_c$ Eqs. (9.113) and (9.114) are satisfied but *not* for $R \le R_c$. It implies that the branch point is located somewhere on a circle that is centered around $(\lambda_1^{c}, \lambda_2^{c})$ in the 2D parameter plane with radius is $R = R_c$. One should repeat these steps of the calculation where now the contour of the φ-adiabatic calculations is a circle centered at $(\lambda_1^{c2}, \lambda_2^{c2}) = (\lambda_1^{c} + R_c\sin\varphi_0, \lambda_2^{c} + R_c\cos\varphi_0)$ (the value of φ_0 can be taken arbitrarily between 0 and 2π) and its radius $R \le 2R_c$ is gradually reduced to a value R_{c2} such that for $R > R_{c2}$ Eqs. (9.113) and (9.114) are satisfied but *not* for $R \le R_{c2}$. One of the two intersection points of the two circles is the desired branch point $(\lambda_1^{bp}, \lambda_2^{bp})$. Namely, λ_1^{bp} and λ_2^{bp} are one pair out of the two pairs of solutions of the two coupled equations,

$$\begin{aligned}(\lambda_1^{bp} - \lambda_1^{c})^2 + (\lambda_2^{bp} - \lambda_2^{c})^2 &= R_c^2\,,\\ (\lambda_1^{bp} - \lambda_1^{c2})^2 + (\lambda_2^{bp} - \lambda_2^{c2})^2 &= R_{c2}^2\,.\end{aligned} \tag{9.115}$$

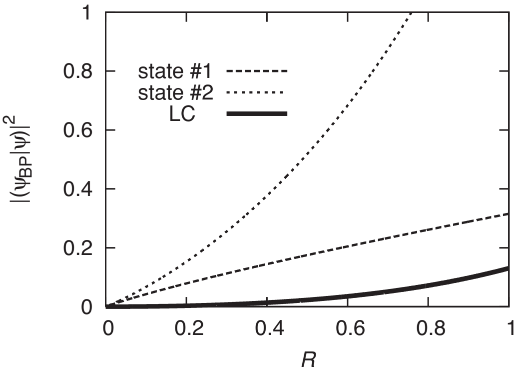

Figure 9.9 The projection of two almost-degenerate eigenstates and a linear combination (LC) of them on the self-orthogonal eigenstate (obtained for $R = 0$) of our model potential as defined in Eq. (9.56).

Exercise 9.7

For the model Hamiltonian given in Eq. (9.10) show that a superposition of the two non-normalized almost-SO eigenvectors given in Eq. (9.12)

$$\mathbf{c}_{\mathrm{LC}}(\lambda) \equiv \frac{\mathbf{c}_{+}(\lambda) + \mathbf{c}_{-}(\lambda)}{\sqrt{2}} \to \mathbf{c}_{\mathrm{bp}} \tag{9.116}$$

as $\lambda \to \mathrm{i}$, where $\mathbf{c}_{\mathrm{bp}}$ is a self-orthogonal vector which is associated with a branch point where the two eigenvectors merge. Moreover, prove that

$$\left\{\frac{\partial}{\partial\lambda}\left|\mathbf{c}_{\mathrm{bp}}^{\mathrm{T}}\mathbf{c}_{\mathrm{LC}}(\lambda)\right|^2\right\}_{\lambda=\mathrm{i}} = 0\,, \tag{9.117}$$

while

$$\left\{\frac{\partial}{\partial\lambda}\left|\mathbf{c}_{\mathrm{bp}}^{\mathrm{T}}\mathbf{c}_{\pm}(\lambda)\right|^2\right\}_{\lambda=\mathrm{i}} = 2\,. \tag{9.118}$$

For the simple analytical solvable problem with the complex 1D potential which is given in Eq. (9.56) we calculated the almost-SO states as functions of the potential parameter $\Gamma = \Gamma_{\mathrm{bp}} + R$. Γ is the potential parameter λ that appears above in our discussion for the most general case and $\lambda_{\mathrm{bp}} = \Gamma_{\mathrm{bp}}$, and therefore $\lambda - \lambda_{\mathrm{bp}} = R$ is the small parameter in our problem which determines how far the two almost SO states are from the branch point where they coalesce.

The results presented in Fig. 9.9 show clearly that for a broad range of values of R *a linear combination of two eigenstates provides the self-orthogonal eigenfunctions* (in a very good approximation). Moreover, the first derivative

$\mathrm{d}[(\Psi_{\mathrm{bp}}|\Psi_{\mathrm{LC}}(R \equiv \lambda - \lambda_{\mathrm{bp}}))]/\mathrm{d}R = 0$ at $R = 0$. Note that here we omit the label "res" from the two almost-SO states and from the SO solution since the non-Hermitian Hamiltonian in this case results from the use of a complex potential and because of the use of one of the complex scaling transformations that are applied for the calculation of the square integrable resonance states.

Exercise 9.8

Consider a system interacting with a laser field with frequency ω_{L} and a maximum field amplitude of ϵ_0. Assume that for specific values of the field parameters ϵ_0^{bp} and $\omega_{\mathrm{L}}^{\mathrm{bp}}$ two resonance eigenvalues, $E_\pm$, and their corresponding eigenvectors coalesce.

(1) Prove that the functional dependence close to the branch point of the two nearly degenerate resonance eigenvalues is given by

$$E_\pm = E_{\mathrm{bp}} \pm \sqrt{a(\omega_{\mathrm{L}} - \omega_{\mathrm{L}}^{\mathrm{bp}}) + b(\epsilon_0 - \epsilon_0^{\mathrm{bp}})}\,. \tag{9.119}$$

(2) Now consider a straight line $\epsilon_0(\omega_{\mathrm{L}}) = \epsilon_0^{\mathrm{bp}} + \alpha(\omega_{\mathrm{L}} - \omega_{\mathrm{L}}^{\mathrm{bp}})$, where $\alpha = -\frac{\mathrm{Im}(a)}{\mathrm{Im}(b)}$, which passes through the branch point $(\omega_L^{\mathrm{bp}}, \epsilon_0^{\mathrm{bp}})$ in the laser parameters' space. Show that close to the branch point along this line either the widths of the two resonance states $E_\pm$ are equal, i.e. $\mathrm{Im}(E_+) = \mathrm{Im}(E_-)$, or their energy positions are equal, i.e. $\mathrm{Re}(E_+) = \mathrm{Re}(E_-)$. At the branch point both of these conditions are satisfied and the two resonances are degenerate.

(3) Show that along the above-mentioned line in the $(\omega_{\mathrm{L}}, \epsilon_0)$ parameter space, when $\omega_{\mathrm{L}} \geq \omega_{\mathrm{L}}^{\mathrm{bp}}$, the resonance widths of $E_\pm$ are identical, i.e., $\mathrm{Im}(E_+ - E_-) = 0$, while when $\omega_{\mathrm{L}} \leq \omega_{\mathrm{L}}^{\mathrm{bp}}$, $\mathrm{Re}(E_+ - E_-) = 0$.

(4) Show that the condition that $[\mathrm{Re}(E_+ - E_-)]^2 = [\mathrm{Im}(E_+ - E_-)]^2$ is satisfied on the straight line $\epsilon_0(\omega_{\mathrm{L}}) = \epsilon_0^{\mathrm{bp}} + \tilde{\alpha}(\omega_{\mathrm{L}} - \omega_L^{\mathrm{bp}})$, where $\tilde{\alpha} = -\frac{\mathrm{Re}(a)}{\mathrm{Re}(b)}$.

9.7 Concluding remarks

(1) The self-orthogonality (SO) condition implies that for specific and unique parameters two or more orthogonal eigenfunctions of the non-Hermitian Hamiltonian coalesce and $(\Psi_{\mathrm{SO}}|\Psi_{\mathrm{SO}}) = 0$, where the c-product is used. The coalescence happens at a branch point in the complex energy plane where the spectrum of the non-Hermitian Hamiltonian becomes incomplete. This branch point is considered as an exceptional point in the energy spectrum.

(2) When the Hamiltonian is represented by a non-Hermitian finite $N \times N$ matrix, upon coalescence the number of linearly independent eigenvectors is smaller than N.

(3) The closure relations can be reconstructed from the SO state and the other eigenfunctions (eigenvectors) of the non-Hermitian Hamiltonian which has an incomplete

spectrum by adding additional $N_{\text{bp}} - 1$ functions (vectors). N_{bp} stands for the number of eigenfunctions (eigenvectors) which coalesce.

(4) The fingerprints of the SO phenomenon appear when the Hamiltonian has a complete spectrum but is sufficiently close to the SO situation that several (usually two) eigenfunctions (eigenvectors) are almost-SO states. Being almost-SO states implies that they are very much alike although they are orthogonal. By normalizing these states to unity their amplitudes (components of eigenvectors) become extremely large as one nears the SO situation.

(5) The self-orthogonal state can be recovered even when the non-Hermitian Hamiltonian has a complete spectrum and all eigenfunctions (eigenvectors) are normalizable.

(6) The effects of the SO phenomenon on observable quantities is measurable even when the spectrum of the non-Hermitian is complete and there is no SO eigenstate. These effects are hard or even impossible to predict by carrying out calculations within the framework of the Hermitian formalism of quantum mechanics.

9.8 Solutions to the exercises

Answer to Exercise 9.1

This problem has been taken from a paper published by Moiseyev, Kventsel and Katriel.[12]

The eigenvalues of the given matrix are obtained by taking $\det(\mathbf{H} - E\mathbf{I}) = 0$, which leads to the the following cubic equation for the characteristic polynomial:

$$E^3 - xE^2 - \left(\frac{3a^2}{2} + \frac{9}{16}\right)E + \left(x + \frac{7}{8}\right)a^2 + \frac{x+2}{16} = 0\,. \tag{9.120}$$

The solutions of the cubic equation

$$E^3 + a_1E^2 + a_2E + a_3 = 0 \tag{9.121}$$

depend on the discriminant, $D = Q^3 + R^2$, where Q and R are given by

$$Q = \frac{3a_2 - a_1^2}{9}\,; \qquad R = \frac{9a_1a_2 - 27a_3 - 2a_1^3}{54}\,. \tag{9.122}$$

For $a = 1/\sqrt{2}$ we find that the coefficients of the cubic equation are $a_1 = -x$, $a_2 = -21/16$ and $a_3 = 9(x+1)/16$.

(1) A crossing of two eigenvalues is obtained when the discriminant is equal to zero. Substituting in the discriminant leads to a polynomial for x with a root at $x = 1/4$. Substituting $x = 1/4$ in the characteristic polynomial in Eq. (9.120) gives $a1 = -1/4$,

---

[12] N. Moiseyev, G. F. Kventsel and J. Katriel, *Chem. Phys. Lett.* **57**, 477 (1978).

$a2 = -21/16$ and $a3 = 45/64$. The solutions to the cubic equation are given by

$$E_1 = S + T - a_1/3\,, \tag{9.123}$$

$$E_{2,3} = (S+T)/2 - a_1/3 \pm \mathrm{i}\sqrt{3}(S-T)/2\,, \tag{9.124}$$

where

$$S = \sqrt[3]{R + D^{1/2}}\,; \qquad T = \sqrt[3]{R - D^{1/2}}\,. \tag{9.125}$$

Since $D = 0$, in this case we get that $S = T = -2/3$. Accordingly, the eigenvalues at the crossing point are $E_1 = -5/4,\ E_2 = 3/4$ and $E_3 = 3/4$.

(2) The plot of $|E_3(x) - E_2(x)|$ as function of x exhibits a cusp at the point of crossing since the two eigenvalues at this point are equal.

(3) Any infinitesimally small change in the values of the matrix elements (as for example by changing a to $a = 1/\sqrt{2.001}$) will change the cusp behavior of $|E_3(x) - E_2(x)|$ to an analytical function with a minimum.

(4) By adding 1/4 to the diagonal of **H** we get the same eigenvalues as for the matrix **M**. Therefore,

$$\mathbf{U}^{\mathrm{T}}\mathbf{M}\mathbf{U} = \mathbf{H}(x = 0.25) + 0.25\mathbf{I} \tag{9.126}$$

and the unitary matrix **U** is given by

$$\mathbf{U} = \mathbf{C}\mathbf{D}^{\mathrm{T}}\,, \tag{9.127}$$

where **C** and **D** are correspondingly the eigenvector matrices of **M** and $\mathbf{H}(x = 0.25) + 0.25\mathbf{I}$ which have the same eigenvalue spectra. That is, $\mathbf{C}^{\mathrm{T}}\mathbf{M}\mathbf{C} = \mathbf{D}^{\mathrm{T}}[\mathbf{H}(x = 0.25) + 0.25\mathbf{I}]\mathbf{D}$. The matrix **U** is obtained from Eq. (9.127),

$$\mathbf{U} = \begin{pmatrix} 1/2 & a & 1/2 \\ a & 0 & -a \\ 1/2 & -a & 1/2 \end{pmatrix}, \tag{9.128}$$

where $a = 1/\sqrt{2}$.

Answer to Exercise 9.2

The $N \times N$ non-symmetric matrix is denoted by **H** and the transformed tri-diagonal symmetric matrix by **T**. The right and left Lanczos recursion vectors are defined as $\mathbf{U}^{\mathrm{L,R}} = \left(\mathbf{U}_1^{\mathrm{L,R}}, \mathbf{U}_2^{\mathrm{L,R}}, \ldots, \mathbf{U}_N^{\mathrm{L,R}}\right)$ such that

$$\begin{aligned} &[\mathbf{U}^{\mathrm{L}}]^{\mathrm{T}}\mathbf{U}^{\mathrm{R}} = \mathbf{I}\,, \\ &[\mathbf{U}^{\mathrm{L}}]^{\mathrm{T}}\mathbf{H}\mathbf{U}^{\mathrm{R}} = \mathbf{T}\,, \\ &\mathbf{H}\left[\mathbf{U}_1^{\mathrm{L}}, \mathbf{U}_2^{\mathrm{L}}, \ldots, \mathbf{U}_N^{\mathrm{L}}\right] = \left[\mathbf{U}_1^{\mathrm{R}}, \mathbf{U}_2^{\mathrm{R}} \ldots, \mathbf{U}_N^{\mathrm{R}}\right]\mathbf{T}\,, \end{aligned} \tag{9.129}$$

where **I** is an $n \times N$ unit matrix and

$$T_{n,n} \equiv \alpha_n \,,$$
$$T_{n,n+1} \equiv T_{n+1,n} = \beta_n \,. \tag{9.130}$$

By considering the sequence of vector multiplications $\mathbf{U}_1^{\mathrm{L,R}}, \mathbf{U}_2^{\mathrm{L,R}}, \ldots, \mathbf{U}_N^{\mathrm{L,R}}$ onto **H** and **T** in Eq. (9.129) it is easy to see that

$$\mathbf{H}\mathbf{U}_n^{\mathrm{R}} = \beta_{n-1}^{\mathrm{R}}\mathbf{U}_{n-1}^{\mathrm{R}} + \alpha_n \mathbf{U}_n^{\mathrm{R}} + \beta_n^{\mathrm{R}}\mathbf{U}_{n+1}^{\mathrm{R}} \,,$$
$$\mathbf{H}^{\mathrm{T}}\mathbf{U}_n^{\mathrm{L}} = \beta_{n-1}\mathbf{U}_{n-1}^{\mathrm{L}} + \alpha_n \mathbf{U}_n^{\mathrm{L}} + \beta_n \mathbf{U}_{n+1}^{\mathrm{L}} \,. \tag{9.131}$$

Apart from initial left and right eigenvectors which must be supplied (and can be taken to be equal, e.g, $U_{\mathrm{i},1}^{\mathrm{L}} = U_{\mathrm{i},1}^{\mathrm{R}} = 1/\sqrt{N}$) the recursions involve only two adjacent $\mathbf{U}^{\mathrm{L,R}}$ at a time. Rearrangements of Eqs. (9.131) give the residue vectors $\rho_n^{\mathrm{L,R}}$ and the operational recursion formula,

$$\rho_{n+1}^{\mathrm{R}} = [\mathbf{H} - \alpha_n]\,\mathbf{U}_n^{\mathrm{R}} - \beta_{n-1}\mathbf{U}_{n-1}^{\mathrm{R}} \,,$$
$$\rho_{n+1}^{\mathrm{L}} = \left[\mathbf{H}^{\mathrm{T}} - \alpha_n\right]\mathbf{U}_n^{\mathrm{L}} - \beta_{n-1}\mathbf{U}_{n-1}^{\mathrm{L}} \,, \tag{9.132}$$

from which each successive off-diagonal matrix element $\beta_n = T_{n,n+1} = T_{n+1,n}$ and vectors $\mathbf{U}_{n+1}^{\mathrm{L,R}}$ are constructed:

$$\beta_n = \left([\left(\rho_{n+1}^{\mathrm{L}}\right)^{\mathrm{T}} \cdot \rho_{n+1}^{\mathrm{R}}\right]^{1/2} \,,$$
$$\mathbf{U}_{n+1}^{\mathrm{L,R}} = \rho_{n+1}^{\mathrm{L,R}}/\beta_n \,. \tag{9.133}$$

The diagonal matrix elements, $\alpha_n = T_{n,n}$, are obtained from the projection

$$\alpha_n = \left(\mathbf{U}_{n+1}^{\mathrm{L}}\right)^{\mathrm{T}}\mathbf{H}\mathbf{U}_{n+1}^{\mathrm{R}} \,. \tag{9.134}$$

Note that in principe it is possible that $\left(\mathbf{U}_n^{\mathrm{L}}\right)^{\mathrm{T}}\mathbf{U}_n^{\mathrm{R}} = 0$ and $\mathbf{U}_n^{\mathrm{L,R}} \neq 0$ for a bi-orthogonal vector. However, rounding errors in the computations will always allow a normalization such that $\left(\mathbf{U}_n^{\mathrm{L}}\right)^{\mathrm{T}}\mathbf{U}_n^{\mathrm{R}} = 1$.[13]

Answer to Exercise 9.3

Let us carry a similarity transformation of **H**,

$$\mathbf{L} = \mathbf{A}^{-1}\mathbf{H}\mathbf{A} \,, \tag{9.135}$$

---

[13] On the use of the Lanczos recursion method for calculating complex resonance eigenvalues see K. F. Milfeled and N. Moiseyev, *Chem. Phys. Lett.* **130**, 180–186 (1986).

where

$$\mathbf{A} = \begin{pmatrix} a & b \\ c & d \end{pmatrix} \tag{9.136}$$

and

$$\mathbf{A}^{-1} = \frac{1}{\det(A)} \begin{pmatrix} d & -b \\ -c & a \end{pmatrix} . \tag{9.137}$$

Therefore,

$$\mathbf{L} = \frac{1}{ad - bc} \begin{pmatrix} ad + bc + \mathrm{i}(cd - ab) & 2bd + \mathrm{i}(d^2 - b^2) \\ -2ac + \mathrm{i}(a^2 - c^2) & -(ad + bc) + \mathrm{i}(ab - cd) \end{pmatrix} . \tag{9.138}$$

Since the matrix is one Jordan block we are left with the following equations:

$$-2ac + \mathrm{i}(a^2 - c^2) = 0 , \tag{9.139}$$

$$2bd + \mathrm{i}(d^2 - b^2) = ad - bc , \tag{9.140}$$

$$ad + bc + \mathrm{i}(cd - ab) = \lambda(ad - bc) , \tag{9.141}$$

$$-(ad + bc) + \mathrm{i}(ab - cd) = \lambda(ad - bc) , \tag{9.142}$$

where λ is the eigenvalue of the matrix. From Eqs.(9.141) and (9.142) it is immediately evident that $\lambda = 0$, which is indeed the eigenvalue of this matrix. Thus the transformed matrix **L** is

$$\mathbf{L} = \begin{pmatrix} 0 & 1 \\ 0 & 0 \end{pmatrix} \tag{9.143}$$

and we have proved here that the matrix **H** is a Jordan matrix of order 2.

Similarly, one can show that the matrix

$$\mathbf{L} = \begin{pmatrix} \alpha & 0 \\ \gamma & \beta \end{pmatrix} \tag{9.144}$$

can be transformed into a symmetric non-Hermitian matrix, **H**, by using the transformation matrix

$$\mathbf{A} = \begin{pmatrix} \pm \mathrm{i}a & -a \\ -b & \mp \mathrm{i}b \end{pmatrix} \tag{9.145}$$

and the exceptional point associated with the self-orthogonal eigenvector is obtained when $\alpha = \beta$.

Answer to Exercise 9.4

The zero-order eigenvector matrix of the diagonal matrix $\mathbf{H_0}$ is $\mathbf{C}^{(0)} = \mathbf{I}$. We set the diagonal elements of $\mathbf{C}^{(n>0)}$ to be equal to zero. That is, $C_{k,k}^{(n)} = \delta_{n,0}$. As usual in the Rayleigh–Schrödinger perturbation theory, the first-order correction term to the k-th eigenvalue of $\mathbf{H}$ is given by

$$E_k^{(1)} = H_{k,k}^{(0)} \tag{9.146}$$

and the components of the corresponding first-order correction vector to the k-th eigenvector of $\mathbf{H}$ are given by

$$C_{k,i}^{(1)} = \frac{V_{i,k}}{E_k^{(0)} - E_i^{(0)}}\,, \quad \{k, i\} = 1, 2, \ldots, N\,. \tag{9.147}$$

Let us denote the $(n > 1)$-order correction terms to the eigenvalues as

$$E_k^{(n+1)} = \sum_{i=0}^{N} V_{k,i} C_{k,i}^{(n)}\,. \tag{9.148}$$

We will prove that

$$C_{k,i \neq k}^{(n)} = \frac{\sum_{j=0}^{N} (V_{i,j} - E_k^{(1)} \delta_{i,j}) C_{k,j}^{(n-1)} - \sum_{p=1}^{n-2} E_k^{(n-p)} C_{k,i}^{(p)}}{E_k^{(0)} - E_i^{(0)}}\,, \tag{9.149}$$

where $\{k, i\} = 1, 2, \ldots, N$.

Proof of Eq. (9.149)

The Rayleigh–Schrödinger perturbation equation is given by

$$(\mathbf{H}^{(0)} - E_k^{(0)})\mathbf{C}_k^{(n)} - \sum_{q=1}^{n} E_k^{(q)} \mathbf{C}_k^{(n-q)} + \mathbf{V}\mathbf{C}_k^{(n-1)} = 0\,. \tag{9.150}$$

Let us multiply on the left-hand side of Eq. (9.150) by $[\mathbf{C}_i^{(0)}]^{\mathrm{T}}$, where $i \neq k$,

$$(E_i^{(0)} - E_k^{(0)}) C_{k,i}^{(n)} - \sum_{q=1}^{n} E_k^{(q)} C_{k,i}^{(n-q)} + \sum_{j=0}^{N} C_{k,j}^{(n-1)} V_{i,j} = 0\,. \tag{9.151}$$

By defining $q = n - p$, where $p = 1, \ldots, (n-1)$, one gets that

$$\sum_{q=1}^{n} E_k^{(q)} C_{k,i}^{(n-q)} = \sum_{p=1}^{n-1} E_k^{(n-p)} C_{k,i}^{(p)}\,. \tag{9.152}$$

By substituting Eq. (9.152) into Eq. (9.151) one gets Eq. (9.149).

Answer to Exercise 9.5

The time-dependent Hamiltonian for the interaction of an atom/molecule with an intense linearly polarized laser field and an additional weak field is given within the dipole approximation by

$$\hat{H}(\mathbf{r},t) = \hat{H}_{\text{system}}(\mathbf{r}) + f(t)\mathbf{e}_x \cdot \mathbf{r}[\epsilon_0 \cos(\omega_0 t) + \epsilon_1 \cos(\omega_1 t)]\,, \tag{9.153}$$

where $f(t)$ is the envelope of the laser pulse. The solution of the time-dependent Schrödinger equation (using atomic units where $\hbar = 1$, $e = 1$ and $m_\text{e} = 1$),

$$\hat{H}(\mathbf{r},t)\psi((\mathbf{r},t) = \mathrm{i}\partial_t \psi((\mathbf{r},t)\,, \tag{9.154}$$

can be expressed as a special case of a more general solution:

$$\psi(\mathbf{r},t) = \left[\Psi(\mathbf{r},t',t)\right]_{t'=t}\,. \tag{9.155}$$

$\Psi(\mathbf{r},t',t)$ is the (t,t') solution for the t-independent Hamiltonian $\mathcal{H}(\mathbf{r},t')$,

$$\mathcal{H}(\mathbf{r},t') = -\mathrm{i}\partial_{t'} + \hat{H}(\mathbf{r},t')\,, \tag{9.156}$$

and

$$\Psi(\mathbf{r},t',t) = \mathrm{e}^{-\mathrm{i}\mathcal{H}(\mathbf{r},t')t}\Psi(\mathbf{r},t',t=0)\,. \tag{9.157}$$

The use of the (t,t') method enables us to evaluate an analytical expression for the time-evolution operator for the time-dependent Hamiltonian. The reason is clear since t' serves as an additional coordinate. The duration of the two laser pulses is τ and thus we look for quasi-stationary solutions of the time-dependent Schrödinger equation of the form

$$\begin{aligned}\Psi(\mathbf{r},t',t) &= \exp(-\mathrm{i}Et)\Phi_E(\mathbf{r},t')\,,\\ \Phi_E(\mathbf{r},t') &= \Phi_E(\mathbf{r},t'+\tau)\,.\end{aligned} \tag{9.158}$$

By substituting Eq. (9.158) into $\hat{H}(t)\Psi(\mathbf{r},t) = \mathrm{i}\partial_t\Psi(\mathbf{r},t)$ one gets

$$\mathcal{H}(\mathbf{r},t')\Phi_E(\mathbf{r},t') = E\Phi_E(\mathbf{r},t')\,, \tag{9.159}$$

where $\{E + (2\pi/\tau)n\}_{n=\pm1,\pm2,\ldots}$ are also eigenvalues of $\mathcal{H}(\mathbf{r},t)$ which are associated with the eigenfunctions $\exp[\mathrm{i}(2\pi/\tau)n]\Phi_E(\mathbf{r},t)$. For this reason we refer to the eigenvalues of the Floquet-type operator $\mathcal{H}(\mathbf{r},t)$ as quasi-energies (QE). When $\mathbf{r}$ is a contour in the complex coordinate plane (read in Chapter 5 on the complex scaling transformations for which the resonance eigenfunctions are square integrable), the eigenvalues E get *complex discrete* values. Therefore Eq. (9.159) should be replaced by

$$\mathcal{H}(\mathbf{r}_\theta,t')\Phi^\theta_{E_\alpha}(\mathbf{r},t') = E^\theta_\alpha\Phi^\theta_{E_\alpha}(\mathbf{r},t')\,, \tag{9.160}$$

where $\alpha = 1,2,\ldots$ and $\mathbf{r}_\theta$ is one of the contours in the complex coordinate plane described in Chapter 5. The resonance solutions are associated with square integrable eigenfunctions, i.e., $\lim_{r\to\infty}\Phi^{\theta}_{E_\alpha}(\mathbf{r},t')=0$, provided that θ exceeds a certain value (see Chapter 5), and the corresponding photo-induced resonance eigenvalues,

$$E^{\theta}_{\alpha}=\mathcal{E}_{\alpha}-\frac{\mathrm{i}}{2}\Gamma_{\alpha}\,, \tag{9.161}$$

are θ-independent (as long as $\Phi^{\theta}_{E_\alpha}$ is square integrable). We can add additional coordinates to the problem by using a similar procedure to that used in the formulation of the (t,t') method. That is,

$$\begin{aligned}\mathcal{H}(\mathbf{r}_\theta,t',t'',t''')&=-\mathrm{i}\partial_{t'}-\mathrm{i}\partial_{t''}-i\partial_{t'''}+\hat{H}_{\text{system}}(\mathbf{r}_\theta)\\&\quad+f(t''')\mathbf{e}_x\cdot\mathbf{r}_\theta[\epsilon_0\cos(\omega_0t')+\epsilon_1\cos(\omega_1t'')]\,.\end{aligned}\tag{9.162}$$

Since the envelope of the laser pulse, $f(t)$, is a slowly varying function we can apply the adiabatic theorem (read more on it in Chapter 8) where $-\mathrm{i}\partial_{t'''}$ is the non-adiabatic coupling potential,

$$\begin{aligned}\mathcal{H}^{\text{ad}}(\mathbf{r}_\theta,t',t'')&=-\mathrm{i}\partial_{t'}+\hat{H}_{\text{system}}(\mathbf{r}_\theta)\\&\quad+f(t''')\mathbf{e}_x\cdot\mathbf{r}_\theta[\epsilon_0\cos(\omega_0t')+\epsilon_1\cos(\omega_1t'')]\,.\end{aligned}\tag{9.163}$$

We will take a laser pulse which supports many optical cycles and thus we can set $f(t''')=1$, assuming that the envelope of the laser pulse has a trapezoidal shape such that most of the time the laser pulse is at its maximal field amplitude. The adiabatic Floquet-type operator can be further simplified:

$$\begin{aligned}\mathcal{H}^{\text{ad}}(\mathbf{r}_\theta,t',t'')&=-\mathrm{i}\partial_{t''}+\mathcal{H}^{\text{ad}}_0(\mathbf{r}_\theta,t')+\epsilon_1\mathcal{H}^{\text{ad}}_1(\mathbf{r}_\theta,t'')\,,\\\mathcal{H}^{\text{ad}}_0(\mathbf{r}_\theta,t')&=-\mathrm{i}\partial_{t'}+\hat{H}_{\text{system}}(\mathbf{r}_\theta)+\epsilon_0\mathbf{e}_x\cdot\mathbf{r}_\theta\cos(\omega_0t')\,,\\\mathcal{H}^{\text{ad}}_1(\mathbf{r}_\theta,t'')&=\mathbf{e}_x\cdot\mathbf{r}_\theta\cos(\omega_1t'')\,.\end{aligned}\tag{9.164}$$

When

$$\epsilon_1\ll\epsilon_0 \tag{9.165}$$

we can simplify the calculations of the spectrum of $\mathcal{H}^{\text{ad}}(\mathbf{r}_\theta,t',t'')$ by assuming that the second weak laser couples the two resonance quasi-energy states, $\alpha=1,2$, which are associated with the ground and first excited electronic states of the field-free system (e.g., an atom). These states are solutions of $\mathcal{H}^{\text{ad}}_0(\mathbf{r}_\theta,t')$ and are given by

$$\begin{aligned}\mathcal{H}^{\text{ad}}_0(\mathbf{r}_\theta,t')\Phi^{\theta}_{\alpha}(\mathbf{r},t')&=E^{\text{ad}}_{\alpha}\Phi^{\theta}_{\alpha}(\mathbf{r},t')\,,\\E^{\text{ad}}_{\alpha}&=\mathcal{E}_{\alpha}-\frac{1}{2}\Gamma_{\alpha}\,.\end{aligned}\tag{9.166}$$

Using these photo-induced ionizing resonance states as a basis set the 2 × 2 Hamiltonian matrix of an atom (or a molecule) which interacts with a combined strong and weak laser fields is given by

$$\boldsymbol{H}^{\mathrm{ad}}(t'') = \begin{pmatrix} -\mathrm{i}\partial_{t''} + E_1^{\mathrm{ad}} & \epsilon_1 d_{12}\cos(\omega_1 t'') \\ \epsilon_1 d_{12}\cos(\omega_1 t'') & -\mathrm{i}\partial_{t''} + E_2^{\mathrm{ad}} \end{pmatrix}, \tag{9.167}$$

where

$$d_{12} = \frac{\omega_1}{2\pi}\int_0^{2\pi/\omega_1} \mathrm{d}t'' \langle \Phi_1^{-\theta_1}(t'')|\mathbf{r}_\theta \cdot \mathbf{e}_x|\Phi_2^{\theta_2}(t'')\rangle_{\mathbf{r}} = \langle \Phi_1^{-\theta}(0)|\mathbf{r}_\theta \cdot \mathbf{e}_x|\Phi_2^{\theta}(0)\rangle_{\mathbf{r}}\,. \tag{9.168}$$

Since $\boldsymbol{H}^{\mathrm{ad}}(t'') = \mathcal{H}^{\mathrm{ad}}(t'' + 2\pi/\omega_1)$ the eigenfunctions of $\mathcal{H}^{\mathrm{ad}}(t'')$ are periodic functions and can be expanded in a Fourier series of $\{\exp(\mathrm{i}\omega_1 n t'')\}_{n=0,\pm1,\pm2,\ldots}$. The Hamiltonian $\mathcal{H}^{\mathrm{ad}}(t'')$ is thereby recast as

$$\boldsymbol{H}^{\mathrm{ad}}(t'') = \sum_{n',n} |\mathrm{e}^{+\mathrm{i}\omega_1 n' t''}\rangle\langle \mathrm{e}^{-\mathrm{i}\omega_1 n' t''}|\mathcal{H}^{\mathrm{ad}}(t'')|\mathrm{e}^{+\mathrm{i}\omega_1 n t''}\rangle_{t''}\langle \mathrm{e}^{-\mathrm{i}\omega_1 n t''}|\,. \tag{9.169}$$

The Hamiltonian matrix elements are defined accordingly by

$$\begin{aligned}
[\boldsymbol{H}^{\mathrm{ad}}]_{n',n} &= \langle \mathrm{e}^{-\mathrm{i}\omega_1 n' t''}|\boldsymbol{H}^{\mathrm{ad}}(t'')|\mathrm{e}^{+\mathrm{i}\omega_1 n t''}\rangle_{t''} \\
&= \frac{\omega_1}{2\pi}\int_0^{2\pi/\omega_1} \mathrm{d}t'' \mathrm{e}^{-\mathrm{i}\omega_1 n' t''}\boldsymbol{H}^{\mathrm{ad}}(t'')\mathrm{e}^{+\mathrm{i}\omega_1 n t''} \\
&= \begin{pmatrix} \omega_1 n + E_1^{\mathrm{ad}} & 0 \\ 0 & \omega_1 n + E_2^{\mathrm{ad}} \end{pmatrix}\delta_{n,n'} + \epsilon_1 \begin{pmatrix} 0 & d_{12}/2 \\ d_{12}/2 & 0 \end{pmatrix}\delta_{n,n'\pm1}\,.
\end{aligned} \tag{9.170}$$

Since the second laser intensity is too weak to support multi-photon processes, we can restrict ourselves to effective one-photon processes where $n', n = 0, \pm1$. In such a case, the Hamiltonian matrix is given by

$$\mathcal{H}^{\mathrm{ad}} = \begin{pmatrix}
E_2^{\mathrm{ad}} + \omega_1 & \epsilon_1 d_{12}/2 & 0 & 0 & 0 & 0 \\
\epsilon_1 d_{12}/2 & E_1^{\mathrm{ad}} + \omega_1 & \epsilon_1 d_{12}/2 & 0 & 0 & 0 \\
0 & \epsilon_1 d_{12}/2 & E_2^{\mathrm{ad}} & \epsilon_1 d_{12}/2 & 0 & 0 \\
0 & 0 & \epsilon_1 d_{12}/2 & E_1^{\mathrm{ad}} & \epsilon_1 d_{12}/2 & 0 \\
0 & 0 & 0 & \epsilon_1 d_{12}/2 & E_2^{\mathrm{ad}} - \omega_1 & \epsilon_1 d_{12}/2 \\
0 & 0 & 0 & 0 & \epsilon_1 d_{12}/2 & E_1^{\mathrm{ad}} - \omega_1
\end{pmatrix}.$$

When $E_2^{\mathrm{ad}} - \omega_1 \simeq E_1^{\mathrm{ad}}$ and ϵ_1 is sufficiently small then it is a good approximation to take into consideration only the coupling between the two almost-degenerate quasi-energy (photo-induced) ionizing resonance states. Under this approximation (which is equivalent to the rotating wave approximation),

$$\boldsymbol{H}^{\mathrm{ad}} = \begin{pmatrix} E_1^{\mathrm{ad}} & \epsilon_1 d_{12}/2 \\ \epsilon_1 d_{12}/2 & E_2^{\mathrm{ad}} - \omega_1 \end{pmatrix} = E_1^{\mathrm{ad}}\mathbf{I} + \begin{pmatrix} 0 & \epsilon_1 d_{12}/2 \\ \epsilon_1 d_{12}/2 & \Delta E \end{pmatrix}, \tag{9.171}$$

where

$$\Delta E = E_2^{\mathrm{ad}} - \omega_1 - E_1^{\mathrm{ad}} = [\mathcal{E}_2 - \mathcal{E}_1 - \omega_1] - \frac{\mathrm{i}}{2}[\Gamma_2 - \Gamma_2]\,. \tag{9.172}$$

This expression is identical to that of

$$\begin{aligned} \mathbf{H} &= \mathbf{H}_0 + \epsilon_1 \mathbf{V}\,, \\ \mathbf{H}_0 &= \begin{pmatrix} 0 & 0 \\ 0 & \Delta E \end{pmatrix}, \\ \mathbf{V} &= \begin{pmatrix} 0 & d/2 \\ d/2 & 0 \end{pmatrix} \end{aligned} \tag{9.173}$$

up to the addition of $E_1^{\mathrm{ad}}\mathbf{I}$ which is equivalent to adding a constant to the eigenvalues.

The time-independent Schrödinger equation is

$$\mathbf{H}\mathbf{C}_\pm = \lambda_\pm \mathbf{C}_\pm\,. \tag{9.174}$$

The two eigenvalues of $\mathbf{H}$ are given by

$$\lambda_\pm = \frac{\Delta E}{2} \pm \frac{1}{2}\sqrt{(\Delta E)^2 + \epsilon_1^2 d^2}\,. \tag{9.175}$$

The two corresponding (c-product) orthogonal vectors are given by

$$\mathbf{C}_\pm = \mathcal{N}_\pm \begin{pmatrix} 1 \\ [\epsilon_1 d/2]/[\Delta E - \lambda_\pm] \end{pmatrix}. \tag{9.176}$$

The pre-factors can be taken (with some caution, as will be explained soon) as the normalization factors for which

$$[\mathbf{C}_\pm]^{\mathrm{T}}\mathbf{C}_\pm = \mathbf{I} \tag{9.177}$$

and therefore for $\Delta E \neq 0$ and $\epsilon_1 d \neq 0$,

$$\mathcal{N}_\pm = \sqrt{\frac{1}{1 + \epsilon_1^2 d^2/(\Delta E - \lambda_\pm)^2}}\,. \tag{9.178}$$

When

$$\Delta E = \mathrm{i}\epsilon_1 d\,. \tag{9.179}$$

degenerate eigenvalues are obtained:

$$\lambda_+ = \lambda_- = \frac{\Delta E}{2}\,. \tag{9.180}$$

Here we proved that for non-zero off-diagonal matrix element $\epsilon_1 d$ degenerate eigenvalues can be obtained for a non-Hermitian matrix (note that any matrix can be transformed to be complex and symmetric). It is, however, immediately seen that as the two eigenvalues coalesce *also the corresponding eigenvectors coalesce*. When we denote the value of ϵ_1 for which Eq. (9.179) is satisfied by

$$\epsilon_1^{\text{bp}} = -\text{i}\frac{\Delta E}{d}\,, \tag{9.181}$$

then Eq. (9.176) is reduced

$$\mathbf{C}_+ = \mathbf{C}_- = \mathcal{N}_\pm \begin{pmatrix} 1 \\ \text{i} \end{pmatrix}. \tag{9.182}$$

Using the c-normalization condition for $\epsilon_1 \neq \epsilon_1^{\text{bp}}$ as given in Eq. (9.178) one gets that the components of the unit normalized eigenvectors for which $[\mathbf{C}_\pm]^{\text{T}}\mathbf{C}_\pm = \mathbf{I}$ become large and go to ∞ as ϵ_1 approaches the value of ϵ_1^{bp}.

Only for very special values of the Hamiltonian matrix elements is the branch point, where a single self-orthogonal eigenvector obtained, associated with a real value of ϵ_1,

$$\epsilon_1^{\text{bp}} = \frac{\text{Re}(\Delta E)}{\text{Im}(d)} = \frac{\text{Im}(\Delta E)}{\text{Re}(d)}\,. \tag{9.183}$$

The requirement of a real value for ϵ_1^{bp} results from a a physical realization of this case where an atom or a molecule interacts with a combination of strong and weak laser fields. The intensity of the strong laser field I_0 is much larger than the intensity of the weak almost monochromatic laser field, $[\epsilon_1^{\text{bp}}]^2 \ll I_0$ with the fundamental frequency ω_{bp} (using Eq. (9.183)) which is defined by

$$\hbar\omega_{\text{bp}} = \text{Re}(E_2^{\text{QE}} - E_1^{\text{QE}}) - \text{Im}(E_2^{\text{QE}} - E_1^{\text{QE}})\frac{\text{Im}(d)}{\text{Re}(d)}\,, \tag{9.184}$$

where E_1^{QE} and E_2^{QE} are the two complex resonance quasi-energy states that are coupled by the weak laser field.

Answer to Exercise 9.6

(a) Following the explanation in the text, if $\mathbf{c}$ is a defective (self-orthogonal) eigenfunction (eigenvector) of an operator (complex symmetric matrix) $\mathbf{H}$,

$$(\mathbf{H} - E\mathbf{I})\mathbf{c} = 0\,, \tag{9.185}$$

where

$$\mathbf{c}^{\text{T}} \cdot \mathbf{c} = 0\,, \tag{9.186}$$

we get for the 2×2 matrix in Eq. (9.10) that when $\lambda = \mathrm{i}$ then $E_{\mathrm{bp}} = 0$ and the self-orthogonal vector is

$$\mathbf{c} = \begin{pmatrix} 1 \\ \mathrm{i} \end{pmatrix} . \tag{9.187}$$

Since we have only one eigenvector we can correct the closure relations by adding an additional state $\mathbf{d}$ satisfying

$$(\mathbf{H} - E\mathbf{I})\mathbf{d} = \mathbf{c} , \tag{9.188}$$

which can be easily solved to yield

$$\mathbf{d} = \begin{pmatrix} 1/2 \\ -\mathrm{i}/2 \end{pmatrix} . \tag{9.189}$$

Note that the two non-orthogonal vectors $\mathbf{c}$ and $\mathbf{d}$ are associated with the same eigenvalue E and satisfy $\mathbf{c}^{\mathrm{T}} \cdot \mathbf{d} = 1$. It is easy to see that in our case (due to the absence of other orthonormal vectors) we can express the closure relation using these two vectors only and verify that indeed we obtain a unit operator:

$$\mathbf{I} = \frac{\mathbf{c} \cdot \mathbf{d}^{\mathrm{T}} + \mathbf{d} \cdot \mathbf{c}^{\mathrm{T}}}{\mathbf{c}^{\mathrm{T}} \cdot \mathbf{d}} . \tag{9.190}$$

(b) Another illustrative example is the 3×3 matrix which is given in Eq. (9.55) for which

$$\mathbf{BHB}^{-1} = \begin{pmatrix} 3 & 1 & 0 \\ 0 & 3 & 0 \\ 0 & 0 & 6 \end{pmatrix} , \tag{9.191}$$

where

$$\mathbf{B} = \begin{pmatrix} 0 & -\frac{1}{7} & -3 \\ \mathrm{i} & -\frac{3\mathrm{i}}{7} & -\mathrm{i} \\ -1 & 2\mathrm{i} & 1 \end{pmatrix} \tag{9.192}$$

The first column, $\mathbf{B}_1$, is the self-orthogonal state with eigenvalue of $E_1 = 3 \equiv E_{\mathrm{bp}}$. The third column, $\mathbf{B}_3$, is the regular state with eigenvalue $E_3 = 6$. For the second column $\mathbf{B}_2$, we find:

$$\begin{aligned} (\mathbf{B}_2|\mathbf{B}_3) &= \mathbf{B}_2^{\mathrm{T}}\mathbf{B}_3 = 0 , \\ (\mathbf{B}_2|\mathbf{B}_1) &= \mathbf{B}_2^{\mathrm{T}}\mathbf{B}_1 \neq 0 , \\ \mathbf{B}_1 &= (\mathbf{H} - E_1\mathbf{I})\mathbf{B}_2 \end{aligned} \tag{9.193}$$

and one can see that $\mathbf{B}_1$ and $\mathbf{B}_2$ are mixed.

For this specific case of Eq. (9.45), $\mathbf{B}\mathbf{U}\mathbf{B}^{\mathrm{T}} = \mathbf{I}$, which is satisfied when

$$\mathbf{U} = \frac{1}{9}\begin{pmatrix} 8 & -21 & 0 \\ -21 & 0 & 0 \\ 0 & 0 & 1 \end{pmatrix} . \tag{9.194}$$

Answer to Exercise 9.7

We consider the Hamiltonian

$$\mathbf{H} = \begin{pmatrix} +1 & \lambda \\ \lambda & -1 \end{pmatrix} . \tag{9.195}$$

Here λ is a complex parameter. The eigenvalue problem of $\mathbf{H}$ is written as

$$\mathbf{H}\,\mathbf{c}_{\pm} \;=\; E_{\pm}\,\mathbf{c}_{\pm} \; . \tag{9.196}$$

An explicit calculation gives

$$\begin{aligned} E_{\pm} &= \pm\sqrt{\lambda^2 + 1}\,, \\ \mathbf{c}_{\pm} &= \begin{pmatrix} \frac{\lambda}{E_{\pm}-1} \\ 1 \end{pmatrix} . \end{aligned} \tag{9.197}$$

Note that we prefer to keep the eigenvectors un-normalized. The case of $\lambda = \mathrm{i}$ corresponds to the branch point, where both the eigenvalues and eigenvectors are degenerate. At the branch point,

$$\begin{aligned} E_{\mathrm{bp}} &= 0\,, \\ \mathbf{c}_{\mathrm{bp}} &= \begin{pmatrix} -\mathrm{i} \\ +1 \end{pmatrix} . \end{aligned} \tag{9.198}$$

Moreover, the branch point eigenvector is self-orthogonal, that is, $\mathbf{c}_{\mathrm{bp}}^{\mathrm{T}}\,\mathbf{c}_{\mathrm{bp}} = 0$. This explains why we did not implement the usual unit c-normalization.

It is instructive to see how the branch point eigenvector bifurcates into two distinct linearly independent eigenvectors when λ is close to i. By expanding the factor $(E_{\pm} - 1)^{-1}$ into power series one finds after straightforward manipulations that

$$\mathbf{c}_{\pm} = \mathbf{c}_{\mathrm{bp}} \pm \sqrt{\lambda - \mathrm{i}} \begin{pmatrix} 1-\mathrm{i} \\ 0 \end{pmatrix} + (\lambda - \mathrm{i}) \begin{pmatrix} 1 \\ 0 \end{pmatrix} + \mathcal{O}[(\lambda - \mathrm{i})^{3/2}] . \tag{9.199}$$

Consequently,

$$\mathbf{c}_{\mathrm{bp}} = \frac{(\mathbf{c}_{+} + \mathbf{c}_{-})}{2} + \mathcal{O}[(\lambda - \mathrm{i})] . \tag{9.200}$$

Equation (9.200) shows that the branch point eigenvector can actually be determined quite accurately by combining the two non-degenerate eigenvectors for λ

close to i. While the difference between $\mathbf{c}_{\mathrm{bp}}$ and $\mathbf{c}_{\pm}$ is of the order $\mathcal{O}[(\lambda - \mathrm{i})^{1/2}]$, the combination in Eq. (9.200) approximates $\mathbf{c}_{\mathrm{bp}}$ much better, with an error estimate $\mathcal{O}[(\lambda - \mathrm{i})^{1}]$. Let us elaborate this point in an alternative way, without directly using the power series expansion of Eq. (9.199). For any $\lambda \neq 0$ we have

$$\mathbf{c}_{\mathrm{LC}} = \frac{(\mathbf{c}_{+} + \mathbf{c}_{-})}{2} = \begin{pmatrix} \lambda^{-1} \\ 1 \end{pmatrix} . \tag{9.201}$$

Hence the projection

$$\mathbf{c}_{\mathrm{bp}}^{\mathrm{T}}\, \mathbf{c}_{\mathrm{LC}} = 1 - \mathrm{i}\,\lambda^{-1} . \tag{9.202}$$

On the other hand, the projection

$$\mathbf{c}_{\mathrm{bp}}^{\mathrm{T}}\, \mathbf{c}_{\pm} = 1 - \frac{\mathrm{i}\,\lambda}{E_{\pm} - 1} . \tag{9.203}$$

It is convenient to set

$$\lambda = \mathrm{i} + R\, \mathrm{e}^{\mathrm{i}\varphi} , \tag{9.204}$$

where the parameters $R \geq 0$ and $\varphi \in [0, 2\pi]$ characterize the deviation of λ from the branch point. Equation (9.202) then boils down to

$$\mathbf{c}_{\mathrm{bp}}^{\mathrm{T}}\, \mathbf{c}_{\mathrm{LC}} = \frac{R\, \mathrm{e}^{\mathrm{i}\varphi}}{\mathrm{i} + R\, \mathrm{e}^{\mathrm{i}\varphi}} = \mathcal{O}(R) , \tag{9.205}$$

whereas the expression in Eq. (9.203) becomes

$$\mathbf{c}_{\mathrm{bp}}^{\mathrm{T}}\, \mathbf{c}_{\pm} = \mp\sqrt{R\, \mathrm{e}^{\mathrm{i}\varphi}\,(2\,\mathrm{i} + R\, \mathrm{e}^{\mathrm{i}\varphi})} + \mathcal{O}(R) . \tag{9.206}$$

This implies that

$$\frac{\partial}{\partial R}\left\{ \left| \mathbf{c}_{\mathrm{bp}}^{\mathrm{T}}\, \mathbf{c}_{\mathrm{LC}} \right|^{2} \right\}_{R=0} = 0 \;, \;\; \text{but} \;\; \frac{\partial}{\partial R}\left\{ \left| \mathbf{c}_{\mathrm{bp}}^{\mathrm{T}}\, \mathbf{c}_{\pm} \right|^{2} \right\}_{R=0} = 2 > 0 , \tag{9.207}$$

demonstrating once again that the linear combination $\mathbf{c}_{\mathrm{LC}}$ is a much better approximation to $\mathbf{c}_{\mathrm{bp}}$ than $\mathbf{c}_{\pm}$ itself.

Answer to Exercise 9.8

(1) The coalescence of two resonance eigenvalues implies that $E_{\pm}(\epsilon_0, \omega_{\mathrm{L}})$ are not analytical functions and thus the Taylor expansions of these functions at the branch point are not applicable. However, the functions $(E_{\pm}(\epsilon_0, \omega_{\mathrm{L}}) - E_{\mathrm{bp}})^2$ are analytical functions, and when the laser parameters attain values which are sufficiently close to the branch point then the Taylor expansion approach is applicable and the leading term of $(E_{\pm}(\epsilon_0, \omega_{\mathrm{L}}) - E_{\mathrm{bp}})^2$ is $a(\omega_{\mathrm{L}} - \omega_{\mathrm{L}}^{\mathrm{bp}}) +$

$b(\epsilon_0 - \epsilon_0^{\mathrm{bp}})$. Consequently we can express the two eigenvalues near the branch point by

$$E_{\pm} = E_{\mathrm{bp}} \pm \sqrt{a\Delta\omega + b\Delta\epsilon}\,, \tag{9.208}$$

where

$$\begin{aligned} \Delta\omega &= \omega_{\mathrm{L}} - \omega_{\mathrm{L}}^{\mathrm{bp}}\,, \\ \Delta\epsilon &= \epsilon_0 - \epsilon_0^{\mathrm{bp}}\,. \end{aligned} \tag{9.209}$$

(2) The condition we wish to fulfill is either

$$\mathrm{Re}(E_+ - E_-) = 0 \tag{9.210}$$

or

$$\mathrm{Im}(E_+ - E_-) = 0. \tag{9.211}$$

At least one of this conditions must be fulfilled when

$$\mathrm{Re}(E_+ - E_-)\mathrm{Im}(E_+ - E_-) = 0\,. \tag{9.212}$$

On the basis of Eq. (9.208) one gets that this last condition is satisfied to the leading order in expansion whenever

$$\frac{\Delta\epsilon}{\Delta\omega} = -\frac{a - a^*}{b - b^*} = -\frac{\mathrm{Im}(a)}{\mathrm{Im}(b)}\,. \tag{9.213}$$

Therefore,

$$\epsilon_0(\omega) = \epsilon_0^{\mathrm{bp}} + \alpha(\omega_{\mathrm{L}} - \omega_{\mathrm{L}}^{\mathrm{bp}})\,, \tag{9.214}$$

where $\alpha = -\frac{\mathrm{Im}(a)}{\mathrm{Im}(b)}$. Along this line we get that

$$E_+ - E_- = 2\Delta\omega^{1/2}\left(\frac{\mathrm{Re}(a)\mathrm{Im}(b) - \mathrm{Re}(b)\mathrm{Im}(a)}{\mathrm{Im}(b)}\right)^{1/2}\,. \tag{9.215}$$

(3) Assuming that $[\mathrm{Re}(a)\mathrm{Im}(b) - \mathrm{Re}(b)\mathrm{Im}(a)]/\mathrm{Im}(b) > 0$ it is immediately evident from Eq. (9.215) that when $\omega_{\mathrm{L}} > \omega_{\mathrm{L}}^{\mathrm{bp}}$ then $\Delta\omega > 0$ and thus $E_+ - E_-$ is real. Thus the only condition which we can satisfy in this case is $\mathrm{Im}(E_+ - E_-) = 0$, leading to equal widths for the two resonances. On the other hand, when $\omega_{\mathrm{L}} < \omega_{\mathrm{L}}^{\mathrm{bp}}$ the behavior changes since $E_+ - E_-$ becomes imaginary. In this regime the only condition which can be satisfied is $\mathrm{Re}(E_+ - E_-) = 0$ and the two resonance have the same energy position. At the branch point both conditions are satisfied and $E_+ - E_- = 0$.

(4) A substitution of Eq. (9.208) into $[\mathrm{Re}(E_+ - E_-)]^2 = [\mathrm{Im}(E_+ - E_-)]^2$ leads to

$$\left[\frac{\sqrt{a\Delta\omega + b\Delta\epsilon} + \sqrt{a^*\Delta\omega + b^*\Delta\epsilon}}{2}\right]^2 = \left[\frac{\sqrt{a\Delta\omega + b\Delta\epsilon} - \sqrt{a^*\Delta\omega + b^*\Delta\epsilon}}{2\mathrm{i}}\right]^2 ,$$

$$a\Delta\omega + b\Delta\epsilon + a^*\Delta\omega + b^*\Delta\epsilon = -[a\Delta\omega + b\Delta\epsilon + a^*\Delta\omega + b^*\Delta\epsilon] .$$

This rearranges to

$$\Delta\epsilon = -\frac{\mathrm{Re}(a)}{\mathrm{Re}(b)}\Delta\omega . \tag{9.216}$$

This is just a straight line in the $(\epsilon_0, \omega_\mathrm{L})$ parameter space given by

$$\epsilon_0 = \epsilon_0^{\mathrm{bp}} + \tilde{\alpha}(\omega_\mathrm{L} - \omega_\mathrm{L}^{\mathrm{bp}}) , \tag{9.217}$$

where

$$\tilde{\alpha} = -\frac{\mathrm{Re}(a)}{\mathrm{Re}(b)} . \tag{9.218}$$

9.9 Further reading

N. Moiseyev, P. R. Certain and F. Weinhold, Resonance properties of complex-rotated Hamiltonians, *Mol. Phys.* **36**, 1613–1630 (1978).

N. Moiseyev and S. Friedland, The association of resonance states with the incomplete spectrum of finite complex-scaled Hamiltonian matrices, *Phys. Rev. A* **22**, 618–623 (1980).

H. P. Breuer, K. Dietz and M. Holthaus, Berry's phase in quantum optics, *Phys. Rev. A* **47**, 725–728 (1993).

O. Latinne, N. J. Kylstra, M. Dörr *et-al*. Laser-induced degeneracies involving autoionizing states in complex atoms, *Phys. Rev. Lett.* **74**, 46–49 (1995).

M. V. Berry and D. H. J. O'Dell, Diffraction by volume gratings with imaginary potentials, *J. Phys. A* **31**, 2093–2101 (1998).

W. D. Heiss, M. Müller and I. Rotter, Collectivity, phase transitions, and exceptional points in open quantum systems, *Phys. Rev. E* **58**, 2894–2901 (1998).

W. D. Heiss, Phases of wave functions and level repulsion, *Eur. Phys. J. D* **7**, 1 (1999).

W. D. Heiss, Repulsion of resonance states and exceptional points, *Phys. Rev. E* **61**, 929–932 (2000).

E. Hernández, A. Jáuregui and A. Mondragón, Degeneracy of resonances in a double barrier potential, *J. Phys. A* **33**, 4507–4523 (2000).

E. Narevicius and N. Moiseyev, Fingerprints of broad overlapping resonances in the e+H2 cross section, *Phys. Rev. Lett.* **81**, 2221–2224 (1998); Trapping of an electron due to molecular vibrations, *Phys. Rev. Lett.* **84**, 1681–1684 (2000).

W. D. Heiss and H. L. Harney, The chirality of exceptional points, *Eur. Phys. J. D* **17**, 149–151 (2001).

P. Serra, S. Kais and N. Moiseyev, Crossover phenomena and resonances in quantum systems, *Phys. Rev. A* **64**, 062502-062507 (2001).

R. Santra and L. S. Cederbaum, Non-Hermitian electronic theory and applications to clusters, *Phys. Rep.* **368**, 1–117 (2002).

M. V. Berry and M. R. Dennis, The optical singularities of birefringent dichroic chiral crystals, *Proc. R. Soc. Lond.* **459**, 1261–1292 (2003).

E. Narevicius, P. Serra and N. Moiseyev, Critical phenomena associated with self-orthogonality in non-Hermitian quantum mechanics, *Europhys. Lett.* **62**, 789–794 (2003).

E. Hernández, A. Jáuregui and A. Mondragón, Jordan blocks and Gamow–Jordan eigenfunctions associated with a degeneracy of unbound states, *Phys. Rev. A* **67**, 022721/1–022721/15 (2003).

W. D. Heiss, Exceptional points: their universal occurrence and their physical significance, *Czechoslovak J. Phys.* **54**, 1091–1099 (2004) and references therein.

A. Mostafazadeh, Quantum mechanics of Klein–Gordon-type fields and quantum cosmology, *Ann. Phys.* **309**, 1–48 (2004).

M. V. Berry, Physics of nonhermitian degeneracies, *Czech. J. Phys.* **54** 1039–1047 (2004).

E. Hernández, A. Jáuregui and A. Mondragón, Energy eigenvalue surfaces close to a degeneracy of unbound states: crossings and anticrossings of energies and widths, *Phys. Rev. E* **72**, 026221/1–026221/11 (2005).

U. Günther, I. Rotter and B. F. Samsonov, Projective Hilbert space structures at exceptional points, *J. Phys. B* **40**, 8815–8833 (2007).

C. M. Bender, Making sense of non-Hermitian Hamiltonians, *Rep. Prog. Phys.* **70**, 947–1018 (2007) and references therein.

S. Klaiman, U. Günther and N. Moiseyev, Visualization of branch points in PT-symmetric waveguides, *Phys. Rev. Lett.* **101**, 080402 (2008).

U. Günther and B. F. Samsonov, Naimark-dilated PT-symmetric brachistochrone, *Phys. Rev. Lett.* **101**, 230404–230408 (2008).

M. V. Berry, Optical lattices with PT symmetry are not transparent, *J. Phys. A* **41**, 244007–244013 (2008).

S. Klaiman and N. Moiseyev, Narrow resonances in complex potential energy surfaces, *J. Phys. B: At. Mol. Opt. Phys.* **42**, 044004 (2009).

O. Peleg, M. Segev, G. Bartal, D. N. Christodoulides and N. Moiseyev, Nonlinear waves in subwavelength waveguide arrays: evanescent bands and the Phoenix Soliton, *Phys. Rev. Lett.* **102**, 163902 (2009).

H. Cartarius, J. Main and G. Wunner, Exceptional points in atomic spectra, *Phys. Rev. Lett.* **99**, 173003 (2007); Exceptional points in the spectra of atoms in external fields, *Phys. Rev. A* **79**, 053408-1-11 (2009).

I. Rotter, A non-Hermitian Hamilton operator and the physics of open quantum systems, *J. Phys. A* **42** 153001–153051 (2009) and references therein.

S. Y. Lee, Decaying and growing eigenmodes in open quantum systems: biorthogonality and the Petermann factor, *Phys. Rev. A* **80**, 042104–042108 (2009).

S. B. Lee, J. Yang, S. Moon *et al.*, Observation of an exceptional point in a chaotic optical microcavity, *Phys. Rev. Lett.* **103**, 134101–134104 (2009).

10

The point where QM branches into two formalisms

Although the standard formalism of quantum mechanics is based on the requirement of the physical operators to be Hermitian, the use of non-Hermitian operators in the study of different types of phenomena is not uncommon. One of the most well-known non-Hermitian potentials is the optical potential where for any given choice of N channels the exact eigenvalue is a solution of a single-channel problem. The optical potential is a non-Hermitian, non-local and energy-dependent operator. In his book on scattering theory Taylor writes: "In practice, the optical potential is far too complicated for exact use in actual calculations".[1] It is often believed that the complex energies which are obtained by the use of optical potentials result from the approximations in the calculations. However, this is not true. The complex energy obtained by solving the one-channel problem with an optical potential is the exact eigenvalue of the original N-channel problem which is obtained by imposing outgoing boundary conditions on the eigenfunctions of the time-independent Schrödinger equation. In this chapter we wish to show that the study of the resonances in multi-channel problems (so-called Feshbach resonances) can be considered as the point where quantum mechanics branches into the standard (Hermitian) and non-standard (non-Hermitan) formalisms.

10.1 Feshbach resonances

Quite a long time ago Feshbach showed that the **exact** energy spectrum of the full physical problem can be obtained by solving two different self-energy problems. In spite of the fact that the two effective Hamiltonians are derived in a similar manner, in one case the exact energy spectrum of the full problem can be either real or complex (depending on the boundary conditions), whereas the exact energy spectrum associated with the second effective Hamiltonian has to be complex

---

[1] J. R. Taylor, *Scattering Theory*, New York, John Wiley & Sons, Inc., p. 385, 1972.

(excluding bound states in the continuum). The focus of this chapter is on the fact that in both cases the complex eigenvalues result from the *same* requirement of an out-going boundary condition. The branching of quantum mechanics into standard (Hermitian) formalism and non-Hermitian formalism is associated with the decision to express the exact energy spectrum for one of the two possible self-consistent-like problems where the use of the Green's operator imposes out-going boundary condition on the solutions of the time-independent Schrödinger equation. Our analysis is made here for the case where an ABC molecule has sufficient energy to dissociate only to $A + BC$ but not to $A + B + C$ or $AB + C$ or $AC + B$.

In this chapter we will focus on the association of the pre-dissociation resonances with the solutions obtained by applying the Feshbach formalism to the closed channels and not to the open ones as is usually done in molecular physics studies. The idea to apply the Feshbach formalism to the closed channels is not new and has been explored before by Feshbach himself for nuclear physics problems. Here we apply this approach to molecular physics problems, emphasizing the role of the Green's function in imposing the outgoing boundary conditions on the solutions which are associated with the open channels and emphasizing the fact that by doing so we get into the non-Hermitian sector of the domain of the Hamiltonian. The derivation and discussion presented here will demonstrate the branching of quantum mechanics into Hermitian and non-Hermitian formalisms when the Feshbach effective Hamiltonians are derived. We stress here the fact that complex eigenvalues are obtained not only by solving the time-independent Schrödinger equation for the closed channel's Feshbach effective Hamiltonian but also for the full physical Hamiltonian when outgoing boundary conditions are imposed on the solutions which are embedded in the continuous part of the spectrum.

In spite of the requirement of physical operators to be Hermitian, non-Hermitian Hamiltonians appear in the standard quantum mechanics formalism when effective Hamiltonians are derived. Let us briefly describe how these are obtained and what the significant results of such a derivation are, and its relevance to a broad range of general physical phenomena known as Feshbach resonances for a multi-dimensional system.

The Hermitian Hamiltonian $\hat{H}$ of the ABC molecular system depends on two types of coordinates: $\mathbf{r}$ which describes the position of the atom B with respect to the atom C in the diatom and the second coordinate $\mathbf{R}$ which gives the position of the atom A with respect to the center of mass of the diatom BC. Upon dissociation where $|\mathbf{R}| \to \infty$ we get that the Hamiltonian behaves as

$$\lim_{|\mathbf{R}|\to\infty} \hat{H} = \hat{T}_{\mathbf{R}} + \hat{H}_{\text{final}}(\mathbf{r})\,, \tag{10.1}$$

where

$$\hat{H}_{\mathrm{final}}(\mathbf{r}) = \hat{T}_{\mathbf{r}} + \lim_{|\mathbf{R}|\to\infty} V(\mathbf{r},\mathbf{R})\,. \tag{10.2}$$

$\hat{T}_{\mathbf{R}}$ and $\hat{T}_{\mathbf{r}}$ are the kinetic energy operators associated respectively with the "dissociative" coordinate **R** and the internal coordinate of the diatom **r**. The BC diatom which is obtained as the molecule ABC dissociates is associated with the Hamiltonian $\hat{H}_{\mathrm{final}}$ that has a discrete spectrum such that

$$\hat{H}_{\mathrm{final}}(\mathbf{r})\chi_n(\mathbf{r}) = E_n^{\mathrm{th}}\chi_n(\mathbf{r})\,, \tag{10.3}$$

where $n = 0, 1, 2, \ldots,$ and $E_0^{\mathrm{th}} < E_1^{\mathrm{th}} \leq E_2^{\mathrm{th}} \leq \cdots$ and the corresponding eigenfunctions $\chi_n(\mathbf{r})$ are the vibrational–rotational bound states of the diatomic molecule BC. The superscript "th" means that these bound states of the diatom BC are the threshold energies in the spectrum of the full Hamiltonian.

The atom A is temporarily trapped by the diatom BC due to the potential of interaction $V(\mathbf{r},\mathbf{R})$. The time-independent Schrödinger equation we solve here is given by

$$\hat{H}\Psi(\mathbf{R},\mathbf{r}) = E\Psi(\mathbf{R},\mathbf{r})\,, \tag{10.4}$$

where E is in the continuous part of the spectrum of $\hat{H}$ which describes the three-atomic system ABC. We can expand the eigenfunction of the full Hamiltonian $\Psi(\mathbf{R},\mathbf{r})$ which depends on the energy E in the continuum by using the eigenfunctions of $\hat{H}_{\mathrm{final}}$ as a basis set,

$$\Psi(\mathbf{R},\mathbf{r}) = \sum_n \phi_n(\mathbf{R})\chi_n(\mathbf{r})\,. \tag{10.5}$$

We can split the summation in Eq. (10.5) into two parts based on the fact that from some channel n_{c} all the channels above $n > n_{\mathrm{c}}$ are closed for "dissociation" since $E < E_{n>n_{\mathrm{c}}}^{\mathrm{th}}$ and the ABC molecule does not have the energy which is required for the dissociation to the atom A and a diatom BC in the vibrational–rotational quantum state $n > n_{\mathrm{c}}$. However, $n \leq n_{\mathrm{c}}$ are channels which are open for "dissociation" since $E > E_{n\leq n_{\mathrm{c}}}^{\mathrm{th}}$. Following the Feshbach formalism we now divide the problem into two subspaces. One subspace $\{Q\}$ will contain the closed channels, and a second subspace $\{P\}$ will contain the open channels. Therefore, $\{Q\} \cong \{\chi_{n>n_{\mathrm{c}}}\}$, and $\{P\} \cong \{\chi_{n\leq n_{\mathrm{c}}}\}$. Using $\chi_n(\mathbf{r})$ which are associated with the closed and the open channels as a basis set, Eq. (10.4) can be represented in the following matrix form:

$$\begin{pmatrix} \mathbf{H}_{\mathrm{QQ}} & \mathbf{H}_{\mathrm{QP}} \\ \mathbf{H}_{\mathrm{PQ}} & \mathbf{H}_{\mathrm{PP}} \end{pmatrix} \begin{pmatrix} \phi^{\mathrm{Q}}(\mathbf{R}) \\ \phi^{\mathrm{P}}(\mathbf{R}) \end{pmatrix} = E \begin{pmatrix} \phi^{\mathrm{Q}}(\mathbf{R}) \\ \phi^{\mathrm{P}}(\mathbf{R}) \end{pmatrix}\,, \tag{10.6}$$

where

$$\begin{aligned}
[\mathbf{H}_{\mathrm{QQ}}]_{n',n}(\mathbf{R}) &= \langle \chi_{n'>n_{\mathrm{c}}} | \hat{H} | \chi_{n>n_{\mathrm{c}}} \rangle_{\mathbf{r}} \,, \\
[\mathbf{H}_{\mathrm{PP}}]_{n',n}(\mathbf{R}) &= \langle \chi_{n'\leq n_{\mathrm{c}}} | \hat{H} | \chi_{n\leq n_{\mathrm{c}}} \rangle_{\mathbf{r}} \,, \\
[\mathbf{H}_{\mathrm{QP}}]_{n',n}(\mathbf{R}) &= \langle \chi_{n'>n_{\mathrm{c}}} | \hat{H} | \chi_{n\leq n_{\mathrm{c}}} \rangle_{\mathbf{r}} \,, \\
[\mathbf{H}_{\mathrm{PQ}}]_{n',n}(\mathbf{R}) &= [\mathbf{H}_{\mathrm{QP}}]^{*}_{n,n'}(\mathbf{R}) \,.
\end{aligned} \tag{10.7}$$

The functions $\phi^{\mathrm{Q}}(\mathbf{R})$ and $\phi^{\mathrm{P}}(\mathbf{R})$ are the projections of the total wavefunction into each of the subspaces given by

$$\begin{aligned}
[\phi^{\mathrm{Q}}(\mathbf{R})]_n &= \phi_{n>n_{\mathrm{c}}}(\mathbf{R}) \,, \\
[\phi^{\mathrm{P}}(\mathbf{R})]_n &= \phi_{n\leq n_{\mathrm{c}}}(\mathbf{R}) \,.
\end{aligned} \tag{10.8}$$

The subscript $\mathbf{r}$ denotes integration over this variable only. Since the eigenfunctions of $\mathbf{H}_{\mathrm{QQ}}(\mathbf{R})$ are bound states they have outgoing boundary conditions with purely imaginary positive valued wavevectors. However, the eigenfunctions of $\mathbf{H}_{\mathrm{PP}}(\mathbf{R})$ are continuum functions. Within the Hermitian formalism of quantum mechanics they have components of outgoing waves as well as components of incoming waves. Therefore, as $[|\boldsymbol{R}| \to \infty]$ the asymptotes of the open channels should be scattering states of the form

$$[\phi^{\mathrm{P}}(\mathbf{R})]_n \equiv \phi_{n>n_{\mathrm{c}}}(\mathbf{R}) \to \sqrt{\frac{M}{\hbar k_n}} \mathrm{e}^{-\mathrm{i}\mathbf{k}_n \mathbf{R}} - \sum_{n'>n_{\mathrm{c}}} S_{n,n'}(E) \sqrt{\frac{M}{\hbar k_{n'}}} \mathrm{e}^{+\mathrm{i}\mathbf{k}_{n'} \mathbf{R}} \,, \tag{10.9}$$

where for $m > n_{\mathrm{c}}$ (m stands for n or n')

$$\frac{(\hbar k_m)^2}{2M} = E - E_m^{\mathrm{th}} \tag{10.10}$$

and the incoming and outgoing waves are flux normalized.

The requirement for the continuum functions $[\phi^{\mathrm{P}}(\mathbf{R})]_n$ to behave only as outgoing waves in the asymptotes implies that $S_{n,n'>n_{\mathrm{c}}}(E) = \infty$. However, the S-matrix elements get infinitely large either when E is equal to the bound state energy of the molecule ABC (this is not the case here since ABC has been prepared in a metastable state where it has sufficient energy for dissociation) or when E is complex. The values for which the S-matrix elements are infinitely large are defined as the poles of the scattering matrix. In the case where the pole of the S-matrix has a complex value, by definition $[\phi^{\mathrm{P}}(\mathbf{R})]_n$ for $n > n_{\mathrm{c}}$ are not in the Hilbert space and can be obtained only by using the non-Hermitian formalism of quantum mechanics.

10.2 The point where QM branches into two formalisms

We are now at a delicate point in our analysis. The system defined by the Hamiltonian in Eq. (10.6) can be reduced to two types of effective Hamiltonians. One is derived only in terms of the ϕ^{P} components when we eliminate the *closed* channels from the problem, while in the other approach an effective Hamiltonian is derived in terms of the ϕ^{Q} components by eliminating the *open* channels from the problem. *In both cases the elimination of one set of channels from the problem is not an approximation and the exact energy spectrum of the problem is obtained.* In the discussion given below we demonstrate how the choice of one of the above basis sets for a derivation of an effective theory leads to the standard formalism of quantum mechanics, while the choice of the other set leads to the formulation of non-Hermitian quantum mechanics where metastable-resonance states are associated with complex eigenvalues of the time-independent Schrödinger equation as given in Eq. (10.4).

The reduction of the Hamiltonian given in Eq. (10.6) to the first type of effective Hamiltonian is achieved by reducing the two coupled equations in Eq. (10.6) to the following self-consistent eigenvalue problem:

$$\left(\mathbf{H}_{\mathrm{PP}} + \mathbf{H}_{\mathrm{PQ}}\mathbf{G}^{+}_{\mathrm{QQ}}(E)\mathbf{H}_{\mathrm{QP}}\right)\phi^{\mathrm{P}}(\mathbf{R}) = E\phi^{\mathrm{P}}(\mathbf{R})\,, \tag{10.11}$$

where

$$\mathbf{G}^{+}_{\mathrm{QQ}}(E) = \lim_{\epsilon\to 0^{+}} \frac{1}{E\mathbf{I} - \mathbf{H}_{\mathrm{QQ}} + \mathrm{i}\epsilon}\,. \tag{10.12}$$

In the transition from Eq. (10.6) to Eq. (10.11) we expressed ϕ^{Q} in terms of ϕ^{P}:

$$\phi^{\mathrm{Q}} = \varphi^{\mathrm{Q}} + \mathbf{G}^{+}_{\mathrm{QQ}}(E)\mathbf{H}_{\mathrm{QP}}\phi^{\mathrm{P}}\,, \tag{10.13}$$

where φ^{Q} is the homogenous solution such that

$$(E\mathbf{I} - \mathbf{H}_{\mathrm{QQ}})\varphi^{\mathrm{Q}} = 0\,. \tag{10.14}$$

Since E is a continuous variable while the spectrum of $\mathbf{H}_{\mathrm{QQ}}$ is discrete, we have chosen as the homogenous solution $\varphi^{\mathrm{Q}} = 0$. Note that ϕ^{Q} is a square integrable function which implies that ϕ^{Q} has an outgoing boundary condition with purely imaginary momentum, and consequently, by taking the homogenous solution as zero, we do not change the boundary condition of ϕ^{Q}. The term $+\mathrm{i}\epsilon$ in the Green's operator ensures that in Eq. (10.13) only outgoing waves will be present in the closed channels ϕ^{Q} (see Eq. (10.8) for the definition of the closed and open channels). The requirement on ϕ^{Q} to have outgoing wave asymptotes does not cause any problem since the asymptotes of bound states are indeed outgoing waves, $\mathrm{e}^{\mathrm{i}\mathbf{kR}}$ with $\mathrm{Re}(\mathbf{k}) = \mathbf{0}$ and $\mathrm{Im}(\mathbf{k}) > \mathbf{0}$.

The self-energy Hamiltonian given in Eq. (10.11) contains a non-local, energy-dependent, *non-Hermitian* operator which is known as the *optical potential*,[2]

$$\mathbf{V}^{\mathrm{P}}_{\mathrm{opt}}(\mathbf{R}, E) = \mathbf{H}_{\mathrm{PQ}}\mathbf{G}^{+}_{\mathrm{QQ}}(E)\mathbf{H}_{\mathrm{QP}}\,. \tag{10.15}$$

The physical meaning of the optical potential is clarified by replacing the full Hamiltonian by an effective Hamiltonian for the open channels only. The optical potential introduces processes by which particles in the closed channels, ϕ^{Q}, are scattered onto one or several open channels.

Exercise 10.1

Explain how the term $\mathrm{i}\epsilon$ in the Green's operator, $\hat{G}^{+}(E) = \lim_{\epsilon\to 0^{+}}(E + \mathrm{i}\epsilon - \hat{H})^{-1}$, introduces outgoing wave boundary conditions into $\Phi = \hat{G}^{+}(E)\phi$.

Let us now return to the self-energy problem in Eq. (10.11). This equation can be solved by an iterative procedure where in every step of the iteration an eigenvalue problem is solved for a non-Hermitian Hamiltonian. Since the original Hamiltonian $\hat{H}$ is a Hermitian operator, the energy E is gets real. Therefore,

$$\hat{H}^{\mathrm{P}}_{\mathrm{eff}}(E)\phi^{\mathrm{P}}(\mathbf{R}) = E\phi^{\mathrm{P}}(\mathbf{R})\,, \tag{10.16}$$

where E is real although the *effective* Hamiltonian is non-Hermitian,

$$\hat{H}^{\mathrm{P}}_{\mathrm{eff}} = \mathbf{H}_{\mathrm{PP}} + \mathbf{V}^{\mathrm{P}}_{\mathrm{opt}}(\mathbf{R}, E)\,. \tag{10.17}$$

Since in the Hermitian formalism of quantum mechanics the amplitude of the incoming waves has non-zero values, the spectrum of $\hat{H}^{\mathrm{P}}_{\mathrm{eff}}$ within the framework of the standard formalism of quantum mechanics is real, just like the spectrum of the full Hamiltonian. The key point in this derivation is in the fact that within the framework of the Feshbach formalism[3] the non-Hermitian optical potential has been derived for the open channels where the $+\mathrm{i}\epsilon$ in the denominator of the Green's operator imposes outgoing boundary conditions on ϕ^{Q} which are associated with the closed channels.

We can summarize the Feshbach formalism by stating that the derivation of the first type of self-energy effective Hamiltonian eliminated the closed channels from the problem. The price we pay for this is that now we do not solve an eigenvalue problem but instead we solve for a non-Hermitian, energy dependent and non-local Hamiltonian. However, since the boundary conditions are kept identical to the original problem, i.e., square integrable bound states are associated with the closed

---

[2] See, for example, J. R. Taylor, *Scattering Theory*, New York, John Wiley & Sons, Inc., 1972.

[3] See Feshbach 1958, in Section 10.5.

channels and scattering states are associated with the open channels, the real energy E and the eigenfunctions of the full Hermitian Hamiltonian are obtained. As we will show below, in contradiction to the derivation of the first type of Feshbach effective Hamiltonian, in the derivation of the second type of a effective Feshbach Hamiltonian when the open channels are eliminated then complex energies E (i.e., complex poles of the scattering matrix) are obtained. These complex energies E can be obtained by solving Eq. (10.16), but *not* within the framework of the standard formalism of quantum mechanics as we did above, but by imposing outgoing boundary conditions on $\phi^{\mathrm{P}}(\mathbf{R})$.

Let us briefly review here how the resonances associated with the poles of the S-matrix are obtained in nuclear systems in a simple approach described by Feshbach.[4] In the process we will emphasize the fact that the outgoing boundary condition are imposed by the Green's function.

Instead of deriving the effective Hamiltonian for the open channels as described above (Feshbach, 1958), the effective Hamiltonian for the closed channels (ϕ^{Q}) will be derived (Feshbach, 1962). As we will show below, this is a crucial point in explaining why complex energies are obtained by solving the self-consistent problem for the effective Hamiltonian of the closed channels. The self-consistent problem for the effective Hamiltonian of the closed channels is given by

$$\hat{H}^{\mathrm{Q}}_{\mathrm{eff}}(E)\phi^{\mathrm{Q}}(\mathbf{R}) = E\phi^{\mathrm{Q}}(\mathbf{R})\,. \tag{10.18}$$

where the effective Hamiltonian is

$$\hat{H}^{\mathrm{Q}}_{\mathrm{eff}} = \mathbf{H}_{\mathrm{QQ}} + \mathbf{V}^{\mathrm{Q}}_{\mathrm{opt}}(\mathbf{R}, E)\,. \tag{10.19}$$

The non-local energy-dependent operator which is associated with the effective Hamiltonian of the closed channels is defined as

$$\mathbf{V}^{\mathrm{Q}}_{\mathrm{opt}}(\mathbf{R}, E) = \mathbf{H}_{\mathrm{QP}}\mathbf{G}^{+}_{\mathrm{PP}}(E)\mathbf{H}_{\mathrm{PQ}}\,, \tag{10.20}$$

where the Green's operator is now associated with the Hamiltonian of the open channels' Hamiltonian and *not* with the that of the closed channels,

$$\mathbf{G}^{+}_{\mathrm{PP}}(E) = \lim_{\epsilon\to 0^{+}} \frac{1}{E\mathbf{I} - \mathbf{H}_{\mathrm{PP}} + \mathrm{i}\epsilon}\,. \tag{10.21}$$

Here we come to the subtle point in our derivation. In the transformation of the original full problem in Eq. (10.4) into Eq. (10.18) we used the following identity:

$$\phi^{\mathrm{P}} = \mathbf{G}^{+}_{\mathrm{PP}}(E)\mathbf{H}_{\mathrm{PQ}}\phi^{\mathrm{Q}}\,. \tag{10.22}$$

---

[4] See Feshbach, 1962, in Section 10.5.

In writing Eq. (10.22) we set the homogenous solution φ^{P} which is an eigenfunction of $\mathbf{H}_{\mathrm{PP}}$ to be equal to *zero* although the eigenvalue of $\mathbf{H}_{\mathrm{PP}}$ is a continuous variable E and its corresponding eigenfunction can be taken as the homogeneous solution. *This is the point where we have to choose between adhering to the standard formalism or digressing to the non-Hermitian formalism of quantum mechanics.* As we proved in Ex. (9.1), if

$$\lim_{x\to\infty}\Phi(x)=\int_{-\infty}^{+\infty}\mathrm{d}k'[A(k')\mathrm{e}^{\mathrm{i}k'x}+B(k')\mathrm{e}^{-\mathrm{i}k'x}] \tag{10.23}$$

then the limit of $\hat{G}(E=k^2/2)\Phi(x)$ as $x\to\infty$ is an outgoing wave,

$$\lim_{x\to\infty}\hat{G}(E)\Phi(x)\propto\mathrm{e}^{\mathrm{i}kx}\,. \tag{10.24}$$

Consequently, as will be explained below, by taking the homogenous solution of ϕ^{P} that has incoming and outgoing wave components to be equal to zero, we impose on the non-homogeneous solution of ϕ^{P} outgoing boundary conditions which imply complex values of E, and thereby making ϕ^{P} an exponentially divergent function which is in the non-Hermitian sector of the domain of the Hamiltonian. Note, however, that by keeping the homogeneous solution, ϕ^{P}, just as defined in standard quantum mechanics we get that the non-homogeneous solution ϕ^{P} also has incoming and outgoing wave components. In such a case the self-consistent solutions of Eq. (10.19) get only real values just as in the standard formalism of quantum mechanics.

The explanation above for the point of bifurcation of quantum mechanics into an Hermitian formalism and a non-Hermitian formalism is based on the fact that the term $\mathrm{i}\epsilon$ in the Green's operator, $\hat{G}^+(E)=\lim_{\epsilon\to 0^+}(E+\mathrm{i}\epsilon-\hat{H})^{-1}$ introduces outgoing wave boundary conditions on $|\Phi\rangle=\hat{G}^+(E)|\Psi\rangle$ for any wavepacket $|\Psi\rangle$ which can be described as a linear combination of incoming and outgoing waves. Let us explain this in detail. The term $+i\epsilon$ appearing in Eq. (10.21) ensures that in Eq. (10.22) only outgoing waves will be represented in ϕ^{P}. The problem from the point of view of the Hermitian formulation of quantum mechanics is that ϕ^{P} is associated with the open channels (see Eq. (10.8)). The requirement of ϕ^{P} to have outgoing wave asymptotes implies that the amplitudes of the incoming waves vanish and therefore $S_{n,n'}(E)=\infty$ (see Eq. (10.9)). The scattering state conditions which are needed to conserve the flux (see Eq. (10.9)) are not satisfied. Thus, imposing outgoing wave boundary conditions on $\phi^{\mathrm{P}}(\mathbf{R})$ implies that the flux is not conserved any more. Therefore, when we disregard the possibility of bound states in the continuum, $S_{n,n'}(E)=\infty$ for a *complex* value of $E=E_{\mathrm{res}}$, where $\mathrm{Re}(E_{\mathrm{res}})$ is in the continuum of the spectrum. Since E for which Eq. (10.18) is satisfied is the eigenvalue of the original full problem, Eq. (10.4), this means that $E = E_{\rm res} = E_{\rm r} - {\rm i}/2\Gamma$ is a resonance solution of our problem. We should re-emphasize the fact that the complex resonance eigenvalue $E = E_{\rm res}$ is obtained here by solving Eq. (10.18) where the complex resonance eigenvalue is associated with an eigenfunction embedded in the generalized Hilbert space (i.e., $(\phi^{\rm Q})^2$ is integrable rather than $|\phi^{\rm Q}|^2$ in the Hilbert space).

We can summarize the above discussion in the following points.

(1) The term $+{\rm i}\epsilon$ appearing in Eq. (10.21) ensures that the continuum functions $\phi^{\rm P}(E)$ defined in Eq. (10.22) have outgoing waves only and therefore are associated with complex eigenvalues E. The only situation in which this kind of solution may come about within the framework of standard quantum mechanics is when there are true bound states in the continuum and E has real values only.

(2) Instead of deriving an effective Hamiltonian for the open channels we derive an effective Hamiltonian for the closed channels by eliminating the open channels from our problem. By doing so we change the wave boundary conditions of the original full problem. The obtained continuum states which are associated with the open channels are not scattering states and have outgoing wave boundary conditions which are the same boundary conditions for the bound states associated with the closed channels. This gives a convincing explanation for the text-book result that an optical potential becomes a complex function for energies above the threshold.[5]

If one wishes to define a point where the formulation of quantum mechanics branches into the standard Hermitian formulation and the non-Hermitian formulation, it is the point in our derivation where we decide to construct the effective Hamiltonian for the closed channels rather than for the open channels.

The question now is can the energy E which solves Eq. (10.18) attain a complex value $E = E_{\rm r} - \frac{\rm i}{2}\Gamma$ as proposed above?

The answer to this question is positive. $E = E_{\rm r} - \frac{\rm i}{2}\Gamma$ is a simple pole of the optical potential. Let us prove this claim. The spectral representation of $\mathbf{H}_{\rm PP}$ is

$$\mathbf{H}_{\rm PP} = \int_0^{+\infty} {\rm d}E_{\rm c}\, E_{\rm c}\rho(E_{\rm c})|\phi^{\rm P}_{E_{\rm c}}\rangle\langle\phi^{\rm P}_{E_{\rm c}}|\,, \tag{10.25}$$

where $E_{\rm c}$ stands for the continuum energy spectrum of the open channels and $\rho(E_{\rm c})$ is the density of states in the continuum. When the continuum states are energy normalized such that $\langle E|E'\rangle = \delta(E - E')$ there is no need to introduce $\rho(E_{\rm c})$ into the integration over $E_{\rm c}$. We introduce here $\rho(E_{\rm c})$ since we assume that the continuum eigenfunctions were calculated using the box-quantization condition while taking the limit of the box-size to infinity. The use of the box-quantization condition helped us in the derivation of the Fermi golden rule for the calculations of the resonance widths (see Chapter 3).

---

[5] See, for example, J. R. Taylor, Scattering Theory, New York, John Wiley & Sons, Inc., 1972.

By using the spectral representation of $\mathbf{H}_{\mathrm{PP}}$, one gets that

$$\begin{aligned} E &= \langle \phi^{\mathrm{Q}} | \hat{H}_{\mathrm{QQ}} | \phi^{\mathrm{Q}} \rangle + \langle | \phi^{\mathrm{Q}} | \mathbf{V}_{\mathrm{opt}}(\mathbf{R}, E) | \phi^{\mathrm{Q}} \rangle \\ &= \langle \hat{H}_{\mathrm{QQ}} \rangle + \lim_{\epsilon \to 0^+} \int_0^{+\infty} \mathrm{d}E_{\mathrm{c}} \rho(E_{\mathrm{c}}) \frac{\langle \phi^{\mathrm{Q}} | \mathbf{H}_{\mathrm{QP}} | \phi^{\mathrm{P}}_{E_{\mathrm{c}}} \rangle \langle \phi^{\mathrm{P}}_{E_{\mathrm{c}}} | \mathbf{H}_{\mathrm{PQ}} | \phi^{\mathrm{Q}} \rangle}{E - E_{\mathrm{c}} + i\epsilon}, \end{aligned} \tag{10.26}$$

assuming that all poles of the Green's function are at a finite "distance" from the real E_{c} axis so that the contour of integration along the real E_{c} (E_{c} varies from 0 to ∞) can be replaced by a closed contour of integration in the complex E_{c} plane with radius $|E^0_{\mathrm{c}}|$. Thus we integrate along the real axis from 0 to $2|E^0_{\mathrm{c}}|$, and return to the origin on a semi-circle on the lower half of the energy plane centered around $|E^0_{\mathrm{c}}|$. The replacement of the contour of integration from the real axis to a closed contour in the complex plane is possible when the integrand is exponentially small in the lower half complex plane of E_{c} where $|E_{\mathrm{c}}| > |E^0_{\mathrm{c}}|$.

By using the definition of a delta function as the limit of a function which exhibits a sharp peak about E, while its integral over all space is equal to 1, one gets that

$$\lim_{\epsilon \to 0^+} \frac{1}{E - E_{\mathrm{c}} + \mathrm{i}\epsilon} = \mathrm{PV}\left[\frac{1}{E - E_{\mathrm{c}}}\right] \mp \mathrm{i}\pi\delta(E - E_{\mathrm{c}}), \tag{10.27}$$

where PV stands for the (Cauchy) principal value.

By substituting Eq. (10.27) into Eq. (10.26) one obtains

$$\begin{aligned} E = \langle \phi^{\mathrm{Q}} | \hat{H}_{\mathrm{QQ}} | \phi^{\mathrm{Q}} \rangle + \mathrm{PV} \int_0^{\infty} \mathrm{d}E_{\mathrm{c}} \rho(E_{\mathrm{c}}) \frac{|\langle \phi^{\mathrm{Q}} | \mathbf{H}_{\mathrm{QP}} | \phi^{\mathrm{P}}_{E_{\mathrm{c}}} \rangle|^2}{E - E_{\mathrm{c}}} \\ - \mathrm{i}\pi\rho(E) \langle \phi^{\mathrm{Q}} | \mathbf{H}_{\mathrm{QP}} | \phi^{\mathrm{P}}_{\mathrm{E}} \rangle \langle \phi^{\mathrm{P}}_{\mathrm{E}} | \mathbf{H}_{\mathrm{PQ}} | \phi^{\mathrm{Q}} \rangle . \end{aligned} \tag{10.28}$$

Note in passing that since E becomes complex,

$$\langle \phi^{\mathrm{P}}_{\mathrm{E}} | \mathbf{H}_{\mathrm{PQ}} | \phi^{\mathrm{Q}} \rangle \neq [\langle \phi^{\mathrm{Q}} | \mathbf{H}_{\mathrm{QP}} | \phi^{\mathrm{P}}_{\mathrm{E}} \rangle]^* \tag{10.29}$$

and one should carry out analytical continuation of E from the real axis (where the equality holds) to the complex E plane in order to evaluate the third term in Eq. (10.28).

Exercise 10.2

Solve Eq. (10.18) for a two-channel problem where the potential in the closed channel (Q) is defined as $V_1(x) = V_0 - V_1\delta(x)$, the potential in the open channel (P) is given by $V_2(x) = 0$ and the coupling between the two (Q and P) channels is given by $V_{1,2} = \lambda\delta(x)$. Obtain a transcendental equation for the complex energy E which is associated with the Feshbach resonance positions, E_{r}, and widths, Γ. Use the fact that a delta potential well, $-\alpha\delta(y)$, supports a single outgoing wave eigenstate which is associated with an eigenvalue $E = -\alpha^2/2$.

Since Eq. (10.27) holds only for real values of E it implies that in the derivation of Eq. (10.28) we make an approximation where in the right-hand side of Eq. (10.28) we have to introduce the real part of E. Another approximation we can apply in order to simplify Eq. (10.28) is by assuming that:

(1) there is only one closed channel which supports a single bound state, $|E_b\rangle$ and in the right-hand side of Eq. (10.28) we can replace E by E_b since E is embedded close enough to the real axis (the resonance state is a narrow resonance which has sufficiently long lifetime to justify this approximation);
(2) there is only one open channel with the threshold energy $E_1^{\text{th}} = 0$, and $\hat{H}_{PQ} = \hat{V}_{\text{coup}}$. We also assume here that the continuum of the open channel is structure-less. Specifically, the density of states, $\rho(E_c)$, varies monotonically with $E_c > 0$.

Under these assumptions Eq. (10.28) reduces to

$$E = E_r - \frac{i}{2}\Gamma\,, \tag{10.30}$$

where the resonance position is defined as $E_r = E_b + \Delta$ and the shift from the bound energy value is given by

$$\Delta = \text{PV}\int_0^\infty dE_c\,\rho(E_c)\frac{|\langle\phi^Q|\hat{V}_{\text{coup}}|\phi^P_{E_c}\rangle|^2}{E_b - E_c}\,. \tag{10.31}$$

The resonance width Γ is given by

$$\Gamma = 2\pi\rho(E_b)|\langle\phi^Q|\hat{V}_{\text{coup}}|\phi^P_{E_b}\rangle|^2\,, \tag{10.32}$$

where $\rho(E_b)$ is the density of states in the open channel. Here we neglect the shift of the resonance position from E_b. In the case of one-dimensional problems or in the case of three-dimensional problems with s-wave symmetry, or when photo-ionization is induced by a linearly polarized laser which takes place primely along one direction, then $\rho(E_b) \simeq 1/\sqrt{E_b}$. Therefore, as the bound state in the closed channel approaches the threshold energy of the open channel $\Gamma(\text{Feshbach}) \to \infty$ (provided $|\langle\phi^Q|\hat{V}_{\text{coup}}|\phi^P_{E_b}\rangle|^2$ does not decay to zero faster or as fast as $\rho(E_b)$ when $E_b \to 0$) . This behavior is very different from the behavior of shape-type resonances where the tunneling through the potential barrier is suppressed as the position of the resonance state approaches the threshold energy.

We can have a better estimate for the value of the decay rate Γ of the Feshbach resonance when E_b is varied as it approaches the threshold energy of the open channel from above (just before it becomes a bound state) by calculating the value of E_b for which $E_\mathrm{b} + \Delta = 0$. Using the approximate expression for the Feshbach resonance position given in Eq. (10.57) we can estimate the value of E_b for which the resonance coincides with the threshold energy of the open channel. For example, for $\alpha = 1$ the resonance position is at the threshold energy when $E_\mathrm{b} = E_\mathrm{b}^\mathrm{th} = 0.28309$. Since $\rho(E_\mathrm{b}^\mathrm{th})$ has a finite value then $\Gamma(\text{Feshbach}) \to$ finite value as well when the resonance position approaches the threshold energy of the open channel. The expression in Eq. (10.32) we obtained for the resonance decay rate Γ is identical to that of the Fermi golden rule expression (see the derivation of the Fermi golden rule in Ex. 3.2).

It is important to realize that the complex energies E obtained by solving Eq. (10.18) with the non-Hermitian effective Hamiltonian given in Eq. (10.19) are also eigenvalues of the physical Hamiltonian given in Eq. (10.4). It implies that the corresponding eigenfunctions are not in the Hilbert space as in the conventional formulation of quantum mechanics. The change of the boundary conditions in the solutions of the time-independent Schrödinger equation is "responsible" for the non-Hermitian property of the physical Hamiltonian. *We may say that the solutions obtained in conventional quantum mechanics calculations are embedded in the Hermitian sector of the domain of the operator, whereas the resonance solutions are embedded in the non-Hermitian sector of the domain of the same physical operator.*

It is a point of interest that the resonance solutions which are embedded in the non-Hermitian sector of the domain of the Hamiltonian are obtained from a very common application of the Green's function method to the Hermitian formulation of quantum mechanics where the outgoing boundary conditions are imposed by the Green's operator.

Exercise 10.3

One-dimensional model Hamiltonians for atoms in laser fields are commonly used in the literature since the oscillating field breaks the spherical symmetry of the atom and the electrons are ionized along a direction determined by the ac field.

Calculate the value of the shift in the resonance position from the bound state energy in the closed channel for the case where the density of states in the continuum of the open channel is $\rho(E_\mathrm{c}) = \sqrt{1/E_\mathrm{c}}$, the free electron functions are flux normalized, the bound state in the closed channel is the ground state of a one-dimensional harmonic potential, and $\hat{V}_\mathrm{coup} = \mathcal{E}_0 x \mathrm{e}^{-(x/\sigma)^2}$, where σ is much larger than the size of the system under consideration (e.g., an atom or a molecule, or an artificial mesoscopic structure).

In this model $\hat{V}_\mathrm{coup}$ is the coupling between the bound state of the atom and the continuum due to the effective absorption of one photon (no multi-photon absorption processes) when a weak ac field of linearly polarized light is applied. Therefore, by using the dressed picture formalism one gets that $\mathcal{E}_0$ is the maximum field amplitude of the laser field divided by 2. The Gaussian window function introduces into the calculations the fact that the laser beam has a finite width σ and therefore the dipole introduced by the laser field is effective only in a finite spatial region.

10.3 Concluding remarks

We have shown here that the Hamiltonian becomes non-Hermitian by imposing outgoing boundary conditions resulting from the use of the Green's operator $G^+(E)$. We showed that Feshbach resonances are associated with complex eigenvalues of an effective Hamiltonian which is non-Hermitian while the associated eigenfunctions of the closed channels are square integrable and are in the Hilbert space. However, the corresponding open channel functions are not in the Hilbert space. The derivation of an effective Hamiltonian provides a method for calculating Feshbach resonances which avoids the need to overcome the computational difficulties due to the exponential divergence of the open channel functions. In addition it shows that the non-Hermitian formulation of quantum mechanics comes about in a very natural way. It is very important to notice that the complex eigenvalues are are not only associated with the effective Hamiltonian but they are also those of the full problem and are not obtained by a truncation of the number of channels which are taken into consideration.

10.4 Solutions to the exercises

Answer to Exercise 10.1

The spectral representation of the Green's operator is given by

$$\hat{G}^+(E) = \frac{1}{E - \hat{H} + \mathrm{i}\epsilon} = \int \mathrm{d}E' \frac{|\Psi_{E'}\rangle\langle\Psi_{E'}|}{E - E' + \mathrm{i}\epsilon}\,, \tag{10.33}$$

where $\epsilon \to 0^+$ (we omit the use of $\lim_{\epsilon\to 0^+}$ for brevity) and

$$\hat{H}|\Psi_{E'}\rangle = E'|\Psi_{E'}\rangle\,. \tag{10.34}$$

The continuum functions are energy normalized and therefore the density of states does not appear in the integration over the energy as it would in the case when the box-quantization is applied.

The asymptote of the energy normalized eigenfunctions $\Psi_{E'}$ consists of incoming and outgoing waves, $\frac{1}{\sqrt{2\pi k}}\mathrm{e}^{\pm \mathrm{i}kx}$, which are respectively associated with negative and positive momentum $p = \hbar k$. The energy is related to the momentum through $E' = (\hbar k)^2/2$ (here we use for simplicity a one-dimensional Hamiltonian for non-interacting particles). We will use the atomic units where $m_{\mathrm{e}} = \hbar = 1$. Since we wish to show that the asymptote of $\Phi = \hat{G}^+(E)\phi$ is an outgoing wavepacket we will calculate

$$\lim_{x\to\infty} \Phi(x) = \hat{\mathcal{G}}^+_\infty(E)\phi_\infty(x)\,, \tag{10.35}$$

where $\phi_\infty(x) = \lim_{x\to\infty}\phi(x)$, $\hat{\mathcal{G}}^+_\infty(E) = (E^+ + \frac{1}{2}\frac{\mathrm{d}^2}{\mathrm{d}x^2})^{-1}$, and $E^+ = E + \mathrm{i}\epsilon$. Therefore,

$$\lim_{x\to\infty} \Phi(x) = \int_{-\infty}^{+\infty} \mathrm{d}x' \mathcal{G}^+_E(x,x')\phi_\infty(x')\,, \tag{10.36}$$

where

$$\begin{aligned}\mathcal{G}^+_E(x,x') &= \frac{1}{2\pi}\int_{-\infty}^{+\infty} \mathrm{d}k \frac{\mathrm{e}^{\mathrm{i}k(x-x')}}{E^+ - k^2/2} \\ &= \frac{1}{2\pi}\int_{-\infty}^{+\infty} \mathrm{d}k\, \mathrm{e}^{\mathrm{i}k(x-x')} \frac{1}{\sqrt{2E^+}}\left[\frac{1}{\sqrt{2E^+}-k} + \frac{1}{\sqrt{2E^+}+k}\right].\end{aligned} \tag{10.37}$$

Next we will employ the residue theorem (note that $E' = k^2/2$ and E is a free parameter in our derivation, where $E' = E + \mathrm{i}\epsilon$ such that $\mathrm{Im}(E') > 0$),

$$\int_{-\infty}^{+\infty} \mathrm{d}k \frac{\mathrm{e}^{\mathrm{i}k(x-x')}}{\sqrt{2E^+} \pm k} = -2\pi \mathrm{i}\mathrm{e}^{\mp \mathrm{i}\sqrt{2E^+}(x-x')}\,. \tag{10.38}$$

Notice that $\mathrm{e}^{-\mathrm{i}\sqrt{2E^+}(x-x')} \to 0$ when $x < x'$ and diverges exponentially when $x > x'$. Conversely, $\mathrm{e}^{+\mathrm{i}\sqrt{2E^+}(x-x')} \to 0$ when $x > x'$ and diverges exponentially when $x < x'$. Consequently, by applying the Green's operator on $\phi(x)$,

$$\begin{aligned}\lim_{x\to\infty} \Phi(x) = \frac{1}{\mathrm{i}\sqrt{2E}}\Bigg[&\mathrm{e}^{+\mathrm{i}\sqrt{2E}x}\int_{-\infty}^{x} \mathrm{d}x' \mathrm{e}^{\mathrm{i}\sqrt{2E^+}x'}\phi_\infty(x') \\ &+ \mathrm{e}^{-\mathrm{i}\sqrt{2E}x}\int_{x}^{\infty} \mathrm{d}x' \mathrm{e}^{-\mathrm{i}\sqrt{2E^+}x'}\phi_\infty(x')\Bigg].\end{aligned} \tag{10.39}$$

Since as $x \to \infty$ the second term in the r.h.s of Eq. (10.39) vanishes,

$$\lim_{x\to\infty} \Phi(x) = \frac{1}{\mathrm{i}\sqrt{2E}}\left[\int_{-\infty}^{+\infty} \mathrm{d}x' \mathrm{e}^{\mathrm{i}\sqrt{2E}x'}\phi_\infty(x')\right]\mathrm{e}^{+\mathrm{i}\sqrt{2E}x}\,. \tag{10.40}$$

Equation (10.40) shows that the wavepacket $\Phi = \hat{G}^+(E)\phi$ is indeed constructed of outgoing waves only. This completes the proof that the $+\mathrm{i}\epsilon$ in the Green's operator, $\hat{G}^+(E) = \lim_{\epsilon\to 0^+}(E + \mathrm{i}\epsilon - \hat{H})^{-1}$, introduces outgoing wave boundary conditions on $\Phi = \hat{G}^+(E)\phi$.

Answer to Exercise 10.2

Following Eq. (10.18), the resonance state of our problem is the complex solution of the self-consistent equation

$$\left[-\frac{1}{2}\partial_x^2 + V_0 - V_1\delta(x)\right]\Phi^{\mathrm{Q}}(x) + \lambda^2\delta(x)\int dx' G_E^{\mathrm{PP}}(x,x')\delta(x')\Phi^{\mathrm{Q}}(x') = E\Phi^{\mathrm{Q}}(x)\,, \tag{10.41}$$

where $G_E^{\mathrm{PP}}(x,x')$ is the Green's's function of a free particle which satisfies

$$\left(E + \frac{1}{2}\partial_x^2\right) G_E^{\mathrm{PP}}(x,x') = \delta(x-x')\,. \tag{10.42}$$

It is straightforward to show that

$$G_E^{\mathrm{PP}}(x,x') = -\frac{\mathrm{i}}{k}\mathrm{e}^{\mathrm{i}k|x-x'|}\,. \tag{10.43}$$

The proof is as follows.

By defining a new variable $y = x - x'$ and substituting the ansatz that $G_E^{\mathrm{PP}}(x,x') = A\mathrm{e}^{\mathrm{i}k|y|}$ into Eq. (10.41), it is clear that for positive values of ϵ

$$\begin{aligned}
&\int_{-\epsilon}^{+\epsilon} \mathrm{d}y \left[\left(E + \frac{1}{2}\partial_y^2\right) G_E^{\mathrm{PP}}(y) - \delta(y)\right] = 0\,,\\
&\frac{1}{2}\left[\partial_y G_E^{\mathrm{PP}}\Big|_{y=+\epsilon} - \partial_y G_E^{\mathrm{PP}}\Big|_{y=-\epsilon}\right] - 1 = 0\,.\\
&\frac{1}{2}\left[\mathrm{i}kA\mathrm{e}^{\mathrm{i}k|\epsilon|} - (-\mathrm{i}kA)\mathrm{e}^{\mathrm{i}k|\epsilon|}\right] - 1 = 0\,.
\end{aligned} \tag{10.44}$$

By taking the limit of $\epsilon \to 0$, Eq. (10.44) reduces to the condition

$$\mathrm{i}kA - 1 = 0 \tag{10.45}$$

and therefore $A = -\mathrm{i}/k$, as given in Eq. (10.43).

The next step in our calculations is to substitute Eq. (10.43) into Eq. (10.41) which leads to

$$\lambda^2\delta(x)\int \mathrm{d}x' G_E^{\mathrm{PP}}(x,x')\delta(x')\Phi^{\mathrm{Q}}(x') = -\lambda^2\delta(x)\frac{\mathrm{i}}{k}\mathrm{e}^{\mathrm{i}k|x|}\Phi^{\mathrm{Q}}(0)\,. \tag{10.46}$$

Since $\delta(x) = 0$, for $x \neq 0$ we can replace $\mathrm{e}^{\mathrm{i}k|x|}\Phi^{\mathrm{Q}}(0)$ in the above equation by $\mathrm{e}^{\mathrm{i}k0}\Phi^{\mathrm{Q}}(x)$. Therefore, Eq. (10.41) can be rewritten as

$$\left[-\frac{1}{2}\partial_x^2 - \alpha\delta(x)\right]\Phi^{\mathrm{Q}}(x) = (E - V_0)\Phi^{\mathrm{Q}}(x)\,, \tag{10.47}$$

where we define $E = k^2/2$, $E - V_0 = q^2/2$ and

$$\alpha = V_1 + \mathrm{i}\frac{\lambda^2}{k}\,. \tag{10.48}$$

The resonance state for our two-coupled-channel problem is the solution of the effective self-consistent equation given above.

Using the given information that a delta potential well, $-\alpha\delta(x)$, supports a single outgoing wave eigenstate which is associated with an eigenvalue for which $q^2 = -\alpha^2$, and thus $q = \mathrm{i}\alpha$, we obtain that the resonance complex energy $E = k^2/2$ is a solution of the following transcendental equation:

$$kq(k) - \mathrm{i}kV_1 + \lambda^2 = 0\,. \tag{10.49}$$

The resonance solution to this transcendental equation can be found using graphical or numerical methods. For a graphical solution, one method is to plot the absolute value of Y:

$$Y = k\sqrt{k^2 - 2V_0} - \mathrm{i}kV_1 + \lambda^2\,, \tag{10.50}$$

as a function of the complex k where the solutions are the values for $|Y| = 0$.

For the sake of completeness of our representation we prove below that indeed the solution of Eq. (10.47) with outgoing asymptote is associated with an eigenvalue $E = -\alpha^2/2$. For real values of α the wavevector q is purely imaginary, i.e., $q = \mathrm{i}|q|$, and $\Phi^{\mathrm{Q}}(x)$ is a bound state, whereas for complex values of α complex eigenvalues (decay resonance poles of the scattering matrix) are obtained. We substitute the anzatz that $\Phi^{\mathrm{Q}}(x) = A\mathrm{e}^{\mathrm{i}q|x|}$ in Eq. (10.47) and integrate over x from $-\epsilon$ to $+\epsilon$. Resulting from this integration one gets

$$-\frac{1}{2}\left[\left.\frac{\mathrm{d}\Phi^{\mathrm{Q}}}{\mathrm{d}x}\right|_{x=\epsilon} - \left.\frac{\mathrm{d}\Phi^{\mathrm{Q}}}{\mathrm{d}x}\right|_{x=-\epsilon}\right] - \alpha\Phi^{\mathrm{Q}}(0) = 0\,. \tag{10.51}$$

After the integration we substitute our anzatz for the solution and take the limit of $\epsilon \to 0$. This mathematical operations yields the following equation:

$$-\frac{1}{2}\left[2\mathrm{i}q\Phi^{\mathrm{Q}}(0)\right] - \alpha\Phi^{\mathrm{Q}}(0) = 0\,, \tag{10.52}$$

which is reduced to the final result $q = \mathrm{i}\alpha$ and consequently to

$$E = \frac{q^2}{2} = E_{\mathrm{r}} - \frac{\mathrm{i}}{2}\Gamma\,, \tag{10.53}$$

where

$$E_{\mathrm{r}} = -\frac{\mathrm{Re}(\alpha^2)}{2}\,,$$

$$\Gamma = \mathrm{Im}(\alpha^2)\,. \tag{10.54}$$

Answer to Exercise 10.3

For convenience in solving this problem we use atomic units with $m_{\mathrm{e}} = \hbar = 1 = a_0$, where the mass of the electron is m_{e} and and the Bohr radius is defined as $a_0 = \hbar^2/(m_{\mathrm{e}}e^2) = 1$. Therefore, $E_{\mathrm{c}} = k_{\mathrm{c}}^2/2$, where k_{c} is the wave vector of the continuum function of a free particle in the open channel. The threshold energy of the open channel is taken here as 0. Accordingly, the bound state energy in the closed channel is positive, i.e. $E_{\mathrm{b}} > 0$. Since the singularity in the expression for the resonance shift given in Eq. (10.31) is at $E_{\mathrm{c}} = E$, the PV of the divergent integral is obtained by calculating the limit of the integral outside the interval $(E_{\mathrm{b}} - \epsilon, E_{\mathrm{b}} + \epsilon)$ as $\epsilon \to 0$. Specifically, the shift in the resonance position from the bound state energy in the closed channel, E_{b}, is defined as

$$\Delta = \lim_{\epsilon \to 0} \left[\int_0^{E_{\mathrm{b}}-\epsilon} \mathrm{d}E_{\mathrm{c}} \frac{|\langle \phi^{\mathrm{Q}}_{\mathrm{bound}} | \hat{V}_{\mathrm{coup}} | \phi^{\mathrm{P}}_{E_{\mathrm{c}}} \rangle|^2}{\sqrt{E_{\mathrm{c}}}(E_{\mathrm{b}} - E_{\mathrm{c}})} + \int_{E_{\mathrm{b}}+\epsilon}^{\infty} \mathrm{d}E_{\mathrm{c}} \frac{|\langle \phi^{\mathrm{Q}}_{\mathrm{bound}} | \hat{V}_{\mathrm{coup}} | \phi^{\mathrm{P}}_{E_{\mathrm{c}}} \rangle|^2}{\sqrt{E_{\mathrm{c}}}(E_{\mathrm{b}} - E_{\mathrm{c}})} \right]. \tag{10.55}$$

The ground state in the closed channel is defined by $\phi^{\mathrm{Q}}_{\mathrm{bound}}(x) = (\alpha/\pi)^{1/4} \mathrm{e}^{-\alpha x^2/2}$.

Within the interval $-L/2 < x < +L/2$, where $L > 1/\alpha$ is the size of the system under consideration, $\hat{V}_{\mathrm{coup}} \simeq \mathcal{E}_0 x$. The matrix element $\langle \phi^{\mathrm{Q}}_{\mathrm{bound}} | \hat{V}_{\mathrm{coup}} | \phi^{\mathrm{P}}_{E_{\mathrm{c}}} \rangle$ (where the continuum functions are fluxed normalized) is equal to

$$\langle \phi^{\mathrm{Q}}_{\mathrm{bound}} | \hat{V}_{\mathrm{coup}} | \phi^{\mathrm{P}}_{E_{\mathrm{c}}} \rangle = \mathcal{E}_0 \int_{-\infty}^{+\infty} \mathrm{d}x \mathrm{e}^{-\frac{\alpha x^2}{2}} x \mathrm{e}^{+\mathrm{i}k_{\mathrm{c}}x} k_{\mathrm{c}}^{-1/2} = \mathrm{i}\mathcal{E}_0 \frac{\sqrt{2\pi}}{\alpha^{3/2}} \sqrt{k_{\mathrm{c}}} \mathrm{e}^{-\frac{k_{\mathrm{c}}^2}{2\alpha} k_{\mathrm{c}}} . \tag{10.56}$$

Therefore (note that $\sqrt{E_{\mathrm{c}}} = k_{\mathrm{c}}/\sqrt{2}$)

$$\begin{aligned} \Delta &\simeq \mathcal{E}_0^2 \frac{2\pi\sqrt{2}}{\alpha^3} \lim_{\epsilon \to 0} \left[\int_0^{E_{\mathrm{b}}-\epsilon} \mathrm{d}E_{\mathrm{c}} \frac{\mathrm{e}^{-\frac{2E_{\mathrm{c}}}{\alpha}}}{E_{\mathrm{b}} - E_{\mathrm{c}}} + \int_{E_{\mathrm{b}}+\epsilon}^{\infty} \mathrm{d}E_{\mathrm{c}} \frac{\mathrm{e}^{\frac{-2E_{\mathrm{c}}}{\alpha}}}{E_{\mathrm{b}} - E_{\mathrm{c}}} \right] \\ &= \mathcal{E}_0^2 \frac{4\pi\sqrt{2}}{\alpha^3} \mathrm{e}^{-\frac{E_{\mathrm{b}}}{\alpha}} \, \mathrm{Ei}(E_{\mathrm{b}}/\alpha), \end{aligned} \tag{10.57}$$

where Ei is the second exponential-integral function.[6]

10.5 Further reading

H. Baumgärtel, *Analytic Perturbation Theory for Matrices and Operators*, Berlin, Akademie-Verlag, 1984 and *Operator Theory: Adv. Appl.* **15** (1985).

P. A. M. Dirac, *The Principles of Quantum Mechanics*, 4th edn., Oxford, Clarendon Press, 1958.

---

[6] Equation (5.1.2) in Abramowitz and Stegun, *Handbook of Mathematical Functions*, New York, Dover Publications, Inc., 1970.

H. Feshbach, *Theoretical Nuclear Physics*, New York, John Wiley & Sons, Inc., 1992.

H. Feshbach, Unified theory of nuclear reactions, *Ann. Phys*. **5**, 357–390 (1958).

H. Feshbach, Unified theory of nuclear reactions: II, *Ann. Phys*. **19**, 287–313 (1962).

N. Moiseyev, Feshbach resonances: the branching of quantum mechanics into Hermitian and non-Hermitian formalisms, *J. Phys. Chem. A*. **113**, 7660–7666 (2009).

Index